# THE SYNTHESIS AND STUDY OF BRIDGING HETEROCYCLIC LIGANDS

A thesis
submitted in partial fulfilment
of the requirements for the Degree
of
Doctor of Philosophy in Chemistry
in the
University of Canterbury
by
Christopher J. Sumby


University of Canterbury
Christchurch
New Zealand
2003

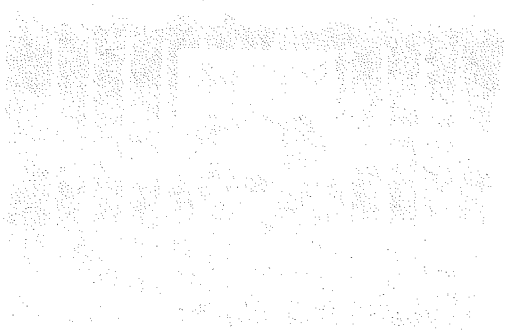

# Acknowledgements

First and foremost I would like to acknowledge my supervisor, Prof. Peter Steel, who seeded my mind with a project that has captivated my interest and expanded my knowledge and experience these past three years; his guidance, supervision and encouragement have made this thesis possible.

My thanks to many of the academic staff in the Chemistry Department for their open door policy, in particular Dr Alison Downard, Dr Jonathan Morris, Prof. Ward Robinson and Dr Jan Wikaira for their time and expertise. I would particularly like to express my gratitude to Dr Dave McMorran; his efforts were the equal of another supervisor. Further thanks to Prof. Richard Keene for his assistance early on in my project, and to Deanna D'Alessandro, for her skilful synthetic work. My thanks also to the technical staff in the department who work diligently away, often unseen. Particular thanks to Bruce Clark for mass spectrometric analysis, and to the technical staff who maintain the diffractometer.

The Steel group lab, and the department as a whole, has been a friendly and enjoyable environment in which to study. It has been a pleasure to share a lab with Dave, Chris F., William, Thomas, Nick, Stephan, Muna, Robert, Philip and more recently, Jon, Jennifer, Justine and Neroli.

My family has supported me throughout my studies and I thank them for their love and encouragement. Special thanks must go to my fiancé, Krista, who allowed me to put things into perspective on many occasions; her never-ending love, friendship and understanding helped me to where I am today.

# Table of Contents

# Abbreviations

| | |
|---|---|
| BINAP | 2,2'-bis(diphenylphosphino)-1,1'-binaphthyl |
| bpy | 2,2'-bipyridine |
| dmb | 4,4'-dimethyl-2,2'-bipyridine |
| CIS | coordination induced shift |
| COSY | correlation spectroscopy |
| dba | dibenzylideneacetone |
| DDQ | 2,3-dichloro-5,6-dicyano-1,4-benzoquinone |
| DMF | N,N-dimethylformamide |
| DMSO | dimethylsulfoxide |
| DPV | differential pulse votammetry |
| ES-MS | electrospray mass epectrometry |
| FAB-MS | fast atom bombardment mass spectrometry |
| HMPA | hexamethylphosphoric triamide |
| IR | infrared |
| M | molar |
| MLCT | metal-to-ligand charge-transfer |
| NMR | nuclear magnetic resonance |
| NOESY | nuclear Overhauser effect spectroscopy |
| PMD | photochemical molecular device |
| SCE | saturated calomel electrode |
| THF | tetrahydrofuran |
| TOCSY | total correlation spectroscopy |
| tpy | 2,2':6',2"-terpyridine |

# Abstract

This thesis describes the synthesis and study of thirty four multidentate heterocyclic bridging ligands, twenty four of which are new compounds. A majority of these ligands incorporate a di-2-pyridyl coordination motif and are capable of chelation to a metal centre with the formation of a six-membered chelate ring, in contrast to the five-membered chelate rings formed by the majority of bridging ligands previously described in the literature. Four ligands were synthesised that represent the first examples of bridging heterocyclic ligands incorporating a [3]radialene core. The ligands described in this thesis are divided into three sections: those prepared from dipyridylmethane precursors, ligands with a di-2-pyridylamine chelating motif, and tripodal ligands, which are capable of facial coordination to an octahedral metal atom.

The coordination and metallosupramolecular chemistry of these ligands were investigated with several different metal atoms, predominantly silver(I), copper(II) and palladium(II). With the dipyridylmethyl ligands and the di-2-pyridylamine-based ligands, both discrete and polymeric structures were obtained, including dinuclear complexes, [2+2] dimeric complexes, molecular polyhedra and one-dimensional coordination polymers. Some novel structures, including a hexanuclear silver cage with an encapsulated fluoride anion and a triply cyclopalladated compound, are described. The tripodal ligands showed a preference for forming discrete complexes with $M_2L$ and $M_2L_2$ compositions, which included a new type of helicate.

Bis(2,2'-bipyridyl)ruthenium complexes of the di-2-pyridylmethane-based and di-2-pyridylamine-based ligands are described and structurally characterised. Despite forming dinuclear complexes in many cases with palladium and copper, all the multidentate di-2-pyridylmethane-based ligands were surprisingly resistant to chelating their intended number of ruthenium atoms. Visible absorption spectroscopy and cyclic voltammetry was used to probe the nature of the metal-ligand and metal-metal interactions in these complexes.

In combination with NMR spectroscopy, mass spectrometry and elemental analysis, X-ray crystallography was used to characterise many of the complexes and metallosupramolecular species produced. The crystal structures of five ligands and fifty one complexes are described.

# *Chapter 1*

# *Introduction*

# Chapter 1

## 1. Introduction

### 1.1. Background

In the traditional field of coordination chemistry nitrogen heterocycles are one of the most important classes of ligand.[1-4] Aromatic nitrogen heterocycles can be classified into two main groups on the basis of ring size, the six-membered azines and five-membered azoles.[1] Both these types of heterocycle form strong coordination bonds resulting in stable complexes with many transition metals. The azines, such as pyridine, **1.1**, are π-electron deficient heterocycles, which form stable complexes because of metal to ligand back-bonding from metal d-orbitals into low lying π*-orbitals on the azine. In contrast, azoles are π-excessive donor ligands and deprotonation of acidic NH groups results in anionic donors that also lead to stable complexes.[1] An example of an azole ring system is pyrazole, **1.2**. Introduction of further heteroatoms into either the azine, or azole ring systems, provides ligands with very different electronic and coordination properties.


**1.1** **1.2**

**Figure 1.1.** Examples of π-deficient (**1.1**) and π-excessive heterocycles (**1.2**).

The incorporation of two or more aromatic nitrogen heterocycles within one molecule has resulted in the synthesis and study of numerous chelating and bridging ligands (Figure 1.2a).[1, 2] Ligands possessing more than one heteroatom and coordination site have the potential to link a number of metal atoms. These bridging ligands have attracted much attention in recent years

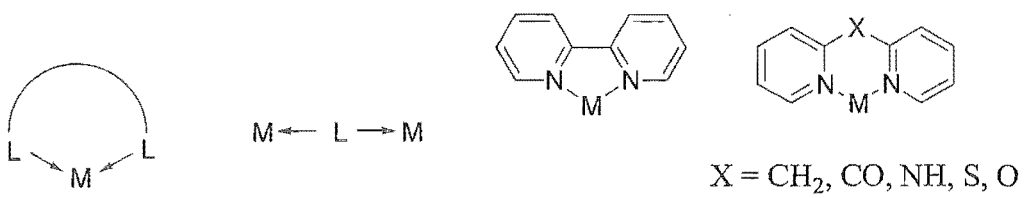


(a) (b)

**Figure 1.2.** (a) Chelating and bridging modes of coordination, and (b) examples of ligands forming five- and six-membered chelate rings.

because they enable the formation of multinuclear complexes with desirable structural and functional properties.[2-4] The stabilising effect of chelation to a metal atom can be achieved through either a five- or six-membered chelate ring (Figure 1.2b). While ligands forming five-membered chelate rings, such as 2,2'-bipyridine (bpy), have been extensively studied in coordination chemistry,[4] the related ligands, with a spacer atom, X, between the pyridine donors have, by comparison, been somewhat neglected.

## 1.2. Nitrogen heterocycles as bridging ligands

In coordination chemistry, the simplest bridging mode is doubly monodentate (non-chelating) coordination to two metal atoms. An example of a ligand displaying this motif is the well-studied diazine, pyrazine, **1.3**, which forms complexes with metals from all regions of the periodic table,[1-3] including the well-known mixed-valence Creutz-Taube ion.[5, 6] The metal-metal distance in complexes bridged by pyrazine is *ca.* 6.9 Å. Two other diazines, pyrimidine, **1.4**, and pyridazine, **1.5**, have also been investigated as bridging ligands, but not to the same extent as pyrazine.[1, 2] Dinuclear complexes of pyrimidine have been prepared and characterised with metal-metal distances of *ca.* 6.0 Å. Pyridazine displays quite variable metal-metal distances depending on whether it bridges across metal-metal bonds or between two separate metal atoms.

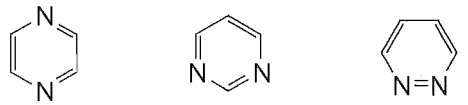

**1.3** **1.4** **1.5**

**Figure 1.3.** The diazines: pyrazine (**1.3**), pyrimidine (**1.4**) and pyridazine (**1.5**).

The distance between the bridged metal atoms can significantly affect the properties of the resulting complex. 4,4'-Bipyridine, **1.6** (Figure 1.4), is a bridging ligand in which the metal-metal distance is *ca.* 11.2 Å, in contrast to the considerably shorter distances for dinuclear complexes bridged by the diazine ligands.[2, 3] To further increase and tailor the metal-metal

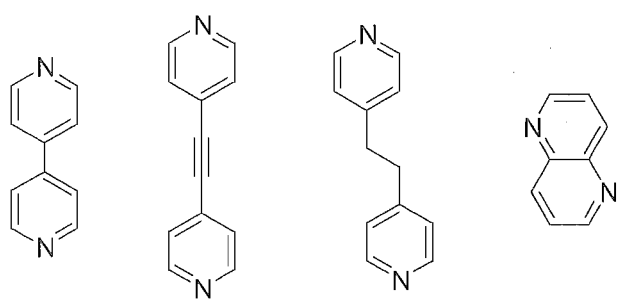

**1.6** **1.7** **1.8** **1.9**

**Figure 1.4.** Increasing the metal-metal distances with rigid and flexible ligands.

distances, various spacer atoms or groups can be inserted between the pyridine rings in **1.6**. For example, a rigid alkyne connector has been incorporated into ligand **1.7**, whereas a flexible spacer group is used in **1.8**.[2, 3] Heterocycles like 1,5-naphthyridine, **1.9**, where the donor atoms are staggered, introduce further structural differences.

Bridging ligands with the potential to chelate at both metal centres result in complexes with greater stability and potentially enhanced metal-metal interaction. Doubly bidentate ligands like 2,2'-bipyrimidine,[2, 3] **1.10**, and various linked bpy-based ligands[3, 4] (**1.11** and **1.12**) are examples of such chelating ligands (Figure 1.5). 2,2'-Bipyrimidine is a well investigated ligand and has been shown to form complexes with short metal-metal distances, on average *ca.* 5.5 Å. In contrast, bpy-based ligands allow large variation in metal-metal distances, through the variable spacer and have been the subject of a recent extensive review.[4] Other common doubly bidentate bridging ligands include, 2,3-di(2-pyridyl)pyrazine,[2, 3] **1.13**, and the related pyrimidine derivative, 4,6-di(2-pyridyl)pyrimidine, **1.14**.[2, 7] There are fewer examples of triply bidentate ligands like hexaazatriphenylene, **1.15**, which can bridge up to three metal atoms.[2, 3]

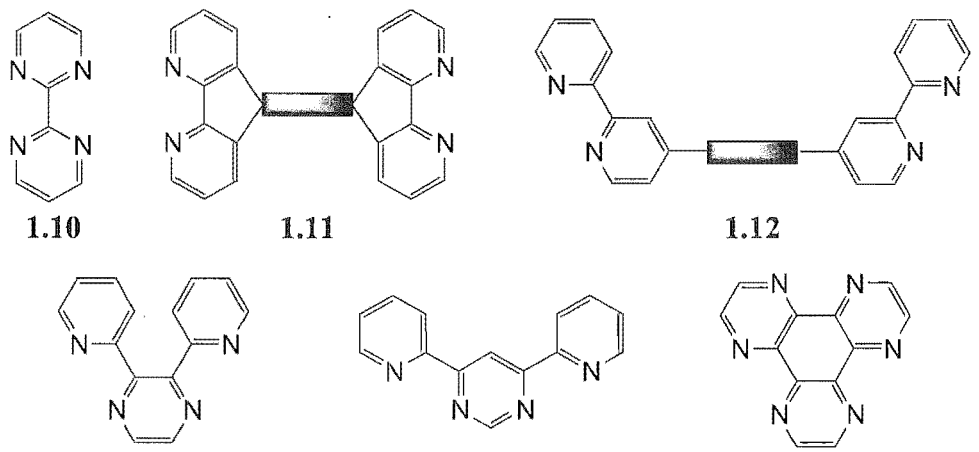


**Figure 1.5.** Selected examples of doubly bidentate ligands.

Tridentate ligands offer further stability through the addition of a third donor atom. This can be either as a meridional donor set, such as in 2,2',6',2"-terpyridine (tpy),[2, 3] or as a tripodal

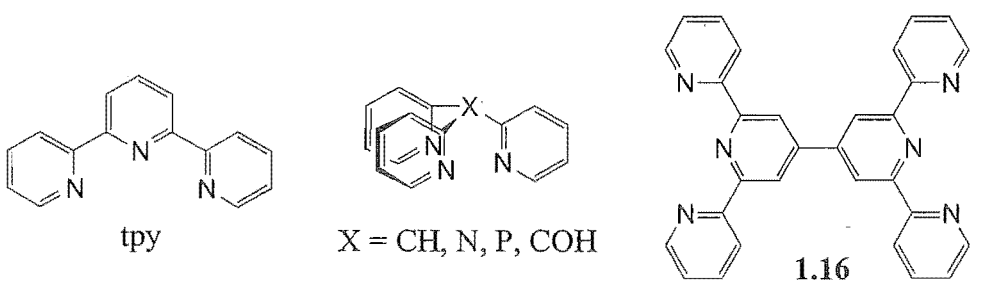


**Figure 1.6.** Selected examples of some tridentate ligands with azine donor atoms.

donor set, which can chelate facially to an octahedral metal centre.[8] The former type has been extensively investigated with many different ligands based around a tpy core utilised in coordination chemistry (for example **1.16**). Simple tripodal ligands, as shown in Figure 1.6, have been well investigated,[8] as have their pyrazole analogues.[9]

The ligands described above have been extensively employed in coordination chemistry and have also found use in the rapidly evolving field of metallosupramolecular chemistry. The ligands described above are all six-membered azines, or constructed from azines. An analogous survey could be made of ligands incorporating the five-membered azoles as donors for which there are examples with related structures, denticities and binding sites. However, the electronic properties of azole-containing ligands are somewhat different due to the π-excessive nature of the heterocycles.

## 1.3. Metallosupramolecular chemistry

Traditional chemistry relies on covalent bonds to hold together atoms within molecules. As such, the building blocks of conventional chemistry are the atoms, and the covalent bonds connecting the atoms represent the inter-atomic 'glue' that holds those atoms together. Covalent bonds are typically very strong. Thus, the formation of a covalent bond during the course of a reaction is usually irreversible. Consequently, conventional synthesis often results in mixtures, which must be separated and the products purified by chromatography and/or recrystallisation.

Nature, on the other hand, has routinely employed other weaker bonding interactions in the formation of large and very stable molecules. These assemblies are utilised as functional (enzymes and DNA) and structural (proteins) components in living cells. The weaker interactions holding such biological assemblies together include hydrogen bonding, dipole-dipole, π-π stacking and ion-pairing interactions. Using nature as inspiration, chemists have developed another approach to synthesising large aggregates with novel structures and functional properties. This area, called supramolecular chemistry,[10, 11] is where the building blocks are themselves molecules and the connecting 'glue' that holds these molecules together are the weak interactions used by nature. Supramolecular chemistry has been defined as "...chemistry beyond the molecule, bearing on the organised entities of higher complexity that results from the association of two or more species held together by intermolecular forces."[10, 12]

With conventional chemistry, complexity is built into a molecule one reaction at a time throughout a multistep synthesis. Unless each reaction is very high yielding, over a process of several steps the overall yield will be low. Supramolecular chemistry relies on the self-assembly of simple, pre-programmed components into large complicated aggregates in a single process.[12]

The interactions holding the structure together are weaker than covalent bonds, allowing the aggregate to form, as a single thermodynamically stable species, in high yield, by a corrective process of built-in error checking.

As in nature, the weak interactions commonly employed in supramolecular chemistry are hydrogen bonding, ion-dipole, dipole-dipole, and π-π stacking interactions. Hydrogen bonding interactions are ubiquitous in nature and supramolecular chemistry, but in comparison to a covalent bond are relatively weak, typically of the order of 5 - 50 $kJmol^{-1}$.[13, 14] A hydrogen bond occurs between a hydrogen atom bonded to an electronegative or electron deficient atom and another such acceptor atom. Another type of interaction routinely utilised in supramolecular chemistry is π-π stacking interactions.[15] There are two forms of such interactions, face-to-face and edge-to-face interactions (Figure 1.7), which are thought to be electrostatic in nature,[16] and relatively weak, ranging in energy from 0 - 20 $kJmol^{-1}$.

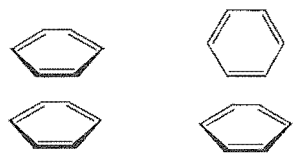

(a) (b)

**Figure 1.7.** (a) Face-to-face and (b) edge-to-face π-π stacking interactions.

Other forces utilised by the supramolecular chemist include hydrophilic or hydrophobic interactions, van der Waals forces and host-guest interactions. While individually all of these interactions are relatively weak, the combination of multiple interactions can provide a strong 'glue' to bind large aggregates together.

A more recent development of supramolecular chemistry, which has blurred the definitions between the complementary fields of coordination and supramolecular chemistry, is to incorporate metal ions into the supramolecular structures. In this area, which has been called metallosupramolecular chemistry,[17] metal atoms are the intermolecular 'glue' used to bind together organic components. These coordinate bonds work in tandem with other weaker interactions previously described, to provide access to an even greater diversity of structures and properties. Much of this work has been dominated by nitrogen containing heterocyclic ligands for reasons of stability, predictability, availability and because they offer an extensive number of denticities and bridging geometries.

The combinations of metal atoms and heterocyclic ligands available provide access to a large variation of bond strengths, ranging from the strength of hydrogen bonds through to covalent bonds. Organic molecules rely on carbon atoms, which are limited to linear, trigonal and four-

coordinate tetrahedral geometries. Transition metal ions offer a greater diversity of both coordination numbers and geometries (Figure 1.8). The choice of either labile or inert transition metals can be used to tailor the self-assembly process.

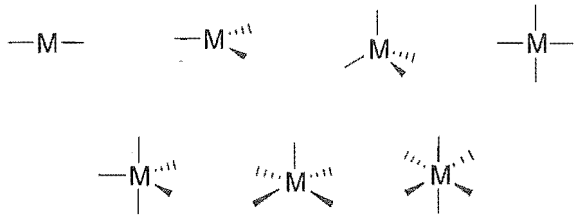


**Figure 1.8.** Some of the coordination geometries available to transition metals.

Silver(I) is a $d^{10}$ transition metal atom that is flexible in both its coordination number and geometry, but which shows a preference for two-coordinate (linear or bent) and three-coordinate (trigonal or T-shaped) geometries.[18] Silver has been extensively employed in metallosupramolecular chemistry[19, 20] and was used throughout the present research project to investigate both the coordination chemistry and metallosupramolecular chemistry of the new ligands. Different anions were utilised in tandem with silver to gauge the anion dependency of certain complexes and assemblies. Copper(II) is also employed in the formation of complexes and metallosupramolecular assemblies that may have interesting properties as a consequence of magnetic interactions between paramagnetic metal ions. Copper(II) has some flexibility in its coordination modes ranging from four-coordinate to six-coordinate.[21] It shows a preference for five-coordinate square-pyramidal or trigonal-bipyramidal geometries with the donor sets employed in this research project.

Compared with the flexibility available with silver and copper, other metal atoms allow more strict control over the coordination numbers and geometries. Palladium(II), for example, has a dependable square-planar geometry with almost no flexibility and, by using different precursors and ancillary ligands, the stereochemistry can be limited to *cis* or *trans* geometries (Figure 1.9a). For example, Fujita has used the *cis* precursor, shown in Figure 1.9(a), in the formation of a discrete molecular square,[22] as described below. Other metals employed in this research project have octahedral geometries, for example nickel(II) and ruthenium(II). The relative inertness of the common oxidation states of ruthenium towards substitution allows the coordination sphere of ruthenium to be tailored to the demands of the ligand. Thus, ruthenium can provide a *cis*-bidentate, a meridional or a facial tripodal binding site, as shown in Figure 1.9(b). A 'naked' ruthenium precursor, $[Ru(DMSO)_4Cl_2]$ can also be used if all six coordination sites are required.

Using the methodology of combining mixtures of pre-programmed multidentate bridging ligands and transition metal ions, the controlled self-assembly of a large number of

metallosupramolecular aggregates has been achieved. These one-, two- and three-dimensional architectures, which can be either discrete or polymeric have many applications.

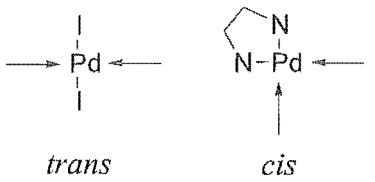


(a)

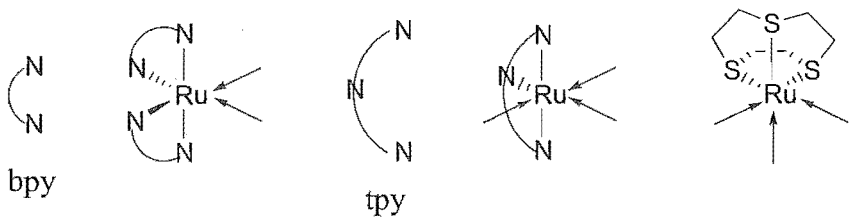


(b)

**Figure 1.9.** Examples of the use of anions and ancillary ligands to control the metal ion geometry, and potentially the structure of the assembly by pre-organising the donor sites.

The rational design of such species involves a consideration of the type of structure required. For example, one method of preparing a polygon, such as a square, is to combine four right-angled components and four linear components.[23-25] This can be achieved in two ways; the linear component can be a linear bridging ligand, like 4,4'-bipyridine, **1.6**, and the metal ion can be the right-angled component (Figure 1.10),[22] or the roles can be reversed and the angular component satisfied by a ligand like pyrimidine, **1.4**, and the linear component by a more flexible transition metal like silver.[26] Using similar methodology, other two-dimensional polygons such as triangles, pentagons and hexagons with varying sizes have been prepared.[23-25]

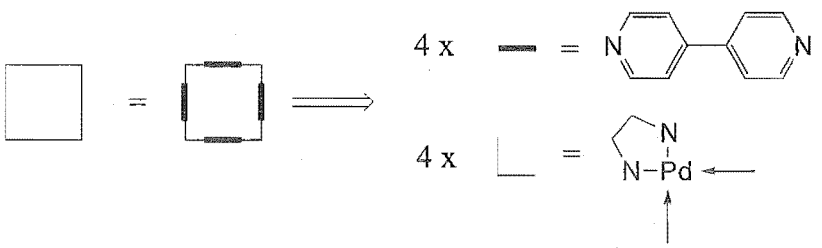


**Figure 1.10.** Retrosynthetic analysis of a molecular square.

As shown in Figure 1.11, three-dimensional polyhedra, such as a cube, can be constructed in a similar manner by combining eight angular and twelve linear components. The angular precursor can be a facially capped octahedral transition metal and the linear component a bridging ligand, such as **1.6**, which were used by Thomas and co-workers to prepare the first example of a molecular cube.[27] Polyhedra of varying shapes and dimensions can be prepared by

changing the linear and angular components.[23-25] Similar approaches are used in the formation of other molecular cages and containers with interesting properties.[23, 28-30]

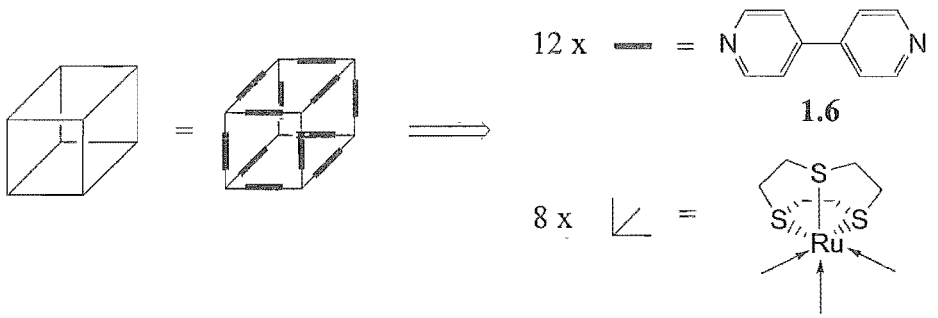


**Figure 1.11.** The synthetic strategy for preparing a molecular cube.

Polymeric structures like coordination polymers,[31, 32] grids[30, 33] and network structures[34, 35] have been prepared using both rigid and flexible bridging ligands. A ladder-like coordination polymer, shown in Figure 1.12, can be obtained by combining T-shaped and linear precursors.[36] Again, either the linear, as in Figure 1.12, or the T-shaped component could be a heterocyclic ligand. Coordination polymers with linear and zigzag topologies may have applications as molecular scale wires, while network structures might be used as storage devices or as biomimetic zeolite alternatives. Network structures can be interpenetrating or contain occluded guest molecules, which may be able to be reversibly exchanged.[34]

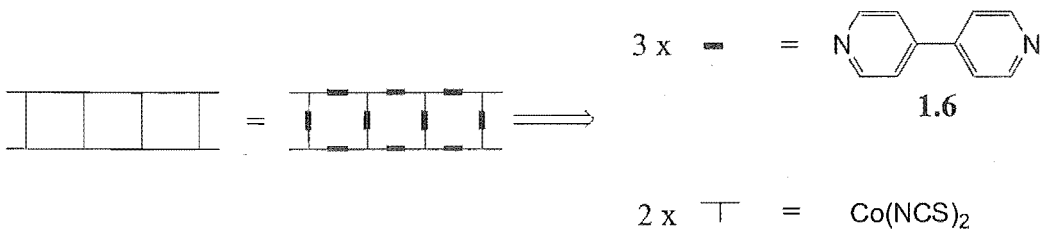


**Figure 1.12.** One approach for the construction of a molecular ladder.

Other interesting metallosupramolecular structures include helicates,[37, 38] catenanes and rotaxanes,[39, 40] which have been instrumental in founding many of the concepts upon which supramolecular chemistry is based.[37] A helicate can be defined as a metal-containing helix, where a number of ligands wrap around two or more metal atoms. Double, triple and quadruple stranded helicates have been prepared as has been covered in two extensive reviews.[37, 38] In most of the metallosupramolecular architectures outlined above, including helicates, the components are chemically bonded together, whereas in species such as catenanes and rotaxanes, the components are mechanically interlocked, but without any chemical interaction between the components. A catenane is a compound consisting of two or more interlocked rings that cannot be separated without breaking a chemical bond. Rotaxanes are comprised of a rigid rod-like structure inserted through a macrocyclic or metallomacrocyclic ring. Bulky end groups prevent

the ring from slipping off the rod. Such assemblies have been prepared in metallosupramolecular chemistry in very high yields, compared to their organic counterparts, by using the self-assembly principles of supramolecular chemistry.

## 1.4. Ruthenium chemistry, metal-ligand and metal-metal interactions

The importance of ruthenium in coordination and metallosupramolecular chemistry is a consequence of its favourable chemical and physical properties, and the potential for the use of species incorporating ruthenium in novel applications. The archetypal bidentate chelating ligand, bpy, forms a very stable mononuclear complex, $[Ru(bpy)_3]^{2+}$.[41] This complex is probably the most well studied complex in coordination chemistry, because of a combination of its chemical stability, redox chemistry, and excited state and luminescence properties.[42-44] This chemical stability originates because ruthenium is inert to ligand substitution in both its common oxidation states. In addition to significant absorption bands in the visible region of the absorption spectrum, $[Ru(bpy)_3]^{2+}$ has a relatively long-lived and stable excited state that makes it, and related complexes, ideal for applications as potential photocatalysts. It has been claimed that $[Ru(bpy)_3]^{2+}$ may have potential as a photocatayst in the process of splitting water to hydrogen and oxygen.[45] By using different heterocycles with different donor-acceptor properties the physical properties of the subsequent complexes can be tuned.[42-44]

The use of additional metal atoms and more elaborate bridging ligands pushes such compounds into the realm of metallosupramolecular chemistry, where new interactions and properties arise related to the aggregate as a whole, and which are greater than the sum of its constituent parts.[3] Such interactions include energy and electron transfer, magnetic interactions and photoinduced charge separation.[3, 42, 46] These types of interaction between the metal centres are transmitted by way of the ligand $\pi$-system and, thus, the extent of such metal-metal interactions can be controlled and altered by appropriate selection of the bridging ligand. Different bridging ligands allow control of the metal-metal distance, the donor set and the spatial arrangement of the metal atoms about the bridging ligand. However, the use of the octahedral metal centres, and incorporation of more than one metal atom into a complex, require due consideration of the stereochemical problem.

## 1.5. The stereochemical problem

In coordination chemistry, and in the field of metallosupramolecular chemistry, many of the polymetallic complexes investigated are based around octahedral metal centres – often ruthenium(II). When bidentate chelating ligands are used, stereochemical ambiguities may arise

in the products, which have been shown to affect the electrochemistry and photophysical behaviour of the complex. This is termed the "stereochemical" or "isomer" problem.[47-49] For mononuclear complexes the ambiguity arises because symmetrical ligands like bpy can form two enantiomeric tris-bidentate complexes (Figure 1.13). In the case of unsymmetrical ligands, further geometric isomers can result. For dinuclear complexes bridged by a doubly bidentate ligand, two diastereomeric forms are possible (Figure 1.13); a $C_2$-symmetric racemic isomer, which exists in two enantiomeric forms ($\Delta\Delta/\Lambda\Lambda$) and a $C_s$-symmetric meso isomer ($\Delta\Lambda$). Extension to polymetallic complexes based around octahedral centres leads to an exponential increase in stereoisomeric possibilities. These stereochemical differences are transferred into the three-dimensional structures of such complexes.

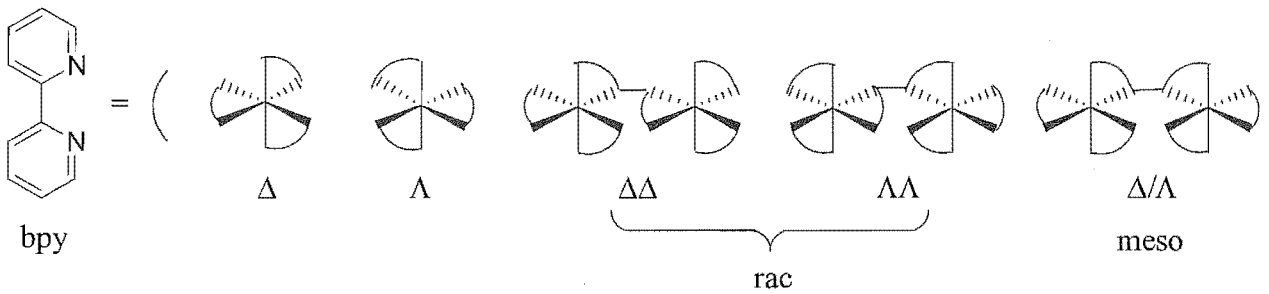


**Figure 1.13.** The potential isomers of mononuclear and dinuclear complexes with symmetrical bidentate ligands.

The stereochemical problem described can be addressed in several ways.[47] Attempting to prevent the formation of stereoisomers by incorporating chirality into bidentate chelating ligands is one approach. The chiragen family of chelating ligands, which are derived from pinanoid monoterpenes, prepared by von Zelewsky and co-workers,[49, 50] are the most well studied examples. Camphor has also been incorporated into ligands in attempts to predetermine the chirality of metal centres.[51] More recently, the incorporation of nicotine and other alkaloids has been pursued to create a further series of chiral ligands.[52]

While there is a large pool of natural products from which to draw chiral precursors, it is not a trivial matter to incorporate the group into the ligand without affecting the coordination properties of the ligand. Thus, a more practical approach is to prepare complexes through a controlled coordination strategy,[44] and to separate mixtures of diastereoisomers formed from available bridging and chelating ligands. This approach, which was pioneered by Keene and co-workers,[47, 48, 53] relies on the differential passage of the different stereoisomers down a Sephadex cation exchange resin column. The different rates of elution for the stereoisomers is achieved by differential interactions between the anion and each stereoisomeric form.[48]

A third approach, akin in some respects to using chiral ligands because it prevents the formation of isomers, is to use isomerically pure starting materials; i.e. a stereospecific synthesis.[49] The resolution of a racemic complex, such as $[Ru(bpy)_2(1.1)_2]^{2+}$, with a chiral auxiliary to give the two enantiomers has been described.[54] This can be substituted in a stereospecific way to give multinuclear species in an isomerically pure form, but requires precautions to prevent racemisation during the synthesis. A related approach, which does not require substitution of the ruthenium centre, is to elaborate functionalised ligands that are coordinated to a resolved ruthenium complex.[55]

A fourth approach is to remove the possibility of forming isomers by utilising tridentate ligands based around the 2,2':6',2"-terpyridine structure.[47, 56] These ligands coordinate in a meridional fashion resulting in an achiral product, thereby avoiding the stereochemical problem. However, a consequence of this approach is that to avoid further introduction of isomerism the linking of the tpy subunits must occur through the 4'-position of the central ring of the tpy; thus multinuclear species of this type must be necessarily linear.[47] This restricts the resulting geometries of the multinuclear complexes, and has led some authors to propose that the formation of multinuclear assemblies in more than one dimension requires the use of bidentate chelating ligands.[7]

## 1.6. Applications

The interest in coordination complexes and metallosupramolecular assemblies of bridging ligands, in particular nitrogen heterocycles, spans a number of areas in modern chemistry, as has been alluded to above. Interest in the structural properties of such complexes and assemblies is one important area. This includes general coordination chemistry[1, 2, 57] and novel coordination properties, such as the stabilisation of unusual oxidation states in coordination complexes;[58] the use of aromatic nitrogen heterocycles for the construction of structural and functional models of enzyme active sites and other biologically relevant assemblies;[59-61] and the synthesis of new materials, such as luminescent compounds for use in electroluminescent displays and chemosensors.[3, 62-65] As highlighted above, nitrogen heterocyclic ligands have also been used as structural and functional components in metallosupramolecular chemistry and as components of artificial molecular machines.[40]

There is further interest in the electrochemical, photophysical and magnetic properties of multinuclear complexes bridged by nitrogen heterocycles.[3, 6, 42, 46, 47, 66, 67] This is centred around metal-ligand and metal-metal interactions, which allow the tuning of the properties of such complexes. Control of these types of interactions is important for designing potential

photochemical molecular devices (PMDs). PMDs may be capable of information storage, solar energy conversion, multielectron catalysis and act as molecular switches.[40, 47, 68]

## 1.7. Thesis coverage

Di-2-pyridylmethane and di-2-pyridylamine (Figure 1.14) are two easily accessible starting materials that have seldom been incorporated, as a chelating motif, into bridging ligands. Using these precursors, three sets of bridging ligands were prepared and an investigation of their coordination chemistry and metallosupramolecular chemistry was completed. In Chapters 2 and 3, a range of multitopic bidentate bridging ligands that were prepared from di-2-pyridylmethane and di-2-pyridylamine, respectively, are described, which are capable of chelating to two or more metal atoms, with the formation of a six-membered chelate rings. These incorporate different spacer groups between the chelating regions that provide control over both the metal-metal distances in multinuclear complexes, and the orientation and arrangement of the metal centres relative to each other.

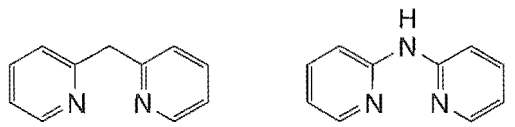


**Figure 1.14.** The two chelating motifs used in this research project, di-2-pyridylmethane and di-2-pyridylamine.

The coordination and metallosupramolecular chemistry of these two sets of bridging ligands were investigated with a range of relatively labile transition metals. Different anions were used to probe the influence the anion has on the complexes and assemblies that were prepared. The lability of the transition metal atoms employed dictated that X-ray crystallography be extensively used for the structural characterisation of the products. In contrast, since the nitrogen-ruthenium bond is much more inert to ligand substitution, the ruthenium complexes that were prepared have been readily characterised in solution. Mass spectrometry, NMR spectroscopy, visible absorption spectroscopy and electrochemistry were used to investigate the properties of these ruthenium complexes, and the nature of the metal-ligand and metal-metal interactions. In complexes where the stereochemistry was deemed to be influential, through a collaboration with Prof. Keene and Deanna D'Alessandro at James Cook University in Townsville, Australia, the diastereoisomers of these complexes were separated. This allowed the stereochemical problem to be addressed.

A second approach used to address the stereochemical problem was to prepare a series of doubly tridentate bridging ligands, capable of bridging two metal atoms with tripodal coordination at each metal centre. This new variation of the tridentate approach to the stereochemical problem involved the synthesis of some new ligands, revisited several previously

reported ligands and provided access to new three-dimensional coordination motifs. These ligands, in contrast to the tpy ligands, chelate with the formation of six-membered chelate rings. The coordination and metallosupramolecular chemistry of these ligands were investigated with an emphasis on forming symmetrical tripodal complexes by facial coordination of two octahedral metal atoms. Some preliminary investigations into $d^6$ transition metal complexes of these ligands are also discussed.

# *Chapter 2*

# *Multidentate ligands derived from isomeric dipyridylmethanes*

# Chapter 2

## 2. Multidentate ligands derived from isomeric dipyridylmethanes

### 2.1. Introduction

In this chapter a study of ligands that are derived from di-2-pyridylmethane, **2.1**, and some related precursors is described. In all compounds in this chapter the chelating pyridines of the ligand are bonded to, and incorporated into the ligand through a carbon atom. As covered in Chapter 1, 2,2'-bipyridine (bpy) is the classical, chelating, bidentate ligand that has been investigated for over a century[69] and shown to form stable complexes with most metals of the periodic table.[43] Compound **2.1** is closely related to this well studied ligand, as shown in Figure 2.1, but possesses an extra carbon atom between the two pyridine rings. It is part of the larger class of compounds containing two pyridine rings separated by a single atom spacer (X). This extra atom means that **2.1** forms six-membered chelate rings, while bpy forms stable five-membered chelate rings.[2] In addition, the spacer atom acts to insulate the two rings from one another, thus removing the conjugation between the two heterocyclic rings.


X = $CH_2$ = **2.1**
= NH, S, O

bpy

**Figure 2.1.** Two different types of chelating ligand that form six- and five-membered chelate rings, respectively.

In recent years, many new ligands have been prepared that incorporate two, or more, bpy subunits and can thus bridge two, or more, metal centres to produce dinuclear and multinuclear coordination complexes and metallosupramolecular assemblies.[3, 4] Such species have been investigated with regard to their structural, stereochemical,[47, 48] electrochemical and photophysical properties.[3, 42, 66] When alkyl or conjugated spacers separate the bpy centres, these allow systematic variation of the spatial orientation, metal-metal distance and the degree of interaction between the metal centres. For example, such variations include methylene, ethylene and propylene spacers, ethenyl and buta-1,3-diene spacers, as shown in Figure 2.2.

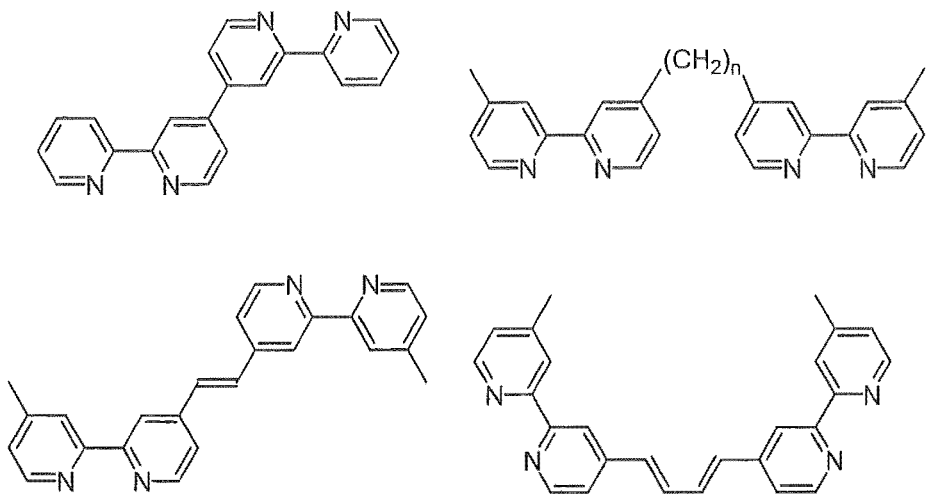


**Figure 2.2.** Examples of bridging ligands incorporating two bpy subunits.

In contrast to bpy-based ligands, bridging ligands that contain two or more dipyridylmethane subunits have been virtually ignored. Some of these ligands, which are investigated in this chapter, represent a further evolution of the potentially doubly monodentate bridging ligands like 1,2-bis(2-pyridyl)ethane and *trans*-1,2-bis(2-pyridyl)ethene that have previously been used in coordination chemistry.[70] Compared to these doubly monodentate bridging ligands, the compounds investigated in this research project incorporate the potential for a bidentate bridging mode of coordination, and extra stability imposed by the chelate effect, through the addition of two extra pyridine donors. There are one or two reported examples of such ligands, including 1,1,2,2-tetra(2-pyridyl)ethane, **2.2**, shown in Figure 2.3, which was prepared by Canty and Minchin,[71, 72] but limited reports of the coordination chemistry of such ligands.

The ligands prepared and investigated in this chapter are grouped and described in three sections with the di-2-pyridylmethane-based ligands (Figure 2.3) described first in Section 2.2.1. Compound **2.2** and 1,2-diphenyl-1,2-bis(2-pyridyl)ethane, **2.5** have previously been prepared,[71, 72] but very little of their coordination chemistry investigated. Ligands **2.3** and **2.4**, 1,1,2,2-tetra(2-pyridyl)ethanol and tetra(2-pyridyl)ethene respectively, have not been directly prepared, but have been characterised as copper complexes.[73] Attempts to prepare the novel ligands **2.6**, **2.7** and **2.9** are also described. The azine ligand, di-2-pyridylketone azine, **2.8**, has previously been prepared as an analytical reagent,[74, 75] but little of its coordination chemistry studied. All these ligands, with the exception of **2.5**, incorporate di-2-pyridylmethane chelating units, and can all potentially form dinuclear complexes with chelation, or in the case of **2.5**, cyclometallation, to two metal centres.

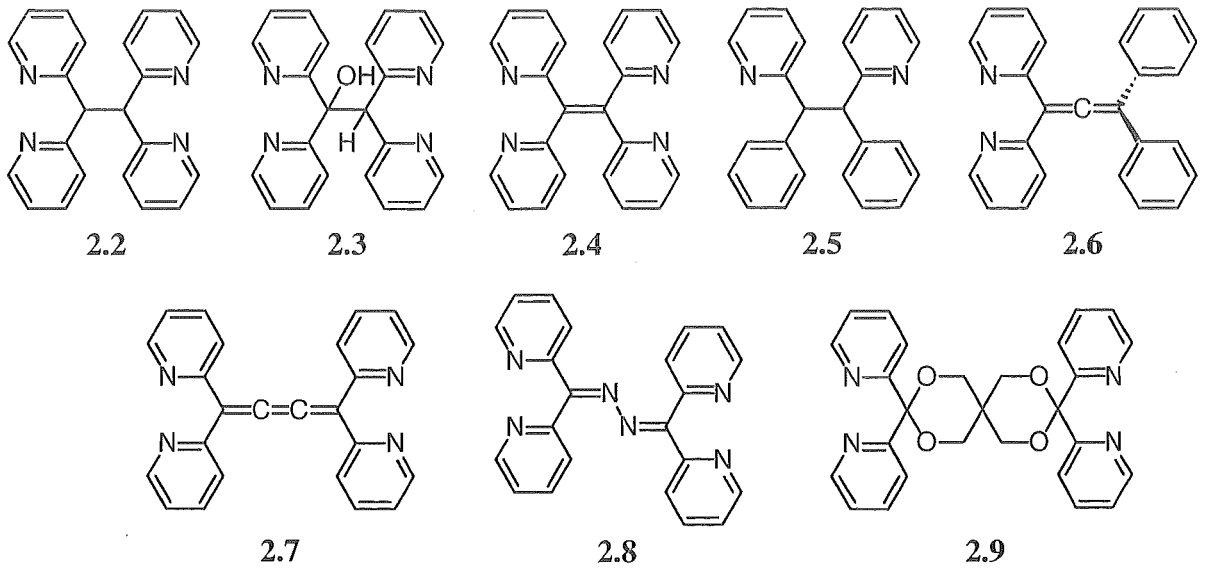

**Figure 2.3.** Examples of dinucleating ligands related to and, for the most part, prepared from the starting material, **2.1**.

The second series of ligands investigated in this chapter (Section 2.2.2) were formed from 4,5-diazafluorene, **2.10**, and have the dipyridylmethane unit locked in a planar conformation by a carbon-carbon bond between the two pyridine rings. Such ligands can also be thought of as rigid bpy-based ligands. 9,9'-Bi-(4,5-diazafluorenyl), **2.11**, and 9,9'-bi-(4,5-diazafluorenylidene), **2.12**, are two such compounds that have previously been prepared.[76-78] However, as **2.11** was obtained as part of the synthesis of the novel ligand spiro[3,3]heptane-2,6-dispiro-4,5-diazafluorene, **2.13**, and **2.12** by a one step oxidation of **2.11**, they were both investigated as a comparison for **2.13** and the previously introduced di-2-pyridylmethane-based ligands.

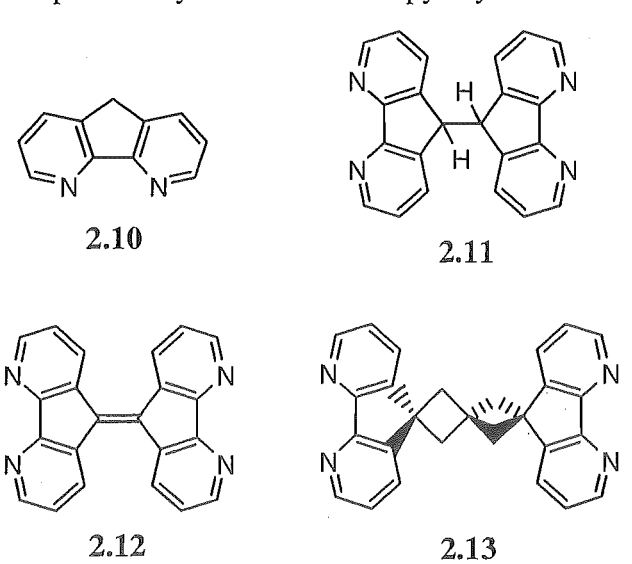

**Figure 2.4.** 4,5-Diazafluorene, **2.10**, and related dinucleating ligands formed from this compound.

The third series of ligands investigated in this research project and described in this chapter is constructed around a [3]radialene core. The [3]radialene core is part of a larger group of

compounds called radialenes.[79, 80] These consist of a cycloalkane core to which exocyclic methylene groups are appended to all ring carbon atoms. The parent radialenes with the general formula $C_nH_n$ are shown in Figure 2.5. Radialenes have attracted the interest of both theorists and experimentalists, because of their fascinating structures and the potential for novel electronic properties.[79, 81, 82] No pyridine containing [3]radialene ligands had previously been prepared, prompting the preparation of compounds **2.14** - **2.18**, shown in Figure 2.6. The synthesis and properties of these compounds, and some examples of the coordination chemistry of these novel ligands are described.

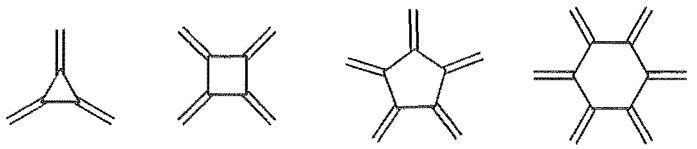

**Figure 2.5.** The structures of the first four parent radialenes.

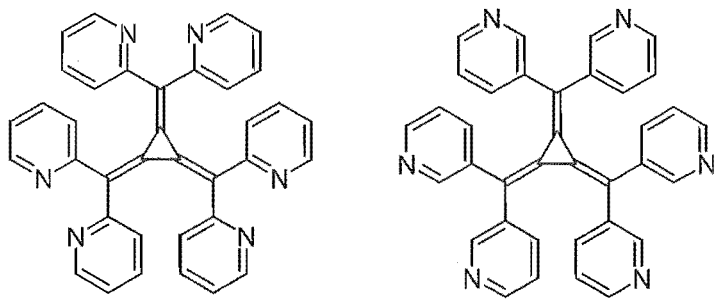

**2.14** **2.15**

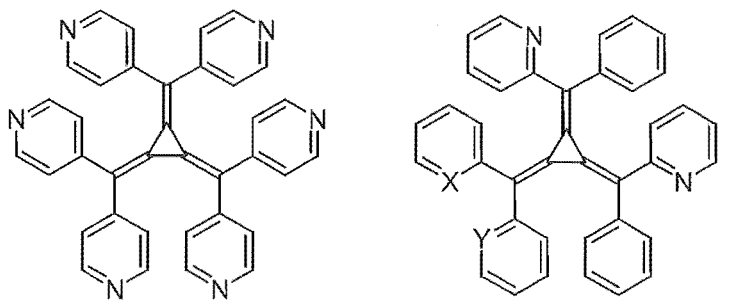

**2.16** **2.17:** X=N, Y=CH
**2.18:** X=CH, Y=N

**Figure 2.6.** The structures of the [3]radialene-based ligands.

The syntheses of the three groups of ligands are described in the next section of this chapter, followed by individual sections covering an investigation of the coordination chemistry and metallosupramolecular chemistry of the three different sets of ligands. The ruthenium complexes of selected ligands are described separately in Section 2.6.

## 2.2. Syntheses of the ligands

### 2.2.1 Di-2-pyridylmethane-based ligands

The precursor to a considerable number of the ligands investigated, both in this chapter and this thesis as a whole, di-2-pyridylmethane, **2.1**, is itself a potential ligand.[73, 83] Therefore, **2.1** was prepared as a reactant for subsequent preparations throughout this thesis, and as a model ligand. It is not commercially available, but can be readily prepared from a commercially available starting material, di-2-pyridylketone, by a Wolff-Kishner reduction as shown in step (a) of Scheme 2.1.[72] This procedure is a modification of a literature procedure and is straightforward, reproducible and high yielding, with relatively pure **2.1** easily afforded by extraction of the reaction mixture with benzene. The purity of the material obtained by extraction was suitable for most purposes and it was, unless otherwise stated, used without subsequent distillation. Vacuum distillation can be used to purify the extract, resulting in a colourless oil that darkens slowly on standing.[72]

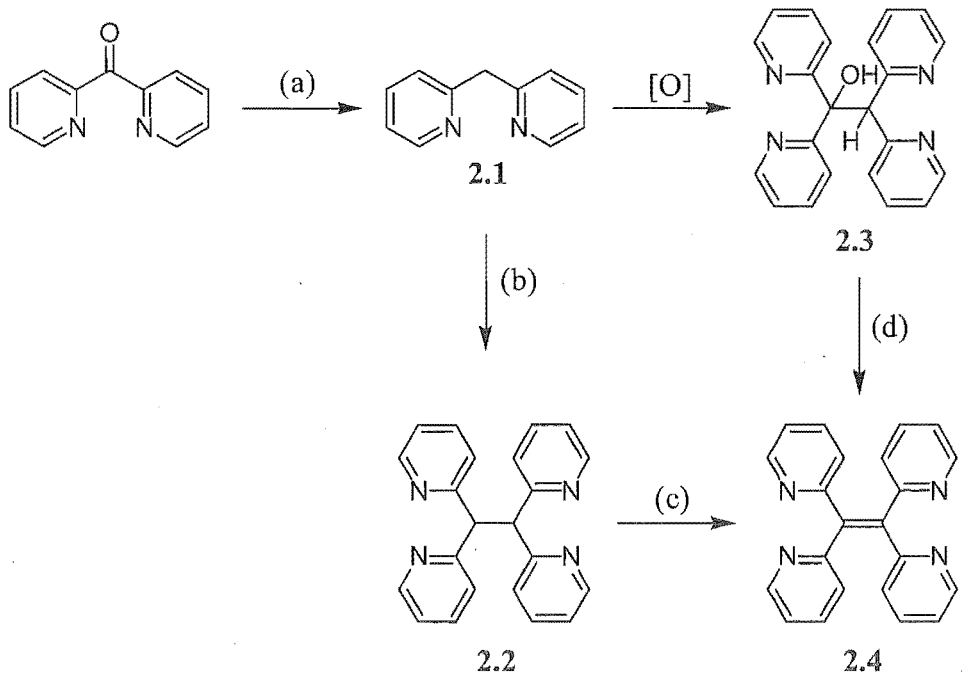


(a) KOH, $NH_2NH_2.H_2O$, 94%; (b) n-BuLi, $I_2$, 53%; (c) DDQ, 25%;
(d) $SOCl_2$, pyridine, 81%.

**Scheme 2.1.**

As mentioned, **2.1** is not only a useful ligand, but also an important precursor for the synthesis of a majority of the other ligands that are described and investigated in this work. Therefore efforts were made to prepare **2.1** from less expensive precursors on a larger scale, by

coupling of appropriately substituted pyridine compounds. Previous work by other researchers reported that **2.1** could be prepared by reaction of lithiated 2-methylpyridine with either 2-bromopyridine,[84] or, simply pyridine[85]. Both methods were tried, but only low yields of the desired compound were obtained. Compound **2.1** was also difficult to isolate in pure form from the complex mixture of isomerically substituted products and insoluble polymeric materials that formed. The failure of these two methods could be attributed to multiple pathways for reaction, in particular for nucleophilic aromatic substitution of pyridine.

1,1,2,2-Tetra(2-pyridyl)ethane, **2.2**, has previously been prepared by Canty and Minchin[71, 72] by the general method outlined in Scheme 2.1 involving deprotonation of **2.1** with n-butyllithium, followed by oxidative dimerisation with mercuric iodide. This was reported to give **2.2** in good yield, but the reaction was found not to be completely reliable and the synthesis was modified to maintain a reasonable yield for the reaction. After an identical deprotonation step using n-butyllithium, the resulting anion was oxidised with iodine, instead of mercuric iodide, to give **2.2** in 53% yield. Despite this modification, the high yields obtained previously by Canty and Minchin could not be achieved. Nonetheless, the use of iodine has the bonus of avoiding the production of undesirable and toxic mercury.

In the paper where they describe the preparation of **2.1**, Canty and Minchin[72] note that they observe the formation of a dimeric adduct of this compound on standing that was not characterised. As noted above, freshly prepared **2.1** is a colourless oil that is pure by NMR and mass spectrometry. However, on standing over extended periods, a colourless solid precipitates from the oil. This compound, labelled **2.3** in Scheme 2.1, has previously been reported as a ligand that was formed during the synthesis of a copper complex.[86] The solid material obtained is insoluble in ether and can be isolated by filtration of the oil, and subsequent washing with ether to remove the ether-soluble **2.1**. $^{1}$H NMR spectroscopy confirmed that this solid is neither **2.1**, nor the initial starting material for the Wolff-Kishner reduction, di-2-pyridylketone. The $^{1}$H NMR spectrum consists of the signals for two non-equivalent pyridine rings, a singlet at 6.28 ppm and a broad singlet, consistent with hydroxy or amino proton, in a 2:2:1:1 ratio, respectively. On the basis of the $^{1}$H NMR spectrum, and corroborating evidence from the $^{13}$C NMR spectrum, it was proposed that the solid was 1,1,2,2-tetra(2-pyridyl)ethanol, **2.3**. Elemental analysis supported the proposed structure, although mass spectrometry was not entirely consistent with this compound. However, two of the ions detected in the mass spectrum are **2.1** and di-2-pyridylketone, possibly originating from decomposition of **2.3**.

The dimerisation of related compounds has been shown to occur in the course of, or following, similar reactions. For instance, the Clemmenson reduction of benzophenone has been

shown to produce 1,1,2,2-tetraphenylethanol as a side product under certain conditions.[87] As an aside, diphenylmethane was synthesised by a Wolff-Kishner reaction, but was not observed to undergo the same transformation on standing to form 1,1,2,2-tetraphenylethanol.

One of the major targets in this section of work was the synthesis of the novel ligand tetra(2-pyridyl)ethylene, **2.4**, which was prepared by two different methods (Scheme 2.1). In the first method, **2.4** was synthesised by treating **2.2** with 2,3-dichloro-5,6-dicyano-1,4-benzoquinone (DDQ) in refluxing toluene, to give a 25% yield of **2.4**. Decomposition of **2.2** to give the original starting material, di-2-pyridylketone, coupled with the fact that the reaction does not go to completion, considerably reduces the yield of this reaction. Addition of extra DDQ to the reaction ensures the reaction proceeds to completion, but significantly increases the decomposition of **2.2**.

The failure of the above reaction to provide a satisfactory method for preparing **2.4** led to an investigation of other possible routes. Manzur et al. reported the synthesis of **2.4** by a copper-catalysed condensation reaction of di-2-pyridylmethane and di-2-pyridylketone. However, the ligand was only isolated as the copper complex.[73] Attempts to repeat this procedure with the intention of complexing and removing the copper with cyanide were unsuccessful. However, as described, a serendipitous supply of 1,1,2,2-tetra(2-pyridyl)ethanol, **2.3**, is available, which can be dehydrated to produce **2.4**. Thus, treatment of **2.3**, as shown in Scheme 2.1, with thionyl chloride and pyridine gave **2.4** in an excellent 81% yield. The limiting aspect of this route is its reliance on the availability of **2.3**.

A compound closely related to **2.2**, and also previously reported by Canty and Minchin[72] has the potential to form dinuclear complexes by being doubly cyclometallated. Therefore, **2.5** was prepared as a potential ligand and also as the precursor to the synthesis of *E/Z*-1,2-bis(2-pyridyl)-1,2-diphenylethylene (Scheme 2.2). Iodine oxidation of the anion of 2-benzylpyridine, formed by deprotonation with n-butyllithium, gave **2.5**, as a mixture of the two diastereoisomers, in 40% yield.

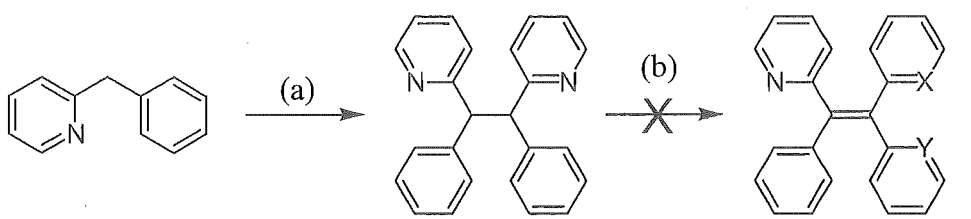


**2.5** *trans*: X=CH, Y=N
*cis*: X=N, Y=CH

(a) n-BuLi, THF, 40%; (b) DDQ.

**Scheme 2.2**

The ethylene analogue of **2.5** also has the potential to be doubly cyclometallated. Unfortunately, the oxidation of **2.5** with DDQ to give *E/Z*-1,2-bis(2-pyridyl)-1,2-diphenylethylene was unsuccessful, with only starting material being recovered from the reaction (Scheme 2.2). Nonetheless, despite not having the desired ethylene ligand for comparison, some of the coordination chemistry of **2.5** was investigated, as described later, along with attempts at cyclopalladation of this compound.

Having successfully synthesised ligand, **2.4**, the next step was to prepare ligands that would provide an increase in the metal-metal distance while still maintaining the conjugation. Therefore the synthesis of two very closely related ligands, 1,1,3,3-tetra(2-pyridyl)propa-1,2-diene, **2.6**, and 1,1,4,4-tetra(2-pyridyl)buta-1,2,3-triene, **2.7** was investigated. The insertion of one extra carbon atom to give an allene-based ligand, **2.6**, would not only increase the metal-metal distance in dinuclear complexes, but would also incorporate a 90° twist into the ligand. The cummulene-based ligand, **2.7**, has been previously reported, but unfortunately demonstrated to be unstable,[88] and thus, was not pursued.

Two possible routes were proposed for the synthesis of **2.6** from available starting materials. The first method requires the synthesis of the Meldrum's acid derivative, shown in Scheme 2.3, which could be then treated with methyllithium in THF/HMPA solution to form the allene. This approach has been used for the synthesis of a related compound, 2,4-bis(4-pyridyl)penta-2,3-diene.[89] However, the second reaction was never attempted because the required Meldrum's acid

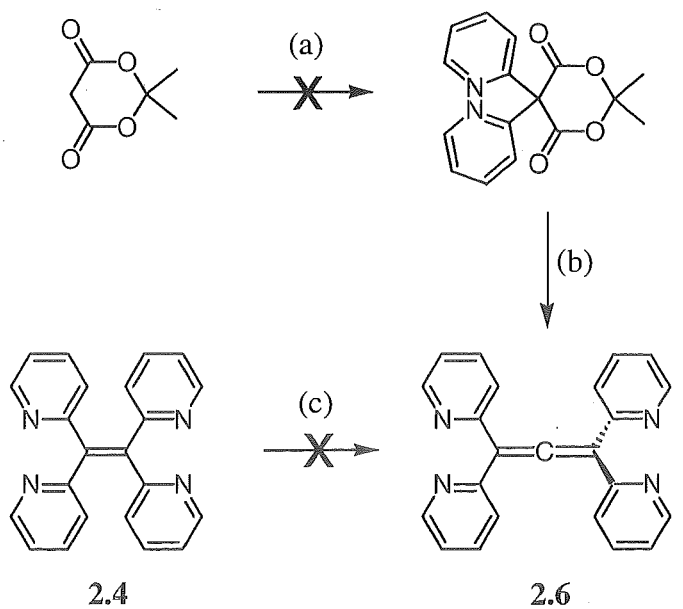


(a) 2-bromopyridine, acetic anhydride; (b) MeLi, THF, HMPA; (c) $CBr_4$, MeLi.

**Scheme 2.3**

derivative could not be definitively prepared. A second and more common route to allenes involves reaction of an alkene with dibromocarbene, which can be generated from the reaction of tetrabromomethane with methyllithium.[90] However, when this reaction was carried out on the alkene, **2.4**, only starting material was recovered following work up of the reaction.

To provide examples of ligands with longer spacer groups, two ligands were prepared directly from commercially available di-2-pyridylketone. Di-2-pyridylketone azine, **2.8**, has previously been reported.[75] It was prepared by reaction of di-2-pyridylketone with hydrazine hydrate in the presence of a catalytic quantity of acetic acid[91] (Scheme 2.4). This gave ligand **2.8** as a yellow solid in 89% yield. The second ligand, **2.9**, was synthesised by the condensation of pentaerythritol with di-2-pyridylketone, using a Dean-Stark apparatus and 4 Å molecular sieves to remove the water that was produced (Scheme 2.4). The isolated material was shown to be consistent with the expected product by mass spectrometry and $^1$H NMR spectroscopy, but rapidly decomposed by hydrolysis during subsequent work up.

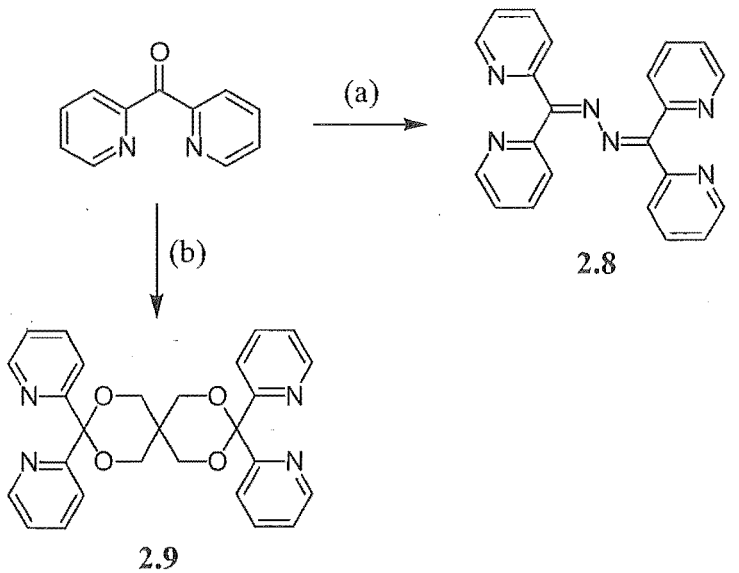


**2.8**

**2.9**

(a) $NH_2NH_2.H_2O$, AcOH, MeOH, 89%; (b) pentaerythritol, $Na_2CO_3$, 4A sieves.

**Scheme 2.4**

### 2.2.2 4,5-Diazafluorene-based ligands

The synthesis and structural characterisation of dinuclear complexes (Section 2.3) of the series of di-2-pyridylmethane-based ligands, revealed that the six-membered chelate rings of complexes incorporating these ligands adopt a boat-conformation, both in solution and in the solid state. This disrupts the conjugation within the π-system of the ligand and is likely to minimise the metal-metal interactions within dinuclear complexes. Thus, a second series of

ligands, in which the pyridine rings are forced to be co-planar, were prepared to complement the previously synthesised ligands. Other researchers have previously prepared two such compounds, **2.11** and **2.12**,[76-78] but there are no reported crystal structures of coordination complexes of these two ligands.

Preparation of the spirolene, **2.13**, requires 4,5-diazafluorene, **2.10**, which was prepared in two steps. In the first step, 4,5-diazafluorenone was prepared by a literature procedure,[76, 92] by reaction of 1,10-phenanthroline with potassium permanganate and potassium hydroxide, as shown in scheme 2.5. This reaction gave 4,5-diazafluorenone in variable yields ranging from 7-33% yield. In the second step, heating 4,5-diazafluorenone with hydrazine hydrate gave **2.10** in 36% yield.[76] Unfortunately these reactions are problematic, as shown by the variable and relatively low yields. The first step to prepare 4,5-diazafluorenone is unreliable, and because the second step only provides **2.10** in low yield, only relatively limited amounts of **2.10** were available to prepare **2.13**.

One of the reasons the key intermediate, **2.10**, is only obtained in 36% yield is because during the Wolff-Kishner reduction 9,9'-bi(4,5-diazaflurorenyl), **2.11**, is formed as a major by-product (26% yield). The closely related ligand, 9,9'-bi(4,5-diazaflurorenylidene), **2.12**, can then be easily prepared from **2.11**, following the method of von Zelewsky,[77] in 95% yield (Scheme 2.5). An interesting comparison is apparent here with a large contrast between the reactivity of

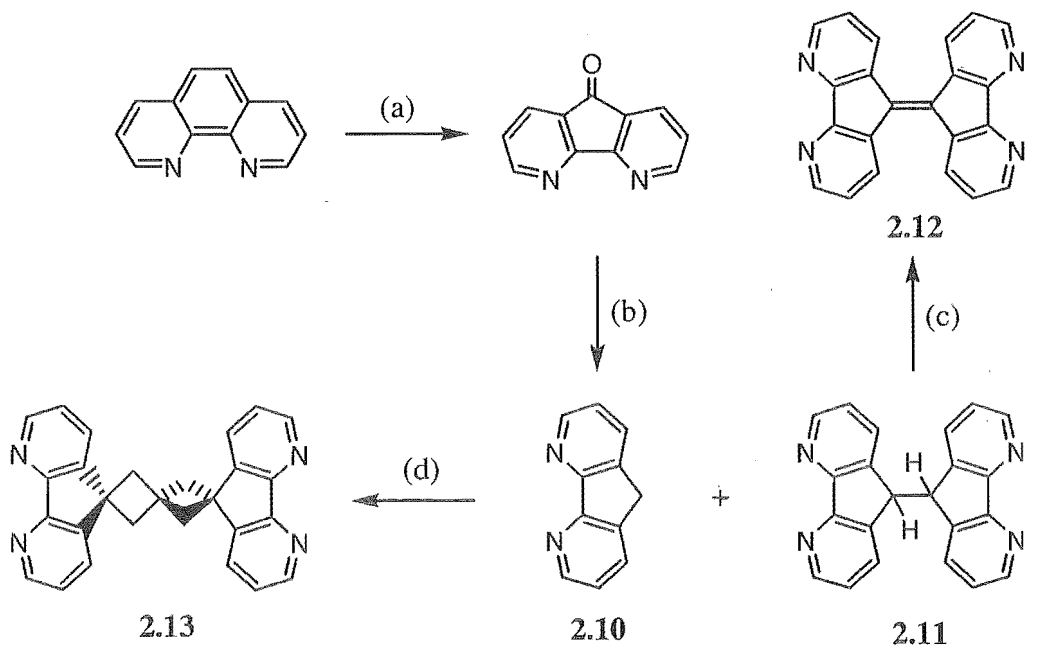


(a) $KMnO_4$, KOH, 33%; (b) $NH_2NH_2.H_2O$, **2.10**: 36%, **2.11**: 26%; (c) DDQ, toluene, 95%; (d) K, pentaerythrityl tetrabromide, 18%.

**Scheme 2.5.**

**2.11** and 1,1,2,2-tetrakis(2-pyridyl)ethane, **2.2**, towards oxidation with DDQ. As noted earlier, compound **2.2** undergoes a very slow and incomplete reaction with DDQ, whereas the reaction for the synthesis of **2.12** proceeds almost quantitatively.

The spirolene ligand, **2.13**, was then prepared by the reaction shown in Scheme 2.5. This reaction illustrates an interesting manifestation of the neopentanyl effect. The *in situ* prepared potassium salt of **2.10** was reacted with pentaerythrityl tetrabromide to give **2.13** in 18% yield. Unfortunately, the reaction requires four equivalents of **2.10**, which, for the reasons outlined above, has been difficult to obtain and thus, the low yield of **2.13** could not be improved. The formation of the spirolene core appears to be very specific for the fluorene ring system, because a similar reaction with di-2-pyridylmethane gave no analogous product. Another interesting observation, made by other workers, is that the related cyclobutane compound, shown in Figure 2.7, cannot be prepared from 1,3-dibromopropane.[93] Instead, the product is a compound with a propane spacer between two 4,5-diazafluorenyl moieties.

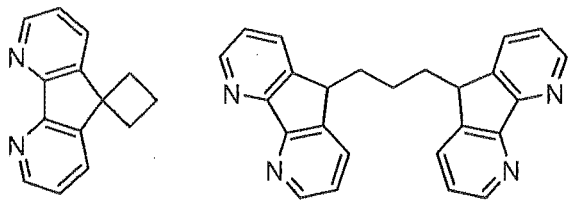


**Figure 2.7.** The anticipated and actual products from the reaction of 1,3-dibromopropane with 4,5-diazafluorene.

Crystal Structure of **2.13**

Crystals of **2.13**, which were suitable for X-ray crystallography, were obtained during recrystallisation. The compound crystallises in the chiral, orthorhombic space group $P2_12_12_1$. The compound is not in itself chiral, but in the solid state it packs with a twist in the two cyclobutane rings that makes it chiral. The two cyclobutane rings are twisted by 9.1° and 16.8°, leading to a curvature of the spiroheptane backbone in the solid state. As shown in Figure 2.8, the meanplanes of the two 4,5-diazafluorene subunits are twisted at an angle of 89.5° because of the spiro-carbon at the centre of the spirolene backbone, but are still ideally placed to chelate to two metal atoms. The strain within this structure is apparent in the large deviations of the bond angles about C(1) from the tetrahedral value. A consideration of the packing reveals that molecules of **2.13** pack in a herringbone arrangement, with edge-to-face $\pi$-$\pi$ interactions between adjacent molecules.

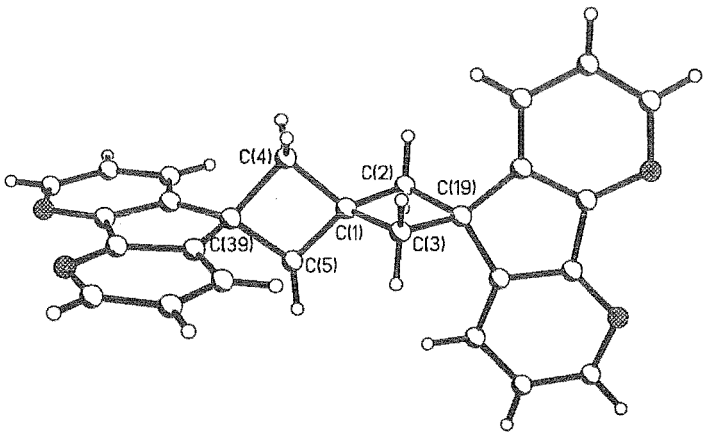


**Figure 2.8.** A perspective view of **2.13** shows the perpendicular arrangement of the two 4,5-diazafluorenyl ring systems. Selected bond lengths (Å) and angles (°): C(1)-C(2) 1.542(2), C(1)-C(5) 1.544(2), C(1)-C(4) 1.545(2), C(1)-C(3) 1.552(2), C(2)-C(1)-C(5) 121.19(15), C(2)-C(1)-C(4) 121.86(15), C(5)-C(1)-C(4) 88.84(12), C(2)-C(1)-C(3) 89.21(12), C(5)-C(1)-C(3) 119.20(14), C(4)-C(1)-C(3) 119.97(14).

### 2.2.3 Radialene-based ligands

While several [3]radialene compounds are known, the synthesis of the first hexaaryl[3]radialene was reported only relatively recently.[82] Since then two groups have developed different methods for the preparation of hexaaryl[3]radialenes, which can be prepared either by reaction of diarylmethyl anions with tetrachlorocyclopropene,[82, 94] or by cyclisation of dibromo[3]dendralenes.[81]

Hexa(2-pyridyl)[3]radialene, **2.14**, was prepared using the former approach, by reacting six equivalents of **2.1** with a slight excess of n-butyllithium, followed by addition of one equivalent of neat tetrachlorocyclopropene and then *in situ* oxidation of the resulting dianion with molecular oxygen (Scheme 2.6). An initial attempt to synthesise this compound following the exact methodology of Enomoto et al.[82] was unsuccessful. However, using just THF as the solvent, as opposed to a mixed DMSO/THF solvent system used for preparing other hexaaryl[3]radialenes, furnished the new hexadentate ligand **2.14** in 72% yield. During the course of this research, the work described here on the synthesis of hexapyridyl[3]radialenes was published concurrently with that of Matsumoto et al.[95-98]

The isomeric ligands, hexa(3-pyridyl)[3]radialene, **2.15**, and hexa(4-pyridyl)[3]radialene, **2.16**, were also prepared using the same procedure. However, these two compounds require the

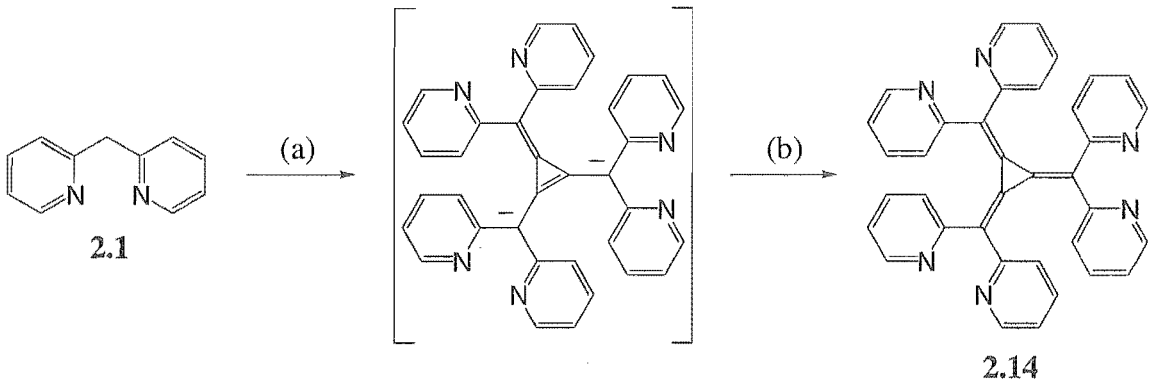


2.1 2.14

(a) n-BuLi, tetrachlorocyclopropene, THF; (b) oxygen gas, 72%.

**Scheme 2.6.**

preparation of either di-3-, or di-4-pyridylketone from the appropriately substituted bromopyridine and cyanopyridine starting materials, as illustrated for compound **2.15** (Scheme 2.7). The first step in which di-3-pyridylketone is prepared is relatively straightforward, proceeding in 73% yield. Using a similar method to the preparation of **2.1**, di-3-pyridylmethane was obtained in 41% yield. Subsequent reaction of di-3-pyridylmethane with tetrachlorocyclopropene, as described above, gave **2.15** in 43% yield.

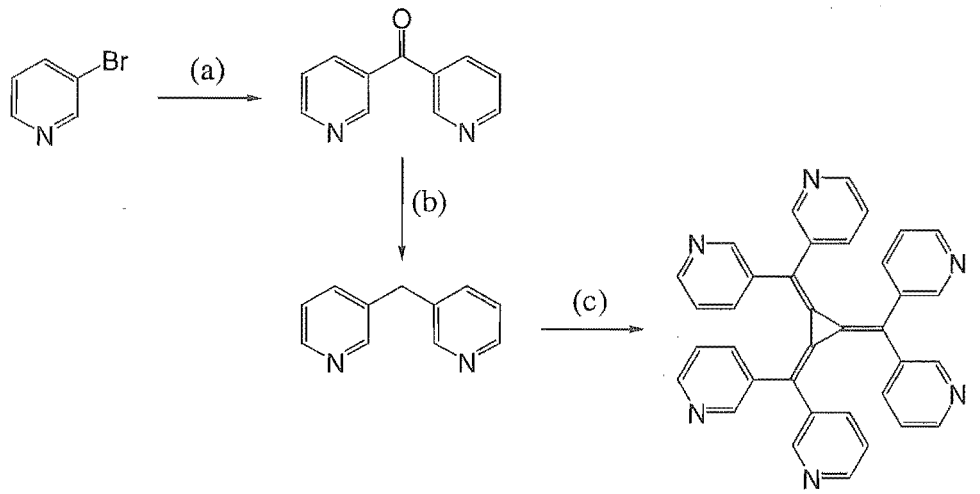


2.15

(a) n-BuLi, 3-cyanopyridine, 73%; (b) $NH_2NH_2$, KOH, 41%; (c) n-BuLi, tetrachlorocyclopropene, $O_2$, 43%.

**Scheme 2.7**

In comparison to the preparation of di-3-pyridylketone, the synthesis of di-4-pyridylketone is more problematic because the starting material, 4-bromopyridine is unstable. When required, the hydrochloride salt of 4-bromopyridine can be converted to its free base, and once deprotonated it must be rigorously maintained below -78°C to prevent polymerisation. Di-4-pyridylketone was prepared following a literature procedure,[99] and then reduced by a Wolff-Kishner reaction, in a

modification of the procedure for **2.1**, to give di-4-pyridylmethane in 85% yield following distillation.[100] Then di-4-pyridylmethane was reacted with tetrachlorocyclopropene, as previously described, to give the [3]radialene **2.16** in 16% yield. Unfortunately this reaction proceeds in a poor yield, which could not be improved.

Two other [3]radialene-based ligands, *unsym*- and *sym*-triphenyltri(2-pyridyl)[3]radialene, **2.17** and **2.18**, were prepared from commercially available 2-benzylpyridine by an analogous procedure. The two isomers are formed as a 3:1 mixture of *unsym*- and *sym*-triphenyltri(2-pyridyl)[3]radialene in a total yield of 31%. Unfortunately the two isomers have proven impossible to separate. The *unsym* isomer represents the first example of an unsymmetrically substituted [3]radialene.

Crystal Structure of **2.17** and **2.18**

An X-ray crystal structure determination was carried out on a crystal obtained by recrystallisation of the mixture of isomers **2.17** and **2.18**. The novel [3]radialene crystallises in the triclinic space group P-1 with one complete molecule in the asymmetric unit. The structure, shown in Figure 2.9, is very similar to that found for related hexaaryl[3]radialenes in the solid state with the aromatic rings twisted out of the plane of the [3]radialene core.[82] The mean twist

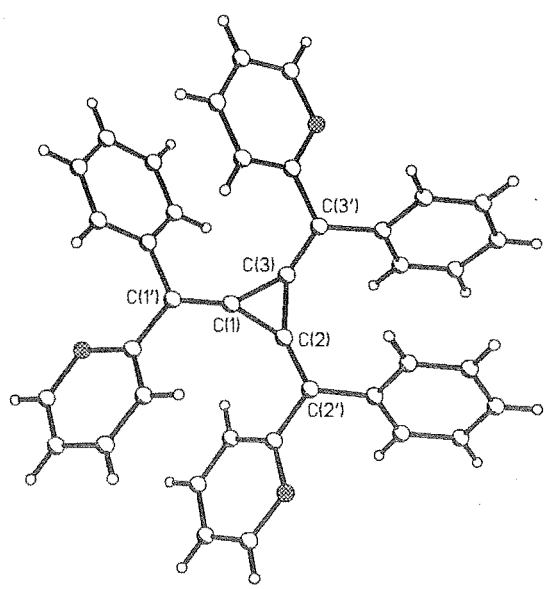


**Figure 2.9.** A perspective view of one of the major contributors of **2.17** in the crystal structure. Selected bond lengths and angles: C(1')-C(1) 1.362(3), C(1)-C(3) 1.448(3), C(1)-C(2) 1.450(3), C(2')-C(2) 1.342(3), C(2)-C(3) 1.454(3), C(3')-C(3) 1.353(3), C(3)-C(1)-C(2) 60.22(13), C(1)-C(2)-C(3) 59.82(14), C(1)-C(3)-C(2) 59.96(13).

out of the plane of the [3]radialene core for the pyridine and phenyl rings is 45.0(1)°. The bond lengths and angles are consistent with the [3]radialene core; C(1), C(2) and C(3) have a highly strained geometry, with bond angles of 60.22(13), 59.82(13) and 59.96(13), respectively. The positions of the nitrogen atoms are heavily disordered and it is difficult to unambiguously determine the absolute positions of the nitrogen atoms.

The extended π-system means that the hexapyridyl[3]radialene compounds are bright red solids and give bright red solutions. The UV-visible absorption spectrum shows a strong absorbance at *ca.* 463 nm, accounting for the bright red colour of solutions of these compounds. The values for the absorbance maxima, shown in Table 2.1, are similar to other hexaaryl[3]radialenes synthesised by other workers.[81, 82, 94]

A study of the electrochemistry of these compounds revealed that they undergo two reductions, the first reversible and the second quasi-reversible, to give the mono- and dianions, respectively (Table 2.1). This is similar to the redox behaviour observed for related hexaaryl[3]radialenes. These novel pyridine containing [3]radialenes were expected to possess lower reduction potentials then the previously studied hexaaryl[3]radialenes, in line with the strong electron withdrawing nature of the pyridine substituents. However, they were not as easily reduced as had been expected. This may be due to the propeller like conformation that hexaaryl[3]radialenes adopt in solution, which prevents the resonance withdrawing effects of the pyridine rings from significantly affecting the reduction potentials.

**Table 2.1.** Visible absorption maxima and redox potentials for compounds **2.14** - **2.18**.

| Compound | λ (nm)[a] | $E_{red(1)}$[b,c] | $E_{red(2)}$[b,c] |
|---|---|---|---|
| **2.14** | 463 | -1.23 | -1.59 |
| **2.15** | 464 | -1.31 | -1.78[d] |
| **2.16** | 463 | -1.32 | -1.63[d] |
| **2.17/2.18** | 469 | -1.47 | -1.80[d] |

[a] Measured in $CH_2Cl_2$ (±2 nm)

[b] Potentials (V) measured in $CH_2Cl_2$/0.1 mol.$L^{-1}$ [(*n*-$C_4H_9$)$_4$]$PF_6$ (the ferrocene/ferrocenium couple occurred at +0.16 V).

[c] Uncertainty in $E_{1/2}$ values *ca.* ± 0.01 V.

[d] Irreversible (approximate value estimated from anodic half-scan).

The aromatic region of the $^1$H NMR spectrum of **2.14** is shown in Figure 2.10, highlighting the significant upfield shifts that arise because of the propeller conformation that hexaaryl[3]radialenes adopt in solution. In the hexaaryl[3]radialenes the protons of the aromatic

rings lie over the shielding region of the adjacent rings and are shifted upfield. This is consistent with the solid state structures and the electrochemical studies of these compounds.

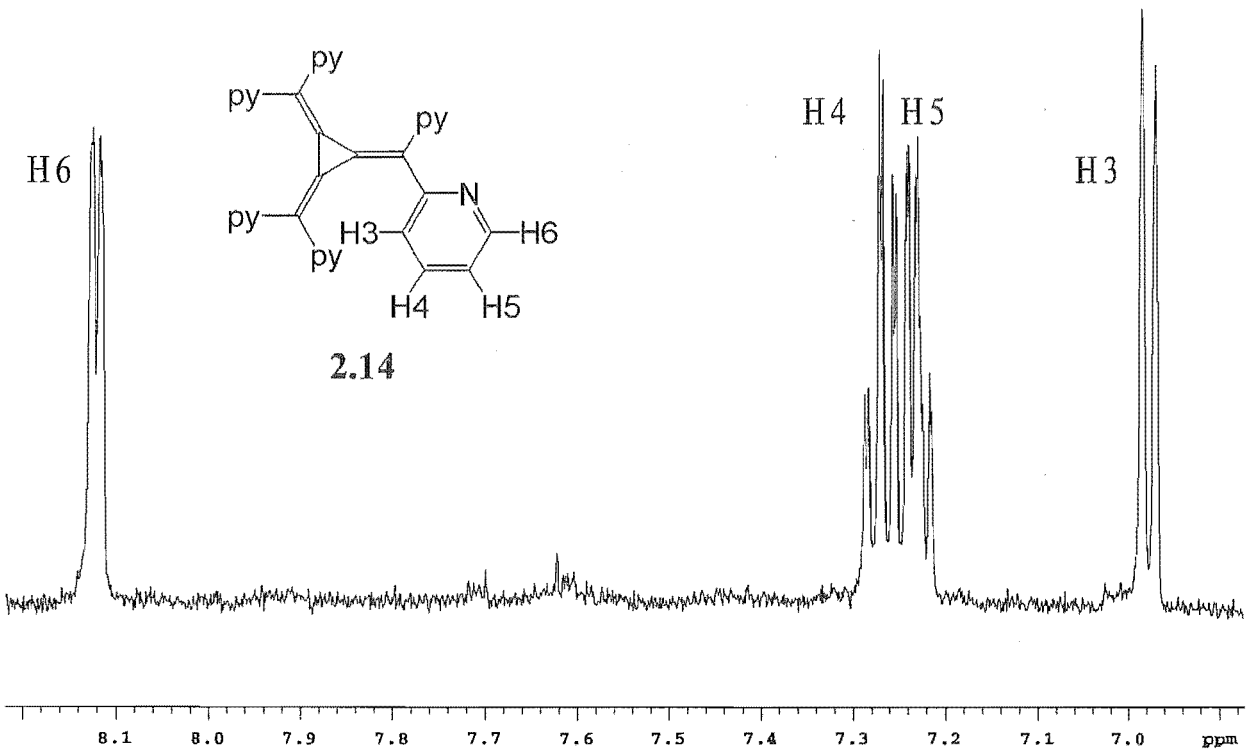





**2.14**

**Figure 2.10.** The $^{1}$H NMR spectrum of **2.14** showing the significant upfield shifts of the pyridyl protons.

## 2.3. Coordination and metallosupramolecular chemistry of the dipyridylmethane-based ligands

### 2.3.1 Complexes of di-2-pyridylmethane, 2.1

Compound **2.1** is expected to act primarily as a chelating ligand, as previously encountered in several structurally characterised complexes, and not as a bridging ligand (Figure 2.11). In all the structurally characterised complexes of **2.1** encountered in a search of the Cambridge Structural Database (CSD), **2.1** acts only as a chelating ligand.[73, 83] To further study the coordination chemistry of **2.1** it was reacted with a range of metal salts previously not investigated. Several silver salts with both coordinating and non-coordinating anions were used, as were copper and zinc nitrate. All of these were used throughout this research project to investigate the coordination chemistry of the various ligands. Ruthenium complexes of **2.1** were also prepared and these are discussed later (Section 2.6), serving as models for the study of ruthenium complexes of the structurally related bridging ligands.

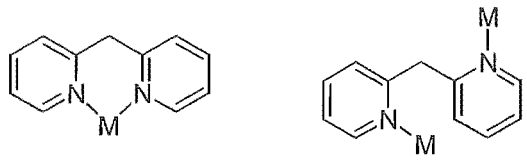


**Figure 2.11.** The chelating and bridging coordination modes of **2.1**.

The reactions investigated for **2.1** are summarised in Scheme 2.8. Reaction of **2.1** with silver nitrate in a 1:1 stoichiometry provided colourless crystals of a complex, **2.19**, which analysed with the anticipated 1:1 metal-ligand ratio. These crystals were suitable for X-ray crystallography and were studied to ascertain whether **2.1** was functioning as a bridging or chelating ligand. To probe the effect the anion has on the structure, **2.1** was also reacted in a 1:1 stoichiometry with both silver tetrafluoroborate and silver hexafluorophosphate. The former complex, **2.20**, was characterised as [Ag(**2.1**)]($BF_4$) and has the same composition, and potentially the same structure, as **2.19**, while the latter complex, **2.21**, analyses as [Ag(**2.1**)$_2$]($PF_6$).2$H_2O$. Unfortunately, no crystals were obtained, which were suitable for X-ray crystallography, despite several attempts at recrystallising these complexes.

A zinc nitrate complex, **2.22**, that analyses as [Zn(**2.1**)($NO_3$)$_2$] was also prepared by reacting a 1:1 mixture of zinc nitrate and **2.1** in methanol. A copper nitrate complex, **2.23**, was obtained by reaction of copper nitrate with **2.1** in 63% yield, but did not provide satisfactory elemental analysis for the expected 1:1 metal-ligand complex. Fortunately blue crystals were obtained of the complex which partially explained some of the difficulties with the elemental analysis. The ligand, **2.1**, had undergone oxidation in the presence of the copper to give di-2-pyridylmethanediol (**L'**).

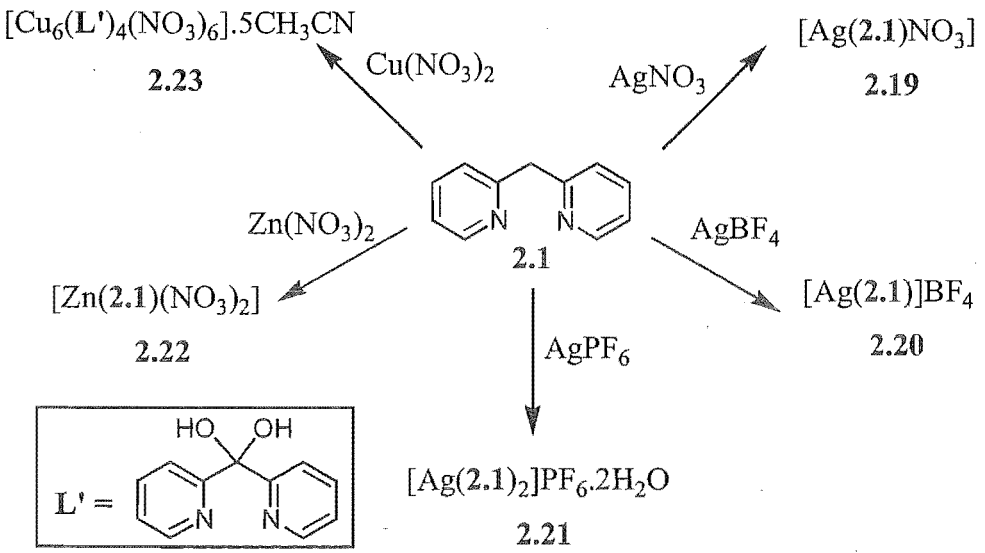


**Scheme 2.8**

Crystal Structure of **2.19**

Complex **2.19** crystallises in the monoclinic space group P2/c with one half of a ligand molecule, half a silver atom and half a nitrate anion in the asymmetric unit. One two-fold rotation axis passes through the silver nitrate and another through the methylene carbon of the ligand. The geometry of the silver atom is almost linear, but it makes two weak bonds to the oxygen atoms of the weakly coordinating nitrate anion with a Ag-O distance of 2.630(5) Å. A perspective view of the extended structure, shown in Figure 2.12, reveals that complex **2.19** is a one-dimensional coordination polymer. There are very weak π-π stacking interactions (3.740(9) Å) between the pyridine rings of adjacent coordination polymers. As highlighted earlier, there are no examples of structurally characterised complexes where di-2-pyridylmethane bridges between two metal centres and therefore, the complex characterised here is the first example of such a coordination mode for **2.1**.

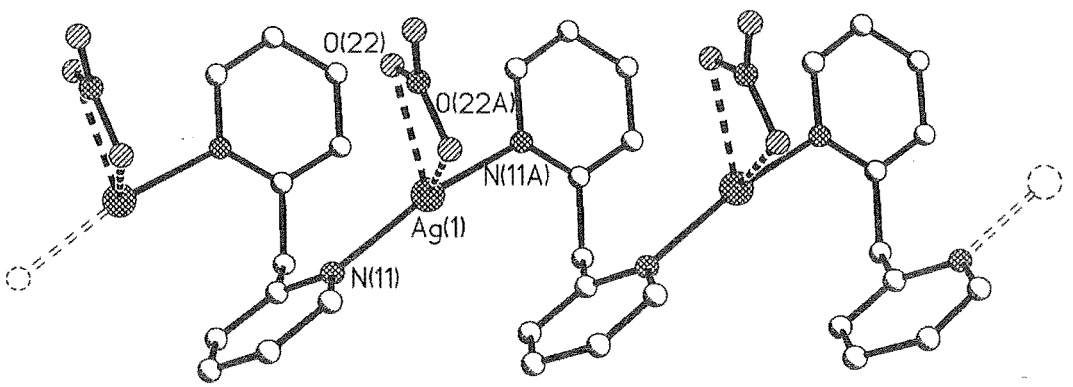


**Figure 2.12.** A perspective view of the one-dimensional coordination polymer **2.19**, formed from silver nitrate and **2.1**. Selected bond length (Å) and angle (°): Ag(1)-N(11) 2.235(5), N(11A)-Ag(1)-N(11) 162.9(2).

Crystal Structure of **2.23**

Crystals of the copper nitrate complex, **2.23**, were obtained by vapour diffusion of ether into an acetonitrile solution of the complex. The complex crystallises in the monoclinic space group $P2_1/c$, with a complete $M_6L'_4$ cluster and five acetonitrile molecules in the asymmetric unit. This $M_6L'_4$ cluster is constructed from two different $M_2L'_2$ components, orientated at 90° relative to each other, and two additional capping copper atoms. The asymmetric unit of the complex, **2.23**, excluding hydrogen atoms and solvate molecules, is shown in Figure 2.13. The most obvious feature of the structure is that the original ligand has undergone oxidation, in the presence of the copper ions, to give di-2-pyridylmethanediol (L').

The coordination environments of the copper atoms are very different. Excluding the copper-copper interaction, Cu(1) and Cu(2) both have a trigonal-bipyramidal geometry, with coordination by two pyridine nitrogen atoms and three deprotonated $\mu_2$-bridging oxygen atoms of the ligand. Two of the $\mu_2$-bridging oxygen atoms bridge only across the Cu(1)-Cu(2) dimer, while a third one bridges between these copper atoms and one of the capping copper atoms (Cu(5) and Cu(6)). The latter oxygen atoms are two of the links holding the two dimeric units together. The coordination geometry of both Cu(3) and Cu(4) is square-pyramidal when the copper-copper interaction is excluded. In this copper dimer, both copper atoms are coordinated in the basal plane by two $\mu_2$-bridging oxygen atoms, a pyridine nitrogen and a monodentate nitrate anion. The $\mu_2$-bridging oxygen atoms of the lower (Figure 2.13), Cu(1)-Cu(2) dimer, make weak contacts (2.472(6) and 2.476(6) Å) to the axial coordination sites of Cu(3) and Cu(4). Cu(5) and Cu(6) both possess distorted octahedral coordination geometries with typical Cu-N and Cu-O bond lengths to the atoms in the square plane. Both copper atoms make two longer

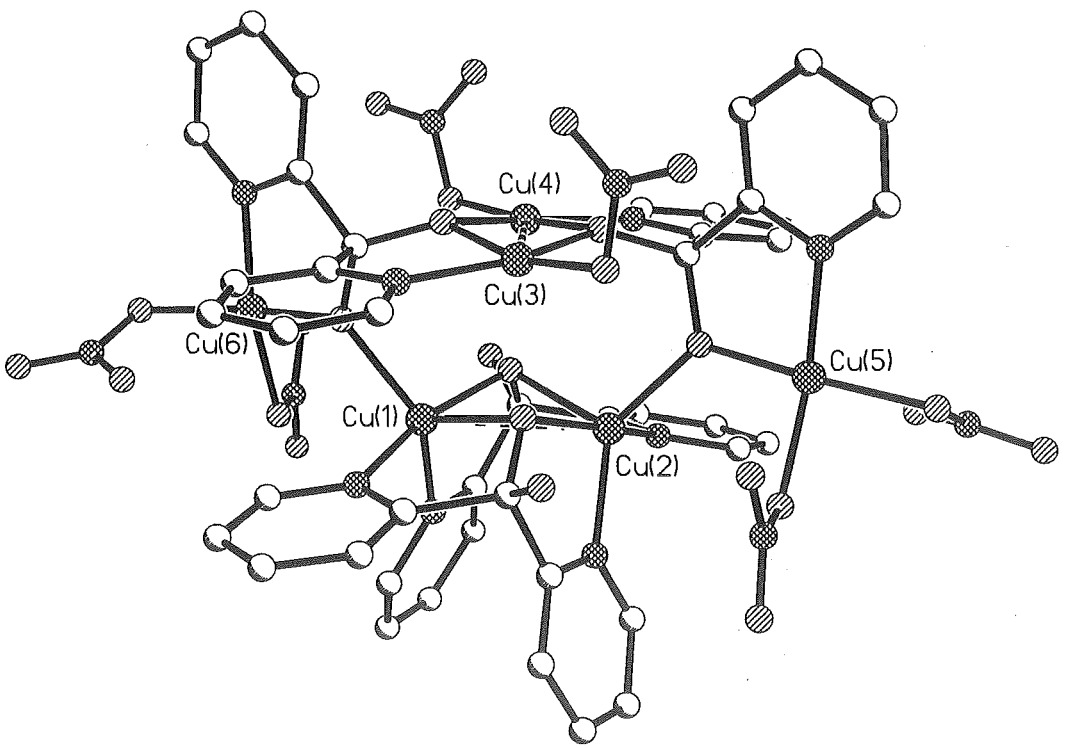


**Figure 2.13.** The $M_6L'_4$ cluster **2.23** formed from di-2-pyridylmethane and copper nitrate. Selected metal-metal distances (Å): Cu(1)-Cu(2) 2.928(1), Cu(3)-Cu(4) 3.015(1), Cu(1)-Cu(6) 3.440(1), Cu(2)-Cu(5) 3.471(1).

axial contacts, with Cu-O distances ranging between 2.484(6) and 2.559(7) Å, to the second oxygen atoms of the coordinated nitrate anions (not shown in Figure 2.13).

The geometry of the $M_2L'_2$ dimer involving Cu(3) and Cu(4), which is almost planar, is shown in Figure 2.14(a), while the other $M_2L'_2$ copper dimer, between Cu(1) and Cu(2), adopts a puckered butterfly conformation (Figure 2.14(b)). The metal-metal distances in these two dimers are 3.015(1) and 2.928(1) respectively, a value typical for such interactions. These $Cu_2O_2$ squares are part of a larger family of $Cu_2X_2$ squares, where X is a range of monatomic bridges, and have been the subject of an exhaustive review.[101] $Cu_2X_2$ squares like the ones observed here are of interest from a number of perspectives, but in particular in the context of magnetic behaviour of such complexes.[101]

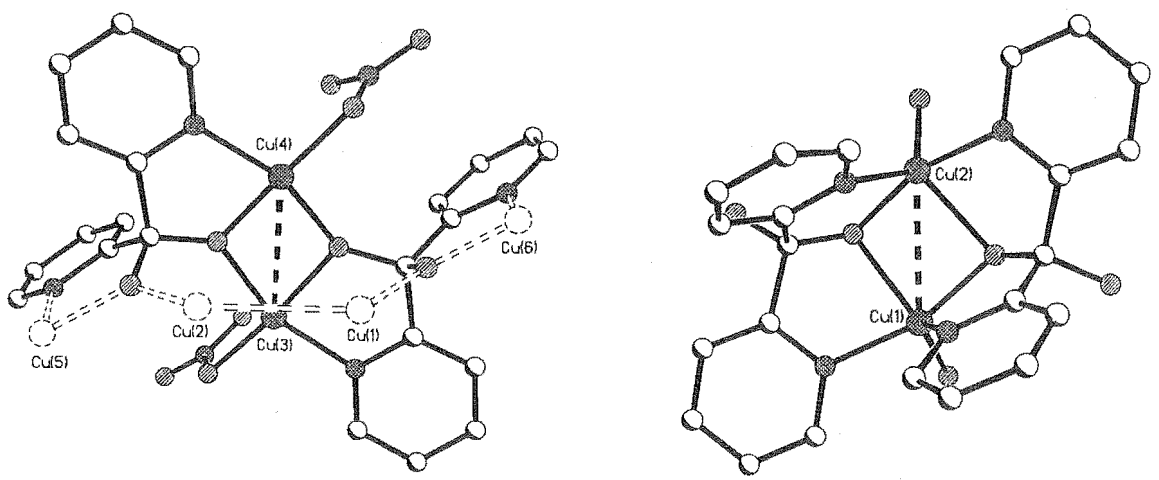


**Figure 2.14.** (a) A perspective view of the planar $M_2L'_2$ copper dimer involving Cu(3) and Cu(4) and (b) the butterfly shaped $M_2L'_2$ copper dimer involving Cu(1) and Cu(2).

An interesting aspect of this structure, mentioned earlier, is that **2.1** has undergone oxidation to produce both the singly and doubly deprotonated forms of di-2-pyridylmethanediol. The two molecules of L' bridging Cu(1) and Cu(2) are present as the monoanionic form, while the two molecules bridging Cu(3) and Cu(4) are dianions. Di-2-pyridylmethane is relatively stable in the presence of acids and bases, but has been shown to react with di-2-pyridylketone in the presence of copper ions by other workers.[73] When copper perchlorate was reacted with a mixture of di-2-pyridylketone and **2.1**, the formation of a copper complex of ligand **2.4** was observed after short periods of reaction at room temperature. Subsequently, after longer reaction times at elevated temperature, the formation of a copper complex of **2.3** was observed.[86] The former complex was

characterised by X-ray crystallography and UV-visible spectroscopy.[73] In the present case, **2.1** has undergone oxidation to a hydrated form of di-2-pyridylketone.

### 2.3.2 Complexes of 1,1,2,2-tetra(2-pyridyl)ethane, 2.2

This ligand was investigated from a number of standpoints. The ethane ligand has $sp^3$-hybridised carbon atoms in the backbone, in contrast to ligand **2.4**, and dinuclear complexes of this ligand were prepared to provide a comparison for complexes of **2.4**. Also of interest was a comparison of the coordination chemistry of **2.2** and **2.5**, the latter of which had been shown to form a complex[72] containing a seven-membered chelate ring as represented in Figure 2.15. Ligand **2.2** could potentially chelate through the vicinally substituted pyridine rings, but would be expected to coordinate through the geminally substituted pyridine rings (Figure 2.15). Therefore **2.2** was reacted with various silver salts, copper nitrate, palladium chloride and zinc acetate, as shown in Scheme 2.9, to investigate these various possibilities.

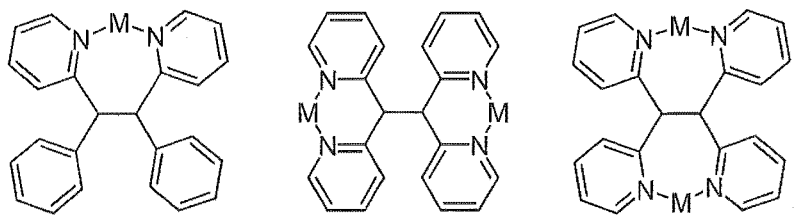

**Figure 2.15.** Some of the possible bridging coordination modes of ligands **2.5** and **2.2**.

Silver nitrate was reacted with **2.2** to give a complex with the composition $[Ag(\mathbf{2.2})NO_3]$, as shown by elemental analysis. An X-ray structure determination supported this composition,

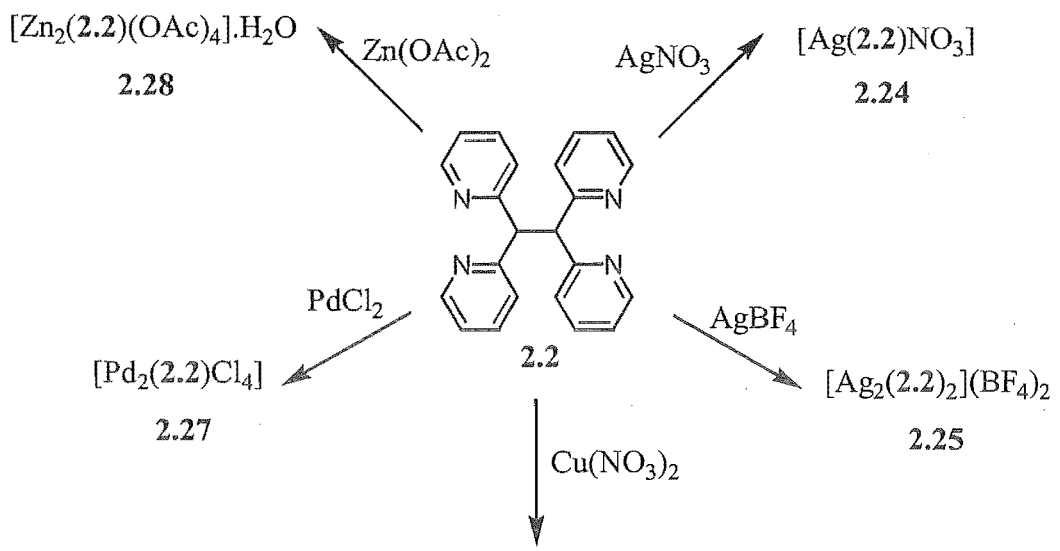


**Scheme 2.9**

revealing that simply mixing silver nitrate and **2.2** had led to the self-assembly of an undulating one-dimensional coordination polymer with a 1:1 metal-ligand ratio, despite the reaction being carried out with a 2:1 stoichiometry. With a labile metal such as silver, the stoichiometry and reaction conditions can strongly influence the type of structure obtained. To investigate the effect of the anion on the formation of complex **2.24**, ligand **2.2** was reacted with a different silver salt, namely silver tetrafluoroborate. This provided a second silver complex, **2.25**, also with a 1:1 metal-ligand ratio.

To demonstrate that ligand **2.2** could also form discrete dinuclear complexes it was reacted with copper nitrate in a metal-ligand ratio of 2:1. On standing, dark blue crystals of complex **2.26** were obtained, which analysed with the desired composition of $[Cu_2(\mathbf{2.2})(NO_3)_4]$ by elemental analysis. To further investigate the coordination chemistry of **2.2**, it was reacted with palladium chloride, but the complex, **2.27**, proved to be insoluble in common NMR solvents and could not be examined by NMR spectroscopy. This insolubility also prevented recrystallisation of the complex, which was found to have a $[Pd_2(\mathbf{2.2})Cl_4]$ composition by elemental analysis. Like the corresponding palladium acetate complex of **2.2**, which was prepared by Canty and Minchin,[72] the complex would be expected to show a square planar geometry at each palladium centre. A zinc complex, **2.28**, was prepared by reaction of zinc acetate with **2.2** in a 2:1 stoichiometry. Slow evaporation of the methanol reaction mixture gave crystals, analysing as $[Zn_2(\mathbf{2.2})(OAc)_4].H_2O$, which were suitable for X-ray crystallography.

Crystal Structure of **2.24**

Complex **2.24** crystallises in the monoclinic space group Cc. The asymmetric unit of **2.24**, which contains one molecule of **2.2**, a silver atom and a nitrate anion, is shown in Figure 2.16 and a perspective view of the extended coordination polymer in Figure 2.17. The geometry of the silver atom is distorted trigonal-bipyramidal, with coordination by four pyridine rings of two crystallographically related ligand molecules and an oxygen of the nitrate anion. The nitrate anion makes another long contact with the silver atom, and hence the geometry could be described as highly distorted octahedral. The silver-nitrogen distances range from 2.312(4)-2.635(3) Å, while the nitrate oxygen atoms are slightly further distant at 2.672(3) and 2.786(3) Å; the later distance to O(12), representing a very long and weak interaction. The Ag-N bonds to the pyridine nitrogen atoms N(21) and N(41A) in the trigonal plane are longer than the bonds to the nitrogen atoms of the pyridine rings in the axial coordination sites. The silver-silver distance in this complex is 6.835(1) Å.

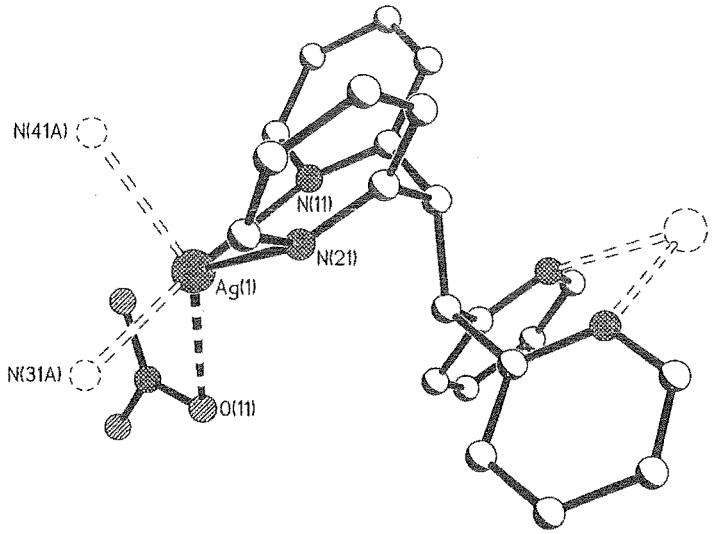


**Figure 2.16.** A perspective view of the asymmetric unit of **2.24** shows the highly distorted geometry around the silver atom. Selected bond distances (Å) and angles (°): Ag(1)-N(11) 2.312(4), Ag(1)-N(21) 2.635(3), Ag(1)-N(31A) 2.343(4), Ag(1)-N(41A) 2.469(3), Ag(1)-O(11) 2.671(3), N(11)-Ag(1)-N(31A) 170.04(12), N(11)-Ag(1)-N(41A) 96.59(10), N(31A)-Ag(1)-N(41A) 84.62(10), N(11)-Ag(1)-N(21) 84.44(10), N(31A)-Ag(1)-N(21) 85.92(10), N(41A)-Ag(1)-N(21) 82.44(8).

While the complex demonstrates the potential for a number of bimetallic complexes, the extended structure of **2.24** is an interesting one-dimensional coordination polymer. The coordination polymer is helical and extends down the crystallographic *c*-axis of the unit cell. The nitrate anion alternates on opposite sides of the coordination polymer at each silver atom, while

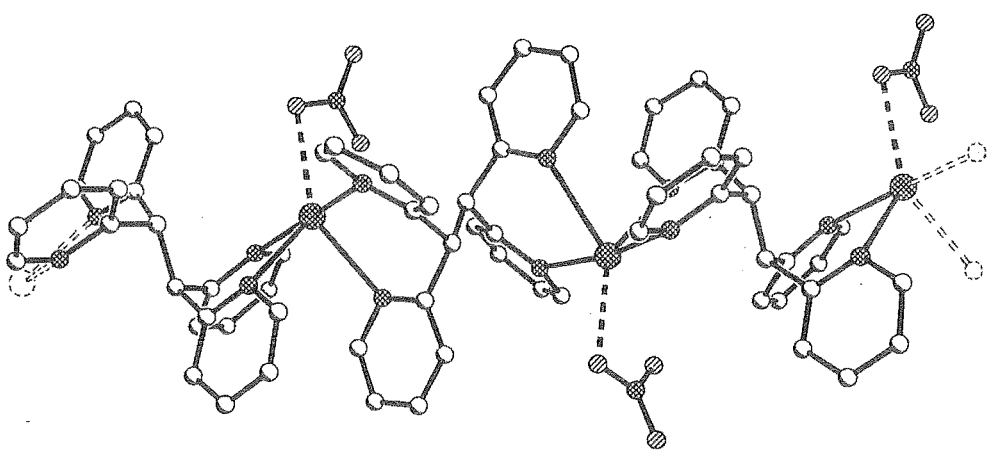

**Figure 2.17.** A perspective view of the structure of the coordination polymer **2.24**.

the ligand twists by approximately 90° at each repeat. No significant interactions occur between the different coordination polymers in the crystal with only weak interactions by the non-coordinated oxygen atom of the nitrate anions with the pyridine hydrogen atoms of adjacent polymer chains.

Crystal Structure of **2.25**

As was mentioned, the choice of anion often plays a pivotal role in the solid-state structure of silver complexes and, thus, despite having the same stoichiometry as **2.24**, an X-ray crystal structure determination was undertaken on complex **2.25**. This revealed that complex, **2.25**, does indeed have a different structure to **2.24**. It crystallises in the space group $P2_1/c$, with one ligand molecule, one disordered silver atom, a tetrafluoroborate counterion and an acetonitrile solvate molecule in the asymmetric unit. The overall structure of **2.25** is a [2+2]-dimetallomacrocycle, as shown in Figure 2.18. Each silver atom is trigonal-planar with coordination by one pyridine ring of one ligand and chelation by two pyridine rings of the second ligand molecule. The bond distances are 2.302(2) and 2.344(3) Å for the chelating pyridine rings, and slightly shorter

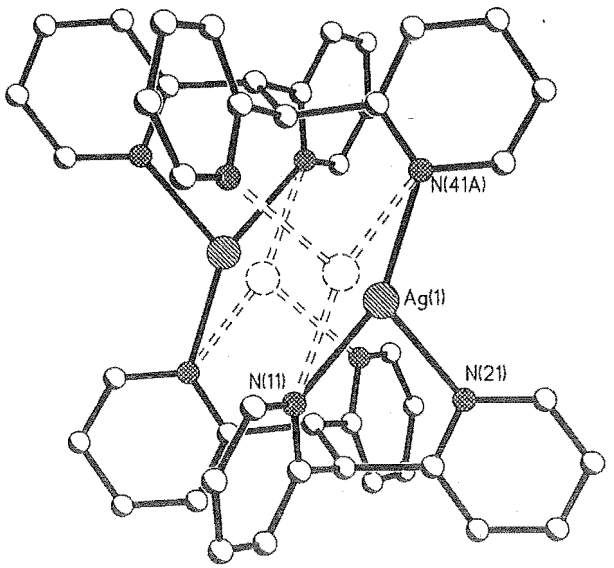


**Figure 2.18.** A perspective view of complex **2.25** shows the two positions of the silver atom. The dashed bonds and atoms show the minor component of the structure. Selected bond distances (Å) and angles (°): Ag(1)-N(41A) 2.266(3), Ag(1)-N(11) 2.302(2), Ag(1)-N(21) 2.344(3), N(41A)-Ag(1)-N(11) 150.62(10), N(41A)-Ag(1)-N(21) 122.62(11), N(11)-Ag(1)-N(21) 85.87(10).

(2.266(3) Å) for the monodentate pyridine donor (N(41A)) of the other ligand. The geometry of the silver atom is distorted away from trigonal-planar because the angle between the chelating pyridine rings is acute, and consequently, this opens up the angle between N(11) and N(41A). One of the pyridine ring nitrogen atoms is not involved in coordination to the silver atoms, and the ligand can therefore be described as hypodentate.

The silver atom is disordered over two sites, as indicated in Figure 2.18, with a 7:3 ratio of site occupancies. One site is less favored because it is a more sterically demanding binding site, with a close contact with the ethylene bridge proton of the ligand. The silver-silver distance in this complex is 3.893(1) Å, and because of the nature of the complex, considerably shorter than that in complex **2.24**. The discrete [2+2]-dimetallomacrocyclic complexes pack in the crystal with no significant interactions between the individual [2+2] complexes. There are weak contacts with the tetrafluoroborate anions, which are located in the spaces between the [2+2]-dimetallomacrocycles.

Crystal Structure of **2.26**

Complex **2.26** crystallises in the monoclinic space group C2/c, with four molecules of **2.26** in the unit cell. The asymmetric unit consists of one metal atom, half the ligand, one coordinated methanol molecule, two coordinated nitrate anions and one non-coordinated methanol solvate molecule, with the latter three units each disordered over two sites. A perspective view of **2.26** is shown in Figure 2.19, with the non-coordinated solvate molecules and the disorder of the nitrate anions omitted for clarity. The copper atoms have a square-pyramidal geometry ($\tau$ value[#] of 0.01) with the coordinated methanol solvate molecule occupying the apical coordination position. The Cu-N distances are typical (1.992(2) and 2.000(2) Å), as are the Cu-O bond distances to the monodentate nitrate anions, while the methanol solvate molecule is coordinated at a longer distance of 2.269(2) Å. The copper-copper distance is 6.698(1) Å, similar to that in the previous silver nitrate complex, **2.24**.

[#] The $\tau$ value ($\tau = (\beta-\alpha)/60°$ where $\alpha$ and $\beta$ are the angles between the atoms in the basal plane of a square-pyramidal geometry and $\beta$ is greater than $\alpha$) is a measure of the geometry of five-coordinate complexes. Strictly tetragonal geometries have a $\tau$ value of zero, while trigonal-bipyramidal geometries will have a $\tau$ value of one.[102]

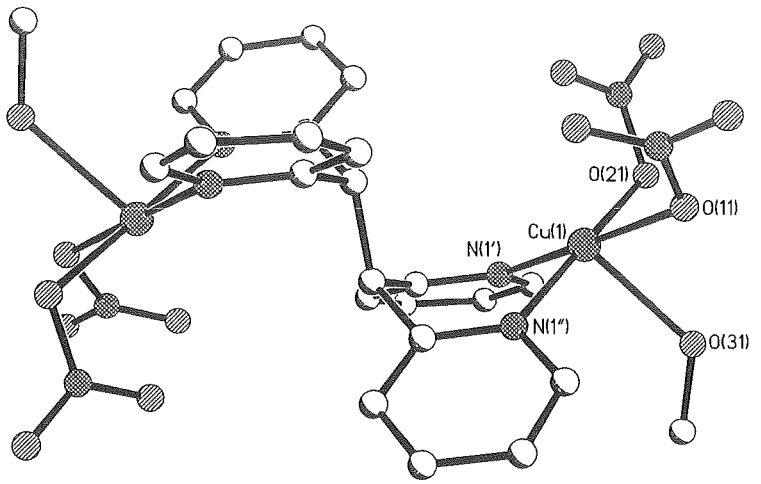


**Figure 2.19.** A perspective view of the dinuclear copper complex **2.26**. Selected bond lengths (Å) and angles (°): Cu(1)-N(1') 1.992(2), Cu(1)-N(1") 2.000(2), Cu(1)-O(21) 2.006(15), Cu(1)-O(11) 1.967(8), Cu(1)-O(31) 2.269(2), O(11)-Cu(1)-N(1') 175.0(4), O(11)-Cu(1)-N(1") 96.7(3), N(1')-Cu(1)-N(1") 88.32(7), O(11)-Cu(1)-O(21) 87.3(7), N(1')-Cu(1)-O(21) 87.7(6), N(1")-Cu(1)-O(21) 175.6(6), O(11)-Cu(1)-O(31) 78.7(3), N(1')-Cu(1)-O(31) 99.97(7), N(1")-Cu(1)-O(31) 96.82(7), O(21)-Cu(1)-O(31) 82.1(5).

Crystal Structure of **2.28**

Complex **2.28** crystallises in the monoclinic space group $P2_1/c$ with $Z = 2$. The asymmetric unit contains one zinc atom, half the ligand and two monodentate acetate anions. The zinc atom has a tetrahedral geometry, with chelation by the ligand to give a six-membered chelate ring, with a boat conformation, characteristic of complexes where this ligand chelates to a metal centre. A perspective view of **2.28** is shown in Figure 2.20, with selected bond lengths and angles given in the caption. The oxygen atoms of the acetate anions are held closer to the zinc, with bond lengths of 1.946(2) and 1.974(2) Å, than the pyridine nitrogen donors (2.094(2) and 2.119(2) Å). The geometry of the zinc atom is distorted away from a strict tetrahedral geometry by the chelation to **2.2** with the bond angle for N(21)-Zn-N(11) of 89.57(7)°. The zinc-zinc distance in **2.28** is 6.571(1) Å, a value that is very similar to the metal-metal distance in complex **2.26** (6.698(1) Å).

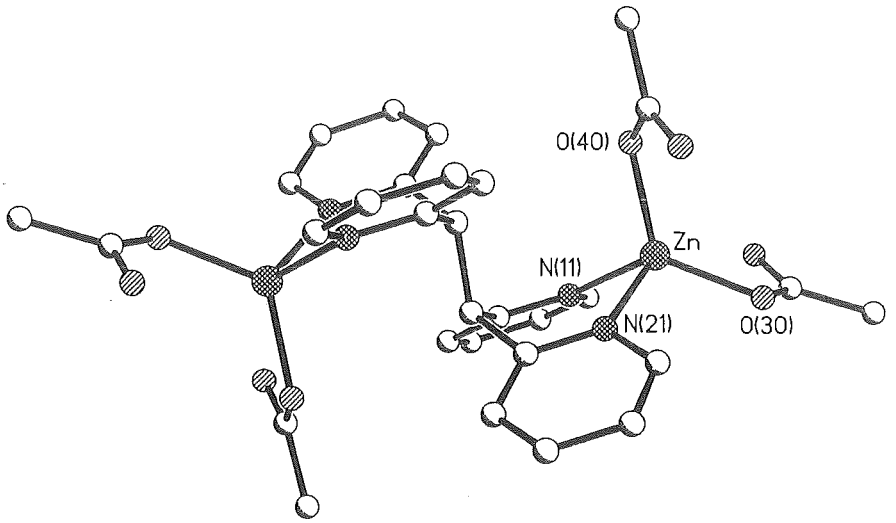


**Figure 2.20.** A perspective view of complex **2.28** with the hydrogen atoms omitted for clarity. Selected bond lengths (Å) and angles (°): Zn-N(21) 2.094(2), Zn-N(11) 2.119(2), Zn-O(30) 1.946(2), Zn-O(40) 1.974(2), O(30)-Zn-O(40) 123.91(8), O(30)-Zn-N(21) 98.20(8), O(40)-Zn-N(21) 121.04(7), O(30)-Zn-N(11) 122.66(8), O(40)-Zn-N(11) 97.85(7), N(21)-Zn-N(11) 89.57(7).

### 2.3.3 Complexes of 1,1,2,2-tetra(2-pyridyl)ethanol, 2.3

The ditopic ligand **2.3** has a number of different potential coordination modes. It possesses two different metal binding domains; one bidentate, like ligand **2.2**, and the other potentially tridentate with two pyridine nitrogen donors and the oxygen of the alcohol as possible donor atoms. To investigate the various coordination modes, several complexes of **2.3** were prepared by reaction with copper, silver, palladium and ruthenium precursors (Scheme 2.10). Reaction of **2.3** with silver nitrate furnished colourless crystals, **2.29**, for which X-ray crystallography was used to determine the structure. The crystal structure of complex **2.29**, discussed below, revealed an interesting feature of **2.3** with regards to its stability. During the synthesis of this complex, **2.3** undergoes a retro-Knoevenagel reaction to form di-2-pyridylmethane and di-2-pyridylketone. Aside from the decomposition of **2.3**, the crystal structure shows di-2-pyridylmethane again acting as a bridging, as opposed to a chelating, ligand. $^1$H NMR spectroscopy on the bulk sample from the above reaction confirmed the decomposition of **2.3** and revealed a mixture of two components; one corresponding to di-2-pyridylmethane and the second to di-2-pyridylketone.

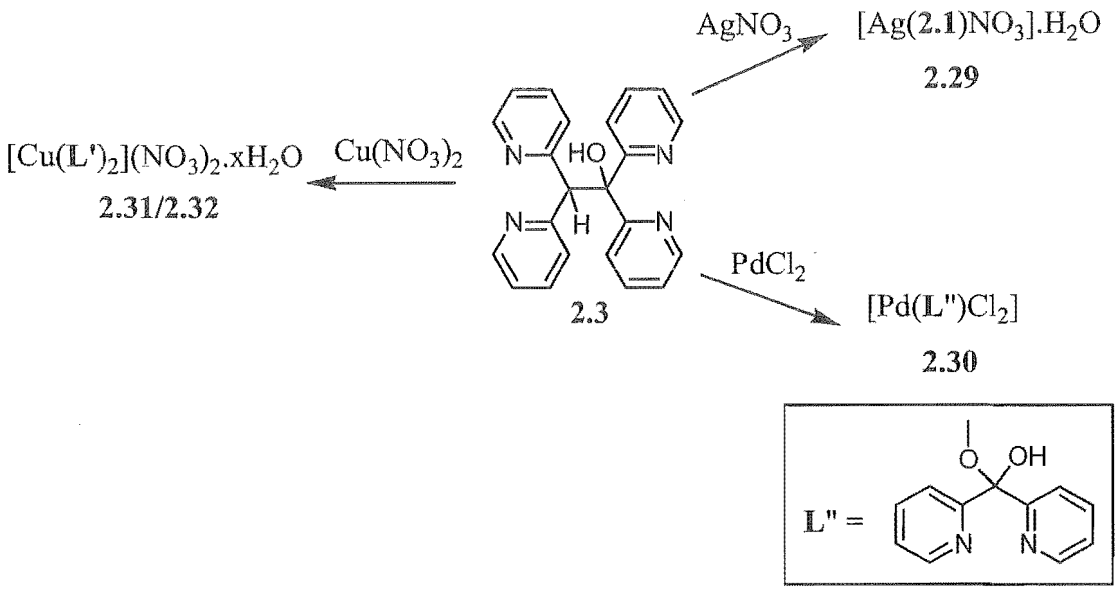


**Scheme 2.10**

In an effort to prevent the decomposition of **2.3**, which is stable enough to dehydrate in the preparation of ligand **2.4**, a palladium chloride complex was prepared under weakly acidic conditions. Orange-yellow crystals were obtained by concentrating the reaction mixture, leading to an X-ray structure of a palladium complex, **2.30**, that revealed a further unexpected twist. This time, while the ligand had again decomposed, the structure was that of the hemiacetal of di-2-pyridylketone (**L"**) coordinated to a palladium atom. A similar decomposition was also noted during the synthesis of a copper nitrate complex and in the formation of a ruthenium complex of **2.3**. Reaction of copper nitrate with **2.3**, followed by recrystallisation, gave a mixture of two different coloured crystals; purple crystals, **2.31**, and blue crystals, **2.32**. These were shown to have a similar composition by X-ray crystallography, $[Cu(\mathbf{L'})_2](NO_3)_2.xH_2O$ (where **L'** is the previously encountered di-2-pyridylmethanediol and x = 1 or 2). The bulk sample was not separated and the elemental analysis was consistent with the blue monohydrate form (**2.32**).

Crystal Structure of **2.29**

As mentioned above, the structure of complex **2.29** is a coordination polymer comprised of bridging di-2-pyridylmethane ligands and silver nitrate. The complex crystallises in the monoclinic space group $P2_1/c$ with the asymmetric unit, shown in Figure 2.21, containing one molecule of di-2-pyridylmethane, one silver atom and one nitrate anion. This is an identical composition to that reported earlier for complex **2.19**, which was formed directly from reaction of **2.1** and silver nitrate. However, that complex crystallises in the space group P2/c, possesses a slightly different conformation of the ligand and, more importantly, different packing interactions (Figure 2.22).

The Ag-N bond lengths and angles about the silver atom are 2.183(2) and 2.184(2) Å with an angle between the two pyridine donors of 164.46(9)°. These bond distances and angles are similar to those found in the previous complex, **2.19**. The silver also makes weak Ag-O interactions with two different nitrate anions. The bifurcated oxygen atoms, O(22) and O(22A), bridge between different coordination polymers, with Ag-O distances of 2.908(4) and 2.758(3) Å, respectively. The Ag-O distance for O(21A) is 2.713(3) Å. One of the major differences between the two structures, **2.19** and **2.29**, resides in the weak silver to nitrate anion interactions

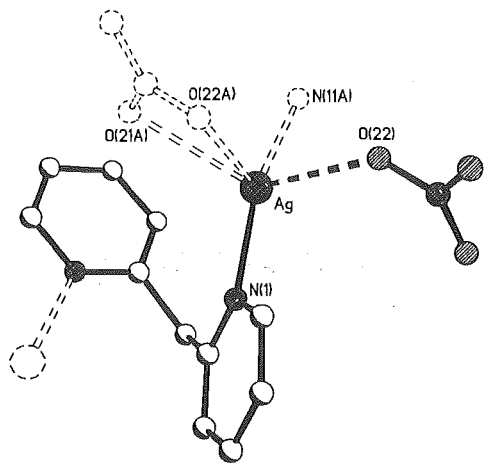


**Figure 2.21.** A perspective view of the asymmetric unit of the coordination polymer, **2.29**, formed from reaction of silver nitrate with **2.3**. Selected bond lengths (Å) and angles (°): Ag-N(1) 2.183(2), Ag-N(11A) 2.184(2), Ag-O(22) 2.908(4), Ag-O(21A) 2.713(3), Ag-O(22) 2.758(3), N(1)-Ag-N(11A) 164.46(9).

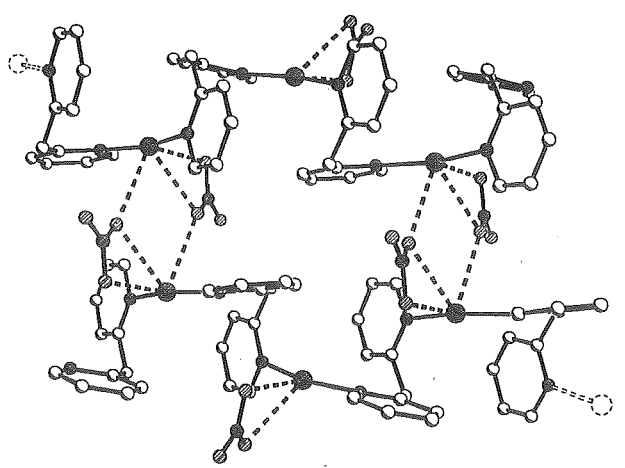

**Figure 2.22.** A perspective view of the extended two-dimensional network structure formed by weak interactions through the nitrate anions.

that connect the one-dimensional coordination polymers. As is shown in Figure 2.22, each one-dimensional coordination polymer is incorporated into two-dimensional sheets by weak interactions through the bifurcated oxygen atom of the nitrate anions.

Crystal Structure of **2.30**

The asymmetric unit of complex **2.30** is shown in Figure 2.23. The palladium atom is square planar with bond lengths and angles typical for such a complex. The oxygen of the methoxy-group of the hemiacetal interacts very weakly (2.755(5) Å) with the palladium atom. Complexes of this ligand, L", prepared directly by solvolysis of di-2-pyridylketone, have previously been characterised by X-ray crystallography with cobalt,[103] copper,[104, 105] zinc[106] and palladium,[107] the latter in the form of a square planar palladium trifluoroacetate complex. In these complexes the interaction with the methoxy oxygen is more significant with M-O distances between 2.371 Å (M = Zn) and 2.614 Å (M = Cu), reflective of the fact that palladium forms very stable square planar complexes. No unusually short intermolecular contacts are present in the structure.

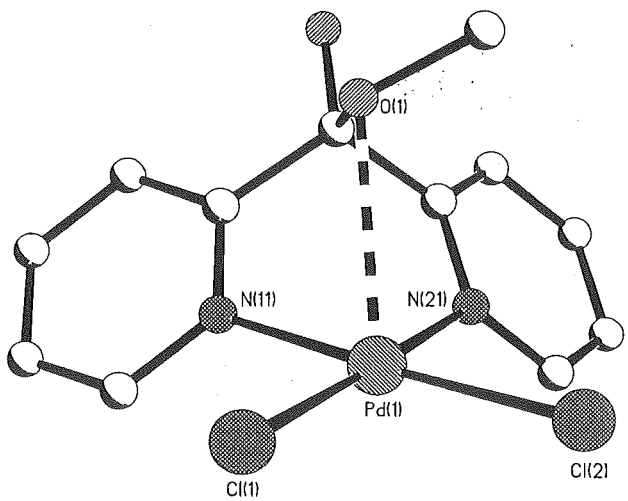


**Figure 2.23.** A perspective view of the decomposition product, **2.30**, formed by reacting palladium chloride with **2.3**. Selected bond lengths (Å) and angles (°): Pd(1)-N(11) 2.028(3), Pd(1)-N(21) 2.044(3), Pd(1)-Cl(2) 2.2891(11), Pd(1)-Cl(1) 2.2953(12), N(11)-Pd(1)-N(21) 86.44(12), N(11)-Pd(1)-Cl(2) 176.91(8), N(21)-Pd(1)-Cl(2) 90.89(9), N(11)-Pd(1)-Cl(1) 91.29(9), N(21)-Pd(1)-Cl(1) 177.74(8), Cl(2)-Pd(1)-Cl(1) 91.37(4).

As previously noted for the synthesis of complex **2.29**, $^{1}$H NMR spectroscopy on the bulk sample from this reaction revealed a mixture of two components corresponding to decomposition of the original ligand. Previous literature reports suggest that the original ligand, **2.3**, probably

decomposed to give a mixture of **2.1** and di-2-pyridylketone, the latter of which, on coordination to a metal atom, is susceptible to nucleophilic attack by methanol.[104]

Crystal Structure of **2.31** and **2.32**

Two different crystalline products were isolated from reaction of copper nitrate with **2.3**; purple crystals (**2.31**) and blue crystals (**2.32**). When crystal structure determinations were undertaken on both sets of crystals it was discovered that the crystals had almost identical compositions. In both cases the ligand, **2.3**, had been hydrolysed to di-2-pyridylmethanediol (**L'**) in the presence of the copper and a Jahn-Teller distorted octahedral complex, $[CuL'_2](NO_3)_2.xH_2O$, of this decomposition product had formed. Perspective views of both structures are shown in Figures 2.24 and 2.25, with selected bond lengths and angles for comparison.

The dihydrate complex, **2.31**, which has one additional water molecule than **2.32** in the structure, crystallises in the space group $P2_1/n$ and has previously been reported.[108] It will be described to provide a comparison with the second complex, the monohydrate form, **2.32**. The asymmetric unit comprises, one molecule of **L'** in its neutral form, half a copper atom, one nitrate anion and one hydrogen bonded water molecule. The copper atom lies on a centre of

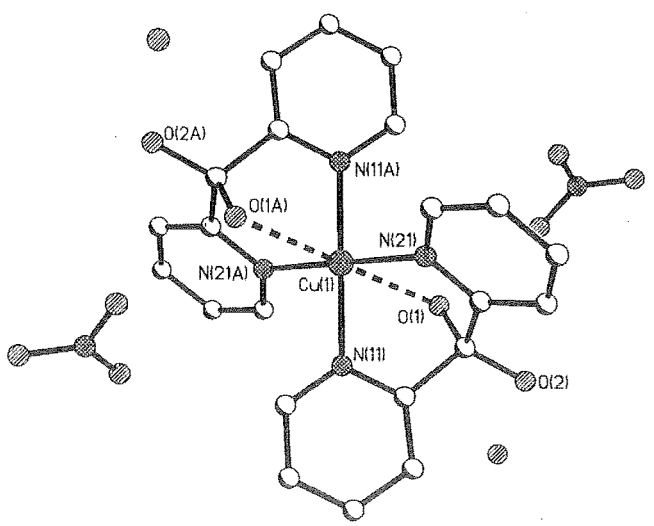


**Figure 2.24.** A perspective view of the purple coloured form of complex **2.31**. Selected bond lengths (Å) and angles (°): Cu(1)-N(11) 1.992(1), Cu(1)-N(21) 2.048(2), Cu(1)-(O1) 2.477(4), N(11A)-Cu(1)-N(11) 180.0, N(11A)-Cu(1)-N(21) 91.59(7), N(11)-Cu(1)-N(21) 88.41(7), N(11)-Cu(1)-(O1) 73.2(7), N(21)-Cu(1)-(O1) 74.4(7), N(11A)-Cu(1)-(O1) 106.8(9), N(21A)-Cu(1)-(O1) 105.6(9), (O1A)-Cu(1)-(O1) 180.0.

inversion and has a distorted octahedral geometry with Jahn-Teller distortion of the weak axial Cu-O bonding interactions. The Cu-N bond lengths of the copper atom in complex **2.31** are 1.992(1) and 2.048(2) Å, while the Cu-O distance is 2.477(4) Å, which represents a weak bond. An intricate hydrogen-bonding network connects the symmetry-related non-coordinated water molecules and nitrate anions to the complex. These water molecules hydrogen bond to O(2) or O(2A) of the ligand, while the two symmetry-related nitrate anions are hydrogen bonded to O(1) or (O1A). The O···O distance for the former two hydrogen bonds is 2.700(8) Å, while for the latter two hydrogen-bonding interactions it is 2.724(8) Å.

The monohydrate complex **2.32** crystallises in the space group Cc, with one full $ML_2$ complex, two non-coordinated nitrate anions and one hydrogen bonded water molecule in the asymmetric unit. The Cu-N bond lengths are fairly similar in both complexes, but by contrast to complex **2.31**, the Cu-O bond lengths in the blue crystals, complex **2.32**, are considerably shorter

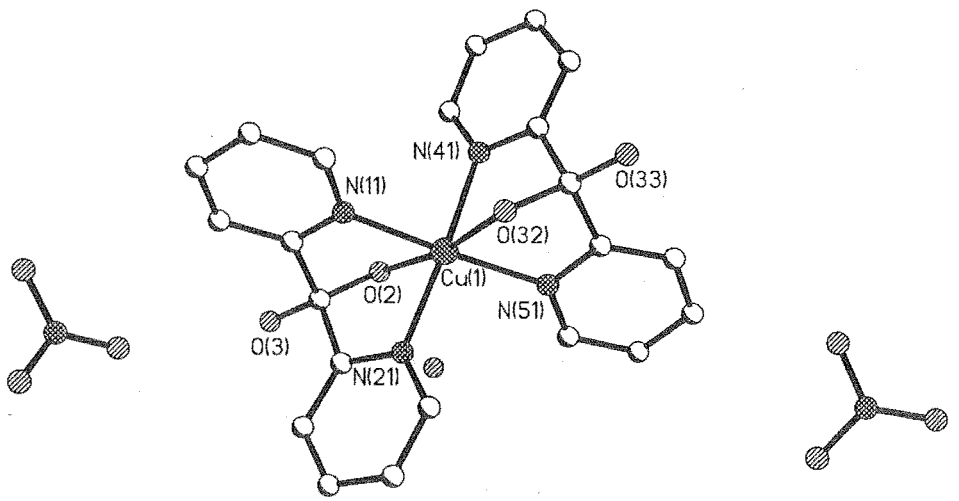


**Figure 2.25.** A perspective view of the blue coloured form of complex **2.32** with hydrogen atoms omitted for clarity. Selected bond lengths (Å) and angles (°): Cu(1)-N(11) 2.014(2), Cu(1)-N(41) 2.015(2), Cu(1)-N(21) 2.029(2), Cu(1)-N(51) 2.033(2), Cu(1)-O(32) 2.323(2), Cu(1)-O(2) 2.394(2), N(11)-Cu(1)-N(41) 90.15(8), N(11)-Cu(1)-N(21) 87.42(8), N(41)-Cu(1)-N(21) 173.59(8), N(11)-Cu(1)-N(51) 174.38(8), N(41)-Cu(1)-N(51) 87.70(9), N(21)-Cu(1)-N(51) 95.24(8), N(11)-Cu(1)-O(32) 98.19(7), N(41)-Cu(1)-O(32) 75.29(7), N(21)-Cu(1)-O(32) 110.93(8), N(51)-Cu(1)-O(32) 76.25(7), N(11)-Cu(1)-O(2) 75.09(7), N(41)-Cu(1)-O(2) 98.37(7), N(21)-Cu(1)-O(2) 75.27(7), N(51)-Cu(1)-O(2) 110.36(7), O(32)-Cu(1)-O(2) 170.93(7).

at 2.323(2) and 2.394(2) Å. This could represent an example of the very interesting, but highly contentious, phenomenon known as bond stretch isomerism.[109] However, like the dihydrate form (**2.31**), the nitrate anions and water molecules participate in an intricate hydrogen-bonding network that surrounds the complex, suggesting the possibility of some form of outer-sphere control of the Jahn-Teller distortion in the solid state. This is a more likely reason for the variability of the Cu-O bond lengths, than the former proposition. Other closely related copper complexes have been described with different anions and solvate molecules that have a range of different bond lengths to the apical hydroxyl groups of ligand **L'**.[108, 110] These M-O distances range from 2.352 to 2.467 Å.

Unfortunately, no examples of ligand **2.3** acting as a bridging ligand in coordination complexes have been observed in this research project. In all examples, it is likely that **2.3** has undergone decomposition to initially give a mixture of di-2-pyridylketone and **2.1**, as described above. Di-2-pyridylketone, its hydrated forms and solvolysis products have been well investigated and many reports of the coordination chemistry of these derivatives described. This is because the ketone is activated in the presence of coordinated metal ions[111] and readily forms several solvated derivatives. This decomposition product, **L'**, was also observed in the formation of an $M_6L'_4$ complex, **2.23**.

### 2.3.4 Complexes of tetra(2-pyridyl)ethylene, 2.4

Having investigated the coordination chemistry of ligands **2.2** and **2.3**, which have a carbon-carbon single bond connecting the chelating units of the ligand, the focus was shifted to complexes of the conjugated analogue, **2.4** (Scheme 2.11). Reacting **2.4** with silver nitrate, silver tetrafluoroborate or silver hexafluorophosphate did not provide any complexes suitable for full

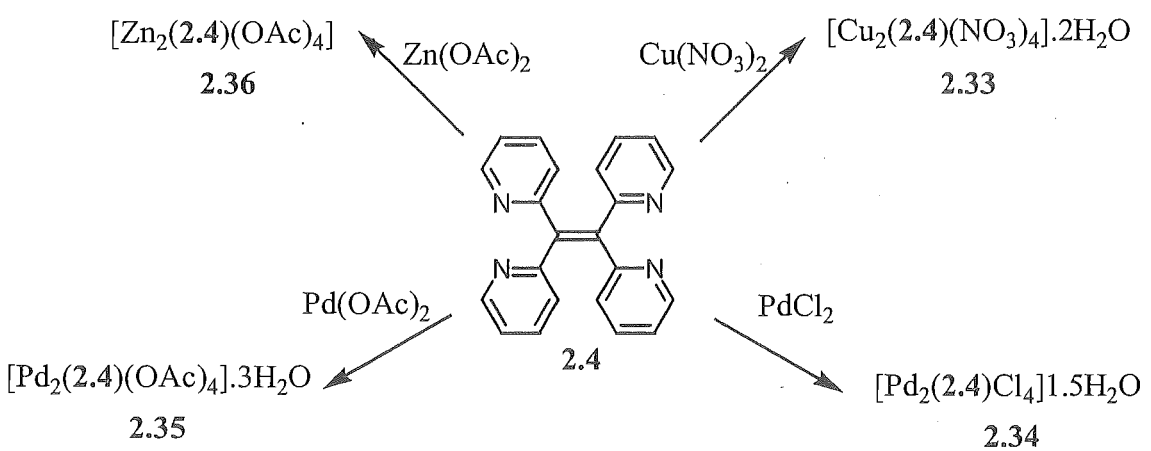


**Scheme 2.11**

characterisation. Reaction of copper nitrate with **2.4** in methanol, under the same conditions as for the preparation of complex **2.26**, gave small blue crystals of a complex **2.33**. These were isolated in 83% yield, analysed as $[Cu_2(\mathbf{2.4})(NO_3)_4].2H_2O$ and the structure determined by X-ray crystallography.

When ligand **2.4** was reacted with palladium chloride in a 1:2 ligand-metal stoichiometry, the complex that was isolated, **2.34**, was soluble in DMSO. A $^1H$ NMR spectrum was obtained, consistent with the expected dinuclear complex. The coordination induced shifts (CIS) for **2.34** are shown in Table 2.2, which show a downfield shift for all the protons of the ligand, as is typical for such complexes.[112] Elemental analysis was also consistent with a dinuclear complex, $[Pd_2(\mathbf{2.4})Cl_4].1\frac{1}{2}H_2O$, but unfortunately, crystals of this dinuclear complex, suitable for X-ray crystallography, could not be obtained.

**Table 2.2.** $^1H$ NMR chemical shifts for **2.4** and **2.34** in DMSO-$d_6$ with the CIS values in italics, showing the downfield shifts that occur on coordination to the metal centre.

| | H6 | H5 | H4 | H3 |
|---|---|---|---|---|
| **2.4** | 8.49 | 7.25 | 7.63 | 7.02 |
| **2.34** | 9.07 | 7.75 | 8.17 | 7.49 |
| *CIS* | *0.58* | *0.50* | *0.54* | *0.47* |

A palladium acetate complex, **2.35**, was also prepared and crystals of this were obtained by evaporation of the acetone-methanol reaction mixture allowing the X-ray crystal structure of the dinuclear palladium acetate complex to be determined. These crystals analysed with the composition $[Pd_2(\mathbf{2.4})(OAc)_4].3H_2O$ by elemental analysis. Reaction of **2.4** with zinc acetate, also in a 1:2 stoichiometry, produced a complex, **2.36**, that analyses as $[Zn_2(\mathbf{2.4})(OAc)_4]$ by elemental analysis. Crystals of **2.36** were also suitable for crystal structure analysis.

Crystal Structure of 2.33

A crystal structure analysis undertaken on complex **2.33** revealed the crystals to have almost identical cell dimensions to those obtained for **2.26**. These two complexes are therefore isomorphous, but not isostructural. The structure only differs in the geometry of the ethene carbon atoms and in the absence of the ethane hydrogen atoms. A perspective view of the structure is shown for comparison in Figure 2.26, with the hydrogen atoms and the non-coordinated methanol solvate molecules omitted for clarity. The copper atom has almost identical bond lengths and angles to the previously described copper complex with ligand **2.2**, and the $\tau$ value for complex **2.33** is 0.02, indicating that the coordination geometry is very

similar to the previous complex **2.26**. Due to the greater rigidity of the ligand core and the similar *trans* arrangement of the metal atoms, the metal-metal distance between the two copper atoms is 7.094(1) Å, which is longer than the corresponding distance for **2.26** (6.698(1) Å).

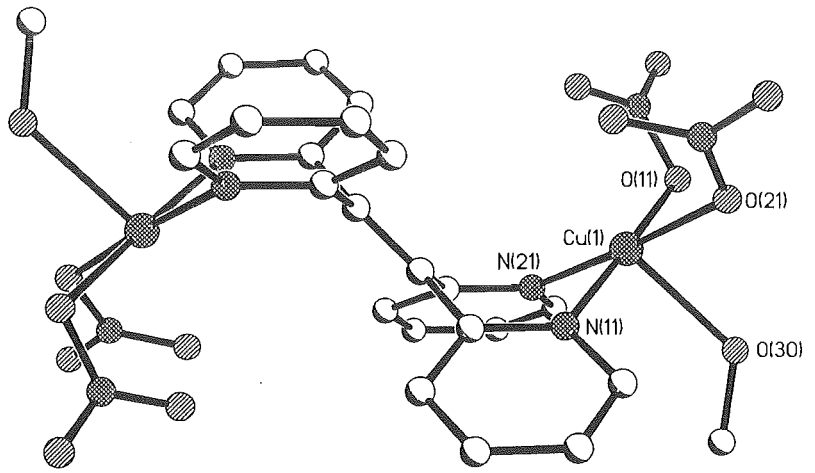


**Figure 2.26.** A perspective view of **2.33** with the hydrogen atoms and the non-coordinated methanol solvate molecules omitted for clarity. Selected bond lengths (Å) and angles (°): Cu(1)-O(21) 1.976(6), Cu(1)-N(21) 1.980(7), Cu(1)-O(11) 2.002(6), Cu(1)-N(11) 2.020(8), Cu(1)-O(30) 2.273(5), O(21)-Cu(1)-N(21) 176.7(2), O(21)-Cu(1)-O(11) 88.7(3), N(21)-Cu(1)-O(11) 89.7(3), O(21)-Cu(1)-N(11) 93.6(3), N(21)-Cu(1)-N(11) 88.0(3), O(11)-Cu(1)-N(11) 177.6(3), O(21)-Cu(1)-O(30) 82.7(2), N(21)-Cu(1)-O(30) 100.1(2), O(11)-Cu(1)-O(30) 85.4(2), N(11)-Cu(1)-O(30) 95.7(2).

A related dinuclear copper perchlorate complex of this ligand has been reported with a hydroxide ligand also bridging the two copper atoms.[73] This was prepared, as noted earlier, by reaction of copper perchlorate, **2.1** and di-2-pyridylketone. The Cu-Cu distance (3.663(3) Å) is considerably shorter than **2.33** because of the $\mu_2$-hydroxide bridge between the copper centres, which enforces a *cis* conformation of the two copper centres.

Crystal Structure of **2.35**

Complex **2.35** is also a dinuclear complex of ligand **2.4**, as suggested by elemental analysis. It crystallises in the monoclinic space group C2/c with four molecules in the unit cell. The asymmetric unit contains one palladium atom, half the ligand, two coordinated acetate anions and three water molecules. A perspective view of the structure is shown in Figure 2.27. As expected the palladium centre is square planar, with bond distances typical for such complexes. The Pd-N and Pd-O bond lengths are between 2.013(3) and 2.026(3) Å. The Pd-Pd distance is 7.002(1) Å, consistent with other complexes bridged only by this ligand.

Like the other complexes of ligand **2.4**, the ethene bridge is planar, but the pyridine rings of the ligand twist significantly out of the plane of the ethene backbone to coordinate and minimise steric hindrance between the H3 protons of the pyridine rings. When viewed down the crystallographic *c*-axis the discrete complexes stack one-on-top-another, and the water solvate molecules and acetate anions participate in an intricate hydrogen-bonding network within the columnar channels formed by molecules of the complex. Specifically, six water solvate molecules form a cyclic hexagonal, hydrogen-bonded ring within this column. This novel 'ring of ice' connects to the complex via hydrogen bonds with the oxygen atoms of the acetate anions.

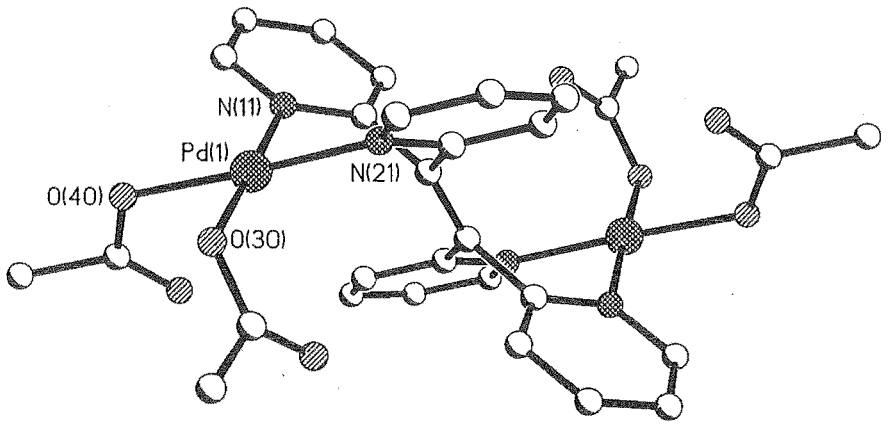


**Figure 2.27.** A perspective view of complex **2.35**, with hydrogen atoms and solvated water omitted for clarity. Selected bond lengths (Å) and angles(°): Pd(1)-O(30) 2.013(3), Pd(1)-N(21) 2.020(3), Pd(1)-N(11) 2.024(3), Pd(1)-O(40) 2.026(3), O(30)-Pd(1)-N(21) 91.13(11), O(30)-Pd(1)-N(11) 178.24(10), N(21)-Pd(1)-N(11) 89.72(11), O(30)-Pd(1)-O(40) 87.52(10), N(21)-Pd(1)-O(40) 176.55(10), N(11)-Pd(1)-O(40) 91.55(10).

Crystal Structure of **2.36**

The structure of complex **2.36** was determined using X-ray crystallography, and confirmed that this complex was dinuclear, with the ligand chelating to two zinc atoms. The asymmetric unit contains one zinc atom, one half of the ligand molecule, two acetate counterions and a coordinated water molecule. A perspective view of the complex, which crystallises in the triclinic space group P-1, is shown in Figure 2.28 with the hydrogen atoms removed for clarity. The geometry about the zinc atoms is distorted trigonal-bipyramidal with one pyridine ring and the coordinated water molecule occupying the axial positions in the primary coordination sphere. The $\tau$ value for the five-coordinate zinc is 0.58, indicating that the geometry is midway between a square-pyramidal and a trigonal-bipyramidal geometry. Molecules of the discrete coordination

complex are linked through two intermolecular hydrogen bonds between the coordinated water molecule and an acetate anion on an adjacent complex. The Zn-Zn distance is 7.354(1) Å, which is slightly longer than in other dinuclear complexes of this ligand, and considerably longer than in complex **2.27** (6.571(1) Å), which is bridged by ligand **2.2**.

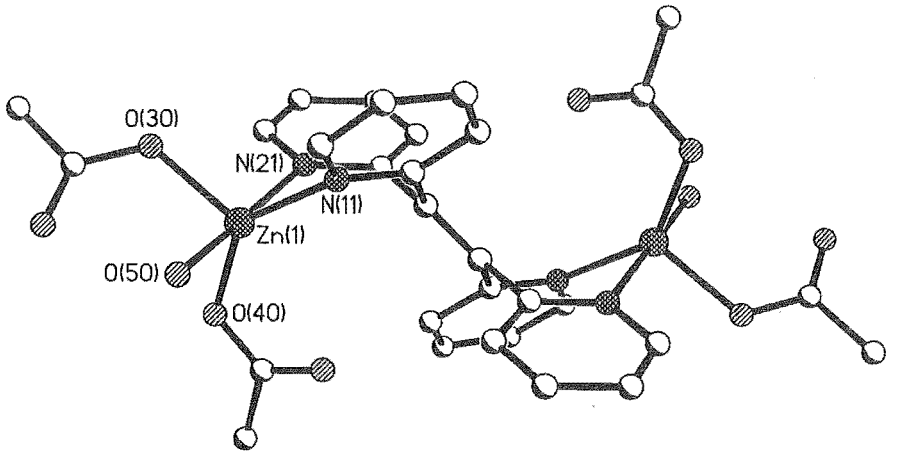


**Figure 2.28.** A perspective view of complex **2.36**, formed from reaction of zinc acetate with **2.4**. Hydrogen atoms are omitted for clarity. Selected bond lengths (Å) and angles (°): Zn(1)-O(40) 1.980(2), Zn(1)-O(30) 1.990(2), Zn(1)-N(11) 2.093(2), Zn(1)-O(50) 2.152(2), Zn(1)-N(21) 2.210(2), O(40)-Zn(1)-O(30) 106.10(7), O(40)-Zn(1)-N(11) 139.17(7), O(30)-Zn(1)-N(11) 114.63(7), O(40)-Zn(1)-O(50) 92.98(7), O(30)-Zn(1)-O(50) 90.63(6), N(11)-Zn(1)-O(50) 89.46(6), O(40)-Zn(1)-N(21) 93.12(7), O(30)-Zn(1)-N(21) 88.85(6), N(11)-Zn(1)-N(21) 85.12(6), O(50)-Zn(1)-N(21) 173.78(6).

A study of the coordination chemistry of **2.2**, **2.3**, and **2.4** has revealed a number of possible coordination modes and structures. A commonly observed structure was a discrete dinuclear complex, but a coordination polymer and a [2+2]-dimetallomacrocycle was characterised for **2.2**. While not described, a coordination polymer was also observed for ligand **2.4**. The coordination chemistry of ligands **2.2** and **2.4** is very similar, with only slight differences in the M-M distances, which originate because of the rigidity of the conjugated bridge between the chelating units in ligand **2.4**. Both **2.2** and **2.4** are considerably more stable than ligand **2.3**, which was not reacted without undergoing some form of decomposition.

### 2.3.5 Complexes of 1,2-bis(2-pyridyl)-1,2-diphenylethane, 2.5

Ligand **2.5** was prepared as a mixture of diastereoisomers as described above. Previously, a palladium acetate complex of this ligand (*rac* isomer) has been prepared and characterised by Canty.[72] This complex was characterised by X-ray crystallography, which revealed the palladium atom was in a square planar coordination environment, formed by chelation of a molecule of ligand **2.5** and two monodentate acetate donors. This required the ligand to form a seven-membered chelate ring. To further investigate coordination complexes of ligand **2.5**, it was reacted with silver and copper nitrate. Reaction of two equivalents of silver nitrate with one equivalent of **2.5** gave a 1:1 complex, **2.37**, which was characterised by X-ray crystallography. Ligand **2.5** was also reacted with copper nitrate, and slow evaporation of the solvent from the reaction mixture, gave blue crystals of a complex, **2.38**. The crystals were suitable for X-ray crystallography, which revealed **2.38** to be a discrete $M_2L_2$ dimer.

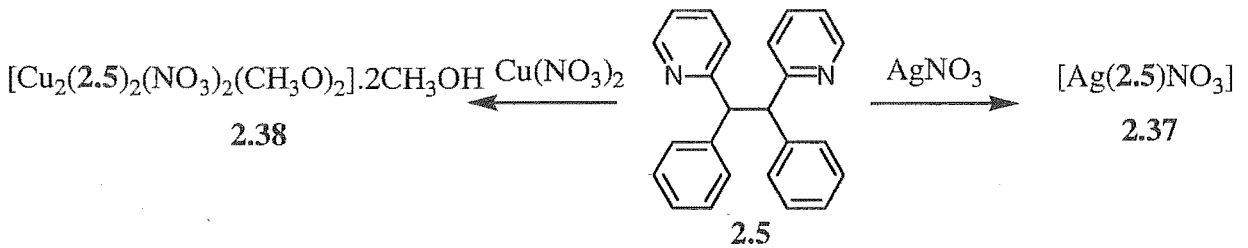


**Scheme 2.12**

Ligand **2.5** also has the potential to be doubly cyclometallated. Attempts to effect such a transformation were carried out by refluxing **2.5** with an excess of palladium acetate in either benzene or acetic acid. Attempts were made to convert the expected acetate complexes into the corresponding chloride complex by stirring with lithium chloride in 3:2 acetone-water. Despite repeated attempts, with several variations of method, no readily characterisable materials were isolated.

Crystal Structure of **2.37**

The overall structure of complex **2.37** is a one-dimensional coordination polymer in which the silver atom acts as a linear connector of the relatively flexible doubly monodentate bridging ligand. A perspective view of complex **2.37** is shown below in Figure 2.29, with selected atom labelling. The coordination geometry of the silver is almost linear with the pyridine nitrogen atoms bonded at distances of 2.198(3) and 2.201(3) Å. There are weak contacts with the oxygen atom of a methanol solvate molecule at a distance of 2.801(4) Å and with an oxygen atom of a non-coordinated nitrate anion 3.124(5) Å. There also appear to be weak interactions between the phenyl rings of the ligand and the silver atom, shielding what is a relatively naked silver atom.

The shortest Ag-C distances to the two phenyl rings that surround each silver atom are 3.061(5) and 3.081(5) Å. These types of interactions are observed for related complexes of silver, and for complexes described later in this thesis. The average distance for an $\eta_1$- or $\eta_2$-interaction such as this is *ca.* 2.82 Å,[20] although considerably longer distances are known for similar alkali metal $\pi$-interactions.[113]

Aside from the very weak contacts involving the non-coordinated nitrate anion, a packing diagram does not reveal any unusually short interactions between the one-dimensional coordination polymers. A feature of this complex is that the ligand has been shown to bridge two metal atoms in preference to forming a seven-membered chelate ring. This is somewhat reflective of the nature of silver, which prefers to adopt linear or trigonal-planar two- and three-coordinate geometries.[19]

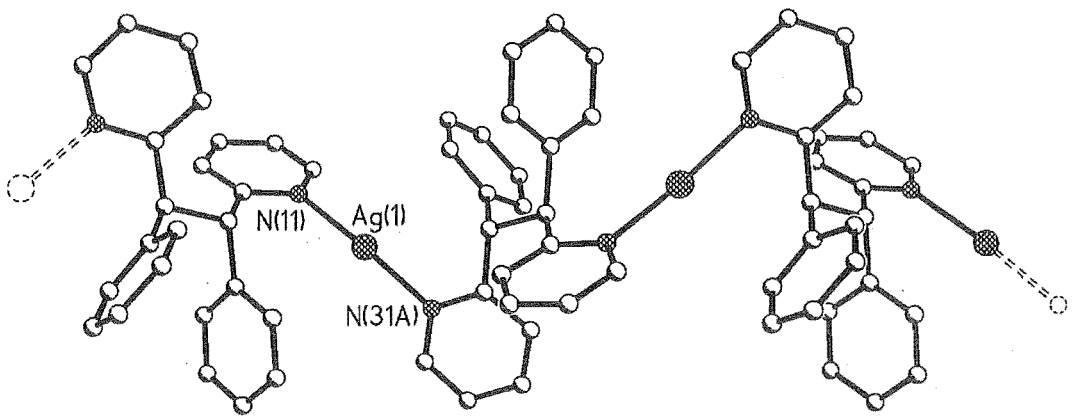


**Figure 2.29.** A perspective view of the extended structure of complex **2.37**, with hydrogen atoms and nitrate anions omitted for clarity. Selected bond lengths (Å) and angles (°): Ag(1)-N(11) 2.198(3), Ag(1)-N(31) 2.201(3), N(11)-Ag(1)-N(31) 170.5(1).

Crystal Structure of **2.38**

The dimeric $Cu_2L_2$ complex, **2.38**, crystallises in the triclinic space group P-1. The asymmetric unit contains two molecules of **2.5**, two copper atoms, a bridging nitrate anion, two bridging methoxide anions, a second nitrate anion (disordered over two positions) and two methanol solvate molecules (one partially occupied). A perspective view of complex **2.38** is shown in Figure 2.30 with hydrogen atoms, and non-coordinated molecules omitted for clarity. One ligand molecule chelates to each copper atom with a previously observed, but relatively uncommon, seven-membered chelate ring. The two CuL units are connected through a bridging nitrate anion and two bridging methoxide anions.

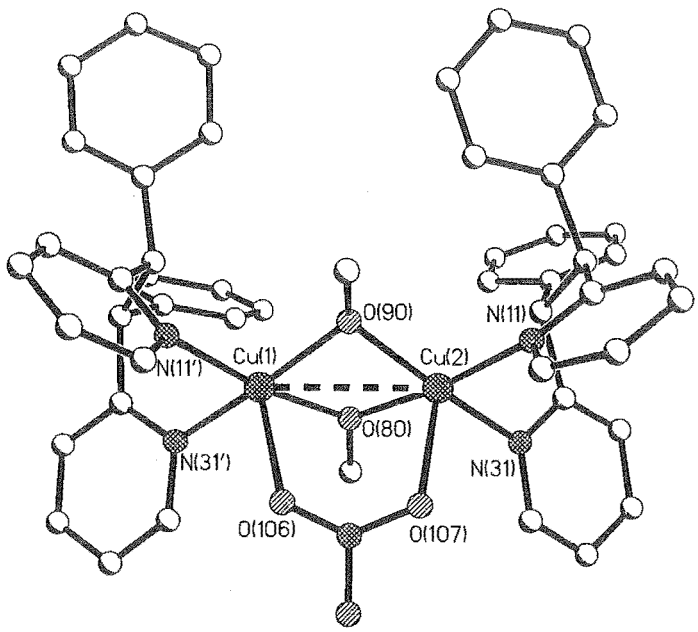


**Figure 2.30.** A perspective view of complex **2.38** with hydrogen atoms, non-coordinated solvate molecules and anions excluded for clarity. Selected bond lengths (Å) and angles (°): Cu(1)-O(90) 1.937(3), Cu(1)-O(80) 1.946(3), Cu(1)-N(11') 2.003(4), Cu(1)-N(31') 2.008(4), Cu(1)-O(106) 2.438(5), Cu(1)-Cu(2) 2.952(1), Cu(2)-O(80) 1.931(3), Cu(2)-O(90) 1.948(3), Cu(2)-N(31) 2.016(4), Cu(2)-N(11) 2.021(4), Cu(2)-O(107) 2.375(4), O(90)-Cu(1)-O(80) 76.89(13), O(90)-Cu(1)-N(11') 97.19(16), O(80)-Cu(1)-N(11') 171.90(18), O(90)-Cu(1)-N(31') 69.70(16), O(80)-Cu(1)-N(31') 97.98(16), N(11')-Cu(1)-N(31') 86.98(17), O(90)-Cu(1)-O(106) 93.06(16), O(80)-Cu(1)-O(106) 91.69(16), N(11')-Cu(1)-O(106) 94.16(19), N(31')-Cu(1)-O(106) 96.03(18).

The two copper atoms have square-pyramidal geometries, if the copper-copper interaction is disregarded. The Cu-N bond lengths are typical ranging from 2.003(4) to 2.021(4) Å. This copper dimer has a similar structure to one of the copper dimers in complex **2.23**, and consequently very similar bond lengths for the Cu-O bonds and the Cu-Cu interaction. The bridging nitrate forms the longer apical bonds to Cu(1) and Cu(2) with distances of 2.438(5) and 2.375(4) Å, respectively.

In addition to the disorder mentioned above, the ethane backbone of both the ligands in the $M_2L_2$ dimer are disordered over two different positions, corresponding to the two different diastereoisomers of the ligand. However this rod-shaped crystal, which was studied by X-ray crystallography, was enriched in the racemic diastereoisomer. The disorder, while not shown in Figure 2.30 (only the major component is represented), was modelled and indicated that the

crystal contains approximately a 9:1 ratio of the racemic and meso diastereoisomers. Attempts to locate a crystal enriched in the other isomer were unsuccessful. There are two different crystal shapes in the sample, but the plate-shaped crystals, which may contain the meso isomer as the dominant fraction, were not large enough for X-ray crystallography. Separation of diastereoisomers in this manner has been observed in other systems, such as a nickel chloride mediated separation of the meso and racemic diastereoisomers of a phosphine ligand.[114]

### 2.3.6 Complexes of di-2-pyridylketone azine, 2.8

While ligand **2.8** has the same di-2-pyridylmethyl coordination motif as the previously investigated ligands, it also possesses an azine backbone that provides two additional imine nitrogen donor atoms. Such imine nitrogen atoms have been shown to coordinate to various metals in complexes of related ligands. For example, in complexes of 2-acetylpyridine azine and 2-formylpyridine azine, both the pyridine nitrogen atoms and azine nitrogen atoms are involved in the formation of coordination complexes with several transition metals.[115, 116]

Ligand **2.8** has been studied before in regard to its potential for selective spectrometric determination of metal ions and these results are described in the literature.[74] However, no complexes of this ligand have been reported for silver salts. Thus, **2.8** was reacted with silver nitrate in a 2:1 ratio to give a yellow crystalline complex, **2.39**, with the composition determined by elemental analysis as $[Ag_2(\mathbf{2.8})(NO_3)_2]$ (Scheme 2.13). The complex was obtained in 51% yield and crystals, suitable for X-ray crystallography, were obtained on slow evaporation of the methanol reaction mixture.

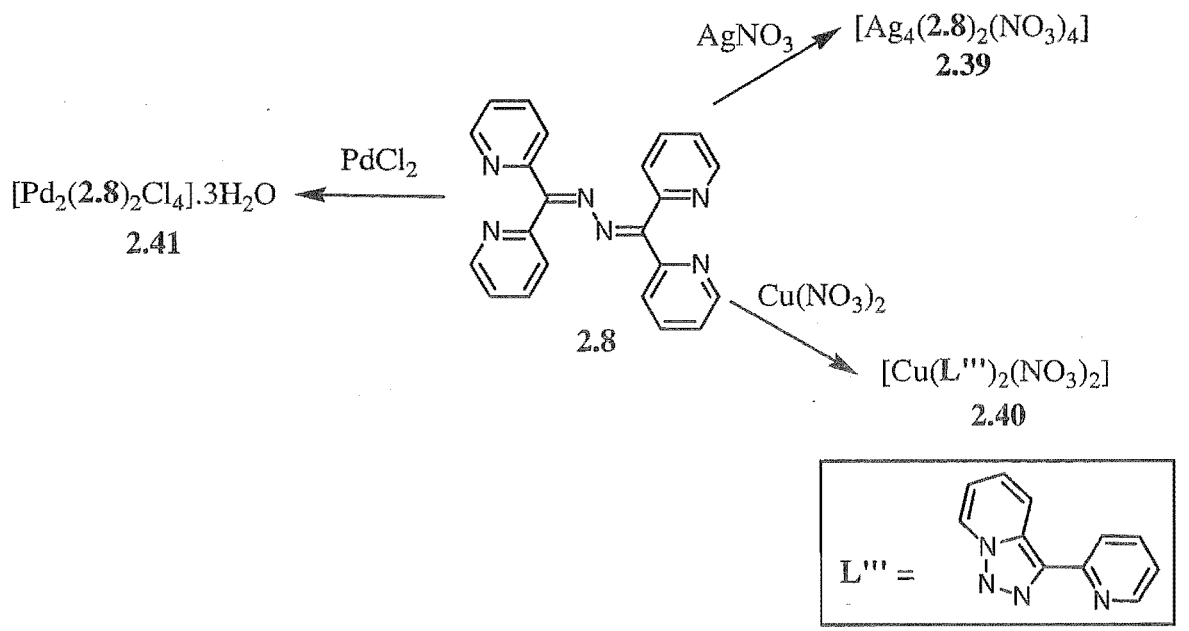


**Scheme 2.13**

Reaction of **2.8** with copper nitrate and palladium chloride provided two complexes, **2.40** and **2.41**, respectively. In complex **2.40**, the ligand underwent decomposition of the imine bond, similar to what has been previously observed with this ligand, and the related compound, 2-benzylpyridineketone azine.[91, 117, 118] Complex **2.40** was isolated as green crystals in 51% yield by slow evaporation of a methanol solution. The crystals were characterised by X-ray crystallography and a structure description is given below. Further evaporation gave blue crystals in 25% yield that were shown to have an identical structure by X-ray crystallography to a previously characterised $[Cu_2L']^{2+}$ complex, **2.32**. The dinuclear palladium chloride complex, **2.41**, of **2.8** immediately precipitated, as a red solid, from the reaction mixture in 49% yield. This analysed with the composition $[Pd_2(\mathbf{2.8})Cl_4].3H_2O$, consistent with a dinuclear complex of ligand **2.8**. Further evaporation gave crystals of another complex that, while twinned, were shown to be a palladium complex of a decomposition product and not the original ligand **2.8**.

Crystal Structure of **2.39**

The structure of complex **2.39** is a discrete $Ag_4L_2$ tetragonal prismate, formed by the self-assembly of four silver atoms and two molecules of **2.8**. The complex crystallises in the monoclinic space group $P2_1/c$, with an asymmetric unit that contains two units of the discrete complex (one of which is shown in Figure 2.31), four non-coordinated nitrate anions and eleven water molecules. The other unit of the discrete complex has the same structure, but has significant disorder of the chelating nitrate anion coordinated to Ag(4) (equivalent of Ag(8) in the pictured complex).

In each discrete $[Ag_4(\mathbf{2.8})_2(NO_3)_2]$ complex the four silver atoms lie in a plane between the two bridging ligands. Each hexadentate ligand utilises all six potential donors in bonding to the four silver atoms, although one of the imine nitrogen donors, N(52'), makes a very weak contact (2.824(5) Å) with Ag(7). When viewed from above (as in Figure 2.31), all the pyridine donors in the top ligand are twisted in an anticlockwise direction, while the pyridine nitrogen donors in the bottom ligand are twisted in a clockwise direction. Therefore each discrete complex is helical and chiral, although the overall crystal is of course racemic. Each discrete complex has this helical tetragonal prismatic structure, where the ligand forms a cap of four silver atoms, which all lie in a central plane. This coordination motif is part of a more general class of $M_xL_2$ prismatic cages[96] that will be discussed in more detail later in this chapter.

There are two different silver coordination environments in this structure; one where the silver is coordinated by pyridine donors and nitrate oxygen atoms (Ag(5) and Ag(8)) and a second where the imine nitrogen atoms coordinate to the silver atoms in place of the nitrate donors (Ag(6) and Ag(7)). Both Ag(5) and Ag(8) occupy four-coordinate environments in which

they are coordinated by two pyridine nitrogen atoms and a nitrate anion. The Ag-N bond lengths are in the range 2.216(5) to 2.238(5) Å, while the closest Ag-O distances are 2.468(4) and 2.456(5) for Ag(5) and Ag(8), respectively. Ag(6) and Ag(7) both have five-coordinate environments, with coordination by two pyridine nitrogen atoms and three other donors. Ag(6) is coordinated by the two imine nitrogen atoms of the azine, with distances of 2.486(4) and 2.581(4) Å, and also makes a weak contact with a non-coordinated nitrate atom with a Ag-O distance of 2.897(5) Å. Ag(7) makes one bond to an imine nitrogen atom (2.487(4) Å) and a

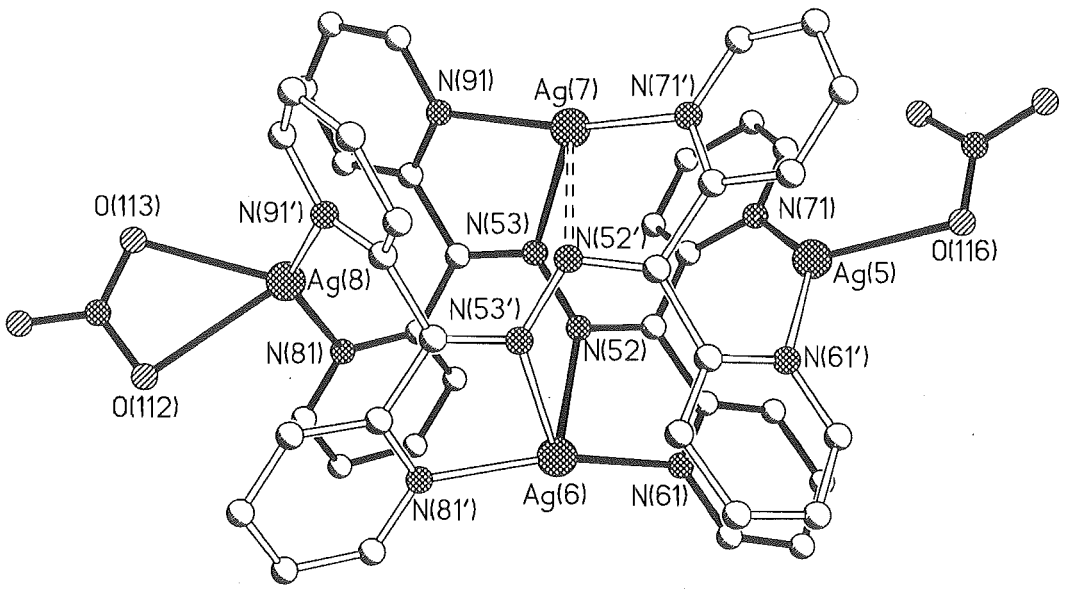


**Figure 2.31.** A perspective view of one discrete complex of structure **2.39** with hydrogen atoms and non-coordinated anions and solvate water molecules omitted for clarity. Selected bond lengths (Å) and angles (°): Ag(5)-N(71) 2.227(5), Ag(5)-N(61') 2.266(4), Ag(5)-O(116) 2.468(4), Ag(6)-N(61) 2.220(5), Ag(6)-N(81') 2.223(4), Ag(6)-N(53') 2.486(4), Ag(6)-N(52) 2.581(4), Ag(7)-N(71') 2.246(5), Ag(7)-N(91) 2.287(4), Ag(7)-N(53) 2.487(4), Ag(8)-N(91') 2.216(5), Ag(8)-N(81) 2.238(5), Ag(8)-O(113) 2.456(5), Ag(8)-O(112) 2.596(4), N(71)-Ag(5)-N(61') 140.17(16), N(71)-Ag(5)-O(116) 128.56(16), N(61')-Ag(5)-O(116) 90.89(15), N(61)-Ag(6)-N(81') 164.68(16), N(61)-Ag(6)-N(53') 124.81(15), N(81')-Ag(6)-N(53') 70.51(15), N(61)-Ag(6)-N(52) 69.18(15), N(81')-Ag(6)-N(52) 116.32(15), N(53')-Ag(6)-N(52) 83.39(14), N(71')-Ag(7)-N(91) 162.07(17), N(71')-Ag(7)-N(53) 126.23(16), N(91)-Ag(7)-N(53) 69.42(15), N(91')-Ag(8)-N(81) 140.99(18), N(91')-Ag(8)-O(113) 106.18(17), N(81)-Ag(8)-O(113) 112.34(17), N(91')-Ag(8)-O(112) 117.30(16), N(81)-Ag(8)-O(112) 92.73(16), O(113)-Ag(8)-O(112) 50.21(15).

weak bond to a non-coordinated nitrate anion (2.671(5) Å) in addition to a weak interaction with the other imine nitrogen as described above. There are many different silver-silver distances within the complex, but none that would be considered even to be a weak bonding interaction.[119] The shortest silver-silver distance (Ag(5)-Ag(7)) is 4.200(1) Å, while Ag(5) and Ag(8) are separated by 8.048(1) Å.

Helical $Ag_2L_2$ complexes with a related ligand have recently been described.[115] When 2-acetylpyridine azine was reacted with AgX salts (X = perchlorate, tetrafluoroborate and nitrate), $[Ag_2(L)_2(X)_2]$ complexes were detected by ESI-MS, and characterised by X-ray crystallography. These complexes are helicates, with the ligand forming the helical part of the complex. This is in contrast to the helical prismate cages, described in this thesis, where the silver atoms form the so-called 'strands'.

Crystal Structure of **2.40**

The crystal structure of complex **2.40** reveals that ligand **2.8** has undergone a copper-catalysed decomposition to form 3-(2-pyridyl)-triazolo[1,5-*a*]pyridine. This ligand has previously been directly prepared and a copper nitrate complex, with almost an identical structure, characterised by X-ray crystallography.[117] Complex **2.40** also has a very similar structure to two copper complexes characterised by Richardson with either benzisoxazole- or benzotriazole-based ligands.[120] The only significant structural difference between **2.40** and the previously characterised examples is that the apical ligands are nitrate anions instead of the water

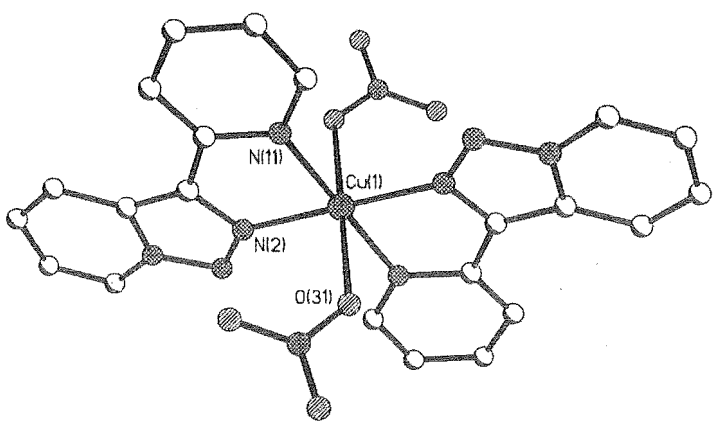


**Figure 2.32.** A perspective view of complex **2.40**. Selected bond lengths (Å) and angles (°): Cu(1)-N(2) 2.0135(17), Cu(1)-N(11) 2.0517(18), Cu(1)-O(31) 2.4324(18), N(2)-Cu(1)-N(11) 80.03(7), N(2)-Cu(1)-O(31) 97.91(7), N(11)-Cu(1)-O(31) 95.53(7).

molecules in the literature examples. The complex crystallises in the triclinic space group, P-1, with the copper atom on a centre of inversion. A perspective view of the complex without hydrogen atoms is shown in Figure 2.32. The bond lengths and angles are similar to the previously reported[117, 120] structures and are typical for a Jahn-Teller distorted copper complex.

## 2.4. Complexes of the 4,5-diazafluorene-based ligands

Recently, transition metal complexes of **2.11** have been prepared with copper(I/II), nickel(II) and zinc(II),[121] and complexes of **2.12** with ruthenium(II),[77] cobalt(II), nickel(II) and zinc(II) reported.[78] However, in contrast to the di-2-pyridylmethane-based ligands investigated in this research project, it appears that the reduced flexibility of these ligands has thus far prevented the crystallisation of such complexes for study by X-ray crystallography. It is also worth noting some interesting differences, in addition to the changes in flexibility, between the two sets of ligands. The closely related ligands **2.2** and **2.4** have the potential to form six- or seven-membered chelate rings, although the former is more likely, whereas the diazafluorene-based ligands can only form a five-membered ring on chelation to a metal centre. The bite angle in ligands **2.2**, **2.4** and archetypal chelating ligand bpy, are considerably different to the diazafluorene-based ligands and this widening of the bite angle in **2.11** and **2.12** may significantly influence the coordination chemistry.

Nonetheless, **2.11** and **2.12** were reacted with a range of metal salts in an effort to provide materials suitable for structural characterisation. No complexes had been reported with silver salts for either ligand and therefore this was the major focus. Unfortunately, no useful results were obtained for either ligand. On reaction of either ligand with zinc nitrate, crystalline materials were formed following slow evaporation of the methanol reaction solvent. Both sets of crystals were suitable for crystal structure analysis. However, both structures were solved to reveal only 4,5-diazafluorenone and neither of the two ligands initially used. This was shown by NMR spectroscopy to be the case for the bulk samples of these reactions.

Ligand **2.13** is a novel compound, and while the results with the two related ligands described above were not encouraging, **2.13** was reacted with both silver nitrate and copper nitrate. Disappointingly, no materials suitable for further analysis were obtained. Once the difficulties with the synthesis of this ligand have been overcome, it would be desirable to prepare dinuclear ruthenium complexes of this novel spiro-ligand to probe the nature of the metal-metal interactions. This would also provide an interesting comparison to the corresponding bis(2,2'-

bipyridyl)ruthenium complexes of **2.11** and **2.12** that have previously been prepared with carbon-carbon single and double bonds separating the chelating subunits.

## 2.5. Coordination and metallosupramolecular chemistry of the [3]radialene-based ligands

### 2.5.1 Complexes of hexa(2-pyridyl)[3]radialene, 2.14

A variety of modes of coordination are available for **2.14** which, despite the rigid [3]radialene core, has significant flexibility in the arrangement of the six pyridine donors (Figure 2.34). The ligand might act as a relatively uncommon tritopic bridging ligand, with three bidentate chelating binding domains. Chelation is possible in two different modes: either the more likely six-, or possibly nine-membered chelate rings can be formed, depending upon whether the metal binds to pyridine donors attached to the same or adjacent arms of the radialene core. Alternatively, the ligand might act as a hexatopic ligand and bind to six different metals, or in a hypodentate manner with incomplete coordination by the six nitrogen donors.

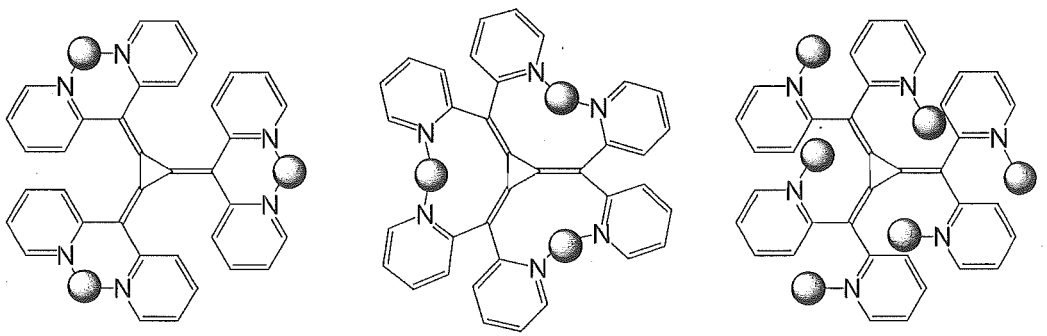

**Figure 2.34.** Some of the potential coordination modes of **2.14**.

Reaction of **2.14** with silver nitrate gave in excellent yield a bright red crystalline complex, **2.42**, which was shown by elemental analysis to have a 2:1 metal to ligand stoichiometry suggesting that not all the donors of **2.14** were being used. Various structural possibilities are available for such a composition, and consequently an X-ray structure determination was carried out on this complex. When **2.14** was reacted with silver hexafluorophosphate, a complex, **2.43**, with the same 2:1 metal to ligand stoichiometry was isolated and characterised by X-ray crystallography to reveal a second mode of coordination. Yet another mode of coordination was observed when **2.14** was reacted with silver tetrafluoroborate, which resulted in the formation of a crystalline product, **2.44**, that was shown to have the constitution $[Ag_6(\mathbf{2.14})_2F(BF_4)_5].11H_2O$ by single crystal X-ray structure analysis. ES-MS was consistent with this composition although only fragmentation of the parent ion was observed.

Ligand **2.14** was also reacted with a diverse range of other late transition metal precursors. This included several metal salts with coordinating and non-coordinating anions. However, despite repeated attempts and different conditions, no further complexes could be formed without causing decomposition. Simply reacting **2.14**, usually in a 3:1 metal-ligand ratio, with copper nitrate, for example, gave a brown oil that could not be crystallised. Similarly for palladium chloride, cadmium nitrate and zinc acetate only decomposition was observed. Fortunately, when **2.14** was reacted with $[Ru(bpy)_2Cl_2]$ a green coloured dinuclear ruthenium complex was obtained that will be described later (Section 2.6).

Crystal Structure of **2.42**

X-Ray crystallography revealed that the reaction of silver nitrate with **2.14** had resulted in the self-assembly of a helical one-dimensional coordination polymer. Complex **2.42** crystallises in the orthorhombic space group Pccn, the asymmetric unit of which is shown, along with selected atom labelling, in Figure 2.35. The asymmetric unit contains one half of the radialene ligand, a silver atom, one coordinated nitrate anion and two solvate water molecules. The silver atom occupies a distorted trigonal environment, with silver-nitrogen distances of 2.201(13) Å and 2.210(12) Å, and a weaker contact (2.591(11) Å) with an oxygen atom of the nitrate anion.

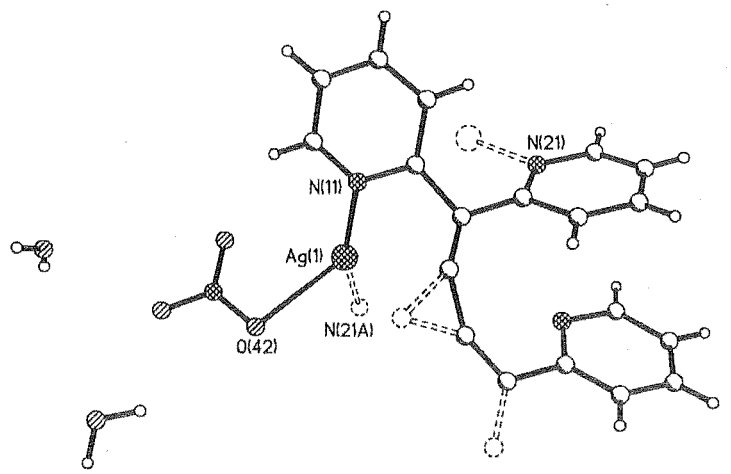


**Figure 2.35.** A perspective view of the asymmetric unit of complex **2.42**. Selected bond lengths (Å) and angles (°): Ag(1)-N(21A) 2.198(13), Ag(1)-N(11) 2.205(12), Ag(1)-O(42) 2.591(11), N(21A)-Ag(1)-N(11) 156.4(5), N(21A)-Ag(1)-O(42) 87.4(4), N(11)-Ag(1)-O(42) 116.1(4).

A perspective view of the repeating polymeric structure of **2.42** is shown in Figure 2.36. In the coordination polymer each radialene ligand **2.14** coordinates to four symmetry-related silver atoms with a helical twist propagating along the coordination polymer. The nitrate anion has the

effect of maintaining the silver atoms on the outside of the polymeric structure, with solvent water molecules filling the voids between the coordination polymers. In this complex the radialene ligand **2.14** acts as a tetradentate bridge with two of the pyridine rings not involved in coordination. There are several different silver-silver distances in **2.42**; the Ag-Ag distance between the two silver atoms in the twelve-membered dimetallocycle is 4.120(1) Å, while the Ag-Ag distance between the silver atoms bridged by different arms of the ligand ranges between 5.643(1) and 9.611(1) Å. None of these are short enough to indicate any silver-silver interactions.[119]

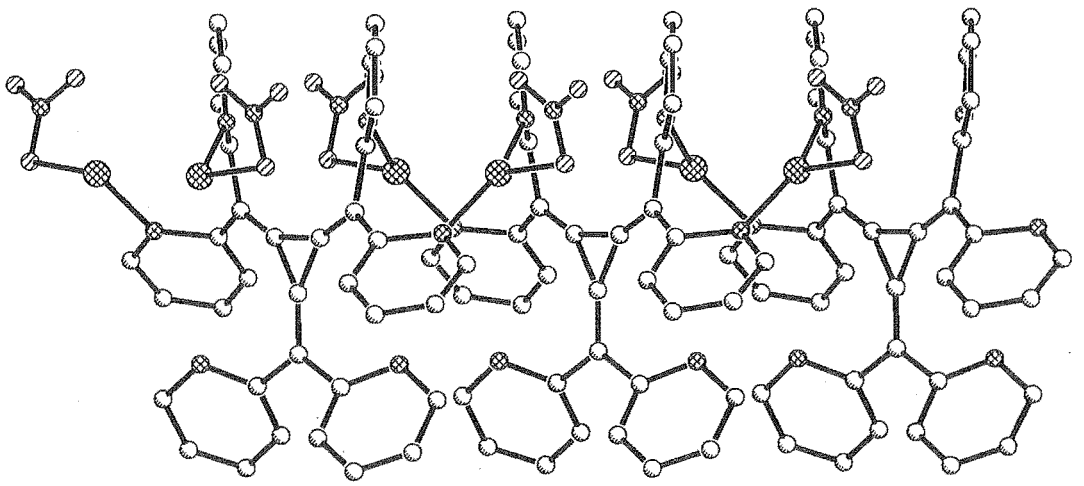

**Figure 2.36.** A perspective view of the extended coordination polymer, **2.42**.

Crystal Structure of **2.43**

The structure of complex **2.43** is a one-dimensional coordination polymer comprised of $M_3L_2$ prismate cages. The asymmetric unit of complex **2.43**, which crystallises in the triclinic space group P-1, contains one molecule of **2.14**, three silver atoms (two of which lie on centres of inversion), two hexafluorophosphate anions and an acetonitrile solvate molecule. A perspective view of the asymmetric unit is shown in Figure 2.37, with the non-coordinated anions and the acetonitrile solvate molecule omitted for clarity.

The silver-nitrogen bonds in complex **2.43** range from 2.120(3) Å for the linear silver atom (Ag(2)-N(21)), to between 2.180(3) Å and 2.321(3) Å for the trigonal-planar silver atoms (Ag1) on the outer of the cage structure. The linear silver atom, Ag(3), that links the $Ag_3L_2$ cages has a Ag-N bond length of 2.140(3) Å. The silver-silver distances are large (>3.695(1) Å), indicating little or no interaction between the silver atoms within the cage. The outer silver atoms of the $M_3L_2$ prismate portion of the structure have distorted trigonal-planar geometry, coordinated by

two pyridine nitrogen atoms of one arm of one ligand and one pyridyl group of the other ligand. The central silver atom has linear geometry and is coordinated by only one pyridyl group of each ligand. A free pyridine ring on the third arm of **2.14** links these $M_3L_2$ cages together via a fourth silver atom to form the polymer. The sixth pyridine ring of each ligand is not coordinated. Thus, the ligand has adopted a hybrid of the coordination modes described above.

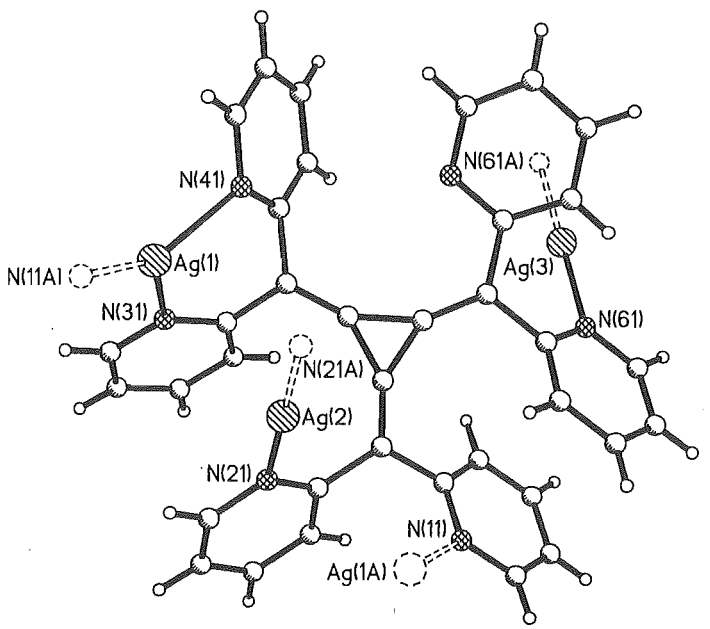


**Figure 2.37.** A perspective view of the asymmetric unit of complex **2.43**, with the non-coordinated hexafluorophosphate anions (one of which is disordered) and the acetonitrile solvate omitted for clarity. Selected bond lengths (Å) and angles (°): Ag(1)-N(11A) 2.180(3), Ag(1)-N(41) 2.262(3), Ag(1)-N(31) 2.321(3), Ag(2)-N(21) 2.120(3), Ag(3)-N(61) 2.140(3), N(11A)-Ag(1)-N(41) 139.90(11), N(11A)-Ag(1)-N(31) 133.88(11), N(41)-Ag(1)-N(31) 86.21(11), N(21A)-Ag(2)-N(21) 180.0, N(61A)-Ag(3)-N(61) 180.0.

A perspective view of the repeating structure is shown in Figure 2.38, which, despite having the same metal-ligand stoichiometry as the silver nitrate complex, has an entirely different spatial arrangement of the atoms. By contrast with **2.42**, where the ligand is tetradentate, in this complex the ligand functions as a pentadentate bridge to four coordinated silver atoms. The coordination polymer consists of $M_3L_2$ prismate cages, which are bridged by linear silver atoms. The polymeric cage structure although not discrete is an interesting example of the trigonal prismatic structures reported by Fujita[122] and others,[123, 124] and represents a rare example of an $M_nL_2$ polyhedron incorporated into a coordination polymer. One other such polymeric structure has recently been reported.[125]

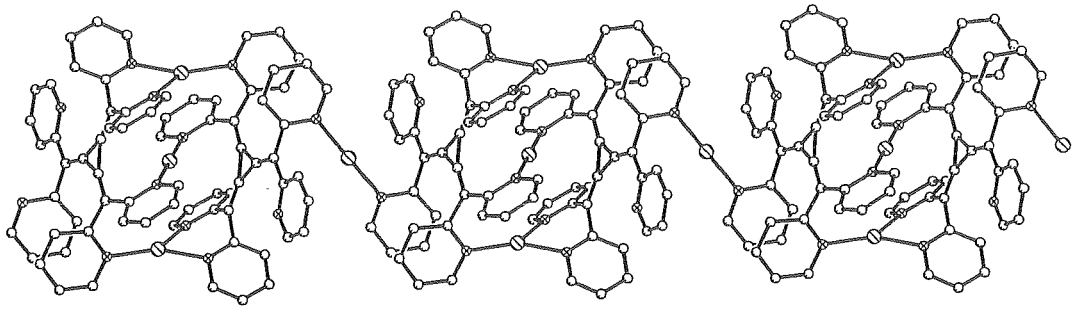

**Figure 2.38.** A perspective view of the polymeric structure of complex **2.43**.

Crystal Structure of **2.44**

Crystal structure analysis revealed that the reaction of **2.14** with silver tetrafluoroborate had produced a discrete $M_6L_2F$ prismate cage complex. Figures 2.39 and 2.40 shows two perspective views of this structure that results from the self-assembly of two molecules of **2.14**, acting in a hexapodal hexadentate mode, and six silver atoms to encapsulate a fluoride anion. External to the cage are five tetrafluoroborate counterions and eleven water molecules, which are not shown in the figures. These tetrafluoroborate anions, which mingle with the water solvate molecules that surround the cage, participate in an intricate hydrogen-bonding network filling the nanoporous voids between the cage molecules.

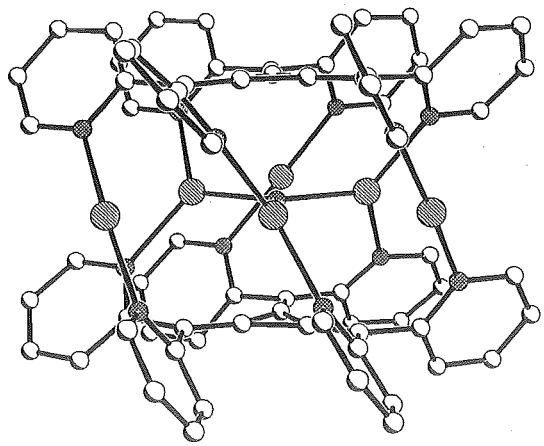

**Figure 2.39.** A perspective view looking through the $Ag_6L_2F$ prismate cage structure at the hexasilver platter sandwiched between two molecules of **2.14**.

Within the structure of **2.44**, the silver platter has a $\mu_3$-fluorido anion at its centre. The fluorine atom is strongly bonded, in a trigonal arrangement, to three internal silver atoms with Ag-F distances of 2.275(3)-2.297(3) Å. The other three silvers are symmetrically disposed at

distances in the range 3.296(1)-3.641(1) Å, which indicate weak Ag-Ag interactions.[119] The Ag-N bond lengths in the complex are unremarkable, with values ranging from 2.166(5) to 2.268(4) Å. The six silver atoms are coplanar (mean deviation from the plane = 0.012 Å). Although hexanuclear silver clusters are not uncommon,[126] they usually involve a three-dimensional arrangement of the atoms. The only planar $Ag_6$ array that was found for comparison is in a silver(I) imidazole perchlorate complex,[127] which has a very different spatial arrangement of the six atoms.

The likely origin of the fluoride anion in **2.44** is from the tetrafluoroborate counterion used in the synthesis. It has previously been observed, with other metal complexes of nitrogen heterocycles, that both tetrafluoroborate and hexafluorophosphate can lose a fluoride ion,[128] although it is more common with tetrafluoroborate anions. In fact, tetrafluoroborate in the presence of either nitrogen heterocycles or amines, is used synthetically as a source of fluoride ions in the synthesis of transition metal fluoride complexes. This is the first example of a $\mu_3$-fluorido silver complex, although, a $\mu_3$-fluorido tricopper(I) complex was recently reported.[129] An interesting possibility exists that the fluoride anion may act as a template[130] for the formation of the hexanuclear cage. This is consistent with the observations made for complexes **2.42** and **2.43**, where no free fluoride ions are available to template such a cage.

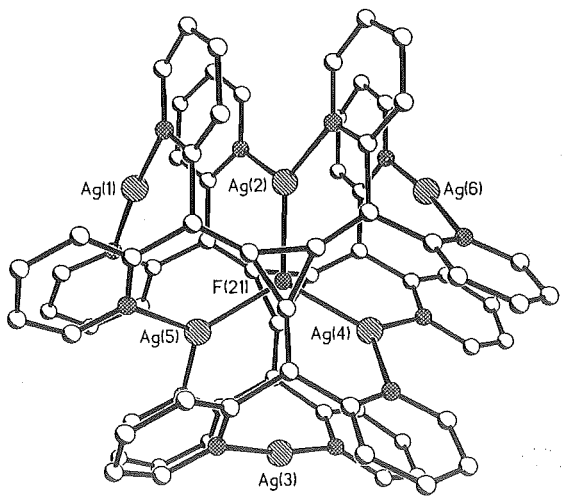


**Figure 2.40.** A perspective view of the $M_6L_2F$ cage complex, **2.44**, looking down on the hexasilver platter. Bond lengths (Å) surrounding the fluoride ion: Ag(2)-F(21) 2.271(3), Ag(4)-F(21) 2.275(3), Ag(5)-F(21) 2.273(3).

The position and orientation of the fluorine atom in the structure also raises the intriguing possibility that, in this compound, there might be a favourable interaction between the filled p-orbital of the relatively electron rich $sp^2$-hybridized fluorine atom and an empty $\pi^*$-orbital of

the [3]radialene ring system, i.e. a new type[131] of "halogen bond".[96] The [3]radialene core is very electron deficient as indicated by the relatively facile two electron reduction observed for this and related [3]radialenes.[81, 82, 95]

The structure has a number of other novel features. It is a new example of a group of compounds, shown in Figure 2.41, called prismates. While there are a few reported examples of $M_3L_2$ and $M_4L_2$ prismates that have been prepared in recent years,[122, 123] complex **2.44** is the first and only example of an $M_6L_2$ prismate cage. Another novel feature is that within each of the ligands in the complex, the six pyridine rings display a co-operative, propeller-like twisting about the central radialene core. This imparts a helical character to the complex and therefore makes it chiral. In comparison, in addition to also being helical and therefore chiral, complex **2.39**, which was described in Section 2.3.6, is also a complicated example of a $M_4L_2$ prismate cage, that is schematically represented in Figure 2.41.

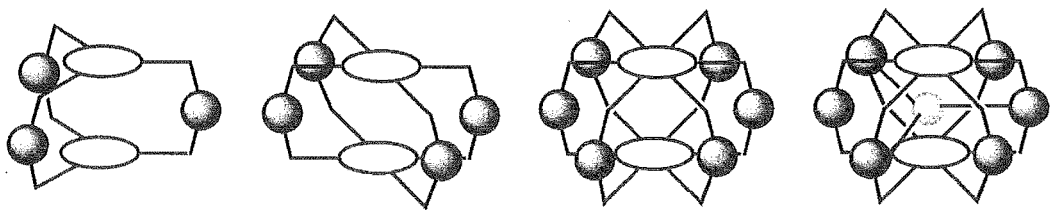

**Figure 2.41.** Schematic representations of some $M_nL_2$ prismates and complex **2.44**.

NMR studies were used to investigate this structure in solution. The $^1$H NMR spectrum indicates that in solution the species present is a symmetrical complex. No evidence was obtained by $^{19}$F NMR spectroscopy for the presence of the fluoride ion, or whether it was located within or external to the cage structure, which appears to hold up in solution. A proposal of what may be occurring in solution is shown in Scheme 2.14. In solution either the fluoride anion is symmetrically encapsulated, or lost completely from the cage. The former proposal is consistent with the ES-MS of the complex that, while not showing the proposed molecular ion, did reveal the presence of an ion corresponding to $[Ag_3(\mathbf{2.14})_2F]^{2+}$.

Another feature that distinguishes this structure from the previously described silver complexes is the arrangement of the pyridine rings about the central radialene core. In complex **2.44** the pyridine rings are all twisted co-operatively out of the plane of the [3]radialene core, but in **2.42** and **2.43** the coordination demands require that, while some pyridine rings are twisted out of the plane of the [3]radialene core, others lie parallel to it. In summary, the coordination chemistry presented here has demonstrated that while ligand **2.14** has a very rigid core, it still possesses significant flexibility in its coordination modes.

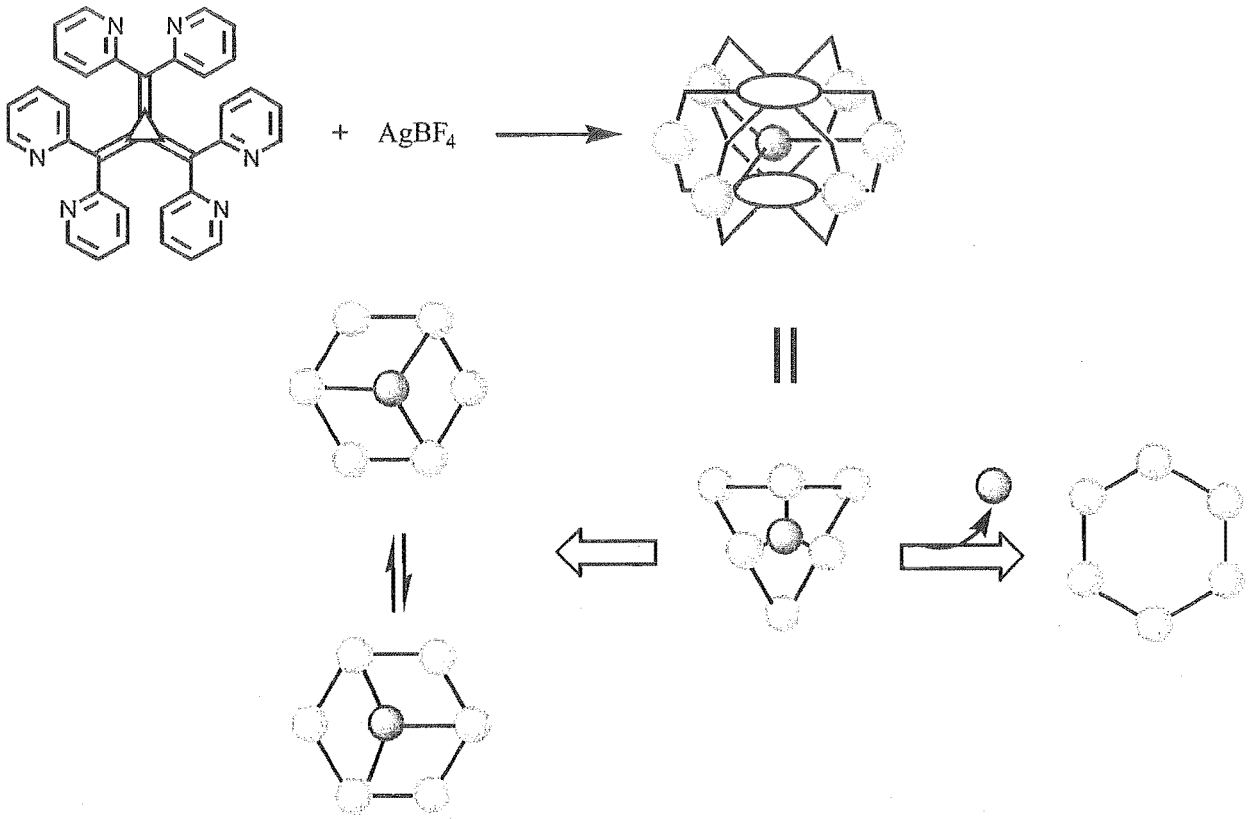


**Scheme 2.14**

### 2.5.2 Complexes of other [3]radialene-based ligands

Four other [3]radialene ligands, **2.15** - **2.18**, were prepared in this work, although disappointingly none of these provided complexes that could be structurally characterised. These ligands are a significant departure from the ligands previously investigated in this chapter because they are more likely to bridge metal ions without chelation. When a dichloromethane solution of ligand **2.15** was layered with a methanol solution of silver nitrate, a bright orange crystalline complex, **2.45**, was isolated in 57% yield. Elemental analysis indicated that complex **2.45** had the composition $[Ag_4(\mathbf{2.15})(NO_3)_4]$. Despite repeated attempts at crystallising this compound, no crystals that were suitable for crystal structure analysis could be obtained. NMR spectroscopy was, as observed for most silver complexes involving ligands incapable of chelation, difficult to interpret and considerably broadened because of the lability of the system.

Following the differences observed when changing the anion in complexes of **2.14**, **2.15** was also reacted with silver tetrafluoroborate and silver hexafluorophosphate. Using the layering method described above, reaction of **2.15** with these metal salts gave two further orange solids, **2.46** and **2.47**, respectively. Complex **2.46** was obtained in 79% yield after slow mixing of the two layers and elemental analysis indicated a composition similar to complex **2.45**. Complex **2.47** was also obtained in high yield and elemental analysis suggested a complex with an unusual

$[Ag_5(\mathbf{2.15})_2](PF_6)_5.4H_2O$ composition. Despite repeated attempts, neither compound could be recrystallised to give crystals suitable for X-ray crystallography. Ligand **2.15** was also reacted with bis(acetonitrile)palladium dichloride by refluxing a dichloromethane-acetonitrile solution of the palladium complex and **2.15** for 24 hours. The complex, **2.48**, was isolated as a very insoluble orange-red precipitate in 91% yield, which analysed as $[Pd_4(\mathbf{2.15})Cl_8]$ by elemental analysis.

Initial attempts to cyclopalladate the mixture of *sym-* and *unsym-*[3]radialene ligands (**2.17/2.18**) were unsuccessful and this was not pursued any further. A silver nitrate complex, **2.49**, was prepared in 64% yield by the layering method used for **2.15**. Elemental analysis suggested a complex with an unusual $[Ag_5(\mathbf{2.17/2.18})_2(NO_3)_5].H_2O$ composition, which despite repeated attempts, could not be satisfactorily recrystallised.

While no complexes were structurally characterised, one feature of these other [3]radialene ligands has become apparent. These ligands have a tendency to bridge multiple metal centres and, thus, are likely to be forming large one- and two-dimensional polymeric structures. The low solubility of the compounds prepared here is consistent with such structures. There is ample room for further investigation of these [3]radialene ligands.

## 2.6. Ruthenium complexes of selected ligands

The high level of interest and myriad of potential applications of ruthenium complexes has meant that the electrochemistry and photophysics of mononuclear and multinuclear ruthenium complexes have been very well studied. A coordinated ligand can affect the redox potentials and spectroscopy of a complex, and likewise, the bridging ligands have a fundamental impact on the properties of multinuclear complexes, because of the control exerted over the metal-metal distances and the extent of interaction between the metal atoms. A handle on the nature of the metal-ligand and metal-metal interactions can be obtained by studying the electrochemistry and spectroscopy. Cyclic voltammetry and visible absorption spectroscopy are routinely employed in this regard.

There is also interest in the structures of such compounds, which have often been investigated by NMR spectroscopy. Dramatic changes in the $^1H$ NMR chemical shifts are sometimes observed when a ligand is coordinated to ruthenium. This is exemplified by the range of coordination induced shift (CIS) values ($CIS = \delta_{complex} - \delta_{ligand}$) that are found for complexes described in this section of work. Previously, a number of factors have been identified that influence the sign and magnitude of the CIS values that are observed when a ligand coordinates to a ruthenium atom.[112, 132] These include ligand-to-metal $\sigma$ donation, metal-to-ligand $\pi$ back-

donation, chelation-imposed conformational changes, disruption of the inter-ring conjugation and inter-ligand through-space ring-anisotropy effects. In some instances the CIS values that a ligand displays on coordination enable conclusions to be formed about the structure of the complex. A series of complexes are discussed in this section; initially the ruthenium chemistry of **2.1** was studied to serve as a model compound for the ruthenium complexes of the bridging ligands **2.2**, **2.4** and **2.14**.

### 2.6.1 Synthesis of the complexes and NMR spectroscopy

The ruthenium complexes were typically prepared by reaction of the ligand with the ruthenium precursor, $[Ru(L)_2Cl_2]$ in a 3:1 ethanol-water solution. In most cases these complexes were isolated as their hexafluorophosphate salts and purified by column chromatography on alumina. In some cases, the more recalcitrant ligands were reacted with $[Ru(L)_2(OTf)_2]$ to attempt to prepare dinuclear complexes, where conventional precursors had failed to give the desired products. Through a collaboration with Prof. Richard Keene, microwave assisted synthesis was also employed with some ligands.

Reaction of $[Ru(bpy)_2Cl_2]$, or $[Ru(dmb)_2Cl_2]$, with **2.1** in ethanol-water gave the expected mononuclear complexes $[Ru(bpy)_2(\mathbf{2.1})](PF_6)_2$, **2.50**, and $[Ru(dmb)_2(\mathbf{2.1})](PF_6)_2$, **2.51** (Scheme 2.15), which were characterised by elemental analysis, mass spectrometry and $^1$H NMR spectroscopy. Compound **2.50** had previously been reported as part of a study of the photochemistry of related complexes.[133] The $^1$H NMR chemical shifts for ligand **2.1** and the ruthenium complexes **2.50** and **2.51** are given in Table 2.3, along with the CIS values in italics. The assignments were made on the basis of spin-spin coupling information, 1-D TOCSY and 1-D NOESY experiments.

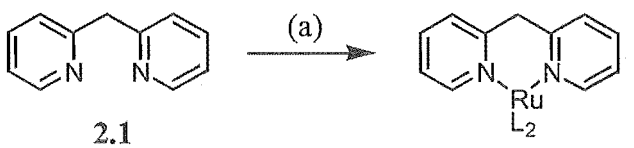


**2.1**

**2.50** L=bpy
**2.51** L=dmb

(a) $Ru(L)_2Cl_2$, EtOH/water, $NH_4PF_6$.

**Scheme 2.15**

In the mononuclear complexes **2.50** and **2.51**, which serve as models for subsequent complexes, the six-membered chelate ring of coordinated **2.1** is expected to exist in a boat conformation. This reduces the symmetry of the complex and would result in separate signals for the diastereotopic protons of the $CH_2$ group and all pyridine rings, unless there were rapid interconversion of the two boat conformers on the NMR timescale. In these two complexes such

interconversions are indeed rapid, as indicated by the $CH_2$ protons appearing as sharp singlets in the $^1H$ NMR spectra. The CIS values (Table 2.2) for the protons of **2.50** and **2.51** are very similar, as expected for the subtle differences of the auxiliary bpy-like ligands. The large negative CIS values for the H6 protons result from inter-ligand through-space ring-anisotropy effects, because on complexation these protons lie over the shielding plane of adjacent bpy rings.

**Table 2.3.** $^1H$ NMR chemical shift values for the ligand **2.1** and the two dinuclear complexes **2.50** and **2.51** recorded in acetonitrile, with the CIS values shown in italics.

| Compound | H3 | H4 | H5 | H6 | $CH_2$ |
|---|---|---|---|---|---|
| **2.1** | 7.33 | 7.71 | 7.22 | 8.53 | 4.32 |
| **2.50** | 7.71 | 7.90 | 7.14 | 7.58 | 4.61 |
| *CIS* | *0.38* | *0.19* | *-0.08* | *-0.95* | *0.29* |
| **2.51** | 7.69 | 7.88 | 7.13 | 7.60 | 4.60 |
| *CIS* | *0.36* | *0.17* | *-0.09* | *-0.93* | *0.28* |

Reaction of **2.2**, a potentially ditopic doubly bidentate ligand, with either ruthenium precursor unexpectedly yielded only the mononuclear complexes, $[Ru(bpy)_2(\mathbf{2.2})](PF_6)_2$, **2.52**, and $[Ru(dmb)_2(\mathbf{2.2})](PF_6)_2$, **2.53**. Despite repeating these reactions several times with substantial excesses of the ruthenium precursors (Scheme 2.16), and a number of variations in method and reaction time, the formation of dinuclear products was not detected. $[Ru(bpy)_2(OTf)_2]$ was also reacted without success with **2.2** in an effort to form dinuclear complexes. This result was rather

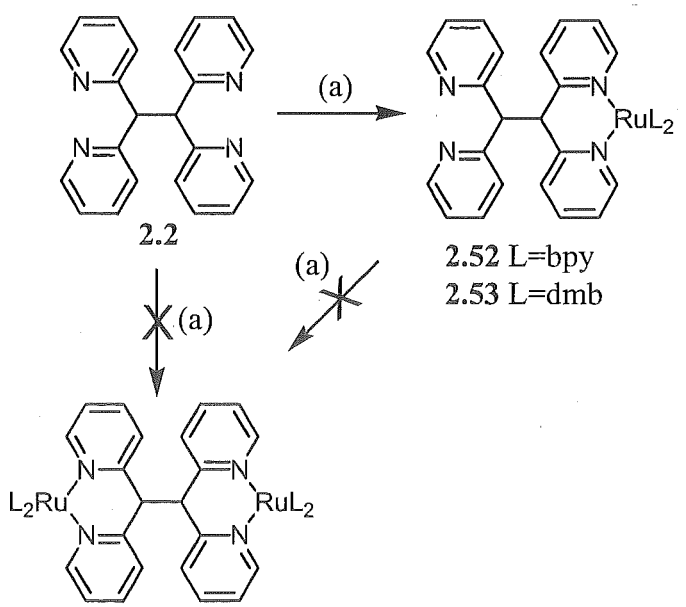


(a) $Ru(L)_2Cl_2$, EtOH/water, $NH_4PF_6$.

**Scheme 2.16**

perplexing, considering that several other dinuclear complexes of this ligand have been described in this work and, as mentioned, a dinuclear palladium complex of this ligand has also been reported by Canty and Minchin.[72] Attempts to react the isolated mononuclear complex, $[Ru(bpy)_2(\mathbf{2.2})](PF_6)_2$, with a further equivalent of $[Ru(bpy)_2Cl_2]$ were also unsuccessful.

The $^1$H NMR spectra of the mononuclear ruthenium complexes **2.52** and **2.53** are somewhat more complicated because the two boat conformations of the six-membered chelate ring are very different. Since the conformer with the CH proton in the flagpole position[†] and the rest of the non-coordinated portion of the ligand in the bowsprit position is much more stable than the other conformer, this complex is locked in one conformation, which has $C_1$ symmetry. As a consequence all eight pyridine rings are non-equivalent, as shown in the $^1$H NMR spectrum of **2.52** (Figure 2.42), and the signals were identified by a combination of 2-D COSY, 1-D TOCSY and 1-D NOESY experiments. The CIS values experienced by ligand **2.2** upon coordination to ruthenium are more pronounced than for complexes **2.50** and **2.51** and range from -1.27 to +0.95 ppm (Table 2.4).

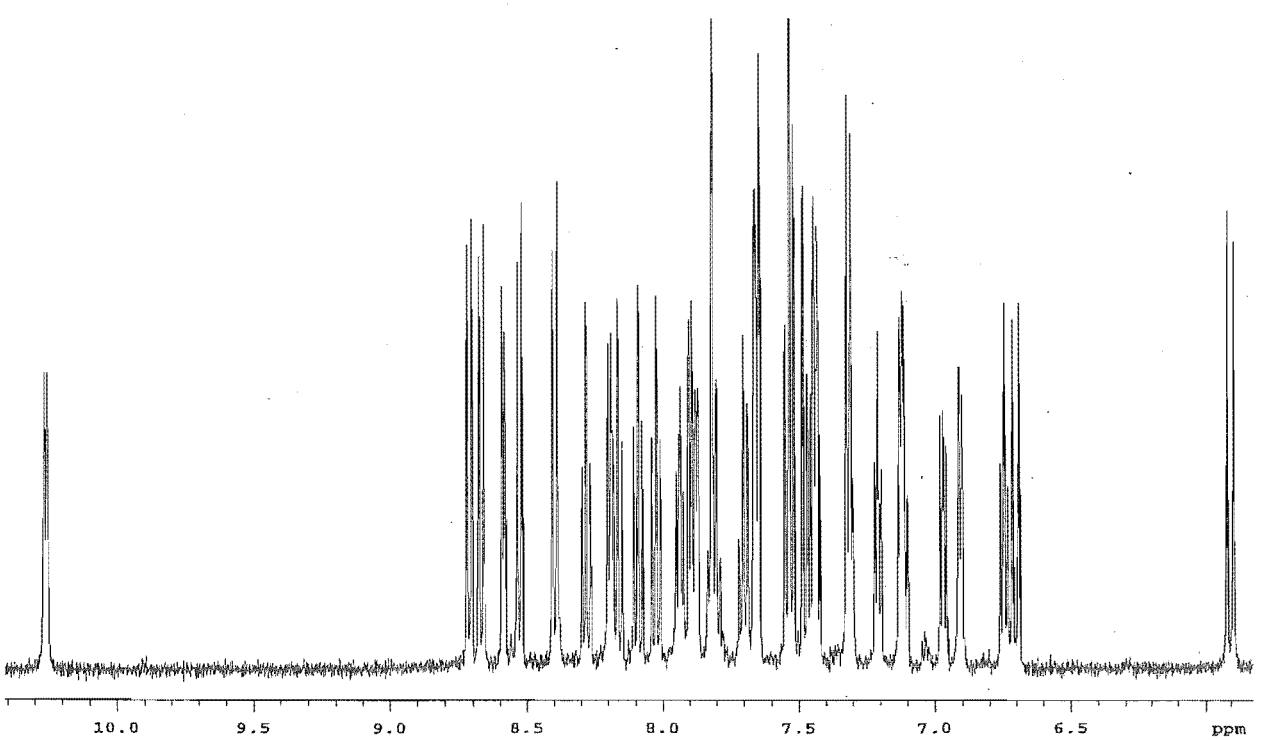


**Figure 2.42.** The aromatic region of the $^1$H NMR spectrum showing the relatively well resolved signals for complex **2.52**.

[†] The terms flagpole and bowsprit are used to refer to the orientation of the geminal substituents on the $sp^3$ carbon atom in a boat conformation of a six-membered chelate ring. The flagpole position refers to the group perpendicular to the plane of the chelate ring, while the bowsprit is approximately in that plane.

**Table 2.4.** $^1$H NMR chemical shift values for ligand **2.2** and the two dinuclear complexes **2.52** and **2.53** recorded in acetonitrile, with the CIS values shown in italics.

| Compound | H3 | H4 | H5 | H6 | CH |
|---|---|---|---|---|---|
| **2.2** | 7.51 | 7.54 | 7.05 | 8.39 | 5.76 |
| **2.52** | 7.81 | 7.83 | 7.20 | 8.59 | 5.90 |
| *CIS* | *0.30* | *0.29* | *0.15* | *0.20* | *0.14* |
| **2.52** | 7.32 | 7.54 | 6.97 | 7.88 | 6.71 |
| *CIS* | *-0.19* | *0* | *-0.08* | *-0.51* | *0.95* |
| **2.52** | 7.67 | 7.72 | 7.12 | 7.91 | |
| *CIS* | *0.16* | *0.18* | *0.07* | *-0.48* | |
| **2.52** | 7.47 | 7.54 | 6.75 | 7.13 | |
| *CIS* | *-0.04* | *0* | *-0.30* | *-1.26* | |
| **2.53** | 7.82 | 7.82 | 7.21 | 8.59 | 5.89 |
| *CIS* | *0.31* | *0.28* | *0.16* | *0.20* | *0.13* |
| **2.53** | 7.28 | 7.53 | 6.98 | 7.89 | 6.67 |
| *CIS* | *-0.23* | *-0.01* | *-0.07* | *-0.50* | *0.91* |
| **2.53** | 7.65 | 7.68 | 7.10 | 7.91 | |
| *CIS* | *0.14* | *0.14* | *0.05* | *-0.48* | |
| **2.53** | 7.46 | 7.52 | 6.74 | 7.12 | |
| *CIS* | *-0.05* | *-0.02* | *-0.31* | *-1.27* | |

Crystal Structure of **2.52**

Crystals of complex **2.52** were obtained by slow evaporation of a methanol solution of the complex. It crystallises in the monoclinic space group $P2_1/n$, with one complete cation (Figure 2.43), two hexafluorophosphate counterions and two methanol solvate molecules in the asymmetric unit. The structure determination confirms the mononuclear nature of **2.52** and unambiguously establishes that the ligand chelates to the ruthenium atom through two *geminally*-substituted pyridine rings (with the formation of a six-membered chelate ring), rather than through two *vicinally*-related rings (and a seven-membered chelate ring). As surmised above the non-coordinated dipyridylmethane substituent exists in the bowsprit position of the chelate ring boat conformation. As shown in Figure 2.43, the non-coordinated pyridine rings are ideally disposed to coordinate to a second ruthenium centre, and thus, steric factors do not appear to be influential in preventing a second equivalent of bis(2,2'-bipyridyl)ruthenium from coordinating. The bonding geometry of the ruthenium atom is unremarkable.

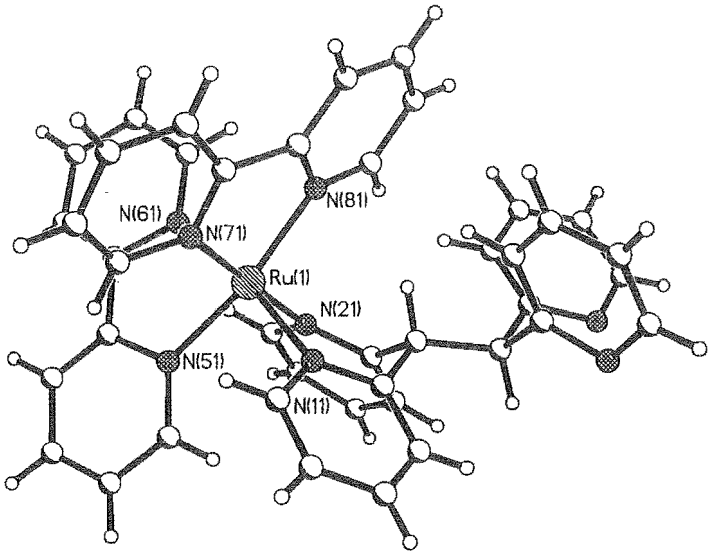


**Figure 2.43.** A perspective view of the structure of complex **2.52**. Hexafluorophosphate counterions and methanol solvate molecules are not shown. Selected bond lengths (Å) and angles (°): Ru(1)-N(61) 2.046(4), Ru(1)-N(51) 2.058(4), Ru(1)-N(71) 2.059(4), Ru(1)-N(81) 2.075(4), Ru(1)-N(21) 2.124(4), Ru(1)-N(11) 2.135(4), N(61)-Ru(1)-N(51) 79.5(2), N(61)-Ru(1)-N(71) 87.1(2), N(51)-Ru(1)-N(71) 95.9(2), N(61)-Ru(1)-N(81) 92.3(2), N(51)-Ru(1)-N(81) 170.4(2), N(71)-Ru(1)-N(81) 78.7(2), N(61)-Ru(1)-N(21) 94.4(2), N(51)-Ru(1)-N(21) 85.7(2), N(71)-Ru(1)-N(21) 178.0(2), N(81)-Ru(1)-N(21) 99.9(2), N(61)-Ru(1)-N(11) 171.7(2), N(51)-Ru(1)-N(11) 92.7(2), N(71)-Ru(1)-N(11) 91.1(2), N(81)-Ru(1)-N(11) 95.3(2), N(21)-Ru(1)-N(11) 87.7(2).

Ligand **2.3** was also reacted with $[Ru(bpy)_2Cl_2]$ to produce a mononuclear ruthenium complex, **2.54**, that was characterised as $[Ru(bpy)_2(L)](PF_6)_2$ (where L=di-2-pyridylketone) by $^1H$ NMR and HRMS. This complex has previously been directly prepared by reaction of $[Ru(bpy)_2Cl_2]$ with di-2-pyridylketone, and thus, no further characterisation was undertaken.[134] The previously characterised complex, **2.50** was also obtained from this reaction. Once again ligand **2.3** has undergone decomposition during the synthesis of a coordination complex.

Similar observations to those made for **2.2** were seen for **2.4**, which again has the potential to bridge two metal atoms. Only the mononuclear complexes, $[Ru(bpy)_2(\mathbf{2.4})](PF_6)_2$, **2.55**, and $[Ru(dmb)_2(\mathbf{2.4})](PF_6)_2$, **2.56**, were formed by conventional synthetic techniques (Scheme 2.17). Through a collaboration with the group of Prof. Keene at James Cook University in Australia, Deanna D'Alessandro carried out microwave assisted syntheses of several complexes in this section of work, and prepared Dreiding models of these complexes to aid the understanding of the structures and CIS values of these complexes. This included attempts, using these more

aggressive conditions, to prepare dinuclear ruthenium complexes of **2.4** (Scheme 2.17). By heating a suspension of $[Ru(bpy)_2Cl_2]$ and **2.4** in ethylene glycol in a modified microwave oven on high power for 45 min, a red-brown solution was obtained. This contained three components that were separated chromatographically, using a column of SP Sepharose Fast Flow cation exchanger and a gradient elution procedure using aqueous 0.1-0.5 $molL^{-1}$ NaCl as the eluent. Disappointingly, the three components were identified by NMR spectroscopy as unreacted $[Ru(bpy)_2Cl_2]$, the mononuclear complex **2.55** and an unsymmetrical mononuclear ruthenium complex containing an unidentified decomposition product of **2.4**, respectively.

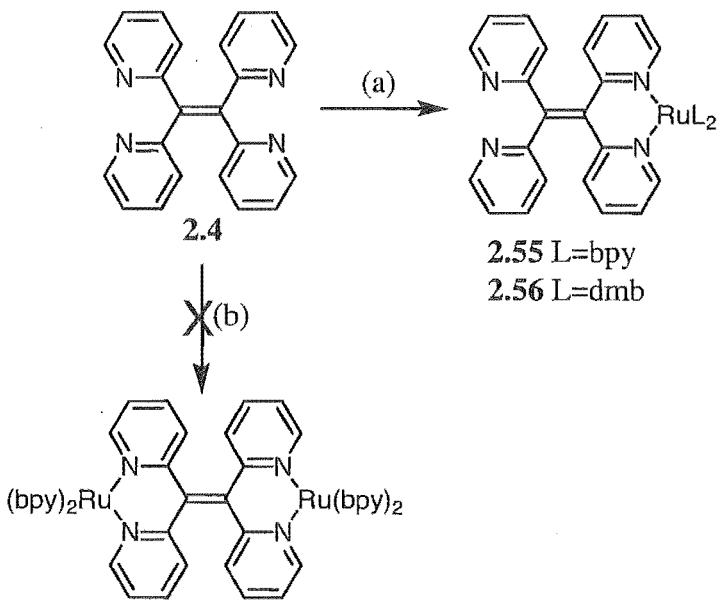


(a) $Ru(L)_2Cl_2$, EtOH/water, $NH_4PF_6$;
(b) $Ru(bpy)_2Cl_2$, ethylene glycol, microwave.

**Scheme 2.17**

Complexes **2.55** and **2.56** have $C_1$ symmetry due to a restricted conformation of the six-membered chelate ring of the coordinated ligand. Interestingly, the $^1H$ NMR spectrum for **2.55**, shown in Figure 2.44 reveals that one H3 proton lies in a strongly shielded environment (5.56 ppm, CIS = -1.49 ppm), while a bpy-H6 proton lies in a strongly deshielded environment (10.43 ppm). A similar, strongly deshielded proton is observed for complex **2.52**, but a strongly shielded proton was not observed in the earlier complex.

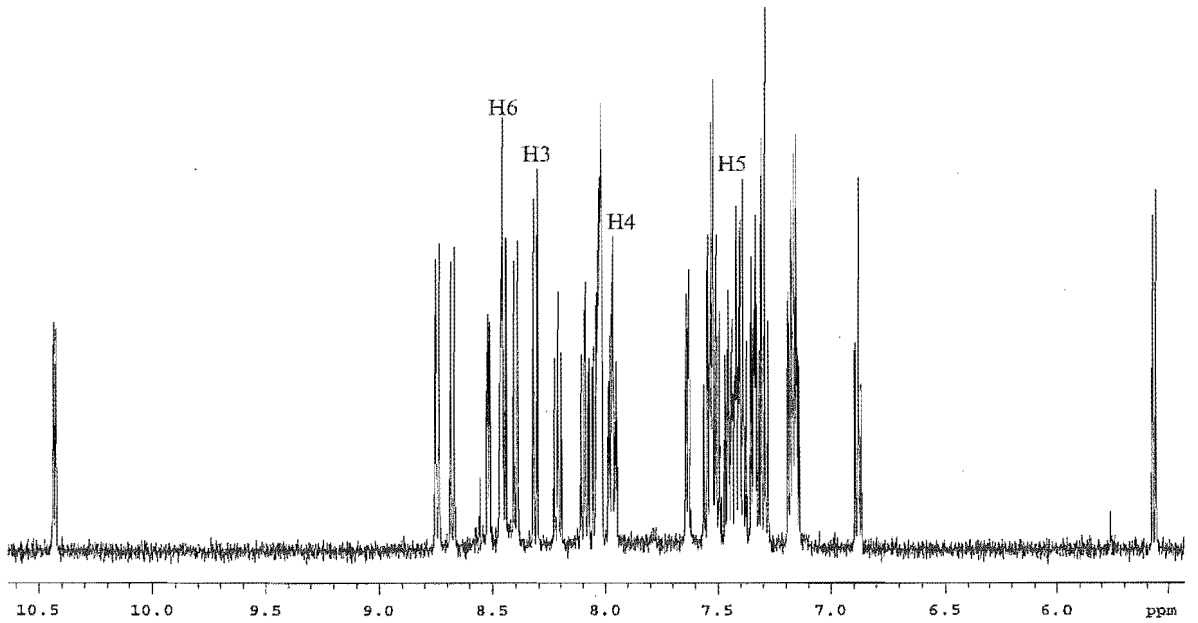


**Figure 2.44.** The aromatic region of the $^{1}$H NMR spectrum shows the relatively well resolved signals for complex **2.55**. The labels indicate the signals assigned by the 1-D TOCSY experiment shown in Figure 2.45.

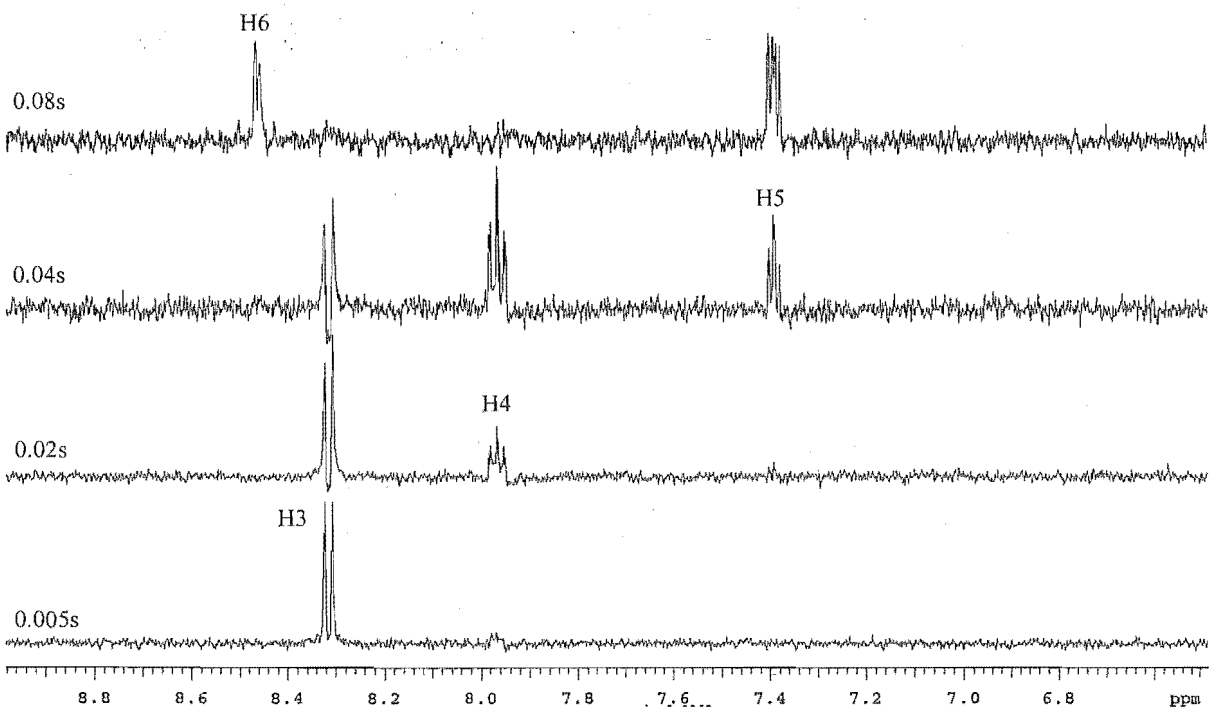


**Figure 2.45.** The spectra obtained from a 1-D TOCSY experiment.

One technique that was used extensively in this research project to resolve the proton chemical shift values of a particular spin system is 1-D total correlation spectroscopy (1-D TOCSY). The 1-D TOCSY experiment involves irradiation of a multiplet of a spin system and then the time-delayed observation of the magnetisation transfer through the spin system. The only requirement is that the protons are coupled, meaning that the heterocyclic compounds used in this work are particularly suited to this technique. When used in this research project, the experiment was usually conducted by irradiation, where possible, of either the H3 or H6 proton, and the magnetisation transfer monitored at time periods of 0.005, 0.02, 0.04 and 0.08 s. As shown in Figure 2.45 (previous page), irradiation of the bpy-H3 proton at 8.32 ppm is then transferred around the spin system of that pyridine ring to reveal first the bpy-H4 proton signal, and then the bpy-H5 and bpy-H6 signals at longer time periods. In this manner, the chemical shifts of very complicated spectra can be assigned and the CIS values calculated.

Crystal Structure of **2.55**

The structure of **2.55** was also determined by X-ray crystallography and served to help understand some of the large CIS values observed. The structure is shown in Figure 2.46 and crystallises in the triclinic space group P-1 with a full cation, two hexafluorophosphate anions, a methanol and a water molecule in the asymmetric unit. The structure and conformation of the complex allows further conclusions to be drawn from the previously assigned $^1$H NMR signals. The boat conformation of the six-membered chelate ring destroys the potential $C_2$ symmetry of the complex. As the structure shows, the strongly shielded H3 proton of one of the non-coordinated rings lies directly over one of the bpy rings. Conversely, the H3 proton of the other non-coordinated ring is in a deshielded environment, lying very close to the nitrogen atom of the aforementioned non-coordinated pyridine ring. The structure also shows that the two H6 protons of the coordinated pyridine rings of the tetradentate ligand both lie over a pyridine ring of the ancillary bpy ligands. Hence these protons are shielded due to through-space ring anisotropy effects. Once again the bonding geometry of the ruthenium atom is normal.

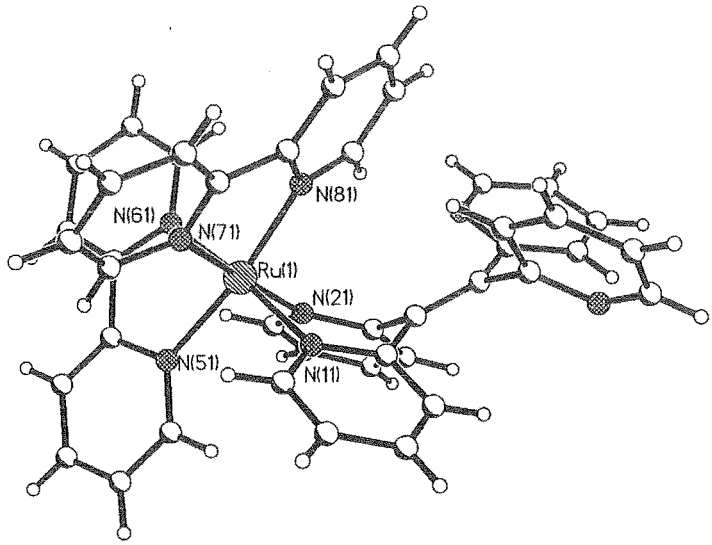


**Fig. 2.46.** A perspective view of the structure of complex **2.55** with counterions and solvate molecules not shown. Selected bond lengths (Å) and angles (°): Ru(1)-N(61) 2.049(5), Ru(1)-N(71) 2.053(7), Ru(1)-N(81) 2.063(6), Ru(1)-N(51) 2.078(6), Ru(1)-N(21) 2.111(6), Ru(1)-N(11) 2.116(5), N(61)-Ru(1)-N(71) 90.9(2), N(61)-Ru(1)-N(81) 95.4(2), N(71)-Ru(1)-N(81) 77.7(3), N(61)-Ru(1)-N(51) 78.8(2), N(71)-Ru(1)-N(51) 96.5(3), N(81)-Ru(1)-N(51) 171.8(2), N(61)-Ru(1)-N(21) 92.7(2), N(71)-Ru(1)-N(21) 175.8(2), N(81)-Ru(1)-N(21) 99.8(2), N(51)-Ru(1)-N(21) 86.3(2), N(61)-Ru(1)-N(11) 175.6(3), N(71)-Ru(1)-N(11) 89.8(2), N(81)-Ru(1)-N(11) 89.0(2), N(51)-Ru(1)-N(11) 96.8(2), N(21)-Ru(1)-N(11) 86.7(2).

Using a combination of spin-spin coupling information from the $^1$H NMR spectrum, 2-D COSY, 1-D TOCSY and 1-D NOESY experiments, the $^1$H NMR chemical shifts for ligand **2.2** and the ruthenium complexes **2.55** and **2.56** were assigned. These are given in Table 2.5, along with the CIS values in italics. The sign and magnitude of the CIS values observed for **2.55** and **2.56** indicate that while some effects of the coordination are similar for the mononuclear complexes of both the methane and ethane ligands, other effects are more significant for **2.4**, possibly because of the extra rigidity of this ligand. On examination of the crystal structure shown above and Dreiding models, the strongly shielded proton at 5.56 ppm is assigned as the H3 proton of the non-coordinated ring *b* of **2.4**, which lies directly over the shielding region of bpy ring *a* of the complex (Figure 2.47). The resonance at 10.43 ppm is assigned to the H6 proton of bpy ring *a*, which lies close to the nitrogen atom and the deshielding region of the non-coordinated ring *c* of **2.4**. This rationale is based on the assumption that the solid state and solution phase structures of complex **2.55** are similar. This similarity of the two structures may

be assisted by a stabilising hydrogen bond-type interaction between the nitrogen atom of ring *b* and the H3 proton of ring *c* as is found in the crystal structure (*vide infra*). Such C-H···N interactions are now well recognised as offering significant energetic stabilisation.[14, 135] The CIS values for the ligand **2.4** in complex **2.55** range from -1.49 to +1.27 ppm and, as expected, are similar to those observed for **2.56**.

**Table 2.5.** $^1$H NMR chemical shift values for the ligand **2.4** and the two dinuclear complexes **2.55** and **2.56** recorded in acetonitrile, with the CIS values shown in italics.

| Compound | H3 | H4 | H5 | H6 |
|---|---|---|---|---|
| **2.4** | 7.05 | 7.54 | 7.17 | 8.45 |
| **2.55** | 5.56 | 7.30 | 7.17 | 8.52 |
| *CIS* | *-1.49* | *-0.24* | *0.00* | *0.07* |
| **2.55** | 8.32 | 7.97 | 7.39 | 8.46 |
| *CIS* | *1.27* | *0.43* | *0.22* | *0.01* |
| **2.55** | 7.35 | 7.52 | 6.88 | 7.19 |
| *CIS* | *0.30* | *-0.02* | *-0.29* | *-1.26* |
| **2.55** | 7.31 | 7.55 | 7.16 | 8.04 |
| *CIS* | *0.26* | *0.01* | *-0.01* | *-0.41* |
| **2.56** | 5.31 | 7.30 | 7.18 | 8.56 |
| *CIS* | *-1.74* | *-0.24* | *0.01* | *0.11* |
| **2.56** | 8.34 | 7.97 | 7.39 | 8.45 |
| *CIS* | *1.29* | *0.43* | *0.22* | *0* |
| **2.56** | 7.30 | 7.48 | 6,87 | 7.19 |
| *CIS* | *0.25* | *-0.06* | *-0.30* | *-1.26* |
| **2.56** | 7.30 | 7.53 | 7.15 | 8.02 |
| *CIS* | *0.25* | *-0.01* | *-0.02* | *-0.43* |

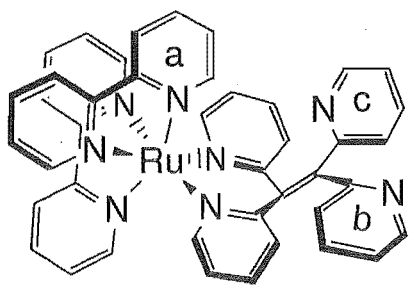


**Figure 2.47.** A three-dimensional representation of **2.55**.

The microwave-assisted reaction of $[Ru(bpy)_2Cl_2]$ with **2.14** in ethylene glycol, carried out by Deanna D'Alessandro, as shown in Scheme 2.18, produced a green/brown solution that was separated into the mononuclear and dinuclear products by a gradient elution procedure using aqueous 0.1-0.5 molL$^{-1}$ NaCl as the eluent. Four bands were eluted: Band 1 (light red, 0.2 molL$^{-1}$ NaCl), Band 2 (purple, 0.3 molL$^{-1}$ NaCl), Band 3 (green, 0.4 molL$^{-1}$ NaCl) and Band 4 (green, 0.4 molL$^{-1}$ NaCl). These were identified by a combination of ES-MS and 1-D and 2-D NMR techniques. Band 1 was identified by ES-MS as a mixture of $[Ru(bpy)_2L]^{2+}$ complexes, where

L = di(2-pyridyl)ketone and its ethylene acetal. Band 2 was unreacted $[Ru(bpy)_2Cl_2]$. Bands 3 and 4 were identified by ES-MS and NMR as the two diastereoisomeric forms of $[\{Ru(bpy)_2\}_2(\mathbf{2.14})](PF_6)_4$. The significance of being able to separate the two diastereoisomers cannot be emphasised enough. Apart from being able to investigate the electrochemistry and photophysics of separate diastereoisomers (later), the $^1$H NMR spectrum of the mixture of compounds, initially prepared, was almost impossible to interpret, with 84 overlapping signals.

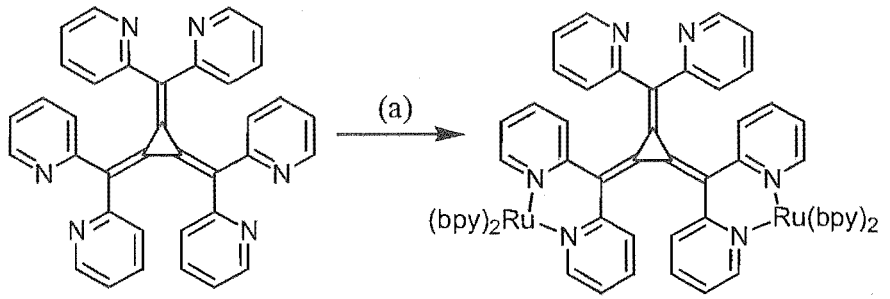


**2.14** **2.57** ΔΛ/ΛΔ
**2.58** ΔΔ/ΛΛ

(a) $Ru(bpy)_2Cl_2$, ethylene glycol, microwave.

**Scheme 2.18**

Mass spectrometry had shown that complexes **2.57** and **2.58** were isomers of dinuclear complexes in which the radialene ligand bridges two $Ru(bpy)_2$ subunits. Normally,[47, 48] the linking of two chiral $Ru(bpy)_2$ moieties by a symmetrical bridging ligand leads to two diastereoisomers: a ΔΛ (*meso*) diastereoisomer, with $C_s$ point group symmetry, and a ΔΔ/ΛΛ (*rac*) isomer with $C_2$ point group symmetry. Surprisingly, however, the $^1$H NMR of **2.57** (Figure 2.48) was significantly more complicated than that of **2.58** (Figure 2.49), with complex **2.57** displaying 56 unique aromatic proton resonances, whereas **2.58** showed only (28) signals. This clearly indicated that one of the isomers has reduced (i.e. $C_1$) symmetry. Despite the complexity of both spectra, the individual pyridine ring spin systems were identified by standard 1- or 2-D NMR experiments. The signals for the two non-coordinated pyridine ring spin systems were observed to slightly overlap and thus the signals of the sixth pyridine ring spin system was difficult to resolve. The $^1$H NMR chemical shifts in acetonitrile for ligand **2.14** and the two diastereoisomers of the dinuclear ruthenium complex, **2.57** and **2.58**, along with the CIS values are shown in Table 2.6.

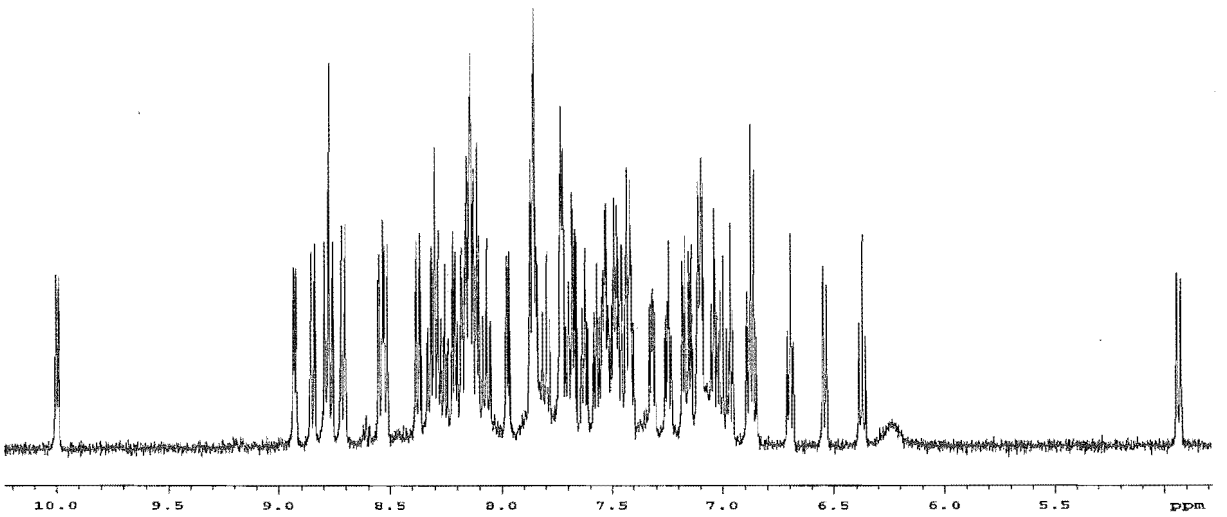


**Figure 2.48.** The $^1$H NMR spectrum of compound **2.57**.

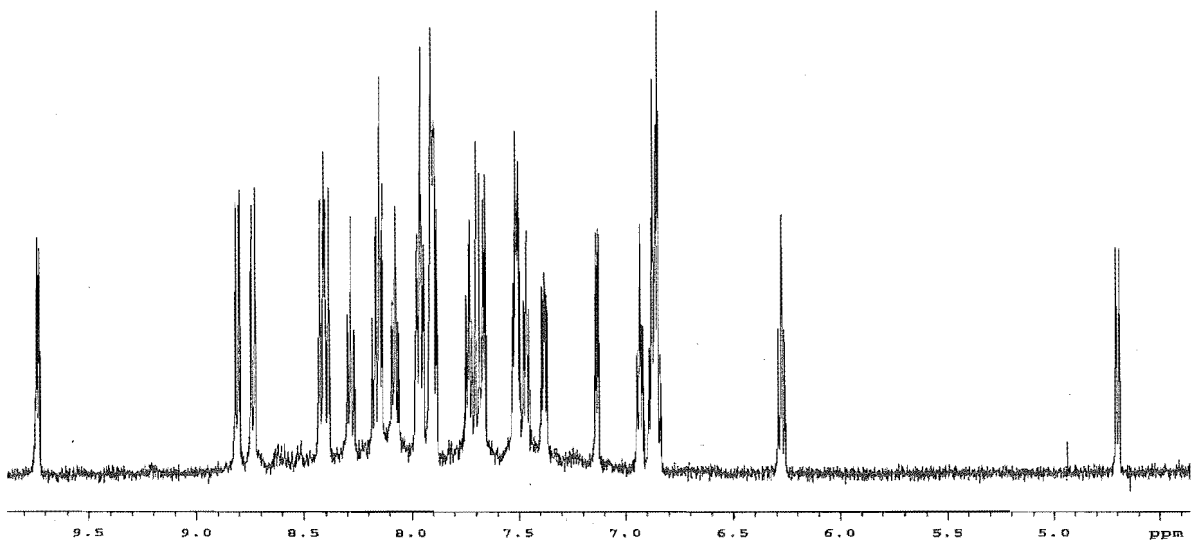


**Figure 2.49.** The $^1$H NMR spectrum of compound **2.58** (*rac*).

The use of Dreiding models of the diastereoisomeric forms of $[\{Ru(bpy)_2\}_2(\mathbf{2.14})]^{4+}$ proved to be of considerable assistance in rationalising the differences observed in the $^1$H NMR spectra. Assuming that the [3]radialene core is planar,[79, 96, 97] the six-membered chelate rings are required to adopt boat conformations on opposite faces of this core, with one boat "up" and the other "down" with respect to the plane of the three-membered ring. All other conformations can be excluded on steric grounds. As a consequence, the ΔΛ diastereoisomer **2.57** possesses $C_1$ symmetry (lacking the mirror plane of the more common *meso* isomers), while the ΔΔ/ΛΛ (*rac*) isomer **2.58** possesses the expected $C_2$ symmetry. The different symmetries of the diastereoisomeric forms account for the observation of 56 and 28 proton signals in the $^1$H NMR spectra of the ΔΛ and ΔΔ/ΛΛ (*rac*) diastereoisomers, respectively.

**Table 2.6.** $^1$H NMR chemical shift values for the ligand **2.14** and the two diastereomeric complexes **2.57** and **2.58** recorded in acetonitrile, with the CIS values shown in italics.

| Compound | H3 | H4 | H5 | H6 |
|---|---|---|---|---|
| **2.14** | 6.91 | 7.16 | 7.15 | 8.16 |
| **2.57** | 7.44 | 7.86 | 7.31 | 7.74 |
| *CIS* | *0.53* | *0.70* | *0.16* | *-0.52* |
| **2.57** | 7.11 | 7.46 | 7.25 | 8.12 |
| *CIS* | *0.20* | *0.30* | *0.10* | *-0.04* |
| **2.57** | 4.93 | 6.37 | 6.70 | 7.15 |
| *CIS* | *-1.98* | *-0.79* | *-0.45* | *-1.01* |
| **2.57** | 6.54 | 6.88 | 7.05 | 7.84 |
| *CIS* | *-0.37* | *-0.28* | *-0.10* | *-0.32* |
| **2.57** | 7.00 | 6.87 | 6.99 | 7.17 |
| *CIS* | *0.09* | *-0.29* | *-0.16* | *-0.99* |
| **2.58** | 4.69 | 6.27 | 6.85 | 7.90 |
| *CIS* | *-2.22* | *-0.92* | *-0.30* | *-0.26* |
| **2.58** | 6.86 | 6.87 | 6.95 | 7.13 |
| *CIS* | *-0.05* | *-0.32* | *-0.20* | *-1.03* |
| **2.58** | 7.69 | 7.96 | 7.38 | 7.92 |
| *CIS* | *0.78* | *0.77* | *0.23* | *-0.24* |

Examination of the Dreiding models also aid in the interpretation of some unusual chemical shifts observed in the $^1$H NMR spectra. The $C_1$-symmetric ($\Delta\Lambda$) diastereoisomer **2.57** has signals at 4.93 ppm (1H) and 10.00 ppm (1H), whilst the $C_2$-symmetric (*rac*) isomer **2.58** has signals at 4.69 ppm (2H) and 9.73 ppm (2H). In the more symmetrical *rac* diastereoisomer **2.58**, the H3 protons of rings *e* and *e'* (Figure 2.50) lie directly over the shielding regions of rings *b'* and *b*, respectively, of the ancillary bpy ligands and are shifted upfield, giving rise to the signal at the remarkably high field position of 4.69 ppm (2H). In the less symmetrical $\Delta\Lambda$ isomer **2.57**, the H3 proton of ring *j* is similarly shielded by bpy ring *b*, but the H3 proton of ring *e* lies in a relatively

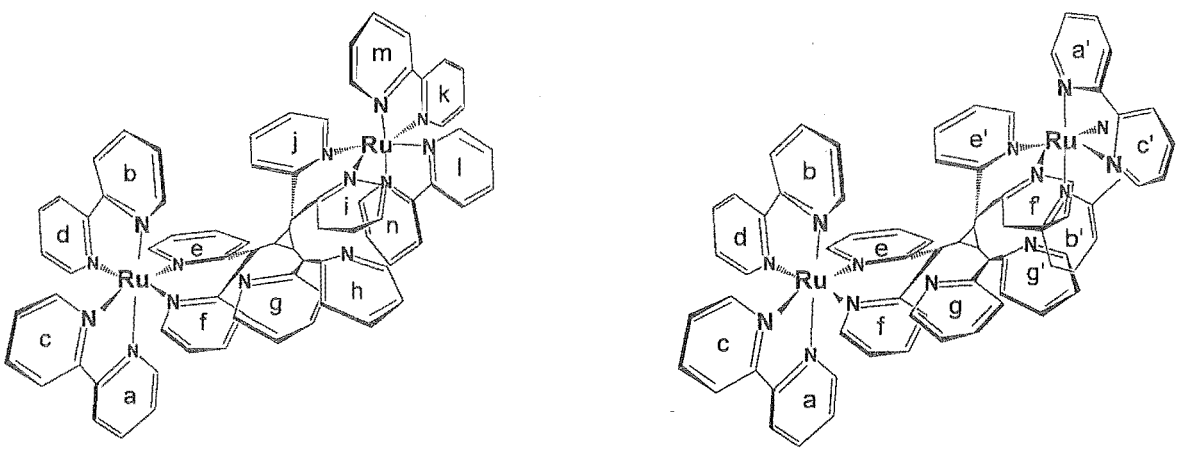


**Figure 2.50.** The structures of the two diastereoisomers, **2.57** ($\Delta\Lambda$) and **2.58** $\Delta\Delta/\Lambda\Lambda$ (*rac*).

less shielded environment due to the opposite chiralities of the two metal centres. Thus, the upfield signal at 4.93 ppm in this diastereoisomer is attributed to the single H3 proton of ring *j*.

A similar rationale accounts for the unusual downfield signals. Whereas the signal at 9.73 ppm in the *rac* diastereoisomer **2.58** is associated with two H6 protons, the signal at 10.00 ppm in the other isomer **2.57** is attributed to a single H6 proton. This suggests that the protons must be associated with the *axial* pyridine rings of the ancillary bpy ligands which lie over the bridging ligand (*e.g. a* or *b* rather than *c* or *d*). Examination of the Dreiding model for **2.58** reveals that the H6 protons of rings *b* and *b'* lie very close to the nitrogen atoms of the non-coordinated rings *g* and *g'*, respectively, and are thus strongly deshielded. By contrast, the H6 protons of rings *a* and *a'* lie in relatively more shielded environments. In the diastereoisomer **2.57**, the opposite chiralities of the two metal centres are such that *only* the H6 proton of ring *b* lies close to the nitrogen atom of the non-coordinated ring *g*. Hence, the downfield signal at 10.00 ppm is attributed to a single proton. This rationale is based on the assumption that the non-coordinated pyridine rings of the bridging ligand are oriented as shown in Figure 2.50, which may again be due to the existence of stabilising C-H···N intramolecular interactions.

### 2.6.2 Absorption Spectra and Redox Properties

The electrochemistry and visible absorption spectroscopy of eight of the ruthenium complexes described above was studied. An example of a cyclic voltammogram, recorded for complex **2.55**, is shown in Figure 2.51. This complex exhibits a reversible one-electron oxidation

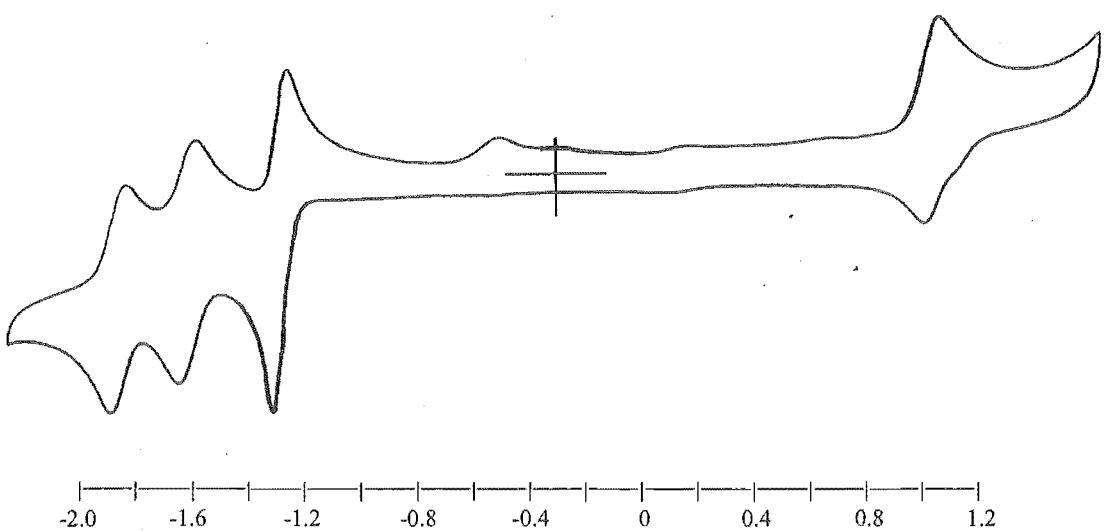


**Figure 2.51.** A picture of a cyclic voltammogram for complex **2.55** showing the metal centred oxidation wave and the three ligand-based reduction waves.

wave at +1.17 V that is well known to be metal centred. Correspondingly, the reductions, of which there are three reversible one-electron waves at -1.25, -1.60 and -1.86 V, have been shown to be ligand localised.[42]

Table 2.7 lists the electronic absorption maxima and redox potentials recorded in acetonitrile solutions for the complexes **2.50** - **2.56**. The mononuclear complexes all exhibit a lowest energy MLCT absorption at a similar wavelength to that of $[Ru(bpy)_3]^{2+}$ (452 nm).[42] However, the redox potentials reveal that the $Ru(bpy)_2$ complexes **2.50** and **2.52** of the non-conjugated ligands are slightly easier to oxidise and more difficult to reduce than $[Ru(bpy)_3]^{2+}$ (+1.26, -1.33 V).[42] This may result because these ligands provide less $\pi$-backbonding stabilisation than bpy. In contrast, the mononuclear complexes of the conjugated ligand **2.4** undergo reduction at a lower potential, whilst still being slightly easier to oxidise. For the series of mononuclear complexes the redox potentials of the dmb complexes are shifted by *ca.* 100 mV related to those of the analogous bpy complexes, consistent with the known[136] electron donating effect of *ca.* 25 mV per methyl group.

**Table 2.7.** Visible absorption maxima and redox potentials for $[Ru(bpy)_3](PF_6)_2$ and complexes **2.50** - **2.56**.

| | $\lambda$ (nm)[a,b] | $E_{ox}$[c,d] | $E_{red(1)}$[c,d] | $E_{red(2)}$[c,d] | $E_{red(3)}$[c,d] |
|---|---|---|---|---|---|
| $[Ru(bpy)_3](PF_6)_2$ | 452 | +1.26 | -1.33 | -1.51 | -1.75 |
| **2.50** | 434(sh), 451 | +1.19 | -1.45 | -1.64 | -1.86 |
| **2.51** | 434, 452(sh) | +1.09 | -1.54[e] | -1.71 | -1.95 |
| **2.52** | 433, 455 | +1.20 | -1.45 | -1.67 | |
| **2.53** | 436, 455 | +1.09 | -1.54 | -1.73 | |
| **2.55** | 454 | +1.17 | -1.25 | -1.60 | -1.86 |
| **2.56** | 456 | +1.07 | -1.33[e] | -1.68 | -1.93 |

[a] The MLCT band measured in $CH_3CN$ (± 2 nm)

[b] sh = shoulder.

[c] Potentials quoted in V *vs.* SCE in $CH_3CN$/0.1 mol.$L^{-1}$ $[(n\text{-}C_4H_9)_4]PF_6$ (the ferrocene/ferrocenium couple occurred at +310 mV *vs.* SCE).

[d] Uncertainty in $E_{1/2}$ values *ca.* ± 0.01 V.

[e] Irreversible (approximate value estimated from anodic half-scan).

The cyclic voltammetry of complexes **2.57** and **2.58** were recorded by Deanna D'Alessandro as part of the collaboration between the groups of Profs. Steel and Keene. The green dinuclear complexes also exhibit MLCT visible absorption maxima associated with the bpy ligands at *ca.* 452 nm, as shown in Table 2.8. However, the lowest energy transitions occur near 630 nm and correspond to electron transfer into the bridging radialene ligand. Both diastereoisomers are oxidised at a similar potential to that of $[Ru(bpy)_3]^{2+}$, but undergo two sequential one-electron

reductions at a much lower potential, consistent with the fact that the radialene ligand **2.14** is known to have very low energy LUMO and SLUMO orbitals.[95] Despite the potential conjugation provided by this ligand for interaction between the metal centres, the simultaneous two-electron oxidation event suggests a lack of communication between ruthenium centres in these dinuclear complexes.

**Table 2.8.** Visible absorption maxima and redox potentials for complexes **2.57** and **2.58**.

| | $\lambda$ (nm)[a] | $E_{ox}$[b,c] | $E_{red(1)}$[b,c] | $E_{red(2)}$[b,c] | $E_{red(3)}$[b,c] | $E_{red(4)}$[b,c] | $E_{red(5)}$[b,c] |
|---|---|---|---|---|---|---|---|
| **2.57** | 452, 632 | +1.24(2e$^-$) | -0.30(1e$^-$) | -0.77(1e$^-$) | -1.51(2e$^-$) | -1.80(2e$^-$) | -2.08(2e$^-$) |
| **2.58** | 453, 628 | +1.25(2e$^-$) | -0.43(1e$^-$) | -0.80(1e$^-$) | -1.53(2e$^-$) | -2.20(2e$^-$) | -2.38(2e$^-$) |

[a] The MLCT band measured in $CH_3CN$ (± 2 nm)

[b] Potentials quoted in V *vs.* SCE in $CH_3CN$/0.1 mol.L$^{-1}$ $[(n\text{-}C_4H_9)_4]PF_6$ (the ferrocene/ferrocenium couple occurred at +310 mV *vs.* SCE).

[c] Uncertainty in $E_{1/2}$ values *ca.* ± 0.01 V.

## 2.7. Summary

This chapter has described the syntheses and study of a range of bridging ligands incorporating a dipyridylmethyl motif. Included in this are a series doubly bidentate bridging ligands that were prepared from di-2-pyridylmethane and 4,5-diazafluorene. A novel ligand incorporating a spirolene backbone, **2.13**, was prepared from 4,5-diazafluorene, with the chelating units fixed perpendicular to each other. Four different ligands incorporating a [3]radialene core were also described in this chapter. These represent the first use of the [3]radialene core to prepare a nitrogen heterocyclic bridging ligand, and are themselves particularly interesting compounds as, like their arene homologues, they are bright red solids, and able to undergo two reductions to give the radical monoanion and the dianion.

The series of doubly bidentate bridging ligands incorporating di-2-pyridylmethane chelating groups (in particular **2.2** and **2.4**) readily bridged two metal atoms usually as discrete dinuclear complexes, or as part of a coordination polymer. With copper, zinc and palladium, dinuclear complexes were characterised, which indicated the possibility of preparing the corresponding ruthenium complexes. However, despite extensive efforts, dinuclear ruthenium complexes of **2.2** and **2.4** could not be prepared. Studies on the silver complexes of these ligands revealed some interesting three-dimensional structures. With ligand **2.2**, both a one-dimensional coordination polymer and a [2+2] dimer were characterised when the ligand was reacted with silver nitrate and silver tetrafluoroborate, respectively. This demonstrates the extent of the structural changes that an anion can induce in the formation of a metallosupramolecular complex.

Ligand **2.3** is readily hydrolysed on reaction with metal atoms that prevented any complexes being characterised whereby **2.3** coordinated to a metal atom, or bridged two metal atoms. An

interesting range of solvolysis products were characterised though. With the previously known ligand, **2.8**, which has, in addition to the two chelating di-2-pyridylmethane units, two azine nitrogen atoms, an $Ag_4L_2$ prismate structure with a helical twist was obtained. All six nitrogen atoms were involved in coordination. In other instances, **2.8** also underwent hydrolysis.

In stark contrast to the di-2-pyridylmethane-based ligands, ligands incorporating two 4,5-diazafluorene moieties proved resistant to forming any solid materials that could be crystallised. Complexes of the ethane- and ethylene-based ligands, **2.11** and **2.12**, have been previously characterised by elemental analysis, but very little is known about the coordination modes of these ligands. An interesting experiment would be to prepare the dinuclear ruthenium complex of **2.13**, which would provide and interesting comparison to the ruthenium complexes of the ethane and ethylene analogues (**2.11** and **2.12**) previously prepared by other workers.

The three silver complexes of the [3]radialene ligand **2.14** reinforced the importance of controlling all aspects of the self-assembly process. Using the three different silver salts, three different structures were obtained, which were in part dependent on the anion. By using silver tetrafluoroborate a $[Ag_6(\mathbf{2.14})_2F]$ prismate cage was formed around a templating fluoride anion. When no free fluoride was present, two coordination polymers were obtained, implicating the fluoride anion as a template for the synthesis of the cage, and demonstrating the affect the anions have on the assembly process and structures.

As noted, the doubly bidentate ligands, **2.2** and **2.4** were particularly resistant to forming dinuclear ruthenium complexes despite considerable efforts to carry out these reactions. Therefore no comparison could be made of the difference in the ethane and ethylene bridge has on metal-metal interactions. The ethylene bridge makes mononuclear ruthenium complexes of **2.4** easier to reduce than the corresponding non-conjugated complexes. The electrochemistry of the two diastereoisomers of the dinuclear bis(2,2'-bipyridyl)ruthenium complexes of **2.14** was very similar, and revealed no significant metal-metal interactions. These observations are likely to be a consequence of the twisting of the ruthenium centres out of the plane of the [3]radialene core.

# *Chapter 3*

# *Multidentate ligands derived from di-2-pyridylamine*

# Chapter 3

## 3. Multidentate ligands derived from di-2-pyridylamine

### 3.1. Introduction

This chapter describes two closely related series of ligands, the first containing di-2-pyridylamine units directly connected to a variety of arene cores and a second where the di-2-pyridylamine units are connected to a benzene core through a methylene spacer. These compounds build upon earlier successes of several groups,[124, 137-144] including the Steel group,[145-156] in the preparation of ligands and anion receptors, based upon multisubstituted arene cores. Such compounds have found use as structural components in assemblies with specified topologies in supramolecular and metallosupramolecular chemistry and applications in diverse areas such as crystal engineering,[24, 32, 33, 35, 157] as molecular receptors and hosts,[29, 158] and in the construction of molecular containers and flasks.[23, 28, 30]

The generalised structure shown in Figure 3.1(a) represents a large range of heterocyclic bridging ligands, with variation at four points within the structure. The arene core may be a multitude of different aromatic rings, including benzene,[145, 147, 149, 150, 152, 155] naphthalene,[154] anthracene,[153] or even another heterocycle for example.[159, 160] The linker atom or spacer group, X, can be varied by changing both the type of atom and the length of the spacer. The latter change allows alterations to the flexibility of the ligand,[142, 152, 153, 161] whilst the former will allow the incorporation of further donors, such as oxygen or sulfur atoms.[142-145, 149] The heterocyclic group can also be varied, with a range of possibilities including pyridine, pyrazole and more recently quinoline.[155, 162] Finally, the number of groups (n), which are appended to the central ring system can be varied. The ligands investigated in this chapter have a structure that is schematically represented in Figure 3.1(b) and could incorporate all of the above variations.

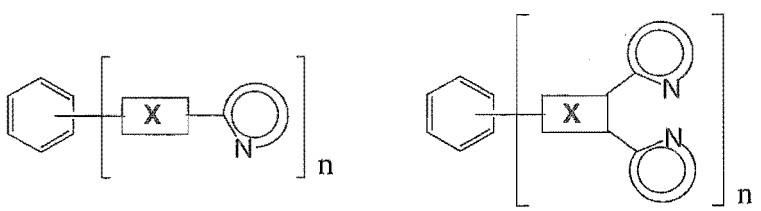


(a) (b)

**Figure 3.1.** (a) A generalised representation of the arene-based ligands previously prepared and (b) the extension to incorporate a symmetrical chelating group.

Using these types of ligands (Figure 3.1(a)), a large array of discrete one-, two- and three-dimensional metallosupramolecular aggregates have been prepared by simply mixing together the ligand with an appropriate metal salt. For example, reaction of silver salts with 1,4-bis(2-pyridyloxy)benzene (Figure 3.2(a)) leads to the self-assembly of a [2+2] dimer with intimate stacking of the central benzene rings of both ligands.[147] The naphthalene-based ligand, 1,5-bis(2-pyridyloxy)naphthalene, on mixing with silver nitrate, readily assembles into a one-dimensional coordination polymer with a zigzag shape.[163] In another example, the ligand 1,3-bis(3-pyridyloxy)benzene (Figure 3.2(c)) was employed in the first reported synthesis of a quadruple helicate by reaction with a palladium precursor.[152] This robust helicate can encapsulate anions of varying sizes, with a preference for perchlorate, by relaxation of the twisting of the helicate strands.

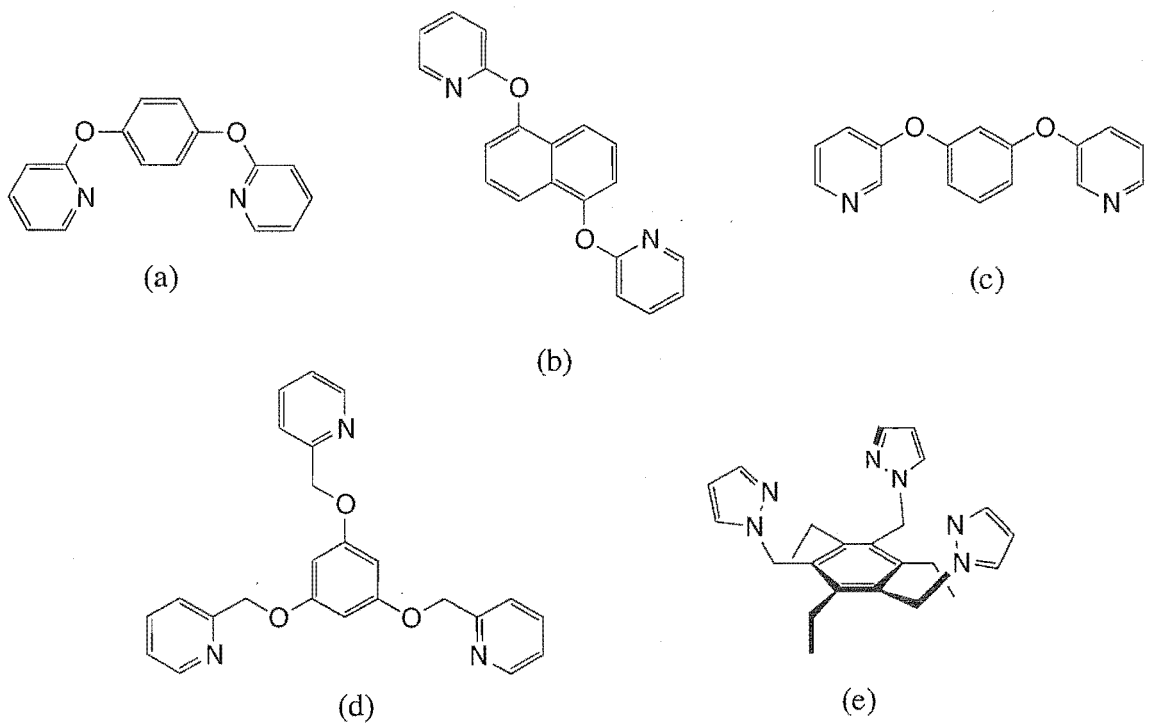


**Figure 3.2.** Some ligands from the Steel group with multisubstituted heteroaryl arenes.

Multisubstituted heteroaryl benzene ligands have also been prepared with greater conformational freedom. Using the phloroglucinol-based ligand (Figure 3.2(d)), Fitchett has demonstrated the formation of a dimetallomacrocyclic structure and a [6,3]-coordination net.[161] With another tri-substituted ligand, 1,3,5-tris(1-pyrazolylmethyl)-2,4,6-triethylbenzene (Figure 3.2(e)), Hartshorn has reported the formation of a highly symmetric $M_6L_4$ cage with the palladium centres in a pseudo-octahedral arrangement, and the benzene cores of the ligand creating a cavity with internal dimensions of 4.7 Å.[148] As many as eight arms have been appended to a central core, with the recent synthesis of octakis(2-pyridylsulfanylmethyl)biphenylene.[164]

One interesting feature of this chemistry is the potential for pre-organisation of the donors by using multisubstituted benzene cores, in particular the triethyl-core incorporated into both the compounds shown in Figure 3.3 and also in Figure 3.2(e). These, so-called, facially segregated cores have been employed in the synthesis of a range of ligand components for metallosupramolecular chemistry and in the synthesis of receptors.[141] The group of Raymond used the compound labelled (a) as a receptor for Fe(III), which was shown to have a selectivity toward Fe(III) that exceeded the iron scavenging siderophore, enterobactin.[137, 165] In contrast, the other compound was designed as an anion receptor, capable of being used as a chemosensor for quantifying citrate concentrations in beverages.[166]

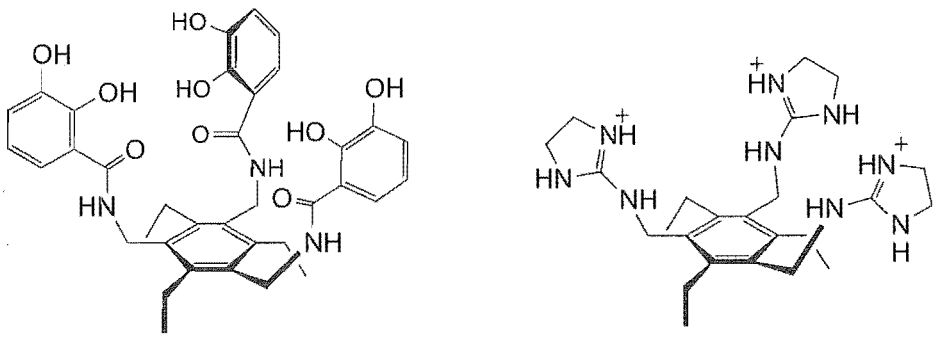


(a) (b)

**Figure 3.3.** Examples of the use of facially segregated arene cores.

One aspect of the arene-based ligands that has not been as extensively pursued is the incorporation of a symmetrical chelating group onto the arene core, through an individual linker atom. One such example of this coordination motif is the hexadentate ligand shown in Figure 3.4(a), which has been shown to form complexes with bidentate chelation of three copper atoms.[167] The use of unsymmetrical chelating groups has been described previously; for example 3-(2-pyridyl)pyrazole, which has been appended to benzene[156, 168] (Figure 3.4(b)), and the incorporation of thioethers into the arms of the ligand to provide further donor sites (c).[142, 144] Some arene-based ligands with flexible arms can function as chelating ligands, forming large chelate rings between adjacent arms of the ligand, as shown for the complex in Figure 3.4(d).[150]

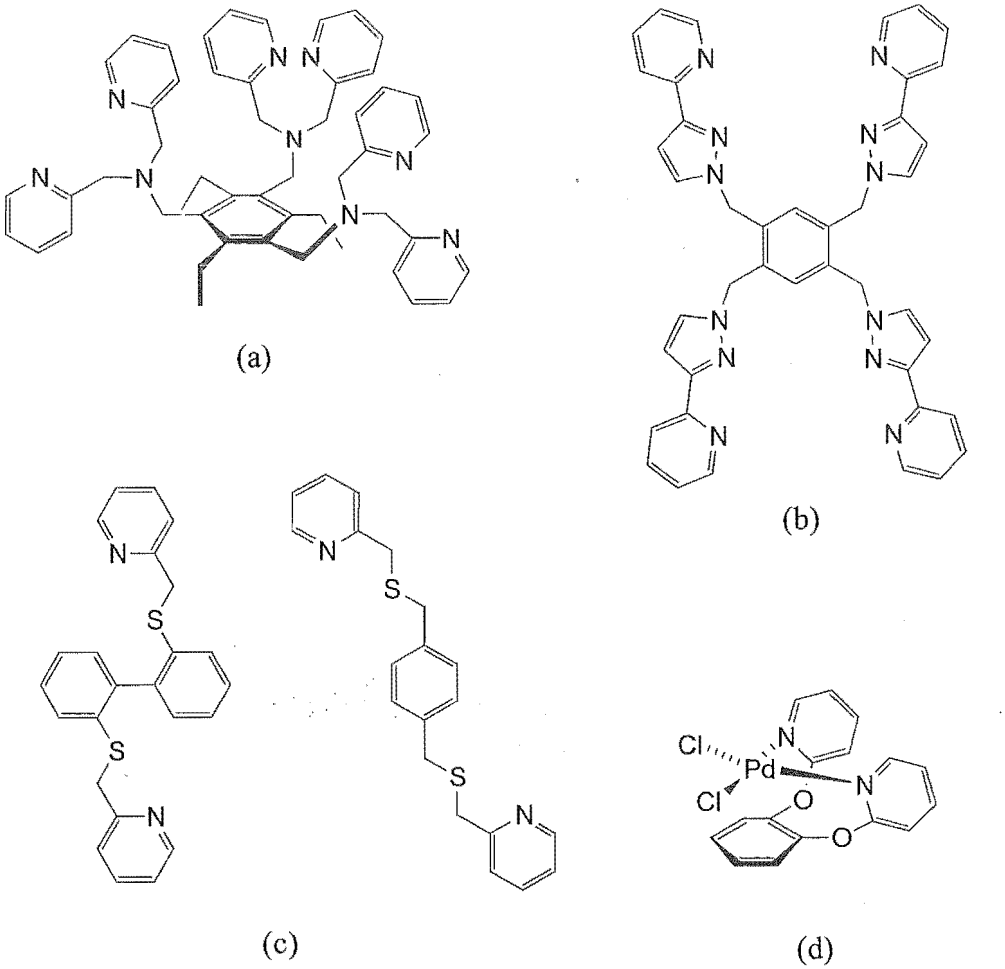


**Figure 3.4.** Some arene-based ligands with chelating heterocyclic groups appended.

The chelating subunit used in this chapter, di-2-pyridylamine, **3.1**, is a commercially available ligand that has been extensively used in coordination chemistry. It displays rich coordination chemistry and forms complexes with metals from all regions of the periodic table.[169] Until recently,[64, 65, 138, 139, 170, 171] there were limited reports of its use as a chelating unit in multidentate bridging ligands.

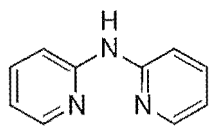

**3.1**

The first series of ligands described in this chapter, compounds **3.2** - **3.8**, are shown in Figure 3.5. All are based around arene cores to which have been appended two di-2-pyridylamine substituents to produce a series of potentially doubly bidentate bridging ligands. The first two examples, 1,4-bis(di-2-pyridylamino)benzene, **3.2**, and 4,4'-bis(di-2-pyridylamino)biphenyl, **3.3**, have been previously reported, and were prepared by condensing di-2-pyridylamine with the appropriate dibromo-substituted arene core.[64] The synthetic methodology used by these workers suggested that a range of potential ligands, with different structural arrangements of the di-2-

pyridylamine units about an aromatic core, could be prepared by variation of both the arene core and the substitution pattern.

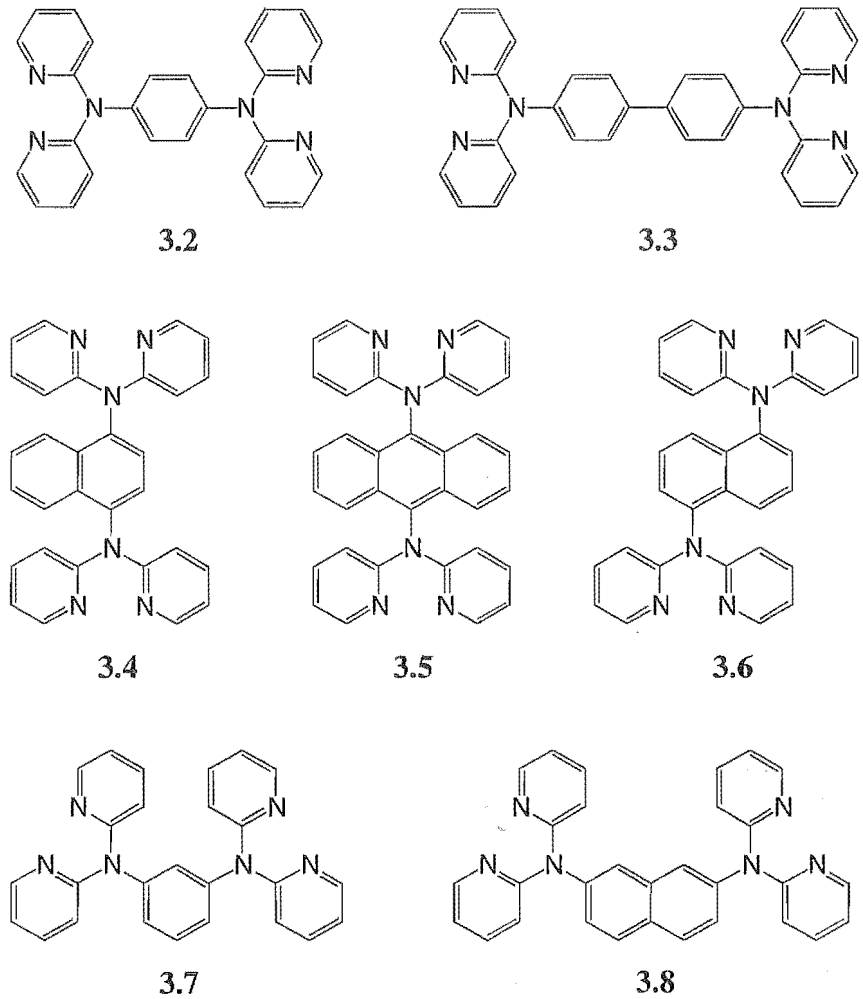


**Figure 3.5.** The doubly bidentate di-2-pyridylamino-based (N-linked) bridging ligands.

Therefore, the synthesis of some further examples of these ligands, 1,3-bis(di-2-pyridylamino)benzene, **3.7**, and 1,4-, 1,5- and 2,7-bis(di-2-pyridylamino)naphthalene, (**3.4**, **3.6**, and **3.8**, respectively) are described. The first five ligands in Figure 3.5, compounds **3.2** - **3.6**, all have the chelating unit on opposite sides of the central core. In contrast, compounds **3.7** and **3.8** have these units closer in space, which may introduce some degree of cooperativity into subsequent complexes of these compounds. Two attempted syntheses of compound **3.5** by different routes are also described in this chapter. An investigation of the coordination and metallosupramolecular chemistry of these ligands is described in Section 3.3, whilst in Section 3.5, the synthesis, NMR spectroscopy and electrochemistry of ruthenium complexes of these ligands are described.

Closely related to the above compounds are the two tritopic ligands, 1,3,5-tris(di-2-pyridylamino)benzene, **3.9**, and 2,4,6-tris(di-2-pyridylamino)-1,3,5-triazine, **3.10** (Figure 3.6). The synthesis of the tritopic ligand, **3.10**, is described in this chapter. During the course of this

research work, two alternative syntheses of **3.10** were reported in the literature.[139, 172] In one of these papers, the preparation of the closely related ligand, **3.9**, was also described.[139] Ligand **3.9** was prepared by this method and a study of the coordination and metallosupramolecular chemistry of both **3.9** and **3.10** is described in this chapter (Section 3.3).

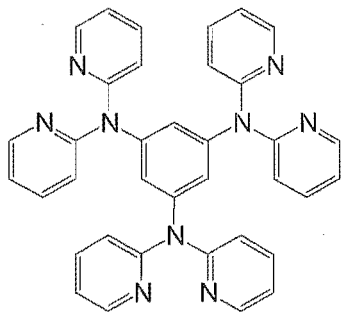

**3.9**

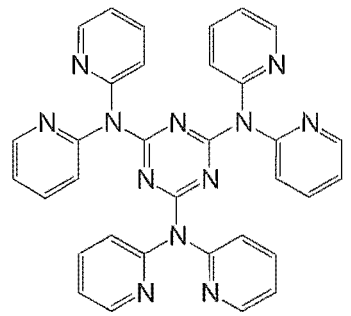

**3.10**

**Figure 3.6.** The tritopic bidentate bridging ligands prepared from di-2-pyridylamine.

Increasing the length of the spacer group leads to more flexible ligands, which, when used in coordination chemistry, can adopt many different conformations that are responsive to external stimuli, such as crystallisation.[142, 160, 173] These flexible ligands can lead to new and unusual structures, such as interpenetrating nets. Recently, highly flexible ligands with monodentate donor arms have been extensively investigated by Fitchett, who described a series of ligands with multi-atom spacer groups.[161] The compounds shown in Figure 3.7 all have aminomethyl

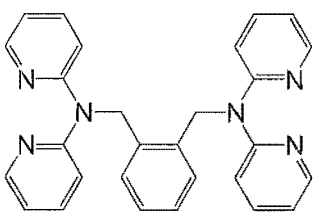

**3.11**

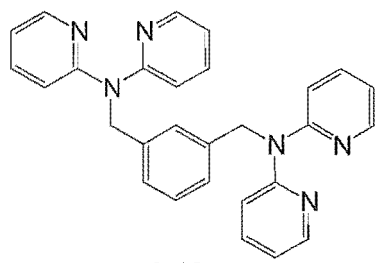

**3.12**

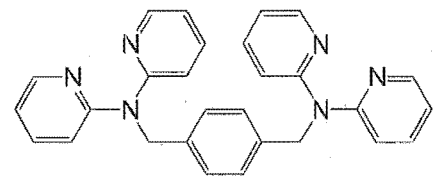

**3.13**

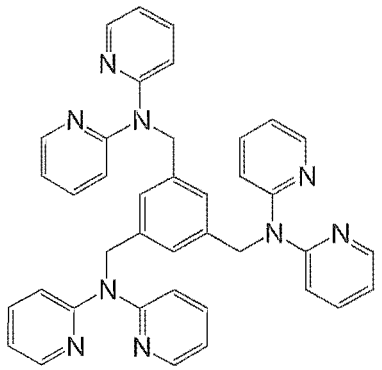

**3.14**

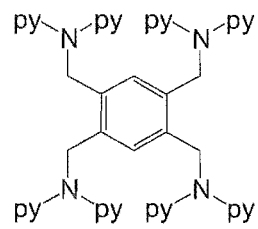

**3.15**

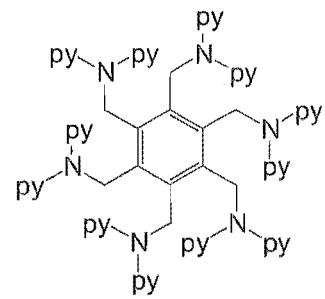

**3.16**

where py = 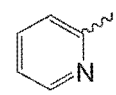

**Figure 3.7.** The aminomethyl-linked (N-$CH_2$) ligands **3.11** – **3.16**.

($N-CH_2$) spacer groups between the pyridine donors and the arene core of the ligand. The synthesis, coordination and metallosupramolecular chemistry of five of these ligands (**3.11** - **3.15**) is described, along with an attempted synthesis of the hexasubstituted benzene compound, **3.16**. Preliminary investigations into the syntheses of some potentially facially segregated analogues of **3.14** were also made, and these are briefly described.

## 3.2. Syntheses of the ligands

### 3.2.1 Synthesis of the amino-linked (N) ligands

The two ligands 1,4-bis(di-2-pyridylamino)benzene, **3.2**, and 4,4'-bis(di-2-pyridylamino)biphenyl, **3.3**, were prepared by literature procedures.[64] This involved a melt reaction of 1,4-dibromobenzene, or 4,4'-dibromobiphenyl, with **3.1**, potassium hydroxide and copper sulfate to give each ligand in *ca.* 30% yield.

The 1,4-disubstituted naphthalene-based ligand, 1,4-bis(di-2-pyridylamino)naphthalene, **3.4**, differs only in the fusion of an extra benzene ring to the core of the ligand. Using a similar melt reaction procedure, this new compound was synthesised by a two step process. Despite prolonged reaction times, this compound could not be prepared in a single step. Thus, the mono-substituted compound was prepared by the method shown in Scheme 3.1, in 31% yield, and then reacted under identical conditions to give a 33% yield of **3.4**. The yields for these two reactions were not entirely satisfactory, but the simplicity of the chemistry means that ample material was easily prepared for an investigation of the coordination and metallosupramolecular chemistry.

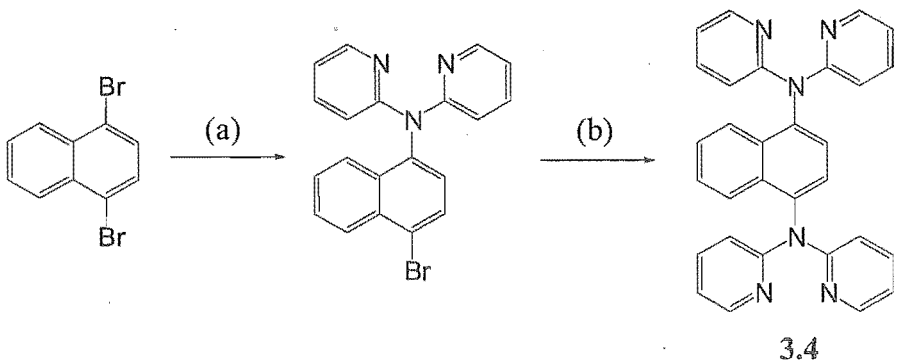


**3.4**

(a) di-2-pyridylamine, $CuSO_4$, KOH, 31%; (b) di-2-pyridylamine, $CuSO_4$, KOH, 33%.

**Scheme 3.1**

The analogous reaction for the synthesis of 9,10-bis(di-2-pyridylamino)anthracene, **3.5**, failed to give any product. This may be due to two factors; one applicable to the general reaction and a second, more specific problem with the desired compound. The latter problem is that

nucleophilic attack by di-2-pyridylamine on the anthracene core may be sterically hindered, more so than for the naphthalene core in compound **3.4**. However, the more general problem is the type of reaction that was used for the synthesis of compounds **3.2**, **3.3** and **3.4**. Nucleophilic substitution of arenes is a relatively unfavourable reaction, usually requiring the presence of strongly electron withdrawing substituents. While nucleophilic substitution of the arenes has succeeded for the three compounds prepared above, a more logical approach would be the alternative process where nucleophilic substitution occurs at the π-deficient pyridine ring. Therefore, another method was sought for the synthesis of the remaining compounds.

Palladium-catalysed amination of heterocycles has been extensively investigated[174, 175] and reviewed.[176] The amination chemistry has been utilised by a number of groups in natural product synthesis, in materials science and in the synthesis of chelating ligands for use in coordination chemistry.[176, 177] The initial catalysts, designed and used for the amination of aryl systems, used weakly coordinating phosphine ligands that were easily displaced by the better pyridine donors.[174] However, in recent years chelating phosphine ligands like 2,2'-bis(diphenylphosphino)-1,1'-binaphthyl (BINAP) and 1,3-bis(diphenylphosphino)propane (DPPP) have been used to generate more robust palladium catalysts for reactions involving heterocycles.

Therefore, a $[Pd_2(dba)_3]$/BINAP catalyst system was employed for the synthesis of 1,5-bis(di-2-pyridylamino)naphthalene, **3.6**, as shown in Scheme 3.2. All reactants, except 2-bromopyridine, were dissolved in dry toluene under an argon atmosphere. After several minutes stirring, 2-bromopyridine was added and the reaction heated at 80°C for 4 days. Despite a relatively high catalyst loading (2 mol% Pd), the reaction proceeded to give **3.6** in 54% yield. The reaction was not optimised, but by altering the co-ligands for the catalyst and optimising the reaction conditions, there is potential to improve the yields of this, and later reactions.

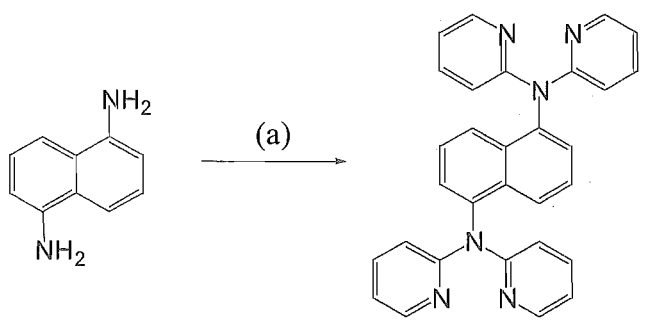


**3.6**

(a) 2-bromopyridine, BINAP, $[Pd_2(dba)_3]$, toluene, 54%.

**Scheme 3.2.**

Crystal Structure of **3.6**

Crystals of **3.6** were obtained during recrystallisation and the structure was determined by X-ray crystallography. The compound crystallised in the monoclinic space group $P2_1/n$ with two molecules of **3.6** contained in the unit cell. It was anticipated that the potential ligand would pack in a relatively flat conformation in the solid state, with slight twists of the pyridine rings to relieve steric hindrance between the H3 protons of the pyridine ring and the arene core. Instead, the di-2-pyridylamine units twist almost perpendicular to the naphthalene core, as shown in Figure 3.8, and adopt a similar conformation to that reported for **3.3** in a crystal structure described by Wang and coworkers.[64] One pyridine ring on each arm of the ligand twists away to relieve the lone-pair repulsion between the nitrogen atoms. The pyridine rings of adjacent molecules of **3.6** pack on either face of the naphthalene ring, within the cavity formed by pairs of pyridine rings.

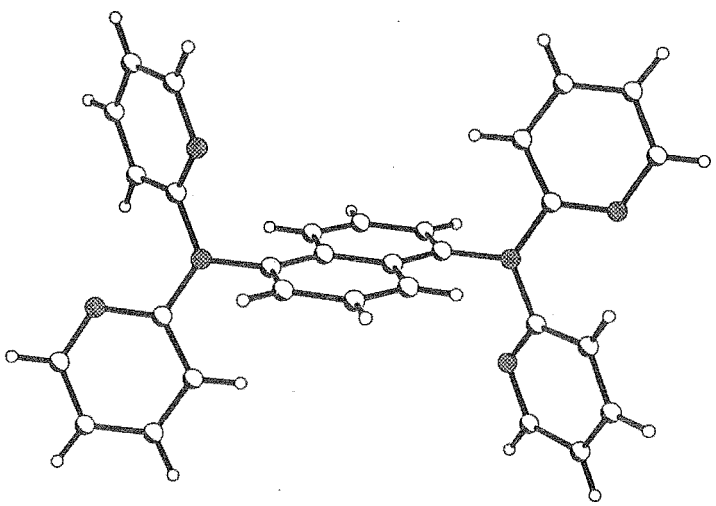

**Figure 3.8.** A perspective view of **3.6** illustrating the dramatic twisting of the di-2-pyridylamine fragments relative to the arene core.

Using the same methodology as above, the ligands **3.7** and **3.8** were prepared in 48% and 50% yield, respectively (Scheme 3.3). In contrast to the other compounds described above, both these ligands have the di-2-pyridylamine substituents on the same side of the arene core, which may have some interesting consequences in coordination complexes of these compounds. However, **3.8** has the di-2-pyridylamine groups on separate rings of the naphthalene core, whereas **3.7** has both di-2-pyridylamine groups located on the same ring, which may lead to co-operative binding between the two coordination sites.

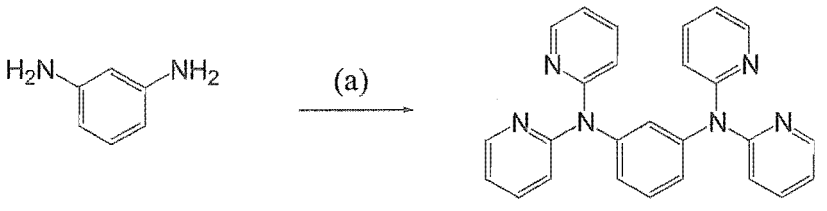

**3.7**

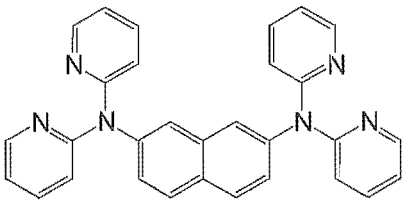

**3.8**

(a) 2-bromopyridine, BINAP, $[Pd_2(dba)_3]$, toluene, **3.7**: 48%; **3.8**: 50%.

**Scheme 3.3.**

The trisubstituted benzene and triazine ligands described in this chapter have a very similar arrangement of the pyridine rings about a central core as the [3]radialene ligands discussed in Chapter 2. 1,3,5-Tris(di-2-pyridylamino)benzene, **3.9**, and 2,4,6-tris(di-2-pyridylamino)-1,3,5-triazine, **3.10**, can be prepared by reaction of di-2-pyridylamine with 1,3,5-tribromobenzene and cyanuric chloride, respectively. Ligand **3.10** was prepared by heating a mixture of di-2-pyridylamine, cyanuric chloride, sodium carbonate, copper powder and potassium bromide in mesitylene to give **3.10** in 27% yield (Scheme 3.4). Compound **3.9** was prepared by a literature procedure[139] in a similar manner to **3.10**, starting with 1,3,5-tribromobenzene in place of cyanuric chloride, and using copper sulfate, instead of copper powder, as the catalyst. In a paper concerning 'starburst' compounds,[139] the crystal structures of both **3.9** and **3.10** revealed that the compounds not only have closely-related structures, but also adopt solid-state conformations that are very similar to those observed for the [3]radialene based-compounds previously discussed in Chapter 2.

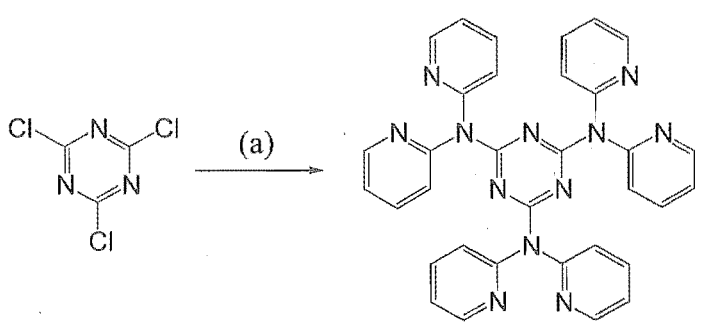

**3.10**

(a) di-2-pyridylamine, $Na_2CO_3$, Cu powder, KBr, mesitylene, 29%.

**Scheme 3.4.**

### 3.2.2 Synthesis of the aminomethyl-linked (N-$CH_2$) ligands

The aminomethyl-linked series of ligands, **3.11**-**3.15**, shown earlier in Figure 3.5, are readily prepared from the appropriately substituted bromomethylbenzene compounds in one step. These compounds incorporate an aminomethyl spacer that provides greater flexibility to the ligand than the series of amino-linked ligands described in the preceding section.

The starting material for the synthesis of **3.11**, 1,2-bis(bromomethyl)benzene, is commercially available, whereas the starting materials for the synthesis of the other related ligands were prepared by literature procedures.[178-180] The synthesis of **3.13** is shown in Scheme 3.5, typifying the approach used here. Starting with *p*-xylene, which was brominated by reaction with N-bromosuccinimide (NBS) in water, 1,4-bis(bromomethyl)benzene was obtained in 42% yield. This compound was reacted with 2.2 equivalents of **3.1** in DMSO solution, using potassium hydroxide as the base. Addition of water led to a bright yellow precipitate that was collected, and washed with water and ethyl acetate, to give **3.13** in 40% yield. The other two bis(di-2-pyridylaminomethyl)benzene compounds, **3.11** and **3.12**, were prepared in moderate yields of 25% and 53%, respectively. The trisubstituted compound, **3.14**, was obtained by a similar procedure in 49% yield, while **3.15** was isolated in 34% yield. The isolated yields of these reactions may be lowered by the solubility of the products in DMSO.

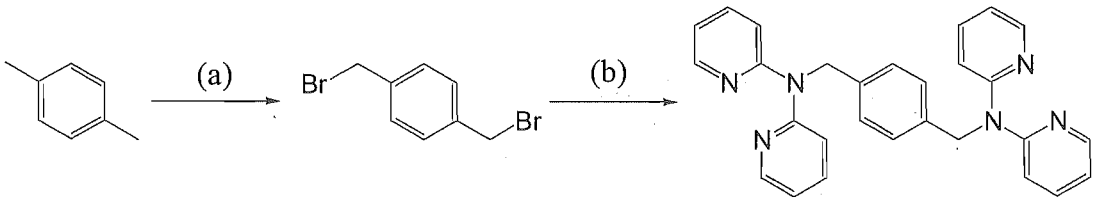


**3.13**

(a) $Br_2$, NBS, water, 42%; (b) di-2-pyridylamine, KOH, DMSO, 40%.

**Scheme 3.5.**

Crystal Structures of **3.11** and **3.13**

Crystals of the majority of these ligands were obtained by recrystallisation, or in the process of studying their coordination chemistry. However, by comparison to rigid bridging ligands, only limited information can be drawn from the crystal structures of flexible compounds such as these. Thus, the structures are not described in any significant detail. The structure of **3.11**, which crystallises in the triclinic space group, P-1, is shown in Figure 3.9. Like the amino-linked ligand, **3.6**, in the preceding section, the di-2-pyridylamine substituents are twisted perpendicular to the arene core of the ligand. One feature of these ligands worth noting is that, like other ligands with an amine nitrogen linker atom described in this thesis, the nitrogen atom has an $sp^2$-

geometry, with bond angles for N(11) and N(12) of between 114.03(12) and 124.06(13)°. The other bond lengths and angles are typical for such a compound. Weak intramolecular (pyridine)N···H-C(methylene) interactions, with N···H distances of between 2.24(7) and 2.44(7) Å, may stabilise this conformation and complementary intermolecular contacts of this nature also occur between adjacent molecules in the structure. This type of hydrogen-bonding synthon has been recently reviewed.[14]

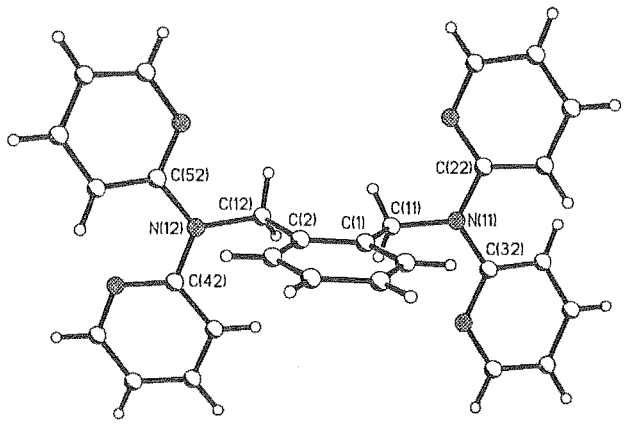


**Figure 3.9.** A perspective view of **3.11** showing the perpendicular arrangement of the di-2-pyridylamine substituents relative to the benzene core. Selected bond lengths (Å) and angles (°): N(11)-C(32) 1.405(2), N(11)-C(22) 1.418(2), N(11)-C(11) 1.4674(19), N(12)-C(42) 1.404(2), N(12)-C(52) 1.419(2), N(12)-C(12) 1.4689(19), C(32)-N(11)-C(22) 122.67(13), C(32)-N(11)-C(11) 118.75(13), C(22)-N(11)-C(11) 118.11(12), N(11)-C(11)-C(1) 114.92(12), C(42)-N(12)-C(52) 124.06(13), C(42)-N(12)-C(12) 117.49(13), C(52)-N(12)-C(12) 118.15(13), N(12)-C(12)-C(2) 114.03(12).

The structure of ligand **3.13** is shown in Figure 3.10. Compound **3.13** crystallises in the monoclinic space group $P2_1/n$, with half a molecule in the asymmetric unit. The same twisting of the chelating fragment of the molecule is observed in this structure, but the packing appears to be governed by weak C-H···π interactions rather than C-H···N interactions. Adjacent molecules make complementary C-H···π interactions (D = 3.746 Å, d = 2.881 Å) between the pyridine-H6 of one molecule and the benzene ring of another. The same planarity of the $sp^2$ nitrogen linker atom is observed in this structure.

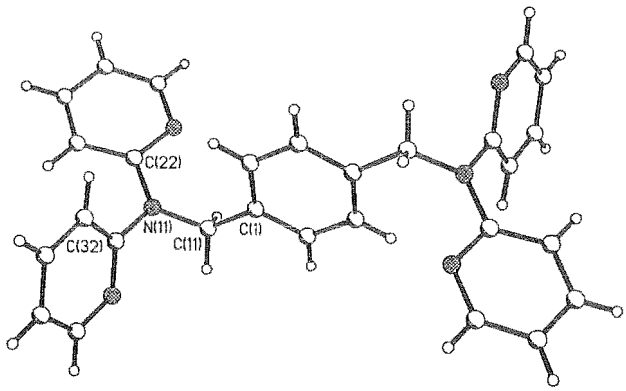


**Figure 3.10.** A perspective view of **3.13** showing the perpendicular arrangement of the di-2-pyridylamino substituents relative to the benzene core. Selected bond lengths (Å) and angles (°): N(11)-C(22) 1.3944(16), N(11)-C(32) 1.4157(15), N(11)-C(11) 1.4666(15), C(22)-N(11)-C(32) 122.03(10), C(22)-N(11)-C(11) 120.32(10), C(32)-N(11)-C(11) 117.55(10), N(11)-C(11)-C(1) 114.39(10).

The syntheses of four further potential ligands were also attempted. The synthesis of the multi-armed ligand, hexakis(di-2-pyridylaminomethyl)benzene, **3.16**, was tried using the standard methodology. Unfortunately, the product of this reaction is an extremely insoluble solid, the identity of which could not be confirmed. Other examples of multi-substituted ligands have been prepared, combining this core with relatively bulky substituents, without any solubility problems. Attempts at preparing complexes of this compound to aid characterisation were unsuccessful.

The syntheses of three related compounds, shown in Figure 3.11, were attempted using similar methodology. The synthesis of 1,2,3,4-tetrakis(di-2-pyridylaminomethyl)benzene, **3.17**, was problematic, with mixtures of lesser substituted compounds forming in preference to the desired compound. The interest in compounds, **3.18** and **3.19**, arises from the potential for pre-

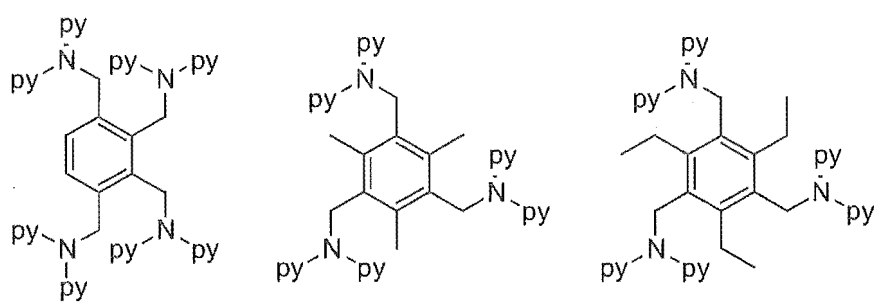

**3.17** **3.18** **3.19**

**Figure 3.11.** An example of potential ligands incorporating cores allowing for pre-organisation and facial segregation of the donor arms.

organisation that has been shown to occur in related ligands. Unfortunately however, the synthesis of the less sterically demanding of the two compounds, **3.18**, was unsuccessful under the reaction conditions used for the synthesis of the other N-$CH_2$ ligands, even when the reaction was heated under nitrogen for prolonged periods. For that reason, the synthesis of **3.19** was not attempted by that method. An improved method might be to use the amination methodology described above to couple the appropriate triamine with 2-bromopyridine. This was not attempted.

## 3.3. Coordination and metallosupramolecular chemistry of the N-linked ligands

The ligands described in this chapter were investigated from two perspectives. They all possess the di-2-pyridyl chelating motif that characterises most ligands in this thesis, and thus, the coordination chemistry was investigated for comparison to the ligands in Chapter 2. The amine linker atom is $sp^2$-hybridised and unlikely to be a potential donor in these complexes. However, all the ligands have an arene core, which may play a role in controlling the types of structures formed with these ligands through weak $\pi$-$\pi$ and silver-arene $\pi$-interactions, leading to some interesting supramolecular chemistry. To study these aspects, the potential ligands were each reacted with a range of different metal salts, where both the metal ion and the anion were varied. Silver salts with coordinating and non-coordinating anions were used to probe the anion dependency of certain structures where possible. Changing from silver to copper, palladium or zinc varied the geometry and coordination number of the metal component.

### 3.3.1 Complexes of 1,4-bis(di-2-pyridylamino)benzene, 3.2

In the paper where the authors reported the synthesis of compound **3.2**, they also described the synthesis and characterisation, by X-ray crystallography, of a praseodymium complex. In this complex the ligand acts as a symmetrical tetradentate bridge between two praseodymium atoms. The remaining coordination sites of the praseodymium are occupied by three hexafluoroacetylacetonate anions.[64] On the basis of this work, the ligand was expected to form symmetrical dinuclear complexes when reacted with a range of first and second row transition metals. Thus, the coordination chemistry of **3.2** was investigated by the formation of complexes with silver nitrate, silver tetrafluoroborate, silver hexafluorophosphate, copper nitrate, palladium chloride and zinc chloride.

Reaction of silver nitrate with **3.2** provided a silver nitrate complex, **3.20**, with a 1:1 metal-ligand stoichiometry, as determined by elemental analysis. Such a composition suggested that **3.20** was likely to be a discrete [2+2] dimer or polymeric in nature. Fortunately, colourless crystals were obtained directly from the reaction mixture and these were suitable for crystal structure analysis. Reaction of **3.2** with silver tetrafluoroborate also gave colourless crystals by slow evaporation of the acetonitrile reaction medium. This second silver complex, **3.21**, was characterised by elemental analysis and X-ray crystallography with a 2:1 metal to ligand stoichiometry. The reaction of **3.2** with silver hexafluorophosphate resulted only in the formation of black solids and was not pursued.

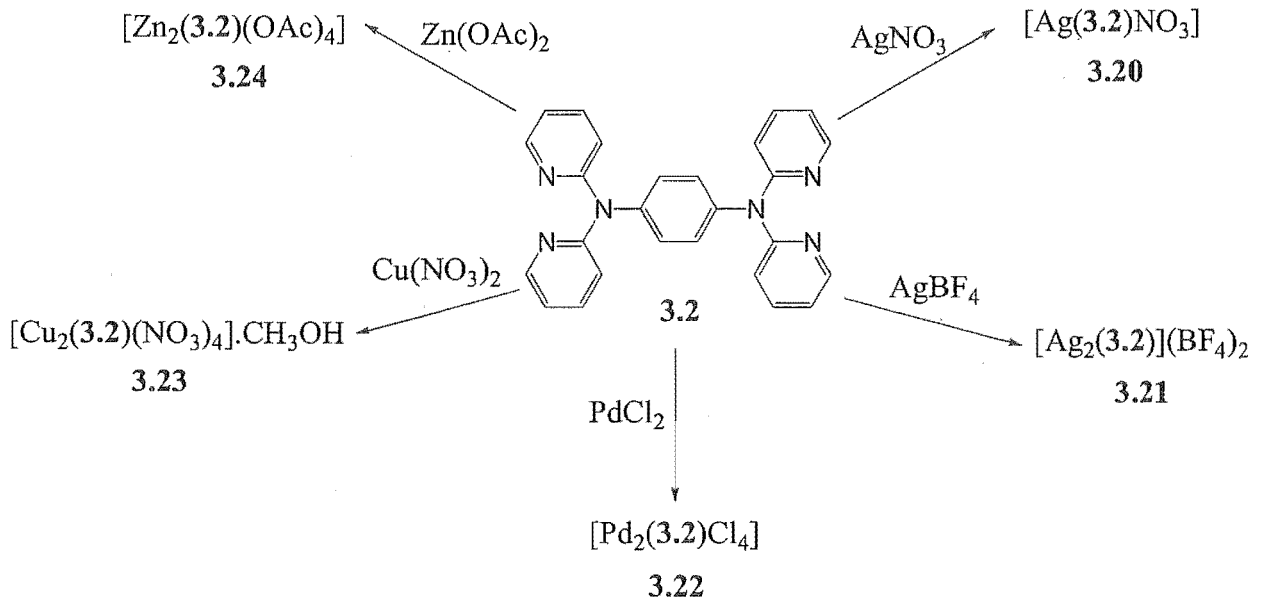


**Scheme 3.6.**

Reaction of **3.2** with palladium chloride, copper nitrate and zinc acetate gave three complexes, **3.22**, **3.23** and **3.24**, respectively. Complex **3.22** was obtained as a bright yellow solid by combining a solution of palladium chloride in 2 M hydrochloric acid with a solution of **3.2** in methanol. This complex gave an elemental analysis consistent with a discrete dinuclear complex, $[Pd_2(\mathbf{3.2})Cl_4]$, but was insoluble in common NMR solvents and no further characterisation was undertaken. The copper nitrate complex, **3.23**, was isolated as a green solid from the methanol reaction medium and small green crystals, suitable for crystal structure analysis, were obtained by vapour diffusion of acetone into a DMSO solution of the complex. Elemental analysis was consistent with a dinuclear copper complex, $[Cu_2(\mathbf{3.2})(NO_3)_4].CH_3OH$. Combining methanol solutions of zinc acetate and **3.2**, followed by slow evaporation of the solvent, provided crystals of complex **3.24**, which was also characterised by X-ray crystallography. However, while the bulk sample gave an elemental analysis more consistent

with a zinc acetate complex, the crystal structure described below, has chloride anions that presumably originate from contamination of either of the two starting materials.

Crystal structure of **3.20**

The overall structure of the silver nitrate complex, **3.20**, is a one-dimensional zigzag coordination polymer with a 1:1 ratio of metal to ligand. The complex crystallises in the triclinic space group P-1, with two half ligand components, one silver atom and a coordinated nitrate anion in the asymmetric unit (Figure 3.12). Both half ligand components lie on centres of inversion, located at the centroids of the benzene rings. Each ligand molecule coordinates to two symmetry-related silver atoms with silver-nitrogen distances of 2.261(3) and 2.263(2) Å, while the oxygen of the coordinated nitrate anion is bonded 2.418(2) Å from the silver atom, which gives a distorted trigonal-planar geometry. Each ligand is hypodentate with only two of the four pyridine rings involved in coordination.

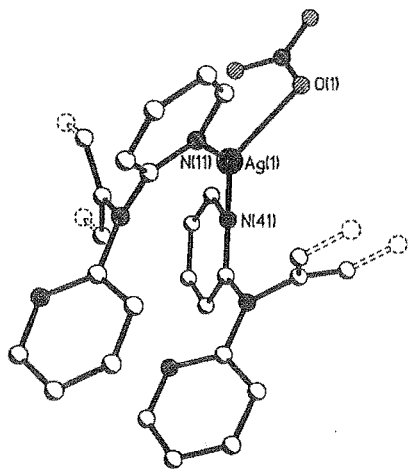


**Figure 3.12.** A perspective view of the asymmetric unit of complex **3.20**. Selected bond lengths (Å) and angles (°): Ag(1)-N(41) 2.261(3), Ag(1)-N(11) 2.263(2), Ag(1)-O(1) 2.418(2), N(41)-Ag(1)-N(11) 147.79(8), N(41)-Ag(1)-O(1) 111.55(9), N(11)-Ag(1)-O(1) 100.37(9).

As Figure 3.13 illustrates, the extended structure is a one-dimensional zigzag coordination polymer. The relatively short distances of 6.832(1) and 6.955(1) Å separate the two silver atoms because the coordinated pyridine rings twist back toward and interact with the core of the ligand. Weak silver-arene $\pi$-interactions may further shield the silver atom, although the shortest Ag-C distance is 2.965 Å, indicating that these are very weak secondary interactions. The average distance for such interactions is *ca.* 2.82 Å.[20, 181] There are no unusually short intermolecular contacts between adjacent polymer chains.

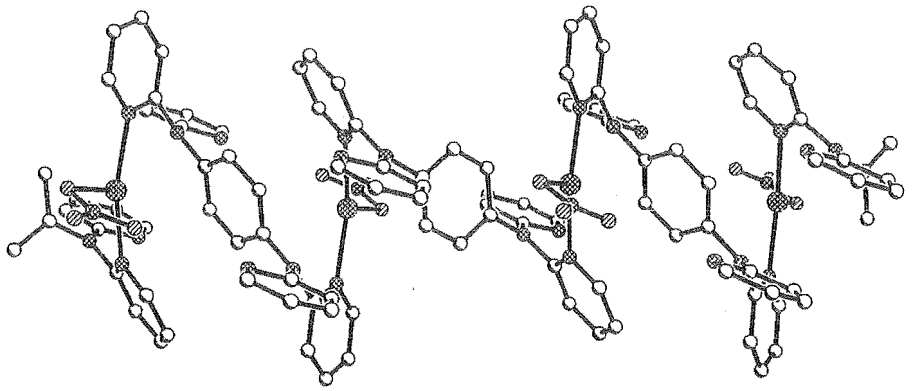

**Figure 3.13.** A perspective view of the one-dimensional zigzag coordination polymer **3.20**, with the nitrate anions alternating on opposite sides of the plane of the page.

Crystal structure of **3.21**

The structure of complex **3.21** is also a one-dimensional coordination polymer like **3.20**, but with a 2:1 metal to ligand stoichiometry. The asymmetric unit of the complex, which crystallises in the space group C2/c, is shown in Figure 3.14, consisting of half a ligand molecule, two half occupied silver atoms that lie on a 2-fold axis, a coordinated acetonitrile and a disordered tetrafluoroborate anion (not shown). The two silver atoms have very different coordination

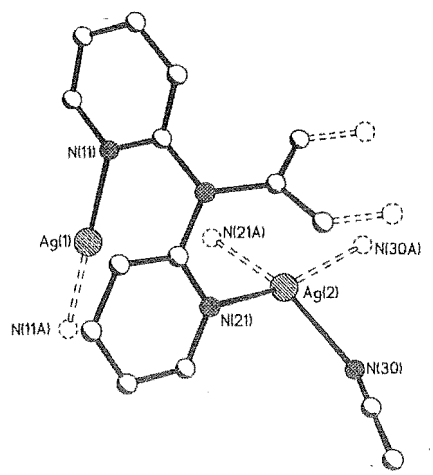


**Figure 3.14.** A perspective view of the asymmetric unit of **3.21** with the hydrogen atoms and the disordered tetrafluoroborate anion omitted for clarity. Selected bond lengths (Å) and angles (°): Ag(1)-N(11) 2.162(2), Ag(2)-N(30) 2.403(3), Ag(2)-N(21) 2.429(2), N(11)-Ag(1)-N(11A) 179.90(10), N(30A)-Ag(2)-N(30) 91.82(12), N(30)-Ag(2)-N(21) 89.72(8), N(30)-Ag(2)-N(21A) 160.20(7), N(21)-Ag(2)-N(21A) 95.46(9).

numbers and geometries; Ag(1) has a linear two-coordinate geometry with a comparatively short Ag-N distance of 2.162(2) Å, whereas Ag(2) has a distorted square-planar geometry. The silver nitrogen distances are considerably longer for the four-coordinate Ag(2), with a Ag(2)-N(21) distance of 2.429(2) Å and a Ag(2)-N(30) distance of 2.403(3) Å.

An extended view of the structure shows that each ligand molecule coordinates to four silver atoms to form a novel one-dimensional 'ladder-like' coordination polymer (Figure 3.15). The ligand molecules lie approximately perpendicular to the direction of propagation of the polymer chain and act as 'rungs', with 12-membered dimetallocycles formed from the two silver atoms acting as the sides of the 'ladder-like' structure. The coordinated acetonitrile molecules occupy the cavities between the benzene rings of the adjacent ligands.

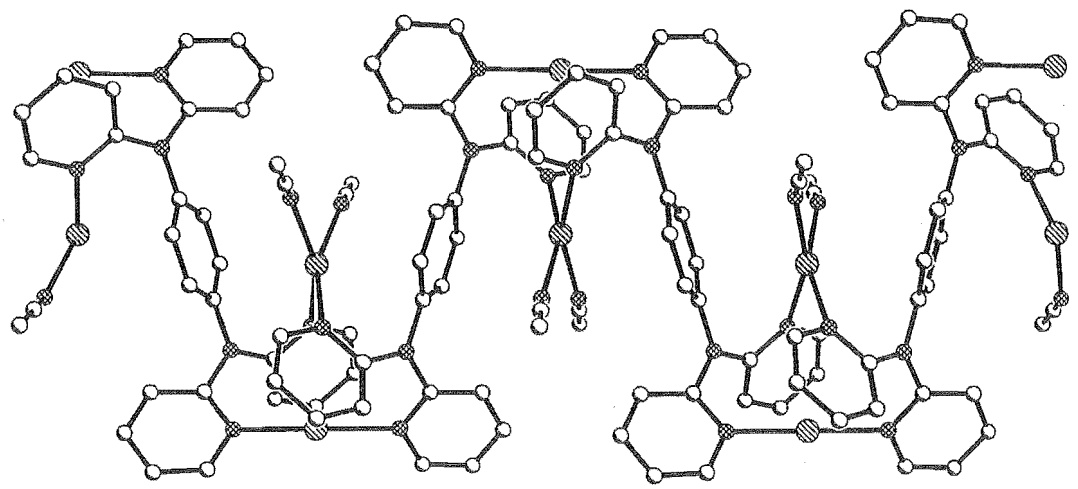

**Figure 3.15.** A perspective view of the extended structure of the one-dimensional 'ladder-like' coordination polymer **3.21**.

There are several unusual and interesting features of this structure. The silver atom, Ag(2) has a relatively unusual square-planar geometry, with silver generally preferring tetrahedral four coordinate geometries.[18] However, when weaker supramolecular interactions are considered, the silver has a pseudo-octahedral geometry, with weak silver-arene π-interactions provided by the benzene rings on either side of Ag(2). The shortest Ag-C distance is 2.975(3) Å to the more electron rich C1 and C4 carbon atoms of the benzene rings. The linear coordination geometry of Ag(1) is also complemented by similar interactions from the surrounding pyridine rings. The shortest Ag-C distance is 2.831(3) Å to the C2 position of the adjacent pyridine ring. These are similar distances to other silver-arene π-interactions.[20]

The silver atoms within the asymmetric unit, Ag(1) and Ag(2), are 4.323(1) Å apart indicating no silver-silver interactions within the complex. The pseudo-octahedral silver atoms are 6.442(1) Å apart, with the vector between these atoms passing directly through the benzene ring of the ligand, lending support to the proposed pseudo-octahedral geometry and the weak silver arene coordination. The silver-silver distance between the two-coordinate silver atoms bridged by a single ligand is 11.386(1) Å.

In the crystal the coordination polymers propagate along the *c*-axis of the unit cell with the non-coordinated tetrafluoroborate anions filling the voids between the polymers. The coordinated acetonitrile molecules protrude out of the polymers and the methyl groups make weak contacts with the fluoride atoms of the tetrafluoroborate anions. These C-H···F hydrogen bonding interactions have H-F distances in the range 2.380 - 2.423 Å, which is similar to other reported examples,[182] and less than the sum of the van der Waals radii for H and F atoms of 2.54 Å.[183]

Crystal Structure of **3.23**

The structure of **3.23** is a discrete dinuclear complex, as shown in Figure 3.16. The asymmetric unit contains half a molecule of **3.2**, a copper atom, two coordinated anions and a coordinated DMSO solvate molecule. The two copper atoms in the structure are related by a

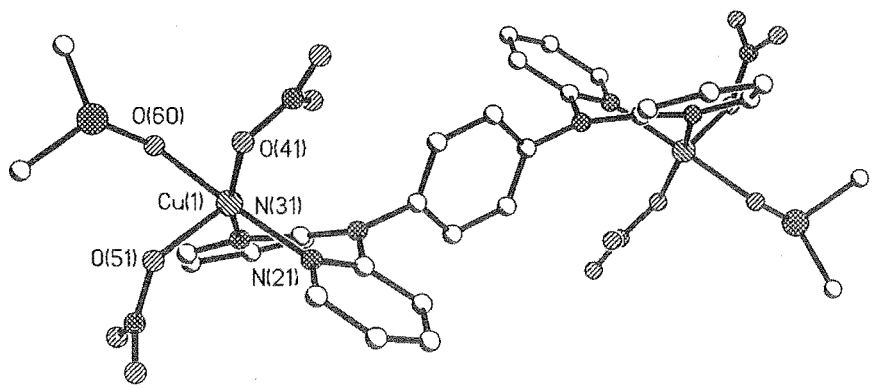


**Figure 3.16.** A perspective view of the copper nitrate structure **3.23**. Selected bond lengths (Å) and angles (°): Cu(1)-O(60) 1.949(6), Cu(1)-N(21) 1.963(6), Cu(1)-N(31) 2.021(7), Cu(1)-O(41) 2.028(6), Cu(1)-O(51) 2.235(6), O(60)-Cu(1)-N(21) 174.2(3), O(60)-Cu(1)-N(31) 88.5(2), N(21)-Cu(1)-N(31), 87.0(2), O(60)-Cu(1)-O(41) 92.4(2), N(21)-Cu(1)-O(41) 90.7(2), N(31)-Cu(1)-O(41) 161.9(2), O(60)-Cu(1)-O(51) 91.5(2), N(21)-Cu(1)-O(51) 93.8(2), N(31)-Cu(1)-O(51) 117.0(2), O(41)-Cu(1)-O(51) 81.0(2).

centre of inversion lying at the centroid of the benzene ring of the ligand. The copper atom has a geometry best described as square-pyramidal, with a $\tau$ value of 0.21. The nitrate oxygen, O(51), is in the apical coordination site with a Cu-O distance of 2.235(6) Å. The copper-copper distance in this complex is 11.179(2) Å, and considerably longer than the silver-silver distance in complex **3.20**, because the pyridine donors are directed away from the core of the ligand.

The six-membered chelate rings have a twist-boat conformation because the amine nitrogen of the ligand is $sp^2$-hybridised and planar. The planes of the chelating domains of the ligand and the benzene core of the ligand are perpendicular, as is observed for related complexes.[65] The ligand uses all its potential donor atoms in this and the subsequent zinc complex, in contrast to the first silver complex, **3.20**, where the ligand is hypodentate. No unusually short contacts dominate the packing of this complex.

Crystal Structure of **3.24**

A perspective view of complex **3.24** is shown in Figure 3.17, with the ligand bridging two symmetry-related zinc atoms. The geometry of the zinc atom is tetrahedral with no unusual bond lengths or angles. The chelating di-2-pyridylamine unit is again perpendicular to the benzene core of the ligand, as was observed in the previous complex, **3.23**. By contrast to the coordination polymer **3.20**, where the monodentate pyridine donors twist back towards the core of the ligand, the metal-metal distance in this complex is considerably longer (11.839(1) Å).

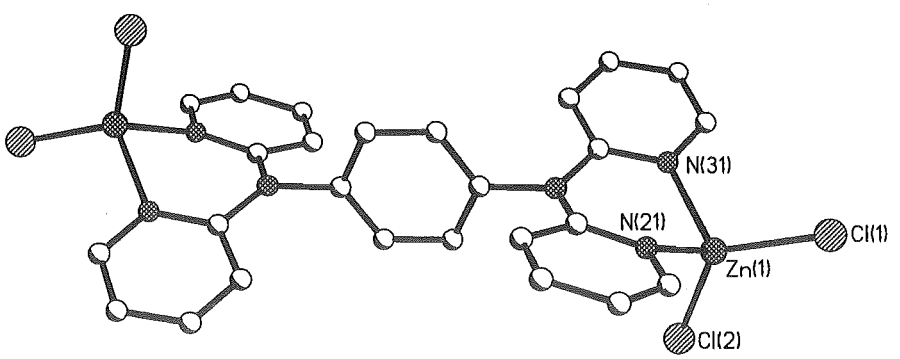


**Figure 3.17.** A perspective view of the structure of the chloro-analogue of complex **3.24** with selected atom labelling. Selected bond lengths (Å) and angles (°): Zn(1)-N(31) 2.033(3), Zn(1)-N(21) 2.065(3), Zn(1)-Cl(1) 2.2371(11), Zn(1)-Cl(2) 2.2462(15), N(31)-Zn(1)-N(21) 88.90(10), N(31)-Zn(1)-Cl(1) 112.62(8), N(21)-Zn(1)-Cl(1) 109.16(8), N(31)-Zn(1)-Cl(2) 109.91(8), N(21)-Zn(1)-Cl(2) 107.73(7), Cl(1)-Zn(1)-Cl(2) 123.04(5).

A consideration of the packing reveals there are no unusually short intermolecular contacts in the structure. During the writing of this thesis, a dinuclear zinc trifluoroacetate complex was described with a closely related ligand that has a diphenylacetylene core.[65] This complex has a very similar metal atom geometry and conformation to the zinc complex described here.

Until this work, no coordination polymers have previously been characterised with **3.2**. The reason they were prepared in this work is in part reflective of the coordination requirements of silver, one of the metals routinely employed for preparing coordination polymers. To produce a coordination polymer with a doubly bidentate bridging ligand, the connecting silver atom must have a four-coordinate geometry, as was observed for **3.21**, or the ligand must be hypodentate, as is the case in **3.20**. With the other metals used, which have coordinating anions, dinuclear complexes are preferred.

Like the previously characterised praseodymium complex,[64] the zinc and copper complexes described in this chapter have the metals in a *trans* conformation. In the praseodymium complex the Pr-Pr distance is 10.090(3) Å, which is a shorter distance than in the two dinuclear complexes described here, because the chelate ring is in a conformation whereby the praseodymium atoms are twisted back toward the core of the ligand. The dinuclear complexes, **3.23** and **3.24**, bear similarities to dinuclear complexes of ligands **2.2** and **2.4** described in Chapter 2. These also have the less sterically hindered *trans* arrangement of the metal centres, but considerably shorter metal-metal distances because of the shorter bridge between the chelating units.

### 3.3.2 Complexes of 4,4'-bis(di-2-pyridylamino)biphenyl, 3.3

Like the benzene-spaced ligand, the coordination chemistry of **3.3** was investigated by the formation of complexes with silver nitrate, silver tetrafluoroborate, silver hexafluorophosphate, copper nitrate, and palladium chloride. Unfortunately, while a number of complexes were isolated, the majority of them were formed in relatively poor yield and often not as crystalline samples. Reaction of **3.3** with silver nitrate and silver tetrafluoroborate led only to decomposition, while with silver hexafluorophosphate a complex was isolated that could not be satisfactorily purified.

Reacting palladium chloride dissolved in 2 M hydrochloric acid with a solution of the ligand in methanol, gave a yellow solid, **3.25**, that was insoluble in common solvents. Analysis of this compound was consistent with the expected dinuclear complex, but a satisfactory agreement between calculated and found values could not be obtained. Previously, Yang et al. had described a dinuclear europium complex of this ligand, which in contrast to the dinuclear complexes of ligand **3.2**, had a *cis* conformation.[64] This may be the conformation adopted by the

palladium complex, **3.25**, and dinuclear ruthenium complexes of this ligand described later in Section 3.5.

### 3.3.3 Complexes of 1,4-bis(di-2-pyridylamino)naphthalene, 3.4

The ligand, **3.4**, was reacted with the usual range of first and second row transition metals. With silver nitrate and silver tetrafluoroborate no readily characterisable products were isolated. However, reacting silver hexafluorophosphate with **3.4** gave a complex, **3.26**, which was isolated as a colourless crystalline solid in 85% yield (Scheme 3.7). Elemental analysis revealed a $M_2L$ composition of the bulk sample of **3.26a**. However, the crystals obtained, as a minor component (**3.26b**) by evaporation of the filtrate, had a different composition and were shown by X-ray crystallography to be composed of a discrete [2+2] metal-ligand dimer. With copper nitrate, a complex, **3.27**, was isolated that analysed as $[Cu_2(\mathbf{3.4})(NO_3)_4]$, but which unfortunately, despite repeated attempts, could not be crystallised. A further dinuclear complex, **3.28**, was obtained by reaction of the ligand dissolved in methanol with palladium chloride dissolved in 2 M hydrochloric acid. Elemental analysis confirmed the composition was $[Pd_2(\mathbf{3.4})Cl_4]$, but unfortunately, the complex was insoluble in common NMR solvents and was not further characterised.

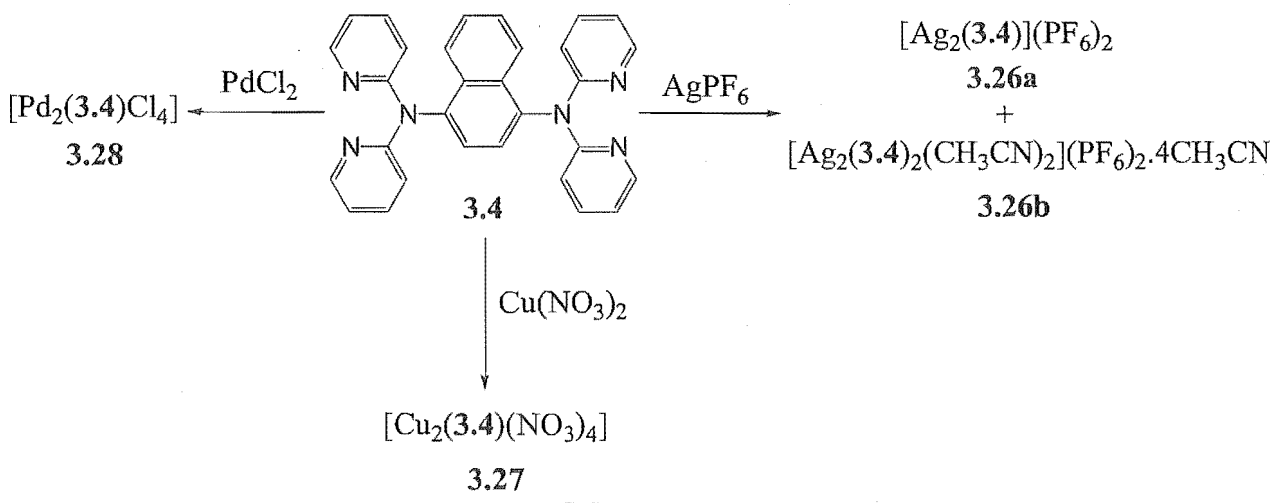


**Scheme 3.7**

Crystal Structure of 3.26b

The plate-like crystals of **3.26b** obtained by evaporation of the filtrate were suitable for X-ray crystallography. Complex **3.26b** crystallises in the monoclinic space group $P2_1/c$ with two complete [2+2] dimers in the unit cell. The asymmetric unit comprises one molecule of **3.4**, one silver atom, one coordinated and two non-coordinated acetonitrile solvate molecules and a non-coordinated hexafluorophosphate anion. In Figure 3.18 a perspective view of the [2+2] dimer is shown, with the non-coordinated solvate molecules, anions and hydrogen atoms omitted for

clarity. The silver atom has a distorted trigonal-planar geometry with bond lengths and angles typical for such a complex. These nitrogen donors are complemented by weak interactions of the non-coordinated pyridine rings with the silver atom and also arene C-H agostic interactions. The metal-metal distance is 10.679(1) Å, and not significantly different to complexes of ligand **3.2**.

The non-coordinated pyridine donors point in toward the centre of the complex and make very weak intramolecular N···H-C interactions with the naphthalene ring. The N···H distance is 2.65(5) Å, and just within the van der Waals radii of N and H.[183] There are no unusually short intermolecular contacts between the non-coordinated acetonitrile solvate molecules and hexafluorophosphate anions that fill the voids surrounding the [2+2] dimers, nor between the discrete dimers.

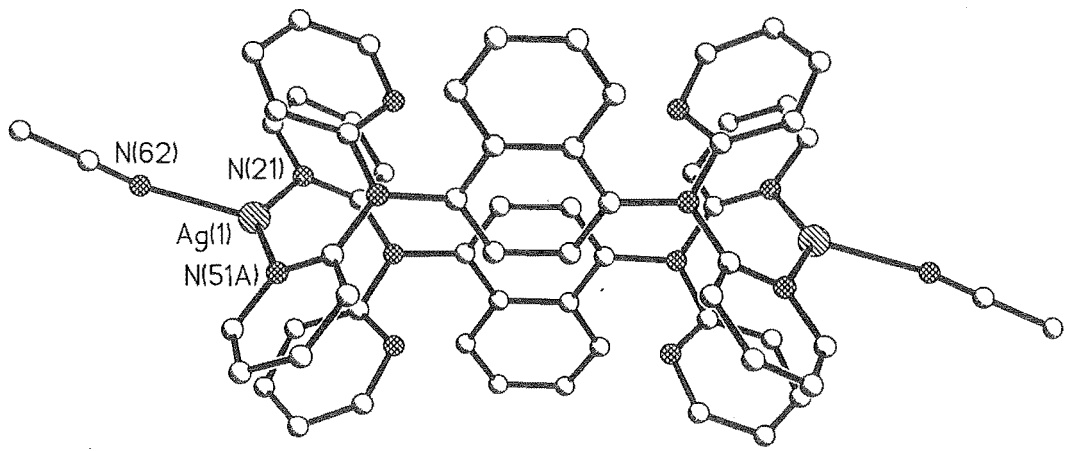


**Figure 3.18.** A perspective view of complex **3.26b** with non-coordinated solvate molecules, hexafluorophosphate anions and hydrogen atoms excluded for clarity. Selected bond lengths (Å) and angles (°): Ag(1)-N(51A) 2.240(5), Ag(1)-N(21) 2.267(4), Ag(1)-N(62) 2.295(5), N(51A)-Ag(1)-N(21) 143.88(15), N(51A)-Ag(1)-N(62) 115.82(17), N(21)-Ag(1)-N(62) 100.15(18).

A closely related silver trifluoroacetate complex has recently been described by Kang et al.[65] with a related rod-like ligand. Reaction of silver trifluoroacetate with 4,4'-bis(di-2-pyridylamino)diphenylacetylene gave a complex that was shown to be a discrete [2+2] dimer by X-ray crystallography. The silver atoms have a trigonal-planar geometry, with monodentate coordination by a pyridine ring from two different ligand molecules and by a trifluoroacetate anion. The overall topology of the structure is almost identical to complex **3.26b**, but, because of the extended core of the ligand, it has a considerably longer metal-metal distance.

### 3.3.4 Complexes of 1,5-bis(di-2-pyridylamino)naphthalene, 3.6

The naphthalene-based ligands, **3.4**, **3.6**, and **3.8**, are less soluble in polar solvents than the benzene-based ligands. This required considerations regarding the formation of complexes with these ligands, in particular with ligand **3.6**. With labile metals like silver, the methods of preparing complexes, which have been used for the related ligands, failed to provide complexes of **3.6**. In most cases the ligand precipitated in preference to the formation of a complex. However, with copper nitrate, a dinuclear complex, **3.29**, which analyses as $[Cu_2(\mathbf{3.6})(NO_3)_4].1½CH_2Cl_2$ was isolated in 62% yield, by vapour diffusion of ether into the methanol-dichloromethane reaction mixture (Scheme 3.8). A palladium chloride complex, **3.30**, was also obtained by the usual procedure in 78% yield. It is also dinuclear and analyses as $[Pd_2(\mathbf{3.6})Cl_4].H_2O$. Once again, it was insoluble in common NMR solvents and not further characterised.

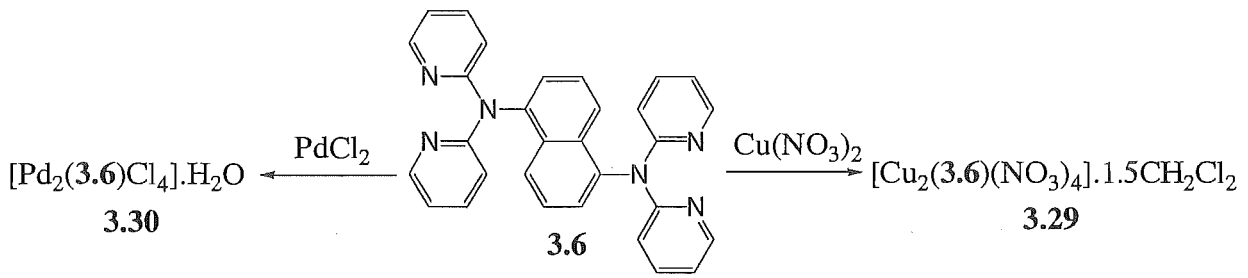


**Scheme 3.8**

### 3.3.5 Complexes of 1,3-bis(di-2-pyridylamino)benzene, 3.7

To investigate the various possible coordination modes of the new ligand, **3.7**, it was reacted with a range of transition metals. Combining acetonitrile solutions of the ligand and silver nitrate gave a complex, **3.31**, with an elemental analysis corresponding to $[Ag_2(\mathbf{3.7})(NO_3)_2]$. A number of structures are possible for such a composition and fortunately crystals were obtained which were suitable for X-ray crystallography. Interestingly, a complex, **3.32**, with an identical metal-ligand composition was obtained by reaction of the same ligand with silver hexafluorophosphate. The structure of **3.32** is described below, alongside complex **3.31**.

With copper nitrate and palladium chloride two dinuclear complexes, **3.33** and **3.34**, were obtained in 59% and 62% yields, respectively. These analyse as $[Cu_2(\mathbf{3.7})(NO_3)_4]$ and $[Pd_2(\mathbf{3.7})Cl_4].CH_3OH.H_2O$. Complex **3.33** was recrystallised by vapour diffusion of ether into a methanol solution of the complex to provide crystals that were characterised by X-ray crystallography. Unfortunately, **3.34** was insoluble in common NMR solvents and was not further characterised.

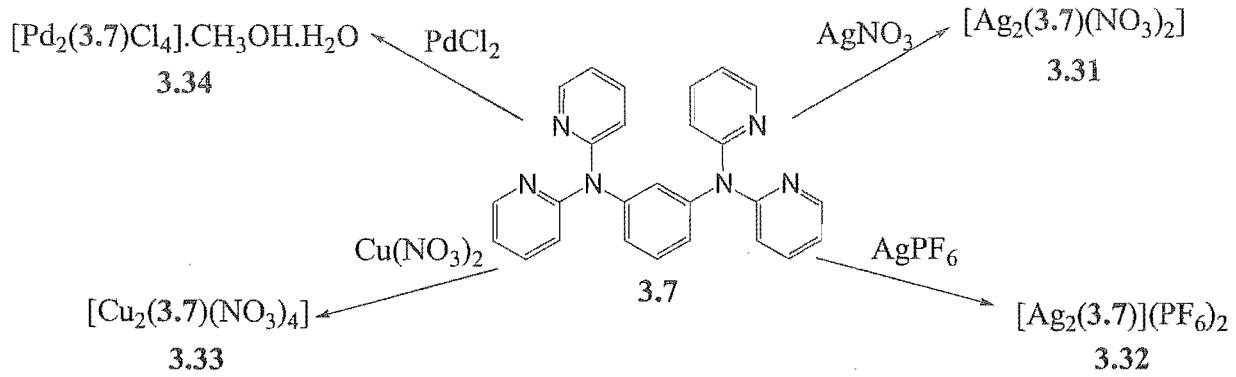


**Scheme 3.9**

Crystal Structures of **3.31** and **3.32**

The structures of both **3.31** and **3.32** will be considered together because they have the same overall structure, despite different anions and differences in the solvate composition. However, while they have the same basic structure, the two complexes crystallise in different monoclinic space groups. Complex **3.31** crystallises in the primitive space group $P2_1/n$ and complex **3.32** in *C*-centred monoclinic space group Cc.

Focussing on structure **3.32**, the large asymmetric unit contains four silver atoms, two molecules of **3.7**, six coordinated acetonitrile molecules, two non-coordinated acetonitrile solvate molecules, a non-coordinated ether molecule and four non-coordinated hexafluorophosphate anions. In Figure 3.19 a perspective view of the asymmetric unit of **3.32** is shown, with non-coordinated solvate molecules, anions and hydrogen atoms omitted for clarity. As depicted the structure appears to have an inversion centre at the centroid of the dimetallocycle. This higher symmetry is destroyed by the hexafluorophosphate anions, and an ether molecule, which lies in the cleft of the polymer between Ag(4) and the dimetallocycle.

The coordination geometry of Ag(1) is distorted trigonal-planar with bond angles of 147.2(2), 108.5(2), and 103.4(2)°, but there are weak silver-arene π-interactions with an adjacent benzene ring (Ag-C distance of 2.994(6) Å) and pyridine ring (2.980(6) Å) from a symmetry-related ligand molecule. Therefore the geometry is better described as pseudo-trigonal-bipyramidal. Ag(2) has a very similar three coordinate geometry with bond angles of 147.5(2), 113.1(2) and 98.2(2)°. The central silver atoms, Ag(3) and Ag(4), also have very similar geometries, both pseudo-octahedral, with two coordinated pyridine rings, two coordinated acetonitrile molecules and weak silver-arene π-interactions from adjacent benzene and pyridine rings. This type of supramolecular interaction has been observed for silver atoms in earlier structures. In a related structure (**3.21**) the two silver-arene π-interactions were *trans*, rather than *cis*. The silver-nitrogen bond lengths for the four silver atoms are typical for such compounds.

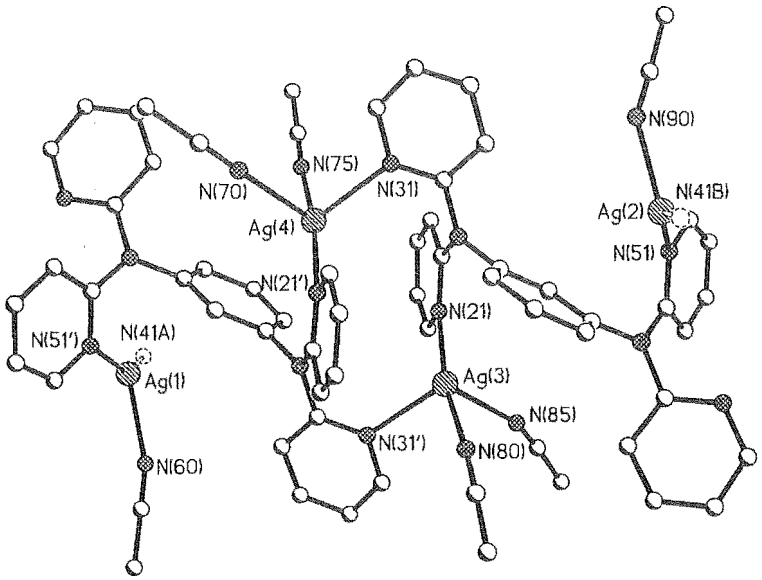


**Figure 3.19.** A perspective view of the asymmetric unit of **3.32**, with non-coordinated solvate molecules, anions and hydrogen atoms omitted for clarity. Selected bond lengths (Å) and angles (°): Ag(1)-N(41A) 2.230(5), Ag(1)-N(51') 2.232(5), Ag(1)-N(60) 2.312(6), Ag(2)-N(41'B) 2.209(5), Ag(2)-N(51) 2.247(5), Ag(2)-N(90) 2.337(6), Ag(3)-N(80) 2.204(6), Ag(3)-N(21) 2.260(5), Ag(3)-N(31') 2.514(6), Ag(3)-N(85) 2.583(7), Ag(4)-N(75) 2.227(6), Ag(4)-N(21') 2.262(5), Ag(4)-N(31) 2.475(5), Ag(4)-N(70) 2.609(8), N(41A)-Ag(1)-N(51') 147.23(18), N(41A)-Ag(1)-N(60) 108.5(2), N(51')-Ag(1)-N(60) 103.4(2), N(41'B)-Ag(2)-N(51) 147.53(18), N(41'B)-Ag(2)-N(90) 113.1(2), N(51)-Ag(2)-N(90) 98.2(2), N(80)-Ag(3)-N(21) 168.5(2), N(80)-Ag(3)-N(31') 98.5(2), N(21)-Ag(3)-N(31') 93.03(18), N(80)-Ag(3)-N(85) 94.2(3), N(21)-Ag(3)-N(85) 85.6(2), N(31')-Ag(3)-N(85) 92.2(3), N(75)-Ag(4)-N(21') 168.2(2), N(75)-Ag(4)-N(31) 96.2(2), N(21')-Ag(4)-N(31) 95.18(17), N(75)-Ag(4)-N(70) 96.5(2), N(21')-Ag(4)-N(70) 86.7(2), N(31)-Ag(4)-N(70) 89.9(2).

A perspective view of the extended structure of **3.32** is shown in Figure 3.20. The overall structure is an undulating one-dimensional coordination polymer, with each ligand molecule forming two different dimetallocyclic rings. Both of the rings are 12-membered dimetallocycles, but with slightly different arrangements of the coordinated pyridine rings above and below the plane of the metallocyclic ring. Within the two different dimetallocyclic rings, the silver-silver distance between Ag(3) and Ag(4) is 5.054(2) Å and between Ag(1) and Ag(2) is 3.976(2) Å. This shows that there are no significant silver-silver interactions within the structure.

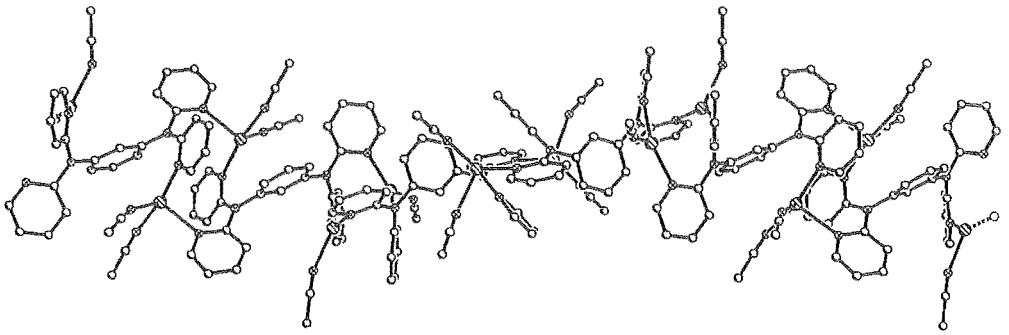

**Figure 3.20.** A perspective view of the extended structure of **3.32**.

While the arrangement and coordination geometry of the silver atoms are slightly different, the overall silver-ligand connectivity of **3.32** is closely related to structure **3.21** obtained with the 1,4-benzene-based ligand, **3.2**. However, because of the differences in silver geometries and in the ligand substitution pattern, the topologies of the one-dimensional coordination polymers are quite different. Schematic representations of the two different types of one-dimensional coordination polymers observed with ligands **3.2** and **3.7** are shown in Figure 3.21.

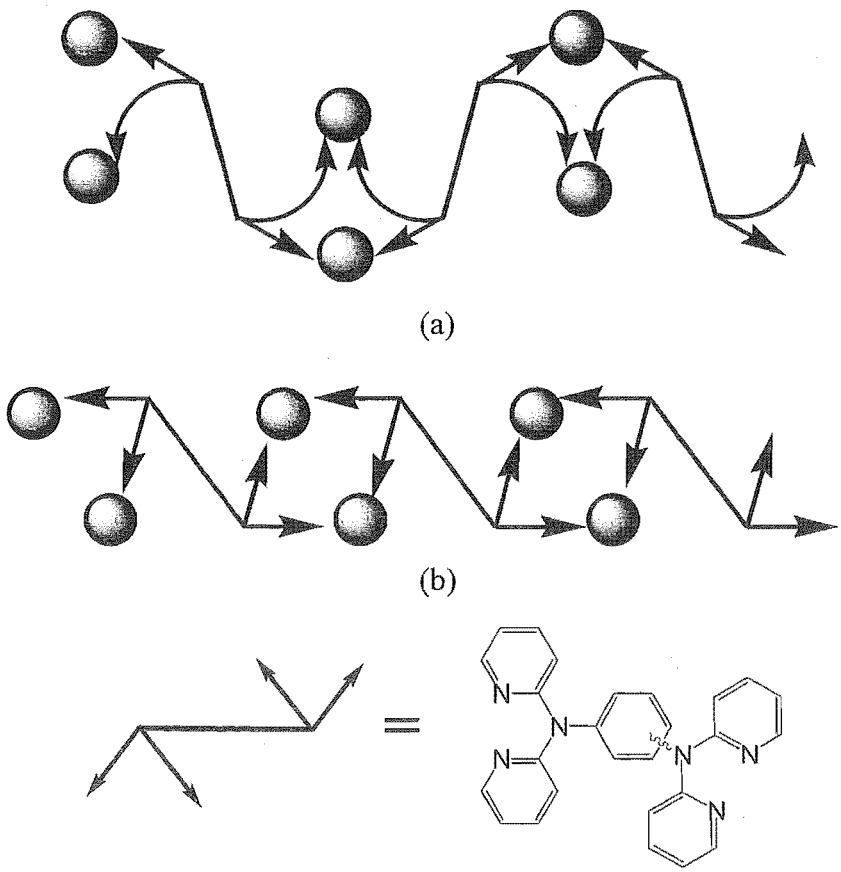


**Figure 3.21.** Schematic representations of complexes (a) **3.21** and (b) **3.31/3.32**.

As outlined, an almost identical complex, **3.31** was obtained by reaction of **3.7** with silver nitrate. In this structure, the asymmetric unit of which is shown in Figure 3.22, the nitrate anions

coordinate in the positions that were occupied by coordinated acetonitrile molecules in the previous complex (**3.32**). The asymmetric unit is shown without the non-coordinated solvate molecules and hydrogen atoms. The coordination environment of all four silver atoms is very similar to that described for complex **3.32**. As with the previous structure, no unusually short intermolecular interactions dominate the packing of the coordination polymers in the crystal.

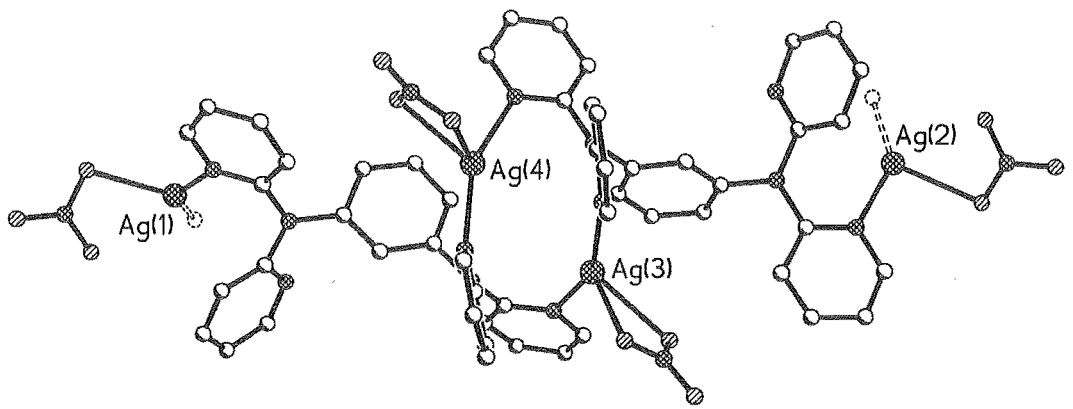


**Figure 3.22.** Asymmetric unit of **3.31**, the $AgNO_3$ analogue of **3.32** for comparison, with nitrate anions replacing the coordinated acetonitrile molecules.

Crystal Structure of **3.33**

As described, crystals of a discrete dinuclear copper complex, **3.33**, were obtained by vapour diffusion of ether into a methanol solution of the complex. The complex crystallises in the monoclinic space group C2/c, with four molecules of the dinuclear complex in the unit cell. A perspective view of the complex is shown in Figure 3.23, with hydrogen atoms omitted for clarity. A two-fold rotation axis passes through C2 and C5 of the central benzene ring. The copper atom has a distorted square-pyramidal geometry ($\tau = 0.19$) with the coordinated methanol solvate molecule bonded 2.265(2) Å from the copper. The other bonds to the copper are also typical for such a geometry, with values ranging from 1.980(2) to 2.004(2) Å for the two coordinated pyridine rings and the nitrate anions.

Like previous structures of these ligands, the chelating units are twisted approximately perpendicular to the benzene ring. The ligand bridges the two copper atoms with a metal-metal distance of 8.785(1) Å. By contrast, ligand **3.2** bridges two copper atoms with a distance of 11.179(1) Å. Thus, the metal-metal distance in later ruthenium complexes for these two ligands will be quite different, although the conformations available to the ligand in solution may minimise this difference.

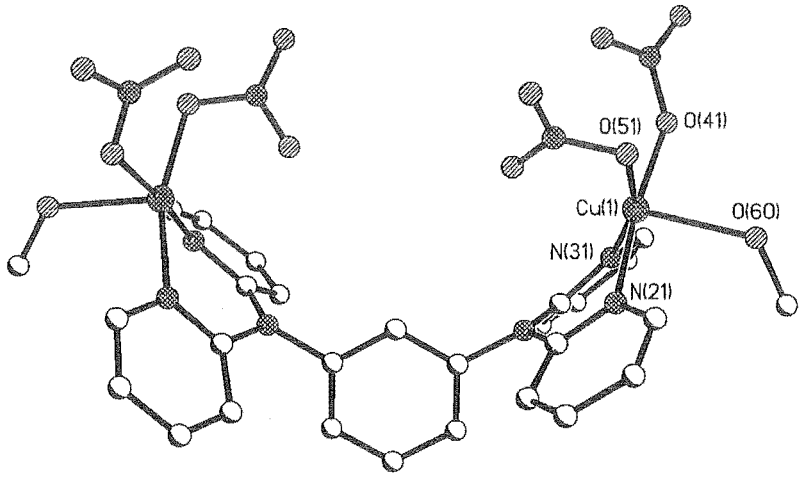


**Figure 3.23.** A perspective view of the complex **3.33** with hydrogen atoms omitted for clarity. Selected bond lengths (Å) and angles (°): Cu(1)-O(41) 1.980(2), Cu(1)-N(21) 1.981(2), Cu(1)-N(31) 1.982(2), Cu(1)-O(51) 2.004(2), Cu(1)-O(60) 2.265(2), O(41)-Cu(1)-N(21) 173.10(8), O(41)-Cu(1)-N(31) 93.45(9), N(21)-Cu(1)-N(31) 87.36(9), O(41)-Cu(1)-O(51) 92.47(8), N(21)-Cu(1)-O(51) 88.87(8), N(31)-Cu(1)-O(51) 161.44(7), O(41)-Cu(1)-O(60) 84.74(8), N(21)-Cu(1)-O(60) 88.36(8), N(31)-Cu(1)-O(60) 97.75(8), O(51)-Cu(1)-O(60) 100.30(7).

The change from a 1,4-substituted benzene ring in ligand **3.2**, to the 1,3-arrangement of the chelating arms in ligand **3.7**, allows for some interesting comparisons. Ligand **3.7** still functions as a bridging ligand and, as shown in Figure 3.21 above, still forms silver complexes with the same connectivity, albeit with different conformations. The dinuclear copper complex described immediately above, **3.33**, has the same connectivity, but a *cis* conformation of the copper atoms, in contrast to complex **3.23** described earlier. This is slightly at odds with the expected steric requirements of the two ligands.

### 3.3.6 Complexes of 2,7-bis(di-2-pyridylamino)naphthalene, 3.8

Ligand **3.8**, which incorporates the naphthalene core, should lead to closely related complexes to the previously described ligand, **3.7**, but with potentially increased metal-metal distances because of the greater size of the naphthalene core. Reaction of **3.8** with silver tetrafluoroborate and silver hexafluorophosphate gave complexes **3.35** and **3.36**, respectively, which had almost identical structures when characterised by X-ray crystallography. Complex **3.35** will be described because the structure refined to a more satisfactory level and complete analysis was obtained. Reaction of silver tetrafluoroborate with **3.8** in acetonitrile provided

complex **3.35** in 62% yield. The complex was recrystallised by vapour diffusion of ether into an acetonitrile solution, and analyses with a 2:1 metal to ligand ratio. A similar approach was used to obtain crystals of complex **3.36**, which was recrystallised by vapour diffusion of pentane into acetonitrile.

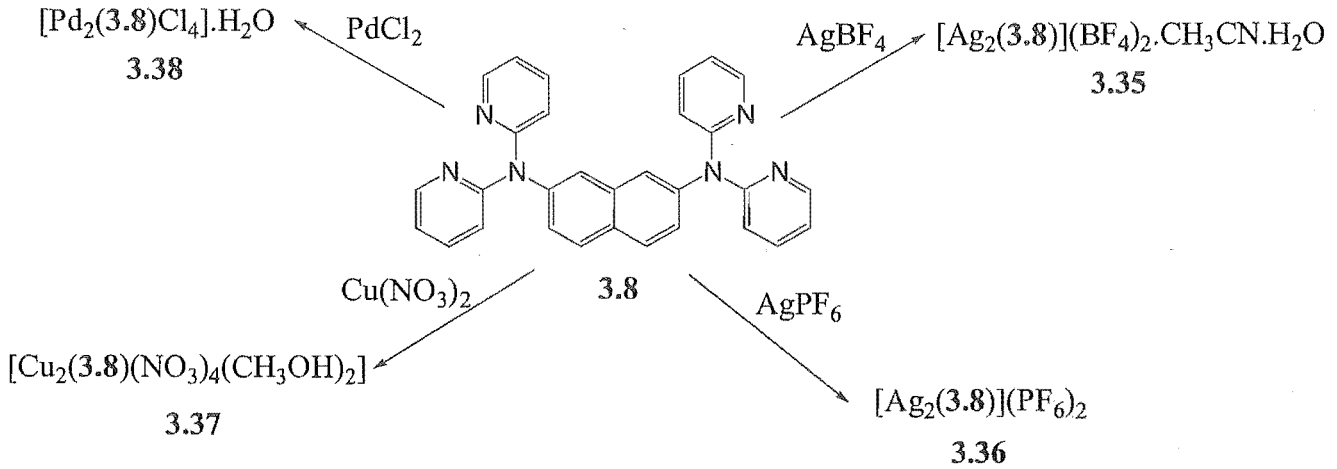


**Scheme 3.10**

Reaction of copper nitrate with **3.8** in methanol gave a green dinuclear copper complex, **3.37**, in 52% yield. The complex analyses as $[Cu_2(\mathbf{3.8})(CH_3OH)_2(NO_3)_4]$ indicating that the complex is likely to have a very similar structure to the copper complex, **3.33**, described above. Reacting the same ligand with palladium chloride in 2 M hydrochloric acid immediately led to a yellow precipitate in 91% yield, which gave an elemental analysis consistent with $[Pd(\mathbf{3.8})Cl_4].H_2O$. This complex, **3.38**, was soluble in DMSO and confirmed to be the symmetrical dinuclear complex by $^1$H NMR. The $^1$H NMR chemical shifts and CIS values for complex **3.38** are shown in Table 3.1. The downfield shift of the pyridine signals is consistent with coordination to the pyridine nitrogen atoms, and the symmetry of the $^1$H NMR spectrum confirms that the ligand chelates to two palladium atoms, with a bridging doubly bidentate coordination mode.

**Table 3.1.** The $^1$H NMR signals and CIS values for **3.38** in DMSO solution.

| | H1/H8 | H3/H6 | H4/H5 | H3' | H4' | H5' | H6' |
|---|---|---|---|---|---|---|---|
| **3.8** | 7.63 | 7.31 | 8.01 | 7.12 | 7.77 | 7.12 | 8.32 |
| **3.38** | 7.57 | 7.57 | 7.90 | 7.57 | 8.44 | 8.16 | 8.90 |
| *CIS* | *-0.06* | *+0.26* | *-0.11* | *+0.45* | *+0.67* | *+1.04* | *+0.58* |

Crystal Structure of 3.35

Complex **3.35** crystallises in the monoclinic space group $P2_1/c$, with one molecule of **3.8**, two silver atoms, three coordinated acetonitrile solvate molecules (one of which is disordered

over two sites) and three tetrafluoroborate anions (two 50% occupied) in the asymmetric unit. A perspective view of the asymmetric unit is shown in Figure 3.24, with hydrogen atoms and non-coordinated anions omitted for clarity. The coordination environment of Ag(1) has an unusual trigonal-pyramidal geometry when only the symmetry-related pyridine donors and the two acetonitrile molecules are considered. However, when the silver-arene π-interaction (2.952(6) Å) is considered, the geometry of Ag(1) can be considered to be trigonal-bipyramidal. The acetonitrile molecule with the nitrogen atom labelled N(71), is disordered over two sites. Ag(2) has a similar five-coordinate geometry when the silver-arene π-interactions are taken into account. Ag(2) coordinates to two pyridine rings, one acetonitrile molecule and makes two silver-arene π-interactions with Ag-C distances of 2.720(6) and 2.958(6) Å. The former Ag-C distance is to the naphthalene ring of a symmetry-related ligand molecule, while the latter distance is to the C2 of the pyridine ring with N(31) labelled. The shortest silver-silver distance in the structure, between Ag(1) and Ag(2) is 4.461(1) Å, indicating no silver-silver interactions within this complex.

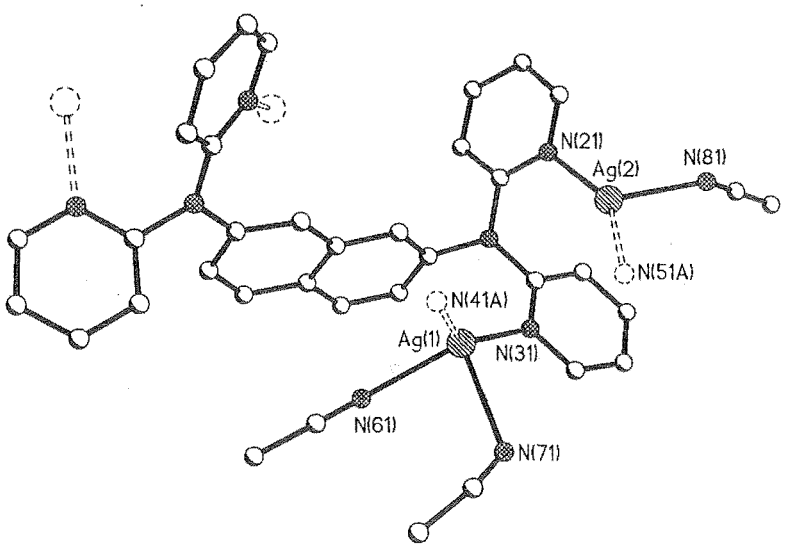


**Figure 3.24.** A perspective view of the asymmetric unit of **3.35**, with hydrogen atoms and non-coordinated tetrafluoroborate anions omitted for clarity. Selected bond lengths (Å) and angles (°): Ag(1)-N(31) 2.304(6), Ag(1)-N(41A) 2.347(7), Ag(1)-N(61) 2.426(7), Ag(1)-N(71) 2.523(10), Ag(2)-N(21) 2.216(6), Ag(2)-N(51A) 2.246(7), Ag(2)-N(81) 2.338(8), N(31)-Ag(1)-N(41A) 139.2(2), N(31)-Ag(1)-N(61) 126.4(2), N(41A)-Ag(1)-N(61) 93.3(2), N(31)-Ag(1)-N(71) 96.1(4), N(41A)-Ag(1)-N(71) 97.9(4), N(61)-Ag(1)-N(71) 83.5(3), N(21)-Ag(2)-N(51A) 150.2(2), N(21)-Ag(2)-N(81) 103.2(2), N(51A)-Ag(2)-N(81) 105.2(3).

Figure 3.25 shows a perspective view of the extended structure of **3.35**. The extended structure is an $M_2L$, one-dimensional coordination polymer, which has similar connectivity to some of the structures described earlier with related ligands. Each ligand is connected by two silver atoms, which are part of a 12-membered dimetallocycle, as was observed in complexes **3.21** and **3.31/3.32**. A diagram showing the connectivity and a simplified representation of the structure is shown in Figure 3.26. The coordination polymers do not make any short intermolecular contacts with adjacent polymer strands, instead being connected by a series of weak interactions between coordinated solvate molecules and the non-coordinated anions. There are no unusually short contacts.

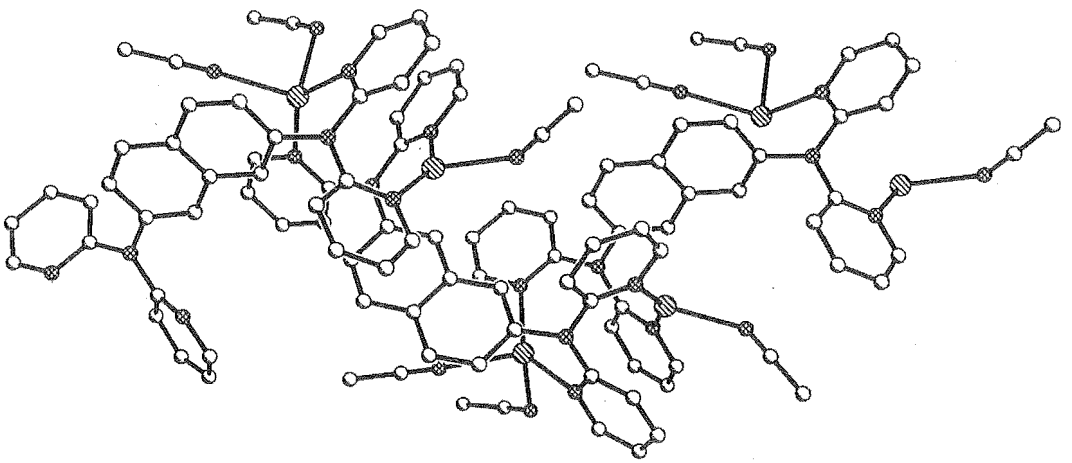

**Figure 3.25.** A perspective view of the extended structure of **3.35**.

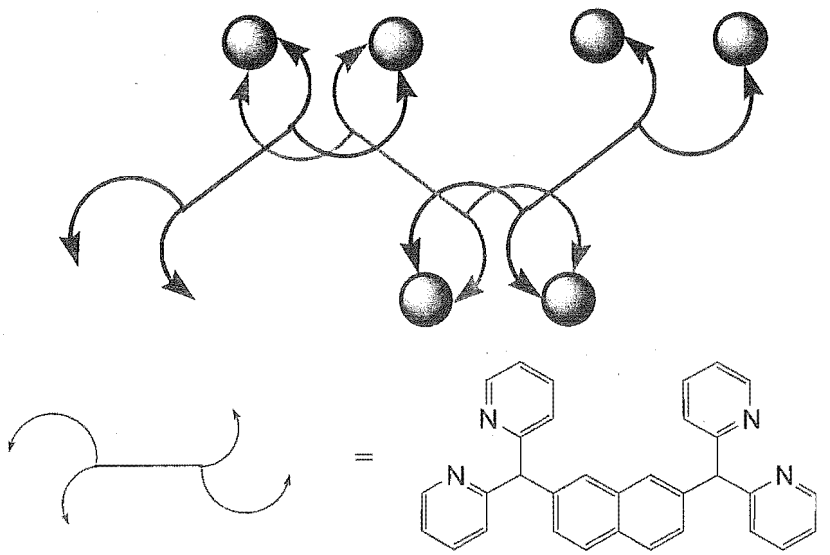


**Figure 3.26.** A schematic representation of complex **3.35**, showing the connectivity within the coordination polymer.

The complexes described above with silver salts have revealed an interesting feature of silver complexes that has not, to the author's knowledge, been commented on before. While the silver atoms in the crystal structures described have coordination numbers and geometries typical of silver, a prevalent feature of these complexes are weaker silver-arene interactions, which further increase the effective coordination number of the atom and shield the silver atom from coordination by solvent. These interactions are only regularly observed here because the metal-ligand nitrogen bonds play a major role in forming the observed structures. Normally such interactions are prevented by coordination of the solvent. These interactions are also reflective of the fact that with silver, the ligands employed above, coordinate to each silver atom through one pyridine donor of the chelating di-2-pyridylamine unit. No chelation by these ligands is observed with silver and a common motif is a twelve-membered dimetallocycle. This has the same enthalpy considerations because the same number of dative covalent bonds are formed per molecule of ligand.

### 3.3.7 Complexes of 1,3,5-tris(di-2-pyridylamino)benzene, 3.9

Ligand **3.9** has been reacted with a variety of metal salts, by Wang and co-workers and in this research project, to demonstrate that it could function as a tritopic connector of three metal ions. Wang et al., who first prepared this ligand, characterised trinuclear coordination complexes with zinc(II) chloride and platinum(II) chloride.[170] In these coordination complexes the ligand bridges three metals with coordination via the three bidentate donor domains. Reactions of **3.9** with silver nitrate, silver tetrafluoroborate and silver hexafluorophosphate, copper nitrate and copper perchlorate, palladium chloride and zinc acetate were attempted to further investigate the coordination chemistry of **3.9**. With silver tetrafluoroborate, a complex, **3.39**, was isolated as an off-white solid that analysed as $[Ag_3(\mathbf{3.9})(BF_4)_3].2CH_3CN$. The analysis and solubility properties suggested that this was a discrete complex. An interesting hypothesis is that this complex may have a similar structure to the hexanuclear silver cage structure reported in Chapter 2. Other than the elemental analysis, there is no evidence to support such a structure, however. With the other silver salts and with the copper and zinc precursors, no readily characterisable materials were obtained.

Reaction with palladium chloride gave what was initially thought to be an unusually soluble palladium coordination complex. The pale yellow product, **3.40**, was analysed by elemental analysis and mass spectrometry, which indicated that the compound had the composition $[Pd_3(\mathbf{3.9}\text{-}3H)Cl_3].2CH_3OH$. The analysis and high symmetry apparent in the $^1H$ and $^{13}C$ NMR spectra, coupled with the absence of any signals for the central benzene ring protons in the $^1H$ NMR spectrum, strongly suggested a triply-cyclopalladated structure, rather than the

expected trinuclear coordination compound. Similarly, the presence of three quaternary carbon signals in the $^{13}C$ NMR spectrum provided further evidence to that end. Eventually, recrystallisation, via vapour diffusion of methanol into a DMSO solution of the complex, gave pale yellow crystals of **3.40**. This complex was characterised by X-ray crystallography to confirm the three-fold cyclopalladated structure. Subsequently, it was found that the yield of the triply cyclopalladated compound could be improved by effecting the conversion in a two step procedure, shown in Scheme 3.11, initially reacting **3.9** with palladium acetate in refluxing benzene, followed by metathesis of the acetate anions with lithium chloride. Even using this procedure the yields proved somewhat variable, ranging between 10-50%.

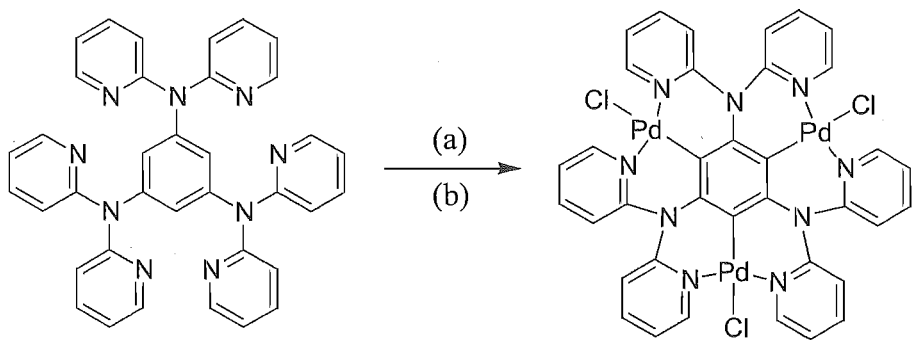


**3.9** **3.40**

(a) $Pd(OAc)_2$, benzene; (b) LiCl, acetone-water, 10-50%.

**Scheme 3.11**

Further cyclometallations were also attempted using mercury and ruthenium. Unfortunately, reaction of **3.9** with mercuric acetate, followed by metathesis with lithium chloride failed to give the desired triply-cyclomercurated product. With $[Ru(tpy)Cl_3]$ similar difficulties were encountered on reaction with **3.9**. The reaction mixture was purified on sephadex cation exchange resin, by elution with sodium chloride solution (0.1 - 0.6 M). Using 0.2 M NaCl solution a red band was eluted that was shown to be the $[Ru(tpy)_2]^{2+}$ dication. Using 0.6 M NaCl solution, the dark brown major component, **3.41**, was eluted. This concentration of eluent would normally be used for a cation of approximately a 6+ charge, and thus, is not likely to be the desired cycloruthenated compound. Characterisation was attempted by NMR spectroscopy and elemental analysis, but the compound could not be identified.

Crystal Structure of **3.40**

As was described, compound **3.40** was proposed to be the first example of three-fold cyclometallation of a benzene ring. Figures 3.27 and 3.28 show two different perspective views of the crystal structure of **3.40**, which confirm that the ligand **3.9** has undergone three-fold cyclometallation. Figure 3.27 shows selected atomic labeling with selected bond lengths and

angles reported in the caption. The complex crystallises about a crystallographic two-fold rotation axis passing through the central benzene ring and one of the PdCl units. The palladium atoms have square-planar geometry with relatively short Pd-C bonds (1.962(2) and 1.956(4) Å). Similar distances are observed in related mononuclear complexes with the same cyclometallation motif.[184]

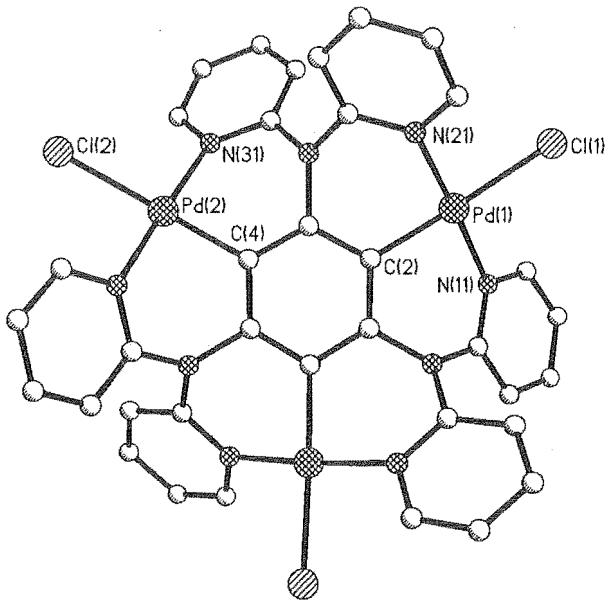


**Figure 3.27.** A perspective view of complex **3.40** looking down on the cyclopalladated benzene ring. Hydrogen atoms and solvate molecules are omitted for clarity. Selected bond lengths (Å) and angles (°): Pd(1)-C(2) 1.962(2), Pd(1)-N(11) 2.035(3), Pd(1)-N(21) 2.036(3), Pd(1)-Cl(1) 2.4017(10), Pd(2)-C(4) 1.956(4), Pd(2)-N(31) 2.036(2), Pd(2)-Cl(2) 2.4030(14), C(2)-Pd(1)-N(11) 88.05(10), C(2)-Pd(1)-N(21) 88.62(10), N(11)-Pd(1)-Cl(1) 92.26(7), N(21)-Pd(1)-Cl(1) 91.24(7), C(4)-Pd(2)-N(31) 88.89(6), N(31)-Pd(2)-Cl(2) 91.11(6).

The N,C,N' cyclometallation motif observed here has been used extensively by van Koten to form a variety of cyclometallated compounds, typically with the formation of five-membered chelate rings.[185] Related mononuclear complexes with a N,C,N' cyclometallation motif, but incorporating two new six-membered rings, have been structurally characterised by Canty.[184] One factor thought to favour cyclometallation in those complexes was the avoidance of the potential strain caused by the Pd···H interaction when only N,N' coordination occurs. This is not likely to be the driving force here because **3.9** is also capable of forming six-membered chelate rings without destabilising interactions. Typically, such cyclometallation reactions of benzene rings occur by an electrophilic aromatic substitution mechanism.[186] Thus, the three-fold

cyclometallation is achieved for **3.9** because the benzene ring is highly activated toward reaction, as a consequence of the three electron donating amine nitrogen atoms.

The three-fold cyclometallation process results in the formation of six new six-membered chelate rings fused to the central benzene ring, which leads to a coronene-type structure. However, unlike coronene, the molecule is far from planar, as shown in the alternative view in Figure 3.28. In order to avoid steric interactions between adjacent pyridine rings, the molecule possesses internal twisting that results in the pyridine rings being positioned on alternating sides of the central benzene ring. This twisting has the effect of making each individual molecule chiral, although, of course, the crystal itself is racemic. There are no unusually short intermolecular interactions in the crystal, although the pyridine rings of the discrete palladacycles weakly π-stack with adjacent molecules. The average C-C distance between the offset-stacked pyridine rings is 3.575(8) Å.

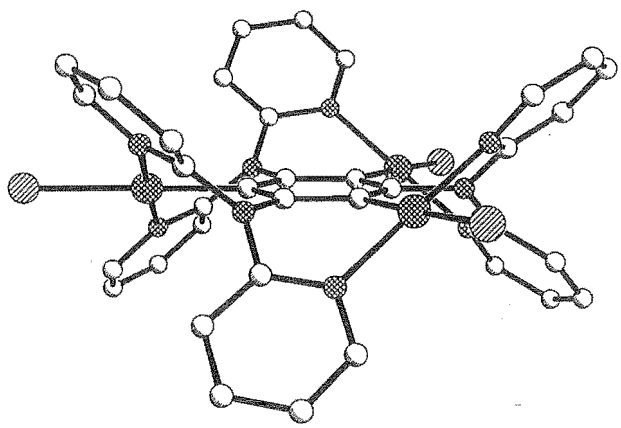

**Figure 3.28.** A perspective view of the structure of **3.40**, viewed from the plane of the benzene ring.

In recent years, there has been much interest in multiply cyclopalladated compounds, with diverse application in many fields.[186-188] For example, a recent review highlighted the potential of palladacycles in homogeneous catalysis.[189] The progression to multiply cyclometallated compounds, like the example above, has been a long and involved process. The first cyclopalladation of a benzene derivative, azobenzene, was described by Cope and Siekman[190] in 1965, and by varying the donor atoms, ring size, and the nature of the carbon donor, a structurally diverse range of cyclopalladated compounds have since been prepared.[186, 187] In 1971, Trofimenko reported the first examples of the double cyclopalladation of a single benzene ring.[191] However, the compound described above is the first example of a triply cyclopalladated benzene ring despite strenuous efforts over several years to prepare such a compound. For comparison, a trimetallated benzene ring was recently reported by Vicente and coworkers.[192]

This was prepared from triiodomesitylene by oxidative addition across the carbon-iodine bonds and also has three palladium atoms appended to a benzene ring.

### 3.3.8 Complexes of 2,4,6-tris(di-2-pyridylamino)-1,3,5-triazine, 3.10

In the same manner as ligand **3.9**, the triazine-based ligand, **3.10**, was reacted with a range of metal salts to investigate its coordination chemistry. Two other groups have independently studied this ligand and described coordination complexes and metallosupramolecular assemblies with several different transition metals. Reaction of **3.10** with zinc chloride and platinum chloride was described by Wang.[170] The trinuclear platinum complex that was described has an intriguing bowl shaped structure, while the mononuclear zinc complex prepared is postulated to undergo an intramolecular 'merry-go-round' exchange process of the zinc unit in solution. By reaction of **3.10** with copper nitrate, Reedijk and co-workers described the spontaneous assembly of a one-dimensional molecular ladder structure, whereby molecules of **3.10** provide the T-shaped connectors.

No complexes have been reported for **3.10** with silver salts and so complexes of this ligand were prepared with silver nitrate, tetrafluoroborate and hexafluorophosphate. The reaction with silver tetrafluoroborate gave a complex, **3.42**, in a low yield that was recrystallised by vapour diffusion of ether into an acetonitrile solution. Complex **3.42** analyses as [Ag(**3.10**)$BF_4$], which is consistent with a polymeric structure. Similarly, reaction with silver hexafluorophosphate gave a complex, **3.43**, which was obtained by an identical method in 23% yield, and was characterised as [Ag(**3.10**)$PF_6$].2$H_2O$. Again such a composition is consistent with a polymeric structure. A reaction was also carried out between **3.10** dissolved in methanol and palladium chloride in 2 M hydrochloric acid to provide a trinuclear palladium complex, **3.44**, in 86% yield. This analysed with the expected metal to ligand ratio of 3:1. Unfortunately, the complex was very insoluble in common NMR solvents and was not further characterised.

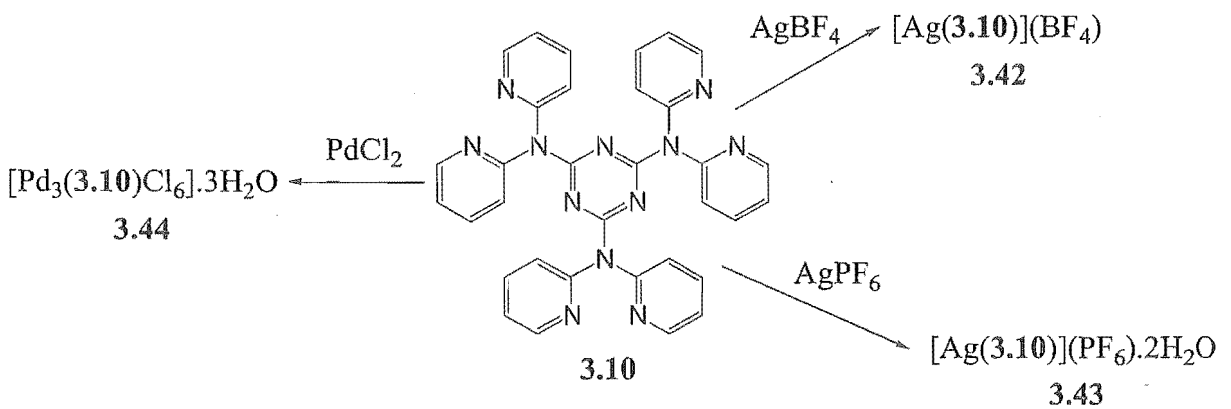


**Scheme 3.12**

## 3.4. Coordination and metallosupramolecular chemistry of the $NCH_2$-linked ligands

As outlined earlier in the chapter, longer spacer groups lead to more flexible ligands that can lead to new and unusual structures because of the greater conformational freedom of the ligand. To exploit this, the coordination chemistry of these ligands was explored primarily with $d^{10}$ metal ions such as silver(I), cadmium(II) and zinc(II). Because of the flexible coordination requirements of these metal atoms, the assembly of the most thermodynamically stable structures is allowed. Disappointingly in this work, the cadmium and zinc salts used provided no examples of complexes that could be adequately characterised.

### 3.4.1 Complexes of 1,2-bis(di-2-pyridylaminomethyl)benzene, 3.11

To amply investigate the coordination chemistry of the novel ligand **3.11**, reactions were carried out with silver nitrate, tetrafluoroborate and hexafluorophosphate, copper nitrate and perchlorate, palladium chloride, cadmium nitrate and zinc acetate. With cadmium nitrate and zinc acetate the ligand precipitated preferentially over the desired coordination complexes under the conditions employed and were not further pursued. Complexes **3.45**, **3.46** and **3.47** were prepared by reaction of the ligand dissolved in 1:1 dichloromethane-methanol solution with silver nitrate, silver tetrafluoroborate and silver hexafluorophosphate, respectively (Scheme 3.13). Complex **3.45** was obtained as colourless crystals in 89% yield and analyses as $[Ag(\mathbf{3.11})NO_3].H_2O$. Many different structures are possible for such a formulation and therefore a crystal structure determination was undertaken. Similarly, complexes **3.46** and **3.47** were

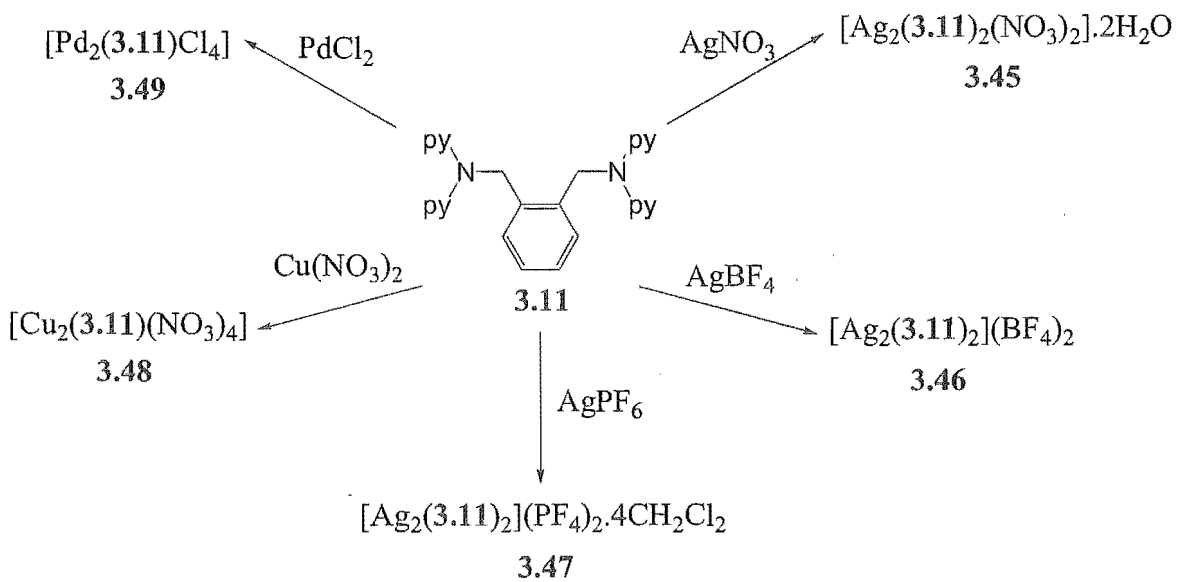


**Scheme 3.13**

obtained as off-white crystals by slow evaporation, in 60% and 68% yield, respectively. These also had the same 1:1 metal-ligand ratio by elemental analysis. Often, as has been demonstrated, the choice of anion strongly influences the type of structure observed, and consequently, both complexes were also analysed by X-ray crystallography.

Reaction of **3.11** dissolved in dichloromethane with copper nitrate dissolved in methanol gave complex **3.48**, as a blue solid in 67% yield that had the composition $[Cu_2(\mathbf{3.11})(NO_3)_4]$ determined by elemental analysis. Despite repeated attempts, this dinuclear complex could not be recrystallised to provide crystals suitable for crystal structure analysis. A dinuclear palladium complex was also prepared in a similar manner to previous palladium chloride complexes, to give **3.49** as a yellow solid in 81% yield. The composition of **3.49** was confirmed by elemental analysis as $[Pd_2(\mathbf{3.11})Cl_4]$, but the complex was highly insoluble and not further studied.

Crystal Structures of **3.45**, **3.46** and **3.47**

The structures of complexes **3.45**, **3.46** and **3.47** are three closely related discrete [2+2] dimetallomacrocycles. Perspective views of two of these structures (**3.45** and **3.46**) are shown in Figures 3.29 and 3.30, respectively, with hydrogen atoms omitted for clarity. Complex **3.45** and **3.46** both crystallise in the monoclinic space group $P2_1/n$ with one ligand molecule, one silver

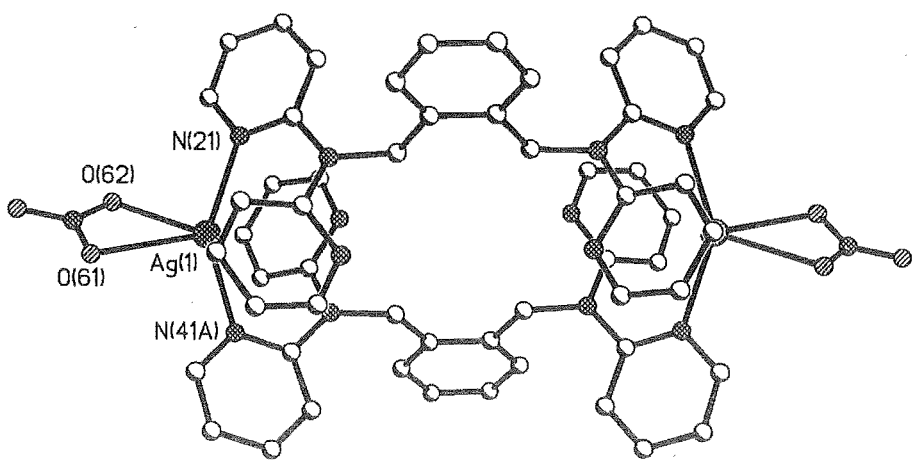


**Figure 3.29.** A perspective view of complex **3.45** with hydrogen atoms omitted for clarity. Selected bond lengths (Å) and angles (°): Ag(1)-N(41A) 2.277(2), Ag(1)-N(21) 2.300(2), Ag(1)-O(62) 2.530(2), Ag(1)-O(61) 2.566(2), N(41A)-Ag(1)-N(21) 144.98(5), N(41A)-Ag(1)-O(62) 123.26(7), N(21)-Ag(1)-O(62) 90.39(7), N(41A)-Ag(1)-O(61) 94.74(6), N(21)-Ag(1)-O(61) 116.81(6), O(62)-Ag(1)-O(61) 49.16(5).

atom and the anion in the asymmetric unit. Complex **3.45** has the silver atoms occupying a pseudo-octahedral environment with coordination by two different pyridine nitrogen atoms, a chelating nitrate anion and weak silver-arene π-interactions with the non-coordinated pyridine rings of the ligand. The silver-nitrogen bonds are 2.277(2) and 2.300(2) Å and the angle between the two pyridine rings is 144.98(5)°. The Ag-C distances for the weak silver-arene π-interactions are 2.917(4) and 3.027(4) Å.

In complex **3.46**, the silver atom adopts a bent geometry with slightly shorter silver-nitrogen distances of 2.223(2) and 2.233(2) Å, and a N(21A)-Ag(1)-N(41) bond angle of 152.84(7)°. However, the silver also makes two close contacts with two of the fluorine atoms of the tetrafluoroborate anion, with silver-fluorine distances of 2.681(2) and 2.686(2) Å. Also, the non-coordinated pyridine rings of the ligand are weakly interacting with the silver atoms. Thus, the coordination geometry is again pseudo-octahedral, as in the previous complex, when all weak interactions have been considered. Like **3.45**, there are weak π-π stacking interactions between the non-coordinated pyridine rings of one ligand molecule and the coordinated pyridine rings of the other ligand. Of interest in both structures is the orientation of the non-coordinated pyridine rings, which have the nitrogen atoms pointing toward the cavity of the metallomacrocycle suggesting the possibility of intramolecular pyridine N···H-C methylene interactions.

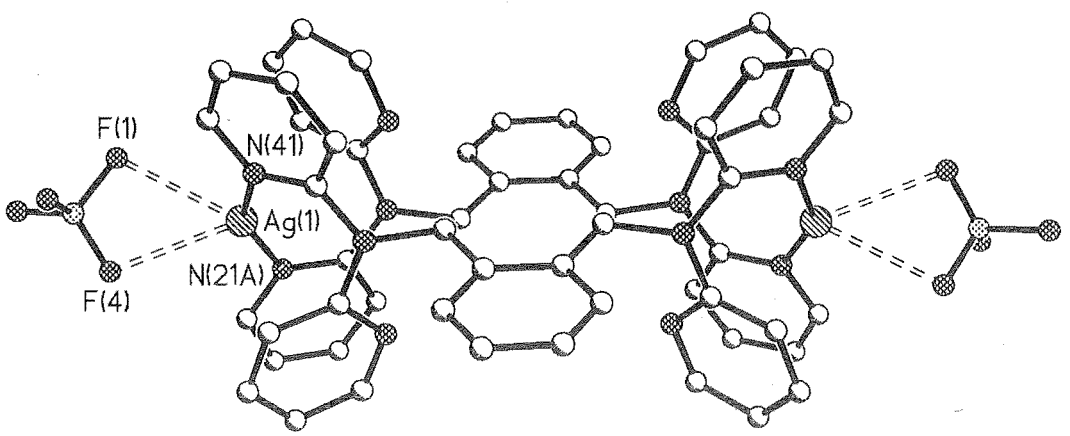


**Figure 3.30.** A perspective view of complex **3.46** showing the weak silver fluorine interactions and with hydrogen atoms omitted for clarity. Selected bond lengths (Å) and angles (°): Ag(1)-N(21A) 2.223(2), Ag(1)-N(41) 2.233(2), Ag(1)-F(1) 2.681(2), Ag(1)-F(4) 2.686(2) N(21A)-Ag(1)-N(41) 152.84(7).

Complex **3.47** crystallises in the triclinic space group P-1 with three ligand molecules, three silver atoms, three hexafluorophosphate anions, one methanol solvate molecule and one disordered dichloromethane molecule in the asymmetric unit. The unit cell thus contains three $M_2L_2$ dimers, each lying on a centre of inversion. The silver atoms have very similar bond lengths to complex **3.46** and the overall complex has the same general structure. The angles about the silver atoms of the coordinated pyridine rings range from 146.17(15) to 150.19(16)° for the three independent complexes in the unit cell. In complex **3.47** the hexafluorophosphate anions are non-coordinated and not interacting, in contrast to the tetrafluoroborate anions in structure **3.46**. However, the pyridine nitrogen coordination of the silver atom is complemented by intermolecular silver-π interactions (Ag-C distance of 2.752(5) Å) with pyridine rings of adjacent [2+2] dimetallocycles. The silver-silver distances in the three complexes **3.45** and **3.46** are 11.201(1) and 10.683(1) Å, while the three silver-silver distances in **3.47** are 10.968(1), 11.039(1) and 11.140(1) Å.

The three silver complexes described here have similarities to a number of related [2+2] dimetallomacrocycles described earlier in this chapter and in the literature. The [2+2] dimetallomacrocycle, **3.26b**, prepared with ligand **3.4**, has a very similar structure and arrangement of the non-coordinated pyridine rings. This type of structure was also observed for a silver trifluoroacetate complex described in the literature.[65] Unlike complexes described by Hartshorn,[147, 150] there is no intimate stacking of the central arene cores, which are parallel to one another, but extend away from the macrocyclic structure on opposite sides of the dimetallomacrocyclic ring. Interestingly, the dimetallomacrocycle is quite a robust structure, which is unaffected by the changes in the anions, in contrast to what has been observed for other complexes in this thesis.

### 3.4.2 Complexes of 1,3-bis(di-2-pyridylaminomethyl)benzene, 3.12

Reaction of a solution of ligand **3.12** dissolved in methanol, with silver nitrate also dissolved in methanol, gave colourless crystals of complex **3.50** in 82% yield. These gave an elemental analysis corresponding to a complex with the formula [Ag(**3.12**)$NO_3$], which would indicate either a discrete 1:1 complex, a [2+2] dimer, or perhaps a 1:1 coordination polymer. The complex was shown by X-ray crystallography to be a discrete ML complex, with a molecule of **3.12** chelating to a silver atom. Complex **3.51** was prepared in 88% yield from silver tetrafluoroborate and **3.12**. The complex provided an elemental analysis indicating an unexpected $M_3L_2$ composition. Unfortunately, no crystals that were suitable for X-ray crystallography could be obtained. When silver hexafluorophosphate was reacted with the ligand

in a 2:1 ratio, a complex, **3.52**, that analysed with a 1:1 composition was isolated in a 31% yield. The crystals that formed in the reaction were suitable for crystal structure analysis and revealed, in contrast to complex **3.50**, a 1:1 coordination polymer.

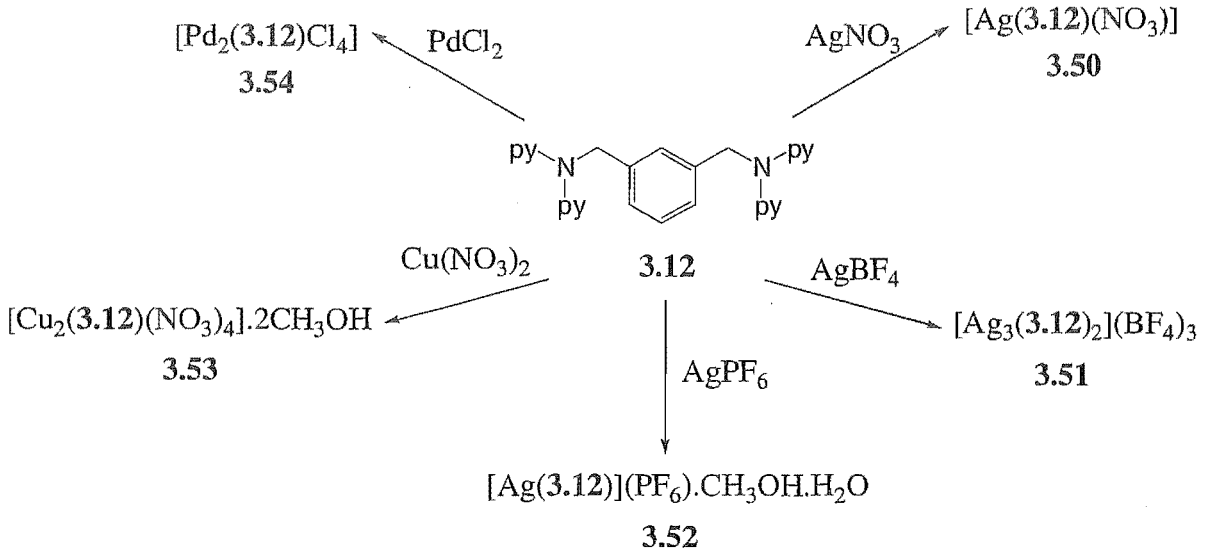


**Scheme 3.14**

Reaction of a solution of **3.12** dissolved in dichloromethane with a methanol solution of copper nitrate in a 2:1 M-L stoichiometry, gave complex **3.53**, as a blue crystalline solid in 54% yield. Complex **3.53** was shown to have the composition $[Cu_2(\mathbf{3.12})(NO_3)_4].2CH_3OH$ by elemental analysis. The dinuclear copper complex was recrystallised by vapour diffusion of ether into a methanol solution of the complex, but the crystals obtained were unsuitable for crystal structure analysis. A dinuclear palladium complex, **3.54**, was prepared by reaction of palladium chloride with the ligand and isolated as a yellow solid in 81% yield. The composition of **3.54** was confirmed by elemental analysis as $[Pd_2(\mathbf{3.12})Cl_4]$, but because the complex was insoluble in common NMR solvents no further characterisation was undertaken.

Crystal Structure **3.50**

Complex **3.50** is a discrete 1:1 complex, with the ligand chelated to the silver atom by a relatively unusual 12-membered chelate ring. It crystallises in the centrosymmetric triclinic space group P-1, with an asymmetric unit consisting of one molecule of **3.12**, one silver atom and a chelating nitrate anion. A perspective view of the structure is shown in Figure 3.31, with hydrogen atoms omitted for clarity. The silver-pyridine nitrogen distances are 2.251(2) and 2.263(2) Å, with the nitrate bonding strongly through one oxygen atom, O(61), and interacting more weakly through a second oxygen atom. The Ag(1)-O(61) and Ag(1)-O(62) bond distances are 2.484(2) and 2.653(2) Å, respectively, with the latter distance representing a weak bond. Weak silver-$\pi$ interactions with the non-coordinated pyridine rings further involve the silver

atom and the silver-arene C-H distance for H2 of the central benzene core is 2.74(1) Å (D = 3.686 Å), indicating a weak M···H-C agostic interaction.

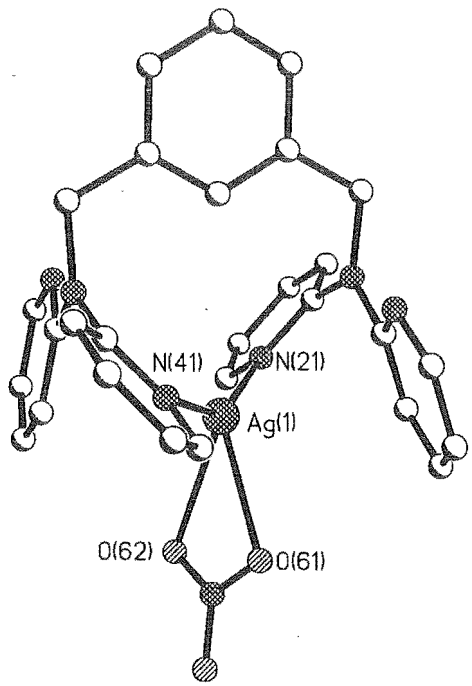


**Figure 3.31.** A perspective view of the discrete ML structure of **3.50** with hydrogen atoms omitted for clarity. Selected bond lengths (Å) and angles (°): Ag(1)-N(21) 2.251(2), Ag(1)-N(41) 2.263(2), Ag(1)-O(61) 2.484(2), Ag(1)-O(62) 2.653(2), N(21)-Ag(1)-N(41) 145.85(5), N(21)-Ag(1)-O(61) 122.55(6), N(41)-Ag(1)-O(61) 90.26(6).

Crystal Structure **3.52**

In stark contrast to the previously described silver complexes of ligand **3.11**, a shift to a non-coordinating anion this time brings about a remarkable change in the structure of the complex. The overall structure of the silver hexafluorophosphate complex, **3.52**, is a one-dimensional coordination polymer rather than the discrete complex described above. Instead of chelating to one silver atom, the ligand now bridges between two trigonal-planar silver atoms to form the polymer. A perspective view of the asymmetric unit of complex **3.52** is shown in Figure 3.32, with a view of the one-dimensional coordination polymer in Figure 3.33.

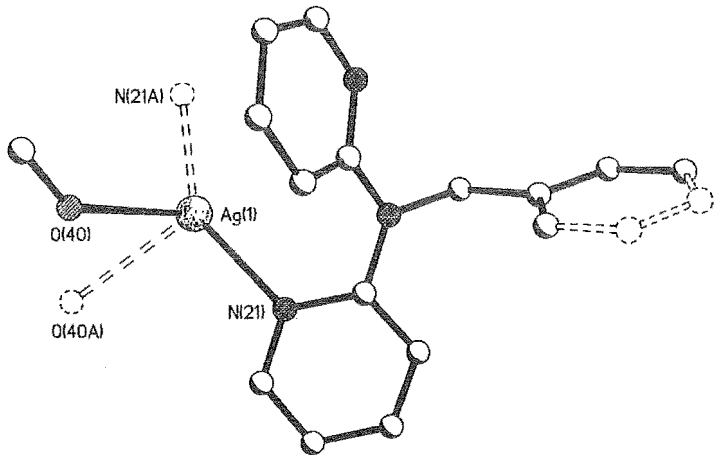


**Figure 3.32.** A perspective view of **3.52** with the two positions of the disordered methanol solvate molecule shown. Hydrogen atoms are omitted for clarity. Selected bond lengths (Å) and angles (°): Ag(1)-N(21) 2.235(4), Ag(1)-O(40) 2.594(7), N(21A)-Ag(1)-N(21) 142.5(2), N(21A)-Ag(1)-O(40A) 113.7(2), N(21)-Ag(1)-O(40A) 98.4(2), N(21A)-Ag(1)-O(40) 98.4(2), N(21)-Ag(1)-O(40) 113.7(2).

Complex **3.52** crystallises in the C-centred monoclinic space group C2/c with the silver atom, benzene ring and hexafluorophosphate anion all lying on 2-fold rotation axes. The coordinated methanol molecule is disordered over two sites. The silver thus sits in a distorted trigonal-planar site composed from the two pyridine nitrogen donors and an oxygen from the disordered methanol molecule. The silver-nitrogen and silver-oxygen bond distances are 2.235(4) and 2.594(7) Å, respectively.

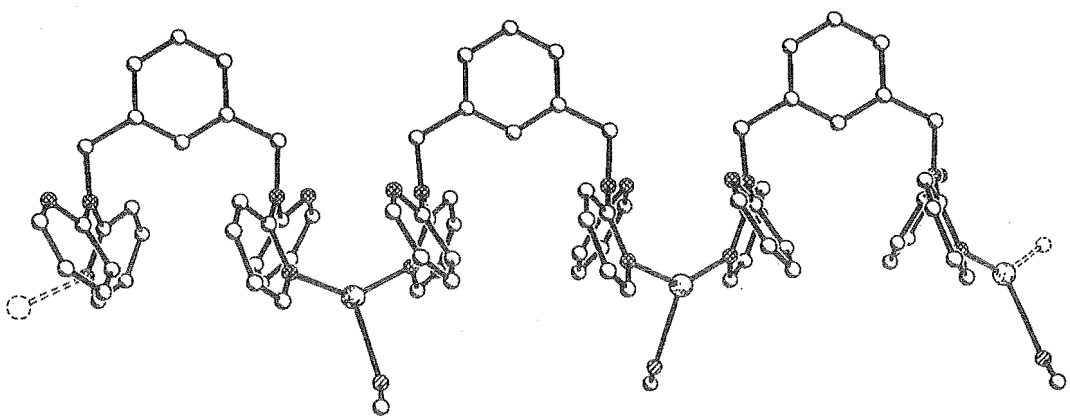

**Figure 3.33.** A perspective view of the extended structure of complex **3.52**.

As the extended structure in Figure 3.33 shows, the trigonal-planar silver atoms also make weak silver-arene π-interactions with the non-coordinated pyridine rings of the ligand. A

consideration of the packing of **3.52** reveals that the non-coordinated hexafluorophosphate anions fit in a cavity formed by the benzene ring, the non-coordinated pyridine rings and the coordinated methanol solvate molecules. Adjacent coordination polymers are connected through a network of weak C-H···F interactions.

An interesting point of comparison can be made between the one-dimensional coordination polymer, **3.52** and the discrete complex **3.50** discussed above. While there are significant changes in the type of structure observed, in both these structures the silver geometry is very similar and the ligand has a similar conformation. However, in **3.52** the coordinated pyridine rings of the ligand are directed away from the benzene core leading to the formation of a one-dimensional coordination polymer, rather than a discrete 1:1 complex.

### 3.4.3 Complexes of 1,4-bis(di-2-pyridylaminomethyl)benzene, 3.13

When the 1,4-substituted ligand, **3.13**, was reacted with silver nitrate, a pale yellow crystalline precipitate was obtained in 97% yield. This complex, **3.55**, analysed with a 1:1 metal-ligand composition suggesting a discrete 1:1 complex, a [2+2] dimer or perhaps a 1:1 coordination polymer. By contrast, when silver tetrafluoroborate was employed, a complex, **3.56**, was isolated as a pale yellow precipitate with the composition $[Ag_2(\mathbf{3.13})](BF_4)_2$, as shown by elemental analysis. Silver hexafluorophosphate was also reacted with a dichloromethane-methanol solution of the ligand to give a yellow crystalline precipitate that was isolated in 95% yield. Elemental analysis indicated that the complex, **3.57a**, had a 1:1 metal to ligand ratio

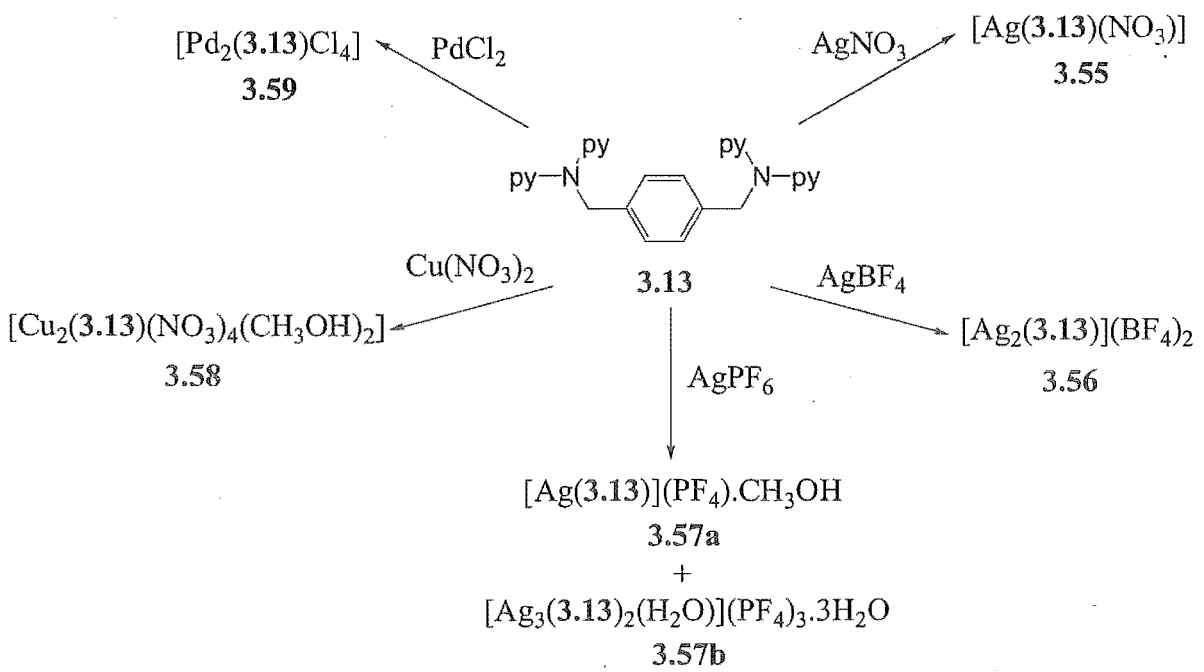


**Scheme 3.15**

and the composition [Ag(**3.13**)]($PF_6$).$CH_3OH$. The filtrate from this reaction yielded, on slow evaporation, colourless crystals, which were shown to have a different stoichiometry by X-ray crystallography. This complex, **3.57b**, had a $M_3L_2$ composition, but could not be obtained in significant quantity for further characterisation by elemental analysis.

A dinuclear copper complex, **3.58**, was obtained in 59% yield by reacting **3.13** dissolved in dichloromethane-methanol with copper nitrate dissolved in methanol. On standing blue crystals precipitated from the solution, which were shown to have the composition [$Cu_2$(**3.13**)$(CH_3OH)_2(NO_3)_4$] by elemental analysis. This composition was confirmed by crystal structure analysis as described below. A dinuclear palladium chloride complex, **3.59**, was prepared by reaction of a 2:1 ratio of palladium chloride dissolved in 2 M hydrochloric acid, with a methanol solution of **3.13**. This complex was isolated as a yellow solid in 80% yield. Elemental analysis confirmed the proposed dinuclear nature of this complex, with a composition of [$Pd_2$(**3.13**)$Cl_4$]. Like many other dinuclear palladium chloride complexes, **3.59** was insoluble in common NMR solvents and no further characterisation was undertaken.

Crystal Structure of **3.57b**

The structure of the $M_3L_2$ complex, **3.57b**, is an interesting hybrid of two different structural motifs, which have been observed for previous complexes of these di-2-pyridylamine-based ligands. At one end of the complex the di-2-pyridylamine units are hypodentate and coordinate to one silver atom, while at the opposite end, a twelve-membered dimetallocycle forms between two silver atoms. Thus, the $M_3L_2$ complex is an unusual 'helicate-like' structure. In the overall complex, the ligand strands have a helical twist between the metal centre Ag(2) and the other, bimetallic, end of the complex (Ag(1)/Ag(3)). The $M_3L_2$ structure is shown in Figure 3.34 with hydrogen atoms, non-coordinated solvate molecules and anions omitted for clarity. Complex **3.57b** crystallises in the monoclinic space group $P2_1/c$, with one complete trication, three water molecules and three hexafluorophosphate anions in the asymmetric unit.

The three silver atoms have very similar, approximately linear geometries when only the pyridine donors are considered. Ag(3) also coordinates to a water molecule (Ag-O distance 2.579(5) Å), but the N(21')-Ag(3)-N(21) angle is 150.40(12)°, consistent with this being a weak interaction. The water molecule, O(60), is hydrogen bonded to a nearby hexafluorophosphate anion and to a non-coordinated water molecule. Ag(3) is also involved in a silver-arene π-interaction with the benzene ring of the ligand (Ag-C distances of 2.844(7) and 2.848(7) Å). Ag(1) and Ag(2) are coordinated by pyridine rings only and have close to linear geometries, but

make weak contacts with the fluorine atoms of nearby hexafluorophosphate anions. The shortest Ag-F distances are 2.826(5) and 2.897(5) Å for Ag(1) and 2.830(5) Å for Ag(2). Silver-arene π-interactions also occupy further coordination sites about Ag(1) and Ag(2).

The silver-silver distances from Ag(2) to Ag(1) and Ag(3) are 8.108(1) and 7.967(1) Å, respectively. Ag(1) and Ag(3) are 3.844(1) Å apart, confirming that there are no significant silver-silver interactions in **3.57b**.[119] Interestingly, the bimetallic end of the complex is not much larger in volume than the other monometallic end. There are no unusually short intermolecular contacts in the structure.

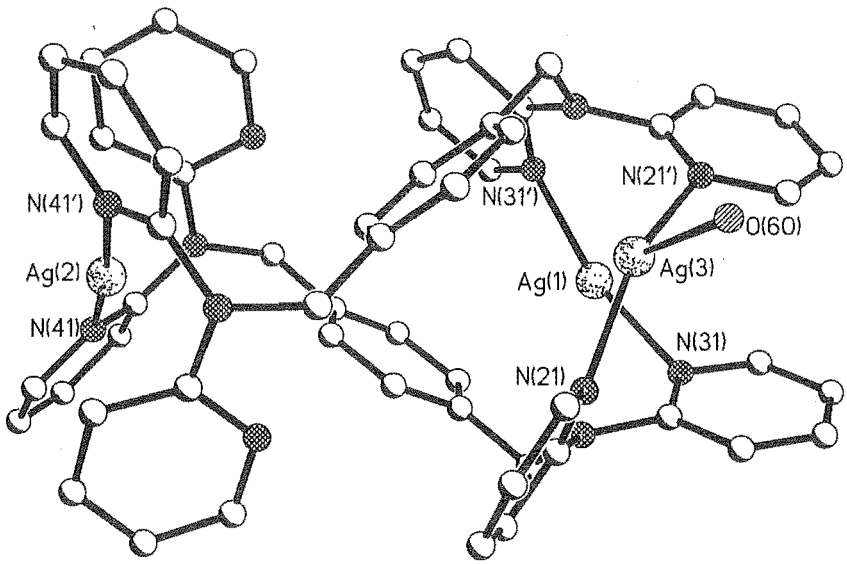


**Figure 3.34.** A perspective view **3.57b** with hydrogen atoms, non-coordinated solvate molecules and anions omitted for clarity. Selected bond lengths (Å) and angles (°): Ag(1)-N(31') 2.151(3), Ag(1)-N(31) 2.156(3), Ag(2)-N(41) 2.166(3), Ag(2)-N(41') 2.175(3), Ag(3)-N(21) 2.195(3), Ag(3)-N(21') 2.204(3), Ag(3)-O(60) 2.579(5), N(31')-Ag(1)-N(31) 163.80(12), N(41)-Ag(2)-N(41') 172.77(11), N(21)-Ag(3)-N(21') 150.40(12), N(21)-Ag(3)-O(60) 94.88(19), N(21')-Ag(3)-O(60) 103.18(17).

Crystal Structure of **3.58**

Reaction of copper nitrate with **3.13** in a 2:1 stoichiometry had provided crystals of complex **3.58**, which were suitable for X-ray crystallography. The complex crystallised in the monoclinic space group $P2_1/n$, with an asymmetric unit that contained half a ligand molecule, one copper atom, two nitrate anions and a coordinated methanol solvate molecule. A perspective view of complex **3.58** is shown in Figure 3.35, with hydrogen atoms omitted for clarity. The copper atom has a square-pyramidal geometry (τ value of 0.02), with the two pyridine nitrogen donors and the

monodentate nitrate anions occupying the basal plane and the coordinated methanol molecule in the apical position. The complex has copper-nitrogen and copper-oxygen distances ranging between 1.985(2) and 2.008(2) Å for the donor atoms in the plane, while the methanol solvate oxygen is bonded at a distance of 2.231(2) Å from the copper atom.

The copper-copper distance in this complex is 11.206(1) Å, and is almost identical to the dinuclear copper complex, **3.23**, of the amino-linked homologue, which has a copper-copper distance of 11.179(1) Å. The two extra atoms in the ligand bridge do not affect the metal-metal distance because of the added flexibility of the ligand. A consideration of the packing shows that the dinuclear complexes are discrete, but that there are weak O-H···O hydrogen bonds between the coordinated methanol of one complex and the oxygen atom of a nitrate anion on an adjacent complex.

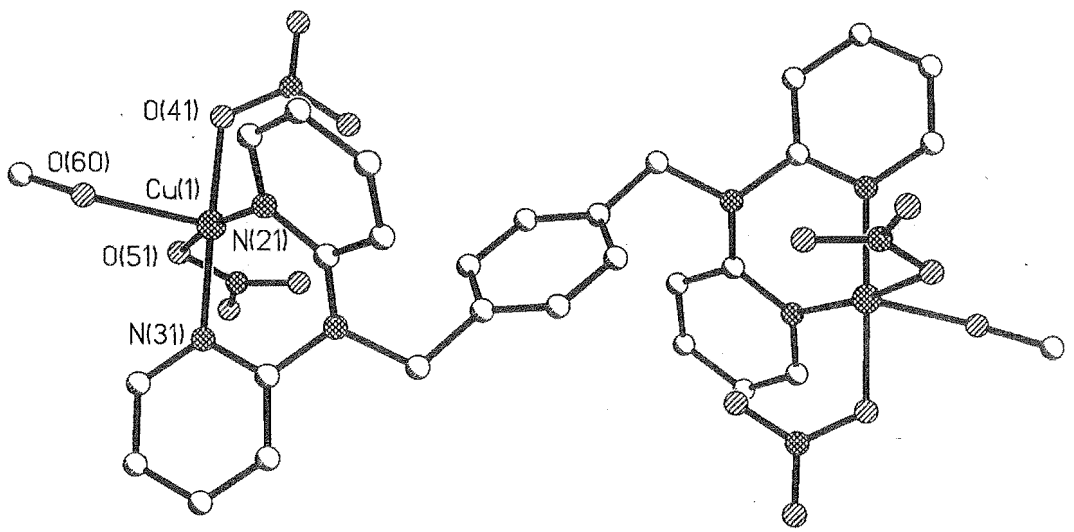


**Figure 3.35.** A perspective view of complex **3.58**. Selected bond lengths (Å) and angles (°): Cu(1)-N(21) 1.985(2), Cu(1)-O(41) 1.998(2), Cu(1)-N(31) 1.999(2), Cu(1)-O(51) 2.008(2), Cu(1)-O(60) 2.231(2), N(21)-Cu(1)-O(41) 95.81(9), N(21)-Cu(1)-N(31) 86.40(9), O(41)-Cu(1)-N(31) 176.52(9), N(21)-Cu(1)-O(51) 170.01(8), O(41)-Cu(1)-O(51) 87.17(8), N(31)-Cu(1)-O(51) 90.21(8), N(21)-Cu(1)-O(60) 100.01(9), O(41)-Cu(1)-O(60) 7.57(10), N(31)-Cu(1)-O(60) 94.71(10).

### 3.4.4 Complexes of 1,3,5-tris(di-2-pyridylaminomethyl)benzene, 3.14

Ligand **3.14** was reacted with a range of different metal salts in an attempt to investigate the various coordination modes of this ligand. Disappointingly, reaction of the ligand with several different silver salts failed to provide any crystalline solids. The employment of different

reaction techniques and crystallisation methods may need to be used to obtain crystalline samples of complexes of this new multi-armed ligand. Fortunately, a trinuclear copper complex was obtained by reaction of copper nitrate with **3.14**, as a blue crystalline solid in 65% yield, which displayed some of the coordination properties of this ligand. However, satisfactory analysis for this complex, **3.60**, could not be obtained to agree with the $[Cu_3(\mathbf{3.14})(NO_3)_4(H_2O)_5](NO_3)_2.5H_2O$ composition, determined by single crystal X-ray crystallography.

Crystal Structure of **3.60**

Complex **3.60** crystallises in the orthorhombic space group, Pbcn, with $Z = 8$. A perspective view of the complex is shown in Figure 3.36, with non-coordinated solvate molecules and anions omitted for clarity. In the discrete complex, each ligand coordinates to three copper atoms with chelation by a six-membered chelate ring. The refinement on this structure is not satisfactory, and despite collecting this data set three times, no improvement could be obtained. As such, while the structure is mentioned because of the interesting conformation, minimal information will be given on bond lengths and angles.

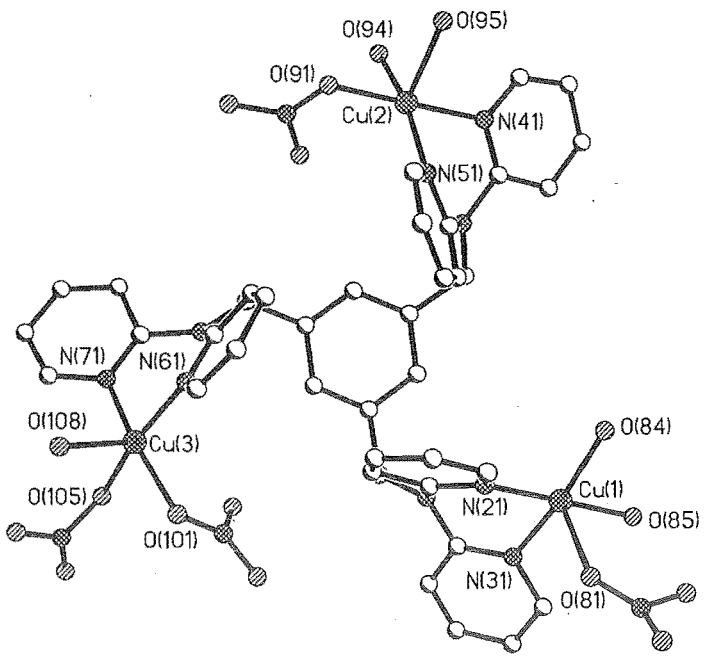


**Figure 3.36.** A perspective view of complex **3.60** looking down on the benzene core of the ligand. Hydrogen atoms, non-coordinated solvate molecules and anions are omitted for clarity.

The three copper atoms have square pyramidal geometries with τ values of 0.12 [Cu(1)], 0.25 [Cu(2)] and 0.12 [Cu(3)]. Cu(1) and Cu(2) are coordinated by two pyridine donors, one monodentate nitrate anion and two water molecules. Cu(3) has two monodentate coordinated nitrate anions and only one coordinated water molecule. The bond lengths for these donor atoms are typical for a square pyramidal copper atom, with slightly longer bonds to the atom in the apical position of the copper.

One of the noteworthy features of this complex is its overall structure and conformation. The copper atoms are all located on one face of the benzene ring (Figure 3.37). The arms of the ligand display some co-operative behaviour, with the di-2-pyridylamino units twisting in one direction. It is relatively uncommon for simple tris-substituted benzene rings to have all the bulky groups on one face of the benzene ring, with the conformational control in these systems being virtually non-existent.[141] One reason for this conformation may be the packing of the complex in the solid state. The benzene cores of the two trinuclear complexes pack back-to-back with very weak π-π stacking interactions (centroid-centroid distance of 3.94(2) Å) between the offset benzene rings. The closest C-C distance is 3.76(2) Å. There is also the possibility that there are three weak edge-to-face C-H···π interactions between the pyridine rings on the top face of the complex (Figure 3.37), which further stabilise such a conformation.

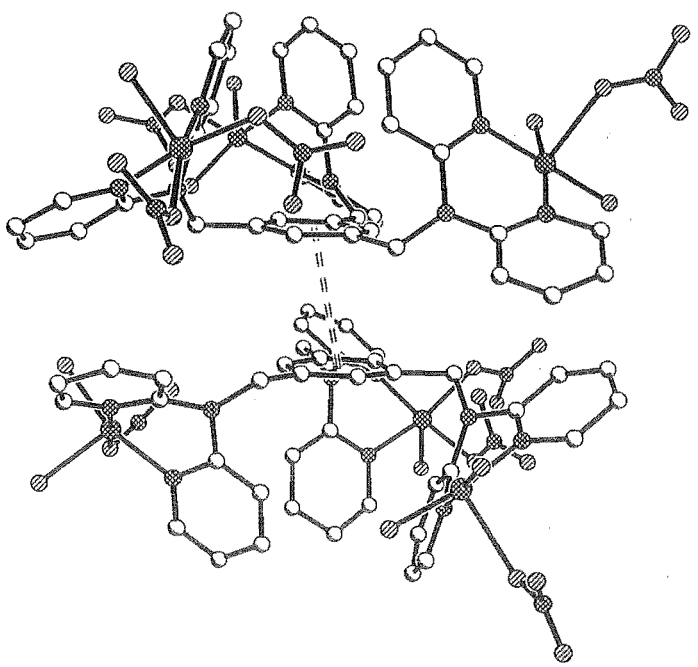

**Figure 3.37.** A perspective view perpendicular of complex **3.60**, showing the co-operative binding and association of two complexes in the solid state.

### 3.4.5 Complexes of 1,2,4,5-tetrakis(di-2-pyridylaminomethyl)benzene, 3.15

Difficulties were encountered in forming coordination complexes of this ligand. The previous ligand, **3.14**, was relatively insoluble, which caused problems in forming coordination complexes. For **3.15**, this problem was more pronounced. Nonetheless, a copper nitrate complex, **3.61**, was prepared in 58% yield by reaction of a methanol solution of copper nitrate with the ligand dissolved in dichloromethane. A green solid precipitated immediately and was shown by elemental analysis to have the composition $[Cu_4(\mathbf{3.15})(NO_3)_8].4H_2O$. This is likely to have a structure very similar to **3.60** in terms of the coordination environment and geometry of the copper atom, but a very different conformation of the ligand. Previous examples of 1,2,4,5-substituted benzene rings generally have the bulky arms arranged on both sides of the central arene core.

## 3.5. Ruthenium complexes of the N-linked ligands

As outlined in Chapter 1, one of the major aims of this thesis was to prepare ruthenium complexes of bridging ligands, and to study the nature of the metal-ligand and any metal-metal interactions within such complexes. The nature of the ligand bridge has a fundamental impact on the electronic interaction between the metals and on the characteristics of the complex by controlling the distance and relative orientations of the metal centres. Another aspect, and an important design factor that needs to be considered when preparing bridging ligands, is the extent of conjugation between the metal centres in the subsequent complexes. The extent of conjugation influences the degree of through-bond communication between the metal centres.

The first series of ligands prepared in this chapter, with di-2-pyridylamine units directly attached to the arene core, presents an interesting contrast to some of the other bridging ligands that have previously been investigated. These ligands chelate to metal atoms via a six-membered chelate ring, like the ligands investigated in Chapter 2, but they incorporate larger spacer groups between the chelating units. The other differentiating factor concerning this series of ligands is that the conjugation is partially disrupted by the amine nitrogen atoms, which are planar and $sp^2$-hybridised. In the second series of ligands, the conjugation is completely disrupted by the introduction of the methylene spacers and thus, the ruthenium complexes of these ligands were not investigated.

### 3.5.1 Synthesis of the complexes and NMR spectroscopy

As shown in Scheme 3.16, reaction of $[Ru(bpy)_2Cl_2]$ or $[Ru(dmb)_2Cl_2]$ with ligand **3.2** in 3:1 ethanol-water, gave the dinuclear complexes, **3.62** and **3.63**, respectively, as their

hexafluorophosphate salts. Both complexes form as a 1:1 mixture of their diastereoisomers and were not separated in this work. Complex **3.62** was isolated in 93% yield following a reaction time of 48 hours, while **3.63** was obtained in 61% yield after 72 hours of refluxing. Using elemental analysis and $^1$H NMR spectroscopy, complexes **3.62** and **3.63** were characterised as $[\{Ru(bpy)_2\}_2(\mathbf{3.2})](PF_6)_4$ and $[\{Ru(dmb)_2\}_2(\mathbf{3.2})](PF_6)_4$, respectively.

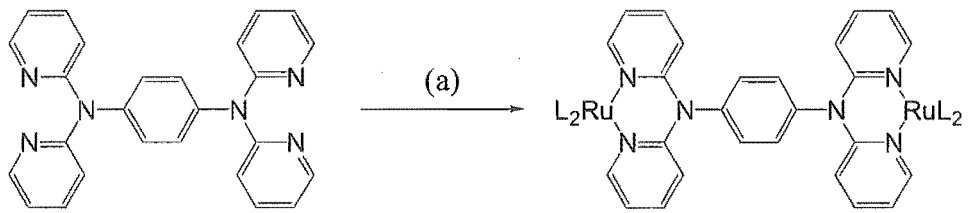


**3.2** **3.62** L=bpy
**3.63** L=dmb

(a) $Ru(L)_2Cl_2$, EtOH/water, $NH_4PF_6$

**Scheme 3.16**

The $^1$H NMR spectrum of **3.62** consists of 13 independent multiplets consistent with a dinuclear complex of ligand **3.2**. The chemical shifts for the pyridine rings of **3.2** and the ancillary bpy rings of the diastereoisomers are partially resolved in some instances and overlapped in other cases indicating slight structural differences between the two diastereoisomers. More clearly resolved are the two singlets for the protons of the benzene ring, corresponding to the two diastereoisomers and indicating there are, as expected, greater structural differences around the central benzene ring. By examination of the spin-spin coupling information and using a combination of 1-D TOCSY and 1D-NOESY NMR techniques, the $^1$H NMR spectrum of **3.62** was assigned. The $^1$H NMR spectrum of **3.63** is likewise consistent with two diastereoisomers, with some multiplets that are partially resolved allowing the chemical shifts of the dmb rings of the two diastereoisomers to be differentiated. The chemical shifts for the pyridine rings of the bridging ligand in the two diastereoisomers were too close to be resolved. The $^1$H NMR chemical shifts for the ligand **3.2** in acetonitrile, and for the two diastereoisomers of the two dinuclear ruthenium complexes **3.62** and **3.63**, are given in Table 3.2, along with the CIS values, which are given in italics.

The CIS values for the two complexes are very similar, which is consistent with the very subtle changes to the ancillary ligands of the complex. No unusual CIS values are observed for either complex. The large negative CIS values for the H6 protons result from inter-ligand through-space ring-anisotropy effects because, in the complexes, these protons lie over the shielding plane of adjacent bpy or dmb rings.

**Table 3.2.** $^1$H NMR chemical shift values for the ligand **3.2** and the two dinuclear complexes **3.62** and **3.63** recorded in acetonitrile, with the CIS values shown in italics. An asterisk differentiates the signals assigned to the two diastereoisomers.

| | H3' | H4' | H5' | H6' | ben. CH |
|---|---|---|---|---|---|
| **3.2** | 7.10 | 7.71 | 7.07 | 8.31 | 7.16 |
| **3.62** | 7.48 | 7.95 | 7.06 | 7.58 | 7.11 |
| *CIS* | *0.38* | *0.24* | *-0.01* | *-0.73* | *-0.05* |
| **3.62*** | 7.47 | 7.93 | 7.05 | 7.58 | 7.09 |
| *CIS* | *0.37* | *0.22* | *-0.02* | *-0.73* | *-0.07* |
| **3.63/3.63*** | 7.43 | 7.89 | 7.01 | 7.57 | 7.20 |
| *CIS* | *0.33* | *0.18* | *-0.06* | *-0.74* | *0.04* |

Ligand **3.3** differs from the previously described ligand by insertion of a second benzene ring between the two chelating domains of the ligand. Reaction of $[Ru(bpy)_2Cl_2]$ or $[Ru(dmb)_2Cl_2]$ with **3.3**, in a 3:1 ethanol-water solvent mixture, gave the dinuclear complexes **3.64** and **3.65**, respectively, as 1:1 mixtures of their diastereoisomers (Scheme 3.17). These were isolated as their hexafluorophosphate salts in 50% and 66% yield, respectively, using the same reaction times as for complexes **3.62** and **3.63**. Using elemental analysis, mass spectrometry and $^1$H NMR spectroscopy, complexes **3.64** and **3.65** were characterised as $[\{Ru(bpy)_2\}_2(\mathbf{3.3})](PF_6)_4$ and $[\{Ru(dmb)_2\}_2(\mathbf{3.3})](PF_6)_4$, respectively.

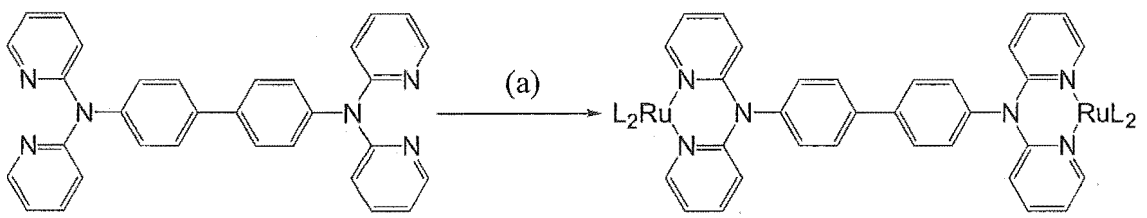


**3.3**

**3.64** L=bpy
**3.65** L=dmb

(a) $Ru(L)_2Cl_2$, EtOH/water, $NH_4PF_6$

**Scheme 3.17**

The $^1$H NMR chemical shifts for the ligand **3.3** in acetonitrile, and for the two diastereoisomers of the two dinuclear ruthenium complexes **3.64** and **3.65**, are given in Table 3.3, along with the CIS values. The $^1$H NMR spectrum of **3.64**, shown in Figure 3.38, is consistent with a mixture of the racemic and meso diastereoisomers of the expected dinuclear complex. There are two different doublets, for the two sets of chemically equivalent H3 and H5 protons of the biphenyl ring, originating from the two diastereoisomers. The chemical shifts of the H2 and H6 protons on the biphenyl core are overlapped with other chemical shifts for pyridine and bpy rings. An unambiguous assignment of the proton chemical shifts of each diastereoisomer could be achieved because chromatography on alumina resulted in enrichment

of some of the column fractions with one diastereoisomer. The $^1$H NMR spectrum of **3.65** is likewise consistent with two diastereoisomers, with some multiplets that are partially resolved allowing the chemical shifts of the pyridine rings of the ligand and the ancillary dmb ligands of the two diastereoisomers to be differentiated.

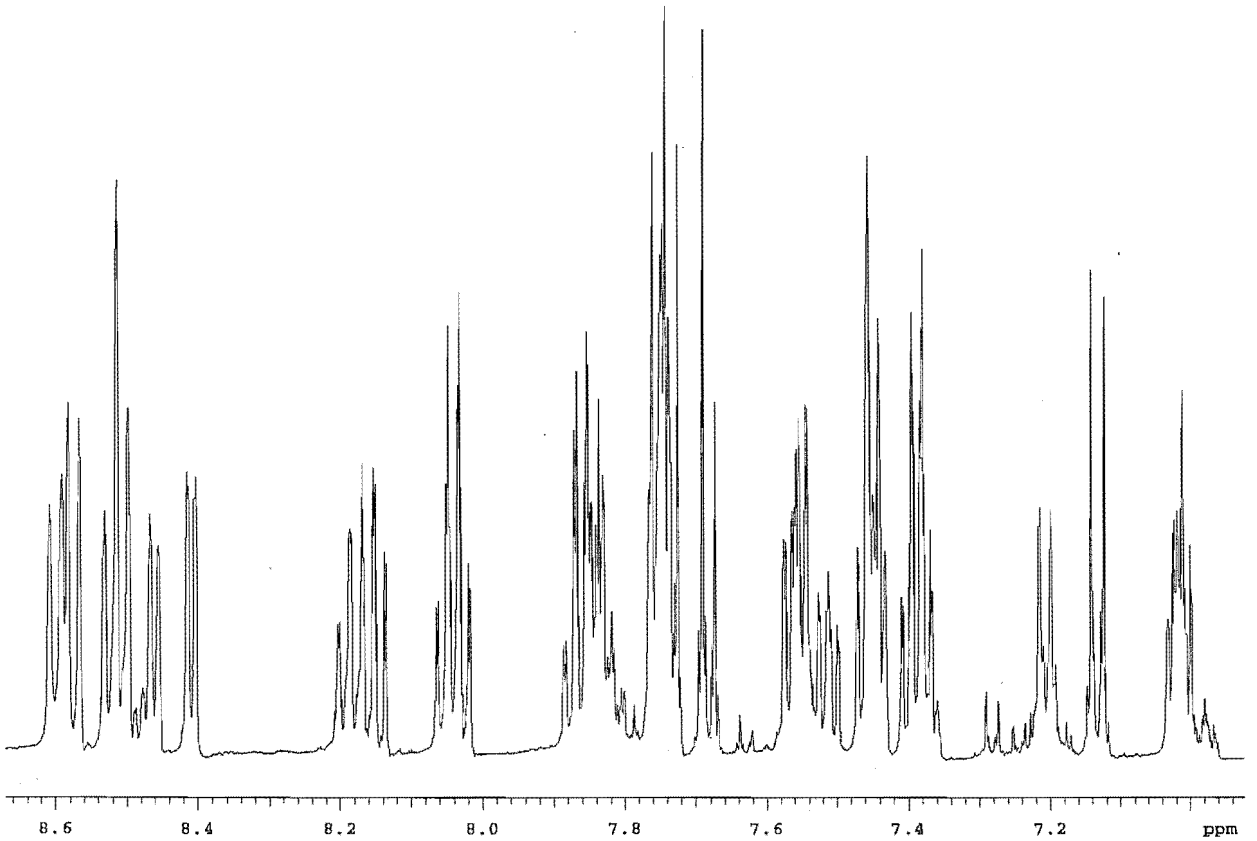


**Figure 3.38.** The aromatic region of the $^1$H NMR spectrum of complex **3.64/3.64***.

**Table 3.3.** $^1$H NMR chemical shift values for **3.3** and the two dinuclear complexes **3.64** and **3.65** recorded in acetonitrile, with the CIS values shown in italics. An asterisk differentiates the signals assigned to the different diastereoisomers of the complexes.

| | H3' | H4' | H5' | H6' | H3/H5 | H2/H6 |
|---|---|---|---|---|---|---|
| **3.3** | 7.06 | 7.69 | 7.07 | 8.30 | 7.23 | 7.68 |
| **3.64** | 7.44 | 7.85 | 7.01 | 7.55 | 7.21 | 7.84 |
| *CIS* | *0.38* | *0.26* | *-0.06* | *-0.75* | *-0.02* | *0.16* |
| **3.64*** | 7.45 | 7.85 | 7.01 | 7.55 | 7.13 | 7.75 |
| *CIS* | *0.39* | *0.26* | *-0.06* | *-0.75* | *-0.10* | *0.07* |
| **3.65** | 7.44 | 7.85 | 7.01 | 7.57 | 7.18 | 7.83 |
| *CIS* | *0.38* | *0.26* | *-0.06* | *-0.73* | *-0.05* | *0.15* |
| **3.65*** | 7.49 | 7.85 | 7.02 | 7.55 | 7.08 | 7.73 |
| *CIS* | *0.43* | *0.26* | *-0.05* | *-0.75* | *-0.13* | *0.05* |

The CIS values for complexes **3.64** and **3.65** are very similar to those observed for the previous set of complexes. Again large negative CIS values occur for the H6 protons of the

coordinated pyridine rings, because they lie over the shielding region of the bpy or dmb rings. The H3 and H5 protons of the biphenyl core are deshielded more so in one of the diastereoisomers than the other, which suggests a greater difference in the two structures around the biphenyl core.

After having prepared dinuclear complexes of ligand **3.3**, which provides an increase in the metal-metal distance over the benzene-based ligand, the ligands possessing a naphthalene core were employed to assess the effect of a more bulky arene core. The 1,4-substituted naphthalene ligand, **3.4** was investigated first. Reaction of either $[Ru(bpy)_2Cl_2]$ or $[Ru(dmb)_2Cl_2]$ with **3.4** in a 2:1 stoichiometry, using the standard reaction medium of 3:1 ethanol-water, provided only the mononuclear complexes **3.66** and **3.67**, respectively. These were isolated as their hexafluorophosphate salts, as shown in Scheme 3.18, in 66% yield for complex **3.66**, while the dmb complex, **3.67**, was obtained in 81% yield. Using elemental analysis, mass spectrometry and $^1H$ NMR spectroscopy, complexes **3.66** and **3.67** were confirmed as $[Ru(bpy)_2(\mathbf{3.4})](PF_6)_2$ and $[Ru(dmb)_2(\mathbf{3.4})](PF_6)_2$, respectively.

To synthesise the dinuclear complex of **3.4**, the ligand was reacted with $[Ru(bpy)_2Cl_2]$ once again, but for a period of 96 hours as opposed to the normal 48 hours (Scheme 3.18). This provided a mixture of the mononuclear and dinuclear complexes that was separated using alumina chromatography to give the above mononuclear complex, **3.66**, in 17% yield, and the

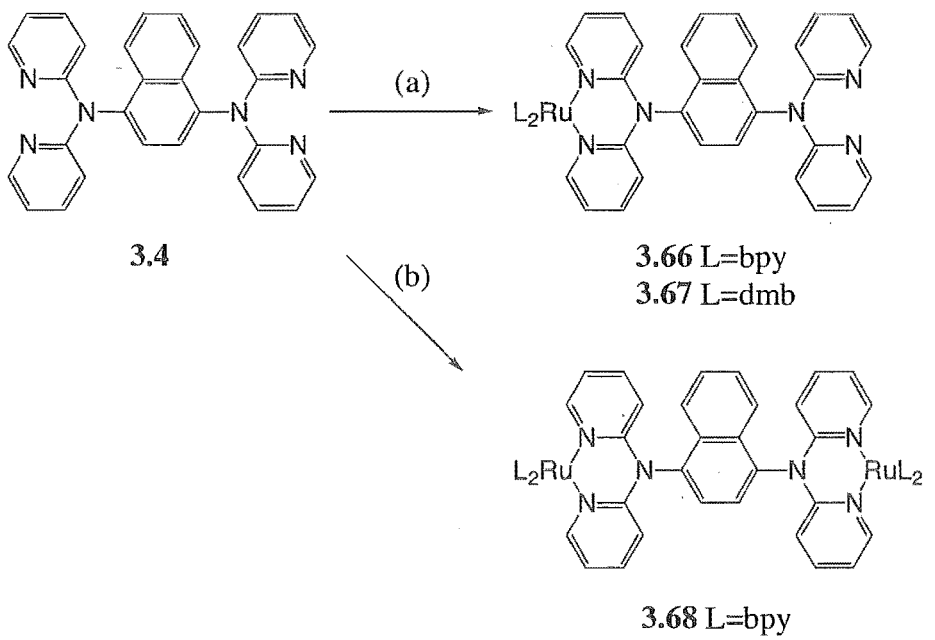


**3.4** **3.66** L=bpy
**3.67** L=dmb

**3.68** L=bpy

(a) $Ru(L)_2Cl_2$, EtOH/water, $NH_4PF_6$, 48hrs; (b) $Ru(L)_2Cl_2$, EtOH/water, $NH_4PF_6$, 96hrs.

**Scheme 3.18**

desired dinuclear complex, **3.68**, in 51% yield. As expected from the previous results, complex **3.68** was obtained as a 1:1 mixture of diastereoisomers and the complex was characterised as $[\{Ru(bpy)_2\}_2(3.4)](PF_6)_4$ in the usual manner.

The $^1$H NMR spectra of **3.66** and **3.67** are complicated by the lower ($C_1$) symmetry of the complexes, which have restricted rotation about the naphthalene-amine nitrogen single bond of the chelated di-2-pyridylamine unit. Thus, the coordinated pyridine rings of the ligand are non-equivalent, but the non-coordinated pyridine rings of the other di-2-pyridylamine unit are equivalent because of free rotation about this naphthalene-amine nitrogen single bond. Employment of the 1-D TOCSY experiment allowed the assignment of all chemical shifts to individual protons for both mononuclear complexes. The $^1$H NMR chemical shifts for the ligand **3.4** in acetonitrile and for the two mononuclear ruthenium complexes **3.66** and **3.67** are given in Tables 3.4a and 3.4b, along with the CIS values, which are given in italics.

**Table 3.4a.** $^1$H NMR chemical shift values for the pyridine rings of ligand **3.4** and the two mononuclear complexes **3.66** and **3.67** in acetonitrile, with the CIS values shown in italics.

| | H3' | H4' | H5' | H6' |
|---|---|---|---|---|
| **3.4** | 7.17 | 7.70 | 7.03 | 8.26 |
| **3.66'** | 6.34 | 7.46 | 6.81 | 7.90 |
| *CIS* | *-0.83* | *-0.24* | *-0.22* | *-0.36* |
| **3.66"** | 6.71 | 7.61 | 6.77 | 7.59 |
| *CIS* | *-0.46* | *-0.09* | *-0.26* | *-0.67* |
| **3.66'"** | 7.22 | 7.73 | 7.09 | 8.29 |
| *CIS* | *0.05* | *0.03* | *0.06* | *0.03* |
| **3.67'** | 6.31 | 7.44 | 6.79 | 7.90 |
| *CIS* | *-0.86* | *-0.26* | *-0.24* | *-0.36* |
| **3.67"** | 6.67 | 7.57 | 6.74 | 7.18 |
| *CIS* | *-0.50* | *-0.13* | *-0.29* | *-1.08* |
| **3.67'"** | 7.22 | 7.74 | 7.09 | 8.29 |
| *CIS* | *0.05* | *0.04* | *0.06* | *0.03* |

**Table 3.4b.** $^1$H NMR chemical shift values for the naphthalene ring system of ligand **3.4** and the two mononuclear complexes **3.66** and **3.67** recorded in acetonitrile, with the CIS values shown in italics.

| | H2 | H3 | H5 | H6 | H7 | H8 |
|---|---|---|---|---|---|---|
| **3.4** | 7.52 | 7.52 | 7.92 | 7.43 | 7.43 | 7.92 |
| **3.66** | 7.18 | 7.46 | 8.11 | 7.59 | 7.57 | 7.72 |
| *CIS* | *-0.34* | *-0.06* | *0.19* | *0.16* | *0.14* | *-0.20* |
| **3.67** | 7.69 | 7.51 | 8.11 | 7.59 | 7.55 | 7.71 |
| *CIS* | *0.17* | *-0.01* | *0.19* | *0.16* | *0.12* | *-0.21* |

The CIS values for the mononuclear complexes **3.66** and **3.67** are larger and more variable than the values observed for the previously described dinuclear complexes. The two coordinated pyridine rings have quite different CIS values, consistent with the restricted rotation of the coordinated arm of the ligand and the different environments for each ring. The naphthalene ring affects one of these coordinated pyridine rings, while the second ring has an environment, and therefore CIS values, similar to the pyridine rings in the dinuclear complexes previously described. The former pyridine ring, denoted with a prime in the table, has a large negative CIS value for the H3 proton because on complexation these protons lie over the shielding region of the adjacent naphthalene ring. The non-coordinated pyridine rings are not affected by coordination and the chemical shifts for these protons are relatively unchanged. The CIS values for the naphthalene ring are consistent with the proposed structure. Very similar observations were made for the dmb complex, **3.67**.

The $^1$H NMR spectrum of **3.68** is much simpler than the spectra for the mononuclear complex **3.66**. The $^1$H NMR spectrum of **3.68** is, like previous spectra of other dinuclear complexes, consistent with two diastereoisomers, with some multiplets that are resolved, which allows the chemical shifts of the pyridine rings and bpy rings of the two diastereoisomers to be differentiated. The various spin systems were not assigned to a specific diastereoisomer because there was no enrichment of any of the column fractions when the complex was purified. The $^1$H NMR chemical shifts for **3.4** in acetonitrile and for the dinuclear ruthenium complex **3.68** in the same solvent are given in Tables 3.5a and 3.5b, along with the CIS values, which are given in italics.

**Table 3.5a.** $^1$H NMR chemical shift values for the pyridine rings of ligand **3.4** and the dinuclear complex **3.68** recorded in acetonitrile, with the CIS values shown in italics. One set of pyridine rings (denoted by primes and the other by double primes) must be assigned to one diastereoisomer and the other set to the second diastereoisomer.

| | H3' | H4' | H5' | H6' |
|---|---|---|---|---|
| **3.4** | 7.17 | 7.70 | 7.03 | 8.26 |
| **3.68'** | 6.42 | 7.46 | 6.86 | 7.94 |
| *CIS* | *-0.75* | *-0.24* | *-0.17* | *-0.32* |
| **3.68"** | 6.84 | 7.66 | 6.83 | 7.24 |
| *CIS* | *-0.33* | *-0.04* | *-0.20* | *-1.02* |
| **3.68'** | 6.47 | 7.52 | 6.87 | 7.95 |
| *CIS* | *-0.70* | *-0.18* | *-0.16* | *-0.31* |
| **3.68"** | 6.74 | 7.60 | 6.80 | 7.22 |
| *CIS* | *-0.43* | *-0.10* | *-0.23* | *-1.04* |

**Table 3.5b.** $^1$H NMR chemical shift values for the naphthalene ring system of ligand **3.4** and the dinuclear complex **3.68** recorded in acetonitrile, with the CIS values shown in italics.

| | H2/H3 | H5/H8 | H6/H7 |
|---|---|---|---|
| **3.4** | 7.52 | 7.92 | 7.43 |
| **3.68** | 7.57 | 7.93 | 7.74 |
| *CIS* | *0.05* | *0.01* | *0.31* |
| **3.68*** | 7.49 | 7.93 | 7.74 |
| *CIS* | *-0.03* | *0.01* | *0.31* |

There are similarities in the NMR spectra and the CIS values of the mononuclear complexes **3.66** and **3.67**, and the dinuclear complex **3.68**. The latter complex has reduced symmetry due to the naphthalene ring and therefore there are two non-equivalent pyridine rings. One of the pyridine rings of each diastereoisomer is located over the naphthalene ring of the ligand and has a large negative CIS value for the H3 proton. Interestingly for both diastereoisomers, one H6 proton of a coordinated pyridine rings has quite a dramatic negative CIS value, whereas the other has a CIS value less than the normal value for an H6 proton of a coordinated pyridine ring in such complexes. There are no significant CIS values for the naphthalene ring.

Given the ability of ligand **3.4** to form both mono- and dinuclear complexes by simply varying the reaction time, the possibility exists of using the mononuclear complex in a 'complexes as ligands' approach[193] to prepare multinuclear assemblies. This would be more easily applied for this system, than for previous mononuclear complexes described in Chapter 2, because the ligand has been shown to form dinuclear ruthenium complexes.

Ligand **3.6** has a 1,5-substituted naphthalene core with the chelating di-2-pyridylamine units of the ligand being attached to different rings of the core. Reaction of either $[Ru(bpy)_2Cl_2]$ or $[Ru(dmb)_2Cl_2]$ with **3.6** in a 2:1 stoichiometry, in the standard reaction medium of 3:1 ethanol-water, provided only the mononuclear complexes **3.69** and **3.70**, respectively. These were isolated as their hexafluorophosphate salts, as shown in Scheme 3.19, in 19% yield for complex **3.69**, while the dmb complex, **3.70**, was obtained in 60% yield. Using mass spectrometry and $^1$H NMR spectroscopy, complexes **3.69** and **3.70** were confirmed as $[Ru(bpy)_2(\mathbf{3.6})](PF_6)_2$ and $[Ru(dmb)_2(\mathbf{3.6})](PF_6)_2$, respectively. Ligand **3.6** is relatively insoluble and this may have lowered the yield of the mononuclear complexes and also hindered the formation of the expected dinuclear complexes. No dinuclear complexes were formed despite efforts using longer reaction times.

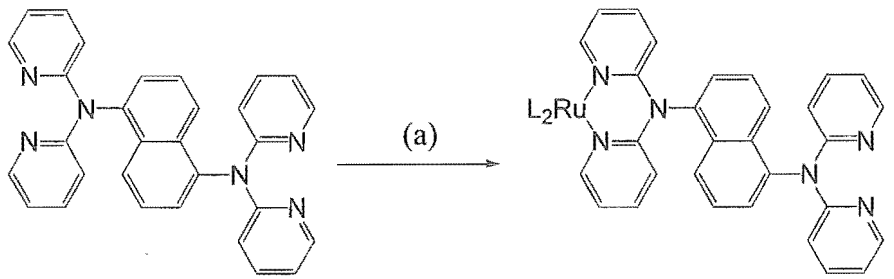


**3.6** **3.69** L=bpy
**3.70** L=dmb

(a) $Ru(L)_2Cl_2$, EtOH/water, $NH_4PF_6$.

**Scheme 3.19**

The $^1$H NMR spectra of **3.69** and **3.70** are again, like the previous mononuclear complexes, complicated by the reduced ($C_1$) symmetry due to restricted rotation of the coordinated arm of the ligand. The coordinated pyridine rings of the ligand are non-equivalent because of this locked conformation, but the non-coordinated pyridine rings are equivalent because of rotation about the naphthalene-nitrogen bond. The 1-D TOCSY technique was used to assign the chemical shifts to individual protons for both mononuclear complexes. The $^1$H NMR chemical shifts for the ligand **3.6** in acetonitrile and for the two mononuclear ruthenium complexes **3.69** and **3.70** are given in Tables 3.6a and 3.6b, along with the CIS values which are given in italics.

**Table 3.6a.** $^1$H NMR chemical shift values for the pyridine rings of ligand **3.6** and the two mononuclear complexes **3.69** and **3.70** recorded in acetonitrile, with the CIS values shown in italics.

| | H3' | H4' | H5' | H6' |
|---|---|---|---|---|
| **3.6** | 7.13 | 7.69 | 7.03 | 8.25 |
| **3.69'** | 6.62 | 7.60 | 6.76 | 7.19 |
| *CIS* | *-0.51* | *-0.09* | *-0.27* | *-1.06* |
| **3.69"** | 6.28 | 7.45 | 6.81 | 7.89 |
| *CIS* | *-0.85* | *-0.24* | *-0.22* | *-0.36* |
| **3.69'"** | 7.19 | 7.72 | 7.07 | 8.28 |
| *CIS* | *0.06* | *0.03* | *0.04* | *0.03* |
| **3.70'** | 6.58 | 7.57 | 6.73 | 7.17 |
| *CIS* | *-0.55* | *-0.12* | *-0.30* | *-1.08* |
| **3.70"** | 6.26 | 7.42 | 6.79 | 7.90 |
| *CIS* | *-0.87* | *-0.27* | *-0.24* | *-0.35* |
| **3.70'"** | 7.19 | 7.72 | 7.07 | 8.28 |
| *CIS* | *0.06* | *0.03* | *0.04* | *0.03* |

**Table 3.6b.** $^1$H NMR chemical shift values for the naphthalene ring system of ligand **3.6** and the two mononuclear complexes **3.69** and **3.70** recorded in acetonitrile, with the CIS values shown in italics.

| | H2 | H3 | H4 | H6 | H7 | H8 |
|---|---|---|---|---|---|---|
| **3.6** | 7.46 | 7.51 | 7.91 | 7.46 | 7.51 | 7.91 |
| **3.69** | 7.13 | 7.67 | 8.25 | 7.35 | 7.66 | 8.21 |
| *CIS* | *-0.33* | *0.16* | *0.34* | *-0.11* | *0.15* | *0.30* |
| **3.70** | 7.28 | 7.68 | 8.18 | 7.41 | 7.68 | 8.21 |
| *CIS* | *-0.16* | *0.17* | *0.27* | *-0.05* | *0.17* | *0.30* |

The CIS values for the mononuclear complexes **3.69** and **3.70** are similar to those obtained for the previous mononuclear complexes of ligand **3.4**. The two coordinated pyridine rings of both complexes have quite different CIS values, consistent with the reduced rotation of the coordinated arm of the ligand and the different environments for each ring. Again, the naphthalene ring affects one pyridine ring of each complex, which has a large negative CIS value for the H3 proton. A second ring of each complex has an environment similar to the pyridine rings in the dinuclear complexes previously described and has a large negative CIS value for the H6 proton. It does however also have a negative CIS value for the H3 proton. The non-coordinated pyridine rings are not affected by coordination and the chemical shifts for these protons are relatively unchanged.

Reaction of $[Ru(bpy)_2Cl_2]$ or $[Ru(dmb)_2Cl_2]$ with **3.7** in 3:1 ethanol-water gave the dinuclear complexes **3.71** and **3.72**, respectively, as 1:1 mixtures of diastereoisomers, which were isolated as their hexafluorophosphate salts (Scheme 3.20). The former complex, **3.71**, was isolated in 48% yield while the latter, **3.72**, was obtained in 61% yield. Using elemental analysis, mass spectrometry and $^1$H NMR spectroscopy, complexes **3.71** and **3.72** were characterised as $[\{Ru(bpy)_2\}_2(\mathbf{3.7})](PF_6)_4$ and $[\{Ru(dmb)_2\}_2(\mathbf{3.7})](PF_6)_4$, respectively. The $^1$H NMR spectra are consistent with the presence of two diastereoisomers for each dinuclear complex. Partial

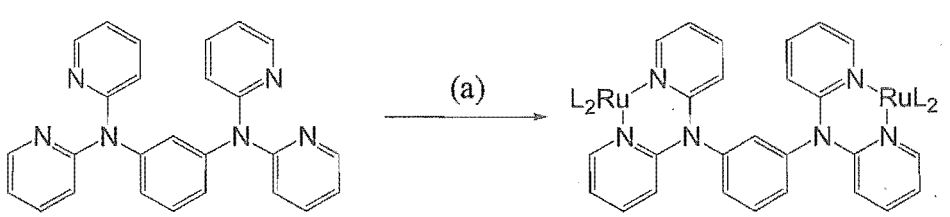


**3.7** **3.71** L=bpy
**3.72** L=dmb

(a) $Ru(L)_2Cl_2$, EtOH/water, $NH_4PF_6$.

**Scheme 3.20**

separation of the diastereoisomers was achieved by alumina chromatography allowing the signals for both diastereoisomers of complexes **3.71** and **3.72** to be assigned to individual spin systems by 1-D TOCSY experiments. The two $^{1}$H NMR spectra of the diastereomerically enriched fractions are shown for comparison in Figure 3.39.

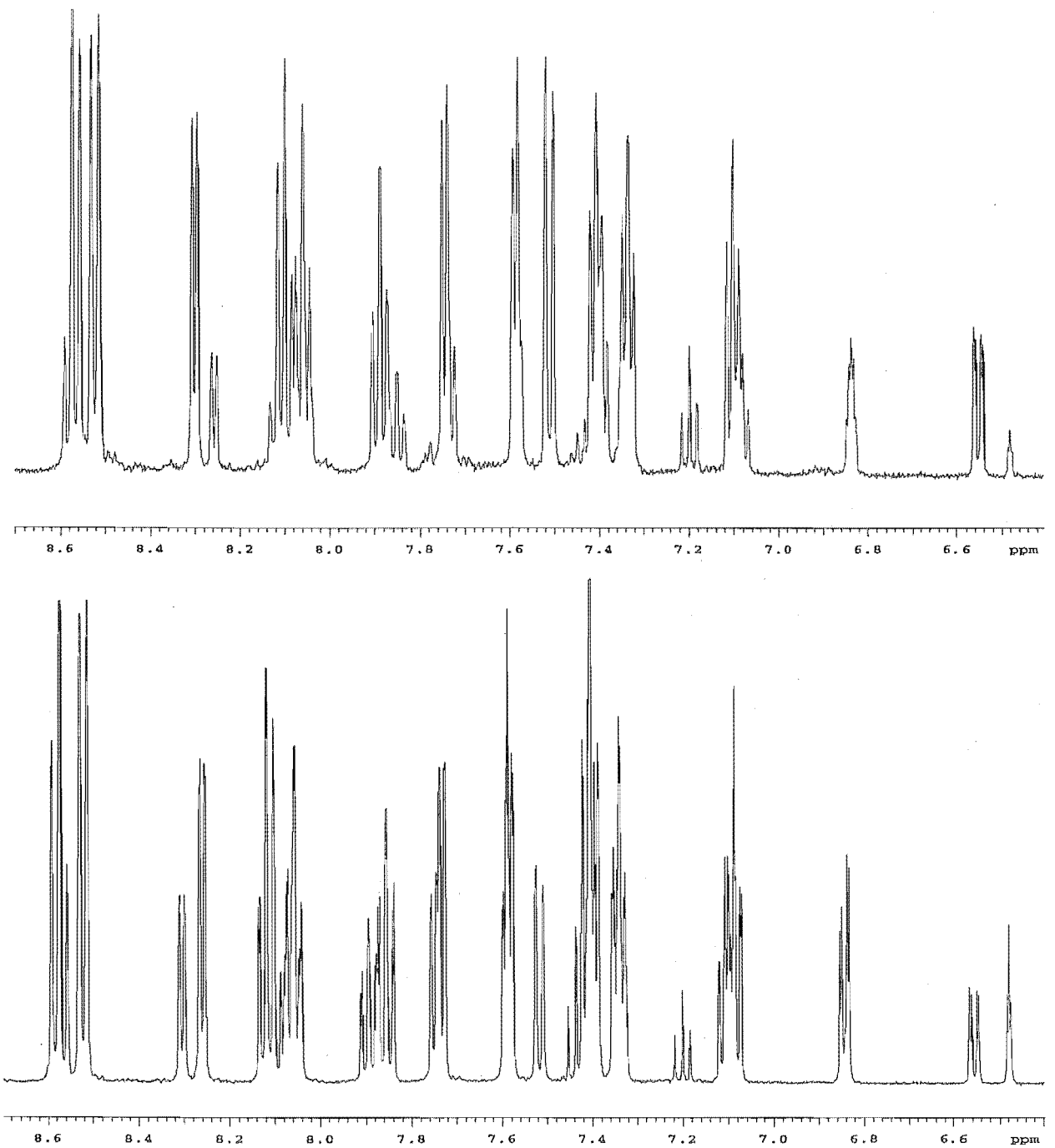


**Figure 3.39.** The aromatic regions of the $^{1}$H NMR spectra of the two fractions obtained by chromatography on alumina for complexes **3.71** and **3.71*** showing the enrichment of each fraction with one of the diastereoisomers. The top spectrum is of a sample enriched with diastereoisomer **3.71**, while the bottom spectrum is of a sample containing more **3.71***.

The different diastereoisomers of complexes **3.71** and **3.72** have quite different chemical shifts, in particular for the central benzene ring of the ligand. This indicates that there are more significant structural differences in the two diastereoisomers above and below the plane of the central benzene ring. The CIS values for complexes **3.71** and **3.72** are shown in Tables 3.7a and 3.7b. While there are differences between the diastereoisomers, the general trend of the CIS values, experienced by the pyridine rings of ligand **3.7** upon coordination to ruthenium, are very similar to dinuclear complexes of ligand **3.2**. The CIS values for the protons of the benzene rings in these two complexes are considerably more dramatic than in the previous complexes with the 1,4-substituted-benzene ligand (**3.62** and **3.63**). These CIS values range from +0.49 to -0.93.

**Table 3.7a.** $^1$H NMR chemical shift values for the pyridine rings of ligand **3.7** and the dinuclear complexes **3.71** and **3.72** recorded in acetonitrile, with the CIS values shown in italics.

| | H3' | H4' | H5' | H6' |
|---|---|---|---|---|
| **3.7** | 7.06 | 7.66 | 7.02 | 8.28 |
| **3.71** | 7.52 | 7.89 | 7.10 | 7.59 |
| *CIS* | *0.46* | *0.23* | *0.08* | *-0.69* |
| **3.71*** | 7.40 | 7.86 | 7.08 | 7.58 |
| *CIS* | *0.34* | *0.20* | *0.06* | *-0.70* |
| **3.72** | 7.45 | 7.84 | 7.09 | 7.58 |
| *CIS* | *0.39* | *0.18* | *0.07* | *-0.70* |
| **3.72*** | 7.33 | 7.80 | 7.03 | 7.57 |
| *CIS* | *0.27* | *0.14* | *0.01* | *-0.71* |

**Table 3.7b.** $^1$H NMR chemical shift values for the naphthalene ring of **3.7** and the dinuclear complexes **3.71** and **3.72** recorded in acetonitrile, with the CIS values shown in italics.

| | H2 | H4/H6 | H5 |
|---|---|---|---|
| **3.7** | 6.90 | 7.37 | 6.95 |
| **3.71** | 6.83 | 6.56 | 7.20 |
| *CIS* | *-0.07* | *-0.81* | *0.25* |
| **3.71*** | 6.48 | 6.84 | 7.43 |
| *CIS* | *-0.42* | *-0.53* | *0.48* |
| **3.72** | 6.86 | 6.44 | 7.17 |
| *CIS* | *-0.04* | *-0.93* | *0.22* |
| **3.72*** | 6.78 | 6.61 | 7.44 |
| *CIS* | *-0.12* | *-0.76* | *0.49* |

For complex **3.71**, the benzene-H2 proton of one diastereoisomer (**3.71***) has a considerably larger negative CIS value than the other diastereoisomer. This is also observed for complex **3.72**,

but the difference is far less dramatic. Inversely, for the equivalent H4 and H6 protons, the effect is reversed, with the other diastereoisomer experiencing larger negative CIS values. Such differences are presumably explained by different conformations around the benzene ring.

Reaction of $[Ru(bpy)_2Cl_2]$ or $[Ru(dmb)_2Cl_2]$ with **3.8** in 3:1 ethanol-water solution gave the dinuclear complexes **3.73** and **3.74**, respectively, as 1:1 mixtures of diastereoisomers. These were isolated as their hexafluorophosphate salts, as shown in Scheme 3.21. Complex **3.73** was isolated in 59% yield, while the latter dmb complex was obtained in 78% yield. ES-MS and $^1$H NMR spectroscopy were use to characterise complexes **3.73** and **3.74** as $[\{Ru(bpy)_2\}_2(\mathbf{3.8})](PF_6)_4$ and $[\{Ru(dmb)_2\}_2(\mathbf{3.8})](PF_6)_4$, respectively.

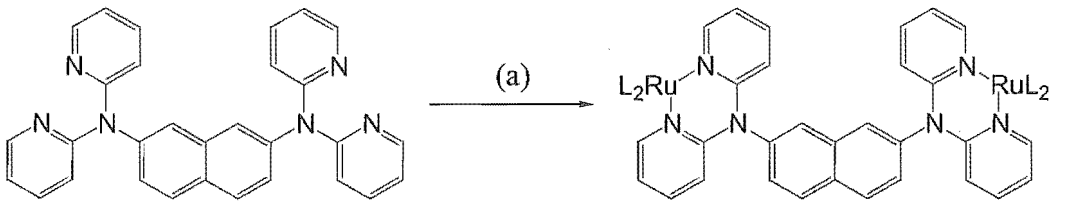


**3.8** **3.73** L=bpy
**3.74** L=dmb

(a) $Ru(L)_2Cl_2$, EtOH/water, $NH_4PF_6$.

**Scheme 3.21**

The $^1$H NMR spectra are consistent with a mixture of the two diastereoisomers for both the bpy and dmb complexes. The signals for both diastereoisomers of complexes **3.73** and **3.74** where able to be assigned to individual spin systems by 1-D TOCSY experiments. The CIS values (Tables 3.8a and 3.8b) experienced by the pyridine and naphthalene rings of ligand **3.8** upon coordination in these complexes are very similar to previous dinuclear complexes. There are subtle differences in the CIS values for the different diastereoisomers, in particular for H1 and H8 of the naphthalene ring of complex **3.73**.

**Table 3.8a.** $^1$H NMR chemical shift values for the pyridine rings of ligand **3.8** and the dinuclear complexes **3.73** and **3.74** recorded in acetonitrile, with the CIS values shown in italics.

| | H3' | H4' | H5' | H6' |
|---|---|---|---|---|
| **3.8** | 7.10 | 7.69 | 7.06 | 8.29 |
| **3.73** | 7.55 | 7.95 | 7.07 | 7.60 |
| *CIS* | *0.45* | *0.26* | *0.01* | *-0.69* |
| **3.73*** | 7.52 | 7.92 | 7.08 | 7.60 |
| *CIS* | *0.42* | *0.23* | *0.02* | *-0.69* |
| **3.74/3.74*** | 7.54 | 7.90 | 7.07 | 7.58 |
| *CIS* | *0.44* | *0.21* | *0.01* | *-0.71* |

**Table 3.8b.** $^1$H NMR chemical shift values for the naphthalene ring system of ligand **3.8** and the dinuclear complexes **3.73** and **3.74** recorded in acetonitrile, with the CIS values shown in italics.

| | H1/H8 | H3/H6 | H4/H5 |
|---|---|---|---|
| **3.2.7** | 7.46 | 7.29 | 7.92 |
| **3.73** | 7.39 | 7.17 | 8.03 |
| *CIS* | *-0.07* | *-0.12* | *0.11* |
| **3.73*** | 7.09 | 7.27 | 8.04 |
| *CIS* | *-0.37* | *-0.02* | *0.12* |
| **3.74** | 7.18 | 7.14 | 8.00 |
| *CIS* | *-0.28* | *-0.15* | *0.08* |
| **3.74*** | 7.18 | 7.19 | 8.02 |
| *CIS* | *-0.28* | *-0.10* | *0.10* |

### 3.5.2 Electrochemistry and UV-visible spectroscopy

The electrochemistry of the ruthenium complexes of the amino-linked ligands (**3.2** - **3.8**) is complicated by the fact that the ligands themselves can undergo two irreversible oxidations. Figure 3.40 shows a cyclic voltammogram for the free ligand **3.2**, showing the two irreversible oxidation waves. These are attributed to the oxidation of the amine nitrogen atoms of the ligand. The potentials for the oxidation of ligands **3.2** and **3.4** are shown in Table 3.9. Upon coordination, the ligands are no longer susceptible to oxidation, and so this is only a consideration for the mononuclear complexes with a non-coordinated di-2-pyridylamine subunit.

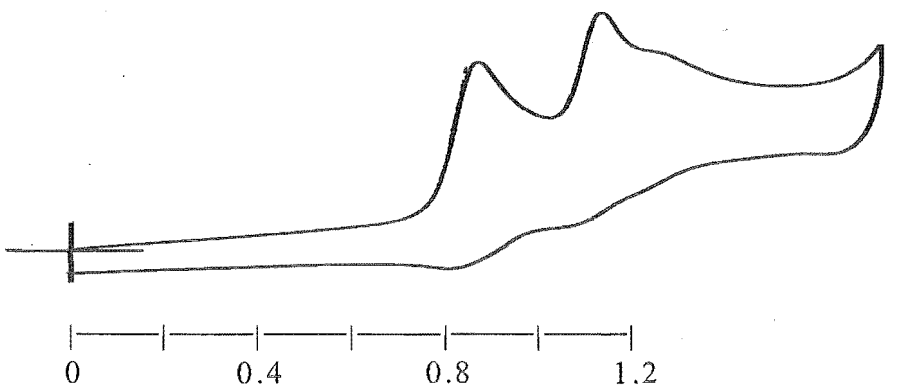


**Figure 3.40.** A cyclic voltammogram of **3.2** showing the two irreversible oxidations.

**Table 3.9.** Redox potentials for ligands **3.2** and **3.4**.

| | $E_{ox}$ [a,b] | $E_{ox(2)}$ [a,b] |
|---|---|---|
| **3.2** | +0.82[c](1e) | +1.13[c](1e) |
| **3.4** | +0.82[c](1e) | +1.14[c](1e) |

[a] Potentials quoted in V *vs.* SCE in $CH_3CN$/0.1 mol.L$^{-1}$ $[(n\text{-}C_4H_9)_4]PF_6$ (the ferrocene/ferrocenium couple occurred at +310 mV *vs.* SCE).

[b] Uncertainty in $E_{1/2}$ values *ca.* ± 0.01 V.

[c] Irreversible (approximate value estimated from cathodic half-scan).

Table 3.10 lists the electronic absorption maxima and redox potentials, recorded in acetonitrile solution, for the mononuclear complexes **3.66**, **3.67** and **3.70**. The mononuclear complexes all have broad absorption maxima at *ca.* 430 nm, with a shoulder at *ca.* 457 nm. The MLCT transitions into the orbitals of the ligand are at a higher energy than for $[Ru(bpy)_3]^{2+}$, while the shoulder may correspond to MLCT into the bpy ligands.

**Table 3.10.** Visible absorption maxima and redox potentials for $[Ru(bpy)_3]^{2+}$ and complexes **3.66**, **3.67** and **3.70**.

| | $\lambda$ (nm)[a,b] | $E_{ox(1)}$[c,d] | $E_{ox(2)}$[c,d] | $E_{red(1)}$[c,d] | $E_{red(2)}$[c,d] |
|---|---|---|---|---|---|
| $[Ru(bpy)_3]^{2+}$ | 452 | +1.26(1e) | | -1.33(1e) | -1.51(1e) |
| **3.66** | 429, 457(sh) | +1.14(2e) | | -1.45(1e) | -1.68(1e) |
| **3.67** | 431, 456(sh) | +1.02(1e) | +1.27[e](1e) | -1.56(1e) | -1.74(1e) |
| **3.70** | 430, 458 (sh) | +1.02(1e) | +1.27[e](1e) | -1.54(1e) | -1.75(1e) |

[a] The MLCT band measured in $CH_3CN$ (± 2 nm)

[b] sh = shoulder.

[c] Potentials quoted in V *vs.* SCE in $CH_3CN$/0.1 mol.$L^{-1}$ $[(n\text{-}C_4H_9)_4]PF_6$ (the ferrocene/ferrocenium couple occurred at +310 mV *vs.* SCE).

[d] Uncertainty in $E_{1/2}$ values *ca.* ± 0.01 V.

[e] Irreversible (approximate value estimated from cathodic half-scan).

The cyclic voltammograms for the mononuclear complexes, **3.66**, **3.67** and **3.70**, all have four one electron redox processes. For complex **3.66**, the reversible oxidation of the ruthenium centre and the irreversible oxidation of the amine on the non-coordinated arm of the ligand are overlapped. For the dmb complexes, the ruthenium oxidation potentials are shifted *ca.* 100 mV less positive and the amine nitrogen becomes *ca.* 100 mV more difficult to oxidise.

The redox potentials reveal that the bpy complex, **3.66**, is both easier to oxidise and more difficult to reduce than $[Ru(bpy)_3]^{2+}$ (+1.26, -1.33 V).[42] This is consistent with the electron-rich nature of these ligands. For the dmb complex, **3.67**, the reduction potentials are shifted by *ca.* 100 mV related to those of the bpy complex, consistent with the electron donating effect of *ca.* 25 mV per methyl group.[136] Linking the ligands through different rings of the naphthalene core, as in complex **3.70**, has a negligible affect on the redox potentials.

The dinuclear complexes **3.62** - **3.65**, **3.68** and **3.71** - **3.74** all exhibit broad visible absorption maxima at *ca.* 440 nm as shown in Table 3.11. For all the complexes these bands can be assigned to a MLCT, as is the case for $[Ru(bpy)_3]^{2+}$. This indicates that the HOMO-LUMO energy gap in these complexes is similar to $[Ru(bpy)_3]^{2+}$.

**Table 3.11.** Visible absorption maxima and redox potentials for dinuclear complexes **3.62** - **3.65**, **3.68** and **3.71** - **3.74**.

| | $\lambda$ (nm)[a,b] | $E_{ox}$[c,d] | $E_{ox(2)}$[c,d] | $E_{red(1)}$[c,d] | $E_{red(2)}$[c,d] | $E_{red(3)}$[c,d] |
|---|---|---|---|---|---|---|
| **3.62** | 442 | +1.13[e](1e) | +1.19[f](1e) | -1.44(2e) | -1.66(2e) | |
| **3.63** | 442 | +1.05(2e) | | -1.52(2e) | -1.75(2e) | |
| **3.64** | 443 | +1.11(2e) | | -1.44(2e) | -1.66(2e) | -2.01(1e) |
| **3.65** | 442 | +1.01(2e) | | -1.54(2e) | -1.76(2e) | -2.06(1e) |
| **3.68** | 445 | +1.13(2e) | | -1.45(2e) | -1.68(2e) | |
| **3.71** | 441 | +1.15[e](1e) | +1.21[f](1e) | -1.41(2e) | -1.71(2e) | -1.94[e](1e) |
| **3.72** | 440 | +1.11(2e) | | -1.54(2e) | -1.77[e](2e) | -2.00[e](1e) |
| **3.73** | 444 | +1.12(2e) | | -1.45(2e) | -1.66(2e) | -1.89[f](1e) |
| **3.74** | 441 | +1.07(2e) | | -1.53(2e) | -1.74(2e) | -1.94[f](1e) |

[a] The MLCT band measured in $CH_3CN$ (± 2 nm)

[b] sh = shoulder.

[c] Potentials quoted in V *vs.* SCE in $CH_3CN$/0.1 mol.$L^{-1}$ $[(n\text{-}C_4H_9)_4]PF_6$ (the ferrocene/ferrocenium couple occurred at +310 mV *vs.* SCE).

[d] Uncertainty in $E_{1/2}$ values *ca.* ± 0.01 V.

[e] Overlapped or irreversible (approximate value estimated from anodic half-scan).

[f] Overlapped or irreversible (approximate value estimated from cathodic half-scan).

A cyclic voltammogram for complex **3.62** is shown in Figure 3.41. It shows the complex undergoes four redox processes (two partially overlapped), including two bpy-centred reductions at -1.44 and -1.66 V. The oxidation wave is complicated either by differences between the two diastereoisomers, or by the interaction between the two metal centres. The flexibility of the ligand suggests that the latter possibility is more likely. From the cyclic voltammogram for **3.62**, it can be seen that these two one-electron processes are occurring *ca.* 60 mV apart. This type of behaviour was also observed for complex **3.71**, although similar separations of the oxidation potentials for the two ruthenium atoms could not be observed in the corresponding dinuclear dmb complexes, **3.63** and **3.72**.

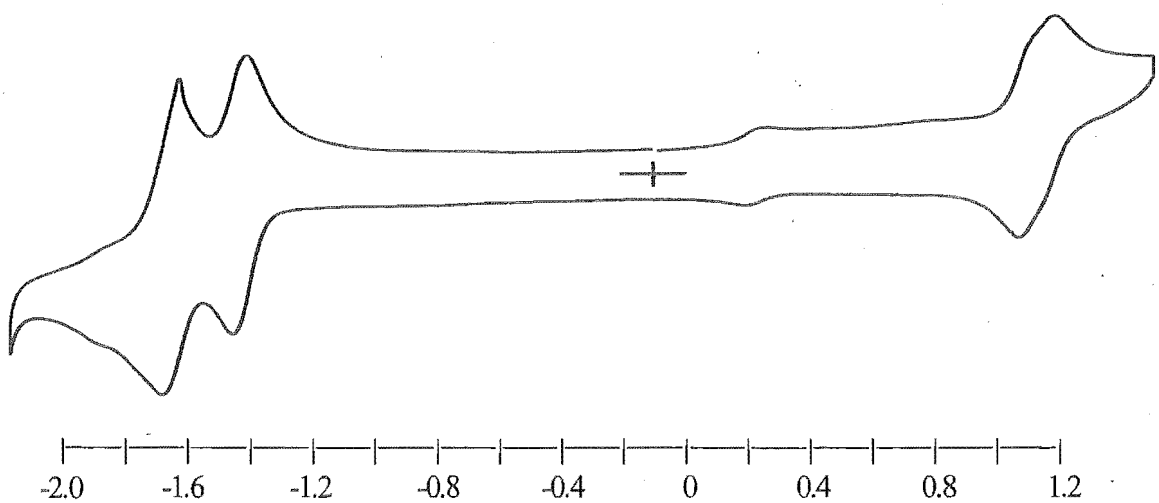


**Figure 3.41.** A cyclic voltammogram for the dinuclear complex **3.62**.

While cyclic voltammetry (CV) is an excellent technique for measuring redox potentials and importantly for confirming reversibility, differential pulse voltammetry (DPV) is far superior when the resolution of two closely separated potentials is required. In cyclic voltammetry a voltage is applied to the sample by scanning forward and backward over a potential range and a current is measured, increasing as the applied potential approaches the oxidation or reduction potential of the compound. Depletion of the sample near the electrode leads to a diminishing of the current and when the potential range is scanned in the opposite direction, the compound that was initially oxidised or reduced undergoes the opposite process. This provides a second wave with an opposite polarity, indicating reversibility and allowing the redox potential to be determined. However, in cases such as the one above, the background current makes it harder to determine the potentials of two closely spaced processes. In DPV the applied potential does not increase linearly as in CV, because superimposed on a constantly increasing applied potential are small pulses. The current is measured just before the beginning of the pulse and just before the end of a pulse and the difference between these values used which gives a significant current only at the redox potential of the compound under study. This minimises the background current and allows the two closely spaced redox potentials to be more easily measured.

The differential pulse voltammograms of complex **3.62** and **3.71** are shown in Figure 3.42. For both the dinuclear bpy complexes, the differential pulse voltammograms confirm two separate, but closely spaced processes, consistent with the observations made by cyclic voltammetry. For both complexes, the voltage separations of these two one-electron redox potentials are at the boundaries of this technique, and thus in both cases, the drop in current between the two potentials is very small.

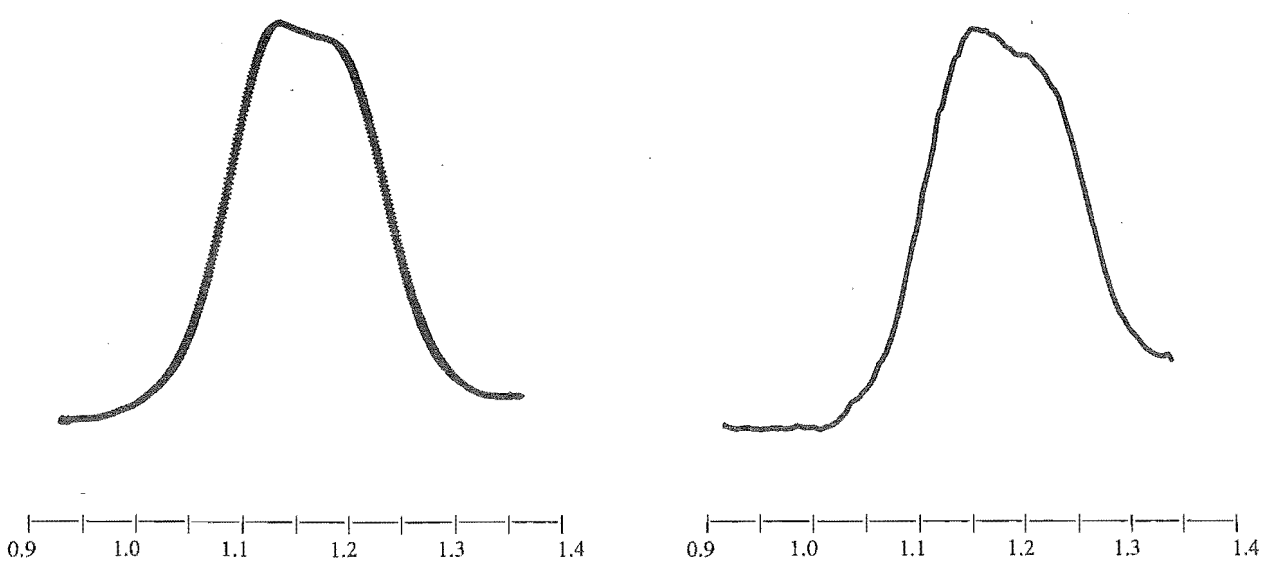


**Figure 3.42.** The differential pulse voltammograms for complexes **3.62** and **3.71**.

The cyclic voltammetry of the other dinuclear complexes revealed three reversible two-electron redox processes for each complex. Unlike the complexes of ligands with a benzene core, the oxidation waves of the dinuclear complexes of the biphenyl- and naphthalene-based ligands are reversible two-electron waves, with a $E_{ox}/E_{red}$ peak separation of approximately 65 mV. Thus, the metal centres do not appear to be interacting to any significant extent because of the combined effects of distance, and possibly greater twisting of the chelating units out of the plane of the ligand core. All the ruthenium complexes studied have oxidation potentials that are similar to the di-2-pyridylamine (**3.1**) ruthenium complex, $[Ru(bpy)(phen)(\mathbf{3.1})]^{2+}$ (+1.06 V),[44] where phen = 1,10-phenanthroline.

The dinuclear bpy complexes **3.62**, **3.64**, **3.68**, **3.71** and **3.73** all undergo ligand centred reductions at about -1.44 V and -1.68 V. These are attributed to the reductions of the ancillary bpy ligands. The di-2-pyridylamine-based ligands are very difficult to reduce, but appear to undergo reductions at potentials between -1.90 and -2.06 V. The potentials of the dinuclear dmb complexes (**3.63**, **3.65**, **3.72** and **3.74**) are shifted by *ca.* 100 mV related to those of the analogous bpy complexes, consistent with the electron donating effect of *ca.* 25 mV per methyl group[136] that was noted earlier.

## 3.6. Summary

This chapter has furthered investigations into a series of ligands which have two di-2-pyridylamine chelating units attached directly to arene rings. In this series, ligands incorporating a naphthalene core have been prepared for the first time with three different substitution patterns. A second series of novel flexible multidentate ligands, with symmetrical bidentate chelating sites, was also prepared and investigated. The ligands were not as flexible as other ligands that have been previously prepared with two atom spacers, because the $sp^2$-hybridised nitrogen atom connecting the two pyridine rings adopts a planar geometry. In all the complexes investigated in this chapter, the ligands were shown to coordinate only through the pyridine nitrogen atoms and no coordination was observed by the amine nitrogen, consistent with the $sp^2$ hybridisation of this atom.

When the two sets of ligands were reacted with silver salts, the mode of coordination was predominantly monodentate by one pyridine ring from each chelating site of a ligand. This led to a number of examples of polymeric structures with the ligand molecules linked through either one or two silver atoms. In the cases where there were two linking silver atoms, twelve-membered dimetallomacrocylic structures formed which connected the two molecules of the ligand. Another common structure observed was a [2+2] dimer, while a further feature of the

silver complexes characterised in this chapter was the existence of intramolecular silver-arene π-interactions. These weaker secondary supramolecular interactions were observed in nearly every silver complex that was characterised by X-ray crystallography.

Despite not utilising the chelating binding motif for the silver complexes, all the ligands formed the expected six-membered chelate rings when coordinated to copper, palladium and ruthenium. This resulted in a twisting of the chelating units out of the plane of the ligand core, which was observed in all structures that were characterised by X-ray crystallography. While no pre-organised, facially segregated ligands were prepared, a trinuclear copper complex of ligand **3.14** was shown to have all three arms of the ligand organised on one face of the benzene core.

Electrochemical studies on the amino-linked series of ligands revealed that they are susceptible to oxidation of the amine nitrogen atoms unless the di-2-pyridylamine subunits were coordinated to a ruthenium centre. A series of mononuclear and dinuclear, bpy and dmb complexes were prepared with these ligands and studied by NMR spectroscopy, visible absorption spectroscopy and electrochemistry. The amino-linked ligands are relatively electron-rich leading to oxidation potentials that are lower than the archetype complex, $[Ru(bpy)_3]^{2+}$. The metal centres in dinuclear complexes of the ligands containing a benzene core were shown to be weakly interacting by cyclic and differential pulse voltammetry.

The electron-rich nature of these ligands was highlighted by the synthesis of the first example of a three-fold cyclopalladated benzene ring. The electron donating properties of the three amine nitrogen atoms in **3.9** activate the ligand toward multiple electrophilic aromatic substitution.

# *Chapter 4*

# *Tripodal ligands*

# Chapter 4

## 4. Tripodal Ligands

### 4.1. Introduction

As described in Chapter 1, it has been demonstrated that when multitopic bidentate chelating ligands are coordinated to octahedral metal centres, the different diastereoisomers of multinuclear complexes can have different electrochemical and photophysical properties. This is termed the stereochemical problem and has been extensively reviewed.[47-50] The stereochemical problem can be addressed by several different methods as outlined earlier. Controlled synthesis and separation of the resulting diastereoisomers, as used for the synthesis of **2.57** and **2.58** in Chapter 2, was an approach pioneered by Keene et al.[47, 48] to address the stereochemical problem. Also the use of chiral ligands to introduce diastereoselectivity into the preparation of the complex has been reported by several workers.[49, 50, 161, 194] This is the concept of asymmetric synthesis applied to coordination chemistry. Using resolved octahedral metal centres as starting materials is another method of addressing the stereochemical problem.

More relevant to the work described in this chapter is the use of tridentate ligands based around the 2,2':6',2"-terpyridine (tpy) structure. These ligands avoid the formation of isomers because they coordinate in a meridional fashion to an octahedral metal centre, resulting in an achiral product (Figure 4.1). However, a limitation of this approach, in the case of polymeric materials, is that to avoid further introduction of isomerism the bridging must occur through the 4'-position of the central ring of the tpy subunits; thus multinuclear species of this type must be necessarily linear.[47] Simple dinuclear complexes with symmetrical ancillary ligands do not suffer

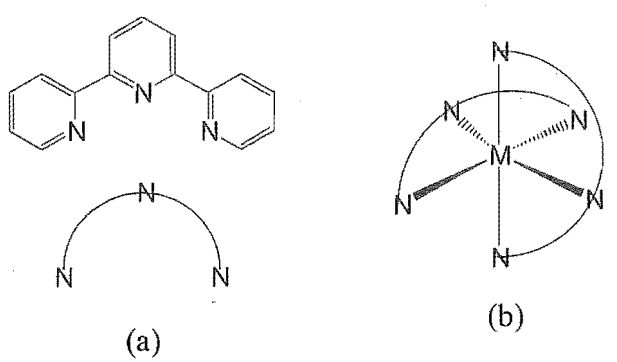


(a) (b)

**Figure 4.1.** (a) 2,2':6',2"-Terpyridine and the formation of an achiral complex (b).

this complication. A further consequence of using meridional tridentate donors is that the excited state lifetimes are shorter and the $[Ru(tpy)_2]^{2+}$ complex does not luminesce at room temperature;[47] problems detrimental to some of the proposed applications of such ruthenium compounds.

A variation on the tridentate approach to addressing the stereochemical problem is to use $C_3$-symmetric tripodal ligands, which are capable of facially coordinating to an octahedral metal atom. Tripodal ligands have been investigated for a number of years with tripyrazolylborate, **4.1**, being the archetypal tripodal ligand.[9, 195] Tripyrazolylborate is a mono-anionic ligand that has been shown to coordinate to metals from all over the periodic table with tripodal coordination.[9, 195] Closely related to this ligand is the neutral carbon analogue tripyrazolylmethane, **4.2**, which is isoelectronic with **4.1**, and has been recently reviewed.[196] Several compounds incorporating three pyridine groups have been shown to be excellent tripodal ligands, in particular tri-2-pyridylmethane, **4.3** and tri-2-pyridylamine, **4.4**.[58, 63, 64, 197-199] A relatively recent review discusses the preparation, coordination chemistry, physical studies and applications of these and related tripodal ligands.[8]

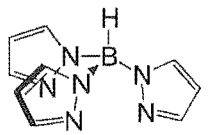

**4.1**

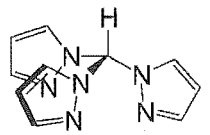

**4.2**

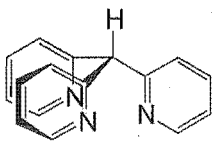

**4.3**

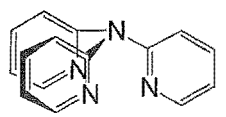

**4.4**

**Figure 4.2.** Some examples of tripodal ligands with pyrazole and pyridine donors.

In addition to the $C_3$-symmetric examples, tripodal ligands incorporating different heterocycles and different substitution patterns (Figure 4.3a), which provide an unsymmetrical donor set, have been investigated.[63, 64, 200] Also, ligands with multiple atom bridges or tethers between the heterocycles have been prepared,[201] but the addition of further atoms into the bridge, or large linking groups such as benzene rings,[140, 145, 146, 148, 202] leads to larger, less stable chelate rings and ultimately to bridging coordination motifs (Figure 4.3b). Other donors, amines and thioethers for example, have been incorporated into macrocycles (Figure 4.3c) and employed as tripodal ligands also.[27, 203]

(a)

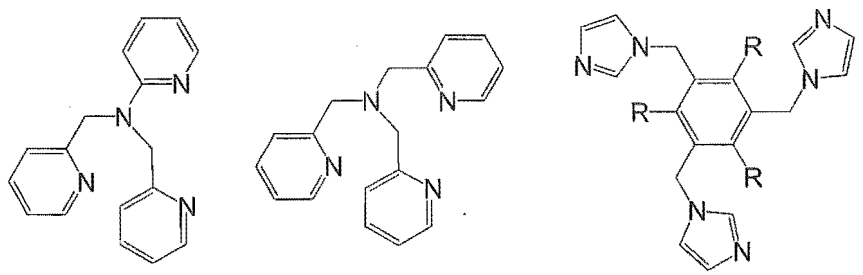

(b)

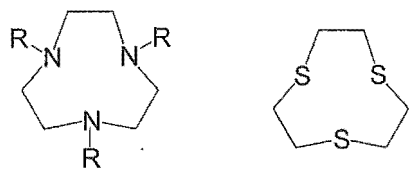

(c)

**Figure 4.3.** Other examples of tripodal ligands with (a) mixed heterocycles, (b) different tether length and (c) macrocyclic tripodal ligands.

While there are many examples of simple tripodal ligands, the extension from tripodal ligands to multitopic tripodal bridging ligands has only been recently explored with the syntheses of several new ligands. These include the doubly tripodal hexadentate ligand, Figure 4.4(a), which has been demonstrated to bridge two metal atoms with tripodal coordination[204, 205] and a series of ligands, an example of which is shown in Figure 4.4(b), prepared by reaction of tris(2-pyrazolyl)methanol with bromomethylbenzenes. These tris(2-pyrazolyl)methyl ligands have been shown to coordinate facially to metal centres in complexes with molybdenum,[206] rhenium[207] and cadmium.[208] However, in complexes with silver, each tripodal unit bridges between two silver atoms.[182, 209]

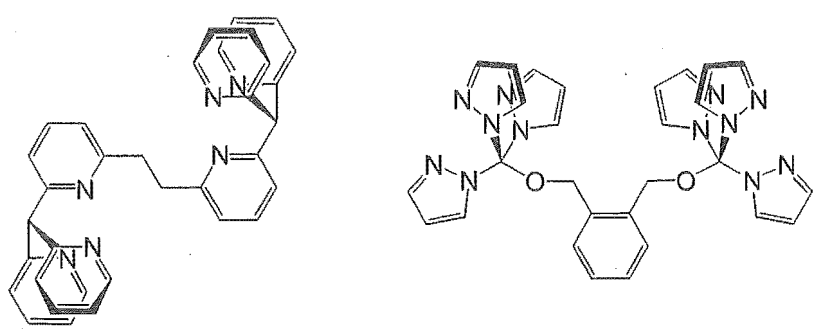

(a) (b)

**Figure 4.4.** Two examples of tripodal ligands prepared by Kodera (a), and by Reger (b).

The two different types of ligands in Figure 4.4 are capable of bridging multiple metal atoms with tripodal coordination at each metal centre. However, a downside of these ligands, in some contexts, is that the metal centres cannot interact through the π-system of the ligand. The ligands of interest in this chapter are represented schematically in Figure 4.5, and have both the metals coordinated to a planar aromatic heterocycle (N-Y-N) that will hopefully allow metal-metal interaction through the ligand π-system. There are several potential points of variation within the structure schematically represented in Figure 4.5, with different pendant heterocyclic donors (N), different linker atoms (X) and bridging heterocyclic cores (N-Y-N) possible. Two examples of ligands with this coordination motif have been described in the literature, which have the structure schematically represented, and these are shown, along with the some of the other ligands investigated in this chapter, in Figure 4.6.

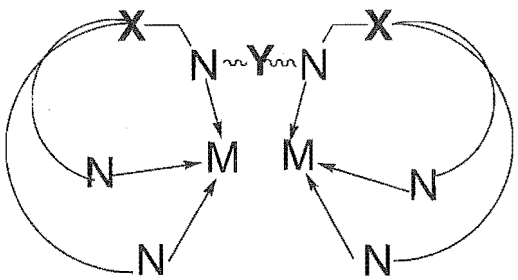


**Figure 4.5.** A schematic representation of the type of ligands investigated in this chapter.

The compounds shown in Figure 4.6 are all capable of bridging two metal ions with tripodal tridentate coordination of each metal centre should all the donor atoms be employed. The first two compounds, **4.5** and **4.6**, are based around a pyrimidine core where the nitrogen donor atoms are separated by a carbon atom. The preparations of both these new ligands are described below. Such ligands, should they bridge two metal atoms, would have metal-metal distances of *ca.* 6.0 Å.[2] Alternatively, a pyridazine core, **4.7** and **4.8**, where the azine nitrogen donors are adjacent in the ring will shorten such metal-metal distances to *ca.* 3.6 Å,[2] while in ligands such as **4.11**, the metal-metal distance will increase to *ca.* 6.9 Å.[2] Ligands **4.7** and **4.9** have previously been prepared by other workers[60, 61, 210-214] and attempts to prepare the novel compounds **4.8** and **4.10** are described. An attempted synthesis of **4.11** is outlined and the reasons for the failure to prepare this compound explained.

One of the aims of this work was to prepare bridging ligands where the metal-metal distance could be systematically varied by altering the core structure of the ligand. Above, the diazine core has been used to bring about small incremental changes in the metal-metal distance. However, using different ring systems can significantly lengthen the metal-metal distance and also alter the spatial arrangement of the metals in the potential complexes (Figure 4.7).[2] Thus, both 1,5-naphthyridine and 4,4'-bipyridine precursors were prepared to attempt the preparations

of ligands **4.12** and **4.13**, respectively. Other extended-reach ligands capable of tripodal coordination are **4.14** and **4.15** (Figure 4.7). Attempted syntheses of ligands **4.12**, **4.13**, and **4.15** are briefly described, along with the successful synthesis of ligand **4.14**.

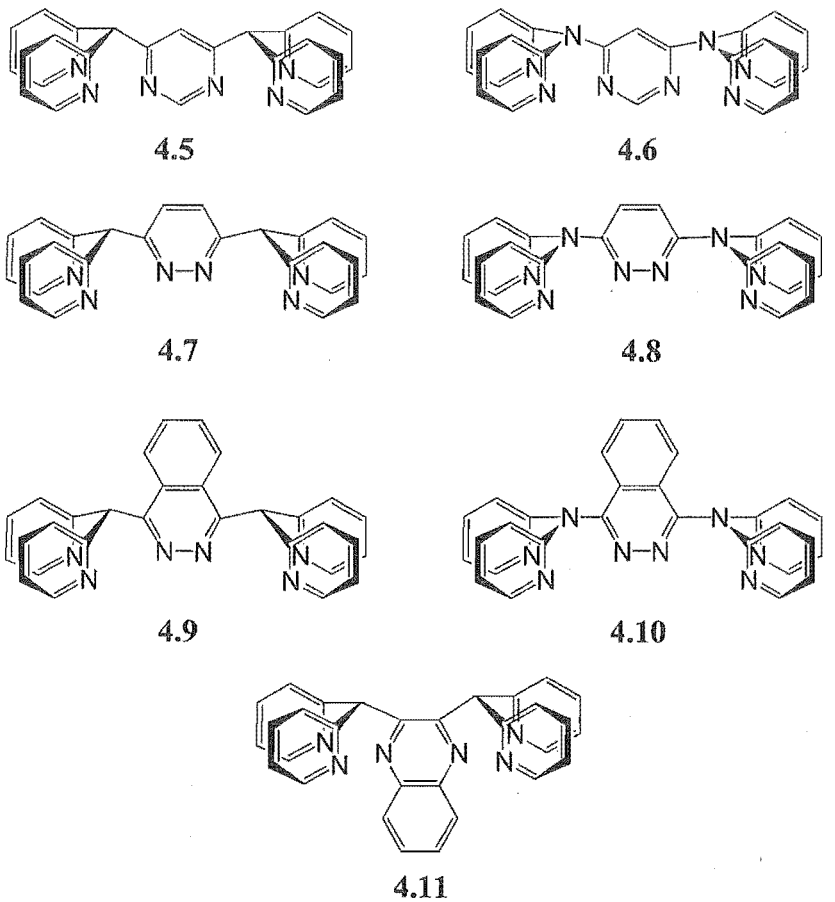

**4.5** **4.6**

**4.7** **4.8**

**4.9** **4.10**

**4.11**

**Figure 4.6.** Some bridging doubly tripodal tridentate ligands based around diazine cores.

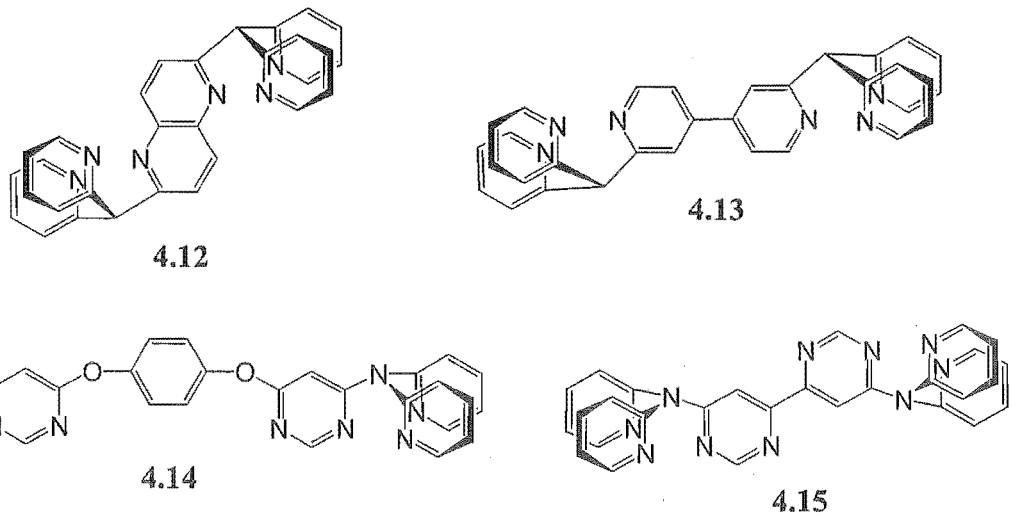

**4.12** **4.13**

**4.14** **4.15**

**Figure 4.7.** Some examples of extended-reach tripodal ligands investigated in this chapter.

## 4.2. Syntheses of the ligands

The general procedure for the synthesis of the tripodal ligands containing a carbon linker atom (X) involved deprotonation of di-2-pyridylmethane with n-butyllithium, followed by reaction with the appropriate dichloro- or diiodo-core. It was discovered that the chloride leaving group caused some problems that could be overcome by using an iodide leaving group. Attempts, using two different methods, at replacing the chlorine in the starting material with iodine were investigated when required.

The method of Mosny and Crabtree[215] for the synthesis of tri-2-pyridylamine, **4.4**, has been adapted for the synthesis of a series of ligands with nitrogen linker atoms. In the case of **4.4**, for example, this involved refluxing di-2-pyridylamine and 2-bromopyridine in mesitylene with a copper(0) catalyst, sodium iodide and sodium carbonate. This method provided tri-2-pyridylamine as described by these workers in moderate yield. A similar method was employed for the syntheses and attempted syntheses of the new nitrogen-linked ligands described in this thesis.

### 4.2.1 Pyrimidine-based ligands

The general method outlined above for the synthesis of carbon-linked ligands was employed for the synthesis of 4,6-bis(di-2-pyridylmethyl)pyrimidine, **4.5**. This method was adapted from the synthesis of 1,4-bis(di-2-pyridylmethyl)phthalazine, **4.9**, by Barrios and Lippard.[213] However, when the *in situ* prepared anion of di-2-pyridylmethane was reacted with 4,6-dichloropyrimidine, none of the desired product was formed. To improve the properties of the leaving group it was changed to iodine, which is both more easily displaced and makes the starting material more soluble. This metathesis reaction was carried out in hydroiodic acid, as shown in Scheme 4.1. Simply stirring a slurry of 4,6-dichloropyrimidine in hydroiodic acid gave the desired 4,6-diiodopyrimidine in 52% yield. Repeating the ligand synthesis reaction, as in Scheme 4.1, on 4,6-diiodopyrimidine gave the desired ligand in 48% yield. The compound is an orange coloured solid and gives bright orange-red coloured solutions.

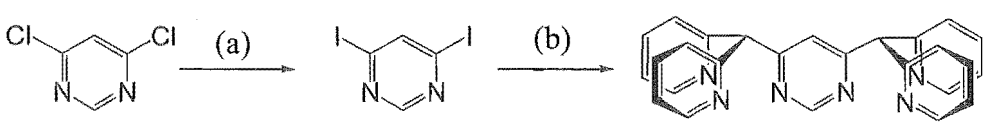


**4.5**

(a) HI, 52%; (b) di-2-pyridylmethane, n-BuLi, THF, 48%.

**Scheme 4.1.**

A second pyrimidine-based ligand, 4,6-bis(di-2-pyridylamino)pyrimidine, **4.6**, with a nitrogen linker atom (X), was prepared by the method adapted from Mosny and Crabtree for the synthesis of **4.4**. This involved reaction of di-2-pyridylamine with 4,6-dichloropyrimidine as shown in Scheme 4.2. The reaction was carried out in refluxing mesitylene and monitored by TLC and $^1$H NMR spectroscopy, which revealed that over several days it progressed to an equilibrium position that consisted of a mixture of starting material, mono-substituted product and the desired compound. Thus, the reaction provided modest yields of the desired product, **4.6** (27%) and the intermediate monoadduct, **4.16** (30%). Both compounds were separated from di-2-pyridylamine by a combination of column chromatography on silica gel and recrystallisation.

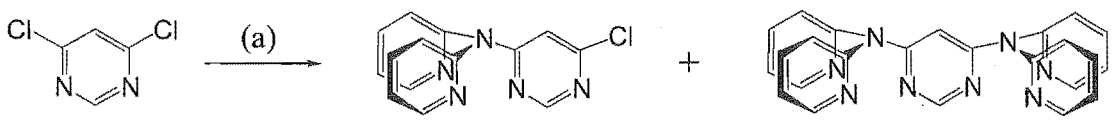

**4.16** **4.6**

(a) di-2-pyridylamine, Cu powder, $Na_2CO_3$, KBr, mesitylene, **4.16**: 30%, **4.6**: 27%.

**Scheme 4.2.**

### 4.2.2 Pyridazine-based ligands

The pyridazine-based ligand 4,6-bis(di-2-pyridylmethyl)pyridazine, **4.7**, which has the nitrogen atoms adjacent in the diazine ring, had been previously prepared and studied by the research group of Manzur et al.[210-212] In the paper reporting the synthesis of this compound,[210] very little detail is provided of the synthetic procedure. The initial synthesis was carried out in ether, but when repeating this reaction THF was found to be a preferable solvent because it is better at dissolving the starting materials. Thus, deprotonation of di-2-pyridylmethane using n-butyllithium, followed by reaction with 3,6-dichloropyridazine, as shown in Scheme 4.3, gave **4.7** in 28% yield. The success in preparing this ligand using a chloride leaving group encouraged the preparation of further ligands from dichloro-substituted starting materials by this methodology.

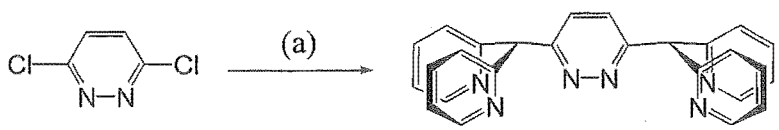

**4.7**

(a) di-2-pyridylmethane, n-BuLi, THF, 28%.

**Scheme 4.3**

The reaction described earlier for the synthesis of **4.6** was then applied to the synthesis of the corresponding ligand possessing a pyridazine core. Reacting a 2:1 ratio of di-2-pyridylamine and 3,6-dichloropyridazine in mesitylene failed to give any **4.8**, despite repeated attempts and extended reaction times. It appears that the extended reaction times and vigorous conditions of the reaction may have led to hydrolysis of 3,6-dichloropyridazine.

While not strictly a pyridazine-based ligand, 1,4-bis(di-2-pyridylmethyl)phthalazine, **4.9**, has the same arrangement of the nitrogen donor atoms, and thus, is likely to possess very similar coordination properties. Ligand **4.9** was prepared by the method of Barrios and Lippard[213] in 48% yield. This was lower than the 80% yield reported by these workers. The general method to produce nitrogen-linked ligands was applied for the synthesis of **4.10**, but again was unsuccessful, possibly for the reasons outlined above for **4.8**.

### 4.2.3 Pyrazine-based ligands

Having prepared both pyridazine and pyrimidine based ligands, the logical progression was to prepare a ligand based around a pyrazine core. However, a pyrazine-based ligand presents several difficulties, notably the synthesis of a suitably substituted starting compound. Pyrazine can be treated with hydrogen peroxide and glacial acetic acid to give the pyrazine-di-N-oxide. However, reaction of pyrazine-di-N-oxide with phosphorous oxychloride does not provide any 2,5-dichloropyrazine. Instead, the reaction gives almost exclusively 2,6-dichloropyrazine,[216] which would not allow the synthesis of a ligand with two tripodal, tridentate binding domains. A multi-step literature method is outlined in Scheme 4.4 that would allow for the preparation of 2,5-dichloropyrazine.[216, 217] However, the individual steps of the synthesis are relatively low yielding and consequently this route to a pyrazine-based ligand was abandoned.

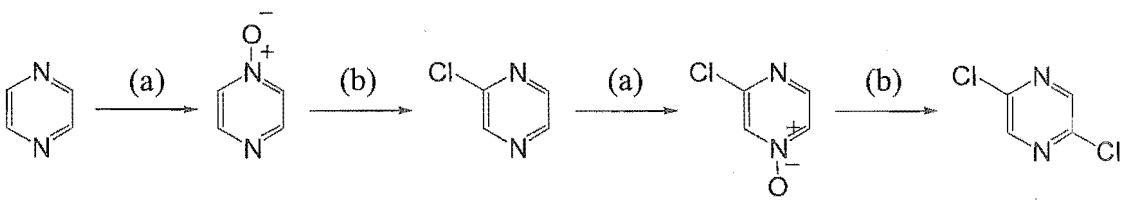


(a) AcOH, $H_2O_2$; (b) $POCl_3$.

**Scheme 4.4.**

Another core that may allow the same separation of the metal atoms in dinuclear complexes as pyrazine, is the quinoxaline ring system. Using methodology described by Iwata,[218] 2,3-dichloroquinoxaline was prepared in two steps from 1,2-phenylenediamine and oxalic acid, as shown in Scheme 4.5. The first step provided 1,4-dihydro-2,3-quinoxalinedione as a pale green solid in 91% yield, which was then converted quantitatively to 2,3-dichloroquinoxaline.

However, deprotonation of di-2-pyridylmethane using n-butyllithium, and subsequent reaction with 2,3-dichloroquinoxaline in a 2:1 stoichiometry, failed to give any of the expected di-substituted product, **4.11**. The monosubstituted compound, 2-chloro-3-(di-2-pyridylmethyl)quinoxaline was isolated as part of a mixture of two different compounds from this reaction.

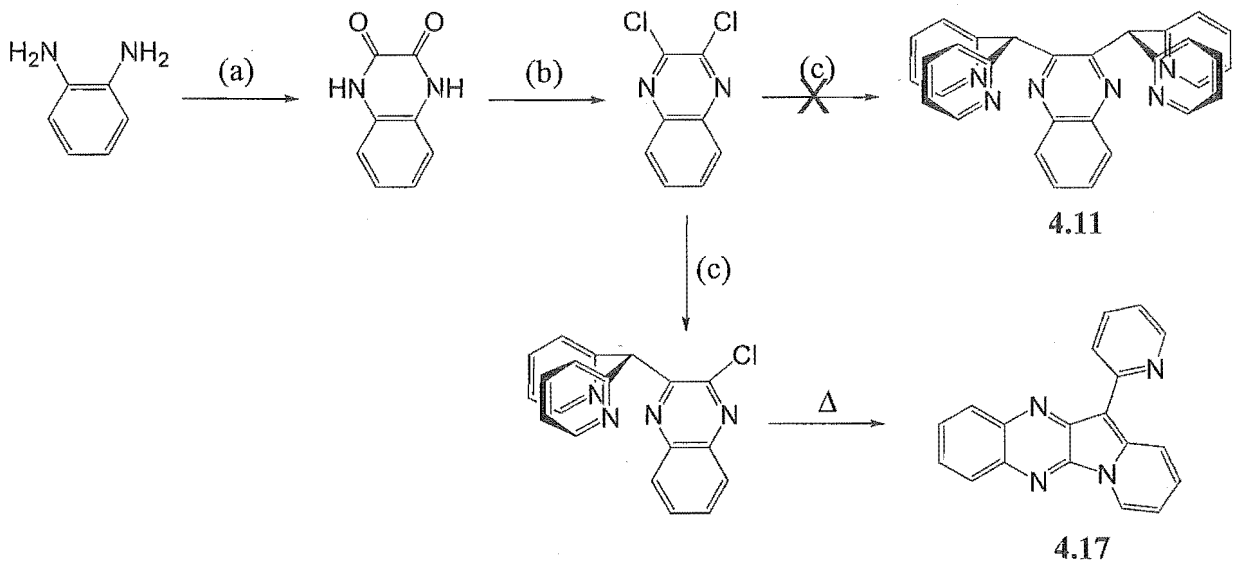


(a) $(COOH)_2$, 91%; (b) $SOCl_2$, DMF, 99%; (c) di-2-pyridylmethane, n-BuLi, THF, 90%.

**Scheme 4.5.**

The steric hindrance of the second chloride substitution was thought to be a problem and therefore the reaction was repeated under more forcing conditions. This did not produce any compounds corresponding to the desired di-adduct, **4.11**. However, a bright purple solid, that was the other component of the mixture isolated from the initial reaction attempt, was obtained in high yield. The purple solid was characterised by mass spectrometry and NMR spectroscopy. Mass spectrometry indicated a compound that had a mass corresponding to the loss of HCl from the monosubstituted intermediate, suggesting the possibility that it had the structure shown for **4.17**. This was confirmed by NMR spectroscopy, which indicated 12 proton environments and 19 carbon signals with chemical shifts consistent with the proposed structure.

The structure of compound **4.17** is a relatively unusual heterocyclic system for which there are limited examples reported in the literature. Compound **4.17** has not previously been described but is based on a known heterocyclic ring system.[219] The conformation of **4.17** is likely to be planar with three intramolecular C-H···N hydrogen bonds holding the pyridine ring in the plane of the indolizino[2,3-b]quinoxaline. This is consistent with the very intense colour of the compound.

Another feature of note is that compound **4.17** has a structure closely related to a class of potential anti-cancer drugs called variolins, for example variolin B [Figure 4.8(a)].[220] The variolins are based on the pyrido[3',2':4,5]pyrrolo[1,2-c]pyrimidine core and have been shown to be potential anti-cancer compounds. Thus, **4.17** was submitted for anti-cancer testing against the P388 murine leukaemia cell line. Compound **4.17** showed no activity in this assay but, because it was prepared in three steps from commercially available compounds, the method is going to be modified for the synthesis of other analogues more closely related to the active variolin B.

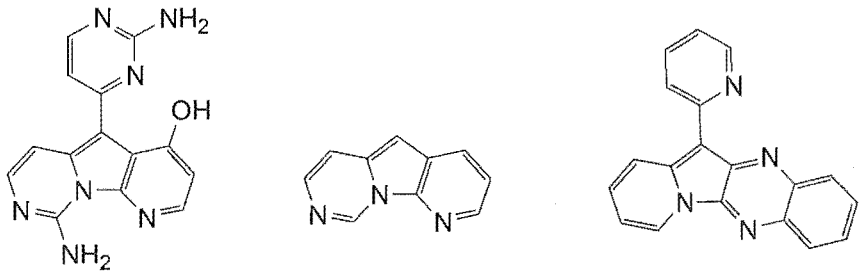

(a) (b) **4.17**

**Figure 4.8.** An example of a variolin (a) and the variolin core (b), to compare with **4.17**.

### 4.2.4 Other bridging cores

It was initially proposed to prepare the novel ligand, **4.12**, in four steps, beginning with commercially available 3-aminopyridine. Using the Skraup reaction,[221] 1,5-naphthyridine was prepared in 31% yield from 3-aminopyridine and glycerol (Scheme 4.6). The di-N-oxide of 1,5-naphthyridine was then prepared using acetic acid and hydrogen peroxide, before it was converted to 2,6-dichloro-1,5-naphthyridine by refluxing in phosphorus oxychloride.[222] Reaction under the conditions used to form other carbon-linked ligands was tried, without success, to prepare **4.12**. The problems with this reaction were thought to stem from substitution of the chloride leaving group and the low solubility of 2,6-dichloro-1,5-naphthyridine.

Both these problems could be corrected by replacing the chlorines with iodine. Stirring 2,6-dichloro-1,5-naphthyridine in hydroiodic acid failed to effect such a transformation. A second method to prepare iodopyridines from chloro- and bromopyridines has been reported by Corcoran and Bang.[223] Refluxing 2-chloro- or 2-bromopyridine with sodium iodide and acetyl chloride in acetonitrile was shown to effect the iodination of these compounds in high yields, especially for the bromo-substituted starting material. However, this reaction did not cleanly effect the iodination reaction on 2,6-dichloro-1,5-naphthyridine and gave a mixture of the starting material, mono- and di-substituted products. Unfortunately, the mixture could not be

adequately separated to give 2,6-diiodo-1,5-naphthyridine in a pure form for the subsequent reaction.

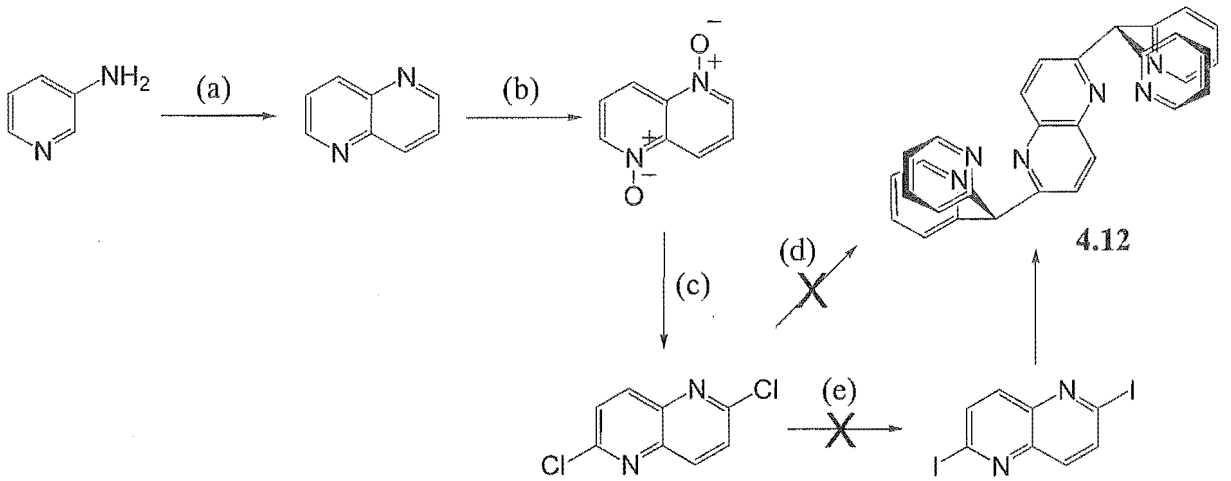


(a) glycerol, sodium *m*-nitrobenzenesulphonate, $H_2O$, $H_2SO_4$, 31%; (b) $H_2O_2$, AcOH, 33%; (c) $POCl_3$, 46%; (d) di-2-pyridylmethane, n-BuLi, THF; (e) NaI, $CH_3COCl$, $CH_3CN$.

**Scheme 4.6.**

A similar set of problems to those encountered in the synthesis of **4.12** applies to the synthesis of ligand **4.13**. The precursor, 2,2'-dichloro-4,4'-bipyridine was prepared as shown in Scheme 4.7.[224, 225] Reaction of this with di-2-pyridylmethane failed to give any of the desired product. A colourless solid was isolated when the reaction was heated for extended periods under argon, but this compound could not be identified. The iodination reaction was equally

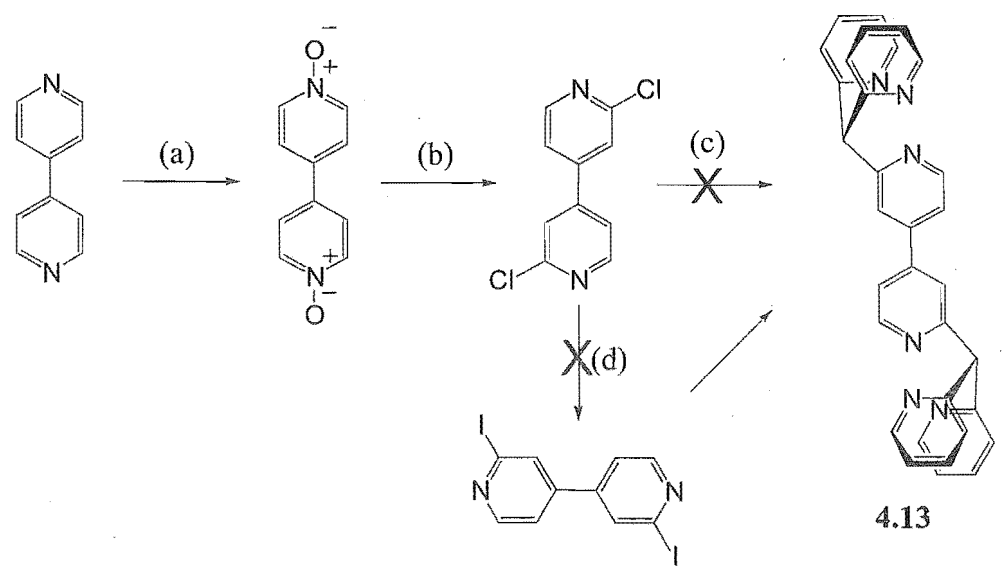


(a) $H_2O_2$, AcOH, 87%; (b) $POCl_3$, 23%; (c) di-2-pyridylmethane, n-BuLi, THF; (d) NaI, $CH_3COCl$, $CH_3CN$.

**Scheme 4.7.**

problematic, with difficulties in converting 2,2'-dichloro-4,4'-bipyridine to the diiodo-derivative, and in separating the mixture formed from the incomplete substitution reaction.

As was noted earlier, the synthesis of **4.6** also provided a significant amount of 4-chloro-6-(di-2-pyridylamino)pyrimidine, **4.16**. This can be reacted to form 'extended-reach' tripodal ligands, analogous to the work of Kodera[204] and Reger,[208] by reaction with various substituted benzene cores. An example of such a reaction is shown in Scheme 4.8. Simply heating **4.16**, hydroquinone and potassium carbonate overnight in DMF gave **4.14** in 59% yield. As noted though, a disadvantage with such ligands is that the metal centres of potential dinuclear complexes are no longer connected via a conjugated core.

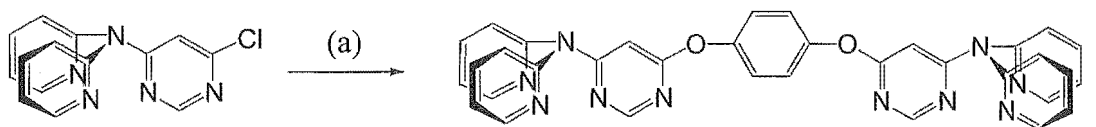


**4.16** **4.14**

(a) Hydroquinone, $K_2CO_3$, DMF, 59%.

**Scheme 4.8.**

Attempts to employ either a nickel or palladium catalysed cross-coupling reaction[226] in the synthesis of ligand **4.15** failed to provide any product (Scheme 4.9). Phillips has used this nickel catalysed cross-coupling reaction to couple related pyrimidine compounds before.[225] The palladium catalysed cross-coupling has also been used within the Steel group previously.[161] Unfortunately, neither method was able to successfully prepare **4.15** by coupling two equivalents of **4.16**.

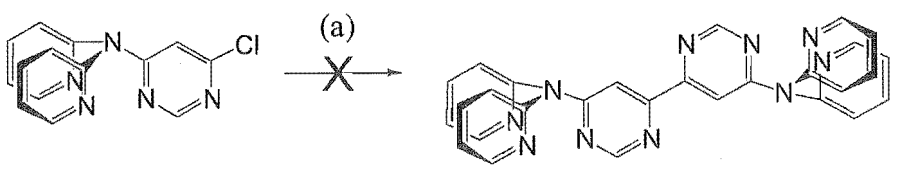


**4.15**

(a) $Ni(PPh_3)_2Cl_2$, Zn, DMF or $K_2CO_3$, $Pd(OAc)_2$, $(n\text{-}Bu)_4NI$, DMF, isopropanol.

**Scheme 4.9.**

## 4.3. Investigation of the coordination and metallosupramolecular chemistry

The studies into the coordination chemistry of these doubly tridentate tripodal ligands were intended to investigate the different possible coordination modes for these compounds. Particular emphasis was applied to finding octahedral metals to which the ligand could coordinate with tripodal tridentate coordination at two metal centres. Therefore, these ligands were reacted with an extensive range of metals, with primarily octahedral geometries, that had both coordinating and non-coordinating anions. These included rhodium, copper, nickel, chromium, zinc, cobalt, ruthenium and cadmium salts. While there are numerous examples of mononuclear complexes with tripodal tridentate coordination, there are significantly fewer examples of dinuclear complexes with the same tripodal mode of coordination of two metal centres.

### 4.3.1 Complexes of tri-2-pyridylamine, 4.4

A cobalt precursor that should bind with the desired coordination mode to the tripodal ligands described in this chapter is sodium cobaltinitrite. Facial coordination of octahedral cobalt by the tripodal ligand, 1,4,7-triazacyclononane (tacn), has been described when tacn was reacted with sodium cobaltinitrite.[227] Replacement of three of the nitrite groups resulted in a neutral complex that precipitated from the mixed water-methanol solution that this reaction was carried out in. Therefore, a similar reaction was attempted with **4.4** to test the possibility of forming the desired dinuclear complexes with other ligands. Simply mixing a solution of sodium cobaltinitrite in water with a solution of **4.4** dissolved in methanol gave crude **4.18** as an orange precipitate. This suspension was heated for 30 minutes before being filtered and dried *in vacuo* to give **4.18** in 86% yield.

Complex **4.18** was characterised by $^{1}$H NMR spectroscopy as a symmetrical complex and shown by infrared spectroscopy to have all N-bound nitrite groups. The proposed tripodal coordination was confirmed by X-ray crystallography when vapour diffusion of methanol into a DMSO solution of **4.18**, produced orange coloured block shaped crystals. Despite appearing to be beautifully formed crystals, they were horribly twinned, and thus, while the structure could be solved in the triclinic crystal system, the correct space group could not be determined and the solution failed to refine. The complex has, as anticipated, the ligand coordinating with tripodal tridentate coordination to the octahedral cobalt atom and three nitrogen-bound nitrite anions. Rhodium chloride and nickel thiocyanate complexes were prepared with potentially the same coordination motif, but were not further characterised.

An $ML_2$ bis-tripodal coordination motif was also desired for the formation of complexes with the tripodal ligands. There are several examples of such complexes with ligands like **4.3** and **4.4**,[58, 198, 199, 228, 229] When **4.4** was reacted with nickel tetrafluoroborate the anticipated $ML_2$ complex, **4.19**, was obtained as pink crystals, in 51% yield by slow evaporation of the reaction solvent. Elemental analysis confirmed the complex to have the composition $[Ni(\mathbf{4.4})_2](BF_4)_2$. A similar $ML_2$ complex was expected when **4.4** was reacted with copper tetrafluoroborate. However, the complex obtained, **4.20**, analysed with an unexpected $M_2L$ composition, in contrast to the $ML_2$ stoichiometry of **4.19**, despite the reaction being done in a 2:1 stoichiometry.

Crystal Structure of **4.19**

Complex **4.19** does indeed have the desired bis-tripodal coordination of the octahedral nickel centre. A perspective view of the complex, **4.19**, which crystallises in the monoclinic space group $P2_1/n$, is shown in Figure 4.9. The asymmetric unit includes one ligand, a half nickel atom and one tetrafluoroborate anion. The nickel atom has octahedral geometry with slight distortions of the angles of the capped faces, as in other complexes of the nitrogen and carbon-linked ligands, caused by the restricted bite angle of the ligand (bond angles of 85.90(7), 86.56(8) and 87.03(8)°). The bond lengths for the nickel–nitrogen bonds are all very similar, ranging from 2.079(2) Å to 2.104(2) Å, which is typical of such complexes, and shorter than complexes with monodentate pyridine ligands.[8] A nickel nitrate complex, $[Ni(\mathbf{4.3})_2](NO_3)_2$, of ligand **4.3** was characterised by Astley et al. with Ni-N bond lengths of 2.069(2) Å.[199]

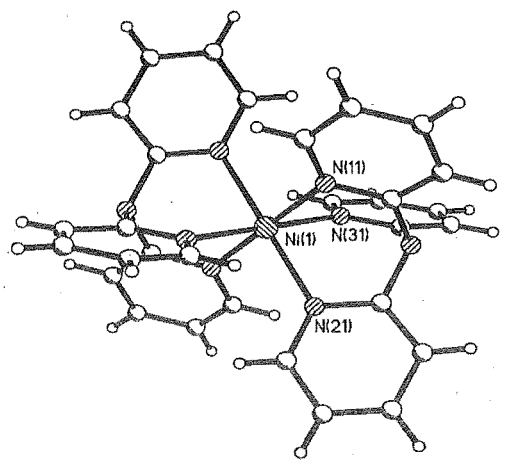


**Figure 4.9.** A perspective view of the nickel tetrafluoroborate complex **4.19** with the tetrafluoroborate anions omitted for clarity. Selected bond lengths (Å) and angles (°): Ni(1)-N(11) 2.079(2), Ni(1)-N(31) 2.082(2), Ni(1)-N(21) 2.104(2), N(11)-Ni(1)-N(31) 87.03(8), N(11)-Ni(1)-N(21) 86.56(8), N(31)-Ni(1)-N(21) 85.90(7).

### 4.3.2 Complexes of 4,6-bis(di-2-pyridylmethyl)pyrimidine, 4.5

Despite many attempts to prepare coordination complexes with **4.5**, very few crystalline products were obtained. Invariably the products of these reactions were oils or oily solids that were not suitable for analysis. Reacting **4.5** with sodium cobaltinitrite resulted in a complicated mixture of products. The mononuclear cobalt complex is insoluble in water-methanol, and thus, does not react to give the expected dinuclear complex. This reaction did not provide the desired dinuclear complex when using other solvents. Similar problems occurred when **4.5** was reacted with rhodium trichloride. Various isomeric mononuclear complexes and polymeric materials were obtained, which did not further react to give a dinuclear compound.

However, reaction of **4.5** with nickel perchlorate and sodium thiocyanate produced an orange solid, which when recrystallised by vapour diffusion of either acetone or ethanol into a DMSO solution of the complex, gave purple coloured crystals in 41% yield. The purple crystals, **4.21**, analysed as $[Ni_2(\mathbf{4.5})(SCN)_4(DMSO)_2]$ and were subsequently characterised by X-ray crystallography. Complexes were also prepared with copper, nickel and cobalt tetrafluoroborate, which were expected to give $M_2L_2$ dimers. Despite repeated attempts and many variations of the conditions, these reactions gave only oily solids that were not characterised.

Attempts were made to prepare dinuclear ruthenium complexes with ligand **4.5**, as shown in Scheme 4.10. This was attempted in two ways, either by reacting with two equivalents of $[Ru(\mathbf{4.4})Cl_3]$, or in two steps, by first reacting with ruthenium trichloride and then with tri-2-pyridylamine. Using both methods low yields of insoluble solids were isolated that could not be adequately characterised. A major problem with using tri-2-pyridylamine is that it is a bulky ligand and may make, for steric reasons, forming the desired ruthenium complexes very difficult.

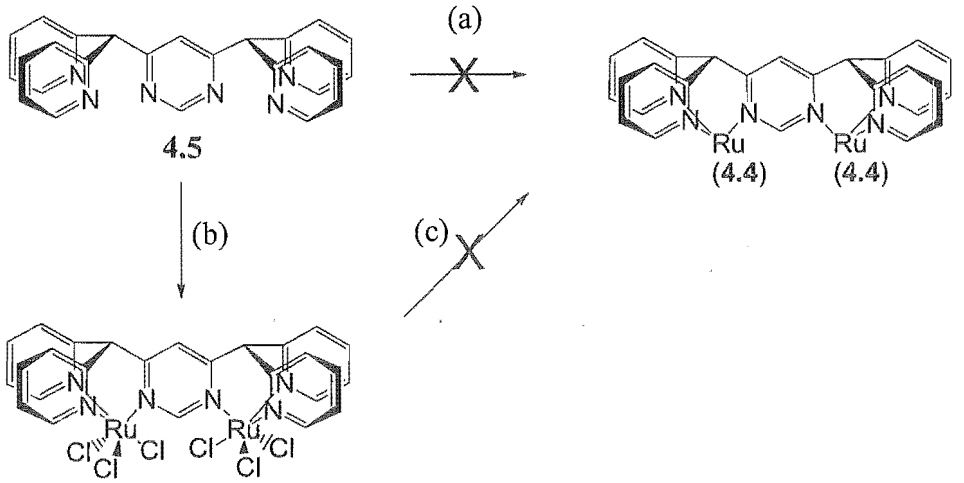


(a) $[Ru(\mathbf{4.4})Cl_3]$, EtOH/water; (b) $RuCl_3.2H_2O$, EtOH; (c) **4.4**, EtOH/water.

**Scheme 4.10.**

Crystal Structure of 4.21

The structure of complex **4.21** is a discrete $M_2L$ dinuclear complex in which, pleasingly, the ligand coordinates in a tripodal fashion to each nickel atom (Figure 4.10). Complex **4.21** crystallises in the monoclinic space group $P2_1/n$, with one molecule of **4.5**, two nickel atoms, four thiocyanate anions, two coordinated and four non-coordinated DMSO molecules and three water molecules in the asymmetric unit. The ligand acts as a ditopic doubly tripodal donor to the two nickel atoms, with two thiocyanate anions and a coordinated DMSO molecule completing the coordination environment of each nickel atom. The metal-metal distance in **4.21** is 5.951(2) Å, which is similar to previous bimetallic units bridged by pyrimidine.[2]

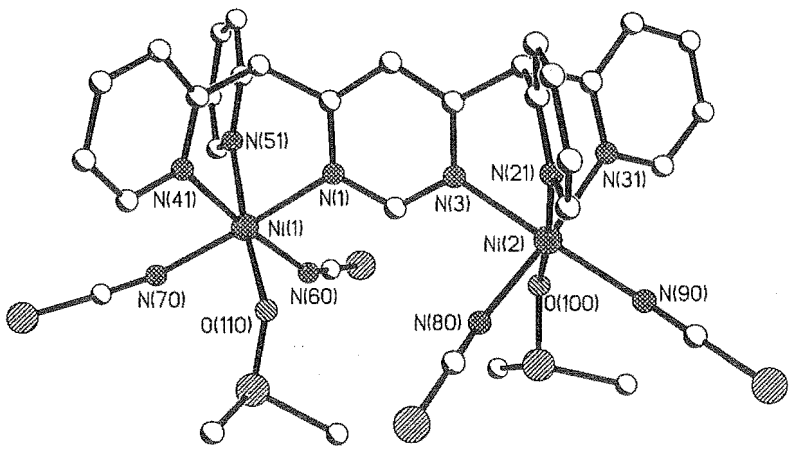


**Figure 4.10.** A perspective view of the nickel thiocyanate complex, **4.21** showing tripodal coordination at each metal. Hydrogen atoms and non-coordinated solvent molecules are omitted for clarity. Selected bond lengths (Å): Ni(1)-N(70) 2.033(5), Ni(1)-O(110) 2.085(4), Ni(1)-N(60) 2.086(5), Ni(1)-N(51) 2.092(4), Ni(1)-N(1) 2.100(4), Ni(1)-N(41) 2.108(4), Ni(2)-N(90) 2.036(5), Ni(2)-N(80) 2.067(5), Ni(2)-N(3) 2.084(4), Ni(2)-N(31) 2.089(4), Ni(2)-O(100) 2.103(4), Ni(2)-N(21) 2.113(4).

The bond lengths for the nickel atoms range from 2.033(5) to 2.113(4) Å, with the two shortest bonds of 2.033(5) and 2.036(5) Å to the thiocyanate nitrogen atoms (N(70) and N(90)), which are *trans* to the pyrimidine nitrogen atoms. The nickel atoms have an octahedral geometry with slight distortions of the angles of the capped faces caused by the bite angles of the ligand. The O-bound DMSO co-ligands coordinate to the nickel atoms on opposite faces of the pyrimidine ring. All the thiocyanate anions coordinate to the nickel atom through a nitrogen donor, as expected, rather than the softer sulfur donors. This is consistent with the infrared

spectrum of the complex, which has a stretch at 2100 $cm^{-1}$, indicating N-bound thiocyanate. There are no unusually short intermolecular interactions between the dinuclear complexes.

A feature of the ligand conformation in this complex that will be compared to other ligands in related complexes is the geometry of the linker atom. The carbon atoms have a tetrahedral geometry with bond angles to the carbon atoms of the arene rings between 107.9(4) and 112.7(4)°. This allows all three of the nitrogen donors that are connected to that carbon atom to coordinate to the metal centre with the desired tripodal coordination.

### 4.3.3 Complexes of 4,6-bis(di-2-pyridylamino)pyrimidine, 4.6

By contrast to **4.5**, ligand **4.6** was significantly more inclined to form coordination complexes, but unfortunately found to be a poor tripodal tridentate donor. Complexes were prepared and characterised for **4.6** with copper nitrate, copper tetrafluoroborate, copper perchlorate, palladium chloride, and with two different nickel salts (Scheme 4.11). Other complexes with silver, zinc, cobalt and cadmium were investigated, but not fully characterised.

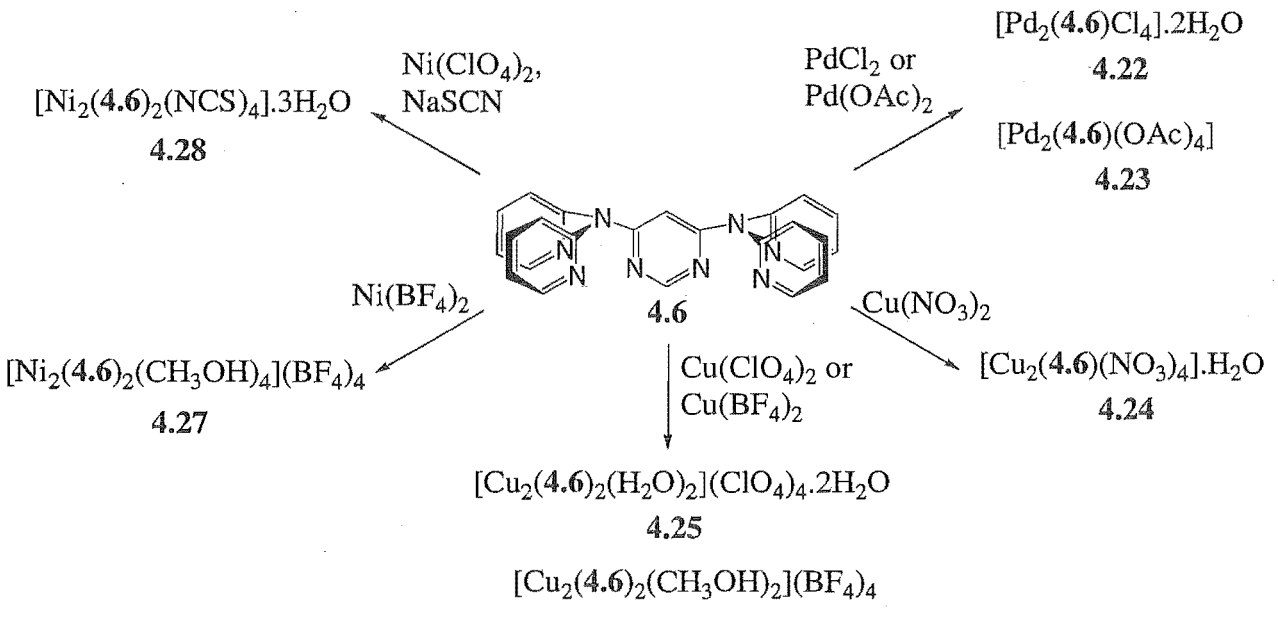


**Scheme 4.11**

Reaction of palladium chloride with **4.6** gave a yellow complex, **4.22**, that was only sparingly soluble in DMSO. Using a combination of elemental analysis and $^1$H NMR spectroscopy, **4.22** was characterised as $[Pd_2(\mathbf{4.6})Cl_4].2H_2O$, with the expected 2:1 metal-ligand ratio. The $^1$H NMR spectrum of the complex shows a number of changes in chemical shifts, (CIS), which result from coordination to the metal ion. These changes originate predominately from ligand-to-metal σ-donation in this complex and are shown in Table 4.1.

**Table 4.1.** The $^1$H NMR signals and CIS values for **4.22**.

| | H2 | H5 | H3' | H4' | H5' | H6' |
|---|---|---|---|---|---|---|
| **4.22** | 8.68 | 6.19 | 8.14 | 8.34 | 7.75 | 8.93 |
| **4.6** | 8.43 | 6.33 | 7.32 | 7.91 | 7.30 | 8.44 |
| *CIS* | *0.25* | *-0.14* | *0.82* | *0.43* | *0.45* | *0.49* |

The significant downfield shifts for the pyridine ring and the symmetry of the complex by NMR, indicate that the ligand forms a symmetrical dinuclear complex, but coordinates only through the pyridine nitrogen atoms. No coordination appears to occur through the pyrimidine ring. Subsequently, reaction of **4.6** with palladium acetate, and slow evaporation from an acetone-methanol solution, gave complex **4.23** as yellow crystals, suitable for X-ray crystallography. Complex **4.23** had the same dinuclear composition by elemental analysis, $[Pd_2(\mathbf{4.6})(OAc)_4]$.

Ligand **4.6** was also reacted with copper nitrate, copper perchlorate and copper tetrafluoroborate to provide three complexes, **4.24**, **4.25** and **4.26**, respectively. Reaction of acetone solutions of copper nitrate and the ligand gave **4.24** as a blue solid in 97% yield. Complex **4.24** gave an elemental analysis consistent with the composition $[Cu_2(\mathbf{4.6})(NO_3)_4].H_2O$, and potentially with the desired doubly tripodal coordination mode for these ligands. Complex **4.25** was isolated in 76% yield by mixing a methanol solution of **4.6**, with an acetonitrile solution of copper perchlorate. Elemental analysis indicated a 1:1 metal-ligand composition that suggests the possibility of either a discrete [2+2] dimer or a coordination polymer. Fortunately, crystals of a closely related complex, **4.26**, with tetrafluoroborate anions were obtained, by slow evaporation of the methanol reaction mixture, in 65% yield. Elemental analysis revealed complex **4.26** had the composition $[Cu_2(\mathbf{4.6})_2(CH_3OH)_2](BF_4)_4$ and was confirmed as a [2+2] dimer by X-ray crystallography. This suggested that the likely composition of the previous complex, **4.25**, is $[Cu_2(\mathbf{4.6})_2(H_2O)_2](ClO_4)_4.2H_2O$, which may also have a [2+2] dimeric structure.

Crystals of two closely related nickel complexes of ligand **4.6** were also obtained. Reaction of **4.6** with nickel tetrafluoroborate in methanol, and then slow evaporation of the methanol reaction mixture, gave pale blue crystals of complex **4.27**. Complex **4.27** analysed with the composition $[Ni_2(\mathbf{4.6})_2(CH_3OH)_4](BF_4)_4$ that was confirmed by X-ray crystallography. Reaction of **4.6** with nickel perchlorate and sodium thiocyanate gave a complex, **4.28**, that also had a metal to ligand ratio of 1:1. This was an unexpected result for a coordinating anion such as thiocyanate, which had been expected to provide a discrete $M_2L$ complex. Crystals of **4.28**, suitable for a structure determination, were obtained from vapour diffusion of methanol into a

DMF solution of the complex, and confirmed the structure to be a closely related [2+2] dimer, like **4.27**.

Attempts were also made to prepare dinuclear ruthenium complexes of this ligand. This was attempted, as for **4.5**, in two ways, either by reacting with two equivalents of [Ru(**4.4**)$Cl_3$] or, in two steps, by first reacting with ruthenium trichloride and then with tri-2-pyridylamine. Unfortunately, similar problems to those encountered for **4.5** prevented the formation and isolation of either $Ru_2L$ or $Ru_2L_2$ complexes by these methods.

Crystal Structure of **4.23**

As was postulated from the NMR spectroscopy and elemental analysis, when ligand **4.6** was reacted with palladium chloride and acetate it forms two dinuclear complexes, **4.22** and **4.23**, with coordination through the pyridine nitrogen atoms only. This was confirmed by crystal structure analysis on complex **4.23**. As suspected, no coordination occurs through the nitrogen atoms on the pyrimidine ring. The complex, shown in Figure 4.11, crystallises in the C-centred monoclinic space group C2/c, with a 2-fold rotation axis running through the C2 and C5 carbon atoms of the pyrimidine ring. Thus, the asymmetric unit contains half the ligand, one palladium atom, two coordinated acetate anions and three water solvate molecules. The coordinated acetate anions and the non-coordinated water molecules are involved in an extensive hydrogen-bonding network that connects adjacent complexes to form infinite one-dimensional chains.

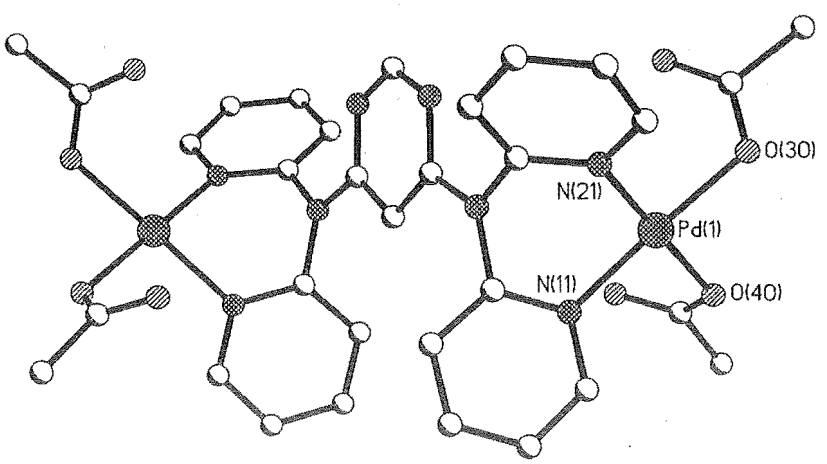


**Figure 4.11.** The palladium acetate complex, **4.23**, showing the ligand acting as a tetradentate bridge. Selected bond lengths (Å) and angles (°): Pd(1)-N(21) 2.010(3), Pd(1)-N(11) 2.011(3), Pd(1)-O(40) 2.024(3), Pd(1)-O(30) 2.026(2), N(21)-Pd(1)-N(11) 87.65(11), N(21)-Pd(1)-O(40) 175.88(10), N(11)-Pd(1)-O(40) 92.59(11), N(21)-Pd(1)-O(30) 91.98(11), N(11)-Pd(1)-O(30) 176.06(10), O(40)-Pd(1)-O(30) 87.51(10).

As expected, the palladium centre is four coordinate, with coordination by two monodentate acetate anions and two pyridine nitrogen atoms. The bond lengths (2.010(3) - 2.026(2) Å) and angles of the palladium atom are typical for such a donor set. The pyrimidine ring does not bridge the metals in complex **4.23**, and so the metal-metal distance is considerably longer than the other complexes of this ligand (9.520(1) Å). The coordination of the ligand is consistent with the CIS values measured for complex **4.22**. The H5 of the pyrimidine ring is in a position to be shielded slightly by the pyridine rings of the ligand in the conformation the complex adopts in the solid state. The same measurements could not be made for **4.23**, which appears to dissociate in solution.

The crystal structure reveals an interesting feature of the triarylamine nitrogen linker atom in these ligands. The nitrogen atom of **4.6** has an $sp^2$ geometry and is almost planar. The bond angles for the nitrogen atom are 121.3(3), 121.8(3) and 116.8(2). This is in contrast to the carbon linker atom of ligand **4.5**, which has a tetrahedral $sp^3$ geometry. This geometry partially explains the difficulty encountered in this work of forming complexes with ligand **4.5**, which have tripodal coordination at two octahedral metal centres.

Crystal Structure of **4.26**

The complex formed from the reaction of **4.6** with copper tetrafluoroborate, **4.26**, crystallises in the tetragonal space group P4/mbn. While the complex is well resolved, the refinement of the overall structure is problematic and incomplete, and thus, the structure will only be discussed in general terms. A perspective view of the [2+2] structure of **4.26** is shown in Figure 4.12. The

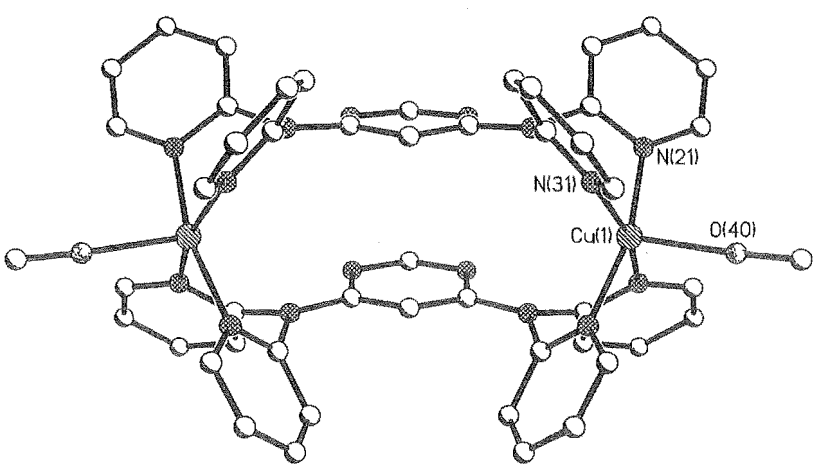


**Figure 4.12.** A perspective view of the complex **4.26**, formed from reaction of copper tetrafluoroborate with ligand **4.6**.

copper atoms have square-pyramidal geometries (τ value of 0.0), with an elongated axial bond (2.19 Å) to the oxygen atom of a coordinated methanol molecule. The triarylamine nitrogen linker atoms of the ligand are approximately planar and again, like complex **4.22** and **4.23**, no coordination by the pyrimidine nitrogen atoms is observed. There is a face-to-face π-π stacking interaction between the two pyrimidine rings (distance 3.47 Å) of the ligand, both of which are unusually orientated in the same direction.

Crystal structure of **4.27**

Simply substituting the metal atom in the previous complex by nickel gave a different, but closely related structure. The [2+2] molecular box structure (Figure 4.13) has nickel atoms in octahedral environments with coordination by two methanol molecules, two pyridine nitrogen atoms of one ligand and a pyridine and pyrimidine donor from a second ligand molecule. Complex **4.27** crystallises in the space group C2/c, with one ligand molecule, a nickel atom, two coordinated methanol solvate molecules, one tetrafluoroborate anion and half a hexafluorosilicate anion in the asymmetric unit. The hexafluorosilicate anion is likely to originate from the action of a hydrofluoric acid (which is formed from decomposition of the tetrafluoroborate anion by water) on the glass container.

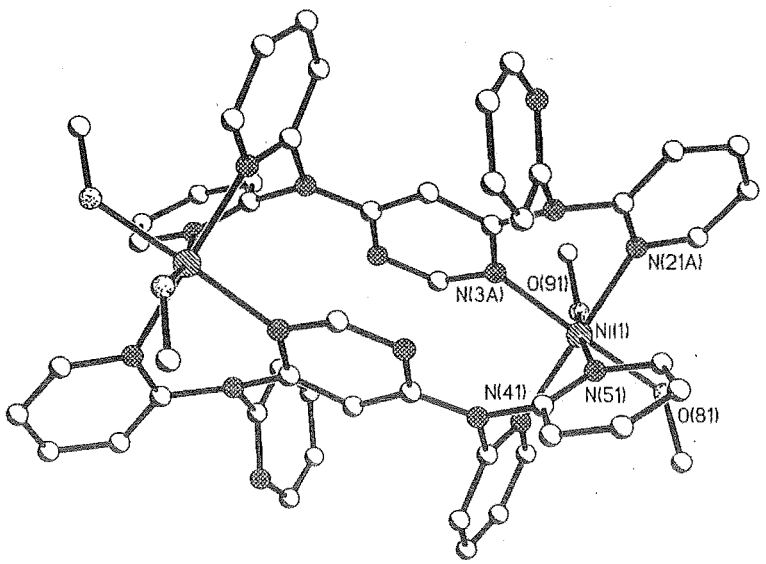


**Figure 4.13.** A perspective view of **4.27** showing the [2+2] molecular box structure with hydrogen atoms and non-coordinated anions omitted. Selected bond lengths (Å): Ni(1)-N(3A) 2.065(2), Ni(1)-O(91) 2.064(2), Ni(1)-N(21A) 2.082(3), Ni(1)-O(81) 2.086(2), Ni(1)-N(51) 2.089(2), Ni(1)-N(41) 2.124(3).

The nickel atom has an octahedral geometry with bond lengths in the range 2.064(2) to 2.124(3) Å. The ligand only utilises four of its six donor atoms in forming this complex, and thus, is hypodentate, with the two non-coordinated pyridine rings oriented away from the metal centres. These non-coordinated pyridine rings cover the open sides of the cavity formed by the pyrimidine rings to form a box-like structure.

Once again the tertiary nitrogen-linker atoms of the ligand are planar, with bond angles in the range 113.2(2) to 124.1(2)°. The metal-metal distance is 7.990(1) Å, considerably shorter than in complex **4.23** and reflective of the coordination of each metal by one of the pyrimidine nitrogen donor atoms from each ligand. There is a relatively strong face-to-face π-π stacking interaction[15] between the two pyrimidine rings (distance 3.410(5) Å) of this complex, and in contrast to **4.26**, the pyrimidine rings are oriented in opposite directions. The π-π stacked pyrimidine rings are also slightly offset in this structure. Non-coordinated tetrafluoroborate and hexafluorosilicate anions fill the voids between the [2+2] molecular box structures, and with the coordinated methanol molecules, participate in an intricate intermolecular hydrogen-bonding network.

Crystal Structure of **4.28**

The structure of complex **4.28** is also a [2+2] molecular box formed from two equivalents of metal and ligand. It has an almost identical structure (Figure 4.14) to the previously described nickel complex, **4.27**, but with the thiocyanate anions replacing the coordinated solvate molecules. Complex **4.28** crystallises in the tetragonal space group $I4_1/a$, with one ligand molecule, a nickel atom, two thiocyanate anions, one non-coordinated water molecule and three non-coordinated DMF solvate molecules in the asymmetric unit. Each nickel atom is octahedral with coordination by two thiocyanate ligands, two pyridine rings from one ligand and one pyridine nitrogen and a pyrimidine nitrogen of the other ligand molecule. Therefore, as observed before, the ligand is not using all its possible coordination sites and is hypodentate. An interesting crystallographic feature of this structure is the presence of a DMF molecule, which is disordered four ways and lies on a four-fold improper rotation axis.

The nitrogen linker atoms again have $sp^2$ geometry with bond angles between 114.5(5) and 125.0(6)°. This has the effect of holding the pyridine rings away from the pyrimidine core of the ligand, and, thus, prevents the ligand from acting as a tripodal donor. The metal-metal distance is 8.044(1) Å and very similar to that in complex **4.27**. There is a strong face-to-face π-π stacking interaction between the two pyrimidine rings (distance 3.313(7) Å) within this complex. This is

quite a short distance, with a typical distance for this type of interaction being in the range 3.3-3.8 Å[15] and the distance in graphite being 3.35 Å.

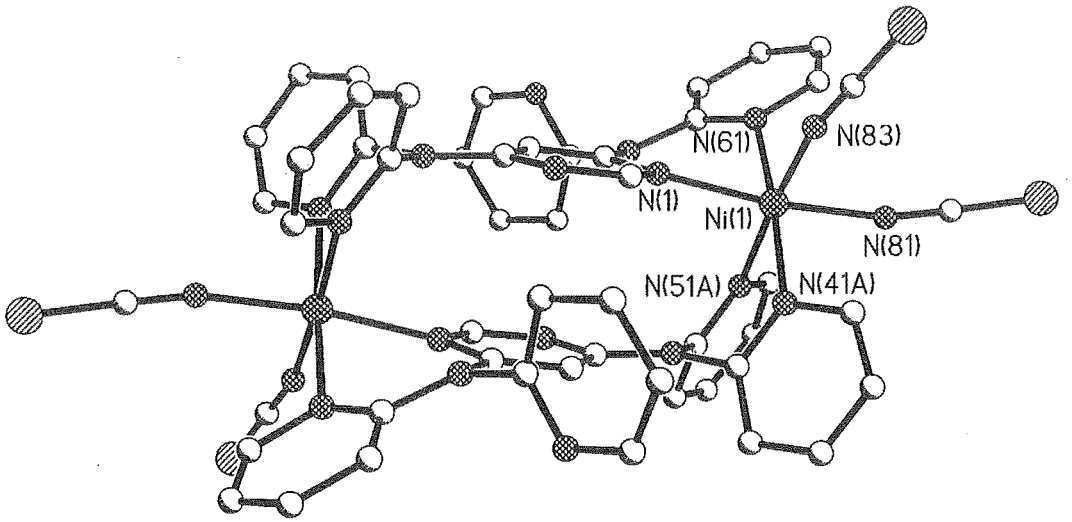


**Figure 4.14.** A perspective view of complex **4.28** with hydrogen atoms and solvate molecules omitted for clarity. Selected bond lengths (Å): Ni(1)-N(83) 2.027(6), Ni(1)-N(81) 2.028(6), Ni(1)-N(1) 2.099(5), Ni(1)-N(61) 2.099(5), Ni(1)-N(41A) 2.122(6), Ni(1)-N(51A) 2.123(5).

In the complexes characterised for ligand **4.6**, the use of coordinating anions and non-coordinating anions has very little effect on the types of structures. In comparison, as will be shown, in complexes of ligands **4.7** and **4.9** the anion influences the coordination motif of the ligand, and thus, the type of structure observed. Ligand **4.6** does not favour the desired tripodal tridentate coordination mode, preferring to be hypodentate, which has led to a predominance of $M_2L_2$ dimers, rather than $M_2L$ complexes.

### 4.3.4 Complexes of 4-chloro-6-(di-2-pyridylamino)pyrimidine, 4.16

Ligand **4.16** is a new tripodal tridentate ligand and is effectively half of ligand **4.6**, but which possesses an extra monodentate coordination site on the pyrimidine ring. To see whether **4.16** would act as a tripodal ligand and coordinate facially to an octahedral centre it was reacted with a range of transition metals. Such complexes provide a comparison to both the doubly tripodal pyrimidine ligands and to simple tripodal ligands like **4.4**. Reaction of **4.16** with rhodium chloride in refluxing methoxyethanol gave complex **4.29** as a yellow solid in 86% yield. $^1$H NMR spectroscopy and elemental analysis were used to characterise the complex as

[Rh(**4.16**)$Cl_3$]. Large positive CIS values for all protons indicate that the complex probably coordinates through both the pyridine and pyrimidine rings to facially cap the rhodium atom.

Ligand **4.16** was also reacted with copper nitrate and copper tetrafluoroborate, but no crystalline solids were obtained. Reaction with nickel tetrafluoroborate was similarly tried without success. However, reaction of the ligand with nickel perchlorate and sodium thiocyanate gave a purple crystalline sample of a complex, **4.30**, that was isolated in 33% yield, following recrystallisation. This complex analysed with the composition [Ni(**4.16**)$_2$$(SCN)_2$].2$H_2O$ that is consistent with the structure determined by X-ray crystallography.

Crystal Structure of **4.30**

A crystal structure of the complex, **4.30**, formed from reaction of **4.16** with nickel thiocyanate is shown in Figure 4.15. The crystals examined here were grown by vapour diffusion of ether into an acetonitrile solution of **4.30**. The complex crystallised in the triclinic space group P-1, and the asymmetric unit contains two ligands and two thiocyanate anions bound to the nickel, along with a non-coordinated acetonitrile molecule. The nickel atom has an octahedral geometry with the two molecules of the ligand coordinated through the pyridine donor atoms only, and the two thiocyanate anions *cis*-coordinated through their nitrogen donor atoms. Again, like complexes of **4.6**, the pyrimidine nitrogen atoms are not involved in coordination, meaning the ligand is hypodentate.

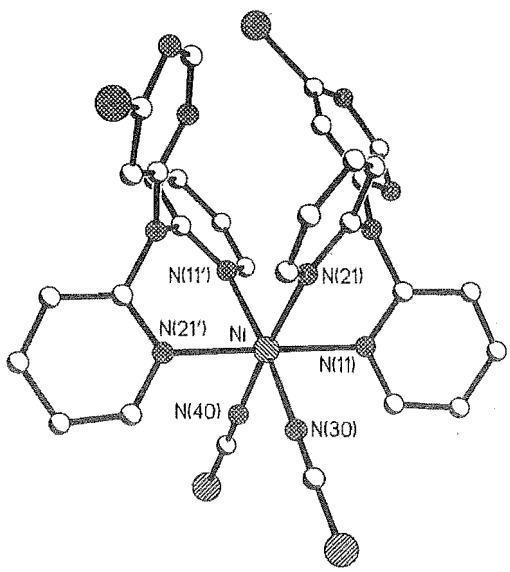


**Figure 4.15.** The nickel thiocyanate complex **4.30**, showing the $ML_2$ structure. Selected bond lengths (Å): Ni-N(40) 2.045(7), Ni-N(30) 2.048(7), Ni-N(21) 2.096(6), Ni-N(11) 2.100(6), Ni-N(21') 2.121(5), Ni-N(11') 2.131(6).

The coordination environment of the nickel precursor used here is quite flexible, and thus, the two molecules of **4.16** can both chelate to the nickel atom in complex **4.30**. In complex **4.29** the ligand is likely to be facially coordinated to the octahedral rhodium centre because the rhodium atom only has three available coordination sites. Hypodentate coordination by **4.16** would require bidentate and monodentate coordination modes in the case of the rhodium complex. The coordination mode employed by the ligand demonstrates the preference the nitrogen-linker atoms have for an $sp^2$ geometry, and the fact that pyridine and thiocyanate donors are preferred over a pyrimidine donor.

### 4.3.5 Complexes of 3,6-bis(di-2-pyridylmethyl)pyridazine, 4.7

Other workers have previously prepared ligand **4.7** and investigated its coordination chemistry by the synthesis of copper complexes with both coordinating and non-coordinating anions.[210-212] The interest of this group was in investigating the magnetic properties of such complexes. With copper chloride and bromide, $Cu_2L$ complexes were obtained with bridging chloride and bromide anions. Similarly, copper chloride and bromide complexes were prepared with the dimethylated analogue of **4.7**, 3,6-bis[(6-methyl-2-pyridyl)(2-pyridyl)methyl]pyridazine.[211] When **4.7** was reacted with copper perchlorate these authors obtained a [2+2] dimeric complex, which was structurally characterised by X-ray crystallography.[210] Subsequently, it was shown that a Cu(I)/Cu(II) mixed valance complex could be prepared, which was also characterised by X-ray crystallography.[212]

As a comparison to the work with the pyrimidine-based ligands, several new complexes were prepared with this ligand (Scheme 4.12). Reaction of **4.7** with palladium chloride gave a complex, **4.31** that was characterised as $[Pd_2(4.7)Cl_4].2H_2O$ by elemental analysis. It is likely

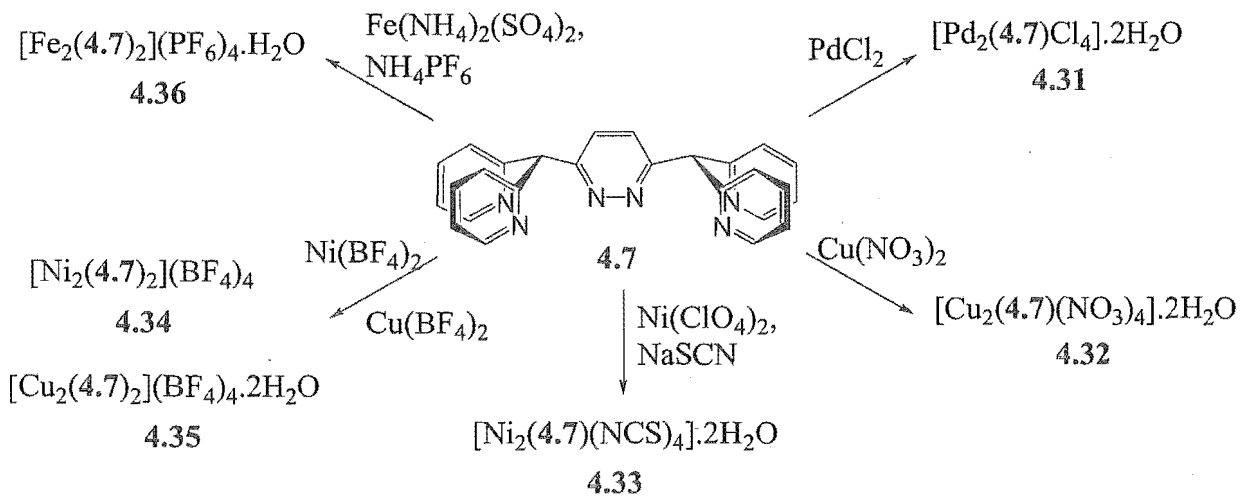


**Scheme 4.12**

that this coordinates through the pyridine nitrogen atoms only, but this could not be confirmed because **4.31** is insoluble in common NMR solvents. The preparation of complexes with rhodium trichloride and sodium cobaltinitrite were also tried, but because the pyridazine nitrogen atoms are closer together than the nitrogen atoms in pyrimidine, it will be more difficult to form $M_2L$ complexes like **4.21**, without incorporating small bridging anions as well. Reacting copper nitrate with **4.7** gave a complex, **4.32**, that is likely to have a very similar structure to the previous copper chloride and bromide complexes characterised by Manzur et al.[210] Complex **4.32** was isolated from the reaction mixture as a blue crystalline solid and characterised as $[Cu_2(\mathbf{4.7})(NO_3)_4].2H_2O$ by elemental analysis. This is consistent with a dinuclear complex with either nitrate anions, or possibly water molecules, bridging between the two copper atoms.

More interesting results were obtained when **4.7** was reacted with two nickel salts. In the first example, reaction of **4.7** with nickel perchlorate and sodium thiocyanate gave a complex, **4.33**, in 91% yield that was successfully recrystallised by vapour diffusion of ethanol into a DMSO solution of the complex. The complex was found, by crystal structure analysis, to have a $M_2L$ composition consistent with the elemental analysis of $[Ni_2(\mathbf{4.7})(NCS)_4].2H_2O$. Ligand **4.7** was also reacted with nickel tetrafluoroborate to give a complex incorporating non-coordinating anions and a different coordination motif. Complex **4.34** was isolated in 43% yield, by slow evaporation of the methanol reaction mixture, and characterised by X-ray crystallography as a novel [2+2] helicate (Figure 4.16). As a result of this interesting structure, **4.7** was also reacted with copper tetrafluoroborate to see if this structural motif was maintained. Complex **4.35** was obtained in 25% yield, by the same method as **4.34**, and characterised as $[Cu_2(\mathbf{4.7})](BF_4)_4.2H_2O$. X-Ray crystallography confirmed that complex **4.35** had a helicate structure (Figure 4.16), closely related to **4.34**, and isomorphous with a previously reported copper perchlorate complex.[210] Reaction with cobalt tetrafluoroborate, which was hoped to provide a third example of a helicate structure, failed to give a solid product.

The results achieved with copper and nickel tetrafluoroborate suggested that the helical structure was a robust coordination motif for this ligand. Therefore, ligand **4.7** was also reacted with $[Ru(DMSO)_4Cl_2]$ to attempt to prepare a helical dinuclear ruthenium complex. This reaction gave a dark red/brown solid in low yield that could not be adequately identified. The complex was not soluble enough for NMR suggesting that it may be polymeric in nature.

Iron(II) is a more labile octahedral transition metal than ruthenium, and thus, it may allow the desired structural motif to form. Reaction of ferrous ammonium sulfate with the ligand, followed by precipitation of the complex with an excess of ammonium hexafluorophosphate,

provided **4.36** in 40% yield. Elemental analysis confirmed the desired stoichiometry, but $^1$H NMR studies provided inconclusive evidence for the formation of the desired helicate. Extensive attempts were made to crystallise **4.36**.

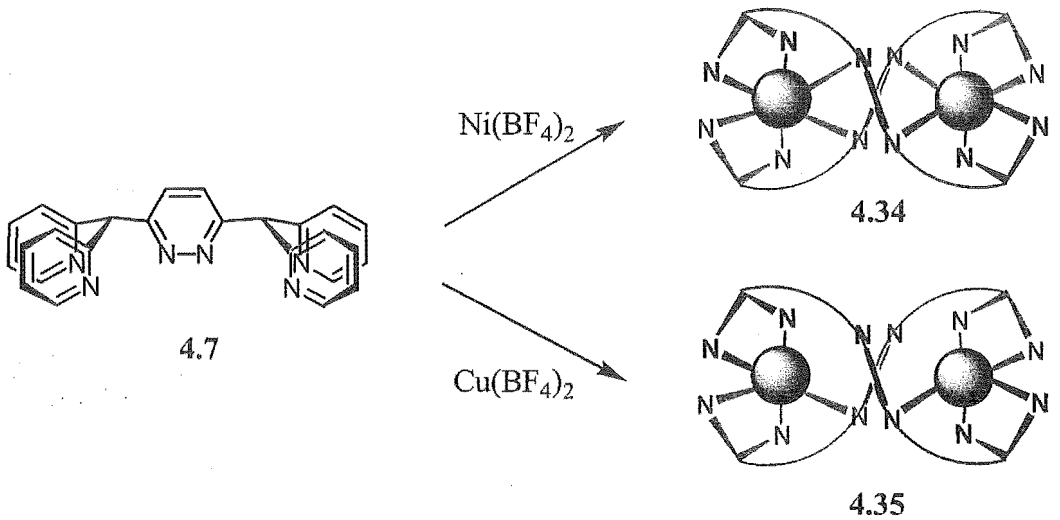


**Figure 4.16.** The synthesis of the two closely related helicates, **4.34** and **4.35**.

Cyclic voltammetry revealed that the complex has one quasi-reversible oxidation wave at +1.13 V (Table 4.2) consistent with nearly simultaneous oxidation of the metal centres. This value for the redox potential is similar to that observed for $[Fe(L)_2]$ complexes of the tridentate ligands, tpy (*ca.* +1.10 V *vs* SCE[230]) and **4.3** (+1.02 V *vs* SCE[229]). The pyridazine donors make this complex harder to oxidise than $[Fe(\mathbf{4.3})_2]$, while all three complexes, with tridentate ligands, are harder to oxidise than $[Fe(bpy)_3]$ (*ca* +0.86 V *vs* SCE in water). Complex **4.36** has three absorption maxima at 375, 407 and 480 nm, which are consistent with charge transfer transitions from the metal to ligand (MLCT).

**Table 4.2.** The visible absorption maxima and redox potential for **4.36**.

| | $\lambda$ (nm)[a,b] | $\varepsilon$ (Lmol$^{-1}$cm$^{-1}$) | $E_{ox}$[c,d] |
|---|---|---|---|
| **4.36** | 375(sh) | | +1.13(2e) |
| | 407 | 5800 | |
| | 480 | 6200 | |

[a] The MLCT band measured in $CH_3CN$ (± 2 nm)

[b] sh = shoulder.

[c] Potentials quoted in V *vs.* SCE in $CH_3CN$/0.1 mol.L$^{-1}$ $[(n\text{-}C_4H_9)_4]PF_6$ (the ferrocene/ferrocenium couple occurred at +310 mV *vs.* SCE).

[d] Uncertainty in $E_{1/2}$ values *ca.* ± 0.01 V.

Crystal Structure of 4.33

Complex **4.33** crystallises in the monoclinic space group $P2_1/c$, with one discrete complex in the asymmetric unit. Unfortunately, the structure is poorly refined as a consequence of very weak intensity data that was not improved by recollection and only a general description will be given. As shown in Figure 4.17, the pyridazine ring of the ligand and two $\mu_2$-thiocyanate anions bridge the two metal atoms, both of which have octahedral coordination geometry. The two different coordination environments for the thiocyanate anions, $\mu_2$-bridging and simple monodentate coordination through nitrogen, are also observed by infrared spectroscopy. In the bulk sample there are two infrared stretches for the C≡N at 2097 $cm^{-1}$ (monodentate) and 1996 $cm^{-1}$ (bridging) that are consistent with the crystal structure.

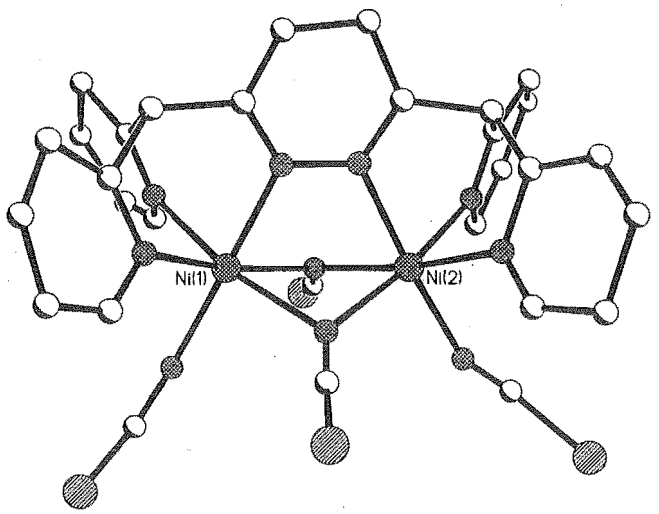


**Figure 4.17.** A perspective view of complex **4.33**, showing the bridging thiocyanate anions, which is a common coordination motif for this ligand.

Several closely related copper complexes have been characterised with this ligand by Manzur.[210] These have either bridging chloride or bromide anions between the two copper atoms with copper-copper distances of 3.511(1) and 3.673(2) Å, respectively. The related phthalazine ligand, **4.9**, also forms very similar dinuclear nickel complexes with bridging water molecules.[60, 61, 213, 214]

Crystal Structure of 4.34

As indicated earlier, when ligand **4.34** was reacted with nickel tetrafluoroborate the crystalline material that formed was shown to be composed of a novel helicate by single crystal X-ray structure determination. It is the first example of a saturated homotopic homostranded

dinuclear helicate with tripodal coordination of both octahedral metal centres. The helicate, crystallises in the non-centrosymmetric space group C2, with an asymmetric unit that contains one metal centre, two independent half-ligand components and two non-coordinated tetrafluoroborate anions. A perspective view of **4.34** is shown in Figure 4.18, showing the ligand acting as a ditopic tripodal ligand to the octahedral nickel atoms, with a crystallographic two-fold rotation axis passing through the two bridging pyridazines.

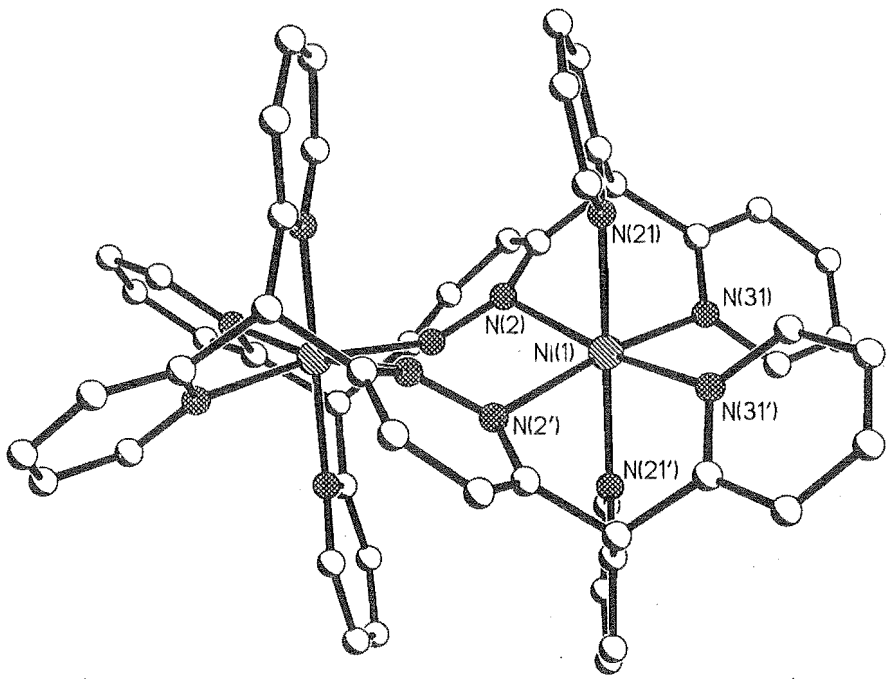


**Figure 4.18.** A perspective view of the saturated homostranded homotopic dinuclear helicate, **4.34**. The non-coordinated tetrafluoroborate counterions are omitted for clarity. Selected bond lengths (Å) and angles (°): Ni(1)-N(31') 2.060(6), Ni(1)-N(31) 2.066(6), Ni(1)-N(21') 2.071(5), Ni(1)-N(21) 2.078(5), Ni(1)-N(2) 2.163(6), Ni(1)-N(2') 2.172(6), N(31')-Ni(1)-N(31) 90.77(17), N(31')-Ni(1)-N(21') 88.5(2), N(31)-Ni(1)-N(21') 92.6(2), N(31')-Ni(1)-N(21) 90.6(2), N(31)-Ni(1)-N(21) 88.3(2), N(21')-Ni(1)-N(21) 178.8(3), N(31')-Ni(1)-N(2) 169.5(2), N(31)-Ni(1)-N(2) 90.9(3), N(21')-Ni(1)-N(2) 101.8(2), N(21)-Ni(1)-N(2) 79.1(2), N(31')-Ni(1)-N(2') 90.4(3), N(31)-Ni(1)-N(2') 170.9(2), N(21')-Ni(1)-N(2') 78.4(2), N(21)-Ni(1)-N(2') 100.8(2), N(2)-Ni(1)-N(2') 89.6(2).

The nickel atom displays a distorted octahedral environment with slightly longer Ni-N bonds to the two *cis*-coordinated pyridazine rings (2.163(6) Å and 2.172(6) Å) than the four pyridine rings (2.060-2.078 Å). To accommodate an octahedral coordination geometry at each nickel atom the pyridazine cores of the two ligand molecules adopt a large torsional twist (Figure 4.19),

with Ni-N-N-Ni torsion angles of 74.9° and 72.5°, respectively. A survey of the Cambridge Structural Database (CSD) reveals that it is not unusual for pyridazine-based ligands to display some twisting when bridging two metal atoms. The CSD contains 122 entries with the structural motif shown in Figure 4.19, but only thirteen of these[61, 231] contain dimetallic pyridazine fragments with torsion angles greater than 20°. None of these have the level of distortion found in **4.34**. The majority of the torsion angles for the metal-pyridazine-metal fragments lie in the range 0-15°, with an average torsion angle for the reported structures of only 9.66°.

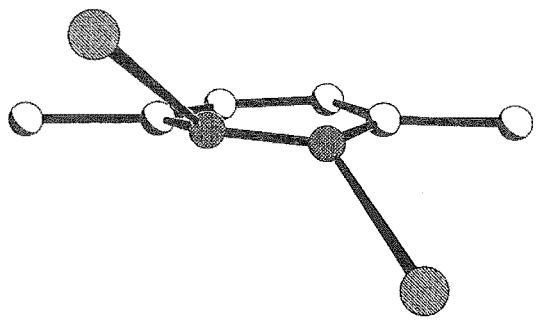

**Figure 4.19.** A view of the extensive twisting about the pyridazine core of **4.34**.

The large torsion angle also lengthens the distance between the metal centres. The metal-metal distances in complexes bridged by pyridazine usually range from 2.57 Å - 3.68 Å,[2, 210] whereas in **4.34** the distance is 4.214(2) Å. This is similar to helicates that have a meridional arrangement of the donor groups, for example the Cd-Cd distance in a sexipyridine-based helicate, reported by Constable and co-workers (4.173 Å).[232] It is a shorter distance than those found for helicates of bulky sexipyridine derivatives, again with meridional coordination, which range from 4.71 Å to 4.89 Å.[233] A septipyridine stranded helicate has a shorter 4.333 Å Zn-Zn distance.[234] The metal-metal distance in the helicate is still shorter than complexes bridged by pyrimidine and those described in this thesis.

Another interesting feature of the complex is that the pyridine rings adjacent to the pyridazine core of the ligand are twisted toward each other. This may be an artefact of the packing, but suggests the possibility that the pyridine rings may be weakly interacting through their $\pi$ systems. The interaction is significantly weaker than typical $\pi$-$\pi$ stacking interactions with C-C distances ranging from 3.666(8) at the closest point to 4.216(8) Å. No unusually short intermolecular interactions dominate the packing of the helicates in the crystal.

Crystal Structure of **4.35**

As discussed above, reaction of **4.7** with copper tetrafluoroborate gave a subtly different dinuclear helicate, as shown by single crystal X-ray crystallography (Figure 4.20). In this

complex, which maintains the same overall structure as **4.34**, only one nitrogen atom from the pyridazine ring of each ligand coordinates. Complex **4.35** crystallises in the centrosymmetric space group $P2_1/c$, with one discrete helicate, four tetrafluoroborate anions and one and a half solvate water molecules in the asymmetric unit. As noted it is isomorphous with the previously reported copper perchlorate structure reported by Manzur et al.[210] A perspective view is shown in Figure 4.19 with anions and solvate molecules omitted for clarity.

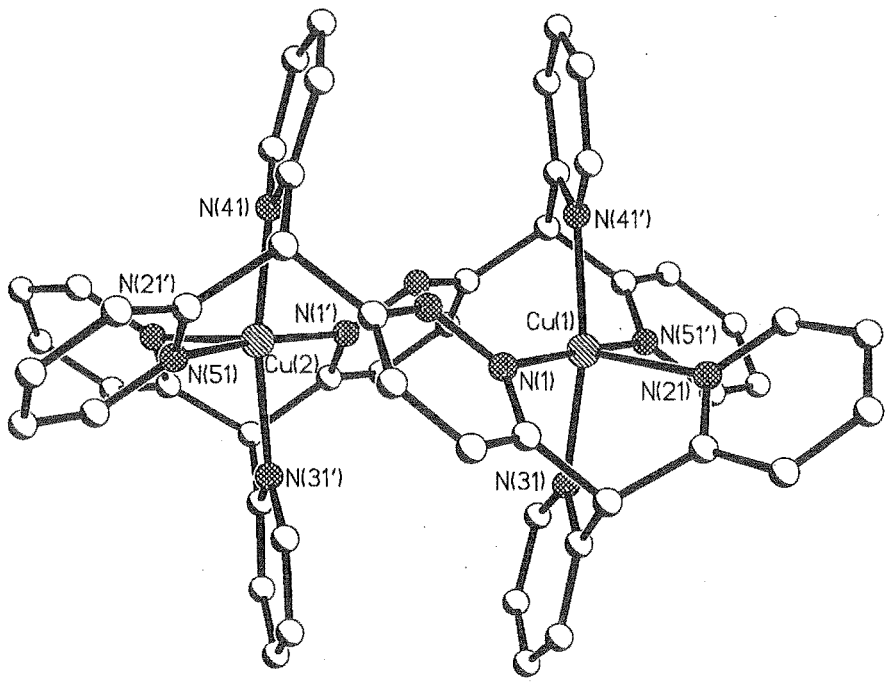


**Figure 4.20.** A view of the saturated homostranded homotopic dinuclear helicate, **4.35**. Selected bond lengths (Å): Cu(1)-N(41') 2.004(5), Cu(1)-N(51') 2.017(5), Cu(1)-N(31) 2.027(5), Cu(1)-N(1) 2.041(5), Cu(1)-N(21) 2.178(5), Cu(2)-N(41) 1.992(4), Cu(2)-N(51) 2.010(5), Cu(2)-N(1') 2.035(4), Cu(2)-N(31') 2.039(5), Cu(2)-N(21') 2.179(5).

The copper atoms lie in a distorted square-pyramidal environment ($\tau$ values of 0.08 and 0.09) with tripodal coordination by one ligand and bidentate coordination by the other ligand molecule. In **4.35** the Cu-N distances are 1.992(4)-2.041(5) Å for the equatorial bonds, while the axial Cu-N distances are slightly longer at 2.178(5) Å and 2.179(5) Å. The relaxation in the twisting of the ligand results in a significant lengthening of the metal-metal distance to 4.801 Å.

The subtle differences between the two helicates **4.34** and **4.35** suggest an extremely delicate balance exists between coordination requirements of the metal atoms and the torsional strain in the ligand. In **4.35** the ligand adopts a more relaxed arrangement by releasing its attachment to one of the metal centres, resulting in non-bonded distances of 3.016 Å and 3.023 Å. As a

consequence, the coordinated metal atom lies closer to the plane of the pyridazine ring to which it is coordinated and the metal-metal distance is increased relative to that in **4.34**.

The two helicates described here with the robust helical motif are novel examples of a class of helicate that appears to have been previously overlooked in the literature.[37, 38, 235] These helicates are saturated homostranded homotopic dinuclear helicates with tridentate-tridentate binding domains, but with a tripodal arrangement of the donor atoms at each octahedral metal centre (Figure 4.21(b)). All previously reported examples of helicates with tridentate-tridentate binding domains have meridional coordination of the octahedral metal centres [Figure 4.21(a)].[37, 38]

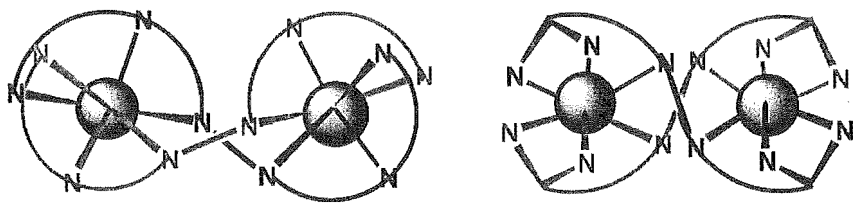


(a) (b)

**Figure 4.21.** Saturated homostranded homotopic dinuclear helicates with (a) meridional and (b) tripodal tridentate coordination at each metal centre.

The helicate structural motif encountered here appears to be a very robust structure. It is possible that this is the structure of the iron complex, **4.36**. To probe this coordination motif further, the related phthalazine-based ligand was investigated, as described below.

### 4.3.6 Complexes of 1,4-bis(di-2-pyridylmethyl)phthalazine, 4.9

Ligand, **4.9**, only differs from the previous ligand by a benzene ring distal from the donor atoms. Thus, the coordination chemistry observed with the previously described ligand should be encountered here. While some of the coordination chemistry of **4.9** has been investigated by the group who first prepared the ligand,[60, 61, 213, 214] the dinuclear helicate structure has not been observed. Previous interest in this ligand lies in its ability to bridge two metal atoms with a coordination motif that mimics the dinuclear catalytic site of some hydrolytic metalloenzymes. Thus, various dinuclear complexes have been prepared with manganese, iron, nickel, copper and zinc.

To further investigate and compare the coordination chemistry of the doubly tripodal ligand, **4.9**, it was reacted with nickel and copper tetrafluoroborate, hoping that these complexes might have structures similar to complexes **4.34** and **4.35**. Reaction, in the manner described for **4.7**, with nickel tetrafluoroborate gave a yellow-brown crystalline solid, **4.37**, in 49% yield that unfortunately did not analyse with the desired $M_2L_2$ composition. Instead, elemental analysis

suggested an $M_2L$ composition for this complex. Crystals were obtained directly from the reaction mixture allowing crystal structure analysis to be employed in determining the structure. With copper tetrafluoroborate a blue crystalline solid, **4.38**, was obtained by slow evaporation of the reaction solvent. This too had the $M_2L$ composition determined by elemental analysis.

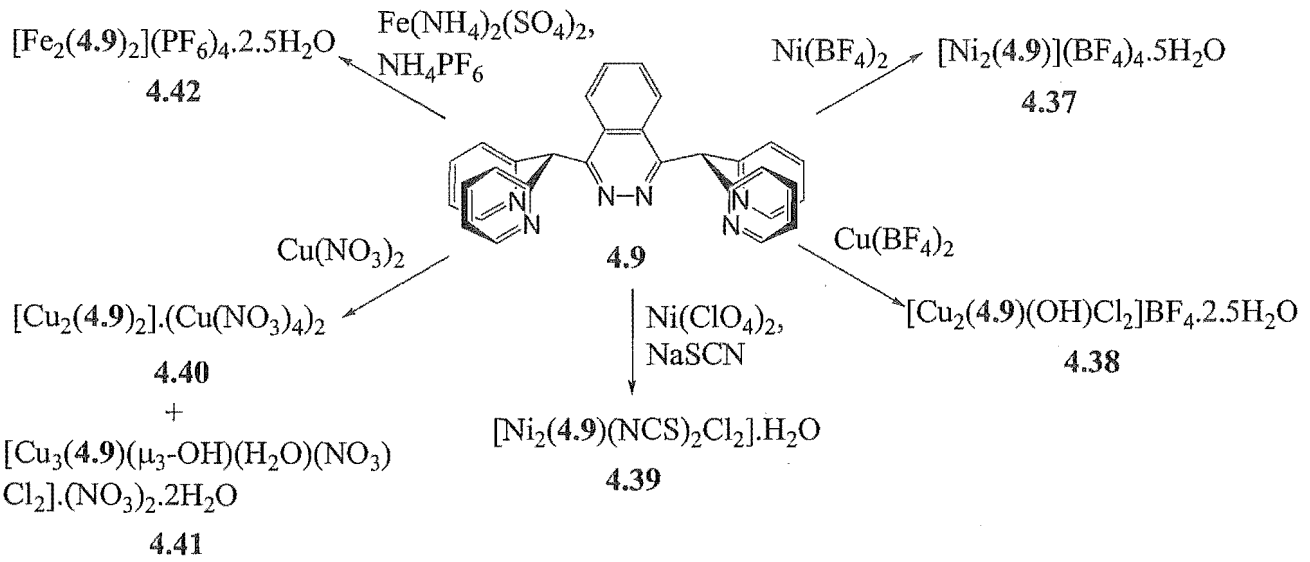


**Scheme 4.13**

As elemental analysis indicated, these two complexes, which were both studied by X-ray crystallography, were not the desired helicates. It also appeared from the composition of these complexes that the ligand was isolated during its synthesis as its hydrochloride salt, because chloride ions were observed in the crystal structure of **4.38**. The crystal structure of **4.37** could not be adequately refined to be included in this thesis, but has an $M_2L$ coordination motif that is very commonly observed for this ligand.[61, 213] Three nitrogen donors from **4.9** and three oxygen donors coordinate each octahedral nickel atom. A very closely related complex, with a similar donor set, is observed when **4.9** is reacted with nickel(II) tosylate in acetonitrile.[213]

Complex **4.39** was prepared by reaction of the ligand with nickel perchlorate and sodium thiocyanate and isolated in 71% yield. Elemental analysis was consistent with an $M_2L$ complex, $[Ni_2(\mathbf{4.9})(NCS)_2Cl_2].H_2O$, with the chloride ions originating from the ligand. This is likely to have a structure similar to the nickel thiocyanate complex of **4.7** with bridging and capping anions.

Two different complexes were obtained by reaction of copper nitrate with **4.9**. When the bulk sample was recrystallised by vapour diffusion of pentane into an acetonitrile solution, initially blue coloured crystals (**4.40**) and then green crystals (**4.41**) were obtained. The blue crystals were shown by elemental analysis to have a metal-ligand ratio of 2:1, but were surprisingly shown, by X-ray crystallography, to still be the desired helicate structure. Complex

**4.41** was shown to have the unusual $M_3L$ composition by elemental analysis and X-ray crystallography.

As tried previously for **4.7**, ligand **4.9** was reacted with $[Ru(DMSO)_4Cl_2]$ to attempt the preparation of a helical dinuclear ruthenium complex. Similar problems occurred in isolating and characterising this complex. Again an iron complex was prepared to avoid these problems, by reaction of ferrous ammonium sulfate with the ligand and then precipitation of the complex with an excess of ammonium hexafluorophosphate. Elemental analysis confirmed the desired composition of $[Fe_2(\mathbf{4.9})_2](PF_6)_4.2½H_2O$ for **4.42**, but $^1H$ NMR spectroscopy was inconclusive for the formation of the desired structure. Cyclic voltammetry revealed that the complex has one quasi-reversible oxidation wave at +0.91 V (Table 4.3) consistent with nearly simultaneous oxidation of the metal centres. This is considerably lower than the potential observed for complex **4.36** indicating that the phthalazine ligand is more easily able to stabilise the Fe(III) oxidation state. Again there are three absorptions in the visible region with maxima at 379, 427 and 504 nm. The lowest energy MLCT absorption occurs at a lower energy in **4.42** than for the pyridazine complex, **4.36**.

**Table 4.3.** The visible absorption maxima and redox potential for **4.42**.

| | $\lambda$ (nm)[a,b] | $\varepsilon$ ($Lmol^{-1}cm^{-1}$) | $E_{ox}$[c,d] |
|---|---|---|---|
| **4.42** | 379 | 7400 | +0.91(2e) |
| | 427 | 7600 | |
| | 504 | 7900 | |

[a] The MLCT band measured in $CH_3CN$ (± 2 nm)

[b] sh = shoulder.

[c] Potentials quoted in V *vs.* SCE in $CH_3CN$/0.1 $mol.L^{-1}$ $[(n\text{-}C_4H_9)_4]PF_6$ (the ferrocene/ferrocenium couple occurred at +310 mV *vs.* SCE).

[d] Uncertainty in $E_{1/2}$ values *ca.* ± 0.01 V.

Crystal Structure of **4.38**

Complex **4.38** crystallises in the monoclinic space group C2/c, with an asymmetric unit containing two discrete molecules of the complex, two tetrafluoroborate anions, five water solvate molecules and a disordered methanol solvate molecule. A perspective view of one molecule of the complex (Figure 4.22) shows the ligand acts as a ditopic tripodal bridge between the two copper atoms, which are also bridged by an hydroxide anion. The other sites of the five coordinate copper atoms are occupied by chloride anions that presumably originate from the hydrochloride salt of the ligand. The copper atoms have a slightly distorted square-pyramidal geometry ($\tau$ values between 0.02 and 0.15 for the four copper atoms in the asymmetric unit)

when the copper-copper interaction is not considered, with a pyridine ring occupying the apical position.

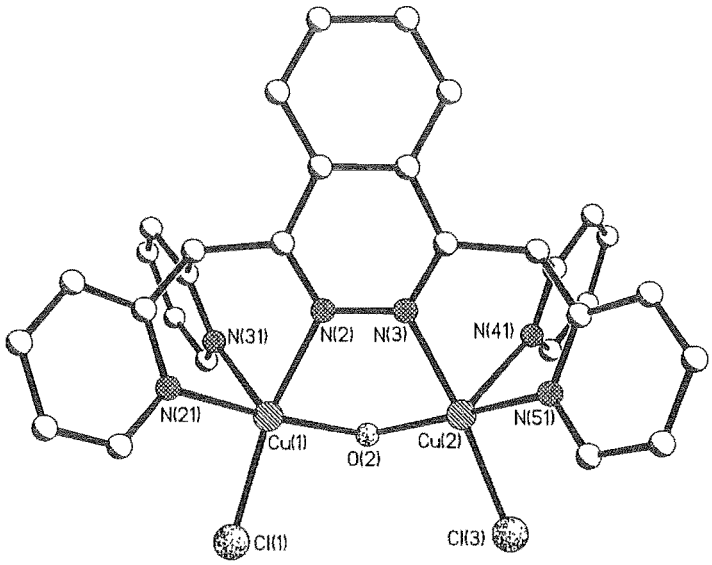


**Figure 4.22.** A perspective view of a molecule of complex **4.38** with hydrogen atoms, non-coordinated anions and solvate molecules omitted for clarity. Selected bond lengths (Å) and angles (°): Cu(1)-O(2) 1.905(3), Cu(1)-N(21) 2.012(3), Cu(1)-N(2) 2.077(4), Cu(1)-N(31) 2.231(4), Cu(1)-Cl(1) 2.265(3), Cu(2)-O(2) 1.881(3), Cu(2)-N(51) 1.981(4), Cu(2)-N(3) 2.052(4), Cu(2)-N(41) 2.285(4), Cu(2)-Cl(3) 2.306(3), Cu(2)-O(2)-Cu(1) 118.28(15).

The copper-copper distances in the two complexes within the asymmetric unit are identical (3.250(2) and 3.251(2) Å). This is typical of the metal-metal distances in related complexes involving pyridazine and phthalazine ligands.[61, 210, 213] The coordination motif observed here has previously been encountered for this ligand in a copper complex reported by Barrios and Lippard, which was prepared from copper tosylate.[61]

Crystal Structure of **4.40**

Having not observed the desired dinuclear helicate with either nickel or copper tetrafluoroborate, it was pleasing to observe that this motif was present in the structure of complex **4.40**. The elemental analysis of a metal-ligand stoichiometry of 2:1 was confirmed by crystallography and explained by the presence of novel tetranitrocuprate anions. A perspective view of the complex is shown in Figure 4.23 with anions, solvate molecules and hydrogen atoms omitted for clarity. The complex crystallises in the monoclinic space group $P2_1/c$, with an asymmetric unit containing one molecule of the helicate, four acetonitrile anions and two tetranitrocuprate anions.

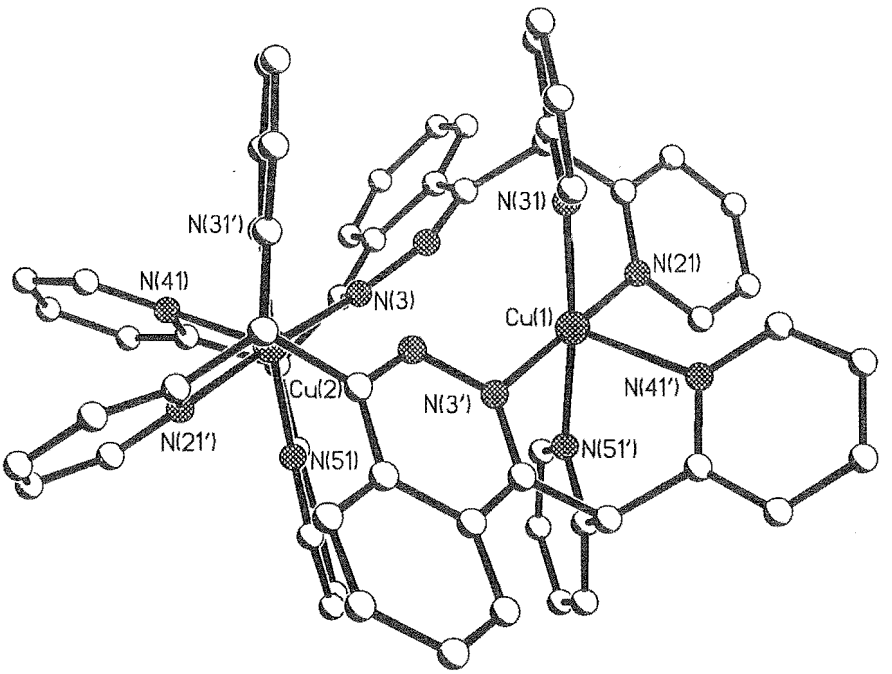


**Figure 4.23.** A perspective view of **4.40** with anions, solvate molecules and hydrogen atoms omitted for clarity. Selected bond lengths (Å): Cu(1)-N(21) 2.028(3), Cu(1)-N(31) 2.028(3), Cu(1)-N(51') 2.031(3), Cu(1)-N(3') 2.036(3), Cu(1)-N(41') 2.243(4), Cu(2)-N(51) 2.015(3), Cu(2)-N(31') 2.022(3), Cu(2)-N(21') 2.026(3), Cu(2)-N(3) 2.042(3), Cu(2)-N(41) 2.255(3).

The copper atoms lie in a square-pyramidal environment ($\tau$ values of 0.07 and 0.00) with tripodal coordination by one ligand and bidentate coordination by the other molecule of **4.9** as was observed for the previous copper helicate, **4.35**. The Cu-N distances are 2.015(3)-2.042(3) Å for the equatorial bonds, while the axial Cu-N distances are longer at 2.243(4) Å and 2.255(3) Å. These are slightly longer than the corresponding distances in the previous dinuclear copper helicate. The metal-metal distance in this complex is intermediate between the two previously characterised helicates at 4.506(1) Å. The preference copper has for a five coordinate geometry means the phthalazine ring is not twisted to bridge the two metal centres as in the dinuclear nickel helicate.

As an aside, the tetranitrocuprate anions observed in this structure have not been reported before. The copper atoms of the anions have a square planar geometry with monodentate coordination by four nitrate anions with Cu-O distances ranging from 1.982(3) to 2.022(3) Å (Figure 4.24). The nitrate anions also make weaker contacts to the copper through a second oxygen atom (*ca.* 2.59 Å).

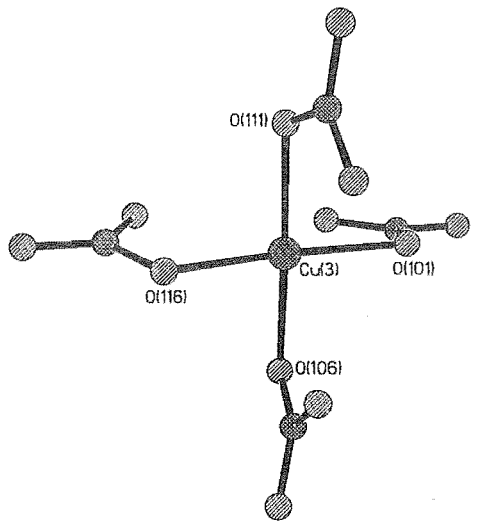


**Figure 4.24.** A perspective view of a tetranitrocuprate anions in the helicate complex, **4.40**.

Crystal Structure of **4.41**

The green crystals of complex **4.41** were also suitable for X-ray crystallography and crystallise in the orthorhombic space group Pnma. The asymmetric unit comprises half the ligand, one and a half copper atoms (one on a mirror plane), three half nitrate anions (all on the mirror plane), a $\mu_2$-chloride anion, a $\mu_3$-bridging hydroxide anion (also located on the mirror plane), a coordinated water molecule (on the mirror plane) and one acetonitrile and one water solvate molecule. A perspective view of the structure is shown in Figure 4.25 with hydrogen atoms, non-coordinated anions and solvate molecules omitted for clarity.

The ligand adopts the expected coordination mode by bridging two copper atoms. However, the complex is very different to other complexes of **4.9** discussed in this report and in the literature[60, 61, 213, 214] because of bridging through the $\mu_2$-chloride anions and the $\mu_3$-hydroxide anion to a third copper atom. This copper atom [Cu(2)] has a very unusual donor set with a chelating nitrate anion, two $\mu_2$-chloride anions, a $\mu_3$-hydroxide anion and a water molecule forming a highly distorted octahedral coordination geometry. The copper atom [Cu(1)] in the binding sites normally provided by the ligand has a square-pyramidal geometry and the two symmetry-related copper atoms [Cu(1)] are bridged by one molecule of **4.9** and a $\mu_3$-hydroxide anion. The water solvate molecule, which is not shown in the figure, is weakly bound to these two copper atoms (Cu-O distance 2.466(3) Å). Thus, the geometry could alternatively be described as pseudo-octahedral.

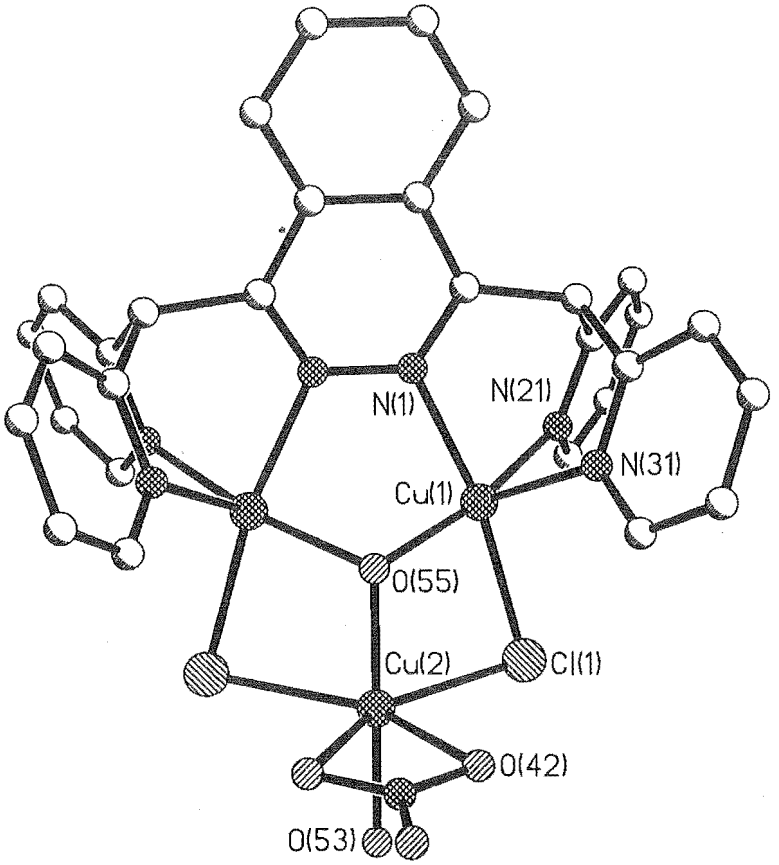


**Figure 4.25.** A perspective view of the unusual trimetallic copper complex, **4.41**. Selected bond lengths (Å): Cu(1)-O(55) 1.978(2), Cu(1)-N(21) 1.978(3), Cu(1)-N(1) 2.062(2), Cu(1)-N(31) 2.228(3), Cu(1)-Cl(1) 2.3407(9), Cu(1)-O(51) 2.466(3), Cu(2)-O(55) 1.924(3), Cu(2)-O(53) 1.942(3), Cu(2)-O(42) 2.309(2), Cu(2)-Cl(1) 2.4477(10).

The $\mu_3$-hydroxide anion oxygen atom has tetrahedral geometry with Cu-O bond lengths of 1.978(2) [Cu(1)] and 1.924(3) [Cu(2)]. Cu(1) and Cu(2) are bridged by a $\mu_2$-chloride anion with Cu-Cl bond lengths of 2.3407(9) and 2.4477(10) to Cu(1) and Cu(2), respectively. The Cu-Cu distance between the symmetry-related Cu(1) atoms is 3.127(1) Å and the Cu(1)-Cu(2) distance is 3.141(1) Å.

The trinuclear copper coordination motif with a $\mu_3$-hydroxide anion is not an uncommon motif with many higher nuclearity clusters having the same connectivity within a larger structure. However, there are no examples of discrete trinuclear copper centres with the donor atoms described here and only one example in the Cambridge Structural Database where copper atoms in such clusters are also connected by a heterocyclic bridging ligand.[236]

### 4.3.7 Complexes of 1,4-bis[6-(di-2-pyridylamino)-4-pyrimidyloxy]benzene, 4.14

The solubility of **4.14** was a major problem in forming complexes of this ligand. Reaction with various transition metal precursors invariably led to precipitation of the ligand. This was overcome to some extent, in certain cases, by adding dichloromethane to the reaction mixtures. When copper tetrafluoroborate was reacted with **4.14**, a blue powder precipitated from the reaction mixture almost immediately. It was induced to crystallise by addition of dichloromethane to the reaction mixture to give **4.43** in 63% yield. By elemental analysis **4.43** was characterised as $[Cu_2(\mathbf{4.14})_2(CH_3OH)_2](BF_4)_4$, a composition confirmed by X-ray crystallography. A similar complex, **4.44**, was prepared by reaction of **4.14** with nickel tetrafluoroborate in methanol and isolated as a pale blue crystalline solid in 27% yield. Elemental analysis characterised **4.44** with a 1:1 metal-ligand stoichiometry and on the basis of complex **4.43**, it is likely to be a [2+2] dimer with the composition $[Ni_2(\mathbf{4.14})_2(H_2O)_4](BF_4)_4.2H_2O$.

Crystal Structure of 4.43

Complex **4.43** is a large [2+2] dimeric structure formed from two molecules of the extended-reach ligand, **4.14**, and two copper atoms. The complex crystallises in the space group P-1, with one molecule of **4.14**, one copper atom, one coordinated methanol molecule, four non-coordinated dichloromethane solvate molecules, one tetrafluoroborate anion and half a hexafluorosilicate anion in the asymmetric unit. A perspective view of the complex is shown in Figure 4.26 with hydrogen atoms and non-coordinated molecules omitted for clarity.

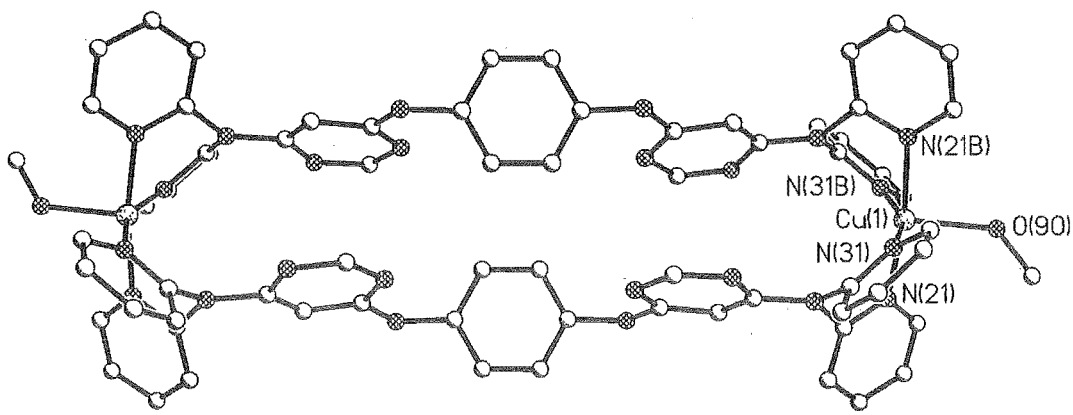


**Figure 4.26.** A perspective view of the [2+2] dimer, **4.43**, with hydrogen atoms, non-coordinated solvate molecules and anions omitted for clarity. Selected bond lengths (Å) and angles (°): Cu(1)-N(21) 2.010(3), Cu(1)-N(21'A) 2.029(3), Cu(1)-N(31) 2.032(3),

Cu(1)-N(31'A) 2.041(3), Cu(1)-O(90) 2.134(3), N(21)-Cu(1)-N(21'A) 170.64(12), N(21)-Cu(1)-N(31) 87.18(13), N(21'A)-Cu(1)-N(31) 90.75(12), N(21)-Cu(1)-N(31'A) 93.26(13), N(21'A)-Cu(1)-N(31'A) 84.99(12), N(31)-Cu(1)-N(31'A) 156.29(12), N(21)-Cu(1)-O(90) 96.45(12), N(21'A)-Cu(1)-O(90) 92.80(12), N(31)-Cu(1)-O(90) 94.32(12), N(31'A)-Cu(1)-O(90) 109.16(12).

The copper atoms have a distorted square-pyramidal coordination geometry ($\tau$ value of 0.24) with the oxygen atom of the methanol solvate in the apical position (2.134(3) Å). Only the pyridine nitrogen atoms participate in coordination of the copper atom and all coordinate in the basal positions with bond lengths that range from 2.010(3) to 2.041(3) Å. Like other structures with a planar tertiary amine-nitrogen atom there is no coordination by the pyrimidine nitrogen donors. There is a weak $\pi$-$\pi$ interaction (3.625(6) Å), like other complexes of the nitrogen linked ligands, between the two sets of non-coordinated pyrimidine rings. In this complex, which incorporates an extended-reach ligand, the Cu-Cu distance is 18.101(1) Å, and considerably longer than previous structures described in this chapter. The structure also has an unusually large 38-membered metallomacrocyclic ring.

## 4.4. Comparison of the structures

An interesting feature of the nitrogen- and carbon-linked ligands described in this chapter is the geometry of the linker atom (X) in complexes of these ligands. A comparison of the geometry and bond distances of the linker atoms in selected complexes described in this chapter, and in complexes of related tripodal ligands from the CSD, highlighted a trend in the preferred geometry and coordination modes of the ligands (Table 4.4).

Typically, the geometry of the carbon-linker atom was closest to tetrahedral, indicating a preference for tripodal coordination by these ligands. The bond lengths and angles for the carbon linker atom in complexes investigated in this chapter are very similar to the corresponding values for complexes of **4.3**. Previously reported complexes of ligands **4.7** and **4.9** have similar tetrahedral geometries for the carbon-linker atom, as do complexes of **4.4**, which has a nitrogen linker atom. In contrast, the ligands other than **4.4** investigated in this chapter, with a bridgehead nitrogen atom, did not have angles close to either a tetrahedral geometry, or to complexes of **4.4**. This planarisation of the nitrogen atom effectively prevents ligands with a nitrogen-linker atom from coordinating tripodally to a metal centre. This may result from the delocalisation of the nitrogen lone pair by the diazine ring forcing a planar arrangement of bonding about the bridgehead nitrogen atom, but is interesting because a similar effect is not observed for **4.4**. This $sp^2$-like nitrogen atom was also observed in complexes of the ligands described in Chapter 3.

**Table 4.4.** The geometry around the linker atom (X) for selected complexes of the tripodal ligands reported in this chapter and for complexes of **4.3**, **4.4**, **4.7** and **4.9**.

| Ligand | Complex | Linker atom (X) | average azine-X bond length (Å) | average bond angle (°) |
|---|---|---|---|---|
| **4.3**[a] | | C | 1.510 | 111.3 |
| **4.7**[a] | | C | 1.517 | 111.3 |
| **4.9**[a] | | C | 1.523 | 110.9 |
| **4.5** | **4.21** | C14 | 1.527 | 110.5 |
| | | C16 | 1.523 | 110.8 |
| **4.7** | **4.34** | C13 | 1.510 | 110.8 |
| | | C13' | 1.496 | 110.9 |
| | **4.35** | C13 | 1.522 | 111.6 |
| | | C13' | 1.517 | 111.8 |
| | | C16 | 1.512 | 111.5 |
| | | C16' | 1.512 | 111.7 |
| **4.9** | **4.38** | C11 | 1.521 | 111.5 |
| | | C11' | 1.518 | 111.0 |
| | | C14 | 1.520 | 111.3 |
| | | C14' | 1.512 | 111.4 |
| | **4.40** | C11 | 1.525 | 111.2 |
| | | C11' | 1.526 | 111.7 |
| | | C14 | 1.530 | 111.4 |
| | | C14' | 1.522 | 111.5 |
| | **4.41** | C2' | 1.530 | 111.0 |
| **4.4**[a] | | N | 1.418 | 112.3 |
| **4.6** | **4.23** | N14 | 1.414 | 120.0 |
| | **4.27** | N14 | 1.427 | 118.9 |
| | | N16 | 1.416 | 120.0 |
| | **4.28** | N4 | 1.419 | 119.9 |
| | | N6 | 1.421 | 118.9 |
| **4.16** | **4.30** | N6 | 1.421 | 120.0 |
| | | N9 | 1.415 | 119.9 |
| **4.14** | **4.43** | N16 | 1.417 | 119.7 |
| | | N16' | 1.420 | 119.5 |

[a] The values reported are from a CSD search on complexes of each of these ligands where the ligand coordinates tripodally and are an average of all structures.

## 4.5. Summary

The interest in preparing stereochemically defined octahedral metal complexes is an area that continues to receive attention from a number of groups in the chemical community. The bridging doubly tripodal ligands investigated in this chapter offer another avenue to address the stereochemical problem. This chapter has described the synthesis of three new bridging doubly tripodal ligands by reaction of both di-2-pyridylmethane and di-2-pyridylamine with a

pyrimidine core. An investigation of the coordination chemistry of these ligands was complemented by studies of two known ligands, which have the same donor set and three-dimensional arrangement of the donor atoms.

From these studies, several conclusions can be drawn about the coordination properties of these ligands with predominantly octahedral metal atoms. Of particular interest was the well-defined set of structures that were obtained with these ligands. With octahedral metal atoms two common structures were observed; either discrete $M_2L$ complexes or [2+2] metal-ligand dimers. The ligands with a carbon linker atom formed either of these structures with octahedral metal atoms. Several $M_2L$ complexes had previously been characterised before for the bridging tripodal ligands, **4.7** and **4.9**, but only two reports existed of [2+2] metal-ligand dimers of ligand **4.7**. The helical [2+2] metal-ligand dimers of **4.7** and **4.9** described in this chapter, are examples of a new class of helicate.

No bridging doubly tripodal ligands with nitrogen linker atoms had previously been described and these were found to predominantly form [2+2] metal-ligand dimers with octahedral metal atoms. The lack of discrete $M_2L$ complexes, with doubly tridentate tripodal coordination, formed with the di-2-pyridylamine-based ligands was reflective of the geometry of the nitrogen linker atoms, which are almost exclusively planar in the complexes described in this thesis.

# *Chapter 5*

# *Conclusions and future prospects*

# Chapter 5

## 5. Conclusions and future prospects

This thesis has described the preparations of a number of new multidentate bridging heterocyclic ligands incorporating di-2-pyridylmethane, **2.1**, and di-2-pyridylamine, **3.1**, as chelating subunits, as well as related ligands with 3-pyridyl and 4-pyridyl donor groups. The coordination and metallosupramolecular chemistry of these ligands has been investigated with a wide range of late transition metal atoms. This allowed metal-ligand bonding to be used in tandem with a range of supramolecular interactions to explore the formation of complexes with novel architectures and properties. The nature of the metal-ligand and metal-metal interactions of two sets of mononuclear and dinuclear bis(2,2'-bipyridyl)ruthenium complexes, prepared by directed syntheses, were probed by cyclic voltammetry and visible absorption spectroscopy. NMR spectroscopy and X-ray crystallography were valuable tools in characterising the complexes obtained in this thesis.

Several different types of bridging heterocyclic ligand, the majority incorporating a di-2-pyridyl chelating motif were prepared, and represent a significant addition to the array of ligands available in coordination and metallosupramolecular chemistry. In Chapter 2, a number of ligands derived from the isomeric dipyridylmethanes were prepared, which included two previously unused and fascinating cores. The [3]radialene-based ligands (**2.14** - **2.18**) represent the first examples of heterocyclic [3]radialenes, while a novel spirolene ligand, **2.13**, was also synthesised. These cores have allowed the synthesis of bridging ligands with unusual three-dimensional structures and bridging modes. In Chapter 3, two different series of ligands were prepared from di-2-pyridylamine. Multi-substituted arene-based ligands have been well studied, but the ligands prepared in Chapter 3 belong to the less common class that is capable of chelating to a number of metal atoms. The tripodal ligands described in Chapter 4 present another possible solution to the stereochemical problem, because they can form achiral dinuclear complexes with octahedral metal atoms, if a suitable ancillary ligand is provided.

The doubly bidentate ligands, in particular **2.2** and **2.4**, readily formed dinuclear complexes with copper, palladium and zinc. Disappointingly, this behaviour was not followed in the syntheses of the ruthenium complexes, as **2.2** and **2.4** proved to be surprisingly resistant to forming dinuclear bis(2,2'-bipyridyl)ruthenium complexes. Nevertheless, their mononuclear

complexes may allow for the synthesis of some mixed metal coordination complexes involving either palladium or platinum.

Another doubly bidentate ligand, **2.13**, described in Chapter 2, did not provide any coordination complexes for characterisation. Ligand **2.13**, and its ethane and ethylene analogues, **2.11** and **2.12**, were prepared from 4,5-diazafluorene, which has a wider bite angle than di-2-pyridylmethane and, thus, may discourage the formation of transition metal complexes with these ligands. One approach to overcoming this may be to examine the coordination chemistry with larger lanthanide salts.

The three isomeric hexapyridyl[3]radialenes and two 2-benzylpyridine analogues, **4.17/4.18**, display a number of different coordination modes and have the potential to lead to other interesting discoveries. Hexa(2-pyridyl)[3]radialene, **2.14**, has the chelating motif, typical of ligands in this thesis, but prefers to bind multiple metal atoms with monodentate coordination. This led to two cage like structures, one incorporated into a coordination polymer and a second discrete structure, which encapsulated a fluoride anion that is likely to be responsible for templating the structure. The discrete hexanuclear silver cage was the first reported example of an $M_6L_2$ prismate. The difficulties encountered in forming complexes of these [3]radialene ligands with transition metals other than silver was a concern, but continued attempts should yield fruitful results. To this end, the 3-pyridyl and 4-pyridyl derivatives proved to be more resistant to decomposition.

The synthesis of a dinuclear bis(2,2'-bipyridyl)ruthenium complex of ligand **2.14** produced some interesting results that served to emphasise a structural problem with ligands forming a six-membered chelate ring. The cyclic voltammetry studies of the two diastereoisomeric complexes, **2.57** and **2.58**, showed no interaction between the metal centres and no significant electrochemical differences between the two diastereoisomers. This can be understood in terms of the conformation of the complex and, in particular, of the six-membered chelate ring. In complexes where a di-2-pyridyl unit chelates to a metal atom, the six-membered chelate ring adopts either a boat or half-chair conformation, which means the metal centre is held out of the plane of the ligand $\pi$-system. This minimises any potential metal-metal interactions within these complexes.

The first series of ligands investigated in Chapter 3 extended upon some recent literature work by providing some analogues of these doubly bidentate ligands, but with non-linear connectivity through the aromatic core. The second series of ligands introduced some flexibility into the ligand core. The coordination and metallosupramolecular chemistry of these ligands revealed a number of different architectures including dinuclear complexes, [2+2]

metallomacrocycles and one-dimensional coordination polymers. With the various silver precursors used an interesting observation was noted. The silver atoms were generally two-, three- and sometimes four-coordinate when only the dative coordinate bonds were considered, but were often supplemented by weaker silver-arene π-interactions. These secondary interactions were similar to, and in some instances slightly longer than, the silver-carbon distances in other reported examples of silver-arene π-interactions. Despite being energetically weak, these interactions appeared to work in tandem with the coordinate bonds in determining the three-dimensional structures of such complexes.

The ligands described in Chapter 3 were readily able to chelate though the di-2-pyridylamine units if the correct transition metal atoms were used. Several such complexes were described with copper and with ruthenium, and with the latter the bis(di-2-pyridylamino)arene ligands readily formed mononuclear and dinuclear complexes. The dinuclear bis(2,2'-bipyridyl)ruthenium complexes of ligands **3.2** and **3.7** showed only weak metal-metal interactions.

An unexpected chelating binding mode was encountered with one of these di-2-pyridylamine-based ligands, 1,3,5-tris(di-2-pyridylamino)benzene (**3.9**). This ligand was expected, and had been shown in the literature, to coordinate to three metals though the chelating di-2-pyridylamine units. Instead, **3.9** was triply cyclopalladated and induced to bond with an N,C,N pincer coordination motif. Presumably the three amine nitrogen atoms strongly activate the ligand toward electrophilic aromatic substitution.

The more flexible tris- and tetrakis(di-2-pyridylaminomethyl)benzene ligands may present interesting possibilities for the synthesis of cage-type complexes, with the potential to encapsulate small templating molecules or anions. This would require the use of octahedral metal atoms that can accommodate chelation by more than one ligand. A further development of such ligands would be the preparation of the 4-pyridyl derivatives (Figure 5.1) from

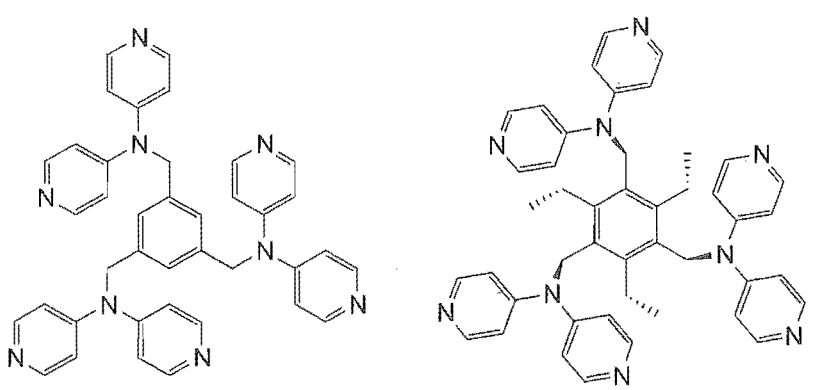

**Figure 5.1.** Some ligands suitable for the controlled assembly of three-dimensional cages.

di-4-pyridylamine, which is commercially available. These new ligands should be ideally suited to the formation of novel three-dimensional cages.

The tripodal ligands described in this thesis were more difficult to prepare than initially expected. Nonetheless, access to a series of ligands based around the two diazines, pyridazine and pyrimidine, with carbon and nitrogen linker atoms, was achieved. A pyrazine-based analogue, **4.11**, could not be prepared, but the synthetic procedure leads instead to an interesting heterocyclic ring system, which has a structure closely related to a potential anti-cancer drug. This emphasises the myriad of potential uses for planar aromatic nitrogen-containing heterocycles.

The coordination chemistry of the five doubly tripodal ligands demonstrated a distinct preference for two metal-ligand compositions, $M_2L$ and $M_2L_2$. Several $M_2L$ complexes were prepared with the carbon linker atom, which had the desired tripodal coordination of two metal centres. In contrast, the nitrogen-linked ligand, **4.6**, would not form complexes with this coordination motif. This was a consequence of the planar $sp^2$ geometry of the nitrogen linker atom, which presented a geometric constraint that prevented the ligand from acting as a tripodal donor. With the $M_2L_2$ complexes two topologies where observed; [2+2] side-by-side dimers and [2+2] helicates. Again these differences could be partially attributed to the different geometries of the linker atoms, but they were also a consequence of the different pyridazine, phthalazine and pyrimidine cores.

The helicates described in Chapter 4 represent a previously overlooked class of helicate, which for ligands **4.7** and **4.9** appears to be a robust motif. An interesting development would be the synthesis of some related ligands that would allow polymers of this helicate motif to be prepared. One such ligand is shown in Figure 5.2, which could be prepared in a three step synthesis.

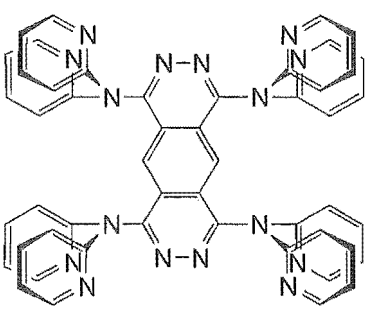

**Figure 5.2.** A multidentate ligand capable of forming a polymer of helicates.

In summary, this thesis has described the synthesis of twenty four new bridging heterocyclic ligands where, in most cases, the pyridine donors are held in defined two-dimensional

geometries, but which still allow some degree of conformational freedom. This has allowed metal atoms to be coordinated by the chelating di-2-pyridyl units with predictable metal-metal distances. An investigation of the coordination chemistry of these bridging ligands revealed that the majority of the doubly bidentate bridging ligands coordinated to two metal atoms in the expected manner. The chelating binding motif was less dependable as further chelating units were added, or more flexibility was introduced into the ligand backbone, but also significantly dependent on the metal atom employed.

The coordination and metallosupramolecular chemistry presented in this thesis has established the coordination properties of these ligands, which will allow for their use in the assembly of larger aggregates with defined structures and properties. As such, it is hoped that other workers in this area will subsequently employ some of these ligands. One foreseeable problem with the use of such ligands is being able to rely upon the conformation of such ligands. The use of metal atoms with more defined geometries and donor sites offers one way of controlling this inherent flexibility.

# *Chapter 6*

# *Experimental*

# Chapter 6

## 6. Experimental

### 6.1. General Experimental

Melting points were recorded on an Electrothermal melting point apparatus and are uncorrected. UV-visible absorption spectra were recorded on a GBC 920 UV-Visible, or Cary 5E UV/Vis/NIR spectrometer, in solutions as described. The UV-visible absorption spectra of all ruthenium complexes were measured in acetonitrile for *ca.* 0.05 - 0.1 mmol solutions. Infrared spectra were measured on a Shimadzu FTIR-8201PC spectrophotometer. The Campbell microanalytical laboratory at the University of Otago performed elemental analyses. Mass spectra (EI and FAB) were recorded using a Kratos MS80RFA mass spectrometer. Electrospray (ES) mass spectra were recorded using a Micromass LCT-TOF mass spectrometer.

NMR spectra were recorded on Varian 300 MHz and Varian 500 MHz spectrometers at 23°C, using a 3 mm probe. $^1$H NMR spectra recorded in $CDCl_3$ were referenced relative to the internal standard $Me_4Si$. $^1$H NMR spectra recorded in other solvents were referenced to the solvent peak: acetonitrile, 2.0 ppm; methanol, 3.3 ppm; DMSO, 2.6 ppm; acetone, 2.17 ppm. $^{13}$C NMR spectra were all referenced to their solvent peaks: $CDCl_3$, 77.0 ppm; acetonitrile, 36.8 ppm; methanol, 49.3 ppm; DMSO, 39.6 ppm. When required, 1-D NOESY, 1-D TOCSY, 1-D ROESY, and 2-D COSY experiments were performed using standard pulse sequences. Unless otherwise stated, the values given for chemical shifts are to the centre of a multiplet. The $^1$H NMR assignments for the compounds are denoted with primes to indicate the different rings of the multidentate ligands and with letters to distinguish the bpy and dmb rings. The different diastereoisomers of the dinuclear complexes are marked with and without an asterisk.

Cyclic voltammetry measurements were performed on a PAR Model 175 Universal Programmer coupled to a PAR Model 173 potentiostat, under argon. The measurements kindly made by D. M. D'Alessandro were performed, under argon, using a Bioanalytical Systems BAS 100A Electrochemical Analyser. Measurements were recorded in either acetonitrile or dichloromethane/0.1 mol dm$^{-3}$ $[(n\text{-}C_4H_9)_4N]PF_6/BF_4$ solution using a glassy carbon working electrode, a platinum wire auxiliary electrode and an $Ag/AgNO_3$ or Ag/AgCl (0.1 mol dm$^{-3}$ $[(n\text{-}C_4H_9)_4N]PF_6/BF_4$ in acetonitrile or dichloromethane) reference electrode. Ferrocene was added as an internal standard on completion of each experiment and tabulated potentials are

given *vs* the saturated calomel electrode [$E°(Fc/Fc^+)$ = 310 mV *vs* SCE (acetonitrile)]. Cyclic voltammetry was performed with a sweep rate of 100 $mVs^{-1}$. Differential pulse voltammetry was recorded with a sweep rate of 4 $mVs^{-1}$ and a pulse amplitude, width, and period of 50 mV, 60 ms and 1 s, respectively.

Unless otherwise stated reagents were obtained from commercial sources and used as received. Solvents were dried by literature procedures and freshly distilled as required. The following compounds were prepared by literature procedures: 1,2-diphenyl-1,2-di(2-pyridyl)ethane, **2.5**,[71, 72] 4,5-diazafluorenone,[76, 92] 4,5-diazafluorene, **2.10**,[76] 9,9'-(bis-4,5-diazafluorenyl), **2.11**,[76] 9,9'-(bis-4,5-diazafluorenylidene), **2.12**,[77, 78] di-4-pyridylketone,[99] 1,4-bis(di-2-pyridylamino)benzene, **3.2**,[64] 4,4'-bis(di-2-pyridylamino)biphenyl, **3.3**,[64] 1,3- and 1,4-bis(bromomethyl)benzene,[180] 1,3,5-tris(bromomethyl)benzene,[180] 1,2,4,5- and 1,2,3,4-tetrakis(bromomethyl)benzene,[179] hexakis(bromomethyl)benzene,[178] 1,3,5-tris(di-2-pyridylamino)benzene, **3.9**,[139] tri-2-pyridylamine, **4.4**,[215] 1,4-bis(di-2-pyridylmethyl)phthalazine, **4.9**,[213] 1,5-naphthyridine,[221] 1,5-naphthyridine-di-N-oxide,[222] 2,6-dichloro-1,5-naphthyridine,[222] 4,4'-bipyridine-di-N-oxide,[224, 225] 2,2'-dichloro-4,4'-bipyridine,[224, 225] dibenzylideneacetone (dba),[237] tris(dibenzylideneacetone)dipalladium(0), $[Pd_2(dba)_3]$,[238] bis(2,2'-bipyridine)ruthenium(II) dichloride, $[Ru(bpy)_2Cl_2]$,[239] bis(2,2'-bipyridine)ruthenium(II) dichloride, $[Ru(dmb)_2Cl_2]$,[240] bis(2,2'-bipyridine)ruthenium(II) carbonate, $[Ru(bpy)_2CO_3]$,[241] bis(2,2'-bipyridine)ruthenium(II) bis(trifluoromethanesulfonate), $[Ru(bpy)_2(OTf)_2]$,[242] and tetrakis(dimethylsulfoxide)ruthenium(II) dichloride, $[Ru(DMSO)_4Cl_2]$.[243]

## 6.2. Preparation of Precursors and Ligands

### 6.2.1 Dipyridylmethane-based ligands

Di-2-pyridylmethane, 2.1

The method of Canty and Minchin[72] was used for the synthesis of di-2-pyridylmethane with some modifications. Potassium hydroxide pellets (1.63 g, 0.029 mol) were crushed and dissolved in ethylene glycol (50 mL). Di-2-pyridylketone (2.52 g, 0.014 mol) was added to this solution, a condenser was fitted and the solution cooled in an ice bath. Hydrazine hydrate (1.55 mL, 0.032 mol) was added dropwise down the condenser and the mixture was refluxed for 4 hours. After cooling to room temperature, water (50 mL) was added and the solution extracted with benzene (7 x 25 mL). The extracts were dried over magnesium sulphate, filtered and taken to dryness. Drying the resultant oil *in vacuo* gave **2.1** as a pale yellow oil. Yield 2.20 g (94%). $^{1}$H NMR ($CDCl_3$) δ 8.52 (d, 2H, H6), 7.59 (t, 2H, H4), 7.26 (d, 2H, H3), 7.12 (dd, 2H, H5), 4.34 (s, 2H, $CH_2$); $^{13}$C NMR ($CDCl_3$) δ 159.5, 149.5, 136.7, 123.7, 121.6, 47.4.

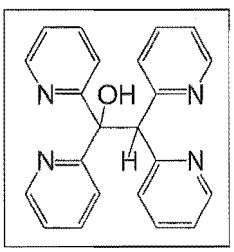


Storage of di-2-pyridylmethane led to the precipitation of a colourless solid within the oil over a period of weeks. By dissolving the oil in ether and collecting the insoluble solid, 1,1,2,2-tetra(2-pyridyl)ethanol, **2.3**, was isolated in various yields, depending on the length of time the sample was left. M.p. 161-164°C. Analysis: calc. for $C_{22}H_{18}N_4O.¾H_2O$ C 71.82, H 5.34, N 15.23; found C 71.84, H 5.08, N 15.23%. ES-MS: 185.1 $[(M+1)-170]^+$, 171.1 $[(M+1)-184]^+$. $^{1}$H NMR ($CDCl_3$) δ 8.45 (d, 2H, H6), 8.34 (d, 2H, H6), 8.24 (bs, 1H, OH), 7.79 (d, 2H, H3), 7.43 (m, 6H), 6.92 (m, 4H), 6.29 (s, 1H, CH). $^{13}$C NMR ($CDCl_3$) δ 163.6, 160.4, 148.0, 147.8, 136.0, 135.8, 125.3, 121.2, 121.1, 121.1, 82.47, 59.49.

1,1,2,2-Tetra(2-pyridyl)ethane, 2.2

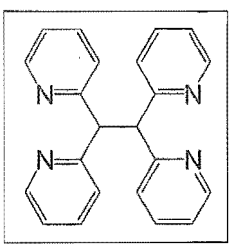


The general method of Canty and Minchin[72] was used for the synthesis of **2.2**, but was adapted as follows to give more consistent yields. To a solution of di-2-pyridylmethane (610 mg, 3.58 mmol) dissolved in THF (10 mL) under argon at -78°C, was added n-butyllithium (2.35 mL, 3.76 mmol). A dark red solution and then an orange solid formed over a period of 30 minutes. Iodine (459 mg, 1.81 mmol) dissolved in THF (20 mL) was added, the solution gradually warmed to room temperature and stirred under argon for 2 days. Water was added to quench the reaction and the solvents were removed *in vacuo*. The remaining solid residue was extracted with ethanol and

filtered, before the filtrate was concentrated to approximately 10 mL by heating and cooled to 0°C. The precipitated solid was collected, and the filtrate was further evaporated to provide more **2.2**. Yield 322 mg (53%). M.p. sublimes >230°C (lit. sublimes >230°C[72]). $^1$H NMR ($CDCl_3$) δ 8.43 (d, 4H, H6'), 7.42 (m, 8H, H3'/H4'), 6.90 (t, 4H, H5'), 5.74 (s, 2H, CH); (DMSO-$d_6$) δ 8.41 (d, 4H, H6'), 7.59 (m, 8H, H3'/H4'), 7.09 (t, 4H, H5'), 5.76 (s, 2H, CH). $^{13}$C NMR ($CDCl_3$) δ 161.1, 149.3, 136.2, 124.4, 121.4, 59.0.

Tetra(2-pyridyl)ethylene, **2.4**

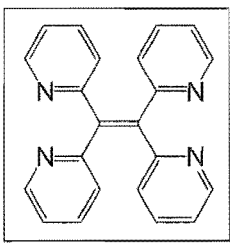

***Method A:*** Compound **2.2** (220 mg, 0.65 mmol) and DDQ (190 mg, 0.85 mmol) were dissolved in 30 mL of dry toluene and refluxed for three hours. The solution was cooled, then filtered, the residue washed with toluene (2 x 5 mL) and the washings combined with the filtrate. The toluene was removed *in vacuo* to give a solid residue. This was dissolved in chloroform (50 mL), washed with 1 M NaOH (50 mL) solution, water (50 mL) and then dried over sodium sulfate. The solvent was removed *in vacuo* and the residue purified on silica gel, eluting with 1:9 methanol-chloroform, to give recovered **2.2** (41 mg, 19%) and **2.4**. Yield 55 mg (25%). Di-2-pyridylketone is also formed in the reaction, but was not recovered.

***Method B:*** Compound **2.3** (160 mg, 0.45 mmol) was dissolved in pyridine (10 mL) and cooled to -10°C. Thionyl chloride (1 mL) was added slowly to give a yellow solution that went red, then brown, over the next three hours. Water was cautiously added to the reaction mixture to quench the remaining thionyl chloride, before it was made alkaline with potassium carbonate. Extraction with dichloromethane (3 x 50 mL) gave a pale brown extract that was dried over sodium sulfate and the solvent removed *in vacuo*. The resultant oily brown solid was triturated with ether and then recrystallised from ether to give **2.4** as an off-white solid. Yield 123 mg (81%).

M.p. 178-180°C (dec.). Analysis: calc. for $C_{22}H_{16}N_4.½H_2O$ C 76.50, H 4.96, N 16.22; found C 77.06, H 5.32, N 16.15%. HRMS: calc. for $C_{22}H_{16}N_4$ 336.1375; found 336.1348. $^1$H NMR ($CDCl_3$) δ 8.48 (d, 4H, H6'), 7.39 (t, 4H, H4'), 7.07 (d, 4H, H3'), 7.03 (dd, 4H, H5'). $^{13}$C NMR ($CDCl_3$) δ 159.8, 149.3, 144.1, 135.7, 126.4, 121.8.

Di-2-pyridylketone azine, **2.8**

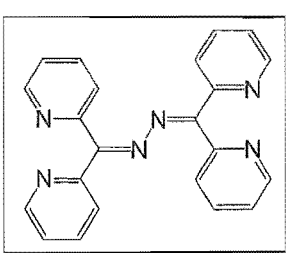

Di-2-pyridylketone (203 mg, 1.10 mmol), hydrazine hydrate (26 μL, 0.53 mmol) and acetic acid (3 drops) were refluxed overnight in methanol (4 mL). The methanol was removed *in vacuo* and the yellow solid, **2.8**, was collected, washed with several portions of ether and dried.

Yield 172 mg (89%). M.p. 176-179°C. Analysis: calc. for $C_{22}H_{16}N_6$ C 72.51, H 4.43, N 23.06; found C 72.51, H 4.45, N 23.00%. $^1$H NMR ($CDCl_3$) δ 8.70 (d, 2H, H6'), 8.55 (d, 2H, H6"), 7.87 (d, 2H, H3"), 7.78 (t, 2H, H4'), 7.70 (m, 4H, H4", H3'), 7.30 (dd, 2H, H5'), 7.27 (dd, 2H, H5"). $^{13}$C NMR ($CDCl_3$) δ 157.0, 155.0, 153.2, 149.1, 148.9, 136.4, 135.9, 125.6, 124.0, 123.6, 123.1.

Spiro[5,5]-2,4,8,10-tetraoxaundecane-3,3,9,9-tetra-2-pyridine, **2.9**

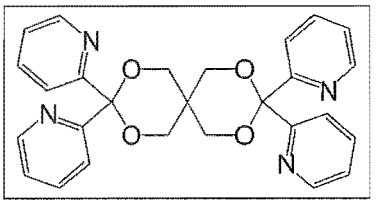

Di-2-pyridylketone (905 mg, 4.91 mmol), erthyritol (334 mg, 2.45 mmol) and sodium carbonate (5 g) were dissolved in methoxyethanol (50 mL) and refluxed in a flask fitted with a Dean-Stark apparatus (containing 4 Å molecular sieves). After 72 hours the solution was filtered, the solvent removed *in vacuo* and the residue extracted with dichloromethane. ES-MS indicated the presence of **2.9** in the crude reaction mix, but the compound was too unstable to purify. $^1$H NMR ($CDCl_3$) δ 8.55 (d, 4H, H6'), 7.65 (t, 4H, H4'), 7.53 (d, 4H, H3'), 7.19 (t, 4H, H5'), 5.90 (d, 4H, CH), 5.86 (d, 4H, CH).

Spiro[3,3]heptane-2,6-dispiro-4,5-diazafluorene, **2.13**

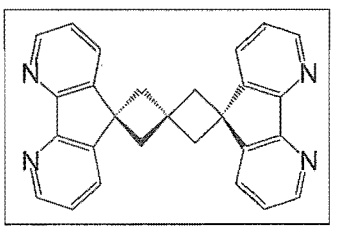

To a suspension of potassium metal (160 mg, 4.09 mmol) in THF (10 mL), under argon, was added compound **2.10** (350 mg, 2.08 mmol), dissolved in THF (15 mL). This gave a purple solution that was stirred for one hour. Pentaerythrityl tetrabromide (205 mg, 0.53 mmol) was then added in THF (15 mL) and the solution refluxed overnight. After cooling, the solvent was removed *in vacuo* and water (20 mL) was added. The reaction mixture was extracted with dichloromethane (3 x 50 mL), the extracts dried over magnesium sulfate and the solvent removed *in vacuo*. The residue was dissolved in dichloromethane, run through a silica gel plug to give a purple solid, from which a significant amount of insoluble material was removed by subsequent elution through an alumina plug. Recrystallisation from dichloromethane-ether gave **2.13** as colourless crystals. Yield 38 mg (18%). M.p. 165-166°C. Analysis: calc. for $C_{27}H_{20}N_4.1½H_2O$ C 75.86, H 5.42, N 13.11; found C 76.60, H 4.69, N 13.12%. HRMS: calc. for $C_{27}H_{20}N_4$ 400.1688, found 400.1693. $^1$H NMR ($CDCl_3$ + 3 drops $CD_3CN$) δ 8.69 (d, 4H, H3'), 8.00 (d, 4H, H1'), 7.37 (dd, 4H, H2'), 3.11 (s, 8H, $CH_2$). $^{13}$C NMR ($CDCl_3$ + 3 drops $CD_3CN$) δ 156.7, 149.2, 145.6, 130.4, 123.2, 44.57, 42.18, 31.00.

General preparation of hexaaryl[3]radialenes

In a three-necked flask under argon, the appropriate dipyridylmethyl compound (1 mol) was dissolved in dry THF (20 mL). After cooling to -78°C in a dry ice-acetone bath, n-butyllithium

(1.05 mol) was added dropwise and stirred for 15 minutes to give a dark red solution. Neat tetrachlorocyclopropene, (58 μL, 0.16 mol) was added and the solution stirred for 60 minutes at -78°C, 0°C for 30 minutes and then at room temperature for a further 30 minutes. The reaction was then cooled again to 0°C, oxygen gas bubbled through for 60 minutes and then for a further 60 minutes at room temperature. Following this, water was added to the reaction mixture, which was extracted with dichloromethane (3 x 50 mL), the extracts dried with sodium sulfate and the solvent removed *in vacuo*. The resultant oil was purified on an alumina column and then on silica gel as described below.

Hexa(2-pyridyl)[3]radialene, **2.14**

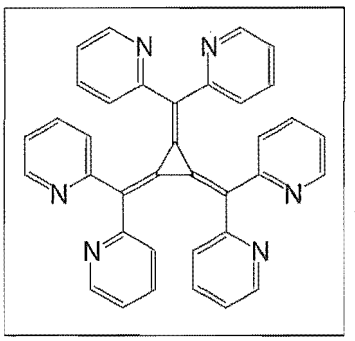

The starting material, **2.1**, (692 mg, 4.07 mmol) was dissolved in dry THF (20 mL), treated with n-butyllithium (1.9 mL, 4.37 mmol) and stirred for 15 minutes to give a dark red solution. Tetrachlorocyclopropene (123 mg, 0.69 mmol) was added and the reaction treated as described above. The resultant oil was run through an alumina column eluting with 1:9 methanol-chloroform and collecting the bright red band, which was then purified on silica gel, eluting again with 1:9 methanol-chloroform to give **2.14** as a bright red solid. Yield 269 mg (72%, based on tetrachlorocyclopropene). M.p. 259-260°C. Analysis: calc. for $C_{36}H_{24}N_6.H_2O$ C 77.40, H 4.69, N 15.04; found C 77.14, H 4.69, N 14.77%. HRMS: calc. for $C_{36}H_{25}N_6^+$ 541.2143; found 541.2141. $^1$H NMR ($CD_3OD$) δ 7.84 (d, 6H, H6'), 6.99 (t, 6H, H4'), 6.95 (dd, 6H, H5'), 6.69 (d, 6H, H3'); ($CDCl_3$) δ 8.28 (m, 6H, H6'), 7.04 (m, 12H), 6.92 (m, 6H). $^{13}$C NMR ($CD_3OD$) δ 158.6, 149.7, 137.5, 128.0, 127.4, 124.3, 123.7. UV-visible ($CH_2Cl_2$): $\lambda_{max}$ 258 nm, log ε 4.40; $\lambda_{max}$ 463 nm, log ε 4.39.

Hexa(3-pyridyl)[3]radialene, **2.15**

***Step 1 - Di-3-pyridylketone:*** 3-Bromopyridine (2.30 g, 14.6 mmol) was dissolved in ether (20 mL) under argon. After cooling to -78°C, n-butyllithium (9.2 mL, 14.7 mmol) was added slowly. To this solution, 3-cyanopyridine (1.52 g, 14.6 mmol) dissolved in THF (20 mL) was added dropwise, over a period of 10 minutes. The reaction was stirred for 30 minutes at -78°C, warmed to -10°C and stirred for a further 30 minutes. Water (15 mL) was added and the solution extracted with 10% sulfuric acid solution (3 x 10 mL). The resulting brown aqueous extracts were decolourised with activated charcoal, filtered and made alkaline with potassium hydroxide solution. The aqueous solution was then extracted with chloroform (5 x 50 mL), dried over

magnesium sulfate and the solvent removed *in vacuo*. The oily solid was purified on silica gel, eluting with 1:19 methanol-dichloromethane solution and recrystallised from ethyl acetate-petroleum ether to give a pale yellow solid. Yield 1.97 g (73%). M.p. 90-93°C. Analysis: calc. for $C_{11}H_{10}N_2O$ C 71.73, H 4.38, N 15.21; found C 71.43, H 4.80, N 15.71%. $^1$H NMR ($CDCl_3$) δ 9.00 (d, 2H, H2), 8.84 (d, 2H, H6), 8.13 (d, 2H, H4), 7.48 (dd, 2H, H5). $^{13}$C NMR ($CDCl_3$) δ 193.0, 153.5, 150.8, 137.1, 132.3, 123.6.

***Step 2 - Di-3-pyridylmethane:*** The reagents: di-3-pyridylketone (1.50 g, 8.15 mmol), potassium hydroxide (1.20 g) and ethylene glycol (30 mL) were combined in a round-bottomed flask. Hydrazine hydrate (1.3 mL) was added and the solution refluxed for four hours. After cooling to room temperature, water (40 mL) was added and the reaction mixture extracted with benzene (5 x 40 mL), dried over magnesium sulfate and the solvent removed *in vacuo* to give an oily pale yellow solid. Yield 566 mg (41%). HRMS: calc. for $C_{11}H_{10}N_2$ 170.0844, found 170.0843. $^1$H NMR ($CDCl_3$) δ 8.48 (m, 4H, H2, H6), 7.44 (d, 2H, H4) 7.22 (dd, 2H, H5). $^{13}$C NMR ($CDCl_3$) δ 150.0, 148.1, 147.8, 136.2, 123.6, 36.18.

***Step 3:*** Di-3-pyridylmethane (367 mg, 2.16 mmol) dissolved in dry THF (30 mL) was reacted with n-butyllithium (1.40 mL, 2.24 mmol). Tetrachlorocyclopropene (44 μl, 0.36 mmol) was added and the reaction treated as described above. The resulting oil was run through an alumina column, eluting with dichloromethane to remove the starting material, then 1:9 methanol-dichloromethane solution, and the bright red band collected. This fraction was chromatographed on silica gel using the same solvent system to give **2.15** as a bright orange solid. Yield 84.5 mg (43%). M.p. >200°C (dec.). Analysis: calc. for $C_{36}H_{24}N_6.2H_2O$ C 74.98, H 4.89, N 14.57; found C 75.38, H 5.25, N 14.31%. HRMS: calc. for $C_{36}H_{24}N_6$ 540.2063; found 540.2066. $^1$H NMR ($CDCl_3$) δ 8.43 (d, 6H, H6), 7.94 (d, 6H, H2), 7.20 (d, 6H, H4), 6.95 (dd, 6H, H5). $^{13}$C NMR ($CDCl_3$) δ 150.4, 148.9, 136.6, 135.4, 122.5, 119.2, 118.6. UV-visible ($CH_2Cl_2$): $\lambda_{max}$ 266 nm, log ε 4.66; $\lambda_{max}$ 464 nm, log ε 4.60.

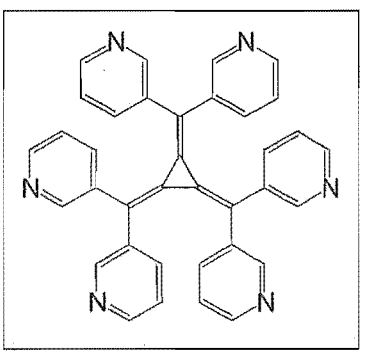


Hexa(4-pyridyl)[3]radialene, **2.16**

***Step 1 - Di-4-pyridylmethane:*** Di-4-pyridylketone (465 mg, 2.52 mmol) and potassium hydroxide (302 mg, 5.38 mmol) were dissolved in ethylene glycol (10 mL). The solution was cooled and hydrazine hydrate (0.3 mL) added, before the reaction mixture was refluxed for 4 hours. After cooling, water (10 mL) was added, the reaction mixture extracted with benzene (6 x 10 mL), dried over magnesium sulfate and the solvent removed *in vacuo*. The oil that was

isolated was distilled to give colourless crystals. Yield 365 mg (85%). M.p. 33-35°C (lit. 36-37°C). $^{1}$H NMR ($CDCl_3$) δ 8.53 (d, 2H, H2/H6), 7.11 (d, 2H, H3/H5). $^{13}$C NMR ($CDCl_3$) δ 150.0, 147.8, 124.2, 40.45.

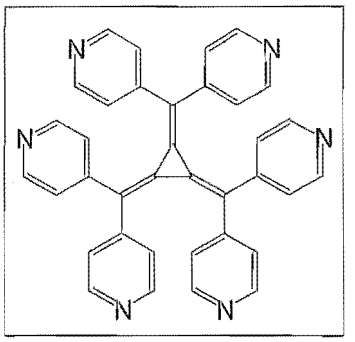

***Step 2:*** Di-4-pyridylmethane (265 mg, 1.56 mmol) dissolved in dry THF (30 mL) was reacted with n-butyllithium (1.02 mL, 1.63 mmol). Tetrachlorocyclopropene (32 μl, 0.26 mmol) was added and the reaction treated as described. The resulting oil was run through an alumina column, eluting with dichloromethane to remove the starting material, then 1:9 methanol-dichloromethane solution, and the bright red band collected. This fraction was purified by gradient elution chromatography on silica gel, eluting with methanol-dichloromethane, to give **2.16** as a oily orange-red solid. Yield 21.9 mg (16%). HRMS: calc. for $C_{36}H_{25}N_6^+$ 541.2141; found 541.2145. $^{1}$H NMR ($CDCl_3$) δ 8.23 (d, 12H, H2/H6), 6.72 (d, 12H, H3/H5). $^{13}$C NMR ($CDCl_3$) δ 148.9, 145.8, 124.4, 124.0, 119.5. UV-visible ($CH_2Cl_2$): $\lambda_{max}$ 263 nm, log ε 4.61; $\lambda_{max}$ 463 nm, log ε 4.62.

*Unsym-* and *sym*-tris(2-pyridyl)triphenyl[3]radialene, **2.17/2.18**

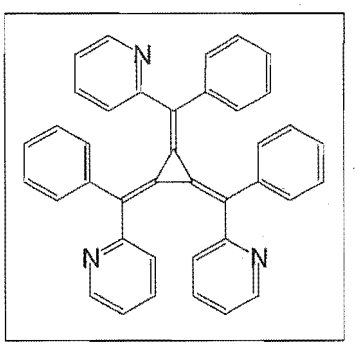

2-Benzylpyridine (1.05 g, 6.20 mmol) was dissolved in dry THF (20 mL) and deprotonated with n-butyllithium (3.9 mL, 6.24 mmol). Tetrachlorocyclopropene (127 μl, 1.04 mmol) was added and the reaction treated as described above. The resulting oil was run through an alumina column, eluting with 1:9 methanol-dichloromethane solution, and the bright red band collected. This fraction was chromatographed on silica gel, with 1:9 methanol-dichloromethane solution as the eluent, but the two isomers could not be effectively separated. This gave a 3:1 mixture of the isomers (*unsym*(**2.17**)-*sym*(**2.18**)) as a bright orange solid. Yield 172mg (31%). Analysis: calc. for $C_{39}H_{27}N_3.H_2O$ C 84.30, H 5.26, N 7.56; found C 84.29, H 4.88, N 7.91%. HRMS: calc. for $C_{39}H_{28}N_3^+$ 538.2294; found 538.2283. $^{1}$H NMR ($CDCl_3$) δ 8.26 (d, 3H, *sym*-H6), 8.25 (d, 1H, *unsym*-H6'), 8.10 (d, 1H, *unsym*-H6"), 8.07 (d, 1H, *unsym*-H6"'), 7.07-7.16 (bm), 6.94-7.02 (bm), 6.80-6.86 (bm). UV-visible ($CH_2Cl_2$): $\lambda_{max}$ 268, log ε 4.66; $\lambda_{max}$ 469, log ε 4.71.

### 6.2.2 Di-2-pyridylamine-based ligands

General synthesis of bis(di-2-pyridylamino)benzenes and naphthalenes

***Method A:*** A mixture of the appropriate dibromo-arene (1 equiv.), di-2-pyridylamine (2 equiv.), potassium hydroxide and copper sulfate were heated at 180°C for 48 hours. After cooling, the residue was dissolved in water and extracted with dichloromethane. The organic layer was washed with water until the washings were neutral, dried over magnesium sulfate and the solvent removed *in vacuo*. Chromatography and/or recrystallisation (as described) were used to purify the crude product.

***Method B:*** The appropriate diamino-arene (1 equiv.), potassium t-butoxide (4.75 equiv.), BINAP (0.15 equiv.) and $[Pd_2(dba)_3]$ (0.07 equiv., 2 mol% Pd) were dissolved in dry toluene under argon. To this mixture was added 2-bromopyridine (4.7 equiv.) and the mixture refluxed for 96 hours. After cooling, ethyl acetate was added and the insoluble material removed by filtration. The filtrate was evaporated to dryness *in vacuo* and the residue purified by chromatography and/or recrystallisation.

1,4-Bis(di-2-pyridylamino)naphthalene, **3.4**

***Step 1 - 1-Bromo-4-(di-2-pyridylamino)naphthalene:*** Using method A, 1,4-dibromonaphthalene (2.86 g, 10 mmol), di-2-pyridylamine (3.42 g, 20 mmol), potassium hydroxide (1.46 g) and copper(II) sulfate (100 mg) were heated at 180°C for 24 hours. Chromatography on alumina with dichloromethane gave the product as a white solid. Yield 1.15 g (31%). M.p. 136-139°C. ES-MS 378.0 $[(M+1)]^+$, 376.0 $[(M+1)]^+$. $^1$H NMR ($CDCl_3$) δ 8.28 (m, 3H, H6', H5/H8), 7.86 (m, 2H, H5/H8, H2), 7.57 (t, 1H, H6/H7) 7.51 (t, 2H, H4'), 7.41 (t, 1H, H6/H7), 7.31 (d, 2H, H3'), 6.88 (d, 2H, H5'). $^{13}$C NMR ($CDCl_3$) δ 157.9, 148.3, 141.0, 137.5, 133.5, 132.7, 130.4, 128.0, 127.9, 127.62, 127.58, 124.2, 122.1, 117.8, 115.7.

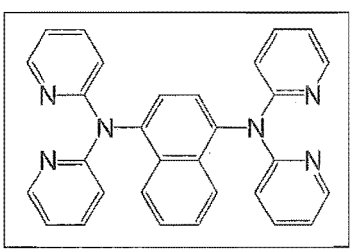

***Step 2:*** Using method A, 1-bromo-4-(di-2-pyridylamino)naphthalene (620 mg, 1.65 mmol), di-2-pyridylamine (340 mg, 2 mmol), potassium hydroxide (200 mg) and copper(II) sulfate (10 mg) were heated at 180°C for 48 hours. Chromatography on alumina, with dichloromethane as the eluent gave **3.4** as a yellow solid that was recrystallised from dichloromethane-ether. Yield 254 mg (33%). M.p. 247-249°C. Analysis: calc. for $C_{30}H_{22}N_6$ C 77.23, H 4.75, N 18.01; found C 76.56, H 4.61, N 18.10%. HRMS: calc. for $C_{30}H_{23}N_6^+$ 467.1984; found 467.1986. $^1$H NMR ($CDCl_3$) δ 8.30 (d, 4H, H6'), 7.92 (dd, 2H,

H5/H8), 7.53 (m, 6H, H4', H2/H3), 7.33 (dd, 2H, H6/H7), 7.01 (d, 4H, H3'), 6.90 (dd, 4H, H5'). $^{13}$C NMR ($CDCl_3$) δ 158.0, 148.2, 140.3, 137.5, 133.0, 128.1, 127.1, 124.4, 117.8, 116.0.

1,5-Bis(di-2-pyridylamino)naphthalene, **3.6**

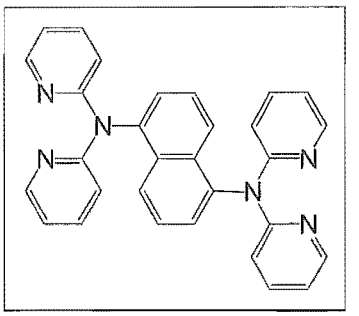

Using method B, 1,5-diaminonaphthalene (127 mg, 0.80 mmol), potassium t-butoxide (426 mg, 3.80 mmol), R-(+)-BINAP (38 mg, 0.06 mmol), [$Pd_2(dba)_3$] (28 mg, 0.03 mmol) and 2-bromopyridine (360 μL, 3.76 mmol) were dissolved in dry toluene (14 mL) and heated at 80°C for 96 hours. The solvent was removed *in vacuo*, the residue dissolved in hot ethanol and cooled to give **3.6** as a brown solid, which was recrystallised from dichloromethane-ether. Yield 200 mg (54%). M.p. 281-283°C. Analysis: calc. for $C_{30}H_{22}N_6$ C 77.23, H 4.75, N 18.01; found C 77.34, H 4.69, N 17.93%. HRMS: calc. for $C_{30}H_{23}N_6^+$ 467.1984; found 467.1989. $^1$H NMR ($CDCl_3$) δ 8.30 (d, 4H, H6'), 7.90 (d, 2H, H4/H8), 7.53 (t, 4H, H4'), 7.43 (m, 4H, H2/H6, H3/H7), 6.98 (d, 4H, H3'), 6.90 (t, 4H, H5'). $^{13}$C NMR ($CDCl_3$) δ 158.2, 148.3, 141.6, 137.5, 133.4, 128.0, 127.2, 123.5, 117.8, 116.1.

1,3-Bis(di-2-pyridylamino)benzene, **3.7**

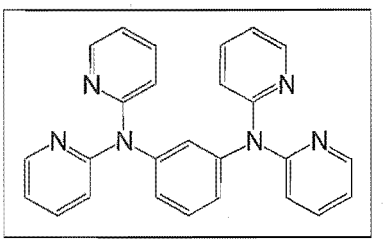

Using method B, 1,3-diaminobenzene (176 mg, 1.63 mmol), potassium t-butoxide (852 mg, 7.59 mmol), *rac*-BINAP (152 mg, 0.24 mmol), [$Pd_2(dba)_3$] (112 mg, 0.12 mmol) and 2-bromopyridine (720 μL, 7.55 mmol) were refluxed in dry toluene (28 mL) for 96 hours. The residue was purified by chromatography on silica gel using 1:9 methanol-dichloromethane eluent to give **3.7**. Yield 325 mg (48%). M.p. 133-136°C. Analysis: calc. for $C_{26}H_{20}N_6.½H_2O$ C 75.77, H 4.87, N 17.67; found C 75.87, H 4.92, N 17.44%. HRMS: calc. for $C_{30}H_{23}N_6^+$ 417.1822; found 417.1828. $^1$H NMR ($CDCl_3$) δ 8.30 (d, 4H, H6'), 7.54 (t, 4H, H4'), 7.33 (t, 1H, H5), 7.05 (d, 4H, H3'), 6.99 (m, 3H, H2, H4/H6), 6.90 (dd, 4H, H5'). $^{13}$C NMR ($CDCl_3$) δ 157.7, 148.3, 145.9, 137.5, 130.5, 125.3, 123.4, 118.3, 117.1.

2,7-Bis(di-2-pyridylamino)naphthalene, **3.8**

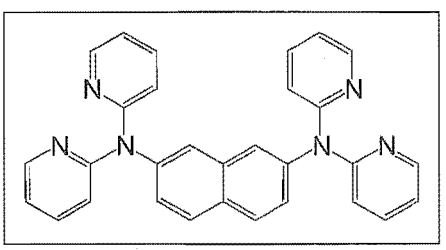

The reagents: 2,7-diaminonaphthalene (254 mg, 1.61 mmol), potassium t-butoxide (856 mg, 7.63 mmol), *rac*-BINAP (152 mg, 0.24 mmol) [$Pd_2(dba)_3$] (112 mg, 0.12 mmol) and 2-bromopyridine (720 μL, 7.55 mmol) were refluxed in dry toluene (28 mL) for 96 hours. The filtrate was purified on a Celite plug before chromatography

on silica gel using 1:9 methanol-dichloromethane as an eluent. Recrystallisation from acetone-water gave **3.8** as a pale brown solid. Yield 375 mg (50%). M.p. 197-199°C. Analysis: calc. for $C_{30}H_{22}N_6.½H_2O$ C 75.77, H 4.87, N 17.67; found C 75.98, H 4.68, N 17.50%. HRMS: calc. for $C_{30}H_{23}N_6^+$ 467.1984; found 467.1983. $^1$H NMR ($CDCl_3$) δ 8.31 (d, 4H, H6'), 7.81 (d, 2H, H4/H5), 7.56 (t, 4H, H4'), 7.46 (d, 2H, H1/H8), 7.26 (d, 2H, H3/H6), 7.02 (d, 4H, H3'), 6.93 (dd, 4H, H5'). $^{13}$C NMR ($CDCl_3$) δ 158.0, 148.5, 143.0, 137.5, 135.3, 129.4, 129.2, 125.7, 124.1, 118.3, 117.2.

2,4,6-Tris(di-2-pyridylamino)-1,3,5-triazine, **3.10**

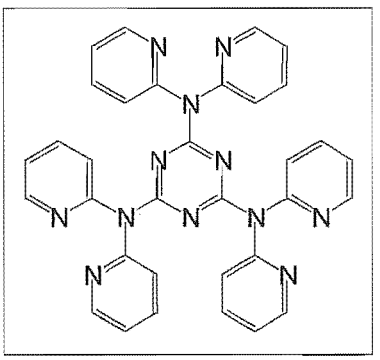

Di-2-pyridylamine (3.51 g, 21 mmol), 2,4,6-trichloro-1,3,5-triazine (1.23 g, 6.7 mmol), sodium carbonate (2 g), copper powder (0.08 g), potassium bromide (trace) and mesitylene were heated at 160°C for 72 hours. The flask was cooled, the mesitylene removed *in vacuo*, dichloromethane added and the mixture stirred for 2 hours. The suspension was filtered through a Celite plug, the solid residues washed with more dichloromethane, the filtrate and washings combined and then taken to dryness *in vacuo*. The residue was purified on an alumina column with 1:9 methanol-dichloromethane to give an oily yellow solid, which was triturated with ethyl acetate and recrystallised from methanol-ether to give pure **3.10**. Yield 1.07 g (27%). M.p. 298-301°C (lit. 299-300°C). HRMS: calc. for $C_{33}H_{25}N_{12}^+$ 589.2319; found 589.2325. Analysis: calc. for $C_{33}H_{24}N_{12}.½H_2O$ C 66.32, H 4.22, N 28.12, found C 66.54, H 4.00, N 28.18%. $^1$H NMR ($CDCl_3$) δ 8.33 (d, 6H, H6'), 7.50 (t, 6H, H4'), 7.40 (d, 6H, H3'), 7.01 (dd, 6H, H5'). $^{13}$C NMR ($CDCl_3$) δ 165.4, 154.9, 148.3, 136.9, 122.7, 120.6.

General synthesis of di-2-pyridylaminomethylbenzenes

Di-2-pyridylamine (1 equiv.) and potassium hydroxide (excess) were stirred in DMSO (25 mL) for one hour. The n-bromomethylbenzene compound (1/n equiv.) was then added and the reaction stirred for 24-48 hours. Water (25 mL) was then added, the yellow solid collected by filtration and washed with water. Purification is as described below for each compound.

1,2-Bis(di-2-pyridylaminomethyl)benzene, **3.11**

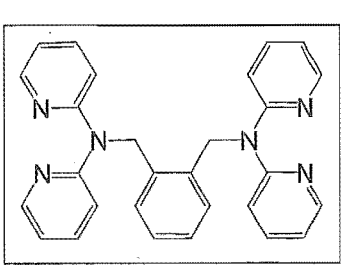

Di-2-pyridylamine (1.00 g, 5.84 mmol) and potassium hydroxide (1.33 g, 23.7 mmol) were stirred in DMSO for one hour, 1,2-bis(bromomethyl)benzene (700 mg, 2.65 mmol) was added and

the reaction mixture stirred for 40 hours. Water was added to give a yellow precipitate, **3.11**, which was recrystallised from ethyl acetate-petroleum ether. Yield 290 mg (25%). M.p. 144-146°C. Analysis: calc. for $C_{28}H_{24}N_6$ C 75.65, H 5.44, N 18.91; found C 75.37, H 5.38, N 19.04%. HRMS: calc. for $C_{28}H_{24}N_6$ 444.2063; found 444.2079. $^1$H NMR ($CDCl_3$) δ 8.32 (d, 4H, H6'), 7.53 (t, 4H, H4'), 7.27 (dd, 2H, arom. H), 7.22 (d, 4H, H3'), 7.04 (dd, 2H, arom. H), 6.86 (dd, 4H, H5'), 5.64 (s, 4H, $CH_2$). $^{13}$C NMR ($CDCl_3$) δ 157.1, 148.2, 137.2, 136.1, 126.5, 117.2, 114.6, 48.62.

1,3-Bis(di-2-pyridylaminomethyl)benzene, **3.12**

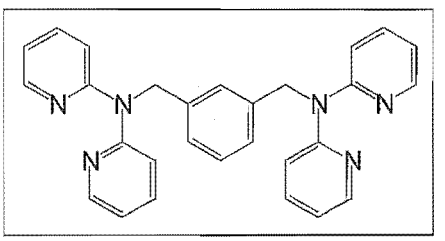

Di-2-pyridylamine (1.00 g, 5.84 mmol) and potassium hydroxide (1.33 g, 23.7 mmol) were stirred in DMSO for one hour, combined with 1,3-bis(bromomethyl)benzene (699 mg, 2.65 mmol) and stirred for 24 hours. Water was added to give a yellow solid, **3.12**, which was filtered washed with a further quantity of water, and then ether. Yield 590 mg (53%). M.p. 133-134°C. Analysis: calc. for $C_{28}H_{24}N_6$ C 75.65, H 5.44, N 18.91; found C 75.46, H 5.49, N 19.03%. HRMS: calc. for $C_{28}H_{24}N_6$ 444.20625; found 444.20638. $^1$H NMR ($CDCl_3$) δ 8.25 (d, 4H, H6'), 7.42 (t, 4H, H4'), 7.27 (s, 1H, arom. H), 7.14 (s, 3H, arom. H), 7.02 (d, 4H, H3'), 6.80 (dd, 4H, H5'), 5.42 (s, 4H, $CH_2$). $^{13}$C NMR ($CDCl_3$) δ 157.0, 148.1, 139.3, 137.1, 128.4, 125.3, 125.1, 117.0, 114.5, 51.20.

1,4-Bis(di-2-pyridylaminomethyl)benzene, **3.13**

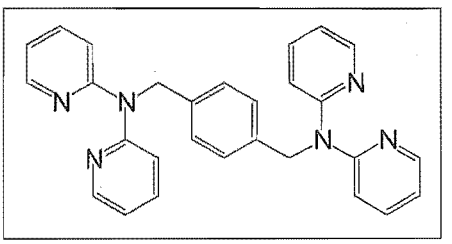

Di-2-pyridylamine (1.00 g, 5.84 mmol) and potassium hydroxide (1.33 g, 23.7 mmol) were stirred in DMSO for one hour, combined with 1,4-bis(bromomethyl)benzene (700 mg, 2.65 mmol) and stirred for 40 hours. Water was added to give a yellow precipitate, **3.13**, which was collected by filtration, washed with water, then ethyl acetate, and dried *in vacuo*. Yield 468 mg (40%). M.p. 181-183°C. Analysis: calc. for $C_{28}H_{24}N_6$ C 75.65, H 5.44, N 18.91; found C 75.47, H 5.44, N 19.01%. HRMS: calc. for $C_{28}H_{24}N_6$ 444.2063; found 444.2078. $^1$H NMR ($CDCl_3$) δ 8.28 (d, 4H, H6'), 7.47 (t, 4H, H4'), 7.22 (s, 4H, H2/H3/H5/H6), 7.13 (d, 4H, H3'), 6.82 (dd, 4H, H5'), 5.43 (s, 4H, $CH_2$). $^{13}$C NMR ($CDCl_3$) δ 157.1, 148.1, 137.6, 137.1, 126.9, 117.1, 114.5, 51.02.

1,3,5-Tris(di-2-pyridylaminomethyl)benzene, **3.14**

Di-2-pyridylamine (1.00 g, 5.84 mmol) and potassium hydroxide (1.31 g, 23.4 mmol) were stirred in DMSO for one hour, combined with 1,3,5-tris(bromomethyl)benzene (675 mg,

1.89 mmol) and stirred for 48 hours. Water was added to give a yellow precipitate, **3.14**, which was washed with water and recrystallised from ethyl acetate-petroleum ether. Yield 583 mg (49%). M.p. 158-160°C. Analysis: calc. for $C_{39}H_{33}N_9$ C 74.62, H 5.30, N 20.08; found C 74.33, H 5.07, N 19.80%. HRMS: calc. for $C_{39}H_{34}N_9^+$ 628.2953; found 628.2937. $^1$H NMR ($CDCl_3$) δ 8.20 (d, 6H, H6'), 7.37 (t, 6H, H4'), 7.07 (s, 3H, H2/H4/H6), 6.91 (d, 6H, H3'), 6.78 (dd, 6H, H5'), 5.34 (s, 6H, $CH_2$). $^{13}$C NMR ($CDCl_3$) δ 157.0, 148.0, 139.4, 137.0, 123.6, 116.9, 114.5, 51.18.

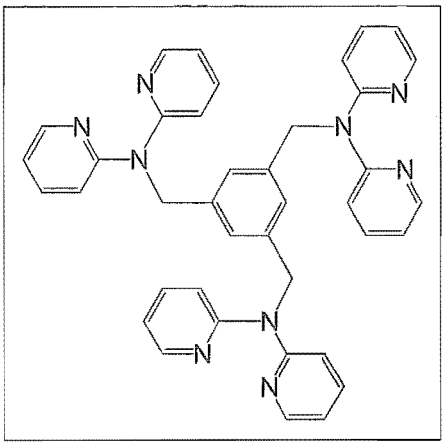

1,2,4,5-Tetrakis(di-2-pyridylaminomethyl)benzene, **3.15**

Di-2-pyridylamine (1.00 g, 5.84 mmol) and potassium hydroxide (1.31 g, 23.4 mmol) were stirred in DMSO for one hour, combined with 1,2,4,5-tetrakis(bromomethyl)benzene (642 mg, 1.89 mmol) and stirred for 48 hours. Addition of water gave a yellow precipitate, **3.15**, which was washed with water and then recrystallised from chloroform-petroleum ether. Yield 396 mg (34%). M.p. 238-241°C. Analysis: calc. for $C_{50}H_{46}N_{12}.2H_2O$ C 70.90, H 5.47, N 19.84; found C 70.68, H 4.84, N 19.68%. HRMS: calc. for $C_{50}H_{43}N_{12}^+$ 811.3729; found 811.3734. $^1$H NMR ($CDCl_3$) δ 8.13 (d, 8H, H6'), 7.28 (t, 8H, H4'), 7.16 (s, 2H, H3/H6), 6.80 (d, 8H, H3'), 6.75 (dd, 8H, H5'), 5.40 (s, 8H, $CH_2$). $^{13}$C NMR ($CDCl_3$) δ 156.8, 147.9, 137.0, 133.7, 124.1, 116.8, 114.4, 48.27.

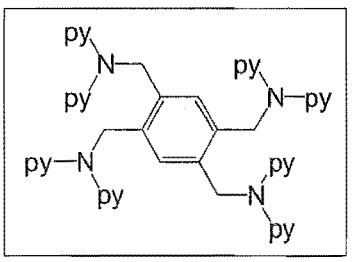

## 6.2.3 Tripodal Ligands

4,6-Bis(di-2-pyridylmethyl)pyrimidine, **4.5**

***Step 1 - 4,6-Diiodopyrimidine:*** 4,6-Dichloropyrimidine (1.00 g, 6.72 mmol) was dissolved in hydroiodic acid (12 mL) to give a brown paste that was stirred for 64 hours. The paste was filtered, the precipitate washed with a small volume of water and then suspended in water (50 mL). After neutralisation with sodium bicarbonate, the solution was extracted with dichloromethane (initially 50 mL, then 3 x 30 mL). The dichloromethane extracts were washed with sodium thiosulfate solution, water and brine before being dried over magnesium sulfate. The solvent was removed to give a white solid, which was recrystallised from petroleum ether. Yield 1.15 g (52%). M.p. 86-89°C. $^1$H NMR ($CDCl_3$) δ 8.54 (s, 1H, H2), 8.27 (s, 1H, H5). $^{13}$C NMR ($CDCl_3$) δ 157.8, 142.9, 128.6.

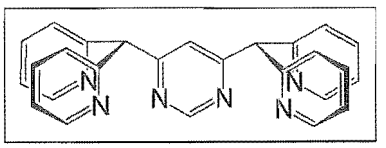

***Step 2:*** Compound **2.1** (650 mg, 3.82 mmol) was dissolved in dry THF (5 mL), under argon, and cooled to -78°C in a dry ice-acetone bath. n-Butyllithium (2.5 mL, 4.00 mmol) was added dropwise and the solution stirred for 15 minutes at -78°C. 4,6-Diiodopyrimidine (634 mg, 1.91 mmol) was dissolved in a further 10 mL of THF and added dropwise to the lithiated di-2-pyridylmethane solution. Over an hour the dark red solution went brown and the solution was left to warm to room temperature, with constant stirring for 48 hours. Water (0.5 mL) was added slowly and the reaction stirred a further hour. The solvents were removed *in vacuo* and the residue extracted into hot ethanol. The ethanol solution was reduced *in vacuo* and triturated with ether (40 mL) to give **4.5** as an orange solid. Yield 379 mg (48%). M.p. 153-155°C (dec.). Analysis: calc. for $C_{26}H_{20}N_6.1½H_2O$ C 70.41, H 5.23, N 18.95; found C 70.11, H 4.87, N 18.94%. $^1$H NMR ($CDCl_3$) δ 9.13 (s, 1H, H2), 8.53 (d, 4H, H6'), 7.62 (t, 4H, H4'), 7.37 (s, 1H, H5), 7.34 (d, 4H, H3'), 7.15 (dd, 4H, H5'), 5.86 (s, 2H, CH); (DMSO-$d_6$) δ 9.09 (s, 1H, H2), 8.55 (d, 4H, H6'), 7.83 (t, 4H, H4'), 7.38 (m, 9H, H5, H3', H5'), 5.95 (s, 2H, CH). $^{13}$C NMR ($CDCl_3$) δ 169.4, 159.5, 158.4, 149.4, 142.5, 136.7, 124.2, 122.1, 63.4.

4,6-Bis(di-2-pyridylamino)pyrimidine, **4.6**

Into a 50 mL round bottom flask 4,6-dichloropyrimidine (1.51 g, 10 mmol), **3.1** (3.5 g, 20 mmol), sodium carbonate (2 g), copper powder (0.05 g), potassium bromide (trace) and mesitylene (5 mL) were placed and then heated to 160°C. Thin layer chromatography and NMR were used to monitor the reaction for five days. After this time, no further reaction occurred, the mesitylene was removed *in vacuo* and the residue redissolved in dichloromethane. The insoluble component was filtered off, and the filtrate, containing a mixture of starting material and products, taken to dryness *in vacuo*. To separate the mixture of starting material, mono-substituted and di-substituted products, the resulting oil was purified on a silica gel column (20 x 5 cm) eluting with 1:40 methanol-chloroform solution. The mono-substituted product, 4-chloro-6-(di-2-pyridylamino)pyrimidine, **4.16**, co-eluted with the starting di-2-pyridylamine. However, this was separated by recrystallisation from a 3:1 mixture of petroleum ether-ethyl acetate to give **4.16** as a creamy yellow solid. Yield 0.86 g (30%). M.p. 145-147°C. Analysis: calc. for $C_{15}H_{10}N_5Cl$ C 59.27, H 3.55, N 24.68, Cl 12.50, found C 59.32, H 3.32, N 24.62, Cl 12.28%. ES-MS 284.1 $[(M+1)]^+$. $^1$H NMR ($CDCl_3$) δ 8.54 (s, 1H, H2), 8.53 (d, 2H, H6'), 7.79 (t, 2H, H4'), 7.23 (m, 4H, H5', H3'), and 6.99 (s, 1H, H5); (DMSO-$d_6$) δ 8.65 (s, 1H, H2), 8.55 (d, 2H, H6'), 7.99 (dd,

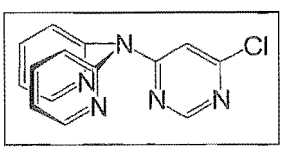

2H, H4'), 7.42 (t, 2H, H5'), 7.36 (d, 2H, H3') and 7.18 (s, 1H, H5). $^{13}$C NMR ($CDCl_3$) δ 160.4, 158.2, 155.0, 149.5, 142.4, 138.6, 121.9, 121.1, 108.8.

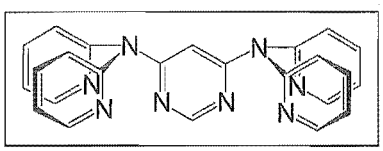

The next fraction contained **4.6** as a pale brown solid that was collected, washed with cold ethyl acetate and recrystallised from ethanol-ether. Yield 1.14 g (27%). M.p. 192-194°C. Analysis calc. for $C_{24}H_{18}N_8$: C 68.89, H 4.34, N 26.79, found C 69.00, H 4.49, N 26.81%. ES-MS 419.2 $[(M+1)]^+$. $^1$H NMR ($CDCl_3$) δ 8.51 (s, 1H, H2), 8.41 (dd, 4H, H6'), 7.70 (t, 4H, H4'), 7.23 (d, 4H, H3'), 7.10 (dd, 4H, H5') and 6.47 (s, 1H, H5); (DMSO-$d_6$) δ 8.43 (m, 5H, H2, H6'), 7.90 (t, 4H, H4'), 7.31 (m, 8H, H3', H5'), and 6.32 (s, 1H, H5). $^{13}$C NMR ($CDCl_3$) δ 162.5, 158.2, 155.9, 149.0, 138.0, 120.9, 120.7, 99.2.

3,6-Bis(di-2-pyridylmethyl)pyridazine, **4.7**

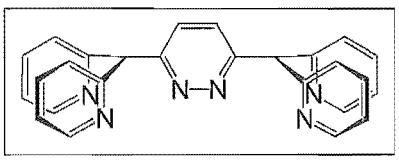

The starting material, **2.1**, (620 mg, 3.64 mmol) was added to a dry flask under argon and dissolved in dry THF (10 ml) to give a pale brown solution. A dry ice/acetone bath was used to cool the reaction to -78°C, before n-butyllithium (2.4 ml, 3.84 mmol) was added dropwise to give a deep red solution that was stirred for 15 minutes. A solution of 3,6-dichloropyridazine (271 mg, 1.82 mmol) in THF (10 mL) was then added dropwise, which caused a precipitate to form and the solution to slowly decolourise. The reaction was allowed to warm to room temperature and then to stir for one hour. The thick brown solution that resulted was treated with distilled water (0.5 mL) and stirred for a further hour. The solids were collected by filtration, washed with a small volume of ice water and ether, before recrystallisation from ethanol-ether solution. This gave **4.7** as a white solid. Yield 210 mg (28%). M.p. 204-206°C (dec.). Analysis: calc. for $C_{26}H_{20}N_6.½H_2O$ C 73.39, H 4.97, N 19.76; found C 73.57, H 4.94, N 19.60%. $^1$H NMR ($CDCl_3$) δ 8.53 (d, 4H, H6'), 7.66 (s, 2H, H4/H5), 7.61 (t, 4H, H4'), 7.35 (d, 4H, H3'), 7.13 (dd, 4H, H5'), 6.17 (s, 2H, CH). $^{13}$C NMR ($CDCl_3$) 161.4, 159.7, 149.2, 136.5, 127.7, 124.0, 121.7, 61.3.

5-(2-Pyridyl)indolizino[2,3-b]quinoxaline, **4.17**

***Step 1 - 1,4-Dihydro-2,3-quinoxalinedione:*** 1,2-Diaminobenzene (2.40 g, 27 mmol) and oxalic acid dihydrate (6.30 g, 49 mmol) were heated at 130°C for 3 hours. The green solid that formed was collected in a filter funnel and washed with 1 M hydrochloric acid and ethanol until the washings were colourless. Yield 3.22 g (91%). M.p. >340°C. $^1$H NMR (DMSO-$d_6$) δ 12.01 (s, 2H, NH), 7.17-7.23 (m, 4H, aromatic H). $^{13}$C NMR (DMSO-$d_6$) δ 155.3, 125.7, 123.1, 115.2.

***Step 2 - 2,3-Dichloroquinoxaline:*** 1,4-Dihydro-2,3-quinoxalinedione (2.28 g, 12.2 mmol) was heated at 100°C with thionyl chloride (5 mL) and DMF (0.5 mL) for two hours. The excess thionyl chloride was removed *in vacuo* and the residue extracted with ethyl acetate. The combined extracts were washed with water and then brine, dried over magnesium sulfate and evaporated to dryness. The solid was recrystallised from ethyl acetate to give a pink powder. Yield 2.40 g (99%). M.p. 147-149°C. $^{1}$H NMR ($CDCl_3$) δ 8.03-8.05 (m, 2H, aromatic H), 7.81-7.83 (m, 2H, aromatic H). $^{13}$C NMR ($CDCl_3$) δ 145.6, 140.8, 131.5, 128.5.

***Step 3:*** In a dry two-necked round-bottomed flask under argon, **2.1** (0.51 g, 3.0 mmol) was dissolved in THF (10 mL). This was cooled to -78°C and n-butyllithium (2 mL, 3.2 mmol) added dropwise to give a dark red solution that was stirred at -78°C for 15 minutes. 2,3-Dichloroquinoxaline (298 mg, 1.50 mmol) was dissolved in THF (10 mL) and added dropwise. The reaction mixture was stirred for 15 minutes at -78°C before allowing warming to room temperature over an hour, during which time the solution turned violet. The violet solution was then heated and stirred for a further three hours, quenched with water, and the solvent was removed *in vacuo*. The crude product was purified on silica gel using 1:19 methanol-chloroform solution to give **2.17** as a purple solid that was recrystallised from ethanol. Yield 400 mg (90%). M.p. 236-238°C. HRMS: calc. for $C_{19}H_{12}N_4$ 296.1062; found 296.10630. $^{1}$H NMR ($CDCl_3$) δ 9.15 (d, 1H, H4), 9.09 (d, 1H, H3'), 8.97 (d, 1H, H6'), 8.69 (d, 1H, H1), 8.37 (d, 1H, H7), 8.24 (d, 1H, H10), 7.86 (t, 1H, H3), 7.82 (t, 1H, H8), 7.73 (t, 1H, H9), 7.42 (dd, 1H, H4'), 7.12 (dd, 1H, H2), 6.78 (t, 1H, H5'). $^{13}$C NMR ($CDCl_3$) δ 154.4, 148.8, 148.4, 143.7, 143.2, 139.9, 136.8, 136.2, 131.1, 129.0, 128.6, 128.3, 126.9, 125.5, 122.5, 121.3, 119.5, 110.2, 100.0.

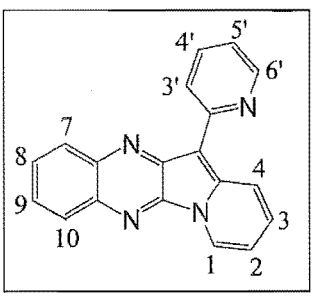


1,4-Bis(6-[di-2-pyridylamino]-4-pyrimidyloxy)benzene, **4.14**

Compound **4.16** (250 mg, 0.88 mmol) and 1,4-dihydroxybenzene (48.5 mg, 0.44 mmol) were dissolved in DMF. Potassium carbonate (122 mg, 0.87 mmol) was added to this solution and the reaction mixture refluxed for 24 hours. The reaction was cooled to room temperature and the DMF removed *in vacuo*. The residue was redissolved in chloroform, filtered through a Celite plug, before the filtrate was washed with brine, then water and dried over magnesium sulfate. The solvent was removed *in vacuo* to give a pale brown solid, which was purified by chromatography on alumina (20 g) to give **4.14** as a cream solid. Yield 314 mg

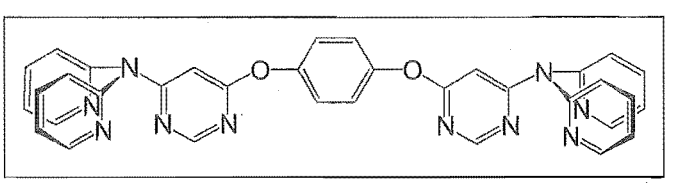

(59%). M.p. 237-239°C. Analysis: calc. for $C_{34}H_{24}N_{10}O_2.½H_2O$ C 66.55, H 4.11, N 22.83; found C 66.66, H 3.78, N 22.73%. ES-MS: 605.3 $[(M+1)]^+$. $^1$H NMR ($CDCl_3$) δ 8.50 (d, 4H, H6"), 8.44 (s, 2H, H2'), 7.75 (t, 4H, H4"), 7.22 (d, 4H, H3"), 7.18 (t, 4H, H5"), 7.16 (s, 4H, H2/H3/H5/H6), 6.49 (s, 2H, H5'). $^{13}$C NMR ($CDCl_3$) δ 170.0, 163.9, 158.1, 155.7, 149.7, 138.4, 122.6, 121.4, 121.0, 94.89.

## 6.3. Preparation of complexes with the di-2-pyridylmethane-based ligands

### 6.3.1 Complexes of 2.1

With silver nitrate, *viz* **2.19**

Ligand **2.1** (10.0 mg, 0.059 mmol) and silver nitrate (10.2 mg, 0.060 mmol) were both dissolved in methanol and the solutions mixed. Slow evaporation gave colourless crystals, suitable for X-ray crystallography. Yield 12.6 mg (63%). M.p. >160-161°C (dec.). Analysis: calc. for $C_{11}H_{10}N_3O_3Ag$ C 38.85, H 2.96, N 12.36; found C 39.10, H 2.83, N 12.37%.

With silver tetrafluoroborate, *viz* **2.20**

To a methanol solution of **2.1** (10.0 mg, 0.059 mmol) was added silver tetrafluoroborate (11.5 mg, 0.059 mmol) dissolved in methanol. Slow evaporation gave a colourless crystalline solid. Yield 12.4 mg (58%). M.p. 115°C (dec.). Analysis: calc. for $C_{11}H_{10}BN_4F_4Ag$ C 36.21, H 2.76, N 7.68; found C 36.63, H 2.56, N 7.64%.

With silver hexafluorophosphate, *viz* **2.21**

Ligand **2.1** (10.0 mg, 0.059 mmol) dissolved in methanol was combined with a methanol solution of silver hexafluorophosphate (15.0 mg, 0.059 mmol). A white precipitate formed after two days. Yield 11.1 mg (60%). M.p. 170°C (dec.). Analysis: calc. for $C_{22}H_{24}N_4O_2F_6PAg$ C 41.99, H 3.84, N 8.90; found C 42.32, H 3.52, N 8.52%.

With zinc nitrate, *viz* **2.22**

Both **2.1** (10.0 mg, 0.059 mmol) and zinc nitrate (17.5 mg, 0.059 mmol) were dissolved in methanol, mixed and the resulting solution slowly evaporated to dryness. The residue was recrystallised by vapour diffusion of ether into an acetonitrile solution of the complex giving a colourless crystalline solid. Yield 10.1 mg (48%). M.p. >192°C (dec.). Analysis: calc. for $C_{11}H_{10}N_4O_6Zn$ C 36.74, H 2.80, N 15.58; found C 36.89, H 2.71, N 15.66%.

With copper nitrate, *viz* **2.23**

Copper nitrate (14.2 mg, 0.059 mmol) dissolved in methanol was added to a methanol solution of **2.1** (10.0 mg, 0.059 mmol). Evaporation of the solution gave a blue oil that was crystallised, by vapour diffusion of ether into an acetonitrile solution of the complex, to give X-ray quality crystals. Yield 16.3 mg (63%). M.p. 110-112°C. Analysis: calc. for $C_{54}H_{49}N_{19}O_{26}Cu_6$ C 36.82, H 2.80, N 15.11, found C 40.60, H 3.25, N 15.83%.

With bis(2,2'-bipyridine)ruthenium(II) dichloride, *viz* **2.50**

Bis(2,2'-bipyridine)ruthenium(II) dichloride (77 mg, 0.16 mmol) and **2.1** (31 mg, 0.18 mmol) were refluxed in degassed 3:1 ethanol-water solution (16 ml) for 36 hours. This was taken to dryness *in vacuo*, redissolved in water, filtered and the complex precipitated with an excess of ammonium hexafluorophosphate. The resulting orange precipitate was recrystallised from methanol to give a dark red solid. Yield 69 mg (49%). M.p. 207-209°C. Analysis: calc. for $C_{31}H_{26}N_6F_{12}P_2Ru$ C 42.62, H 3.00, N 9.62; found C 42.73, H 3.23, N 9.46%. $^1$H NMR ($CD_3CN$) δ 8.58 (d, 2H, bpyH3A), 8.49 (d, 2H, bpyH3B), 8.24 (d, 2H, H6), 8.20 (t, 2H, bpyH4A), 8.03 (t, 2H, bpyH4B), 7.90 (t, 2H, H4), 7.72 (m, 4H, H3, bpyH6B), 7.58 (m, 4H, H5, bpyH6A), 7.39 (t, 2H, bpyH5B), 7.14 (t, 2H, bpyH5A), 4.61 (s, 2H, $CH_2$).

With bis(4,4'-dimethyl-2,2'-bipyridine)ruthenium(II) dichloride, *viz* **2.51**

Bis(4,4'-dimethyl-2,2'-bipyridine)ruthenium(II) dichloride (131 mg, 0.24 mmol) and **2.1** (42 mg, 0.25 mmol) were refluxed in degassed 3:1 ethanol-water solution (16 ml) for 36 hours. This was taken to dryness *in vacuo*, redissolved in water, filtered and the complex precipitated with an excess of ammonium hexafluorophosphate. The resulting precipitate was purified on alumina with 1:9 methanol-dichloromethane solution. Yield 137 mg (61%). M.p. 203-206°C. Analysis: calc. for $C_{31}H_{26}N_6F_{12}P_2Ru$ C 45.22, H 3.69, N 9.04; found C 45.16, H 3.95, N 8.96%. $^1$H NMR ($CD_3CN$) δ 8.44 (s, 2H, dmbH3A), 8.35 (s, 2H, dmbH3B), 8.06 (d, 2H, dmbH6A), 7.88 (t, 2H, H4), 7.69 (d, 2H, H3), 7.60 (d, 2H, H6), 7.54 (d, 2H, dmbH6B), 7.41 (d, 2H, dmbH5A), 7.24 (d, 2H, dmbH5B), 7.13 (t, 2H, H5), 4.60 (s, 2H, $CH_2$), 2.66 (s, 6H, dmbCH$_3$A), 2.54 (s, 6H, dmbCH$_3$B).

### 6.3.2 Complexes of 2.2

With silver nitrate, *viz* **2.24**

Both **2.2** (10.2 mg, 0.03 mmol) and silver nitrate (10.1 mg, 0.06 mmol) were dissolved in hot acetonitrile, the solutions mixed and allowed to cool overnight. Small colourless crystals

precipitated that were suitable for X-ray crystallography. Yield 14 mg (92%). M.p. 274°C (dec.). Analysis: calc. for $C_{22}H_{18}N_5O_3Ag$ C 51.99, H 3.57, N 13.78; found C 51.42, H 3.47, N 13.54%.

With silver tetrafluoroborate, *viz* **2.25**

Ligand **2.2** (10 mg, 0.03 mmol) was dissolved in methanol and silver tetrafluoroborate (13 mg, 0.067 mmol) was dissolved in hot acetonitrile, the solutions were mixed together and left to slowly evaporate. Yield 15.6mg (80%). M.p. >181°C (dec.). Analysis: calc. for $C_{44}H_{36}B_3N_8F_{12}Ag_3.2H_2O$ C 40.75, H 3.11, N 8.64; found C 40.68, H 2.97, N 8.77%. The above precipitate was recrystallised by vapour diffusion of ether into acetonitrile to provide colourless crystals of a [2+2] dimer.

With copper nitrate, *viz* **2.26**

Both **2.2** (10.6 mg, 0.031 mmol) and copper nitrate (16.0 mg, 0.066 mmol) were dissolved in methanol, mixed and the resulting solution allowed to slowly evaporate. Dark blue crystals formed that were suitable for X-ray crystallography. Yield 13.0 mg (59%). M.p. 278°C (dec.). Analysis: calc. for $C_{22}H_{18}N_8O_{12}Cu_2$ C 37.03, H 2.54, N 15.70; found C 36.82, H 2.69, N 15.42%.

With palladium chloride, *viz* **2.27**

Palladium chloride (11.5 mg, 0.065 mmol) was dissolved in 2 mL of 2 M hydrochloric acid and added slowly to a hot methanolic solution of **2.2** (10.0 mg, 0.03 mmol). The resulting solution turned yellow and a fine yellow solid precipitated. This was collected by filtration and dried *in vacuo*. Yield 12.8 mg (63%). M.p. > 310°C (dec.). Analysis: calc. for $C_{22}H_{18}N_4Cl_4Pd_2$ C 38.13, H 2.62, N 8.08, Cl 20.46; found C 37.80, H 2.85, N 7.49, Cl 20.26%. The complex was insoluble in common NMR solvents.

With zinc acetate, *viz* **2.28**

Zinc acetate (13.7 mg, 0.062 mmol) and **2.2** (10.0 mg, 0.03 mmol), were both dissolved in methanol, the solutions combined and the resulting solution allowed to slowly evaporate. Colourless crystals formed which were suitable for X-ray crystal structural analysis. Yield 13 mg (60%). M.p. 275°C (dec.). Analysis: calc. for $C_{30}H_{30}N_4O_8Zn_2.H_2O$ C 49.81, H 4.46, N 7.75; found C 49.66, H 4.11, N 7.65%.

With bis(2,2'-bipyridine)ruthenium(II) dichloride, *viz* **2.52**

Ligand **2.2** (21.8 mg, 0.06 mmol) and bis(2,2'-bipyridine)ruthenium(II) dichloride (63.0 mg, 0.13 mmol) were refluxed in 3:1 ethanol-water for 48 hours. After cooling the solvent was

removed *in vacuo*, the residue dissolved in water and filtered. The resulting red solution was treated with an excess of ammonium hexafluorophosphate to give a red precipitate. The solid was chromatographed on alumina with 1:9 mixture of methanol-dichloromethane. The bright red band was recrystallised from methanol to give red crystals. Yield 47 mg (75%). M.p. 237-239°C. Analysis: calc. for $C_{42}H_{34}N_8F_{12}P_2Ru$ C 48.42, H 3.29, N 10.76; found C 48.37, H 3.35, N 10.87%. HRMS: calc. for $C_{42}H_{34}N_8F_{12}P_2Ru$ 897.1592, found 897.1586. $^1$H NMR ($CD_3CN$) δ 10.27 (d, 1H, bpyH6A), 8.72 (d, 1H, bpyH3B), 8.68 (d, 1H, bpyH3C), 8.59 (d, 1H, H6), 8.53 (d, 1H, bpyH3A), 8.40 (d, 1H, bpyH3D), 8.28 (t, 1H, bpyH4A), 8.21 (d, 1H, bpyH6C), 8.17 (t, 1H, bpyH4B), 8.09 (t, 1H, bpyH4C), 8.03 (t, 1H, bpyH4D), 7.95 (t, 1H, bpyH5A), 7.91 (d, 1H, H6'), 7.88 (d, 1H, H6"), 7.83 (m, 1H, H4), 7.81 (m, 1H, H3), 7.72 (t, 1H, H4'), 7.67 (m, 2H, H3', bpyH6D), 7.54 (t, 2H, H4", H4"'), 7.45 (m, 3H, H3"', bpyH5D, bpyH5C), 7.33 (m, 2H, bpyH5B, H3"), 7.20 (t, 1H, H5), 7.13 (m, 2H, H6"', H5'), 6.97 (dd, 1H, H5"), 6.91 (d, 1H, bpyH6B), 6.75 (t, 1H, H5"'), 6.71 (d, 1H, CH), 5.90 (d, 1H, CH).

With bis(4,4'-dimethyl-2,2'-bipyridine)ruthenium(II) dichloride, *viz* **2.53**

Ligand **2.2** (20.1 mg, 0.059 mmol) and bis(2,2'-bipyridine)ruthenium(II) dichloride (67.0 mg, 0.124 mmol) were refluxed in 3:1 ethanol-water for 48 hours. After cooling the solvent was removed *in vacuo*, the residue dissolved in water and filtered. The resulting red solution was treated with an excess of ammonium hexafluorophosphate to give a red precipitate. The solid was purified on alumina with 1:9 mixture of methanol-dichloromethane to give a red-black solid. Yield 36.7 mg (57%). M.p. 235-238°C. Analysis: calc. for $C_{46}H_{42}N_8F_{12}P_2Ru.H_2O$ C 49.51, H 3.97, N 10.04; found C 49.30, H 3.89, N 9.80%. $^1$H NMR ($CD_3CN$) δ 10.06 (d, 1H, dmbH6A), 8.59 (d, 1H, H6), 8.56 (s, 1H, dmbH3C), 8.52 (s, 1H, dmbH3D), 8.39 (s, 1H, dmbH3A), 8.25 (s, 1H, dmbH3B), 7.97 (d, 1H, dmbH6D), 7.90 (m, 2H, H6', H6"), 7.79 (m, 3H, dmbH5A, H4, H3), 7.66 (m, 2H, H4", H3"), 7.52 (m, 2H, H4', H4"'), 7.45 (m, 2H, dmbH6B, H3"'), 7.27 (m, 3H, dmbH5D, dmbH5B, H3'), 7.21 (t, 1H, H5'), 7.11 (m, 3H, dmbH5C, H5", H6"'), 6.98 (dd, 1H, H5'), 6.73 (m, 2H, dmbH6C, H5"'), 6.67 (d, 1H, CH), 5.89 (d, 1H, CH), 2.71 (dmbMeA), 2.62 (dmbMeC), 2.58 (dmbMeD), 2.53 (dmbMeB).

### 6.3.3 Complexes of 2.3

With silver nitrate, *viz* **2.29**

Ligand **2.3** (10.2 mg, 0.029 mmol) and silver nitrate (10.0 mg, 0.059 mmol) were both dissolved in warm methanol, the solutions mixed and on standing for several days colourless crystals formed. Recrystallisation from methanol gave larger crystals suitable for crystal structure

analysis. Yield 8.4 mg (88%). M.p. 171-173°C (dec.). Analysis: calc. for $C_{11}H_{10}N_3O_3Ag.H_2O$ C 37.85, H 3.18, N 12.04; C 37.75, H 2.21, N 11.77%.

With palladium chloride, *viz* **2.30**

Palladium chloride (9.6 mg, 0.059 mmol) was dissolved in hot 2 M hydrochloric acid and added dropwise to a methanol solution of **2.3** (10.0 mg, 0.028 mmol). Yellow crystals, suitable for X-ray crystallography, formed during slow evaporation of the reaction mixture. Yield 10.3 mg (88%). M.p. 276°C (dec.). Analysis: calc. for $C_{12}H_{12}N_2O_2Cl_2Pd$ C 36.62, H 3.07, N 7.12; found C 36.88, H 2.77, N 7.39%. $^1$H NMR (DMSO) δ 9.19 (d, 2H, H6), 8.46 (t, 2H, H4), 8.27 (d, 2H, H3), 8.01 (t, 2H, H4), 3.27 (s, 3H, $CH_3$).

With copper nitrate, *viz* **2.31/2.32**

Methanol solutions of **2.3** (10.2 mg, 0.029 mmol) and copper nitrate (13.7 mg, 0.057 mmol) were mixed and left to slowly evaporate. The blue precipitate that resulted was dissolved in acetonitrile and vapour diffusion of ether into this solution gave a mixture of purple (**2.31**) and blue crystals (**2.32**). Both sets of crystals were suitable for X-ray crystallography. Combined yield: 11.4 mg (66%). M.p. 270°C (dec.) (**2.31**); 246-248°C (dec.) (**2.32**). Analysis: calc. for $C_{22}H_{20}N_6O_{10}Cu.H_2O$ C 43.61, H 2.99, N 13.87; C 37.96, H 2.90, N 14.17%.

With bis(2,2'bipyridine)ruthenium(II) dichloride, *viz* **2.54**

Bis(2,2'-bipyridine)ruthenium(II) dichloride (18 mg, 0.037 mmol) and **2.3** (6.8 mg, 0.019 mmol) were refluxed in degassed 3:1 ethanol-water solution (8 ml) for 48 hours. This was taken to dryness *in vacuo*, redissolved in water, filtered and the complex precipitated with an excess of ammonium hexafluorophosphate. The crude product was purified to give the major component, **2.54**, as a dark red solid. Yield 8.3 mg (49%). M.p. 314-316°C. HRMS: calc. for $C_{31}H_{24}N_6OF_6PRu$ 743.0697; found 743.0693. $^1$H NMR ($CD_3CN$) δ 8.57 (d, 2H, H3A), 8.49 (d, 2H, H3B), 8.24 (d, 2H, H6A), 8.28 (d, 2H, H3), 8.24 (t, 2H, H4A), 8.13 (t, 2H, H4), 8.08 (t, 2H, H4B), 7.80 (d, 2H, H6), 7.75 (d, 2H, H6B), 7.66 (dd, 2H, H5A), 7.43 (m, 4H, H5, H5B). The second component was identified as **2.50**.

### 6.3.4 Complexes of 2.4

With copper nitrate, *viz* **2.33**

Ligand **2.4** (5.8 mg, 0.017 mmol) and copper nitrate (8.8 mg, 0.036 mmol) were both dissolved in hot methanol and the solutions combined. During slow evaporation of the methanol reaction

mixture, small blue crystals formed that were suitable for X-ray crystallography. Yield 10.5 mg (83%). M.p. >278°C (dec.). Analysis: calc. for $C_{22}H_{16}N_8O_{12}Cu_2.2H_2O$ C 35.35, H 2.70, N 14.99; found C 35.42, H 2.80, N 14.71%.

With palladium chloride, *viz* **2.34**

Palladium chloride (10.5 mg, 0.059 mmol) was dissolved in 2 mL of 2 M hydrochloric acid and added slowly to a hot methanolic solution of **2.4** (10.0 mg, 0.030 mmol). The solution turned yellow and a fine yellow solid precipitated immediately. This was collected by filtration and dried *in vacuo*. Yield 12 mg (56%). M.p. >330°C. Analysis: calc. for $C_{22}H_{16}N_4Cl_4Pd_2.1½H_2O$ C 36.80, H 2.67, N 7.80; found C 36.46, H 2.08, N 7.81%. $^1$H NMR (DMSO) δ 9.07 (d, 4H, H6), 8.17 (t, 4H, H4), 7.54 (t, 4H, H5), 7.49 (d, 4H, H3).

With palladium acetate, *viz* **2.35**

Palladium acetate (13.5 mg, 0.06 mmol) dissolved in hot methanol was added to a methanolic solution of **2.4** (10.1 mg, 0.03 mmol). During slow evaporation of the resulting solution, initially a black precipitate formed that was removed by filtration, followed by yellow crystals that were suitable for X-ray crystallography. Yield 11 mg (44%). M.p. 235-38°C. Analysis: calc. for $C_{30}H_{28}N_4O_8Pd_2.3H_2O$ C 42.93, H 4.08, N 6.67; found C 43.20, H 4.09, N 6.75%.

With zinc acetate, *viz* **2.36**

Two colourless solutions of **2.4** (10.0 mg, 0.03 mmol) and zinc acetate (12.9 mg, 0.059 mmol) dissolved in methanol were mixed to give a white crystalline precipitate. The precipitate was filtered off and the filtrate allowed to slowly evaporate giving large colourless crystals, suitable for a crystal structure determination. Yield 19 mg (90%). M.p. >269°C (dec.). Analysis: calc. for $C_{30}H_{28}N_4O_8Zn_2$ C 51.23, H 4.01, N 7.97; found C 50.92, H 3.93, N 8.03%.

With bis(2,2'-bipyridine)ruthenium(II) dichloride, *viz* **2.55**

***Method A:*** Ligand **2.4** (10.9 mg, 0.032 mmol) and bis(2,2'-bipyridine)ruthenium(II) dichloride (33.6 mg, 0.069 mmol) were refluxed in 3:1 ethanol-water for 48 hours. Silver nitrate was added to precipitate chloride anions. After cooling, the silver chloride was removed by filtration, the solvent removed *in vacuo*, the residue redissolved in water and filtered. The resulting red solution was treated with an excess of ammonium hexafluorophosphate to give a red/orange precipitate. The solid was chromatographed on alumina with 1:9 solution of methanol-dichloromethane. The bright red band was recrystallised from methanol to give red crystals. Yield 22.9 mg (69%).

*Method B (synthesis carried out by D. M. D'Alessandro, James Cook University):* A suspension of bis(2,2'-bipyridine)ruthenium(II) dichloride (40.2 mg, 0.0773 mmol) and **2.4** (6.5 mg, 0.0193 mmol) in ethylene glycol (0.5 mL) was heated at reflux in a modified microwave oven (Sharp Model R-2V55; 600 W, 2450 MHz) on high power for 45 min. Upon cooling, the resultant red/brown solution was diluted with distilled water (10 mL) and loaded onto a column (approximately 15 cm long × 2 cm in diameter) of SP Sepharose Fast Flow cation exchanger. Separation of the products from the crude mixture was achieved via a gradient elution procedure using aqueous 0.1-0.5 $molL^{-1}$ NaCl as the eluent. Three bands were subsequently eluted: these were Band 1 (dark purple, 0.1 $molL^{-1}$ NaCl), Band 2 (orange, 0.2 $molL^{-1}$ NaCl) and Band 3 (brown, 0.4 $molL^{-1}$ NaCl). On addition of a saturated solution of aqueous $KPF_6$ to each band, the products were extracted into dichloromethane and the solvent removed *in vacuo*. The solid residues were dissolved in a minimum volume of acetone and loaded onto a short column of silica gel (2 cm × 2 cm), washed with acetone, water and acetone and then eluted with acetone containing 5% $NH_4PF_6$. Addition of water and removal of the acetone under reduced pressure afforded the pure **2.55** (Band 2). Yield 10.5 mg (52%). Band 1 was identified as unreacted starting material, while band 3 was thought, but not confirmed, to be a dinuclear compound.
M.p. >318°C (dec.). Analysis: calc. for $C_{42}H_{32}N_8F_{12}P_2Ru$ C 48.52, H 3.10, N 10.78; found C 48.29, H 3.06, N 10.58%. HRMS: calc. for $C_{42}H_{32}N_8F_6PRu$ 895.1435, found 895.1463. $^1H$ NMR ($CD_3CN$) δ 10.43 (d, 1H, bpyH6A), 8.74 (d, 1H, bpyH3C), 8.67 (d, 1H, bpyH3D), 8.52 (d, 1H, H6), 8.45 (m, 2H, bpyH3A, H6'), 8.40 (d, 1H, bpyH3B), 8.31 (d, 1H, H3'), 8.21 (t, 1H, bpyH4C), 8.09 (t, 1H, bpyH4D), 8.02 (m, 3H, bpyH6D, bpyH4B, H6'''), 7.97 (m, 2H, bpyH4A, H4'), 7.63 (d, 1H, bpyH6B), 7.53 (m, 3H, bpyH6C, H4", H4'''), 7.43 (m, 4H, bpyH5B, bpyH5C, bpyH5D, H5'), 7.31 (m, 4H, bpyH5A, H4', H3", H3'''), 7.17 (m, 3H, H5, H6", H5'''), 6.88 (t, 1H, H5"), 5.56 (d, 1H, H3').

With bis(4,4'-dimethyl-2,2'-bipyridine)ruthenium(II) dichloride, *viz* **2.56**

The ligand, **2.4**, (11.0 mg, 0.033 mmol) and bis(2,2'-bipyridine)ruthenium(II) dichloride (38.1 mg, 0.070 mmol) were refluxed in 3:1 ethanol-water for 48 hours. After cooling the solvent was removed *in vacuo*, the residue dissolved in water and filtered. The resulting red solution was treated with an excess of ammonium hexafluorophosphate to give a red precipitate. The solid was purified on alumina with 1:19 solution of methanol-dichloromethane to give a red solid. Yield 25.6 mg (71%). M.p. 211-214°C. Analysis: calc. for $C_{46}H_{40}N_8F_{12}P_2Ru$ C 49.51, H 3.97, N 10.04; found C 49.30, H 3.89, N 9.80%. HRMS: calc. for $C_{46}H_{42}N_8F_6PRu$ 951.2061, found 951.2044. $^1H$ NMR ($CD_3CN$) δ 10.26 (d, 1H, dmbH6C), 8.60 (s, 1H, dmbH3A), 8.56 (d, 1H,

H6), 8.54 (s, 1H, dmbH3B), 8.45 (d, 1H, H6'), 8.34 (d, 1H, H3'), 8.31 (s, 1H, dmbH3C), 8.25 (s, 1H, dmbH3D), 8.02 (d, 1H, H6"), 7.96 (t, 1H, H4'), 7.85 (d, 1H, dmbH6B), 7.53 (t, 1H, H4"), 7.48 (t, 1H, H4'"), 7.45 (d, 1H, dmbH6D), 7.37 (m, 2H, dmbH6A, H5'), 7.27 (m, 6H, dmbH5A, dmbH5B, dmbH5D, H4, H3", H3'"), 7.17 (m, 4H, dmbH5C, H5, H5", H6'"), 6.87 (t, 1H, H5'") 5.51 (d, 1H, H3), 2.66 (dmbMeA), 2.58 (dmbMeB), 2.54 (dmbMeD), 2.43 (dmbMeC).

### 6.3.5 Complexes of 2.5

With silver nitrate, *viz* **2.37**

The ligand, **2.5**, (10.2 mg, 0.03 mmol) in methanol was reacted with silver nitrate (10.6 mg, 0.062 mmol) dissolved in hot methanol. Slow evaporation of the resulting solution gave unstable colourless block shaped crystals, which were suitable for X-ray crystallography. Yield 11.3mg (66%). M.p. 143-146°C. Analysis: calc. for $C_{24}H_{20}N_3O_3Ag$ C 56.93, H 3.98, N 8.30; found C 52.36, H 3.74, N 8.32%.

With copper nitrate, *viz* **2.38**

Copper nitrate (15.0 mg, 0.062 mmol) and **2.5** (10.1 mg, 0.03 mmol) were both dissolved in methanol and the solutions mixed. Slow evaporation of the reaction mixture gave a mixture of blue plate and rod shaped crystals. The crystals with the plate morphology were suitable for X-ray crystallography. Yield 14.3 mg (90%). M.p. 242-245°C (dec.). Analysis: calc. for $C_{50}H_{46}N_6O_8Cu_2.4H_2O$ C 56.76, H 5.14, N 7.94; found C 55.99, H 4.86, N 7.67%.

### 6.3.6 Complexes of 2.8

With silver nitrate, *viz* **2.39**

Ligand **2.8** (20.6 mg, 0.056 mmol) was dissolved in methanol and reacted with silver nitrate (20.2 mg, 0.112 mmol) also dissolved in methanol. Slow evaporation of the resulting solution gave a yellow crystalline precipitate, which contained some yellow crystals suitable for X-ray crystallography. Yield 20.3 mg (51%). M.p. 235°C. Analysis: calc. for $C_{22}H_{16}N_8O_6Ag_2$ C 37.53, H 2.29, N 15.91; found C 37.09, H 2.31, N 15.72%.

With copper nitrate, *viz* **2.40**

Copper nitrate (27.7 mg, 0.115 mmol) and **2.8** (20.5 mg, 0.056 mmol) were both dissolved in methanol and mixed together. Slow evaporation initially gave green crystals (**2.40**), followed by blue crystals (**2.32**), when the solution was evaporated to dryness. Both sets of crystals were suitable for X-ray crystallography. Complex **2.40**: Yield 8.3 mg (51%). M.p. 257°C (dec.).

Analysis: calc. for $C_{22}H_{18}N_{10}O_6Cu$ C 45.56, H 2.78, N 24.15; found C 45.79, H 2.76, N 23.74%. Complex **2.32**: Yield 4.6 mg (26%). M.p. 254-256°C (dec.).

With palladium chloride, *viz* **2.41**

Palladium chloride (21.3 mg, 0.120 mmol) was dissolved in 2 M hydrochloric acid (5 mL) and added slowly to a hot methanolic solution of **2.8** (20.1 mg, 0.055 mmol). The solution turned yellow and a red-orange solid precipitated immediately. This was collected by filtration and dried *in vacuo*. Yield 21.0 mg (49%). M.p. >220°C (dec.). Analysis: calc. for $C_{22}H_{16}N_6Cl_4Pd_2.3H_2O$ C 34.18, H 2.87, N 10.87; found C 33.85, H 2.51, N 10.40%. Red crystals of a second palladium complex formed in the filtrate and were shown, by X-ray crystallography, to be a palladium complex of a decomposition product.

### 6.3.7 Complexes of 2.14

With silver nitrate, *viz* **2.42**

Ligand **2.14** (12 mg, 0.022 mmol) and silver nitrate (13 mg, 0.077 mmol) were both dissolved in hot acetonitrile, the solutions combined and left to cool. Crystalline material deposited overnight providing crystals suitable for X-ray crystallography. Yield 16 mg (79%). M.p. 278-279°C. Analysis: calc. for $C_{36}H_{24}N_8O_6Ag_2.2H_2O$ C 47.18, H 3.08, N 12.23; found C 47.15, H 2.92, N 11.97%. $^1$H NMR (DMSO-$d_6$) δ 8.18 (d, 6H, H6), 7.32 (t, 6H, H4), 7.27 (dd, 6H, H5) 6.96 (d, 6H, H3).

With silver hexafluorophosphate, *viz* **2.43**

The ligand, **2.14** (5.1 mg, 0.009 mmol) was dissolved in dichloromethane. A methanolic solution of silver hexafluorophosphate (7.4 mg, 0.029 mmol) was layered overtop and the solutions left to equilibrate. Overnight a fine yellow powder precipitated from this solution (yield 10.3 mg). The solid was recrystallised by vapour diffusion of methanol into an acetonitrile solution of the complex, which yielded large red blocks suitable for X-ray crystallography. M.p. 271-273°C (dec.). Analysis: calc. for $C_{36}H_{24}Ag_2F_{12}N_6P_2.CH_3CN$ C 41.98, H 2.50, N 9.02; found C 42.65, H 2.56, N 8.92%. $^1$H NMR ($CD_3CN$) δ 8.90 (d, 6H, H6), 7.40 (t, 6H, H4), 7.27 (dd, 6H, H5), 6.97 (d, 6H, H3).

With silver tetrafluoroborate, *viz* **2.44**

Ligand **2.14** (13.5 mg, 0.025 mmol) was dissolved in dichloromethane and a methanol solution of silver tetrafluoroborate (15.0 mg, 0.078 mmol) was layered overtop. Mixing by diffusion over

several days, followed by slow evaporation, of the reaction mixture resulted in the formation of orange crystals, suitable for X-ray crystallography. Yield 18.9 mg (64%). M.p. >250°C (dec.). ES-MS 1578.5 ($[Ag_3(\mathbf{2.14})_2](BF_4)_2^+$), 1423.4 ($[Ag_3(\mathbf{2.14})_2F]^{2+}$), 1383.2 ($[Ag_2(\mathbf{2.14})_2](BF_4)^+$), 647.1 ($[Ag_2(\mathbf{2.14})_2]^{2+}$). 541.2 (**2.14**). $^1$H NMR ($CD_3CN$) δ 8.09 (d, 6H, H6), 7.39 (t, 6H, H4), 7.26 (dd, 6H, H5), 6.97 (d, 6H, H3). $^{13}$C NMR ($CD_3CN$) δ 161.5, 156.9, 149.9, 137.2, 128.0, 126.7, 124.7, 123.8.

With bis(2,2'-bipyridine)ruthenium(II) dichloride, *viz* **2.57/2.58** *(reaction carried out by D. M. D'Alessandro, James Cook University)*

A suspension of bis(2,2'-bipyridine)ruthenium(II) dichloride (19.3 mg, 0.037 mmol) and **2.14** (5.0 mg, 0.009 mmol) in ethylene glycol (0.5 mL) was heated at reflux in a modified microwave oven (Sharp Model R-2V55; 600 W, 2450 MHz) on high power for 25 min. Upon cooling, the resultant green/brown solution was diluted with distilled water (10 mL) and loaded onto a column (approximately 15 cm long × 2 cm in diameter) of SP Sepharose Fast Flow cation exchanger. Separation of the mononuclear and dinuclear products from the crude mixture was achieved via a gradient elution procedure using aqueous 0.1-0.5 $molL^{-1}$ NaCl as the eluent. Four bands were eluted: Band 1 (light red, 0.2 $molL^{-1}$ NaCl), Band 2 (purple, 0.3 $molL^{-1}$ NaCl), Band 3 (green, 0.4 $molL^{-1}$ NaCl) and Band 4 (green, 0.4 $molL^{-1}$ NaCl). On addition of a saturated solution of aqueous $KPF_6$ to each band, the products were extracted into dichloromethane and the solvent removed *in vacuo*. The solid residues were dissolved in a minimum volume of acetone and loaded onto a short column of silica gel (2 cm × 2 cm), washed with acetone, water and acetone and then eluted with acetone containing 5% $NH_4PF_6$. Addition of water and removal of the acetone under reduced pressure afforded the pure products. The electronic absorption spectra of the four bands in $CH_3CN$ permitted the identification of Band 2 as unreacted $[Ru(bpy)_2Cl_2]$ precursor, while the composition of Bands 1, 3 and 4 were established by ES-MS. Analysis of Band 1 revealed the presence of two mononuclear ruthenium species: a major species, $[Ru(bpy)_2L]^{2+}$ (L = di-2-pyridylketone), and a minor species (L = di-2-pyridylketone ethylene acetyl). Bands 3 and 4 were identified as the diastereoisomeric forms of $[\{Ru(bpy)_2\}_2(\mathbf{2.14})](PF_6)_4$. Yields: Band 3 (**2.57**), 3.5 mg (19%); Band 4 (**2.58**), 3.2 mg (18%). Complex **2.57**: ES-MS 829.1 (24%, $[\{Ru(bpy)_2\}_2(\mathbf{2.14})](PF_6)_2^{2+}$), 504.4 (100%, $[\{Ru(bpy)_2\}_2(\mathbf{2.14})](PF_6)^{3+}$), 342.0 (73%, $[\{Ru(bpy)_2\}_2(\mathbf{2.14})]^{4+}$). $^1$H NMR ($CD_3CN$) δ 10.00 (d, 1H, bpyH6A), 8.93 (d, 1H, bpyH3B), 8.85 (d, 1H, bpyH3C), 8.78, m, 2H, H6)), 8.71 (d, 1H, bpyH3D), 8.54 (m, 2H, bpyH3B, bpyH3F), 8.38 (d, 1H, bpyH3E), 8.34-8.10 (m, 10H, bpyH3A, bpyH4B, bpyH4C, bpyH4D, bpyH4F, bpyH4G, bpyH4H, bpyH6D, bpyH6H, H6'), 8.07 (t, 1H,

bpyH4E), 7.98 (d, 1H, bpyH6C), 7.88-7.82 (m, 3H, bpyH6G, H4, H6"'), 7.80 (t, 1H, bpyH4A), 7.76-7.66 (m, 4H, bpyH5B, bpyH3E, bpyH3F, H6), 7.64, t, 1H, bpyH5A), 7.58 (t, 1H, bpyH5C), 7.55-7.40 (m, 7H, bpyH5D, bpyH5E, bpyH5F, bpyH5G, bpyH5H, H3, H4'), 7.31 (dd, 1H, H5), 7.25, t, 1H, H5'), 7.17 (d, 1H, H6""), 7.15 (d, 1H, H6"), 7.13-7.06 (m, 2H, H3'), 7.05 (t, 1H, H5"'), 7.00 (d, 1H, H3""), 6.99 (t, 1H, H5""), 6.89-6.84 (m, 2H, H4"', H4""), 6.70 (t, 1H, H5"), 6.54 (d, 1H, H3"'), 6.37 (t, 1H, H4"), 4.93 (d, 1H, H3").

Complex **2.58**: ES-MS 829.1 (43%, $[\{Ru(bpy)_2\}_2(\mathbf{2.14})](PF_6)_2^{2+}$), 504.4 (100%, $[\{Ru(bpy)_2\}_2(\mathbf{2.14})](PF_6)^{3+}$), 342.0 (42%, $[\{Ru(bpy)_2\}_2(\mathbf{2.14})]^{4+}$). $^1$H NMR ($CD_3CN$) δ 9.73 (d, 2H, H6A), 8.81 (d, 2H, H3C), 8.73 (d, 2H, H3D), 8.43 (d, 2H, H3B), 8.40 (d, 2H, H3A), 8.28 (d, 2H, H4C), 8.16-8.13 (m, 4H, H4D, H6D), 8.08 (t, 2H, H4B), 7.96 (m, 4H, H4A, H4"), 7.91 (m, 6H, H6C, H6, H6"), 7.75-7.65 (m, 6H, H5A, H6B, H3"), 7.51 (m, 4H, H5B, H5C), 7.47 (t, 2H, H5D), 7.38 (t, 2H, H5"), 7.13 (d, 2H, H6'), 6.95 (t, 2H, H5'), 6.90-6.83 (m, 6H, H3', H4', H5), 6.27 (t, 2H, H4), 4.69 (d, 2H, H3).

### 6.3.8 Complexes of 2.15

With silver nitrate, *viz* **2.45**

Ligand **2.15** (13 mg, 0.024 mmol) was dissolved in dichloromethane and overlaid with a methanol solution of silver nitrate (12.3 mg, 0.072 mmol). Slow evaporation of the resulting solution gave orange crystalline material. Yield 16.7 mg (57%). M.p. >198°C (dec.). Analysis: calc. for $C_{36}H_{24}N_{10}O_{12}Ag_4$ C 35.44, H 1.98, N 11.48; found C 35.67, H 2.34, N 11.15%.

With silver tetrafluoroborate, *viz* **2.46**

Ligand **2.15** (12 mg, 0.023 mmol) was dissolved in dichloromethane and overlaid with a methanol solution of silver tetrafluoroborate (13.0 mg, 0.067 mmol). Slow mixing by diffusion over several days, followed by evaporation of the resulting solution led in the formation of an orange precipitate. Yield 22 mg (79%). M.p. >255°C (dec.). Analysis: calc. for $C_{36}H_{24}N_6B_3F_{12}Ag_3.4H_2O$ C 36.13, H 2.70, N 7.02; found C 34.29, H 2.55, N 6.99%.

With silver hexafluorophosphate, *viz* **2.47**

The ligand, **2.15**, (14 mg, 0.026 mmol) was dissolved in dichloromethane. This was overlaid with a methanolic solution of silver hexafluorophosphate (19.5 mg, 0.077 mmol) and the solutions left to equilibrate. After several days a fine orange powder precipitated from this solution. Yield 23 mg (73%). M.p. >204°C (dec.). Analysis: calc. for $C_{72}H_{48}N_{12}P_5F_{30}Ag_5.4H_2O$ C 35.77, H 2.33, N 6.95; found C 35.53, H 2.76, N 7.30%.

With bis(acetonitrile)palladium dichloride, *viz* **2.48**

Ligand **2.15** (9.9 mg, 0.018 mmol) was dissolved in dichloromethane. A acetonitrile solution of bis(acetonitrile)palladium dichloride (30.0 mg, 0.118mmol) was added to give an orange-red precipitate, which was refluxed for 24 hours. The precipitate was collected, washed with methanol and dried *in vacuo*. Yield 20.5 mg (91%). M.p. >280°C (dec.). Analysis: calc. for $C_{36}H_{24}N_6Cl_8Pd_4$ C 34.59, H 1.94, N 6.72; found C 35.12, H 2.36, N 6.66%.

### 6.3.9 Complex of 2.17/2.18

With silver nitrate, *viz* **2.49**

A mixture of the isomeric ligands **2.17/2.18** (10.6 mg, 0.014 mmol) were dissolved in dichloromethane and overlaid with a methanol solution of silver nitrate (10.2 mg, 0.060 mmol). Slow evaporation of the resulting solution gave crystalline material. Yield 15 mg (64%). M.p. 215-217°C (dec.). Analysis: calc. for $C_{78}H_{58}N_{11}O_{15}Ag_5.H_2O$ C 48.12, H 3.11, N 7.91; found C 48.02, H 2.87, N 7.81%.

## 6.4. Preparation of complexes with the di-2-pyridylamine-based ligands

### 6.4.1 Complexes of 3.2

With silver nitrate, *viz* **3.20**

Both **3.2** (20.0 mg, 0.048 mmol) and silver nitrate (15.9 mg, 0.093 mmol) were dissolved in hot acetonitrile, the solutions combined and allowed to cool. Crystalline material precipitated overnight, which contained crystals suitable for X-ray crystallography. Yield 22 mg (78%). M.p. 235°C (dec.). Analysis: calc. for $C_{26}H_{20}N_7O_3Ag$ C 53.26, H 3.44, N 16.72; found C 53.56, H 3.53, N 16.87%.

With silver tetrafluoroborate, *viz* **3.21**

Both **3.2** (20.0 mg, 0.048 mmol) and silver tetrafluoroborate (21.1 mg, 0.108 mmol) were dissolved in hot acetonitrile, the solutions combined and allowed to slowly evaporate. Small plate-like crystals were obtained, which were suitable for X-ray crystallography. Yield 34 mg (76%). M.p. >120°C (dec.). Analysis: calc. for $C_{30}H_{26}N_8B_2F_8Ag_2.3CH_3CN$ C 33.62, 2.17, 9.05; found C 33.76, H 2.01, N 9.44%.

With palladium chloride, *viz* **3.22**

Palladium chloride (17.1 mg, 0.096 mmol) was dissolved in 2 M hydrochloric acid (2 mL) and added slowly to a hot methanolic solution of **3.2** (20.1 mg, 0.048 mmol). The solution turned yellow and a fine yellow solid precipitated. After heating for 30 minutes, the precipitate was collected by filtration and dried *in vacuo*. Yield 34 mg (92%). M.p. >330°C. Analysis: calc. for $C_{26}H_{20}N_6Cl_4Pd_2$ C 40.50, H 2.61, N 10.90; found C 40.50, H 2.69, N 10.76%. The complex was insoluble in common NMR solvents.

With copper nitrate, *viz* **3.23**

Ligand **3.2** (20.2 mg, 0.043 mmol) and copper nitrate (25.1 mg, 0.104 mmol) were both dissolved in methanol and combined. Slow evaporation of the resulting solution gave a green precipitate. Yield 32 mg (83%). M.p. >282°C (dec.). Analysis: calc. for $C_{26}H_{20}N_{10}O_{12}Cu_2.CH_3OH$ C 40.25, H 2.89, N 16.76; found C 39.85, H 2.90, N 17.12%. Crystals, suitable for X-ray crystallography, were obtained by vapour diffusion of acetone into a DMSO solution of the complex.

With zinc acetate, *viz* **3.24**

Ligand **3.2** (20.0 mg, 0.048 mmol) and zinc acetate (22.2 mg, 0.100 mmol) were dissolved in methanol, the solutions combined and left to slowly evaporate. This gave colourless crystalline plates suitable for X-ray crystallography. X-ray crystal structure analysis revealed that contamination with chloride ions had occurred, although this was not confirmed by analysis. Yield 10.6 mg (28%). M.p. 194-196°C. Analysis: calc. for $C_{34}H_{32}N_6O_8Zn_2$ C 52.13, H 4.12, N 10.73; found C 51.82, H 3.41, N 13.83%.

With bis(2,2'-bipyridine)ruthenium(II) dichloride, *viz* **3.62**

Ligand **3.2** (20 mg, 0.048 mmol) and bis(2,2'-bipyridine)ruthenium(II) dichloride (59 mg, 0.12 mmol) were refluxed in 3:1 ethanol-water for 72 hours. After cooling the solvent was removed *in vacuo* and the residue redissolved in water and filtered. The resulting red solution was treated with an excess of ammonium hexafluorophosphate to give a red precipitate of **3.62** as a 1:1 mixture of the two diastereoisomers. Yield 81 mg (93%). M.p. 207-211°C. Analysis: calc. for $C_{66}H_{52}N_{14}F_{24}P_4Ru_2.H_2O$ C 43.05, H 2.96, N 10.65; found C 42.71, H 2.51, N 10.27%. $^1$H NMR ($CD_3CN$) δ 8.61 (d, 4H, bpyH3A), 8.60 (d, 4H, bpyH3A*), 8.53 (d, 8H, bpyH3B/B*), 8.42 (d, 8H, bpyH6A/A*), 8.20 (t, 4H, bpyH4A), 8.18 (t, 4H, bpyH4A*), 8.05 (t, 8H, bpyH4B/B*), 7.95 (t, 4H, H4'), 7.93 (t, 4H, H4'*), 7.75 (d, 8H, bpyH6B/B*), 7.58 (d, 8H, H6', H6'*), 7.53 (dd, 4H, bpyH5A), 7.52 (dd, 4H, bpyH5A*), 7.48 (d, 4H, H3'), 7.47 (d, 4H, H3'*), 7.40 (t, 8H,

bpyH5B/B*), 7.11 (s, 4H, H2/H3/H5/H6), 7.09 (s, 4H, H2*/H3*/H5*/H6*), 7.06 (t, 4H, H5'), 7.05 (t, 4H, H5'*).

With bis(4,4'-dimethyl-2,2'-bipyridine)ruthenium(II) dichloride, *viz* **3.63**

Ligand **3.2** (21.1 mg, 0.051 mmol) and bis(4,4'-dimethyl-2,2'-bipyridine)ruthenium(II) dichloride (59.6 mg, 0.110 mmol) were refluxed in 3:1 ethanol-water for 72 hours. After cooling the solvent was removed *in vacuo* and the residue redissolved in water and filtered. The resulting red solution was treated with an excess of ammonium hexafluorophosphate to give a red precipitate, which was purified on alumina to give **3.63** as a 1:1 mixture of the two diastereoisomers. Yield 59.8 mg (61%). M.p. 265-268°C. Analysis: calc. for $C_{74}H_{68}N_{14}F_{24}P_4Ru_2$ C 45.92, H 3.54, N 10.13; found C 46.40, H 3.66, N 9.85%. $^1$H NMR ($CD_3CN$) δ 8.46 (s, 4H, dmbH3A), 8.45 (s, 4H, dmbH3A*), 8.37 (s, 8H, dmbH3B/B*), 8.26 (d, 8H, dmbH6A/A*), 7.89 (m, 8H, H4', H4'*), 7.57 (m, 8H, H6', H6'*), 7.55 (d, 8H, dmbH6B/B*), 7.43 (m, 4H, H3', H3'*), 7.37 (m, 8H, dmbH5A/A*), 7.23 (d, 8H, dmbH5B/B*), 7.20 (s, 4H, H2/H3/H5/H6), 7.18 (s, 4H, H2*/H3*/H5*/H6*), 7.01 (t, 4H, H5', H5'*), 2.64 (s, 12H, dmbMeA), 2.58 (s, 12H, dmbMeA*), 2.55 (s, 24H, dmbMeB/B*).

### 6.4.2 Complexes of 3.3

With palladium chloride, *viz* **3.25**

Palladium chloride (14.6 mg, 0.082 mmol) was dissolved in 2 M hydrochloric acid (2 mL) and added to a methanol solution of **3.3** (20.0 mg, 0.043 mmol). Immediately a pale yellow precipitate formed, which was collected and dried *in vacuo*. Yield 30.0 mg (79%). M.p. 218-220°C (dec.). Analysis: calc. for $C_{32}H_{24}N_6Cl_4Pd_2$.MeOH C 45.08, H 3.21, N 9.56; found C 46.46, H 2.89, N 7.96%.

With bis(2,2'-bipyridine)ruthenium(II) dichloride, *viz* **3.64**

Ligand **3.3** (20.0 mg, 0.044 mmol) and bis(2,2'-bipyridine)ruthenium(II) dichloride (50.0 mg, 0.103 mmol) were refluxed in 3:1 ethanol-water for 48 hours. After cooling, the solvent was removed *in vacuo*, the residue redissolved in water and filtered. The resulting red solution was treated with an excess of ammonium hexafluorophosphate to give a red precipitate of **3.64**, as a 1:1 mixture of the two diastereoisomers, that was purified on alumina eluting with 1:19 methanol-dichloromethane solution. Yield 55.7 mg (66%). M.p. 234-238°C. Analysis: calc. for $C_{72}H_{56}N_{14}F_{24}P_4Ru_2$ C 45.53, H 2.97, N 10.32; found C 45.84, H 3.12, N 9.82%. $^1$H NMR ($CD_3CN$) δ 8.60 (d, 4H, bpyH3A), 8.57 (d, 4H, bpyH3A*), 8.51 (m, 8H, bpyH3B/B*), 8.46 (d,

4H, bpyH6A), 8.41 (d, 4H, bpyH6A*), 8.16 (m, 8H, bpyH4A/A*), 8.04 (m, 8H, bpyH4B/B*), 7.85 (m, 12H, H4', H4'*, H2/H6), 7.75 (m, 12H, bpyH6B/B*, H2/H6*), 7.55 (m, 8H, H6', H6'*), 7.51 (t, 4H, bpyH5A), 7.45 (m, 12H, bpyH5A*, H6'*, H6'), 7.39 (m, 8H, bpyH5B/B*), 7.21 (d, 4H, H3/H5), 7.13 (d, 4H, H3/H5), 7.01 (m, 8H, H5', H5'*).

With bis(4,4'-dimethyl-2,2'-bipyridine)ruthenium(II) dichloride, *viz* **3.65**

Ligand **3.3** (24.9 mg, 0.051 mmol) and bis(4,4'-dimethyl-2,2'-bipyridine)ruthenium(II) dichloride (56.7 mg, 0.105 mmol) were refluxed in 3:1 ethanol-water for 72 hours. After cooling, the solvent was removed *in vacuo*, the residue redissolved in water and filtered. The resulting red solution was treated with an excess of ammonium hexafluorophosphate to give a red precipitate of **3.65** that was purified on alumina eluting with 1:19 methanol-dichloromethane solution. Yield 49.9 mg (50%). M.p. 260-262°C. ES-MS 861.3 (1%, $[\{Ru(dmb)_2\}_2(\mathbf{3.3})](PF_6)_2^{2+}$), 525.9 (27%, $[\{Ru(dmb)_2\}_2(\mathbf{3.3})](PF_6)^{3+}$), 358.1 (66%, $[\{Ru(dmb)_2\}_2(\mathbf{3.3})]^{4+}$). $^1$H NMR ($CD_3CN$) δ 8.43 (s, 4H, dmbH3A), 8.40 (s, 4H, dmbH3A*), 8.36 (s, 4H, dmbH3B), 8.34 (s, 4H, dmbH3B*), 8.24 (d, 4H, dmbH6A), 8.16 (d, 4H, dmbH6A*), 7.84 (m, 12H, H2/H6, H4', H4'*), 7.73 (m, 4H, H2/H6*), 7.55 (m, 16H, dmbH6B/B*, H6', H6'*), 7.49 (d, 4H, H3'*), 7.44 (d, 4H, H3'), 7.29 (d, 4H, dmbH5A), 7.21 (m, 12H, dmbH5B/A*/B*), 7.18 (d, 4H, H3/H5), 7.08 (d, 4H, H3/H5*), 7.01 (m, 8H, H5', H5'*), 2.63 (s, 12H, dmbMeA), 2.59 (s, 12H, dmbMeA*), 2.54 (s, 12H, dmbMeB), 2.53 (s, 12H, dmbMeB*).

### 6.4.3 Complexes of 3.4

With silver hexafluorophosphate, *viz* **3.26a/b**

Both **3.4** (20.0 mg, 0.043 mmol) and silver hexafluorophosphate (24.0 mg, 0.095 mmol) were dissolved in hot acetonitrile, the solutions combined and left to slowly evaporate. A colourless crystalline solid, **3.26a** precipitated from the reaction mixture. **3.26a**: Yield 35.5 mg (85%). M.p. >189°C. Analysis: calc. for $C_{30}H_{22}N_6F_{12}P_2Ag_2$ C 37.06, H 2.28, N 8.64; found C 38.97, H 2.53, N 8.75%. Plate-like crystals formed on the side of the reaction vial when the filtrate was left to evaporate (**3.26b**).

With copper nitrate, *viz* **3.27**

Copper nitrate (21.8 mg, 0.090 mmol) and **3.4** (20.2 mg, 0.043 mmol) were both dissolved in hot methanol, the solutions combined and then cooled. The methanol was allowed to slowly evaporate giving a green precipitate, which was collected and dried *in vacuo*. Yield 20 mg

(55%). M.p. 269-271°C (dec.). Analysis: calc. for $C_{30}H_{22}N_{10}O_{12}Cu_2$ C 42.81, H 2.63, N 16.64; found C 42.57, H 2.53, N 16.46%.

With palladium chloride, *viz* **3.28**

Palladium chloride (14.9 mg, 0.084 mmol) was dissolved in 2 M hydrochloric acid (2 mL) and added slowly to a hot methanolic solution of **3.4** (20.2 mg, 0.043 mmol). The solution turned yellow and a fine yellow solid precipitated. After heating for 30 minutes, the yellow precipitate was collected by filtration and dried *in vacuo*. Yield 30 mg (85%). M.p. >315°C (dec.). Analysis: calc. for $C_{30}H_{22}N_6Cl_4Pd_2$ C 43.88, H 2.70, N 10.23; found C 43.75, H 2.72, N 10.35%. The complex was insoluble in common NMR solvents.

With bis(2,2'-bipyridine)ruthenium(II) dichloride, *viz* **3.66/3.68**

***Attempt A:*** Ligand **3.4** (20.0 mg, 0.043 mmol) and bis(2,2'-bipyridine)ruthenium(II) dichloride (52.0 mg, 0.107 mmol) were refluxed in 3:1 ethanol-water for 48 hours. After cooling, the solvent was removed *in vacuo*, the residue redissolved in water and filtered. The resulting red solution was treated with an excess of ammonium hexafluorophosphate to give a red precipitate of **3.66** that was purified on alumina eluting with 1:19 methanol-dichloromethane solution. Yield 29 mg (58%).

***Attempt B:*** Using the same quantities and procedure as above, but with a reaction time of 96 hours, a mixture of mononuclear and dinuclear compounds were obtained. These were separated and purified on alumina eluting with 1:19 methanol-dichloromethane solution to give two red bands. Band 1 (**3.66**): 9.0 mg (17%); Band 2 (**3.68**): 40.7 mg (51%).

**3.66**: M.p. 234-236°C (dec.). ES-MS 1025.1 (9%, $[Ru(bpy)_2(\mathbf{3.4})](PF_6)^+$), 440.1 (50%, $[Ru(bpy)_2(\mathbf{3.4})]^{2+}$). HRMS: calc. for $C_{70}H_{54}N_{14}F_6PRu_2$ ($[M-(PF_6)_3]^{3+}$) 479.7481; found 479.7471. Analysis: calc. for $C_{50}H_{38}N_{10}F_{12}P_2Ru$ C 51.33, H 3.27, N 11.97; found C 51.09, H 3.58, N 12.25%. $^1$H NMR ($CD_3CN$) δ 8.86 (m, 3H, bpyH6B, bpyH3D, bpyH6D), 8.72 (d, 1H, bpyH3A), 8.43 (d, 1H, bpyH3B), 8.39 (t, 1H, bpyH4D), 8.32 (d, 1H, bpyH3C), 8.29 (d, 2H, H6"'), 8.22 (t, 1H, bpyH4B), 8.11 (d, 1H, H8), 8.07 (t, 1H, bpyH4A), 7.99 (t, 1H, bpyH4C), 7.95 (t, 1H, bpyH5B), 7.90 (d, 1H, H6'), 7.79 (t, 1H, bpyH5D), 7.72 (m, 5H, bpyH6C, H5, H4"', bpyH6A), 7.58 (m, 4H, H6, H7, H4", H6", 7.46 (m, 3H, bpyH5C, H4', H2), 7.30 (t, 1H, bpyH5A), 7.22 (d, 2H, H3"'), 7.18 (d, 1H, H3), 7.09 (dd, 2H, H5"'), 6.81 (t, 1H, H5'), 6.77 (t, 1H, H5"), 6.71 (d, 1H, H3"), 6.34 (d, 1H, H3').

**3.68**: M.p. 279-283°C. ES-MS 792.2 (5%, $[\{Ru(bpy)_2\}_2(\mathbf{3.4})](PF_6)_2^{2+}$), 479.8 (37%, $[\{Ru(bpy)_2\}_2(\mathbf{3.4})](PF_6)^{3+}$), 323.6 (36%, $[\{Ru(bpy)_2\}_2(\mathbf{3.4})]^{4+}$). $^1$H NMR ($CD_3CN$) δ 8.85 (m, 12H, bpyH6A, bpyH3A, bpyH6A*), 8.73 (d, 4H, bpyH3B), 8.49 (m, 4H, bpyH3A*), 8.41 (t, 4H,

bpyH4A), 8.33 (m, 8H, bpyH3B*, bpyH4A*), 8.09 (t, 4H, bpyH4B), 8.02 (m, 8H, bpyH5A*, bpyH4B*), 7.94 (m, 8H, H6/H7, H6*/H7*, H6', H6"), 7.81 (t, 4H, bpyH5A), 7.78 (d, 4H, bpyH6B*), 7.73 (m, 4H, H5/H8, H5*/H8*), 7.71 (d, 4H, bpyH6B), 7.66 (t, 2H, H4'*), 7.60 (d, 2H, H4"*), 7.57 (s, 2H, H2/H3), 7.52 (t, 2H, H4'), 7.47 (m, 8H, H2*/H3*, H4", bpyH5B*), 7.33 (m, 4H, bpyH5B), 7.23 (t, 4H, H6'*, H6"*), 6.83 (m, 10H, H5', H5", H3'*, H5'*, H5"*), 6.74 (d, 2H, H3"*), 6.47 (d, 2H, H3'), 6.42 (d, 2H, H3").

With bis(4,4'-dimethyl-2,2'-bipyridine)ruthenium(II) dichloride, *viz* **3.67**

Ligand **3.4** (17.0 mg, 0.036 mmol) and bis(4,4'-dimethyl-2,2'-bipyridine)ruthenium(II) dichloride (42.2 mg, 0.078 mmol) were refluxed in 3:1 ethanol-water for 72 hours. After cooling, the solvent was removed *in vacuo*, the residue redissolved in water and filtered. The resulting red solution was treated with an excess of ammonium hexafluorophosphate to give a dark red precipitate of **3.67** that was purified on alumina eluting with 1:19 methanol-dichloromethane solution. Yield 35.9 mg (81%). M.p. 258-261°C (dec.). Analysis: calc. for $C_{54}H_{46}N_{10}F_{12}P_2Ru.4H_2O$ C 49.97, H 4.19, N 10.79; found C 49.97, H 3.77, N 10.65%. $^1$H NMR ($CD_3CN$) δ 8.70 (s, 1H, dmbH3B), 8.69 (d, 1H, dmbH6A), 8.67 (d, 1H, dmbH6B), 8.56 (s, 1H, dmbH3C), 8.28 (m, 3H, dmbH3A, H6"'), 8.17 (s, 1H, dmbH3D), 8.11 (d, 1H, H8), 7.90 (d, 1H, H6'), 7.72 (m, 5H, H2, H5, H4"', dmbH5A), 7.59 (m, 5H, dmbH5B, dmbH6D, H6, H7, H4"), 7.51 (d, 1H, H3), 7.45 (m, 2H, dmbH6C, H4'), 7.28 (d, 1H, dmbH5D), 7.22 (d, 2H, H3"'), 7.18 (d, 1H, H6"), 7.13 (d, 1H, dmbH5C), 7.09 (dd, 2H, H5"'), 6.79 (t, 1H, H5'), 6.74 (t, 1H, H5"), 6.67 (d, 1H, H3"), 6.31 (d, 1H, H3'), 2.79 (s, 3H, dmbMeB), 2.66 (s, 3H, dmbMeA), 2.56 (s, 3H, dmbMeC), 2.51 (s, 3H, dmbMeD).

### 6.4.4 Complexes of 3.6

With copper nitrate, *viz* **3.29**

A solution of copper nitrate (21.9 mg, 0.091 mmol) dissolved in methanol and **3.6** (20.1 mg, 0.043 mmol) dissolved in dichloromethane were combined and left to stand. Vapour diffusion of ether into this solution gave a green crystalline precipitate. Yield 25.7 mg (62%). M.p. 281-283°C (dec.). Analysis: calc. for $C_{30}H_{22}N_{10}Cu_2O_{12}.1½CH_2Cl_2$ C 39.04, H 2.60, N 14.45; found C 39.28, H 2.11, N 14.29%.

With palladium chloride, *viz* **3.30**

Palladium chloride (15.5 mg, 0.087 mmol) was dissolved in 2 M hydrochloric acid (2 mL) and added to a methanol solution of **3.6** (19.9 mg, 0.043 mmol). Immediately a pale yellow

precipitate formed, which was collected and dried *in vacuo*. Yield 28.0 mg (78%). M.p. >290°C (dec.). Analysis: calc. for $C_{30}H_{22}N_6Cl_4Pd_2.H_2O$ C 42.94, H 2.88, N 10.01; found C 43.20, H 2.80, N 10.08%.

With bis(2,2'-bipyridine)ruthenium(II) dichloride, *viz* **3.69**

Ligand **3.6** (20.0 mg, 0.044 mmol) and bis(2,2'-bipyridine)ruthenium(II) dichloride (52.1 mg, 0.108 mmol) were refluxed in 3:1 ethanol-water for 48 hours. After cooling, the solvent was removed *in vacuo*, the residue redissolved in water and filtered. The resulting red solution was treated with an excess of ammonium hexafluorophosphate to give a red precipitate of **3.69** that was purified on alumina eluting with 1:19 methanol-dichloromethane solution. Yield 10.0 mg (19%). ES-MS 1025.1 (7%, $[Ru(bpy)_2(\mathbf{3.6})](PF_6)^+$), 440.1 (78%, $[Ru(bpy)_2(\mathbf{3.6})]^{2+}$). $^1$H NMR ($CD_3CN$) δ 8.86 (d, 1H, bpyH3A), 8.83 (d, 1H, bpyH6A), 8.79 (d, 1H, bpyH6C), 8.70 (d, 1H, bpyH3B), 8.46 (d, 1H, bpyH3C), 8.39 (t, 1H, bpyH4A), 8.33 (d, 1H, bpyH3D), 8.28 (d, 2H, H6"'), 8.25 (m, 2H, bpyH4C, H4), 8.21 (d, 1H, H8), 8.06 (t, 1H, bpyH4B), 7.99 (t, 1H, bpyH4D), 7.95 (t, 1H, bpyH5C), 7.89 (d, 1H, H6"), 7.80 (t, 1H, bpyH5A), 7.66 (m, 7H, bpyH6B, bpyH6D, H3, H7, H4', H4"'), 7.46 (m, 2H, bpyH5D, H4"), 7.35 (d, 1H, H6), 7.29 (t, 1H, bpyH5B), 7.19 (d, 3H, H6', H3"'), 7.13 (d, 1H, H2), 7.07 (dd, 2H, H5"'), 6.81 (t, 1H, H5"), 6.76 (t, 1H, H5'), 6.62 (d, 1H, H3'), 6.28 (d, 1H, H3").

With bis(4,4'-dimethyl-2,2'-bipyridine)ruthenium(II) dichloride, *viz* **3.70**

Ligand **3.6** (10.5 mg, 0.023 mmol) and bis(4,4'-dimethyl-2,2'-bipyridine)ruthenium(II) dichloride (25.6 mg, 0.047 mmol) were refluxed in 3:1 ethanol-water for 72 hours. After cooling, the solvent was removed *in vacuo*, the residue redissolved in water and filtered. The resulting red solution was treated with an excess of ammonium hexafluorophosphate to give a dark red precipitate of **3.70** that was purified on alumina eluting with 1:19 methanol-dichloromethane solution. Yield 17.1 mg (60%). M.p. 238-241°C. ES-MS 1080.4 (2%, $[Ru(dmb)_2(\mathbf{3.6})](PF_6)^+$), 468.1 (100%, $[Ru(dmb)_2(\mathbf{3.6})]^{2+}$). HRMS: calc. for $C_{54}H_{46}N_{10}Ru$ ($[M-(PF_6)_2]^{2+}$) 468.1482; found 468.1491. $^1$H NMR ($CD_3CN$) δ 8.69 (s, 1H, dmbH3A), 8.64 (d, 1H, dmbH6A), 8.62 (d, 1H, dmbH6C), 8.55 (s, 1H, dmbH3B), 8.31 (s, 1H, dmbH3C), 8.28 (d, 2H, H6"'), 8.20 (m, 3H, dmbH3D, H4, H8), 7.90 (d, 1H, H6"), 7.76 (d, 1H, dmbH5C), 7.64 (m, 7H, dmbH5A, dmbH6D, H3, H7, H4', H4"'), 7.44 (m, 4H, dmbH6B, dmbH5D, H4",H6), 7.28 (t, 1H, H2), 7.19 (m, 3H, H6', H3"'), 7.12 (d, 1H, dmbH5B), 7.07 (dd, 2H, H5"'), 6.79 (t, 1H, H5"), 6.73 (t, 1H, H5'), 6.58 (d, 1H, H3'), 6.26 (d, 1H, H3"), 2.79 (s, 3H, dmbMeA), 2.69 (s, 3H, dmbMeC), 2.55 (s, 3H, dmbMeB), 2.51 (s, 3H, dmbMeD).

### 6.4.5 Complexes of 3.7

With silver nitrate, *viz* **3.31**

Both **3.7** (20.0 mg, 0.048 mmol) and silver nitrate (17.9 mg, 0.106 mmol) were dissolved in hot acetonitrile, the solutions combined and allowed to cool. Vapour diffusion of ether into the reaction mixture gave crystals suitable for X-ray crystallography. Yield 23.2 mg (63%). M.p. 169-171°C. Analysis: calc. for $C_{26}H_{20}N_8O_6Ag_2$ C 41.30, H 2.67, N 14.82; found C 41.41, H 2.72, N 14.27%.

With silver hexafluorophosphate, *viz* **3.32**

Ligand **3.7** (20.0 mg, 0.48 mmol) and silver hexafluorophosphate (27.3 mg, 0.107 mmol) were dissolved in hot acetonitrile. The solid obtained after evaporation of the resulting solution was recrystallised by vapour diffusion of ether into an acetonitrile solution of the complex, providing crystals suitable for X-ray crystallography. Yield 31.3 mg. M.p. 252-255°C (dec.).

With copper nitrate, *viz* **3.33**

Copper nitrate (25 mg, 0.103 mmol) and **3.7** (20.0 mg, 0.048 mmol) were both dissolved in methanol and combined. Diffusion of ether into the reaction mixture gave green crystals, suitable for X-ray crystallography. Yield 23.5 mg (62%). M.p. 247-250°C (dec.). Analysis: calc. for $C_{26}H_{20}N_{10}O_{12}Cu_2$ C 39.45, H 2.55, N 17.69; found C 39.83, H 2.16, N 17.84%.

With palladium chloride, *viz* **3.34**

Palladium chloride (19.0 mg, 0.107 mmol) was dissolved in 2 M hydrochloric acid (2 mL) and added slowly to a hot methanolic solution of **3.7** (20.1 mg, 0.048 mmol). The solution turned yellow and a fine yellow solid precipitated. After heating for 30 minutes, the precipitate was collected by filtration and dried *in vacuo*. Yield 23.1 mg (59%). M.p. >301°C (dec.). Analysis: calc. for $C_{26}H_{20}N_6Cl_4Pd_2.CH_3OH.H_2O$ C 39.49, H 3.19, N 10.23; found C 39.61, H 2.62, N 9.58%. The complex was insoluble in common NMR solvents.

With bis(2,2'-bipyridine)ruthenium(II) dichloride, *viz* **3.71**

Ligand **3.7** (20.3 mg, 0.049 mmol) and bis(2,2'-bipyridine)ruthenium(II) dichloride (51.6 mg, 0.107 mmol) were refluxed in 3:1 ethanol-water for 72 hours. After cooling, the solvent was removed *in vacuo*, the residue redissolved in water and filtered. The resulting red solution was treated with an excess of ammonium hexafluorophosphate to give a red precipitate of **3.71**. This was purified on alumina, eluting with 1:19 methanol-dichloromethane solution, to provide a

mixture of the two diastereoisomers in a 1:1 ratio. Yield 43.2 mg (48%). M.p. 268-271°C. Analysis: calc. for $C_{66}H_{52}N_{14}F_{24}P_4Ru_2$ C 43.48, H 2.87, N 10.76; found C 43.67, H 3.20, N 10.88%. $^1$H NMR ($CD_3CN$) δ 8.59 (d, 4H, bpyH3A), 8.57 (d, 4H, bpyH3A*), 8.54 (d, 8H, bpyH3B/B*), 8.31 (d, 4H, bpyH6), 8.27 (d, 4H, bpyH6*), 8.10 (t, 8H, bpyH4A/A*), 8.06 (t, 8H, bpyH4B/B*), 7.89 (t, 4H, H4'*), 7.86 (t, 4H, H4'), 7.75 (d, 4H, bpyH6B*), 7.73 (d, 4H, bpyH6B), 7.59 (d, 4H, H6'*), 7.56 (d, 4H, H6'), 7.52 (d, 4H, H3'*), 7.41 (m, 13H, bpyH5B/B*, H3', H5), 7.34 (t, 8H, bpyH5A/A*), 7.21 (t, 1H, H5*), 7.09 (m, 8H, H5', H5'*), 6.84 (m, 3H, H6/H4, H2*), 6.56 (dd, 2H, H6*/H4*), 6.48 (t, 1H, H2).

With bis(4,4'-dimethyl-2,2'-bipyridine)ruthenium(II) dichloride, *viz* **3.72**

Ligand **3.7** (20.5 mg, 0.049 mmol) and bis(4,4'-dimethyl-2,2'-bipyridine)ruthenium(II) dichloride (54.6 mg, 0.101 mmol) were refluxed in 3:1 ethanol-water for 72 hours. After cooling the solvent was removed *in vacuo* and the residue redissolved in water and filtered. The resulting red solution was treated with an excess of ammonium hexafluorophosphate to give a red precipitate of **3.72**, which was purified on alumina, eluting with 1:9 methanol-dichloromethane solution, to give a 1:1 mixture of the two diastereoisomers. Yield 42.3 mg (45%). M.p. 278-282°C. ES-MS 1796.3 (1%, $[\{Ru(dmb)_2\}_2(\mathbf{3.7})](PF_6)_3^+$), 823.3 (40%, $[\{Ru(dmb)_2\}_2(\mathbf{3.7})](PF_6)_2^{2+}$), 500.5 (100%, $[\{Ru(dmb)_2\}_2(\mathbf{3.7})](PF_6)^{3+}$), 339.2 (36%, $[\{Ru(dmb)_2\}_2(\mathbf{3.7})]^{4+}$). HRMS: calc. for $C_{74}H_{68}N_{14}F_6PRu_2$ ($[M-(PF_6)_3)]^{3+}$ 500.4507; found 500.4504. $^1$H NMR ($CD_3CN$) δ 8.45 (s, 4H, dmbH3A), 8.43 (s, 4H, dmbH3A*), 8.37 (s, 8H, dmbH3B/B*), 8.12 (d, 4H, dmbH6A), 8.07 (d, 4H, dmbH6A*), 7.84 (t, 4H, H4'), 7.80 (t, 4H, H4'*), 7.57 (m, 12H, dmbH6B*, H6', H6'*), 7.52 (d, 4H, dmbH6B), 7.44 (m, 5H, H3', H5), 7.33 (d, 4H, H3'*), 7.23 (m, 12H, dmbH5A, dmbH5B/B*), 7.19 (m, 5H, H5, dmbH5A*), 7.09 (t, 4H, H5'), 7.03 (t, 4H, H5'*), 6.86 (t, 1H, H2), 6.81 (dd, 2H, H4/H6), 6.78 (t, 1H, H2), 6.44 (dd, 2H, H4*/H6*), 2.60 (s, 12H, dmbMeA), 2.59 (s, 12H, dmbMeA*), 2.55 (s, 12H, dmbMeB), 2.54 (s, 12H, dmbMeB*).

### 6.4.6 Complexes of 3.8

With silver tetrafluoroborate, *viz* **3.35**

Silver tetrafluoroborate (18 mg, 0.092 mmol) and **3.8** (20 mg, 0.043 mmol) were both dissolved in acetonitrile and combined. Vapour diffusion of ether into the acetonitrile reaction mixture gave colourless crystals, suitable for X-ray crystallography. Yield 24.4 mg (62%). M.p. >180°C (dec.). Analysis: calc. for $C_{30}H_{22}N_6B_2F_8Ag_2.CH_3CN.H_2O$ C 42.01, H 2.97, N 10.72; found C 41.76, H 3.22, N 10.89%.

With silver hexafluorophosphate, *viz* **3.36**

Silver hexafluorophosphate (24 mg, 0.095 mmol) and **3.8** (20 mg, 0.043 mmol) were both dissolved in acetonitrile and the solutions combined. Vapour diffusion of pentane into the reaction mixture gave colourless crystals suitable for X-ray crystallography. Yield 4.0 mg.

With copper nitrate, *viz* **3.37**

Copper nitrate (22 mg, 0.091 mmol) and **3.8** (20 mg, 0.043 mmol) were both dissolved in methanol, the solutions combined and left to stand. Vapour diffusion of ether into this solution gave a green crystalline precipitate. Yield 20.2 mg (52%). M.p. 266-267°C (dec.). Analysis: calc. for $C_{32}H_{30}N_{10}Cu_2O_{14}$ C 42.44, H 3.34, N 15.46; found C 42.27, H 3.11, N 15.77%.

With palladium chloride, *viz* **3.38**

Palladium chloride (16.2 mg, 0.090 mmol) was dissolved in 2 M hydrochloric acid (2 mL) and added to a methanol solution of **3.8** (20 mg, 0.043 mmol). Immediately a pale yellow precipitate formed, which was collected and dried *in vacuo*. Yield 33.0 mg (91%). M.p. >290°C (dec.). Analysis: calc. for $C_{30}H_{22}N_6Cl_4Pd_2.H_2O$ C 42.94, H 2.88, N 10.01; C 43.06, H 2.67, N 9.82%. $^1$H NMR (DMSO-$d_6$) δ 8.90 (d, 4H, H6), 8.44 (t, 4H, H4), 8.16 (t, 4H, H5), 7.91 (d, 2H, arom. CH), 7.57 (m, 8H, H3, arom. CH).

With bis(2,2'-bipyridine)ruthenium(II) dichloride, *viz* **3.73**

Ligand **3.8** (20.3 mg, 0.044 mmol) and bis(2,2'-bipyridine)ruthenium(II) dichloride (45.3 mg, 0.094 mmol) were refluxed in 3:1 ethanol-water for 48 hours. After cooling, the solvent was removed *in vacuo*, the residue redissolved in water and filtered. The resulting red solution was treated with an excess of ammonium hexafluorophosphate to give a red precipitate of **3.73** that was purified on alumina eluting with 1:9 methanol-dichloromethane solution. Yield 48.4 mg (59%). M.p. 208-210°C (dec.). ES-MS 792.5 (6%, $[\{Ru(bpy)_2\}_2(\mathbf{3.8})](PF_6)_2^{2+}$), 479.8 (93%, $[\{Ru(bpy)_2\}_2(\mathbf{3.8})](PF_6)^{3+}$), 323.6 (100%, $[\{Ru(bpy)_2\}_2(\mathbf{3.8})]^{4+}$). $^1$H NMR ($CD_3CN$) δ 8.59 (d, 4H, bpyH3A), 8.56 (d, 4H, bpyH3A*), 8.52 (m, 8H, bpyH3B/B*), 8.44 (d, 4H, bpyH6A) 8.38 (d, 4H, bpyH6A*), 8.12 (t, 4H, bpyH4A), 8.05 (m, 16H, bpyH4A*, bpyH4B/B*, H4, H4*), 7.95 (t, 4H, H4'), 7.91 (t, 4H, H4'*), 7.76 (d, 8H, bpyH6/H6*), 7.60 (d, 8H, H6', H6'*), 7.55 (d, 4H, H3'), 7.52 (d, 4H, H3'*), 7.39 (m, 10H, bpyH5/H5*, H1), 7.36 (t, 4H, bpyH5A), 7.32 (t, 4H, bpyH5A*), 7.27 (dd, 2H, H3*), 7.17 (dd, 2H, H3), 7.07 (m, 10H, H1*, H5', H5'*).

With bis(4,4'-dimethyl-2,2'-bipyridine)ruthenium(II) dichloride, *viz* **3.74**

Ligand **3.8** (20.6 mg, 0.044 mmol) and bis(4,4'-dimethyl-2,2'-bipyridine)ruthenium(II) dichloride (52.3 mg, 0.097 mmol) were refluxed in 3:1 ethanol-water for 48 hours. After cooling, the solvent was removed *in vacuo*, the residue redissolved in water and filtered. The resulting red solution was treated with an excess of ammonium hexafluorophosphate to give a red precipitate of **3.74**, which was purified on alumina eluting with 1:19 methanol-dichloromethane solution. Yield 68.9 mg (78%). M.p. 268-271°C. ES-MS 848.2 (2%, $[\{Ru(dmb)_2\}_2(\mathbf{3.8})](PF_6)_2^{2+}$), 517.1 (22%, $[\{Ru(dmb)_2\}_2(\mathbf{3.8})](PF_6)^{3+}$), 351.6 (20%, $[\{Ru(dmb)_2\}_2(\mathbf{3.8})]^{4+}$). HRMS: calc. for $C_{78}H_{70}N_{14}F_6PRu_2$ ($[M-(PF_6)_3]^{3+}$) 517.1222; found 517.1230. $^1$H NMR ($CD_3CN$) δ 8.42 (s, 4H, dmbH3A), 8.40 (s, 4H, dmbH3A*), 8.37 (s, 4H, dmbH3B), 8.36 (s, 4H, dmbH3B*), 8.15 (m, 8H, dmbH6A/A*), 8.02 (d, 4H, H4, H4*), 7.90 (t, 8H, H4', H4'*), 7.56 (m, 24H, dmbH6B/B*, H3', H3'*, H6', H6'*), 7.22 (d, 8H, dmbH5B/B*), 7.18 (m, 6H, H1, H1*, H3*), 7.14 (dd, 2H, H3), 7.07 (m, 16H, dmbH5A/A*, H5', H5'*), 2.54 (s, 24H, dmbMeB/B*), 2.51 (s, 12H, dmbMeA), 2.49 (s, 12H, dmbMeA*).

### 6.4.7 Complexes of 3.9

With silver tetrafluoroborate, *viz* **3.39**

Silver tetrafluoroborate (21.0 mg, 0.108 mmol) and **3.9** (20.0 mg, 0.034 mmol) were both dissolved in acetonitrile and combined. Vapour diffusion of ether into the resulting solution gave a cream precipitate that was collected by filtration and washed with ether. Yield 11.9 mg (28%). M.p. >255°C (dec.). Analysis: calc. for $C_{36}H_{27}B_3N_9F_{12}Ag_3.2CH_3CN$ C 38.38, H 2.66, N 12.31; found C 38.79, H 2.80, N 11.43%.

With palladium acetate, *viz* **3.40**

Ligand **3.9** (20.1 mg, 0.034 mmol) and palladium acetate (25.7 mg, 0.114 mmol) were refluxed in benzene for 7 days. The benzene was evaporated *in vacuo* and the residue taken up in 3:2 acetone-water solution, filtered, an excess of lithium chloride added and the solution stirred overnight. The resulting precipitate was collected, washed with water, then ether and dried under vacuum (yield 13.5 mg). $^1$H NMR of the precipitate indicated a mixture of cyclopalladated compounds containing approximately 45% of the desired tricyclopalladated compound. Vapour diffusion of methanol into a DMSO solution of the precipitate gave pale yellow crystals, suitable for X-ray crystallography. M.p. 271-273°C. HRMS: calc. for $C_{36}H_{24}N_9Cl_2Pd_3$ ($[M-Cl]^+$) 972.8645, found 972.8638 ($[M-Cl]^+$). Analysis: calc. for $C_{36}H_{24}N_9Cl_3Pd_3.2CH_3OH$ C 42.56, H 3.01, N 11.76; found C 41.79, H 2.63, N 11.83%. $^1$H NMR ($CDCl_3$) δ 7.10 (t, 6H, H5), 7.49

(d, 6H, H3), 7.78 (t, 6H, H4), 9.18 (d, 6H, H6); $^{13}$C NMR ($CDCl_3$) δ 154.1, 147.7, 139.9, 132.6, 125.1, 120.2, 120.0.

With (2,2',6',2"-terpyridine)ruthenium(III) trichloride, *viz* **3.41**

(2,2',6',2"-Terpyridine)ruthenium(III) trichloride (58.1 mg, 0.132 mmol) and silver tetrafluoroborate (80.1 mg, 0.411 mmol) were refluxed in acetone (20 mL) for 3 hours. The solution was cooled, filtered and then the filtrate was taken to dryness. Ligand **3.9** (23.2 mg, 0.040 mmol) was added to the residue, the mixture dissolved in n-butanol and refluxed for 48 hours. The butanol was then evaporated *in vacuo* and the residue redissolved in water. The mixture was purified on Sephadex cation exchange resin to give two bands, band 1 (red, $[Ru(tpy)_2]^{2+}$, 0.1 molL$^{-1}$ NaCl solution) and band 2 (purple, 0.6 molL$^{-1}$ NaCl solution). The purple solution was concentrated *in vacuo* and the resultant precipitate was filtered, washed with water and dried *in vacuo*. Yield 45.4 mg. M.p. 310-315°C.

### 6.4.8 Complexes of 3.10

With silver tetrafluoroborate, *viz* **3.42**

Silver tetrafluoroborate (21 mg, 0.108 mmol) and **3.10** (20.0 mg, 0.034 mmol) were both dissolved in acetonitrile and the solutions combined. Vapour diffusion of ether into the resulting solution gave a colourless precipitate. Yield 8.1 mg (29%). M.p. 264-268°C (dec.). Analysis: calc. for $C_{33}H_{24}N_{12}BF_4Ag$ C 48.26, H 2.95, N 20.47; found C 48.66, H 3.03, N 20.69%.

With silver hexafluorophosphate, *viz* **3.43**

Silver hexafluorophosphate (27 mg, 0.107 mmol) and **3.10** (20.0 mg, 0.034 mmol) were both dissolved in acetonitrile and the solutions combined. Vapour diffusion of ether into the reaction mixture gave a colourless precipitate. Yield 6.9 mg (23%). M.p. >220°C (dec.). Analysis: calc. for $C_{33}H_{24}N_{12}PF_6Ag.2H_2O$ C 45.17, H 3.22, N 19.15; found C 44.81, H 2.78, N 19.06%.

With palladium chloride, *viz* **3.44**

Palladium chloride (18.0 mg, 0.102 mmol) was dissolved in 2 M hydrochloric acid (2 mL) and added to a methanol solution of **3.10** (20.0 mg, 0.034 mmol). Immediately a pale yellow precipitate formed, which was collected and dried *in vacuo*. Yield 34.0 mg (86%). M.p. >330°C (dec.). Analysis: calc. for $C_{33}H_{28}N_{12}Cl_6Pd_3.3H_2O$ C 34.27, H 2.44, N 14.35; found C 34.77, H 2.41, N 14.08%.

### 6.4.9 Complexes of 3.11

With silver nitrate, *viz* **3.45**

Silver nitrate (16.8 mg, 0.099 mmol) was dissolved in methanol and added to a dichloromethane-methanol solution (1:1) of **3.11** (20.1 mg, 0.045 mmol). Colourless crystals, suitable for X-ray crystallography, formed by slow evaporation of the resulting solution, were collected, washed with dichloromethane and methanol, and dried *in vacuo*. Yield 25.2 mg (89%). M.p. 233-235°C (dec.). Analysis: calc. for $C_{28}H_{24}N_7O_3Ag.H_2O$ C 53.18, H 4.14, N 15.50; found C 53.32, H 3.71, N 15.87%.

With silver tetrafluoroborate, *viz* **3.46**

Silver tetrafluoroborate (18.7 mg, 0.096 mmol) was dissolved in methanol and added to a dichloromethane-methanol solution (1:1) of **3.11** (20.2 mg, 0.045 mmol). Colourless crystals formed in the reaction mixture, were collected, washed with dichloromethane and methanol, and dried *in vacuo*. These crystals were suitable for X-ray crystallography. Yield 17.4 mg (60%). M.p. 245°C (dec.). Analysis: calc. for $C_{28}H_{24}N_6BF_4Ag$ C 52.61, H 3.78, N 13.15; found C 52.84, H 3.97, N 13.27%.

With silver hexafluorophosphate, *viz* **3.47**

Silver hexafluorophosphate (23.9 mg, 0.095 mmol) was dissolved in methanol and added to a dichloromethane-methanol solution (1:1) of **3.11** (20.3 mg, 0.046 mmol). Colourless crystals, which formed in the reaction mixture, were collected, washed with dichloromethane and methanol, and dried *in vacuo*. These crystals were suitable for X-ray crystallography. Yield 27.5 mg (68%). M.p. 239-240°C (dec.). Analysis: calc. for $C_{28}H_{24}N_6PF_6Ag.2CH_2Cl_2$ C 41.55, H 3.25, N 9.69; found C 41.76, H 3.09, N 10.27%.

With copper nitrate, *viz* **3.48**

Copper nitrate (23.0 mg, 0.095 mmol) was dissolved in methanol and added to a dichloromethane solution of **3.11** (20.0 mg, 0.045 mmol). On standing a blue solid precipitated, was collected and dried *in vacuo*. Yield 24.6 mg (67%). M.p. 261-263°C (dec.). Analysis: calc. for $C_{28}H_{24}N_{10}O_{12}Cu_2$ C 41.03, H 2.95, N 17.09; found C 40.99, H 3.08, N 17.06%.

With palladium chloride, *viz* **3.49**

Palladium chloride (16.6 mg, 0.094 mmol) was dissolved in 2 M hydrochloric acid solution and added to a dichloromethane-methanol solution of **3.11** (20.2 mg, 0.045 mmol). Immediately a

pale yellow solid precipitated, was collected, washed with methanol and dried under vacuum. Yield 29.3 mg (81%). M.p. >330°C. Analysis: calc. for $C_{28}H_{24}N_6Cl_4Pd_2$ C 42.08, H 3.03, N 10.52; found C 41.85, H 2.81, N 10.24%.

### 6.4.10 Complexes of 3.12

With silver nitrate, *viz* **3.50**

Silver nitrate (15.8 mg, 0.093 mmol) was dissolved in methanol and added to a dichloromethane-methanol solution (1:1) of **3.12** (19.9 mg, 0.045 mmol). Colourless crystals, which formed by slow evaporation, were collected, washed with dichloromethane and methanol and dried *in vacuo*. These crystals were suitable for X-ray crystallography. Yield 22.6 mg (82%). M.p. 232-235°C (dec.). Analysis: calc. for $C_{28}H_{24}N_7O_3Ag$ C 54.74, H 3.94, N 15.96; found C 54.78, H 3.84, N 16.21%.

With silver tetrafluoroborate, *viz* **3.51**

Silver tetrafluoroborate (18.9 mg, 0.097 mmol) was dissolved in methanol and added to a dichloromethane-methanol solution (1:1) of **3.12** (20.0 mg, 0.045 mmol). A colourless crystalline solid precipitated from the reaction mixture, was collected, washed with dichloromethane and methanol, and dried *in vacuo*. Yield 29.3 mg (88%). M.p. >170°C (dec.). Analysis: calc. for $C_{56}H_{48}N_{12}B_3F_{12}Ag_3$ C 45.66, H 3.28, N 11.41; found C 44.98, H 3.70, N 11.21%.

With silver hexafluorophosphate, *viz* **3.52**

Silver hexafluorophosphate (24.4 mg, 0.097 mmol) was dissolved in methanol and added to a dichloromethane-methanol solution (1:1) of **3.12** (20.7 mg, 0.047 mmol). Colourless crystals, which formed in the reaction mixture, were collected, washed with dichloromethane and methanol and dried *in vacuo*. These crystals were suitable for X-ray crystallography. Yield 11.0 mg (31%). M.p. 179-181°C (dec.). Analysis: calc. for $C_{28}H_{24}N_6PF_6Ag.CH_3OH.H_2O$ C 46.60, H 4.05, N 11.24; found C 46.93, H 3.87, N 11.61%.

With copper nitrate, *viz* **3.53**

Copper nitrate (22.8 mg, 0.094 mmol) was dissolved in methanol and added to a dichloromethane solution of **3.12** (20.0 mg, 0.045 mmol). On standing a blue crystalline material precipitated, was collected and then recrystallised by vapour diffusion of ether into a methanol solution of the complex. Yield 21.6 mg (54%). M.p. >175°C (dec.). Analysis: calc. for $C_{28}H_{24}N_{10}O_{12}Cu_2.2CH_3OH$ C 40.77, H 3.65, N 15.85; found C 40.57, H 3.26, N 15.96%.

With palladium chloride, *viz* **3.54**

Palladium chloride (17.5 mg, 0.099 mmol) was dissolved in 2 M hydrochloric acid solution and added to a dichloromethane-methanol solution of **3.12** (20.9 mg, 0.047 mmol). Immediately a pale yellow precipitate formed that was collected, washed with methanol and dried under vacuum. Yield 26.8 mg (81%). M.p. 300-301°C (dec.). Analysis: calc. for $C_{28}H_{24}N_6Cl_4Pd_2$ C 42.08, H 3.03, N 10.52; found C 42.03, H 2.93, N 10.32%.

## 6.4.11 Complexes of 3.13

With silver nitrate, *viz* **3.55**

Silver nitrate (16.7 mg, 0.098 mmol) was dissolved in methanol and added to a dichloromethane-methanol solution (1:1) of **3.13** (20.5 mg, 0.046 mmol). A pale yellow crystalline solid formed following slow evaporation of the reaction mixture. This was collected, washed with dichloromethane and methanol, and dried *in vacuo*. Yield 27.5 mg (97%). M.p. 223-224°C (dec.). Analysis: calc. for $C_{28}H_{24}N_7O_3Ag$ C 54.74, H 3.94, N 15.96; found C 54.85, H 3.87, N 16.02%.

With silver tetrafluoroborate, *viz* **3.56**

Silver tetrafluoroborate (19.3 mg, 0.099 mmol) was dissolved in methanol and added to a dichloromethane-methanol solution (1:1) of **3.13** (19.8 mg, 0.045 mmol). A pale yellow crystalline solid precipitated from the reaction mixture, was collected, washed with dichloromethane and methanol, and then dried *in vacuo*. Yield 14.5 mg (39%). M.p. >145°C (dec.). Analysis: calc. for $C_{28}H_{24}N_6B_2F_8Ag_2$ C 40.33, H 2.90, N 10.08; found C 41.03, H 2.94, N 10.13%.

With silver hexafluorophosphate, *viz* **3.57a/b**

Silver hexafluorophosphate (25.8 mg, 0.102 mmol) was dissolved in methanol and added to a dichloromethane-methanol solution (1:1) of **3.13** (20.5 mg, 0.046 mmol). A yellow crystalline solid precipitated from the reaction mixture, was collected, washed with dichloromethane and methanol, and dried *in vacuo*. **3.57a**: Yield 32.2 mg (95%). M.p. 190-192°C (dec.). Analysis: calc. for $C_{28}H_{24}N_6PF_6Ag.CH_3OH$ C 47.75, H 3.87, N 11.52; C 48.08, H 4.35, N 11.55%. Subsequently, further pale yellow crystals (**3.57b**), suitable for X-ray crystallography, were isolated from the filtrate. These were shown to have a different composition from the bulk sample by X-ray crystallography.

With copper nitrate, *viz* **3.58**

Copper nitrate (23.6 mg, 0.098 mmol) was dissolved in methanol and added to a dichloromethane solution of **3.13** (19.9 mg, 0.045 mmol). On standing blue crystals precipitated, which were suitable for X-ray crystallography. Yield 23.3 mg (59%). M.p. 275-277°C (dec.). Analysis: calc. for $C_{30}H_{32}N_{10}O_{14}Cu_2$ C 40.77, H 3.65, N 15.85; found C 40.81, H 3.46, N 16.03%.

With palladium chloride, *viz* **3.59**

Palladium chloride (16.6 mg, 0.094 mmol) was dissolved in 2 M hydrochloric acid solution and added to a dichloromethane-methanol solution of **3.13** (19.9 mg, 0.045 mmol). Immediately a pale yellow precipitate formed that was collected, washed with methanol and dried under vacuum. Yield 28.6 mg (80%). M.p. >330°C. Analysis: calc. for $C_{28}H_{24}N_6Cl_4Pd_2$ C 42.08, H 3.03, N 10.52; found C 41.97, H 3.01, N 10.24%.

### 6.4.12 Complex of 3.14

With copper nitrate, *viz* **3.60**

Copper nitrate (23.9 mg, 0.099 mmol) was dissolved in methanol and added to a solution of **3.14** (19.9 mg, 0.032 mmol) dissolved in dichloromethane. The solution was concentrated by slow evaporation to give a blue crystalline solid that was collected by filtration and dried *in vacuo*. Yield 28.5 mg (75%). M.p. 195-197°C (dec.). Analysis: calc. for $C_{39}H_{33}N_{15}O_{18}Cu_3$ C 39.35, H 2.79, N 17.65; found (inconsistent with proposed structure) C 45.64, H 4.67, N 14.17%.

### 6.4.13 Complex of 3.15

With copper nitrate, *viz* **3.61**

Copper nitrate (26.3 mg, 0.109 mmol) was dissolved in methanol and added to a solution of **3.15** (20.5 mg, 0.025 mmol) dissolved in dichloromethane. The solution was concentrated by slow evaporation to give a blue crystalline solid that was collected by filtration and dried *in vacuo*. Yield 23.5 mg (58%). M.p. 224-227°C (dec.). Analysis: calc. for $C_{50}H_{42}N_{20}O_{24}Cu_4.4H_2O$ C 36.77, H 3.09, N 17.15; found C 37.20, H 2.78, N 16.75%.

## 6.5. Preparation of complexes with the tripodal ligands

### 6.5.1 Complexes of 4.4

With sodium cobaltinitrite, *viz* **4.18**

Sodium cobaltinitrite (190 mg, 0.47 mmol) was dissolved in water and stirred at room temperature. Ligand **4.4** (103 mg, 0.42 mmol) was dissolved in methanol and added dropwise to this solution, resulting in a copious orange precipitate. This suspension was stirred for 30 minutes at 70°C, cooled in ice, filtered and then washed successively with water, ethanol, and ether. Yield 159 mg (86%). Crystals, suitable for X-ray crystallography, were obtained from vapour diffusion of methanol into a DMSO solution of the complex. M.p. 198-200°C. Analysis: calc. for $C_{15}H_{12}N_7O_6Co.CH_3OH$ C 40.26, H 3.38, N 20.54; found C 40.36, H 3.09, N 20.74%. IR. (nujol mull) 1433.0 (b, N-bound $NO_2$), 1305.7 (s, N-bound $NO_2$), 819.7 (s, N-bound $NO_2$). $^1$H NMR (DMSO-$d_6$) δ 8.80 (d, 3H, H6), 8.42 (t, 3H, H4), 8.17 (d, 3H, H3), 7.87 (t, 3H, H3).

With nickel tetrafluoroborate, *viz* **4.19**

Methanol solutions of nickel tetrafluoroborate (28.1 mg, 0.083 mmol) and **4.4** (20.3 mg, 0.081 mmol) were combined. Slow evaporation of the resulting solution gave pink crystals, suitable for X-ray crystallography. Yield 15 mg, (51%). M.p. >330°C. Analysis: calc. for $C_{30}H_{24}B_2N_8F_8Ni$ C 49.44, H 3.32, N 15.37; found C 49.50, H 3.16, N 15.40%.

With copper tetrafluoroborate, *viz* **4.20**

Copper tetrafluoroborate (28.0 mg, 0.083 mmol) and **4.4** (20.1 mg, 0.081 mmol) were both dissolved in methanol and the solutions combined. Slow evaporation of the resulting solution led to a blue crystalline solid. Yield 33.8 mg, (53%). M.p. 271-273°C. Analysis: calc. for $C_{15}H_{12}B_2N_4F_8Cu_2.2CH_3OH$ C 25.96, H 2.56, N 7.12; found C 26.73, H 2.59, N 7.74%.

### 6.5.2 Complex of 4.5

With nickel perchlorate, *viz* **4.21**

Ligand **4.5** (20 mg, 0.048 mmol) was dissolved in methanol and added to a solution of nickel perchlorate (36 mg, 0.98 mmol) dissolved in water. After stirring for 30 minutes, sodium thiocyanate was added to give an orange precipitate that was collected by filtration and washed with methanol. Recrystallisation, by vapour diffusion of acetone into a DMSO solution of the complex, furnished purple crystals suitable for X-ray crystallography. Yield 18 mg (41%).

M.p. 324°C (dec.). Analysis: calc. for $C_{34}H_{32}N_{10}O_2S_6Ni_2$ C 44.27, H 3.50, N 15.18; found C 43.81, H 3.15, N 16.25%. IR. (nujol mull) 2100.3 (N-bound SCN).

### 6.5.3 Complexes of 4.6

With palladium chloride, *viz* **4.22**

Palladium chloride (36.9 mg, 0.208 mmol) was dissolved in dilute hydrochloric acid (4 mL) and added dropwise to a solution of **4.6** (41.4 mg, 0.099 mmol) in methanol. A yellow precipitate formed, was collected by filtration, washed with cold methanol and dried *in vacuo*. Yield 71 mg (89%). M.p. 310°C (dec.). Analysis: calc. for $C_{24}H_{18}N_8Pd_2Cl_4.2H_2O$ C 35.80, H 2.25, N 13.92, Cl 17.61; found C 35.99, H 2.47, N 13.82, Cl 17.60%. $^1$H NMR (DMSO-$d_6$) δ 8.93 (d, 4H, H6'), 8.68 (s, 1H, H2), 8.36 (t, 4H, H4'), 8.14 (d, 4H, H3'), 7.75 (t, 4H, H5'), 6.19 (s, 1H, H5).

With palladium acetate, *viz* **4.23**

Palladium acetate (24.5 mg, 0.109 mmol) was dissolved in acetone and added dropwise to a solution of **4.6** (21.3 mg, 0.051 mmol), dissolved in methanol, to give an orange solution. Slow evaporation gave orange crystals, suitable for X-ray crystallography, that were collected by filtration and dried *in vacuo*. Yield 23 mg (52%). M.p. 225°C (dec.). Analysis: calc. for $C_{32}H_{30}N_8O_8Pd_2$ C 44.31, H 3.49, N 12.92; found C 44.05, H 3.50, N 12.61%. $^1$H NMR (DMSO-$d_6$) δ 8.67 (s, 1H, H2), 8.55 (d, 4H, H6'), 8.20 (m, 8H, H4', H3'), 7.68 (t, 4H, H5'), 6.20 (s, 1H, H2) and 1.90 (s, 12H, $CH_3$).

With copper nitrate, *viz* **4.24**

To a warm solution of **4.6** (40.0 mg, 0.096 mmol) dissolved in acetone, was added a solution of copper nitrate (47.6 mg, 0.20 mmol) also dissolved in acetone. The resulting solution was heated for 15 minutes during which time a blue precipitate formed. The solid was collected by filtration and dried *in vacuo*. Yield 76 mg (97%). M.p. 210°C. Analysis: calc. for $C_{24}H_{18}N_{12}O_{12}Cu_2.H_2O$ C 35.52, H 2.48, N 20.71; found C 35.87, H 2.89, N 20.31%.

With copper perchlorate, *viz* **4.25**

Copper perchlorate (35.8 mg, 0.097 mmol) was dissolved in acetonitrile (2 mL) and a hot solution of **4.6** (20.1 mg, 0.048 mmol) in methanol (3 mL) was added slowly. A dark blue solution formed, followed by a blue solid, which was collected and recrystallised from acetonitrile-ethanol. Yield 26.3 mg (76%). M.p. 275-278°C (dec.). Analysis: calc. for

$C_{48}H_{36}N_{16}O_{16}Cl_4Cu_2.4H_2O$ C 40.21, H 3.09, N 15.63, Cl 9.89; found C 40.56, H 3.22, N 15.55, Cl 9.86%.

With copper tetrafluoroborate, *viz* **4.26**

Copper tetrafluoroborate (15.9 mg, 0.046 mmol) and **4.6** (20.0 mg 0.048 mmol) were both dissolved in hot methanol and the solutions combined. On standing blue crystals, suitable for X-ray crystallography, precipitated, were collected and dried *in vacuo*. Yield 20 mg (65%). M.p. >255°C (dec.). Analysis: calc. for $C_{48}H_{40}B_4N_{16}O_2F_{16}Cu_2$ C 42.79, H 2.99, N 16.63; found C 42.74, H 3.57, N 16.63%.

With nickel tetrafluoroborate, *viz* **4.27**

Nickel tetrafluoroborate (16.3 mg, 0.048 mmol) and **4.6** (19.9 mg, 0.048 mmol) were both dissolved in hot methanol and combined. On standing pale blue crystals, suitable for X-ray crystallography, precipitated, were collected and then dried *in vacuo*. Yield 17 mg (44%). M.p. >280°C (dec.). Analysis: calc. for $C_{52}H_{52}B_4N_{16}O_4F_{16}Ni_2$ C 43.69, H 3.67, N 15.68; found C 43.22, H 3.85, N 16.25%.

With nickel perchlorate, *viz* **4.28**

A methanolic solution of **4.6** (80.4 mg, 0.192 mmol) was added dropwise to a solution of nickel perchlorate (141.5 mg, 0.387 mmol) in water. After stirring for two hours, sodium thiocyanate was added to give a pale purple precipitate. Yield 155 mg (64%). Recrystallisation by diffusion of acetone into a DMF solution of the complex provided crystals suitable for X-ray crystallography. M.p. >300°C (dec.). Analysis: calc. for $C_{52}H_{36}N_{12}S_4Ni_2.3H_2O$ C 50.34, H 3.41, N 22.58; found C 50.74, H 3.20, N 22.46%. IR. (nujol mull) 2090.7 $cm^{-1}$ (N-bound SCN).

### 6.5.4 Complexes of 4.16

With rhodium trichloride, *viz* **4.29**

Rhodium chloride (51.2 mg, 0.24 mmol) and **4.16** (50.0 mg, 0.18 mmol) were dissolved in methoxyethanol and refluxed for one hour. The yellow precipitate was collected, washed with cold methoxyethanol and dried under vacuum. Yield 76 mg (86%). M.p. 352°C (dec.). Analysis: calc. for $C_{14}H_{10}N_5RhCl_3$ C 34.11, H 2.04, N 14.21, Cl 28.77; found C 34.14, H 2.07, N 13.88, Cl 27.83%. $^1$H NMR (DMSO-$d_6$) δ 9.40 (s, 1H, H2), 9.05 (d, 2H, H6'), 8.85 (s, 1H, H5), 8.40 (t, 2H, H4'), 8.19 (d, 2H, H3'), 7.88 (t, 2H, H5').

With nickel perchlorate, *viz* **4.30**

A methanolic solution of **4.16** (21.4 mg, 0.075 mmol) was added dropwise to a solution of nickel perchlorate (27.7 mg, 0.076 mmol) dissolved in water. After stirring for 30 minutes, sodium thiocyanate was added to give a pale purple crystalline precipitate. The complex was collected by filtration and recrystallised, by vapour diffusion of ether into an acetonitrile solution of the complex, to give crystals suitable for X-ray crystallography. The crystals were filtered, washed with methanol, then ether and dried *in vacuo*. Yield 21.1 mg (33%). M.p. >222°C (dec.). Analysis: calc. for $C_{30}H_{20}N_{12}S_2Ni.2H_2O$ C 48.42, H 3.23, N 21.59; found C 48.28, H 3.11, N 21.91%. IR. (nujol mull) 2090.7 (N-bound SCN).

### 6.5.5 Complexes of 4.7

With palladium chloride, *viz* **4.31**

Palladium chloride (17.9 mg, 0.101 mmol) was dissolved in dilute hydrochloric acid (4 mL) and added dropwise to a solution of **4.7** (19.7 mg, 0.047 mmol) in methanol. An immediate change gave an orange solution from which a yellow precipitate formed, was collected, washed with cold methanol and dried *in vacuo*. Yield 28 mg (74%). M.p. >340°C (dec.). Analysis: calc. for $C_{26}H_{20}N_6Pd_2Cl_4.2H_2O$ C 38.69, H 3.00, N 10.41, Cl 17.57; found C 38.56, H 2.57, N 9.99, Cl 17.20%.

With copper nitrate, *viz* **4.32**

To a warm solution of **4.7** (20.9 mg, 0.050 mmol) in methanol, was added a solution of copper nitrate (24.3 mg, 0.100 mmol) dissolved in methanol. The solution was allowed to cool slowly during which time blue needles of a copper complex precipitated and were collected by filtration. Yield 29.4 mg (71%). M.p. 215-7°C. Analysis: calc. for $C_{26}H_{20}N_{10}O_{12}Cu_2.2H_2O$ C 37.73, H 2.92, N 16.92; found C 38.15, H 3.06, N 15.95%.

With nickel perchlorate, *viz* **4.33**

A methanolic solution of **4.7** (20.1 mg, 0.048 mmol) was added dropwise to a solution of nickel perchlorate (39.6 mg, 0.11 mmol) dissolved in water. The resultant green solution was stirred for 30 minutes and an excess of sodium thiocyanate was added to give a green precipitate. Recrystallisation, by vapour diffusion of ethanol into a DMSO solution of the complex, produced crystals suitable for X-ray crystallography. Yield 35 mg (91%). M.p. 310°C (dec.). Analysis: calc. for $C_{30}H_{20}N_{10}S_4Ni_2.2H_2O$ C 44.92, H 3.02, N 17.46; found C 44.99, H 2.95, N 17.66%. IR. (nujol mull) 2096.5 (N-bound SCN), 1996.2 ($\mu_2$N-bound SCN).

With nickel tetrafluoroborate, *viz* **4.34**

Nickel tetrafluoroborate (16.2 mg, 0.048 mmol) and **4.7** (19.7 mg, 0.47 mmol) were both dissolved in hot methanol and the solutions mixed together. After slow evaporation of the resulting solution, pale green/brown crystals formed that were suitable for X-ray crystallography. Yield 13 mg (43%). M.p. >305°C (dec.). Analysis for this compound was consistently high in carbon and nitrogen and a satisfactory agreement could not be obtained.

With copper tetrafluoroborate, *viz* **4.35**

Copper tetrafluoroborate (16.1 mg, 0.047 mmol) and **4.7** (20.1 mg, 0.048 mmol) were both dissolved in hot methanol and the solutions combined. On cooling a blue crystalline precipitate formed with crystals suitable for X-ray crystallography. Yield 8 mg (25%). M.p. >280°C (dec.). Analysis: calc. for $C_{52}H_{42}B_4Cu_2F_{16}N_{12}.2H_2O$ C 46.49, H 3.30, N 12.51; found C 46.49, H 3.10, N 12.45%.

With ferrous ammonium sulfate **4.36**

An aqueous solution of ferrous ammonium sulfate (18.5 mg, 0.047 mmol) was combined with a solution of **4.7** (20.5 mg, 0.049 mmol) dissolved in acetone. After stirring and heating the solution for 90 minutes, during which time the solution went bright red, an excess of ammonium hexafluorophosphate was added to give a red precipitate. This was collected by filtration, washed first with water, then ether and dried *in vacuo*. Yield 14.5 mg (40%). M.p. >260°C (dec.). Analysis: calc. for $C_{52}H_{40}N_{12}F_{24}P_4Fe_2.H_2O$ C 40.49, H 2.74, N 10.90; found C 40.28, H 3.13, N 10.60%.

### 6.5.6 Complexes of 4.9

With nickel tetrafluoroborate, *viz* **4.37**

Nickel tetrafluoroborate (15 mg, 0.044 mmol) and **4.9** (20 mg, 0.043 mmol) were both dissolved in methanol and the solutions combined. After slow evaporation of the resulting solution, a brown crystalline solid precipitated, was collected and dried *in vacuo*. The precipitate contained some crystals that were suitable for X-ray crystallography. Yield 21.3 mg (49%). M.p. 328°C (dec.). Analysis: calc. for $C_{30}H_{22}B_4N_6F_{16}Ni_2.5H_2O$ C 35.28, H 3.16, N 8.23; found C 34.86, H 2.11, N 8.08%.

With copper tetrafluoroborate, *viz* **4.38**

Copper tetrafluoroborate (15.1 mg, 0.044 mmol) and **4.9** (19.8 mg, 0.043 mmol) were both dissolved in hot methanol and the solutions combined. On cooling a blue crystalline precipitate formed containing crystals suitable for X-ray crystallography. Yield 9.1 mg (26%). M.p. 284-287°C (dec.). Analysis: calc. for $C_{30}H_{23}B_1N_6O_1F_4Cl_2Cu_2.3¼H_2O$ C 43.58, H 3.60, N 10.16; found C 43.51, H 2.96, N 10.02%.

With nickel perchlorate, *viz* **4.39**

To a solution of **4.9** (20 mg, 0.043 mmol) dissolved in methanol was added an aqueous solution of silver perchlorate (34 mg, 0.093 mmol). After 30 minutes sodium thiocyanate was added to this solution resulting in the precipitation of a pale yellow solid. Yield 24 mg (71%). M.p. >295°C (dec.). Analysis: calc. for $C_{32}H_{22}N_8S_2Cl_2Ni_2.H_2O$ C 48.71, H 3.07, N 14.20; found C 48.95, H 3.25, N 13.44%.

With copper nitrate, *viz* **4.40/4.41**

Reaction of **4.9** (20 mg, 0.043 mmol) with copper nitrate (22 mg, 0.091 mmol) in methanol gave a blue precipitate. Recrystallisation by vapour diffusion of pentane into an acetonitrile solution of the precipitate gave blue (**4.40**) and green (**4.41**) crystals, both of which were suitable for X-ray crystallography. **4.40**: Yield 17.6 mg (48%). M.p. >330°C. Analysis: calc. for $C_{60}H_{44}N_{20}O_{24}Cu_4$ C 41.91, H 2.81, N 16.29; found C 42.09, H 2.78, N 15.94%. **4.41**: Yield 7.5 mg (16%). M.p. 198°C (dec.). Analysis: calc. for $C_{30}H_{25}N_{10}O_{14}Cl_2Cu_3.H_2O$ C 35.01, H 2.64, N 13.61; found C 35.01, H 2.63, N 13.85%.

With ferrous ammonium sulfate *viz* **4.42**

An aqueous solution of ferrous ammonium sulfate (16.7 mg, 0.043 mmol) was combined with a solution of **4.9** (20.4 mg, 0.044 mmol) dissolved in acetone. After stirring and heating the solution for 90 minutes, during which time the solution went bright red, an excess of ammonium hexafluorophosphate was added to give a red precipitate. This was collected by filtration, washed first with water, then ether and dried *in vacuo*. Yield 17.4 mg (40%). M.p. >329°C (dec.). Analysis: calc. for $C_{60}H_{44}N_{12}F_{24}P_4Fe_2.2½H_2O$ C 43.16, H 2.96, N 10.07; found C 42.97, H 3.27, N 9.67%.

### 6.5.7 Complexes of 4.14

With copper tetrafluoroborate, *viz* **4.43**

Copper tetrafluoroborate (11.2 mg, 0.032 mmol) and **4.14** (20.0 mg 0.033 mmol) were both dissolved in hot methanol and the solutions combined. Immediately a pale blue solid formed. Addition of dichloromethane to the reaction mixture led to the formation of blue crystals that were suitable for X-ray crystallography. These were collected and dried *in vacuo*. Yield 18.2 mg (63%). M.p.220-223°C (dec.). Analysis: calc. for $C_{70}H_{56}B_4N_{20}O_6F_{16}Cu_2$ C 48.11, H 3.23, N 16.03; found C 48.20, H 3.28, N 16.27%.

With nickel tetrafluoroborate, *viz* **4.44**

Nickel tetrafluoroborate (11.2 mg, 0.033 mmol) and **4.14** (19.9 mg, 0.033 mmol) were both dissolved in hot methanol and the solutions combined. On standing pale blue crystals precipitated from this solution, were collected and then dried *in vacuo*. Yield 8 mg (27%). M.p. >280°C (dec.). Analysis: calc. for $C_{68}H_{52}B_4N_{20}O_4F_{16}Ni_2.6H_2O$ C 45.83, H 3.39, N 15.72; found C 45.68, H 3.84, N 15.39%.

# *Appendices*

# Appendix 1: Crystallography

Tables A1 -A11 list the crystal data and X-ray experimental details for the fifty six fully refined crystal structures discussed in this thesis. Throughout the text, selected bond lengths and angles are discussed and listed under the appropriate figures, while the remaining distances and angles, as well as atom coordinates, anisotropic displacement parameters and hydrogen atom coordinates are available on request from the Department of Chemistry, University of Canterbury.

All measurements were made with a Siemens CCD area detector using graphite monochromatised Mo Kα (λ = 0.71073 Å) radiation at the temperature indicated in the following tables. The data reduction was performed using SAINT.[244] The intensities were corrected for Lorentz and polarisation effects and for absorption using SADABS.[245] The structures were solved by direct methods using either SHELXS,[246] or SIR97[247] and refined on $F^2$ using all data by full-matrix least-squares procedures using SHELXL-97.[248] All non-hydrogen atoms were refined with anisotropic displacement parameters. Aromatic and aliphatic hydrogen atoms were included in calculated positions with isotopic displacement parameters 1.2 and 1.5 times the isotropic equivalent of their carrier carbon atoms, respectively.

**Table A1.** Crystal data and X-ray experimental data for **2.13**, **2.17**, **2.19**, **2.23**, and **2.24**.

| Compound | **2.13** | **2.17** | **2.19** | **2.23** | **2.24** |
|---|---|---|---|---|---|
| Empirical formula | $C_{27}H_{20}N_4$ | $C_{39}H_{27}N_3$ | $C_{11}H_{10}AgN_3O_3$ | $C_{54}H_{49}Cu_6N_{19}O_{26}$ | $C_{22}H_{18}AgN_5O_3$ |
| Formula weight | 400.47 | 537.64 | 340.09 | 1761.36 | 508.28 |
| Temperature (K) | 168(2) | 168(2) | 168(2) | 168(2) | 168(2) |
| Crystal system | Orthorhombic | Triclinic | Monoclinic | Monoclinic | Monoclinic |
| Space group | $P2_12_12_1$ | P-1 | P2/c | $P2_1/c$ | Cc |
| Unit cell dimensions: a (Å) | 10.211(7) | 10.440(6) | 5.477(3) | 14.474(4) | 15.948(6) |
| b (Å) | 10.292(7) | 12.203(7) | 8.370(5) | 24.872(7) | 11.544(5) |
| c (Å) | 18.932(13) | 13.245(7) | 12.711(7) | 20.202(6) | 13.420(5) |
| α (°) | 90 | 105.046(8) | 90 | 90 | 90 |
| β (°) | 90 | 110.742(9) | 93.762(10) | 107.596(4) | 121.083(5) |
| γ (°) | 90 | 105.034(8) | 90 | 90 | 90 |
| Volume ($Å^3$) | 1990(2) | 1403.9(13) | 581.5(6) | 6932(3) | 2116.0(14) |
| Z | 4 | 2 | 2 | 4 | 4 |
| Density (calculated) ($Mg/m^3$) | 1.337 | 1.272 | 1.942 | 1.688 | 1.596 |
| Absorption coefficient ($mm^{-1}$) | 0.081 | 0.075 | 1.737 | 1.901 | 0.987 |
| F(000) | 840 | 564 | 336 | 3552 | 1024 |
| Crystal size ($mm^3$) | 0.55 x 0.39 x 0.16 | 0.70 x 0.28 x 0.06 | 0.55 x 0.21 x 0.08 | 0.50 x 0.50 x 0.33 | 0.20 x 0.18 x 0.10 |
| Theta range for data collection (°) | 2.15 to 26.41 | 2.02 to 26.37 | 2.43 to 26.47 | 1.95 to 26.38 | 2.31 to 26.37 |
| Reflections collected | 26118 | 17764 | 4893 | 50777 | 13344 |
| Independent reflections [R(int)] | 4072 [0.0453] | 5585 [0.0532] | 1175 [0.0346] | 14005 [0.0397] | 3870 [0.0300] |
| Observed reflections [$I>2\sigma(I)$] | 2931 | 2278 | 861 | 8660 | 3445 |
| Data / restraints / parameters | 4072 / 0 / 280 | 5585 / 0 / 379 | 1175 / 0 / 84 | 14005 / 48 / 973 | 3870 / 2 / 281 |
| Goodness-of-fit on $F^2$ | 0.903 | 0.738 | 0.996 | 0.873 | 0.936 |
| $R_1$ [$I>2\sigma(I)$] | 0.0348 | 0.0422 | 0.0509 | 0.0294 | 0.0227 |
| $wR_2$ (all data) | 0.0723 | 0.0909 | 0.1356 | 0.0610 | 0.0407 |

**Table A2.** Crystal data and X-ray experimental data for **2.25**, **2.26**, **2.28**, **2.29**, and **2.30**.

| Compound | **2.25** | **2.26** | **2.28** | **2.29** | **2.30** |
|---|---|---|---|---|---|
| Empirical formula | $C_{48}H_{42}Ag_2B_2F_8N_{10}$ | $C_{26}H_{34}Cu_2N_8O_{16}$ | $C_{30}H_{30}N_4O_8Zn_2$ | $C_{11}H_{10}AgN_3O_3$ | $C_{12}H_{12}Cl_2N_2O_2Pd$ |
| Formula weight | 1148.28 | 841.69 | 705.32 | 340.09 | 393.54 |
| Temperature (K) | 168(2) | 168(2) | 168(2) | 168(2) | 168(2) |
| Crystal system | Monoclinic | Monoclinic | Monoclinic | Monoclinic | Monoclinic |
| Space group | $P2_1/c$ | C2/c | $P2_1/c$ | $P2_1/c$ | $P2_1/n$ |
| Unit cell dimensions: a (Å) | 9.225(3) | 27.086(13) | 9.898(3) | 9.478(3) | 9.106(3) |
| b (Å) | 15.448(6) | 10.055(5) | 7.975(3) | 14.189(4) | 11.784(5) |
| c (Å) | 16.892(6) | 14.324(7) | 18.728(6) | 9.136(3) | 12.625(4) |
| α (°) | 90 | 90 | 90 | 90 | 90 |
| β (°) | 92.551(5) | 119.938(6) | 96.104(4) | 110.702(4) | 91.509(15) |
| γ (°) | 90 | 90 | 90 | 90 | 90 |
| Volume ($Å^3$) | 2404.8(15) | 3380(3) | 1469.8(8) | 1149.3(6) | 1354.2(9) |
| Z | 2 | 4 | 2 | 4 | 4 |
| Density (calculated) ($Mg/m^3$) | 1.586 | 1.654 | 1.594 | 1.966 | 1.930 |
| Absorption coefficient ($mm^{-1}$) | 0.891 | 1.344 | 1.690 | 1.757 | 1.762 |
| F(000) | 1152 | 1728 | 724 | 672 | 776 |
| Crystal size ($mm^3$) | 0.37 x 0.30 x 0.15 | 0.24 x 0.18 x 0.17 | 0.48 x 0.16 x 0.10 | 0.53 x 0.22 x 0.03 | 0.37 x 0.35 x 0.04 |
| Theta range for data collection (°) | 1.79 to 26.37 | 2.20 to 26.41 | 2.19 to 26.37 | 2.71 to 26.39 | 2.36 to 26.45 |
| Reflections collected | 27747 | 21145 | 18324 | 11743 | 9676 |
| Independent reflections [R(int)] | 4818 [0.0517] | 3438 [0.0318] | 2975 [0.0389] | 2245 [0.0326] | 2761 [0.0268] |
| Observed reflections [$I>2\sigma(I)$] | 2844 | 2812 | 2458 | 1795 | 2233 |
| Data / restraints / parameters | 4818 / 0 / 317 | 3438 / 0 / 300 | 2975 / 0 / 205 | 2245 / 0 / 163 | 2761 / 0 / 157 |
| Goodness-of-fit on $F^2$ | 0.926 | 1.034 | 1.055 | 1.045 | 1.044 |
| $R_1$ [$I>2\sigma(I)$] | 0.0440 | 0.0256 | 0.0289 | 0.0269 | 0.0311 |
| $wR_2$ (all data) | 0.1038 | 0.0682 | 0.0749 | 0.0635 | 0.0716 |

**Table A3.** Crystal data and X-ray experimental data for **2.31**, **2.32**, **2.33**, **2.35**, and **2.36**.

| Compound | **2.31** | **2.32** | **2.33** | **2.35** | **2.36** |
|---|---|---|---|---|---|
| Empirical formula | $C_{22}H_{24}CuN_6O_{12}$ | $C_{22}H_{22}CuN_6O_{11}$ | $C_{26}H_{32}Cu_2N_8O_{16}$ | $C_{30}H_{40}N_4O_{14}Pd_2$ | $C_{30}H_{32}N_4O_{10}Zn_2$ |
| Formula weight | 628.01 | 610.00 | 839.68 | 893.46 | 739.34 |
| Temperature (K) | 158(2) | 168(2) | 168(2) | 168(2) | 168(2) |
| Crystal system | Monoclinic | Monoclinic | Monoclinic | Monoclinic | Triclinic |
| Space group | $P2_1/n$ | Cc | C2/c | C2/c | P-1 |
| Unit cell dimensions: a (Å) | 7.538(2) | 8.000(2) | 27.51(2) | 19.644(8) | 8.435(2) |
| b (Å) | 12.048(3) | 32.264(8) | 10.046(7) | 15.938(6) | 8.818(2) |
| c (Å) | 14.550(4) | 9.563(2) | 14.011(10) | 14.847(6) | 10.670(3) |
| α (°) | 90 | 90 | 90 | 90 | 78.723(3) |
| β (°) | 93.479(4) | 97.962(3) | 119.626(10) | 125.925(5) | 82.103(3) |
| γ (°) | 90 | 90 | 90 | 90 | 88.974(3) |
| Volume ($Å^3$) | 1318.9(6) | 2444.5(10) | 3366(4) | 3764(3) | 771.0(3) |
| Z | 2 | 4 | 4 | 4 | 1 |
| Density (calculated) ($Mg/m^3$) | 1.581 | 1.657 | 1.657 | 1.577 | 1.592 |
| Absorption coefficient ($mm^{-1}$) | 0.903 | 0.969 | 1.350 | 1.023 | 1.620 |
| F(000) | 646 | 1252 | 1720 | 1808 | 380 |
| Crystal size ($mm^3$) | 0.53 x 0.24 x 0.11 | 0.61 x 0.60 x 0.50 | 0.20 x 0.15 x 0.05 | 0.55 x 0.43 x 0.21 | 0.56 x 0.40 x 0.29 |
| Theta range for data collection (°) | 2.20 to 26.36 | 2.49 to 26.34 | 2.20 to 22.50 | 1.90 to 25.00 | 2.36 to 26.38 |
| Reflections collected | 16121 | 15172 | 15470 | 12495 | 9413 |
| Independent reflections [R(int)] | 2624 [0.0417] | 4267 [0.0181] | 2193 [0.5997] | 3285 [0.0267] | 3050 [0.0192] |
| Observed reflections [$I>2\sigma(I)$] | 2219 | 4177 | 1203 | 2908 | 2831 |
| Data / restraints / parameters | 2624 / 0 / 176 | 4267 / 2 / 361 | 2193 / 0 / 238 | 3285 / 0 / 226 | 3050 / 0 / 208 |
| Goodness-of-fit on $F^2$ | 1.124 | 1.037 | 0.997 | 1.087 | 1.081 |
| $R_1$ [$I>2\sigma(I)$] | 0.0421 | 0.0250 | 0.0627 | 0.0341 | 0.0286 |
| $wR_2$ (all data) | 0.0952 | 0.0693 | 0.1438 | 0.1067 | 0.0763 |

**Table A4.** Crystal data and X-ray experimental data for **2.37**, **2.38**, **2.39**, **2.40**, and **2.42**.

| Compound | **2.37** | **2.38** | **2.39** | **2.40** | **2.42** |
|---|---|---|---|---|---|
| Empirical formula | $C_{26}H_{28}AgN_3O_5$ | $C_{51.50}H_{52}Cu_2N_6O_{9.50}$ | $C_{88}H_{86}Ag_8N_{32}O_{35}$ | $C_{22}H_{16}CuN_{10}O_6$ | $C_{18}H_{16}AgN_4O_4$ |
| Formula weight | 570.38 | 1034.07 | 3014.84 | 579.99 | 460.22 |
| Temperature (K) | 168(2) | 168(2) | 163(2) | 168(2) | 168(2) |
| Crystal system | Monoclinic | Triclinic | Monoclinic | Triclinic | Orthorhombic |
| Space group | $P2_1/n$ | P-1 | $P2_1/c$ | P-1 | Pccn |
| Unit cell dimensions: a (Å) | 9.008(3) | 13.388(6) | 13.5851(12) | 7.030(3) | 6.718(3) |
| b (Å) | 14.627(5) | 13.474(6) | 16.1634(15) | 9.039(4) | 23.167(11) |
| c (Å) | 19.660(7) | 14.939(6) | 48.468(5) | 9.806(4) | 24.238(12) |
| α (°) | 90 | 74.781(7) | 90 | 76.783(6) | 90 |
| β (°) | 102.566(5) | 77.414(6) | 95.559(1) | 75.962(6) | 90 |
| γ (°) | 90 | 75.730(5) | 90 | 68.600(6) | 90 |
| Volume ($Å^3$) | 2528.4(15) | 2486.1(18) | 10592.6(17) | 556.0(4) | 3772(3) |
| Z | 4 | 2 | 4 | 1 | 8 |
| Density (calculated) ($Mg/m^3$) | 1.498 | 1.381 | 1.890 | 1.732 | 1.621 |
| Absorption coefficient ($mm^{-1}$) | 0.838 | 0.918 | 1.545 | 1.049 | 1.100 |
| F(000) | 1168 | 1074 | 5976 | 295 | 1848 |
| Crystal size ($mm^3$) | 0.48 x 0.38 x 0.09 | 0.63 x 0.21 x 0.13 | 0.64 x 0.35 x 0.11 | 0.37 x 0.16 x 0.05 | 0.30 x 0.15 x 0.05 |
| Theta range for data collection (°) | 2.12 to 26.40 | 1.96 to 25.00 | 1.52 to 26.35 | 2.17 to 26.40 | 1.68 to 24.00 |
| Reflections collected | 31952 | 28374 | 131885 | 7252 | 16385 |
| Independent reflections [R(int)] | 5083 [0.0388] | 8595 [0.0435] | 21441 [0.0887] | 2235 [0.0223] | 2852 [0.1310] |
| Observed reflections [$I>2\sigma(I)$] | 3976 | 5744 | 12468 | 1803 | 1781 |
| Data / restraints / parameters | 5083 / 0 / 328 | 8595 / 8 / 662 | 21441 / 31 / 1546 | 2235 / 0 / 178 | 2852 / 18 / 254 |
| Goodness-of-fit on $F^2$ | 0.914 | 1.019 | 0.972 | 0.989 | 1.093 |
| $R_1$ [$I>2\sigma(I)$] | 0.0454 | 0.0611 | 0.0479 | 0.0295 | 0.0980 |
| $wR_2$ (all data) | 0.1285 | 0.1825 | 0.1042 | 0.0678 | 0.2693 |

Table A5. Crystal data and X-ray experimental data for **2.43**, **2.44**, **2.52**, **2.55**, and **3.6**.

| Compound | **2.43** | **2.44** | **2.52** | **2.55** | **3.6** |
|---|---|---|---|---|---|
| Empirical formula | $C_{38}H_{27}Ag_2N_7F_{12}P_2$ | $C_{72}H_{70}Ag_6B_5F_{21}N_{12}O_{11}$ | $C_{44}H_{42}F_{12}N_8O_2P_2Ru$ | $C_{43}H_{37}F_{12}N_8O_{1.5}P_2Ru$ | $C_{30}H_{22}N_6$ |
| Formula weight | 1087.35 | 2379.67 | 1105.87 | 1080.82 | 466.54 |
| Temperature (K) | 168(2) | 168(2) | 168(2) | 168(2) | 168(2) |
| Crystal system | Triclinic | Monoclinic | Monoclinic | Triclinic | Monoclinic |
| Space group | P-1 | $P2_1/n$ | $P2_1/n$ | P-1 | $P2_1/n$ |
| Unit cell dimensions: a (Å) | 11.627(4) | 21.890(7) | 8.995(3) | 9.361(5) | 6.818(2) |
| b (Å) | 11.825(4) | 15.011(5) | 24.352(11) | 9.996(5) | 10.826(4) |
| c (Å) | 15.340(5) | 27.729(9) | 21.704(11) | 24.314(13) | 15.586(6) |
| α (°) | 104.996(4) | 90 | 90 | 100.296(7) | 90 |
| β (°) | 101.579(4) | 112.604(4) | 100.89(2) | 93.188(8) | 91.271(13) |
| γ (°) | 100.202(5) | 90 | 90 | 91.266(8) | 90 |
| Volume ($Å^3$) | 1936.6(11) | 8412(5) | 4668(4) | 2234(2) | 1150.1(8) |
| Z | 2 | 4 | 4 | 2 | 2 |
| Density (calculated) ($Mg/m^3$) | 1.865 | 1.879 | 1.573 | 1.607 | 1.347 |
| Absorption coefficient ($mm^{-1}$) | 1.193 | 1.481 | 0.500 | 0.519 | 0.083 |
| F(000) | 1072 | 4680 | 2240 | 1090 | 488 |
| Crystal size ($mm^3$) | 0.54 x 0.39 x 0.32 | 0.30 x 0.25 x 0.04 | 0.45 x 0.27 x 0.23 | 0.57 x 0.25 x 0.02 | 0.60 x 0.39 x 0.28 |
| Theta range for data collection (°) | 1.84 to 25.00 | 1.69 to 25.00 | 1.93 to 25.00 | 2.18 to 25.00 | 2.29 to 25.00 |
| Reflections collected | 21665 | 96087 | 54409 | 15868 | 10422 |
| Independent reflections [R(int)] | 6639 [0.0191] | 14791 [0.0747] | 8205 [0.0507] | 7771 [0.0663] | 1968 [0.0328] |
| Observed reflections [$I>2\sigma(I)$] | 5467 | 10121 | 6719 | 3322 | 1685 |
| Data / restraints / parameters | 6639 / 24 / 591 | 14791 / 0 / 1144 | 8205 / 12 / 701 | 7771 / 0 / 616 | 1968 / 0 / 163 |
| Goodness-of-fit on $F^2$ | 1.022 | 1.047 | 1.014 | 0.855 | 1.144 |
| $R_1$ [$I>2\sigma(I)$] | 0.0352 | 0.0493 | 0.0655 | 0.0638 | 0.0468 |
| $wR_2$ (all data) | 0.1084 | 0.0887 | 0.1877 | 0.1556 | 0.1081 |

**Table A6.** Crystal data and X-ray experimental data for **3.11**, **3.13**, **3.20**, **3.21**, and **3.23**.

| Compound | **3.11** | **3.13** | **3.20** | **3.21** | **3.23** |
|---|---|---|---|---|---|
| Empirical formula | $C_{28}H_{24}N_6$ | $C_{28}H_{24}N_6$ | $C_{26}H_{20}AgN_7O_3$ | $C_{30}H_{26}Ag_2B_2F_8N_8$ | $C_{30}H_{32}Cu_2N_{10}O_{14}S_2$ |
| Formula weight | 444.53 | 444.53 | 586.36 | 887.95 | 947.86 |
| Temperature (K) | 168(2) | 168(2) | 168(2) | 168(2) | 168(2) |
| Crystal system | Triclinic | Monoclinic | Triclinic | Monoclinic | Triclinic |
| Space group | P-1 | $P2_1/n$ | P-1 | C2/c | P-1 |
| Unit cell dimensions: a (Å) | 9.205(2) | 8.483(2) | 9.788(3) | 20.917(7) | 9.191(5) |
| b (Å) | 11.066(3) | 16.999(4) | 10.901(3) | 13.665(5) | 9.841(5) |
| c (Å) | 12.355(3) | 8.759(2) | 12.844(3) | 12.791(4) | 11.092(6) |
| α (°) | 104.910(4) | 90 | 69.774(3) | 90 | 84.950(7) |
| β (°) | 95.265(3) | 115.643(3) | 68.357(3) | 114.064(4) | 68.561(9) |
| γ (°) | 108.023(3) | 90 | 79.025(3) | 90 | 86.950(7) |
| Volume ($Å^3$) | 1136.3(5) | 1138.6(5) | 1192.2(5) | 3338.4(19) | 929.9(8) |
| Z | 2 | 2 | 2 | 4 | 1 |
| Density (calculated) ($Mg/m^3$) | 1.299 | 1.297 | 1.633 | 1.767 | 1.693 |
| Absorption coefficient ($mm^{-1}$) | 0.080 | 0.080 | 0.890 | 1.254 | 1.338 |
| F(000) | 468 | 468 | 592 | 1752 | 484 |
| Crystal size ($mm^3$) | 0.65 x 0.39 x 0.16 | 0.61 x 0.53 x 0.35 | 0.60 x 0.15 x 0.13 | 0.48 x 0.37 x 0.05 | 0.35 x 0.11 x 0.10 |
| Theta range for data collection (°) | 2.03 to 26.43 | 2.40 to 26.40 | 2.24 to 26.40 | 2.13 to 26.46 | 2.38 to 22.49 |
| Reflections collected | 14409 | 14413 | 14630 | 20972 | 4182 |
| Independent reflections [R(int)] | 4528 [0.0220] | 2292 [0.0160] | 4743 [0.0436] | 3376 [0.0343] | 2293 [0.0388] |
| Observed reflections [$I>2\sigma(I)$] | 3685 | 2102 | 3967 | 2366 | 1755 |
| Data / restraints / parameters | 4528 / 0 / 307 | 2292 / 0 / 154 | 4743 / 0 / 334 | 3376 / 0 / 265 | 2293 / 0 / 262 |
| Goodness-of-fit on $F^2$ | 1.102 | 1.063 | 1.020 | 0.732 | 1.058 |
| $R_1$ [$I>2\sigma(I)$] | 0.0501 | 0.0403 | 0.0370 | 0.0218 | 0.0714 |
| $wR_2$ (all data) | 0.1252 | 0.1024 | 0.1005 | 0.0508 | 0.1901 |

**Table A7.** Crystal data and X-ray experimental data for **3.24**, **3.26b**, **3.31**, **3.32**, and **3.34**.

| Compound | **3.24** | **3.26b** | **3.31** | **3.32** | **3.34** |
|---|---|---|---|---|---|
| Empirical formula | $C_{26}H_{20}Cl_4N_6Zn_2$ | $C_{72}H_{62}Ag_2F_{12}N_{18}P_2$ | $C_{61}H_{64}Ag_4N_{18}O_{16}$ | $C_{72}H_{74}Ag_4F_{24}N_{20}OP_4$ | $C_{28}H_{28}Cu_2N_{10}O_{14}$ |
| Formula weight | 689.02 | 1685.08 | 1736.78 | 2246.87 | 855.68 |
| Temperature (K) | 168(2) | 168(2) | 168(2) | 168(2) | 168(2) |
| Crystal system | Triclinic | Monoclinic | Monoclinic | Monoclinic | Monoclinic |
| Space group | P-1 | $P2_1/c$ | $P2_1/n$ | Cc | C2/c |
| Unit cell dimensions: a (Å) | 8.329(4) | 18.564(10) | 11.737(5) | 17.656(2) | 22.430(9) |
| b (Å) | 9.597(5) | 14.131(9) | 26.844(10) | 21.334(3) | 9.719(4) |
| c (Å) | 9.755(5) | 14.550(8) | 23.194(9) | 23.747(3) | 16.300(6) |
| α (°) | 98.856(7) | 90 | 90 | 90 | 90 |
| β (°) | 106.025(6) | 107.33(2) | 101.931(6) | 94.719(2) | 100.987(5) |
| γ (°) | 107.965(6) | 90 | 90 | 90 | 90 |
| Volume ($Å^3$) | 688.1(6) | 3644(4) | 7150(5) | 8914.9(18) | 3488(2) |
| Z | 1 | 2 | 4 | 4 | 4 |
| Density (calculated) ($Mg/m^3$) | 1.663 | 1.536 | 1.613 | 1.674 | 1.629 |
| Absorption coefficient ($mm^{-1}$) | 2.160 | 0.668 | 1.156 | 1.042 | 1.302 |
| F(000) | 346 | 1704 | 3488 | 4472 | 1744 |
| Crystal size ($mm^3$) | 0.35 x 0.28 x 0.08 | 0.60 x 0.40 x 0.08 | 0.54 x 0.18 x 0.16 | 0.73 x 0.55 x 0.31 | 0.35 x 0.30 x 0.10 |
| Theta range for data collection (°) | 2.25 to 26.38 | 2.13 to 25.00 | 1.76 to 24.00 | 2.09 to 26.47 | 2.29 to 26.37 |
| Reflections collected | 8180 | 14568 | 73825 | 39624 | 21280 |
| Independent reflections [R(int)] | 2595 [0.0243] | 6383 [0.0450] | 11079 [0.1233] | 13417 [0.0305] | 3521 [0.0451] |
| Observed reflections [$I>2\sigma(I)$] | 1752 | 4015 | 8435 | 12551 | 2612 |
| Data / restraints / parameters | 2595 / 0 / 172 | 6383 / 0 / 481 | 11079 / 3 / 910 | 13417 / 4 / 1136 | 3521 / 0 / 249 |
| Goodness-of-fit on $F^2$ | 0.916 | 1.018 | 1.250 | 1.060 | 1.001 |
| $R_1$ [$I>2\sigma(I)$] | 0.0346 | 0.0506 | 0.1112 | 0.0382 | 0.0330 |
| $wR_2$ (all data) | 0.0761 | 0.1440 | 0.2297 | 0.0985 | 0.0856 |

**Table A8.** Crystal data and X-ray experimental data for **3.35**, **3.40**, **3.45**, **3.46**, and **3.47**.

| Compound | **3.35** | **3.40** | **3.45** | **3.46** | **3.47** |
|---|---|---|---|---|---|
| Empirical formula | $C_{36}H_{31}Ag_2B_2F_8N_9$ | $C_{38}H_{32}Cl_3N_9O_2Pd_3$ | $C_{56}H_{48}Ag_2N_{14}O_6$ | $C_{56}H_{48}Ag_2B_2F_8N_{12}$ | $C_{172}H_{156}Ag_6Cl_4F_{36}N_{36}O_2P_6$ |
| Formula weight | 979.06 | 1072.28 | 1228.82 | 1278.42 | 4418.16 |
| Temperature (K) | 168(2) | 168(2) | 168(2) | 168(2) | 168(2) |
| Crystal system | Monoclinic | Monoclinic | Monoclinic | Monoclinic | Triclinic |
| Space group | $P2_1/c$ | C2/c | $P2_1/n$ | $P2_1/n$ | P-1 |
| Unit cell dimensions: a (Å) | 13.765(4) | 12.696(5) | 12.659(5) | 12.618(4) | 14.361(5) |
| b (Å) | 25.188(7) | 13.416(5) | 12.417(5) | 12.798(4) | 17.001(6) |
| c (Å) | 13.215(4) | 22.649(9) | 17.195(5) | 17.110(6) | 20.092(7) |
| α (°) | 90 | 90 | 90 | 90 | 69.969(4) |
| β (°) | 113.796(4) | 90.887(13) | 106.291(5) | 106.394(4) | 73.690(4) |
| γ (°) | 90 | 90 | 90 | 90 | 86.817(5) |
| Volume ($Å^3$) | 4192(2) | 3857(2) | 2594.3(16) | 2650.8(15) | 4419(2) |
| Z | 4 | 4 | 2 | 2 | 1 |
| Density (calculated) ($Mg/m^3$) | 1.551 | 1.846 | 1.573 | 1.602 | 1.660 |
| Absorption coefficient ($mm^{-1}$) | 1.007 | 1.640 | 0.822 | 0.819 | 0.870 |
| F(000) | 1944 | 2112 | 1248 | 1288 | 2220 |
| Crystal size ($mm^3$) | 0.50 x 0.33 x 0.31 | 0.60 x 0.35 x 0.29 | 0.70 x 0.55 x 0.40 | 0.45 x 0.36 x 0.20 | 0.46 x 0.44 x 0.08 |
| Theta range for data collection (°) | 1.81 to 25.00 | 2.21 to 26.42 | 2.05 to 26.36 | 2.02 to 26.35 | 1.97 to 25.00 |
| Reflections collected | 27661 | 21895 | 31748 | 32363 | 51734 |
| Independent reflections [R(int)] | 7278 [0.0396] | 3960 [0.0191] | 5275 [0.0191] | 5348 [0.0374] | 15404 [0.0952] |
| Observed reflections [$I>2\sigma(I)$] | 4977 | 3716 | 4891 | 4246 | 9767 |
| Data / restraints / parameters | 7278 / 0 / 575 | 3960 / 0 / 263 | 5275 / 0 / 352 | 5348 / 0 / 389 | 15404 / 0 / 1187 |
| Goodness-of-fit on $F^2$ | 1.068 | 1.063 | 1.092 | 0.994 | 0.941 |
| $R_1$ [$I>2\sigma(I)$] | 0.0635 | 0.0268 | 0.0235 | 0.0278 | 0.0496 |
| $wR_2$ (all data) | 0.1842 | 0.0653 | 0.0597 | 0.0663 | 0.1377 |

**Table A9.** Crystal data and X-ray experimental data for **3.50**, **3.52**, **3.57b**, **3.58**, and **4.19**.

| Compound | **3.50** | **3.52** | **3.57b** | **3.58** | **4.19** |
|---|---|---|---|---|---|
| Empirical formula | $C_{28}H_{24}AgN_7O_3$ | $C_{29}H_{28}AgF_6N_6OP$ | $C_{56}H_{55}Ag_3F_{18}N_{12}O_{3.5}P_3$ | $C_{30}H_{32}Cu_2N_{10}O_{14}$ | $C_{30}H_{24}B_2F_8N_8Ni$ |
| Formula weight | 614.41 | 729.41 | 1710.64 | 883.74 | 728.90 |
| Temperature (K) | 168(2) | 168(2) | 168(2) | 168(2) | 168(2) |
| Crystal system | Triclinic | Monoclinic | Monoclinic | Monoclinic | Monoclinic |
| Space group | P-1 | C2/c | $P2_1/c$ | $P2_1/n$ | $P2_1/n$ |
| Unit cell dimensions: a (Å) | 8.8253(18) | 8.623(3) | 14.7918(9) | 8.336(3) | 8.242(4) |
| b (Å) | 10.437(2) | 25.164(9) | 14.7643(9) | 13.148(5) | 17.538(11) |
| c (Å) | 14.732(3) | 14.262(5) | 29.0604(17) | 16.660(6) | 11.023(7) |
| α (°) | 85.759(2) | 90 | 90 | 90 | 90 |
| β (°) | 84.787(2) | 94.626(4) | 94.881(1) | 91.955(5) | 99.77(3) |
| γ (°) | 70.861(2) | 90 | 90 | 90 | 90 |
| Volume ($Å^3$) | 1275.2(4) | 3084.7(18) | 6323.5(7) | 1824.9(11) | 1570.2(16) |
| Z | 2 | 4 | 4 | 2 | 2 |
| Density (calculated) ($Mg/m^3$) | 1.600 | 1.571 | 1.797 | 1.608 | 1.542 |
| Absorption coefficient ($mm^{-1}$) | 0.836 | 0.775 | 1.105 | 1.247 | 0.702 |
| F(000) | 624 | 1472 | 3404 | 904 | 740 |
| Crystal size ($mm^3$) | 0.60 x 0.58 x 0.21 | 0.70 x 0.29 x 0.28 | 0.45 x 0.45 x 0.30 | 0.37 x 0.20 x 0.12 | 0.61 x 0.37 x 0.23 |
| Theta range for data collection (°) | 2.07 to 26.38 | 2.16 to 26.38 | 1.55 to 26.39 | 2.45 to 26.44 | 2.21 to 26.43 |
| Reflections collected | 16279 | 17476 | 47897 | 14750 | 20214 |
| Independent reflections [R(int)] | 5067 [0.0211] | 3121 [0.0289] | 12819 [0.0328] | 3651 [0.0394] | 3201 [0.0255] |
| Observed reflections [$I>2\sigma(I)$] | 4815 | 2833 | 9727 | 2538 | 2737 |
| Data / restraints / parameters | 5067 / 0 / 352 | 3121 / 0 / 212 | 12819 / 0 / 928 | 3651 / 0 / 257 | 3201 / 0 / 223 |
| Goodness-of-fit on $F^2$ | 1.026 | 1.228 | 1.040 | 0.979 | 1.047 |
| $R_1$ [$I>2\sigma(I)$] | 0.0234 | 0.0572 | 0.0395 | 0.0354 | 0.0380 |
| $wR_2$ (all data) | 0.0626 | 0.1457 | 0.0980 | 0.0827 | 0.1046 |

**Table A10.** Crystal data and X-ray experimental data for **4.21**, **4.23**, **4.27**, **4.28**, and **4.30**.

| Compound | **4.21** | **4.23** | **4.27** | **4.28** | **4.30** |
|---|---|---|---|---|---|
| Empirical formula | $C_{42}H_{62}N_{10}Ni_2O_9S_{10}$ | $C_{32}H_{42}N_8O_{14}Pd_2$ | $C_{52}H_{52}B_2F_{14}N_{16}Ni_2O_4Si$ | $C_{65.5}H_{69.5}N_{24.5}Ni_2O_{5.5}S_4$ | $C_{32}H_{23}Cl_2N_{13}NiS_2$ |
| Formula weight | 1289.04 | 975.54 | 1398.23 | 1533.62 | 783.36 |
| Temperature (K) | 168(2) | 168(2) | 168(2) | 168(2) | 168(2) |
| Crystal system | Monoclinic | Monoclinic | Monoclinic | Tetragonal | Triclinic |
| Space group | $P2_1/n$ | C2/c | C2/c | $I4_1/a$ | P-1 |
| Unit cell dimensions: a (Å) | 14.358(5) | 31.798(10) | 22.222(9) | 23.194(13) | 10.399(6) |
| b (Å) | 23.615(7) | 8.539(3) | 10.725(4) | 23.194(13) | 12.577(7) |
| c (Å) | 18.924(6) | 16.420(5) | 23.949(10 | 27.68(2) | 14.147(7) |
| α (°) | 90 | 90 | 90 | 90 | 71.20(2) |
| β (°) | 110.975(4) | 119.099(4) | 96.617(6) | 90 | 82.964(12) |
| γ (°) | 90 | 90 | 90 | 90 | 74.117(10) |
| Volume ($Å^3$) | 5991(3) | 3896(2) | 5670(4) | 14889(17) | 1683.4(16) |
| Z | 4 | 4 | 4 | 8 | 2 |
| Density (calculated) ($Mg/m^3$) | 1.429 | 1.663 | 1.638 | 1.368 | 1.545 |
| Absorption coefficient ($mm^{-1}$) | 1.033 | 0.999 | 0.794 | 0.684 | 0.906 |
| F(000) | 2688 | 1976 | 2856 | 6384 | 800 |
| Crystal size ($mm^3$) | 0.55 x 0.50 x 0.33 | 0.49 x 0.40 x 0.19 | 0.35 x 0.28 x 0.06 | 0.25 x 0.22 x 0.12 | 0.54 x 0.27 x 0.05 |
| Theta range for data collection (°) | 1.72 to 25.00 | 2.48 to 26.42 | 2.11 to 26.42 | 2.10 to 24.99 | 2.34 to 26.41 |
| Reflections collected | 68651 | 24058 | 21968 | 19238 | 10050 |
| Independent reflections [R(int)] | 10537 [0.0390] | 3976 [0.0351] | 5742 [0.0581] | 6526 [0.1361] | 6349 [0.0422] |
| Observed reflections [$I>2\sigma(I)$] | 8654 | 3361 | 2745 | 2140 | |
| Data / restraints / parameters | 10537 / 12 / 700 | 3976 / 0 / 251 | 5742 / 0 / 413 | 6526 / 32 / 468 | 6349 / 0 / 452 |
| Goodness-of-fit on $F^2$ | 1.074 | 1.107 | 0.789 | 0.747 | 1.023 |
| $R_1$ [$I>2\sigma(I)$] | 0.0718 | 0.0361 | 0.0368 | 0.0576 | 0.0796 |
| $wR_2$ (all data) | 0.1962 | 0.0914 | 0.0742 | 0.1309 | 0.2638 |

**Table A11.** Crystal data and X-ray experimental data for **4.34**, **4.35**, **4.38**, **4.40**, and **4.41**.

| Compound | **4.34** | **4.35** | **4.38** | **4.40** | **4.41** |
|---|---|---|---|---|---|
| Empirical formula | $C_{52}H_{40}B_4F_{16}N_{12}Ni_2$ | $C_{52}H_{43}B_4Cu_2F_{16}N_{12}O_{1.5}$ | $C_{30.25}H_{28.5}BCl_2Cu_2F_4N_6O_{3.5}$ | $C_{68}H_{56}Cu_4N_{24}O_{24}$ | $C_{36}H_{36}Cl_2Cu_3N_{12}O_{12}$ |
| Formula weight | 1297.62 | 1334.30 | 816.88 | 1847.53 | 1090.29 |
| Temperature (K) | 168(2) | 168(2) | 168(2) | 168(2) | 168(2) |
| Crystal system | Monoclinic | Monoclinic | Monoclinic | Monoclinic | Orthorhombic |
| Space group | C2 | $P2_1/c$ | C2/c | $P2_1/c$ | Pnma |
| Unit cell dimensions: a (Å) | 22.728(9) | 12.137(4) | 30.35(4) | 23.714(8) | 22.397(5) |
| b (Å) | 11.009(4) | 11.327(3) | 11.912(13) | 15.856(5) | 12.393(3) |
| c (Å) | 11.962(5) | 40.209(13) | 38.96(6) | 20.682(7) | 15.984(4) |
| α (°) | 90 | 90 | 90 | 90 | 90 |
| β (°) | 118.445(5) | 94.360(4) | 109.99(2) | 90.582(5) | 90 |
| γ (°) | 90 | 90 | 90 | 90 | 90 |
| Volume ($Å^3$) | 2631.6(18) | 5512(3) | 13236(31) | 7776(4) | 4436.5(17) |
| Z | 2 | 4 | 16 | 4 | 4 |
| Density (calculated) ($Mg/m^3$) | 1.638 | 1.608 | 1.640 | 1.578 | 1.632 |
| Absorption coefficient ($mm^{-1}$) | 0.824 | 0.880 | 1.514 | 1.172 | 1.619 |
| F(000) | 1312 | 2692 | 6608 | 3760 | 2212 |
| Crystal size ($mm^3$) | 0.62 x 0.30 x 0.05 | 0.70 x 0.64 x 0.49 | 0.39 x 0.33 x 0.09 | 0.58 x 0.52 x 0.08 | 0.20 x 0.33 x 0.60 |
| Theta range for data collection (°) | 2.11 to 25.00 | 2.07 to 25.00 | 1.85 to 26.44 | 1.84 to 26.42 | 2.08 to 25.00 |
| Reflections collected | 9300 | 32581 | 52464 | 59838 | 16243 |
| Independent reflections [R(int)] | 3088 [0.0294] | 9712 [0.0593] | 13534 [0.0920] | 15695 [0.0874] | 3986 [0.0435] |
| Observed reflections [$I>2\sigma(I)$] | 2461 | 7169 | 6806 | 7225 | 3014 |
| Data / restraints / parameters | 3088 / 1 / 389 | 9712 / 132 / 856 | 13534 / 8 / 901 | 15695 / 0 / 1085 | 3986 / 0 / 320 |
| Goodness-of-fit on $F^2$ | 0.986 | 1.069 | 0.791 | 0.851 | 0.997 |
| $R_1$ [$I>2\sigma(I)$] | 0.0491 | 0.0770 | 0.0395 | 0.0477 | 0.0383 |
| $wR_2$ (all data) | 0.1239 | 0.1832 | 0.0738 | 0.1110 | 0.0897 |

**Table A12.** Crystal data and X-ray experimental data for **4.43**.

| Compound | **4.43** |
|---|---|
| Empirical formula | $C_{78}H_{72}B_2Cl_{16}Cu_2F_{14}N_{20}O_6Si$ |
| Formula weight | 2395.55 |
| Temperature (K) | 168(2) |
| Crystal system | Triclinic |
| Space group | P-1 |
| Unit cell dimensions: a (Å) | 10.757(3) |
| b (Å) | 11.718(3) |
| c (Å) | 21.781(6) |
| α (°) | 96.346(4) |
| β (°) | 95.415(4) |
| γ (°) | 111.295(4) |
| Volume ($Å^3$) | 2515.6(13) |
| Z | 1 |
| Density (calculated) ($Mg/m^3$) | 1.581 |
| Absorption coefficient ($mm^{-1}$) | 0.945 |
| F(000) | 1208 |
| Crystal size ($mm^3$) | 0.58 x 0.40 x 0.30 |
| Theta range for data collection (°) | 1.89 to 26.41 |
| Reflections collected | 32825 |
| Independent reflections [R(int)] | 10124 [0.0306] |
| Observed reflections [I>2σ(I)] | 7497 |
| Data / restraints / parameters | 10124 / 4 / 701 |
| Goodness-of-fit on $F^2$ | 1.048 |
| $R_1$ [I>2σ(I)] | 0.0599 |
| $wR_2$ (all data) | 0.1873 |

# Appendix 2: Publications

The following is a list of publications that have resulted from the research work described in this thesis.

1. Peter J. Steel and Christopher J. Sumby, Hexa(2-Pyridyl)[3]Radialene: Self-Assembly of a Hexanuclear Silver Array, *Chem. Comm.*, **2002**, 322.
2. Christopher J. Sumby, Radiating New Directions in Molecular Architecture: the Synthesis and Silver Complexes of Hexa(2-pyridyl)[3]radialene, *Chemistry in NZ, 66*, **2002**, 30.
3. Peter J. Steel and Christopher J. Sumby, Anion-Directed Self-Assembly of Metallosupramolecular Coordination Polymers of the Radialene Ligand, Hexa(2-Pyridyl)[3]Radialene, *Inorg. Chem. Comm., 5*, **2002**, 323.
4. Christopher J. Sumby and Peter J. Steel, 'All Twisted Up': a Dinuclear Helicate with a Highly Contorted Pyridazine Bridge, *Inorg. Chem. Comm., 6*, **2003**, 127.
5. Deanna M. D'Alessandro, F. Richard Keene, Peter J. Steel and Christopher J. Sumby, Ruthenium(II) Complexes of Multidentate Ligands Derived from Di(2-pyridyl)methane, *Aust. J. Chem.*, **2003**, in press.
6. Christopher J. Sumby and Peter J. Steel, Cyclometallated Compounds. XVII. The First Three-fold Cyclopalladation of a Single Benzene Ring, *Organometallics*, *22*, **2003**, 2358.

# *References*

# References


1 J. Reedijk, in 'Comprehensive Coordination Chemistry', ed. G. Wilkinson, R. D. Gillard, and J. A. McCleverty, Pergamon Press, Oxford, 1987, *Vol. 2*, p. 73.

2 P. J. Steel, *Coord. Chem. Rev.*, **1990**, *106*, 227.

3 V. Balzani, A. Juris, M. Venturi, S. Campagna, and S. Serroni, *Chem. Rev.*, **1996**, *96*, 759.

4 C. Kaes, A. Katz, and M. W. Hosseini, *Chem. Rev.*, **2000**, *100*, 3553.

5 C. Creutz and H. Taube, *J. Am. Chem. Soc.*, **1969**, *91*, 3988; W. Kaim, A. Klein, and M. Gloeckle, *Acc. Chem. Res.*, **2000**, *33*, 755.

6 K. D. Demadis, C. M. Hartshorn, and T. J. Meyer, *Chem. Rev.*, **2001**, *101*, 2655; B. S. Brunschwig, C. Creutz, and N. Sutin, *Chem. Soc. Rev.*, **2002**, *31*, 168.

7 I. G. Phillips and P. J. Steel, *Aust. J. Chem.*, **1998**, *51*, 371.

8 L. F. Szczepura, L. M. Witham, and K. J. Takeuchi, *Coord. Chem. Rev.*, **1998**, *174*, 5.

9 S. Trofimenko, *Chem. Rev.*, **1993**, *93*, 943; S. Trofimenko, *Prog. Inorg. Chem.*, **1986**, *34*, 115.

10 J.-M. Lehn, 'Supramolecular Chemistry', VCH, Weiheim, 1995.

11 J. W. Steed and J. L. Atwood, 'Supramolecular Chemistry', John Wiley & Sons Ltd, New York, 2000.

12 J.-M. Lehn, *Proc. Nat. Acad. Sci.*, **2002**, *99*, 4763.

13 G. R. Desiraju, *Acc. Chem. Res.*, **1996**, *29*, 441.

14 G. R. Desiraju, *Acc. Chem. Res.*, **2002**, *35*, 565.

15 C. Janiak, *J. Chem. Soc., Dalton Trans.*, **2000**, 3885.

16 C. A. Hunter and J. K. M. Sanders, *J. Am. Chem. Soc.*, **1990**, *112*, 5525; C. A. Hunter, K. R. Lawson, J. Perkins, and C. J. Urch, *J. Chem. Soc., Perkin Trans. 2*, **2001**, 659.

17 E. C. Constable, *Chem. Ind.*, **1994**, 56.

18 R. J. Lancashire, in 'Comprehensive Coordination Chemistry', ed. G. Wilkinson, R. D. Gillard, and J. A. McCleverty, Pergamon Press, Oxford, 1987, *Vol. 5*, p. 775.

19 M. Munakata, L. P. Wu, and T. Kuroda-Sowa, *Adv. Inorg. Chem.*, **1999**, *46*, 173.

20 A. N. Khlobystov, A. J. Blake, N. R. Champness, D. A. Lemenovskii, A. G. Majouga, N. V. Zyk, and M. Schroder, *Coord. Chem. Rev.*, **2001**, *222*, 155.

21 B. J. Hathaway, in 'Comprehensive Coordination Chemistry', ed. G. Wilkinson, R. D. Gillard, and J. A. McCleverty, Pergamon Press, Oxford, 1987, *Vol. 5*, p. 533.

22 M. Fujita, O. Sasaki, T. Mitsuhashi, T. Fujita, J. Yazaki, K. Yamaguchi, and K. Ogura, *Chem. Commun.*, **1996**, 1535; M. Fujita, J. Yazaki, and K. Ogura, *J. Am. Chem. Soc.*, **1990**, *112*, 5645.

23 P. J. Stang and B. Olenyuk, *Acc. Chem. Res.*, **1997**, *30*, 502; S. Leininger, B. Olenyuk, and P. J. Stang, *Chem. Rev.*, **2000**, *100*, 853.

24 B. Olenyuk, A. Fechtenkotter, and P. J. Stang, *J. Chem. Soc., Dalton Trans.*, **1998**, 1707.

25 B. J. Holliday and C. A. Mirkin, *Angew. Chem., Int. Ed.*, **2001**, *40*, 2022.

26 C. V. K. Sharma, S. T. Griffin, and R. D. Rogers, *Chem. Commun.*, **1998**, 215.

27 S. Roche, C. Haslam, S. L. Heath, and J. A. Thomas, *Chem. Commun.*, **1998**, 1681.

28 T. Kusukawa, T. Nakai, T. Okano, and M. Fujita, *Chem. Lett.*, **2003**, *32*, 284; M. Fujita, K. Umemoto, M. Yoshizawa, N. Fujita, T. Kusukawa, and K. Biradha, *Chem. Commun.*, **2001**, 509; C. J. Jones, *Chem. Soc. Rev.*, **1998**, *27*, 289; G. F. Sweigers and T. J. Malefetse, *Chem. Eur. J.*, **2001**, *7*, 3637.

29 M. Fujita, *Chem. Soc. Rev.*, **1998**, *27*, 417.

30 G. F. Sweigers and T. J. Malefetse, *Chem. Rev.*, **2000**, *100*, 3483.

31 M. Munakata, L. P. Wu, and T. Kuroda-Sowa, *Bull. Chem. Soc. Jpn.*, **1997**, *70*, 1727; R. Robson, *J. Chem. Soc., Dalton Trans.*, **2000**, 3735.

32 J. A. R. Navarro and B. Lippert, *Coord. Chem. Rev.*, **2001**, *222*, 219.

33 M. J. Zaworotko, *Chem. Commun.*, **2001**, 1.

34 S. R. Batten and R. Robson, *Angew. Chem., Int. Ed.*, **1998**, *37*, 1460.

35 B. Moulton and M. J. Zaworotko, *Chem. Rev.*, **2001**, *101*, 1629.

36 K. N. Power, T. L. Hennigar, and M. J. Zaworotko, *New J. Chem.*, **1998**, 177.

37 C. Piguet, G. Bernardinelli, and G. Hopfgartner, *Chem. Rev.*, **1997**, *97*, 2005.

38 M. Albrecht, *Chem. Rev.*, **2001**, *101*, 3457.

39 F. M. Raymo and J. F. Stoddart, *Chem. Rev.*, **1999**, *99*, 1643; M. Fujita, *Acc. Chem. Res.*, **1999**, *32*, 53; D. B. Amabalino and J. F. Stoddart, *Chem. Rev.*, **1995**, *95*, 2725; S. J. Rowan, S. J. Cantrill, G. R. L. Cousins, J. K. M. Sanders, and J. F. Stoddart, *Angew. Chem., Int. Ed.*, **2002**, *41*, 899.

40 V. Balzani, A. Credi, F. M. Raymo, and J. F. Stoddart, *Angew. Chem., Int. Ed.*, **2000**, *39*, 3348.

41 F. H. Burstall, *J. Chem. Soc.*, **1936**, 173.

42 A. Juris, V. Balzani, F. Barigelletti, S. Campagna, P. Belser, and A. von Zelewsky, *Coord. Chem. Rev.*, **1988**, *84*, 85.

43 E. C. Constable, *Adv. Inorg. Chem.*, **1989**, *34*, 1.

44 P. A. Anderson, G. B. Deacon, K. H. Haarmann, F. R. Keene, T. J. Meyer, D. A. Reitsma, B. W. Skelton, G. F. Strouse, N. C. Thomas, J. A. Treadway, and A. H. White, *Inorg. Chem.*, **1995**, *34*, 6145.

45 A. J. Bard and M. A. Fox, *Acc. Chem. Res.*, **1995**, *28*, 141; L. Sun, L. Hammarstrom, B. Akermark, and S. Styring, *Chem. Soc. Rev.*, **2001**, *30*, 36; M. Yagi and M. Kaneko, *Chem. Rev.*, **2001**, *101*, 21.

46 J. A. McCleverty and M. D. Ward, *Acc. Chem. Res.*, **1998**, *31*, 842.

47 F. R. Keene, *Coord. Chem. Rev.*, **1997**, *166*, 121.

48 F. R. Keene, *Chem. Soc. Rev.*, **1998**, *27*, 185.

49 A. von Zelewsky and O. Mamula, *J. Chem. Soc., Dalton Trans.*, **2000**, 219.

50 A. von Zelewsky, *Coord. Chem. Rev.*, **1999**, *190-192*, 811.

51 C. M. Hartshorn, 'The synthesis and study of new nitrogen-containing ligands', Ph.D. thesis, University of Canterbury, Christchurch, 1996; A. A. Watson, 'Synthesis and complexes of new chiral heterocyclic ligands', Ph.D. thesis, University of Canterbury, Christchurch, 1987; G. Baum, E. C. Constable, D. Fenske, C. E. Housecroft, T. Kulke, M. Neuburger, and M. Zehnder, *J. Chem. Soc., Dalton Trans.*, **2000**, 945.

52 W. Lewis, 'Alkaloid-based heterocyclic ligands', 18 Month Ph.D. Progress Report, University of Canterbury, Christchurch, 2002.

53 N. C. Fletcher, P. C. Junk, D. A. Reitsma, and F. R. Keene, *J. Chem. Soc., Dalton Trans.*, **1998**, 133.

54 X. Hua and A. von Zelewsky, *Inorg. Chem.*, **1995**, *34*, 5791.

55 S. Bodige, A. S. Torres, D. J. Maloney, D. Tate, G. R. Kinsel, A. K. Walker, and F. M. MacDonnell, *J. Am. Chem. Soc.*, **1997**, *119*, 10364.

56 E. C. Constable and A. M. W. C. Thompson, *J. Chem. Soc., Dalton Trans.*, **1992**, 3467; E. C. Constable and A. M. W. Cargill Thompson, *J. Chem. Soc., Dalton Trans.*, **1995**, 1615; M. Maestri, N. Armaroli, V. Balzani, E. C. Constable, and A. M. W. C. Thompson, *Inorg. Chem.*, **1995**, *34*, 2759; V. Grosshenny, A. Harriman, M. Hissler, and R. Ziessel, *Platinum Metals Rev.*, **1996**, *40*, 72.

57 F. A. Cotton, *J. Chem. Soc., Dalton Trans.*, **2000**, 1961.

58 K. R. Adam, P. A. Anderson, T. Astley, I. M. Atkinson, J. M. Charnock, C. D. Garner, J. M. Gulbis, T. W. Hambley, M. A. Hitchman, F. R. Keene, and E. R. T. Tiekink, *J. Chem. Soc., Dalton Trans.*, **1997**, 519.

59 D. E. Fenton, *Chem. Soc. Rev.*, **1999**, *28*, 159.

60 A. M. Barrios and S. J. Lippard, *Inorg. Chem.*, **2001**, *40*, 1250.

61 A. M. Barrios and S. J. Lippard, *Inorg. Chem.*, **2001**, *40*, 1060.

62 J. Kido and Y. Okamoto, *Chem. Rev.*, **2002**, *102*, 2357; S. Wang, *Coord. Chem. Rev.*, **2001**, *215*, 79.

63 W. Yang, H. Schmider, Q. Wu, Y.-s. Zhang, and S. Wang, *Inorg. Chem.*, **2000**, *39*, 2397.

64 W.-Y. Yang, L. Chen, and S. Wang, *Inorg. Chem.*, **2001**, *40*, 507.

65 Y. Kang, C. Seward, D. Song, and S. Wang, *Inorg. Chem.*, **2003**, *42*, 2789.

66 C. Richardson, P. J. Steel, D. M. D'Alessandro, P. C. Junk, and F. R. Keene, *J. Chem. Soc., Dalton Trans.*, **2002**, 2775.

67 D. M. D'Alessandro, F. R. Keene, P. J. Steel, and C. J. Sumby, *Aust. J. Chem.*, **2003**, in press.

68 E. C. Constable, *Chem. Commun.*, **1997**, 1073; P. L. Boulas, M. Gomez-Kaifer, and L. Echegoyen, *Angew. Chem., Int. Ed.*, **1998**, *37*, 216; A. Adronov and J. M. J. Frechet, *Chem. Commun.*, **2000**, 1701; V. Balzani, S. Campagna, G. Denti, A. Juris, S. Serroni, and M. Venturi, *Acc. Chem. Res.*, **1998**, *31*, 26.

69 F. Blau, *Chem. Ber.*, **1887**, *20*, 2251.

70 A. T. Baker, J. K. Crass, G. B. Kok, J. D. Orbell, and E. Yuriev, *Inorg. Chim. Acta*, **1993**, *214*, 169; K. Ida, H. Sakiyama, H. Okawa, N. Matsumoto, Y. Aratake, I. Murase, and S. Kida, *Polyhedron*, **1992**, *11*, 65; W. Kleibohmer, B. Krebs, A. T. M. Marcelis, J. Reedijk, and J. L. Van Der Veer, *Inorg. Chim. Acta*, **1983**, *75*, 45; A. T. M. Marcelis, H.-J. Korte, B. Krebs, and J. Reedijk, *Inorg. Chem.*, **1982**, *21*, 4059; M.-L. Tong and X.-M. Chen, *Acta Cryst.*, **2000**, *C56*, 1075; M.-L. Tong, J.-X. Shi, and X.-M. Chen, *New J. Chem.*, **2002**, *26*, 814; S. Kitagawa, S. Matsuyama, M. Munakata, and T. Emori, *J. Chem. Soc., Dalton Trans.*, **1991**, 2869.

71 A. J. Canty and N. J. Minchin, *Inorg. Chim. Acta*, **1985**, *100*, L13.

72 A. J. Canty and N. J. Minchin, *Aust. J. Chem.*, **1986**, *39*, 1063.

73 E. Spodine, J. Manzur, M. T. Garland, M. Kiwi, O. Pena, D. Grandjean, and L. Toupet, *J. Chem. Soc., Dalton Trans.*, **1991**, 365.

74 F. Grases, F. Garcia-Sanchez, and M. Valcarcel, *Anal. Chim. Acta*, **1981**, *125*, 21.

75 M. Valcarcel, M. P. Martinez, and F. Pino, *Analyst*, **1975**, *100*, 33.

76 L. J. Henderson, Jr., F. R. Fronczek, and W. R. Cherry, *J. Am. Chem. Soc.*, **1984**, *106*, 5876.

77 M. Riklin and A. von Zelewsky, *Helv. Chim. Acta*, **1996**, *79*, 2176.

78 M. Riklin, A. von Zelewsky, A. Bashall, M. McPartlin, A. Baysal, J. A. Connor, and J. D. Wallis, *Helv. Chim. Acta*, **1999**, *82*, 1666.

79 H. Hopf and G. Maas, *Angew. Chem., Int. Ed. Engl.*, **1992**, *104*, 953.

80 H. Hopf, 'Classics in hydrocarbon chemistry: syntheses, concepts, perspectives', Wiley-VCH, Weiheim, 2000.

81 M. Iyoda, N. Nakamura, M. Todaka, S. Ohtsu, K. Hara, Y. Kuwatani, M. Yoshida, H. Matsuyama, M. Sugita, H. Tachibana, and H. Inoue, *Tetrahedron Lett.*, **2000**, *41*, 7059.

82 T. Enomoto, N. Nishigaki, H. Kurata, T. Kawase, and M. Oda, *Bull. Chem. Soc. Jpn.*, **2000**, *73*, 2109.

83 A. J. Canty, N. Chaichit, B. M. Gatehouse, E. E. George, and G. Hayhurst, *Inorg. Chem.*, **1981**, *20*, 2414; A. J. Canty, L. A. Titcombe, B. W. Skelton, and A. H. White, *J. Chem. Soc., Dalton Trans.*, **1988**, 35; A. J. Canty, K. Mills, B. W. Skelton, and A. H. White, *J. Chem. Soc., Dalton Trans.*, **1986**, 939; M. T. Garland, J. Y. Le Marouille, E. Spodine, and J. Manzur, *Acta Cryst.*, **1986**, *C42*, 1720; M. T. Garland, D. Grandjean, E. Spodine, and J. Manzur, *Acta Cryst.*, **1987**, *C43*, 643; A. J. Canty, G. Hayhurst, N. Chaichit, and B. M. Gatehouse, *J. Chem. Soc, Chem. Commun.*, **1980**, 316; C. Mock, I. Puscasu, M. J. Rauterkus, G. Tallen, J. E. A. Wolff, and B. Krebs, *Inorg. Chim. Acta*, **2001**, *319*, 109; J. Madureira, T. M. Santos, B. J. Goodfellow, M. Lucena, J. Pedrosa de Jesus, M. G. Santana-Marques, M. G. B. Drew, and V. Felix, *J. Chem. Soc., Dalton Trans.*, **2000**, 4422; E. Spodine, J. Manzur, M. T. Garland, J. P. Fackler, Jr., R. J. Staples, and B. Trzcinska-Bancroft, *Inorg. Chim. Acta*, **1993**, *203*, 73; A. M. Garcia, J. Manzur, E. Spodine, R. F. Baggio, and M. T. Garland, *Acta Cryst.*, **1994**, *C50*, 1882; H. Gornitzka and D. Stalke, *Organometallics*, **1994**, *13*, 4398.

84 C. Osuch and R. Levine, *J. Chem. Soc. A*, **1956**, 1723.

85 E. Leete and L. Marion, *Can. J. Chem.*, **1952**, *30*, 563.

86 J. Manzur, M. T. Garland, A. M. Atria, M. Vera, and E. Spodine, *Bol. Soc. Chil. Quim.*, **1989**, *34*, 229.

87 S. K. Talapatra, S. Chakrabarti, A. K. Mallik, and B. Talapatra, *Tetrahedron Lett.*, **1990**, *46*, 6047.

88 G. R. Newkome, J. D. Sauer, and M. L. Erbland, *J. Chem. Soc, Chem. Commun.*, **1975**, 885.

89 F. C. Y. Chan, M. Jarman, M. F. Wang, and G. A. Potter, *Tetrahedron Lett.*, **2000**, *41*, 2447.

90 K. G. Untch, D. J. Martin, and N. T. Castellucci, *J. Org. Chem.*, **1965**, *30*, 3572.

91 E. Amadei, M. Carcelli, S. Ianelli, P. Cozzini, P. Pelagatti, and C. Pelizzi, *J. Chem. Soc., Dalton Trans.*, **1998**, 1025.

92 I. F. Eckhard and L. A. Summers, *Aust. J. Chem.*, **1973**, *26*, 2727.

93 C. Fritze, G. Erker, and R. Froehlich, *J. Organomet. Chem.*, **1995**, *501*, 41.

94 T. Enomoto, T. Kawase, H. Kurata, and M. Oda, *Tetrahedron Lett.*, **1997**, *38*, 2693.

95 K. Matsumoto, Y. Harada, T. Kawase, and M. Oda, *Chem. Commun.*, **2002**, 424.

96 P. J. Steel and C. J. Sumby, *Chem. Commun.*, **2002**, 322.

97 P. J. Steel and C. J. Sumby, *Inorg. Chem. Commun.*, **2002**, *5*, 323.

98 C. J. Sumby, *Chem. in N.Z.*, **2002**, *66*, 30.

99 F. L. Minn, C. L. Trichilo, C. R. Hurt, and N. Filipescu, *J. Am. Chem. Soc.*, **1970**, *92*, 3600.

100 P. L. Gaus, A. Haim, and F. Johnson, *J. Org. Chem.*, **1977**, *42*, 564.

101 M. Melnik, M. Kabesova, M. Koman, L. Macaskova, J. Garaj, C. E. Holloway, and A. Valent, *J. Coord. Chem.*, **1998**, *45*, 147.

102 A. W. Addison, T. N. Rao, J. Reedijk, J. Van Rijn, and G. C. Verschoor, *J. Chem. Soc., Dalton Trans.*, **1984**, 1349.

103 C. Hemmert, M. Renz, H. Gornitzka, S. Soulet, and B. Meunier, *Chem. Eur. J.*, **1999**, *5*, 1766.

104 C. Tsiamis, A. G. Hatzidimitiou, and L. Tzavellas, *Inorg. Chem.*, **1998**, *37*, 2903.

105 V. Tangoulis, C. P. Raptopoulou, S. Paschalidou, A. E. Tsohos, E. G. Bakalbassis, A. Terzis, and S. P. Perlepes, *Inorg. Chem.*, **1997**, *36*, 5270; Z. E. Serna, R. Cortes, M. K. Urtiaga, M. G. Barandika, L. Lezama, M. I. Arriortua, and T. Rojo, *Eur. J. Inorg. Chem.*, **2001**, 865; C. A. Kavounis, C. Tsiamis, C. J. Cardin, and Y. Zubavichus, *Polyhedron*, **1996**, *15*, 385.

106 E. Katsoulakou, N. Lalioti, C. P. Raptopoulou, A. Terzis, E. Manessi-Zoupa, and S. P. Perlepes, *Inorg. Chem. Commun.*, **2002**, *5*, 719.

107 B. Milani, G. Mestroni, and E. Zangrando, *Croat. Chem. Acta*, **2001**, *74*, 851.

108 S.-L. Wang, J. W. Richardson Junior, S. J. Briggs, R. A. Jacobson, and W. P. Jensen, *Inorg. Chim. Acta*, **1986**, *111*, 67.

109 G. Parkin and R. Hoffmann, *Angew. Chem., Int. Ed. Engl.*, **1994**, *33*, 1462; J. M. Mayer, *Angew. Chem., Int. Ed. Engl.*, **1992**, *31*, 286; G. Parkin, *Acc. Chem. Res.*, **1992**, *25*, 455; M.-M. Rohmer and M. Benard, *Chem. Soc. Rev.*, **2001**, *30*, 340.

110 V. Tangoulis, C. P. Raptopoulou, A. Terzis, S. Paschalidou, S. P. Perlepes, and E. G. Bakalbassis, *Inorg. Chem.*, **1997**, *36*, 3996; G. Yang, M.-L. Tong, X. M. Chen, and S. W. Ng, *Acta Cryst.*, **1998**, *C54*, 732; Z. Serna, M. G. Barandika, R. Cortes, M. K. Urtiaga, and M. I. Arriortua, *Polyhedron*, **1999**, *18*, 249; S. R. Breeze, S. Wang, J. E. Greedan, and N. P. Raju, *Inorg. Chem.*, **1996**, *35*, 6944; O. J. Parker, S. L. Aubol, and G. L. Breneman, *Polyhedron*, **2000**, *19*, 623.

111 A. J. Canty, P. R. Traill, B. W. Skelton, and A. H. White, *Inorg. Chim. Acta*, **1997**, *255*, 117.

112 P. J. Steel and E. C. Constable, *J. Chem. Soc., Dalton Trans.*, **1990**, 1389.

113 E. A. Meyer, R. K. Castellano, and F. Diederich, *Angew. Chem., Int. Ed.*, **2003**, *42*, 1210.

114 D. A. Aubry, S. A. Laneman, F. R. Fronczek, and G. G. Stanley, *Inorg. Chem.*, **2001**, *40*, 5036.

115 G. Dong, H. Cheng, D. Chun-Ying, Q. Chun-Qi, and M. Qing-Jin, *New J. Chem.*, **2002**, *26*, 796.

116 H. W. Smith, *Acta Cryst.*, **1975**, *B31*, 2701; D. A. Edwards, G. M. Hoskins, M. F. Mahon, K. C. Molloy, and G. R. G. Rudolph, *Polyhedron*, **1998**, *17*, 2321; J. Granifo, A. Vega, and M. T. Garland, *Polyhedron*, **1998**, *17*, 1729; J. Granifo, M. E. Vargas, E. S. Dodsworth, D. H. Farrar, S. S. Fielder, and A. B. P. Lever, *J. Chem. Soc., Dalton Trans.*, **1996**, 4369; F. J. Lahoz, A. Tiripicchio, F. Neve, and M. Ghedini, *J. Chem. Soc., Dalton Trans.*, **1989**, 1075; G. Dong, D. Chun-Ying, F. Chen-jie, and M. Quin-jin, *J. Chem. Soc., Dalton Trans.*, **2002**, 834; J. Hamblin, A. Jackson, N. W. Alcock, and M. J. Hannon, *J. Chem. Soc., Dalton Trans.*, **2002**, 1635; C. J. O'Connor, R. J. Romananch, D. M. Robertson, E. E. Eduok, and F. R. Fronczek, *Inorg. Chem.*, **1983**, *22*, 449; P. D. W. Boyd, M. Gerloch, and G. M. Sheldrick, *J. Chem. Soc., Dalton Trans.*, **1974**, 1097.

117 L. P. Battaglia, M. Carcelli, F. Ferraro, L. Mavilla, C. Pelizzi, and G. Pelizzi, *J. Chem. Soc., Dalton Trans.*, **1994**, 2651.

118 H. Mori, K. Sakamoto, S. Mashito, Y. Matsuoka, M. Matsubayashi, and K. Sakai, *Chem. Pharm. Bull.*, **1993**, *41*, 1944.

119 P. Pyykko, *Chem. Rev.*, **1997**, *97*, 597.

120 C. Richardson, 'Synthesis and Complexes of Heterocyclic Ligands', Ph.D. thesis, University of Canterbury, Christchurch, 1999.

121 A. Baysal, J. A. Connor, and J. D. Wallis, *J. Coord. Chem.*, **2001**, *53*, 347.

122 M. Fujita, S. Nagao, and K. Ogura, *J. Am. Chem. Soc.*, **1995**, *117*, 1649.

123 P. L. Jones, J. C. Jeffery, J. P. Maher, J. A. McCleverty, P. H. Reiger, and M. D. Ward, *Inorg. Chem.*, **1997**, *36*, 3088; C. Y. Su, B. S. Kang, C. X. Du, Q. C. Yang, and T. C. W. Mak, *Inorg. Chem.*, **2000**, *39*, 4843; W.-Y. Sun, J. Xie, and K.-B. Yu, *Chem. Lett.*, **2001**, 342; W.-Y. Sun, J. Fan, T.-A. Okamura, J. Xie, K.-B. Yu, and N. Ueyama, *Chem. Eur. J.*, **2001**, *7*, 2557; Z. Zhong, A. Ikeda, S. Shinkai, S. Sakamoto, and K. Yamaguchi, *Org. Lett.*, **2001**, *3*, 1085.

124 H. K. Liu, W. Y. Sun, D. J. Ma, K. B. Yu, and W. X. Tang, *Chem. Commun.*, **2000**, 591.

125 E. Lozano, M. Nieuwenhuyzen, and S. L. James, *Chem. Eur. J.*, **2001**, *7*, 2644.

126 Q. M. Wang and T. C. W. Mak, *Chem. Commun.*, **2000**, 1435; K. Nomiya, S. Takahashi, and R. Noguchi, *J. Chem. Soc., Dalton Trans.*, **2000**, 2091.

127 G. W. Eastland, M. A. Mazid, D. R. Russel, and M. C. R. Symons, *J. Chem. Soc., Dalton Trans.*, **1980**, 1682.

128 R. W. M. Ten Hoedt and J. Reedijk, *Inorg. Chim. Acta*, **1981**, *51*, 23; J. S. Thompson, R. L. Harlow, and J. F. Whitney, *J. Am. Chem. Soc.*, **1983**, *105*, 3522; Y. Zang, H. G. Jang, Y. M. Chiu, M. P. Hendrich, and L. Que, *Inorg. Chim. Acta*, **1993**, *213*, 41; S. Herold and S. J. Lippard, *Inorg. Chem.*, **1997**, *36*, 50.

129 B. F. Straub, F. Rominger, and P. Hofmann, *Inorg. Chem.*, **2000**, *39*, 2113.

130 R. Vilar, *Angew. Chem., Int. Ed.*, **2003**, *42*, 1460.

131 P. Maetrangolo and G. Resnati, *Chem. Eur. J.*, **2001**, *7*, 2511.

132 A. J. Downard, G. E. Honey, and P. J. Steel, *Inorg. Chem.*, **1991**, *30*, 3733; G. Orellana, C. Alvarez Ibarra, and J. Santoro, *Inorg. Chem.*, **1988**, *27*, 1025.

133 L. J. Henderson, Jr., M. Ollino, V. K. Gupta, G. R. Newkome, and W. R. Cherry, *J. Photochem.*, **1985**, *31*, 199.

134 A. Basu, T. G. Kasar, and N. Y. Sapre, *Inorg. Chem.*, **1988**, *27*, 4539.

135 A. Nangia, *CrystEngComm*, **2002**, *4*, 93; T. Steiner, *Angew. Chem., Int. Ed.*, **2002**, *41*, 48; C. B. Aakeroy and A. M. Beatty, *Aust. J. Chem.*, **2001**, *54*, 409.

136 D. L. Jameson, J. K. Blaho, K. T. Kruger, and K. A. Goldsby, *Inorg. Chem.*, **1989**, *28*, 4312.

137 T. D. P. Stack, Z. Hou, and K. N. Raymond, *J. Am. Chem. Soc.*, **1993**, *115*, 6466; B. P. Hay, D. A. Dixon, A. Vargas, J. Garza, and K. N. Raymond, *Inorg. Chem.*, **2001**, *40*, 3922.

138 J. Pang, E. J.-P. Marcotte, C. Seward, R. S. Brown, and S. Wang, *Angew. Chem., Int. Ed.*, **2001**, *40*, 4042.

139 J. Pang, Y. Tao, S. Freiberg, X.-P. Yang, M. D'Iorio, and S. Wang, *J. Mater. Chem.*, **2002**, *12*, 206.

140 H.-K. Liu, W.-Y. Sun, W.-X. Tang, H.-Y. Tan, H.-X. Zhang, Y.-X. Tong, X.-L. Yu, and B.-S. Kang, *J. Chem. Soc., Dalton Trans.*, **2002**, 3886; H.-K. Liu and X. Tong, *Chem. Commun.*, **2002**, 1316; H.-K. Liu, H.-Y. Tan, S. Liao, W. Xiao, H.-X. Zhang, X.-L. Yu, B.-S. Kang, J.-W. Cai, Z.-Y. Zhou, and A. S. C. Chan, *Chem. Commun.*, **2001**, 1008.

141 G. Hennrich and E. V. Anslyn, *Chem. Eur. J.*, **2002**, *8*, 2219.

142 L. R. Hanton and K. Lee, *J. Chem. Soc., Dalton Trans.*, **2000**, 1161.

143 P. L. Caradoc-Davies and L. R. Hanton, *Dalton Trans.*, **2003**, 1754.

144 Z. Atherton, D. M. L. Goodgame, S. Menzer, and D. J. Williams, *Polyhedron*, **1998**, *18*, 237; M. R. Malachowski, M. Adams, N. Elia, A. L. Rheingold, and R. S. Kelly, *J. Chem. Soc., Dalton Trans.*, **1999**, 2177.

145 C. M. Hartshorn and P. J. Steel, *Aust. J. Chem.*, **1995**, *48*, 1587.

146 C. M. Hartshorn and P. J. Steel, *Angew. Chem., Int. Ed. Engl.*, **1996**, *35*, 2655.

147 C. M. Hartshorn and P. J. Steel, *Inorg. Chem.*, **1996**, *35*, 6902.

148 C. M. Hartshorn and P. J. Steel, *Chem. Commun.*, **1997**, 541.

149 C. M. Hartshorn and P. J. Steel, *J. Chem. Soc., Dalton Trans.*, **1998**, 3935.

150 C. M. Hartshorn and P. J. Steel, *J. Chem. Soc., Dalton Trans.*, **1998**, 3927.

151 D. A. McMorran and P. J. Steel, *Chem. Commun.*, **2002**, 2120; P. J. Steel and N. C. Webb, *Eur. J. Inorg. Chem.*, **2002**, 2257; C. M. Hartshorn and P. J. Steel, *Organometallics*, **1998**, *17*, 3487; B. J. O'Keefe and P. J. Steel, *Inorg. Chem. Commun.*, **1998**, *1*, 147.

152 D. A. McMorran and P. J. Steel, *Angew. Chem., Int. Ed.*, **1998**, *37*, 3295.

153 D. A. McMorran and P. J. Steel, *Inorg. Chem. Commun.*, **1999**, *2*, 368.

154 B. J. O'Keefe and P. J. Steel, *Acta Cryst.*, **2000**, *C56*, 1440.

155 M. R. A. Al-Mandhary and P. J. Steel, *Inorg. Chem. Commun.*, **2002**, *5*, 954.

156 D. A. McMorran and P. J. Steel, *Inorg. Chem. Commun.*, **2003**, *6*, 43.

157 D. Braga, F. Grepioni, and G. R. Desiraju, *Chem. Rev.*, **1998**, *98*, 1375.

158 F. P. Schmidtchen and M. Berger, *Chem. Rev.*, **1997**, *97*, 1609; L. R. MacGillivray and J. L. Atwood, *Angew. Chem., Int. Ed.*, **1999**, *38*, 1018; J.-P. Bourgeois and M. Fujita, *Aust. J. Chem.*, **2002**, *55*, 619.

159 D. A. McMorran and P. J. Steel, *J. Chem. Soc., Dalton Trans.*, **2002**, 3321; D. A. McMorran and P. J. Steel, *Supramol. Chem.*, **2002**, *14*, 79; P. L. Caradoc-Davies and L. R. Hanton, *Chem. Commun.*, **2001**, 1098; P. L. Caradoc-Davies, L. R. Hanton, and K. Lee, *Chem. Commun.*, **2000**, 783.

160 P. L. Caradoc-Davies, L. R. Hanton, and W. Henderson, *J. Chem. Soc., Dalton Trans.*, **2001**, 2749.

161 C. M. Fitchett, 'Metallosupramolecular Chemistry', Ph.D. thesis, University of Canterbury, Christchurch, 2002.

162 M. R. A. Al-Mandhary and P. J. Steel, *Aust. J. Chem.*, **2002**, *55*, 705.

163 B. J. O'Keefe, 'Synthesis and Complexes of Heterocyclic Ligands', Ph.D. thesis, University of Canterbury, Christchurch, 1999.

164 D. A. McMorran and P. J. Steel, *Tetrahedron*, **2003**, *59*, 3701.

165 Z. Hou, T. D. P. Stack, C. J. Sunderland, and K. N. Raymond, *Inorg. Chim. Acta*, **1997**, *263*, 341.

166 A. Metzger and E. V. Anslyn, *Angew. Chem., Int. Ed.*, **1998**, *37*, 649; A. Metzger, V. M. Lynch, and E. V. Anslyn, *Angew. Chem., Int. Ed. Engl.*, **1997**, *36*, 862.

167 C. Walsdorff, S. Park, J. Kim, J. Heo, K.-M. Park, J. Oh, and K. Kim, *J. Chem. Soc., Dalton Trans.*, **1999**, 923.

168 J. S. Fleming, K. L. V. Mann, S. M. Couchman, J. C. Jeffery, J. A. McCleverty, and M. D. Ward, *J. Chem. Soc., Dalton Trans.*, **1998**, 2047.

169 S. Youngme, N. Chaichit, C. Pakawatchai, and S. Booncoon, *Polyhedron*, **2002**, *21*, 1279; S. Youngme, N. Chaichit, and N. Koonsaeng, *Inorg. Chim. Acta*, **2002**, *335*, 36; M. J. Plater, M. R. S. J. Foreman, J. M. S. Skakle, and R. A. Howie, *Inorg. Chim. Acta*, **2002**, *332*, 135; S. Youngme and N. Chaichit, *Polyhedron*, **2002**, *21*, 247; H. Zhu, M. Strobele, Z. Yu, Z. Wang, H. J. Meyer, and X. You, *Inorg. Chem. Commun.*, **2001**, *4*, 577.

170 C. Seward, J. Pang, and S. Wang, *Eur. J. Inorg. Chem.*, **2002**, 1390.

171 Y. Kang and S. Wang, *Tetrahedron Lett.*, **2002**, *43*, 3711.

172 P. de Hoog, P. Gamez, W. L. Driessen, and J. Reedijk, *Tetrahedron Lett.*, **2002**, *43*, 6783.

173 M. J. Plater, M. R. S. J. Foreman, T. Gelbrich, and M. B. Hursthouse, *Cryst. Eng.*, **2001**, *4*, 319; M. J. Plater, M. R. S. J. Foreman, and J. M. S. Skakle, *Cryst. Eng.*, **2001**, *4*, 293; M. Fujita, M. Aoyagi, and K. Ogura, *Bull. Chem. Soc. Jpn.*, **1998**, *71*, 1799; M. J. Plater, M. R. S. J. Foreman, T. Gelbrich, and M. B. Hursthouse, *J. Chem. Soc., Dalton Trans.*,

**2000**, 1995; D. A. McMorran, S. Pfadenhauer, and P. J. Steel, *Aust. J. Chem.*, **2002**, *55*, 519.

174 S. Wagaw and S. L. Buchwald, *J. Org. Chem.*, **1996**, *61*, 7240.

175 J. F. Hartwig, *Synlett*, **1996**, 329.

176 J. F. Hartwig, *Angew. Chem., Int. Ed.*, **1998**, *37*, 2046.

177 T. Schareina, G. Hillebrand, H. Fuhrmann, and R. Kempe, *Eur. J. Inorg. Chem.*, **2001**, 2421; J.-S. Yang, L. Yu-Hsi, and C.-S. Yang, *Org. Lett.*, **2002**, *4*, 777.

178 H. J. Backer, *Rec. Trav. Chim. Pays-Bas*, **1935**, *54*, 745.

179 J. T. Stapler and J. Bornstein, *J. Heterocycl. Chem.*, **1973**, *10*, 983.

180 H. Shaw, H. D. Perlmutter, C. Gu, S. D. Arco, and T. O. Quibuyen, *J. Org. Chem.*, **1997**, *62*, 236.

181 M. Munakata, L. P. Wu, T. Kuroda-Sowa, M. Maekawa, Y. Suenaga, T. Ohta, and H. Konaka, *Inorg. Chem.*, **2003**, *42*, 2553; I. Ino, L. P. Wu, M. Munakata, T. Kuroda-Sowa, M. Maekawa, Y. Suenaga, and R. Sakai, *Inorg. Chem.*, **2000**, *39*, 5430.

182 D. L. Reger, R. F. Semeniuc, and M. D. Smith, *Eur. J. Inorg. Chem.*, **2002**, 543; D. L. Reger, R. F. Semeniuc, and M. D. Smith, *Inorg. Chem.*, **2001**, *40*, 6545.

183 A. Bondi, *J. Phys. Chem.*, **1964**, *68*, 441; R. S. Rowland and R. Taylor, *J. Phys. Chem.*, **1996**, *100*, 7384.

184 A. J. Canty, N. J. Minchin, B. W. Skelton, and A. H. White, *J. Chem. Soc., Dalton Trans.*, **1987**, 1477.

185 R. A. Gossage, L. A. van de Kuil, and G. van Koten, *Acc. Chem. Res.*, **1998**, *31*, 423; M. Q. Slagt, H. P. Dijkstra, A. McDonald, R. J. M. Klein Gebbink, M. Lutz, D. D. Ellis, A. M. Mills, A. L. Spek, and G. van Koten, *Organometallics*, **2003**, *22*, 27.

186 A. D. Ryabov, *Chem. Rev.*, **1990**, *90*, 403.

187 I. Omae, *Coord. Chem. Rev.*, **1988**, *83*, 137.

188 B. J. O'Keefe and P. J. Steel, *Organometallics*, **2003**, *22*, 1281; C. J. Sumby and P. J. Steel, *Organometallics*, **2003**, *22*, 2358.

189 J. Dupont, M. Pfeffer, and J. Spencer, *Eur. J. Inorg. Chem.*, **2001**, 1917.

190 A. C. Cope and R. W. Siekman, *J. Am. Chem. Soc.*, **1965**, *87*, 3272.

191 S. Trofimenko, *J. Am. Chem. Soc.*, **1971**, *93*, 1808.

192 R. Vicente, M. Lyakhovych, D. Bautista, and P. G. Jones, *Organometallics*, **2001**, *20*, 4695.

193 G. Denti, S. Campagna, S. Serroni, M. Ciano, and V. Balzani, *J. Am. Chem. Soc.*, **1992**, *114*, 2944.

194 N. C. Fletcher, F. R. Keene, M. Ziegler, H. Stoeckli-Evans, H. Viebrock, and A. von Zelewsky, *Helv. Chim. Acta*, **1996**, *79*, 1192; U. Knof and A. von Zelewsky, *Angew. Chem., Int. Ed.*, **1999**, *38*, 303; A. A. Watson, D. A. House, and P. J. Steel, *Aust. J. Chem.*, **1995**, *48*, 1549; A. A. Watson, D. A. House, and P. J. Steel, *J. Org. Chem.*, **1991**, *56*, 4072.

195 N. Marques, A. Sella, and J. Takats, *Chem. Rev.*, **2002**, *102*, 2137; F. T. Edelmann, *Angew. Chem., Int. Ed.*, **2001**, *40*, 1656; M. Etienne, *Coord. Chem. Rev.*, **1996**, *156*, 201.

196 D. L. Reger, *Comments Inorg. Chem.*, **1999**, *21*, 1.

197 D. Boys, C. Escobar, and W. Zamudio, *Acta Cryst.*, **1992**, *C48*, 1118; G. C. Kulasingam and W. R. McWhinnie, *J. Chem. Soc. A*, **1967**, 1253; G. C. Kulasingam and W. R. McWhinnie, *J. Chem. Soc. A*, **1968**, 254; R. K. Boggess and D. A. Zatko, *Inorg. Chem.*, **1976**, *15*, 626.

198 T. Astley, P. J. Ellis, H. C. Freeman, M. A. Hitchman, F. R. Keene, and E. R. T. Tiekink, *J. Chem. Soc., Dalton Trans.*, **1995**, 595; F. R. Keene, M. R. Snow, P. J. Stephenson, and E. R. T. Tiekink, *Inorg. Chem.*, **1988**, *27*, 2040.

199 T. Astley, M. A. Hitchman, F. R. Keene, and E. R. T. Tiekink, *J. Chem. Soc., Dalton Trans.*, **1996**, 1845.

200 P. K. Byers, A. J. Canty, and R. T. Honeyman, *J. Organomet. Chem.*, **1990**, *385*, 417.

201 S. P. Foxon, O. Walter, and S. Schindler, *Eur. J. Inorg. Chem.*, **2002**, 111; Y. Gultneh, T. B. Yisgedu, Y. T. Tesema, and R. J. Butcher, *Inorg. Chem.*, **2003**, *42*, 1857; M. P. Jensen, S. J. Lange, M. P. Mehn, E. L. Que, and L. Que, Jr., *J. Am. Chem. Soc.*, **2003**, *125*, 2113; H. Borzel, P. Comba, K. S. Hagen, Y. D. Lampeka, A. Lienke, G. Linti, M. Merz, H. Pritzkow, and L. V. Tsymbal, *Inorg. Chim. Acta*, **2002**, *337*, 407; B. de Bruin, T. P. J. Peters, J. B. M. Wilting, S. Thewissen, J. M. M. Smits, and A. W. Gal, *Eur. J. Inorg. Chem.*, **2002**, 2671; D. Mandon, A. Machkour, S. Goetz, and R. Welter, *Inorg. Chem.*, **2002**, *41*, 5364.

202 W. K. Chang, S. C. Sheu, G. H. Lee, Y. Wang, T. I. Ho, and Y. C. Lin, *J. Chem. Soc., Dalton Trans.*, **1993**, 687; J. Fan, B. Sui, T.-A. Okamura, W.-Y. Sun, W.-X. Tang, and N. Ueyama, *J. Chem. Soc., Dalton Trans.*, **2002**, 3868.

203 P. Chaudhuri and K. Wieghardt, *Prog. Inorg. Chem.*, **1987**, *35*, 329; S. Roche, S. E. Spey, H. Adams, and J. A. Thomas, *Inorg. Chim. Acta*, **2001**, *323*, 157; S. Roche, H. Adams, S. E. Spey, and J. A. Thomas, *Inorg. Chem.*, **2000**, *39*, 2385.

204 M. Kodera, H. Shimakoshi, and K. Kano, *Chem. Commun.*, **1996**, 1737; M. Kodera, H. Shimakoshi, M. Nishimura, H. Okawa, S. Iijima, and K. Kano, *Inorg. Chem.*, **1996**, *35*, 4967.

205 M. Kodera, H. Shimakoshi, Y. Tachi, K. Katayama, and K. Kano, *Chem. Lett.*, **1998**, 441; M. Kodera, Y. Tachi, S. Hirota, K. Katayama, H. Shimakoshi, K. Kano, K. Fujisawa, Y. Moro-Oka, Y. Naruta, and T. Kitagawa, *Chem. Lett.*, **1998**, 389.

206 D. L. Reger, R. F. Semeniuc, and M. D. Smith, *J. Organomet. Chem.*, **2003**, *666*, 87.

207 D. L. Reger, K. J. Brown, and M. D. Smith, *J. Organomet. Chem.*, **2002**, *658*, 50.

208 D. L. Reger, T. D. Wright, R. F. Semeniuc, T. C. Grattan, and M. D. Smith, *Inorg. Chem.*, **2001**, *40*, 6212.

209 D. L. Reger, R. F. Semeniuc, and M. D. Smith, *Inorg. Chem. Commun.*, **2002**, *5*, 278.

210 J. Manzur, A. M. Garcia, R. Letelier, E. Spodine, O. Pena, D. Grandjean, M. M. Olmstead, and B. C. Noll, *J. Chem. Soc., Dalton Trans.*, **1993**, 905.

211 E. Spodine, A. M. Atria, J. Manzur, A. M. Garcia, M. T. Garland, A. Hocquet, E. Sanhueza, R. Baggio, O. Pena, and J.-Y. Saillard, *J. Chem. Soc., Dalton Trans.*, **1997**, 3683.

212 J. Manzur, A. M. Garcia, A. Vega, and E. Spodine, *Polyhedron*, **1999**, *18*, 2399.

213 A. M. Barrios and S. J. Lippard, *J. Am. Chem. Soc.*, **1999**, *121*, 11751.

214 A. M. Barrios and S. J. Lippard, *J. Am. Chem. Soc.*, **2000**, *122*, 9172.

215 K. K. Mosny and R. H. Crabtree, *Inorg. Chim. Acta*, **1996**, *247*, 93.

216 B. Klein, N. E. Hetman, and M. E. O'Donnell, *J. Org. Chem.*, **1963**, *28*, 1682.

217 B. Klein and J. Berkowitz, *J. Am. Chem. Soc.*, **1959**, *81*, 5160.

218 S. Iwata, M. Sakajyo, and K. Tanaka, *J. Heterocycl. Chem.*, **1994**, *31*, 1433.

219 S. V. Litvinenko, Y. M. Volovenko, and F. S. Babichev, *Khim. Geterot. Soedi.*, **1993**, 367.

220 R. J. Anderson and J. C. Morris, *Tetrahedron Lett.*, **2001**, *42*, 8697; M. Alvarez, D. Fernandez, and J. A. Joule, *Tetrahedron Lett.*, **2001**, *42*, 315; R. J. Anderson and J. C. Morris, *Tetrahedron Lett.*, **2001**, *42*, 311; G. Trimurtulu, D. J. Faulkner, N. B. Perry, L. Ettouati, M. Litaudon, J. W. Blunt, M. H. G. Munro, and G. B. Jameson, *Tetrahedron*, **1994**, *50*, 3993; N. B. Perry, L. Ettouati, M. Litaudon, J. W. Blunt, M. H. G. Munro, S. Parkin, and H. Hope, *Tetrahedron*, **1994**, *50*, 3987.

221 A. Albert, *J. Chem. Soc.*, **1960**, 1790.

222 E. P. Hart, *J. Chem. Soc.*, **1954**, 1878.

223 R. C. Corcoran and S. H. Bang, *Tetrahedron Lett.*, **1990**, *31*, 6757.

224 D. B. Moran, G. O. Mortan, and J. D. Albright, *J. Heterocycl. Chem.*, **1986**, *23*, 1071.

225 I. G. Phillips, 'Syntheses and Complexes of Heterocyclic Ligands', Ph.D., University of Canterbury, Christchurch, 1995.

226 J. Hassan, V. Penalva, L. Lavenot, C. Gozzi, and M. Lemaire, *Tetrahedron*, **1998**, *54*, 13793; M. Iyoda, H. Otsuka, K. Sato, N. Nisato, and M. Oda, *Bull. Chem. Soc. Jpn.*, **1990**, *63*, 80.

227 F. Galsboel, C. H. Petersen, and K. Simonsen, *Acta Chem. Scand.*, **1996**, *50*, 567.

228 R. T. Jonas and T. D. P. Stack, *Inorg. Chem.*, **1998**, *37*, 6615; E. S. Kucharski, W. R. McWhinnie, and A. H. White, *Aust. J. Chem.*, **1978**, *31*, 2647; P. J. Arnold, S. C. Davies, J. R. Dilworth, M. C. Durrant, D. V. Griffiths, D. L. Hughes, R. L. Richards, and P. C. Sharpe, *J. Chem. Soc., Dalton Trans.*, **2001**, 736; T. Astley, H. Headlam, M. A. Hitchman, F. R. Keene, J. Pilbrow, H. Stratemeier, E. R. T. Tiekink, and Y. C. Zhong, *J. Chem. Soc., Dalton Trans.*, **1995**, 3809; K.-W. Yang, Y.-Q. Yin, Z.-X. Huang, and Y.-H. Wang, *Polyhedron*, **1996**, *15*, 79.

229 P. A. Anderson, T. Astley, M. A. Hitchman, F. R. Keene, B. Moubaraki, K. S. Murray, B. W. Skelton, E. R. T. Tiekink, H. Toftlund, and A. H. White, *J. Chem. Soc., Dalton Trans.*, **2000**, 3505.

230 T. Ayers, S. Scott, J. Goins, N. Caylor, D. Hathcock, S. J. Slattery, and D. L. Jameson, *Inorg. Chim. Acta*, **2000**, *307*, 7.

231 D. T. Cromer and A. C. Larson, *Acta Cryst.*, **1972**, *B28*, 1052; M. G. B. Drew, P. C. Yates, J. Trocha-Grimshaw, A. Lavery, K. P. McKillop, S. M. Nelson, and J. Nelson, *J. Chem. Soc., Dalton Trans.*, **1988**, 347; M. A. A. Miah, D. J. Phillips, and A. D. Rae, *Inorg. Chim. Acta*, **1992**, *201*, 191; M. A. A. Miah, D. J. Phillips, and A. D. Rae, *Inorg. Chim. Acta*, **1996**, *245*, 231; P. N. W. Baxter, H. Sleiman, J.-M. Lehn, and K. Rissanen, *Angew. Chem., Int. Ed. Engl.*, **1997**, *36*, 1294; S.-M. Kuang, Z.-Z. Zhang, Q.-G. Wang, and T. C. W. Mak, *Chem. Commun.*, **1998**, 581; S. Brooker, S. J. Hay, and P. G. Plieger, *Angew. Chem., Int. Ed.*, **2000**, *39*, 1968; Z. Xu, L. K. Thompson, C. J. Matthews, D. O. Miller, A. E. Goeta, C. Wilson, J. A. K. Howard, M. Ohba, and H. Okawa, *J. Chem. Soc., Dalton Trans.*, **2000**, 71; P. N. W. Baxter, J.-M. Lehn, G. Baum, and D. Fenske, *Chem. Eur. J.*, **2000**, *6*, 4510; W. Tsuhada, T. Sato, H. Mori, S. Sugawara, C. Kabuto, S. Miyano, and J. Inoue, *J. Organomet. Chem.*, **2001**, *627*, 121; S. Brooker, J. C. Davidson, S. J. Hay, R. T. Kelly, D. K. Kennepohl, P. G. Plieger, B. Moubaraki, K. S. Murray, E. Bill, and E. Bothe, *Coord. Chem. Rev.*, **2001**, *216*, 3; A. Escuer, R. Vicente, F. A. Mautner, M. A. S. Goher, and M. A. M. Abu-Youssef, *Chem. Commun.*, **2002**, 64.

232 E. C. Constable and M. D. Ward, *J. Am. Chem. Soc.*, **1990**, *112*, 1256; E. C. Constable, M. D. Ward, and D. A. Tocher, *J. Chem. Soc., Dalton Trans.*, **1991**, 1675.

233 K. T. Potts, M. Keshavarz, F. S. Tham, H. D. Abruna, and C. Arana, *Inorg. Chem.*, **1993**, *32*, 4436; R. Chotalia, E. C. Constable, M. Neuburger, D. R. Smith, and M. Zehnder, *J. Chem. Soc., Dalton Trans.*, **1996**, 4207.

234 E. C. Constable, M. Neuburger, D. R. Smith, and M. Zehnder, *Chem. Commun.*, **1996**, 1917.

235 C. J. Sumby and P. J. Steel, *Inorg. Chem. Commun.*, **2003**, *6*, 127.

236 J. Reim, K. Griessar, W. Haase, and B. Krebs, *J. Chem. Soc., Dalton Trans.*, **1995**, 2649.

237 C. R. Conard and M. A. Dolliver, in 'Organic Syntheses', ed. A. H. Blatt, Wiley, New York, 1943, *Coll. Vol. 2*, p. 167.

238 T. Ukai, H. Kawazura, Y. Ishii, J. J. Bonnet, and J. A. Ibers, *J. Organomet. Chem.*, **1974**, *65*, 253.

239 B. P. Sullivan, D. J. Salmon, and T. J. Meyer, *Inorg. Chem.*, **1978**, *17*, 3334.

240 P. A. Mabrouk and M. S. Wrighton, *Inorg. Chem.*, **1986**, *25*, 526.

241 E. C. Johnson, B. P. Sullivan, D. J. Salmon, S. A. Adeyemi, and T. J. Meyer, *Inorg. Chem.*, **1978**, *17*, 2211.

242 M. J. Ridd, D. J. Gakowski, G. E. Sneddon, and F. R. Keene, *J. Chem. Soc., Dalton Trans.*, **1992**, 1949.

243 I. P. Evans, A. Spencer, and G. Wilkinson, *J. Chem. Soc., Dalton Trans.*, **1973**, 204.

244 Bruker-AXS, SAINT+, 1997-1999.

245 G. M. Sheldrick, SADABS, University of Göttingen, Germany, 1998.

246 G. M. Sheldrick, *Acta Cryst.*, **1990**, *A46*, 467.

247 L. J. Farrugia, *J. Appl. Cryst.*, **1999**, *32*, 837.

248 G. M. Sheldrick, SHELXL-97, University of Göttingen, Germany, 1997.